

**DEVELOPMENT AND VALIDATION OF A NOVEL  
CFRP/STEEL HYBRID CRACK REPAIRING  
TECHNIQUE FOR THE STEEL STRUCTURES**



Sampath Abeygunasekara

(138052C)

Degree of Doctor of Philosophy in Civil Engineering

Department of Civil Engineering

University of Moratuwa

Sri Lanka

March 2023

**DEVELOPMENT AND VALIDATION OF A NOVEL  
CFRP/STEEL HYBRID CRACK REPAIRING  
TECHNIQUE FOR THE STEEL STRUCTURES**

Sampath Abeygunasekara

(138052C)

Thesis submitted in partial fulfillment of the requirements for the Degree of  
Doctor of Philosophy in Civil Engineering

Department of Civil Engineering

University of Moratuwa

Sri Lanka

March 2023

## DECLARATION

I declare that this is my own work and this thesis does not incorporate without acknowledgment any material previously submitted for a Degree or a Diploma in any other University or institute of higher learning and to the best of my knowledge and I believe that it does not contain any material previously published or written by another person except where the acknowledgement is made in this text.

Also, I hereby grant University of Moratuwa, the non-exclusive right to reproduce and distribute my dissertation, in whole or in part in print, electronic or other medium. I retain the right to use this content in whole or part in future work (such as articles or books).

---

### ***UOM Verified Signature***

Signature:

Date: 01.03.2023

The above candidate has carried out research for the Doctor of Philosophy dissertation under my supervision.

Name of the supervisors: Prof. J.C.P.H. Gamage

Dr.S.Fawzia

Signature of the supervisor: ***UOM Verified Signature*** Date: 01.03.2023

Signature of the supervisor: ***UOM Verified Signature*** Date: 4/3/2023

## ABSTRACT

Steel structures such as steel bridges greatly contribute to the socio economic development of the world. The current traffic demand has exhausted the service life of steel bridges paving the way for failures without prior warning due to fatigue. In fact, fatigue contributes to change the microstructure of a material which fails below the yield point. Therefore, fatigue could be considered as an issue related to materials, even though it is linked to the area of engineering. Interestingly, several unavoidable stress types on structures occur on steel bridges due to various reasons. As a result, avoiding fatigue on structures has become impossible during their service life. The result of stress fluctuation has caused crack initiation on steel structures while the initial stage is at a micro scale level and not visible to the naked eye. Thus, it should be controlled at the initial stage avoiding adverse effects later. Although the conventional crack repair techniques have extended service lives of structures they have led to numerous drawbacks too.

The crack stop hole technique could be considered as an emergency repairing technique to extend the fatigue life of a cracked steel structures that is quick, simple and economic. This technique was successfully applied in the aerospace industry primarily, however there had been irregularities due to the size of the hole with re-cracking appearing due to continuous service loads. Carbon fiber reinforce polymer (CFRP) materials have become popular as it has potential to replace the conventional repairing techniques with recent research focused on CFRP materials due to its light weight, corrosion resistivity, damping characteristics, fatigue resistivity and high tensile features. Therefore, this study proposes a crack stop hole (CSH) technique combined with a CFRP strengthening method to acquire the lost capacity due to fatigue in old structures with delaying re-cracking by further continue their services by steel bridges in the road and railway network operate at present.

An experimental test program carried out to determine the behavior of strengthened and non-strengthened CSH in steel members subjected to low cycle flexural fatigue. Overall, the test program was focused on estimating yield strength losses and yield strength gained by CFRP. Interestingly, various types of fatigue testing apparatus are available in the open market for a relatively high cost which is not affordable in a university laboratory, thus a hydro-electric controlling fatigue loading apparatus was designed and fabricated as an initiation to this research study to fulfill this vacuum. In this development process, machine operation, and development technique with finite element analysis on the test frame was investigated.

In the next phase of this research, a numerical model was developed using an advanced finite element model (FEM) and results were validated using the laboratory test results. The proposed numerical model was based on the cyclic J-integral method under the detect cyclic mode. The test results agreed with the model results consisting nine key parameters affecting the final results. This CFRP strengthened CSH technique is significantly enhanced fatigue life of the structural members. This investigation reported the yield strength losses; which are in the range of 13.4 % to 25.2 % compared to the non-conditioned and yield strength gains with CFRP; which is in the range of 32.2 % to 45.3 % compared to the non-strengthened CSH with the diameter varies from 4 mm to 25 mm. A considerable amount of strain controlled were recorded by CFRP with respect to non-strengthened CSH. When considering the critical parameter effects, the test results recorded a yield strength gain with respect to off-set distance; which was in the range of 36 % to 131 % compared to the CSH at the midpoint. The yield strength variation recorded due to the length of CFRP layer was in the range of 89 % to 223 % compared to the least length considered. This investigation recommended by CFRP strengthened technique has significantly enhanced fatigue bearing capacity of structural members with CSH. Design guidelines are developed for practical implementations.

**Key words:** steel members, CSH, CFRP, cyclic flexural load, Low cycle fatigue, FEM, cyclic J-integral

## **ACKNOWLEDGEMENTS**

This research paved the way to gain valuable experience on how to apply theoretical knowledge to produce important findings for the well-being and development of the community. Therefore, my gratitude should be conveyed to a number of academics and non-academics of the university of Moratuwa for assisting me to successfully complete this research investigation and dissertation.

First, I wish to express my sincere gratitude to my principal supervisor Dr. J.C.P.H. Gamage, Professor in Civil Engineering, Department of Civil Engineering, University of Moratuwa for her supervision, enthusiastic guidance and continual encouragement throughout the course of my candidature. I am indebted to her understanding, tolerance and precious support. I am very grateful to have a supervisor that believe in my work and always provide me with guidance and valuable suggestions towards completing this thesis. Without her support and guidance none of this would be possible. Furthermore, I highly appreciate the assistance of my associate supervisor Dr. S. Fawzia, Senior lecturer in School of Urban development, Queensland University of technology, Australia, for actively coaching me with her sound knowledge for the experimental work. Her expert technical suggestions and practical assistance were indispensable in improving the quality of this research work. I would like to thank the chairperson of the progress review panel, Prof. Thishan Jayasinghe, Senior Professor and Dr. Sujeewa Lewangama, Senior Lecturer and Prof. Ashoka Perera in the Department of Civil Engineering, University of Moratuwa, guiding me with valuable instructions to progress my research as progress review panel members.

The financial burden on pursuing a PhD program was eased by the department of Civil Engineering by waiving off the course fee.

I gratefully acknowledge the support of the staff in the Mechanical workshop, the Department of Mechanical Engineering at the University of Moratuwa for their valuable support. I would also like to express my gratitude to all non-academic staff members in the department and Mr. D.M.N.L. Dissanayaka, technical officer in the Structural Testing Laboratory, Mr. Yohan technical officer in the Computational

Mechanics Laboratory, Mr. Charaka Satharasinghe, technical officer in the Computer Laboratory for their valuable support extended throughout my research period.

Moreover, I would like to thank Airow Solution (PVT) Ltd and research assistants Mr. Vimukthi, Miss Varakini, Miss. Aruga, Miss Tharika and Miss. Chamodi for their kind support throughout this period. Finally, I wish to acknowledge my wife Thanuja and my daughter Sanjalee, for their love, emotional support and encouragement.

Sampath Abeygunasekara

Department of Civil Engineering

University of Moratuwa

15.02.2023

## LIST OF PUBLICATIONS AND AWARDS

### International Conferences

1. Abeygunasekara.S, Gamage.J.C.P.H, & Fawzia.S. (2021a). Influence of surface preparation on CFRP/Steel bond performance. In *Proceedings of the 12th International Conference on Structural Engineering and Construction Management 2021(ICSECM-2021)*. Earl's Regency Hotel, Kandy, Sri Lanka, December17–19.
2. Abeygunasekara.S, Gamage.J.C.P.H, & Fawzia.S. (2021b). Theoretical model for predicting re-cracking behavior of crack stop holes using J-integral technique. In *Proceedings of the 12th International Conference on Structural Engineering and Construction Management 2021(ICSECM-2021)*. Earl's Regency Hotel, Kandy, Sri Lanka, December17–19.
3. Abeygunasekara.S, Gamage.J.C.P.H, & Fawzia.S. (2020a). Design and demonstration of a low cost small scale flextural cyclic load testing apparatus for composite materials. In *Proceedings of the the International Conference on Architecture and Civil Engineering*, Kuala Lumpur, Malasiya.
4. Abeygunasekara.S, Gamage.J.C.P.H, & Fawzia.S. (2020b). State-of-the-art review influences of environmental factors in CFRP steel bonding. In *Proceedings of the 11<sup>th</sup> International Conference on Sustainable Built Environment (ICSBE)*, Kandy, Sri Lanka,10<sup>th</sup> – 12<sup>th</sup> December.
5. Abeygunasekera, S., Gamage, J. C. P. H., & Fawzia, S. (2019). Low cycle fatigue behaviour of steel/CFRP composite exposed to loads with constant amplitude. In *Proceedings of the International Conference on Civil Engineering and Applications 2019*.University of Moratuwa.
6. Abeygunasekera, S., Gamage, J. C. P. H., & Fawzia, S. (2017). Effects of environmental humidity at installation phase on performance of CFRP strengthen steel I-beam. In *Proceedings of the 8th International Conference on Structural Engineering and Construction Management 2017* (pp. 18-22). *Earl's Regency Hotel, Kandy, Sri Lanka, December 13<sup>th</sup> –15<sup>th</sup>*.
7. Abeygunasekera, S., Gamage, J. C. P. H., & Fawzia, S. (2013). Bond performance of CFRP strengthened steel members subjected to axial compression. In *Proceedings of the 4th International Conference on Structural Engineering and Construction Management 2013* (pp. 161-166). Nethwin Printers (Pvt) Ltd.

### **Indexed journal publications**

1. Abeygunasekara, S., Gamage, J.C.P.H. Fawzia. S (2018) ‘Numerical Modelling of Re-cracking Behaviour in Retrofitted Crack Stop Holes in Steel Structures, *Lecture Notes in Civil Engineering*, Volume 94. pp. 9. DOI 978-981-13-9749-3\_42, © 2020
2. Abeygunasekara.S, Gamage.J.C.P.H, & Fawzia.S. (2022). Investigating the Effects of Offset Distance in CSH on Steel Plates Under Three-Point Flexural Cyclic Loads in the LCF Range. In *Lecture Notes in Civil Engineering 174* (pp. 331–345).

### **Journal papers (under review)**

1. A novel hybrid repairing technique to delay fracture initiation and propagation of steel structures subjected to low cyclic flexural fatigue

### **Awards**

1. Best student presentation awarded to Design and demonstration of a low cost small scale flexural cyclic load testing apparatus for composite materials at the International Conference on Architecture and Civil Engineering, Kuala Lumpur, Malasiya, March 12<sup>th</sup> -13<sup>th</sup>.



# TABLE OF CONTENTS

DECLARATION .....	i
ABSTRACT.....	ii
ACKNOWLEDGEMENTS .....	iii
LIST OF PUBLICATIONS AND AWARDS .....	v
TABLE OF CONTENTS.....	vii
LIST OF FIGURES .....	xvi
LIST OF TABLES .....	xxiv
LIST OF ABBREVIATIONS .....	xxvii
LIST OF SYMBOLS AND NOTATIONS.....	xxviii
LIST OF APPENDICES .....	xxix
<b>1. INTRODUCTION.....</b>	<b>1</b>
1.1 Significance of the study .....	3
1.2 Research background.....	3
1.3 Problem identification and the research gap .....	4
1.4 Objectives .....	4
1.4.1 Primary objectives .....	5
1.4.2 Secondary objectives .....	5
1.5 Methodology.....	5
1.6 Outline of the Thesis .....	6
<b>2. LITERATURE REVIEW .....</b>	<b>9</b>
2.1 Introduction .....	10
2.1.1 Historical development of fatigue investigations .....	10
2.2 Fatigue failure.....	11
2.2.1 Sequence of fatigue failure .....	11
2.2.2 The microscopic explanation of fatigue failure .....	12
2.2.3 Material behavior with fatigue loads .....	13
2.2.4 Characteristics of fatigue .....	14

2.3	Classification of fatigue.....	15
2.3.1	Low cycle fatigue and high cycle fatigue .....	16
2.4	Prediction of fatigue life .....	18
2.4.1	Classification of fatigue life prediction techniques .....	20
2.4.2	Minor rules.....	21
2.4.3	Rain flow counting algorithm .....	22
2.5	CSH method as a repairing technique .....	23
2.5.1	Arrest the crack .....	25
2.5.2	Crack stop hole methods for crack control .....	27
2.5.3	Crack detection and placement of CSH.....	28
2.6	Mechanical treatments for CSH subjected to fatigue.....	29
2.6.1	The bottled CSH .....	29
2.6.2	The pinned CSH.....	30
2.6.3	The cold expanded CSH .....	31
2.6.4	Ancillary holes in added CSH.....	32
2.6.5	Comparison of different methods utilized in CSH strengthening .....	33
2.7	CFRP Material as a crack repairing technique .....	34
2.7.1	Modules of CFRP material .....	37
2.7.2	Flexural strength .....	39
2.7.3	Shear strength.....	39
2.8	Effects of the geometrical dimension of CRFP material .....	39
2.8.1	Effect of CFRP bond length.....	40
2.8.2	Multiple layer of CFRP material.....	40
2.8.3	Thickness of CFRP layer effects.....	40
2.9	Surface preparation.....	40
2.9.1	Surface preparation techniques.....	42
2.9.2	Steps of surface preparation .....	43
2.10	Adhesives and adhesive properties .....	44
2.10.1	Stress concentration of adhesives .....	45
2.10.2	Stiffness effect of adhesives .....	45
2.11	Effects of environmental exposure on CFRP/steel bond performance .....	46

2.11.1	Effects of environment moisture level on CFRP/Steel bond performance .....	46
2.11.2	Cyclic temperature effects on CFRP/Steel bond performance .....	47
2.11.3	Ultraviolet (UV) radiation effects on Steel/CFRP bond performance .....	49
2.11.4	Combined effects of environmental factors on Steel/CFRP bond performance .....	49
2.12	Different types of testing method for Steel/CFRP bond performance .....	51
2.12.1	Tensile load effects related investigations .....	51
2.12.2	Compression load effects related investigations .....	51
2.12.3	Combined effects of bending and compression loads .....	51
2.12.4	Impact load related investigations .....	51
2.12.5	Fatigue load related investigations .....	52
2.13	Testing standards .....	54
2.14	Behavior of fatigue .....	55
2.14.1	Pre-stressed and non- pre-stressed behavior of Steel/CFRP bond under fatigue load .....	57
2.14.2	Failure mechanism of Steel/CFRP bond under fatigue .....	57
2.14.3	Co-relation between geometry specimen's and fatigue .....	58
2.15	Field applications of CFRP strengthened material .....	59
2.15.1	Rectangular Hollow Section (RHS) .....	59
2.15.2	Circular hollow section (CHS) .....	60
2.15.3	Bridge repair related applications .....	61
2.16	Theory of material hardening .....	62
2.16.1	Kinematic hardening .....	63
2.16.2	Isotropic hardening .....	64
2.17	Fatigue related parameter effects on structural element .....	64
2.17.1	Stress intensity factor .....	65
2.17.2	Stress concentration .....	65
2.17.3	Crack tip opening displacement (CTOD) .....	65
2.17.4	Rate of energy release (G) .....	66
2.17.5	Crack growth direction .....	66

2.18	Summary of literature review .....	66
------	------------------------------------	----

### **3. DESIGNING AND FABRICATING A FATIGUE LOADING**

<b>APPARATUS .....</b>	<b>71</b>	
3.1	Introduction of design and fabricated fatigue loading apparatus .....	71
3.1.1	History of fatigue test apparatus .....	71
3.1.2	Types of fatigue loading .....	72
3.2	Classification of existing fatigue loading apparatus.....	73
3.2.1	Rotating bending type fatigue testing apparatus .....	74
3.2.2	Constant deflection amplitude cantilever bending type fatigue testing apparatus.....	75
3.2.3	Axial loading fatigue testing apparatus.....	76
3.2.4	Other types of fatigue testing apparatus.....	77
3.2.5	The modern fatigue testing machine .....	78
3.3	Design and detailing of fatigue loading apparatus .....	79
3.3.1	Considering factors for design fatigue loading apparatus.....	80
3.3.2	Essential components of any fatigue loading apparatus .....	80
3.4	Designing steps of fatigue loading apparatus.....	80
3.4.1	Designing a loading frame .....	81
3.4.2	Loads on the loading frame.....	82
3.4.3	The machining process and assembling of testing apparatus .....	82
3.4.4	Selection of load applying mechanism .....	83
3.4.5	Designing the hydraulic circuit of fatigue loading apparatus .....	84
3.4.6	The controlling system of loading apparatus .....	88
3.5	The test setup and instrumentation of loading apparatus.....	89
3.5.1	Measuring procedure of test apparatus .....	89
3.5.2	Calibration of load .....	90
3.5.3	Calibration of loading frequency .....	91
3.6	Features and benefits of the fatigue loading apparatus.....	92
3.6.1	Cost estimation of fatigue loading apparatus.....	93
3.6.2	Limitations and operating range of fatigue loading apparatus.....	94
3.6.3	Safety aspects of fatigue loading apparatus .....	94

3.6.4	Environmental impact assessment of the fatigue loading apparatus..	95
3.6.5	The maintenance procedure .....	95
3.6.6	Modification for variable loads.....	96
3.7	Summary of design and fabricated fatigue loading apparatus .....	97
<b>4</b>	<b>EXPERIMENTAL INVESTIGATIONS .....</b>	<b>99</b>
4.1	Introduction of experimental investigation relating with CSH/CFRP hybrid system.....	99
4.2	Material selection and specimen preparation .....	100
4.2.1	Selection of steel .....	100
4.2.2	Selection of the adhesive material .....	101
4.2.3	Selection of CFRP material .....	103
4.2.4	Procedure of CFRP installation with steel .....	103
4.2.5	Material properties .....	105
4.3	Test program.....	105
4.3.1	Test setup and instrumentation .....	107
4.3.2	Cyclic flexural loading setup for applying fatigue load on specimen .....	107
4.3.3	Tensile test setup for measuring the retained average strength on specimens .....	108
4.4	Behavior of steel element with respect to loading cycles.....	108
4.4.1	Behavior of non-strengthened steel element without CSH under fatigue load.....	109
4.4.2	Behavior of non-strengthened steel element with CSH under fatigue load.....	111
4.4.3	Behavior of CFRP-strengthened steel element without CSH under fatigue load.....	113
4.4.4	Behavior of CFRP-strengthened steel element with CSH under fatigue load.....	116
4.4.5	Comparison of fatigue behavior with respect to load cycles .....	118
4.5	Effects of CSH diameter on LCF .....	121

4.5.1	Behavior of non-strengthened steel element with CSH under non conditioned.....	121
4.5.2	Behavior of CFRP-strengthened steel element with CSH under a non-conditioned situation .....	123
4.5.3	Behavior of non-strengthened steel element with CSH under fatigue load.....	125
4.5.4	Behavior of CFRP strengthened steel element with CSH under fatigue load.....	127
4.5.5	Comparison of strength variation of non-strengthened and CFRP strengthened CSH .....	129
4.5.6	Strain variation of non-strengthened steel element with CSH under fatigue load.....	131
4.5.7	The Strain variation of CFRP strengthened CSH under fatigue load.....	132
4.5.8	Comparison of strain behavior of non-strengthened and CFRP strengthened CSH .....	133
4.6	Effects due to distance from mid-point to CSH .....	136
4.6.1	Fatigue behavior of non-strengthened CSH with respect to distance from the mid - point .....	137
4.6.2	Fatigue behavior of CFRP-strengthened CSH with respect to distance from the mid-point .....	139
4.6.3	Comparison of fatigue behavior of CSH with respect to distance... ..	141
4.6.4	Strain variation of non-strengthened CSH with respect to offset distance .....	143
4.6.5	Strain variation of CFRP strengthened CSH with respect to offset distance .....	147
4.6.6	Comparison of strain behavior of non-strengthened and CFRP strengthened CSH .....	150
4.7	Fatigue behavior of CFRP strengthened steel element with respect to bond length .....	152
4.7.1	Fatigue behavior of CFRP strengthened CSH with respect to bond length.....	152

4.7.2 Fatigue behavior of CFRP strengthened steel plate with respect to bond length.....	154
4.7.3 Comparison of CFRP length effects .....	157
4.8 Bond stress variation .....	159
4.9 Summary of experimental investigation related to the CSH/CFRP hybrid system.....	160

**5 FINITE ELEMENT MODELLING OF FATIGUE BEHAVIOR OF CSH SUBJECTED TO CYCLIC FLEXURAL LOADING ..... 162**

5.1 Introduction of finite element modelling related to CSH/CFRP hybrid system .....	162
5.1.1 Background of FEM .....	163
5.1.2 Procedure of simulation .....	163
5.2 Detailed steps of simulation .....	165
5.2.1 Geometry of the crack model.....	165
5.2.2 Material properties .....	166
5.2.3 Assembling of geometrical components .....	167
5.2.4 Configuration of the FEM.....	168
5.2.5 Mechanical interaction between contact surfaces.....	168
5.2.6 Loads and boundary conditions .....	169
5.2.7 Meshing of the model and mesh sensitivity analysis .....	169
5.2.8 Analysis and model results .....	173
5.3 Validation of the model .....	174
5.3.1 Non-strengthened and CFRP strengthened CSH.....	176
5.3.2 FEM results compared with experimental results for non-strengthened and CFRP strengthened CSH.....	179
5.3.3 FEM results compared with experimental results for position change of non-strengthened and CFRP strengthened CSH (Stress based) ..	182
5.4 Summary of finite element modelling related with CSH/CFRP hybrid system .....	184

<b>6. THEORETICAL APPROACH FOR EVALUATE RE- CRACKING</b>	
<b>    BEHAVIOR OF CSH.....</b>	<b>186</b>
6.1 Theoretical background of the CSH technique .....	186
6.2 Theory of fracture mechanics.....	187
6.2.1 Linear elastic fracture mechanics (LEFM).....	187
6.2.2 Elastic-plastic fracture mechanics (EPFM).....	188
6.2.3 The fatigue mechanism.....	189
6.3 Theoretical model to predict crack growth .....	191
6.3.1 Total fatigue life.....	191
6.3.2 The Paris law .....	192
6.3.3 The Power law .....	194
6.3.4 Comparison of Paris law and Power law .....	195
6.3.5 Developing a theoretical model to predict the rate of the crack growth .....	195
6.4 Factors that affect re-cracking of the CSH.....	200
6.4.1 Effects of the CSH diameter .....	200
6.4.2 Effects of member thickness .....	201
6.4.3 Effects of the crack length .....	202
6.4.4 Position of the CSH .....	203
6.4.5 Amplitude of the load .....	204
6.4.6 Loading frequency .....	205
6.4.7 Stress ratio effects .....	206
6.4.8 Effects of fiber direction of the CFRP .....	207
6.4.9 Effects of the CFRP length. ....	208
6.5 Summary of the theoretical model relating with the CSH .....	209
<b>7 PARAMETRIC STUDY .....</b>	<b>211</b>
7.1 Introduction of parametric study.....	211
7.2 Fatigue performance of CSH varying with geometry related parameters..	211
7.2.1 Member thickness .....	211
7.2.2 Crack length .....	214
7.3 Load related parameters .....	216



7.3.1 Amplitude of load .....	217
7.3.2 Loading frequency .....	219
7.3.3 The stress ratio .....	221
7.4 Fatigue behavior of CSH varying with Polymer material related parameters.....	224
7.4.1 Fiber direction angle of the CFRP .....	224
7.5 Summary of the parametric study relating to CSH/CFRP hybrid system .	226
<b>8 DISCUSSION AND CONCLUSIONS .....</b>	<b>228</b>
8.1 Conclusions.....	228
8.2 Contributions .....	230
8.3 Future research works.....	231
8.4 Engineering implications.....	232
<b>REFERENCES.....</b>	<b>234</b>
Appendix – A.....	254
Appendix – B .....	262

## LIST OF FIGURES

	Page
Figure 2 1: Main steps of fatigue .....	12
Figure 2 2: Crack growth with number of cycles .....	13
Figure 2 3: HCF to LCF transition.....	13
Figure 2 4: Fatigue bearing capacity variation with number of cycles.....	16
Figure 2 5: Various aspects of fatigue life prediction of steel structures.....	19
Figure 2 6: Methods of fatigue life evaluation.....	20
Figure 2 7: Stress variations with time linked to variable amplitude loads .....	21
Figure 2 8: Stress variation with number of cycles.....	21
Figure 2 9: Rain-flow counting methods related to (a) Pagoda roof (b) stress history .....	23
Figure 2 10: CSH placed at the crack tip (a) schematic view of crack stop hole (b) re-cracking of crack stop hole.....	25
Figure 2 11: Bolted crack stop hole .....	30
Figure 2 12: Pinned crack stop hole.....	31
Figure 2 13: Cold expanded CSH .....	32
Figure 2 14: Schematic diagram of the ancillary holes added CSH .....	33
Figure 2 15: Elephant's foot buckling failure of hollow sections.....	61
Figure 2 16: Uni-axial stress-strain curve .....	63
Figure 2 17: Kinematic hardening curve .....	63
Figure 2 18: Isotropic hardening behavior .....	64
Figure 3 1: The picture of first fatigue testing machine.....	72
Figure 3 2: Rotating Bending Testing Machine .....	75
Figure 3 3: Cantilever bending testing machine .....	76
Figure 3 4: Axial loading fatigue testing machine .....	77
Figure 3 5: Conventional fatigue testing apparatus (a) rotating cantilever bending fatigue testing apparatus (b) rotating bending fatigue testing apparatus .....	78
Figure 3 6: Modern fatigue testing machines .....	78
Figure 3 7: The layout of developed fatigue test apparatus .....	79
Figure 3 8: Different types of energy conversion in each step. ....	80

Figure 3 9: Finite element mesh and stress concentration of loading frame (a) before FEA (b) After FEA.....	82
Figure 3 10: Cyclic flexural test apparatus and loading frame .....	83
Figure 3.11: Cyclic flexural load circuit (a) simulation circuit (b) actual hydraulic circuit .....	87
Figure 3 12: Schematic diagram of spring return single acting cylinder .....	88
Figure 3 13: ARDUINO UNO, open-source electronics circuit used for fatigue test controller (a) development board (b) circuit.....	89
Figure 3 14: Calibration of test apparatus (a)Load measured using load cell (b) Magnifying CSH (c) A data logger with digital display.....	91
Figure 3 15: Complete test setup .....	92
Figure 4 1: Test specimen .....	101
Figure 4 2: Specimen preparation for testing (a) Bare steel plate (b) Grinded steel surface (c) Primer coated steel surface .....	101
Figure 4 3: Two part epoxy adhesive (a) before mixing (b) after mixing with hardner .....	102
Figure 4 4: Normal module of CFRP material .....	103
Figure 4 5: CFRP strengthened specimen schematic view.....	106
Figure 4 6: Typical test specimen .....	106
Figure 4 7: Cyclic flexural test setup for conditioning (a) loading frame (b) specimen fixture .....	107
Figure 4 8: Tensile test setup (a) schematic test layout (scale 1:4) (b) typical test fixture.....	108
Figure 4 9: Schematic diagram (a) elevation (b) Plane view (c) typical specimens of non-strengthened plates without CSH.....	109
Figure 4 10: Variation of retained yield strength with exposure cycles for non-strengthened plate specimen .....	110
Figure 4 11: Failure mode of plane specimens non-strengthened plates without CSH.....	111
Figure 4 12: Schematic diagram (a) elevation (b) plane view (c) typical specimens of non-strengthened plates with CSH .....	112

Figure 4 13: Variation of retained yield strength with exposure cycles for non-strengthened plate specimen with CSH.....	113
Figure 4 14: Failure mode of plane specimens non-strengthened plates with CSH .....	113
Figure 4 15: Schematic diagram (a) elevation (b) Plane view (c) typical specimens of CFRP strengthened plates without CSH.....	114
Figure 4 16: Variation of retained average strength with exposure cycles for CFRP-strengthened plane specimen.....	115
Figure 4 17: Failure mode of CFRP strengthened plane specimens without CSH .....	116
Figure 4 18: Schematic diagram (a) elevation (b) Plane view (c) typical specimens of CFRP strengthened plates with CSH.....	117
Figure 4 19: Average strength variation with number of cycles for CFRP-strengthened steel element with CSH.....	118
Figure 4 20: Failure mode of CFRP-strengthened steel element with CSH.....	118
Figure 4 21: Variation of retained average strength with exposure cycles.....	119
Figure 4 22: Percentage of strength gain by CFRP with respect to loading cycles (a) without CSH (b) with CSH.....	120
Figure 4 23: Schematic view of the non-conditioned and non-strengthened specimen (Scale 1:2) (a) elevation (b) plane view (c) typical specimen.....	121
Figure 4 24: Retained average yield stress variation with diameter to width ratio.....	122
Figure 4 25: Failure mode of non-conditioned non-strengthened CSH.....	123
Figure 4 26: Schematic view of the non-conditioned CFRP-strengthened specimen (Scale 1:2) (a) elevation (b) plane view (c) typical specimen.....	123
Figure 4 27: Retained average strength variation with number of cycles for CFRP - strengthened steel element with CSH.....	124
Figure 4 28: Failure mode of non-conditioned CFRP-strengthened specimen(a) bottom surface (b) top surface .....	125

Figure 4 29: Schematic view of the conditioning steel element with non-strengthened CSH specimen (scale 1:2) (a) elevation (b) plane view (c) typical test specimen .....	125
Figure 4 30: Retained average strength variations with the diameter to width ratio of conditioned non strengthened CSH .....	126
Figure 4 31: Failure mode of conditioned non strengthened steel element with CSH .....	127
Figure 4 32: Schematic diagram of the conditioning steel element with CFRP strengthened CSH (a) elevation (b) plane view (c) typical test specimen .....	127
Figure 4 33: Retained average strength variation of CFRP strengthened conditioned CSH with respect to diameter to width ratio .....	128
Figure 4 34: Failure mode of conditioned CFRP strengthened CSH .....	129
Figure 4 35: Comparison of strength gains for non-strengthened and CFRP strengthened CSH .....	130
Figure 4 36: Average strength with respect to diameter to width ratio (a) losses due to fatigue (b) gain by CFRP.....	131
Figure 4 37: Schematic view of the non-strengthened strain gauge attached CSH specimen (a) elevation (b) plane view (c) typical test specimen .....	132
Figure 4 38: Schematic view of the CFRP strengthened strain gauge attached CSH specimen (a) elevation (b) plane view (c) typical specimen .....	133
Figure 4 39: Strain variations with number of flexural cycles when d/b is ;(a) 0.1 (b) 0.2 (c) 0.3 (d) 0.4 (e) 0.5 (f) 0.6 .....	135
Figure 4 40: Schematic view of the non-strengthened offset CSH specimen (a) elevation (b) plane view (c) typical test specimen .....	137
Figure 4 41: Variation of retained average strength with offset distance for strengthened samples .....	138
Figure 4 42: Failure mechanisms with offset distance for non-strengthened samples.....	139

Figure 4 43: Schematic view of the CFRP strengthened offset CSH specimen (a) elevation (b) plane view (c) typical test specimen .....	140
Figure 4 44: The average strength variation with the location of the CSH.....	141
Figure 4 45: Failure mode of CFRP strengthened offset CSH.....	141
Figure 4 46: Variation of retained average strength gain with offset distance for non-strengthened and CFRP strengthened samples .....	142
Figure 4 47: Percentage strength gain by CFRP strengthened with respect to CSH position.....	143
Figure 4 48: Schematic view of the non-strengthened strain gauge attached offset CSH specimen (a) elevation (b) plane view .....	144
Figure 4 49: Typical specimen of non-strengthened strain gauge attached offset CSH.....	144
Figure 4 50: Strain variations with offset distance of non-strengthened CSH when x is; (a)20 mm (b) 40 mm (c) 60 mm (d) 80 mm (e) 100 mm .....	146
Figure 4 51: Schematic view of CFRP-strengthened strain gauge attached offset CSH.....	147
Figure 4 52: Strain variations with offset distance of CFRP-strengthened CSH when x is; (a) 20 mm (b) 40 mm (c ) 60 mm (d) 80 mm (e) 100 mm .....	149
Figure 4 53: Comparison of strain variations with offset distance for non- strengthened and CFRP strengthened CSH when x is; (a) 20 mm (b) 40 mm (c) 60 mm (d) 80 mm (e) 100 mm.....	151
Figure 4 54: Schematic view of the CFRP strengthen specimen (a) elevation (b) Plane view (c) typical specimen .....	153
Figure 4 55: Retained average strength variation in the length of CFRP layer.....	154
Figure 4 56: Failure mode of CSH due to bond length variation .....	154
Figure 4 57: Schematic view of the CFRP strengthen specimen (a) elevation (b) plane view (c) typical specimen .....	155
Figure 4 58: Retained average strength varies with the length of CFRP .....	156
Figure 4 59: Failure mode of steel member without CSH variation with bond length.....	157

Figure 4 60: Comparison of strength variation by CFRP bond length .....	158
Figure 4 61: Bond stress variation with respect to (a) number of cycles (b) diameter to width ratio (c) bond length.....	159
Figure 5 1: A model view of the specimen after introducing contours and crack seems .....	165
Figure 5 2: The assembly module of the test setup (a) front view (b) plane view.....	167
Figure 5 3: The contour path and crack seams.....	168
Figure 5 4: A loading mode and boundary conditions.....	169
Figure 5 5: Mesh model (a) Front view of the mesh model (b) Bottom view of the mesh model (c) 8 node brick element.....	170
Figure 5 6: Mesh sensitivity anylysis with the mesh size (a) number of nodes (b) wall clock time .....	172
Figure 5 7: Contours with different mesh size (a) 1 mm (b) 2mm (c) 3 mm (d) 4 mm.....	173
Figure 5 8: The Visualization module of specimen (a) test setup (b) bottom view.....	174
Figure 5 9: Stress distribution near the crack stop hole .....	176
Figure 5 10: Average strength variation with diameter to width ratio of CSH .....	177
Figure 5 11: Visualization of the bottom view under fatigue load profile with diameter to width ratio of CFRP strengthened CSH specimen (a) 0.1 (b) 0.2 (c) 0.3 (d) 0.4 (e) 0.5 (f) 0.6 .....	179
Figure 5 12: Numerical models comparing the experimental results for different diameter to width ratio (d/b) under cyclic flexural load (a) 0.1 (b) 0.2 (c) 0.3 (d) 0.4 (e) 0.5 (f) 0.6.....	181
Figure 5.13: Average strength variation with offset distance of CSH.....	182
Figure 5 14: Visualization of the bottom view under fatigue load profile with offset distance. (a) 0 (b) 20 mm (c) 40 mm (d) 60 mm (e) 80 mm .....	183
Figure 6 1: Basic modes of crack deformation. (a) opening; (b) In-plane shear (c) Out- plane shear .....	187

Figure 6 2: Stress distribution at CSH of steel plate .....	190
Figure 6 3: Paris law related curve .....	193
Figure 6 4: Log value of rate of fatigue crack growth with cyclic J-integral .....	197
Figure 6 5: Comparison of Power law with laboratory test results .....	199
Figure 6 6: Number of cycles for crack initiation with the CSH diameter.....	200
Figure 6 7: Number of cycles for crack initiation varies with the thickness to diameter ratio of the specimen.....	201
Figure 6 8: Number of cycles for crack initiation vary with the crack length of the specimen .....	202
Figure 6 9: Number of cycles for crack initiation varies with diameter to offset distance ratio .....	203
Figure 6 10: Number of cycles for crack initiation with respect to diameter to load ratio .....	204
Figure 6 11: Required number of cycle for crack initiation variations with respect to diameter to loading frequency ratio.....	205
Figure 6 12: Number of cycles for crack initiation with respect to ratio of diameter to stress ratio .....	206
Figure 6 13: Fiber direction with respect to the Crack direction.....	207
Figure 6 14: Number of cycles for crack initiation with respect to diameter to bond length ratio .....	208
Figure 7 1: Strength variation with diameter to width ratio of CSH.....	212
Figure 7 2: Visualization of the bottom view under fatigue load profile with diameter to width ratio of CSH specimen (a) 0.1 (b) 0.2 (c) 0.3 (d) 0.4 (e) 0.5 (f) 0.6 .....	213
Figure 7 3: Strength variation with thickness to diameter ratio of member .....	215
Figure 7 4: Visualization of the bottom view under fatigue load profile with thick specimen. (a) 5 mm (b) 6 mm (c) 7 mm (d) 8 mm (e) 9 mm (f) 10 mm .....	216
Figure 7 5: Strength variation with diameter to crack length ratio.....	217



Figure 7 6: Visualization of the bottom view under fatigue load profile with crack length from the mid- point (a) 0 (b)20 mm (c) 40 mm (d) 60 mm (e) 80 mm (f) 100 mm .....	218
Figure 7 7: Strength variation with diameter to offset distance ratio .....	219
Figure 7 8: Visualization of the bottom view under fatigue load profile with offset from the mid point. (a) 20 mm (b) 40 mm (c) 60 mm (d) 80 mm (e) 100 mm.....	221
Figure 7 9: Strength variation of CSH with load.....	222
Figure 7 10: Visualization of the bottom view under fatigue load profile with loaded specimen.(a) 2 kN (b) 4 kN (c) 6 kN (d) 8 kN(e) 10 kN.....	223
Figure 7 11: Strength variation with frequency.....	225
Figure 7 12: Visualization of the bottom view under fatigue load profile with loading frequency at the mid point (a) 1 Hz (b) 2 Hz (c) 4 Hz (d) 5 Hz (e) 8 Hz (f) 10 Hz .....	226

## LIST OF TABLES

	Page
Table 2.1: Summary of results of different crack stop hole treatment methods ....	34
Table 2.2: Properties of CFRP material .....	38
Table 2.3: Characteristics of steel & CFRP .....	38
Table 2.4: Factors affecting the CFRP/ steel bond performance .....	68
Table 2.5: Summary of bond performance characteristics related studies.....	254
Table 2.6: Summary of surface preparation technology related key studies .....	255
Table 2.7: Key research studies related to adhesives and adhesive properties ....	256
Table 2.8: Summary of bonding mechanisms related to key research investigations .....	257
Table 2.9: Key research studies related to humidity effects on CFRP/ steel bond performance .....	259
Table 2.10: Summary of key research investigations related temperature and humidity combination effects on CFRP/steel bond performance .....	260
Table 2.11: Summary of reported bridge retrofitted with CFRP (Nisal Abeetha, 2011) .....	261
Table 3.1: Comparison of the hydraulic ramp and the cam mechanism.....	84
Table 3.2: List of accessories of hydraulic system .....	86
Table 3.3: Expenditure for the fabricate cyclic flexural load test apparatus .....	94
Table 4.1: Measured and manufactures provided material properties.....	105
Table 4.2: Summary of test program .....	106
Table 4.3: Retained average strength of non-strengthened steel element with the number of cycles .....	110
Table 4.4: Retained average strength of non-strengthened steel element with CSH .....	112
Table 4.5: Retained average strength of CFRP-strengthened steel element without CSH.....	115
Table 4.6: Retained average strength of CFRP-strengthened plane specimen with CSH.....	117
Table 4.7: Comparison of strength gain by CFRP .....	119

Table 4.8:	Retained average strength of non-strengthened steel element with the number of cycles .....	122
Table 4.9:	Retained average strength of bare steel varies with the number of cycles .....	124
Table 4.10:	Retained average strength of non- strengthened steel varies with the number of cycles .....	126
Table 4.11:	Retained average strength of CFRP strengthened conditioned CSH varies with the diameter to width ratio.....	128
Table 4.12:	Average strength gained by CFRP material under cyclic flexural loads .....	129
Table 4.13:	Retained average strength variation with the location of the non-strengthened CSH .....	138
Table 4.14:	Retained average strength variation with the location of the CFRP strengthened CSH .....	140
Table 4.15:	Retained average strength, gain with CFRP strengthened offset CSH.....	142
Table 4.16:	Retained average strength varies with the length of CFRP .....	153
Table 4.17:	Retained average strength varies with the length of CFRP .....	156
Table 4.18:	Comparison of retained average strength, variation with bond length.....	157
Table 5.1:	FEM results compared with test results for CSH.....	177
Table 5.2:	FEM result and test results compared with position of CSH.....	182
Table 6.1:	Summary of the fracture mechanics theory .....	188
Table 6.2:	Number of cycles for crack initiation by the Paris law with respect to diameter to width ratio .....	196
Table 6.3:	Log values of the crack growth rate variations with diameter to width ratio of the CSH .....	197
Table 6.4:	Test results comparison with the Power law approximation .....	199
Table 6.5:	Number of cycles for crack initiation with respect to the diameter to width ratio .....	262
Table 6.6:	Number of cycles for crack initiation with respect to the thickness to diameter ratio .....	262

Table 6.7:	Number of cycles for crack initiation with respect to the diameter to crack length ratio.....	263
Table 6.8:	Number of cycles for crack initiation with respect to the diameter to offset distance ratio .....	263
Table 6.9:	Number of cycles for crack initiation with respect to the diameter to load ratio .....	264
Table 6.10:	Number of cycles for crack initiation with respect to the diameter to loading frequency.....	264
Table 6.11:	Number of cycles for crack initiation with respect to the ratio of diameter to stress ratio .....	265
Table 6.12:	Number of cycles for crack initiation with respect to the angle of fiber direction .....	265
Table 6.13:	Number of cycles for crack initiation with respect to the diameter to bond length ratio .....	266
Table 7.1:	Strength variation with respect to the diameter to width ratio .....	212
Table 7.2:	Strength variation with respect to the diameter to crack length ratio	214
Table 7.3:	Strength variation with respect to the diameter to loading amplitude ratio .....	217
Table 7.4:	Strength variation with respect to the diameter to loading frequency ratio .....	219
Table 7.5:	Strength variation with respect to the ratio of diameter to stress ratio	221
Table 7.6:	Strength variation with respect to the fiber direction.....	224
Table 7.7:	Fatigue related design guidelines for CSH .....	227

## LIST OF ABBREVIATIONS

<b>Abbreviation</b>	<b>Description</b>
CCF	Combined Cycle Fatigue
CFRP	Carbon Fiber Reinforced Polymer
CMOD	Crack Mouth Opening Displacement
CSH	Crack Stop Hole
CTOD	Crack Tip Opening Displacement
DB	De-bonding
DBTT	Ductile Brittle Transition Temperature
DCV	Directional Control Valve
DL	De-lamination
EPFM	Elastic Plastic Fracture Mechanics
FCGR	Fatigue Crack Growth Rate
FEM	Finite Element Model
GFRP	Glass Fiber Reinforced Polymer
HCF	High Cycle Fatigue
HLF	Hydraulic Loading Frame
HM	High Module
LCF	Low Cycle Fatigue
LEFM	Linear Elastic Fracture Mechanics
LVDT	Linear Variable Differential Transformer
MCB	Magnetic Circuit Braker
MSC	Microstructural Short Crack
NM	Normal Module
SIF	Stress Intensity Factor
UHM	Ultra High Module
UTM	Universal Tensile Machine

## LIST OF SYMBOLS AND NOTATIONS

Symbol	Description	
$da/dN$	Rate of crack growth (mm/cycle)	mm/cycle
$a$	Crack length	mm
$\Delta K$	Range of stress intensity factor	[MPa $\sqrt{m}$ ]
$C$	Paris law coefficient	
$m$	Paris law exponent	
$\Delta J$	Cyclic J-integral value	
$E$	Elastic modulus of the material	GNm <sup>-2</sup>
$J_{max}$	Maximum value of J–integral	
$J_{min}$	Minimum value of J –integral	
$A$	Ramberg-Osgood coefficient	
$n$	Strain hardening index	
$N_f$	Total number of cycle of fatigue	
$N_i$	Number of cycles for crack initiation	
$N_p$	Number of cycles for crack propagation	
$R$	Stress ratio	
$f$	Loading frequency	Hz
$T_g$	Glass transition temperature	<sup>o</sup> C

## LIST OF APPENDICES

<b>Appendix</b>	<b>Description</b>
Appendix – A	Key finding from literature review
Appendix – B	Results of theoretical model
Appendix – C	Mechanical drawing for fatigue test apparatus
Appendix – D	Copy of publications

## ***Chapter – 1***

---

# ***Introduction to the Research***



# 1. INTRODUCTION

The phenomena of fatigue could be explained as a crack initiation with a crack growth until failure occurs due to effects of repetitive loads. A crack initiation process begins as shear cracks on the material surface. However, all elements of steel structures show fabrication-related discontinuities with stress concentrators such as welds, notches and holes. These stress raisers contribute to accelerate fatigue cracking and they drive, fatigue cracks where failure occurs below the yield point of material. When members of steel structure are stressed by service loads, a crack initiates at a microscopic level. These micro-level cracks gradually rise to a critical level and ultimately the elements of the structures are separate. The whole process begins as an invisible crack initiation at micro scale after that its grows up to a macro scale level. The overall process is called the fatigue life of the structural member.

However, fatigue is not an Engineering problem since it is related to the behavior of any material due to stress fluctuations. The cyclic effect causes to change the mechanical properties of a material which results in failure which occurs below the yield point of the ductile material. Interestingly, quick and sudden failure occurs without any prior warning within a very short duration which causes the loss of lives and properties due to fatigue.

Therefore, fatigue related repairs of steel structures are very important to continue their services within a safety limits. Conventionally steel plates are connected to cracked members used with welding or nut and bolts as a repair technique. However, these methods show limitations which include heavy equipment, skilled labour, self-weight increase, change in micro structure of material due to heat, loss of fatigue durability, discontinuity of the cross section, difficult to use in case of emergency and high down time.

The CSH method is a proven technique for crack control and it has great potential to overcome a majority of the drawbacks mentioned above.

This crack stop hole technique could be considered a quick, simple and cost effective method. The technique of the CSH is done by drilling a hole at the end of crack tip, to convert the crack into a notch. The result is the reduction of stress on the cracked structural elements. This method was successfully utilized in aerospace related applications. At present a few civil engineering applications such as the steel bridge related applications utilizes this technique to control crack propagation. However, reduction of stiffness and re-cracking due to continuous service loads could be considered as major drawbacks of this technology.

CFRP materials have specific features compared to steel including a high tensile strength, corrosion resistivity, fatigue durability and significant strength to weight ratio. However, the repair technique should fulfill the re installation of fatigue loss, controlling the further growth of crack and minimized formation of new cracks. As a result, these kinds of techniques helps to re- install the fatigue capacity of an old structure while in a new structure the capacity would be enhanced. Consequently, the service demand could be fulfilled by these structures in all situations.

Interestingly, the past decade has introduced high performance computing techniques as well as advanced experimental methods to estimate fatigue life under cyclic loading. Such methods are related to material degradation, deformation mechanisms, and modeling concepts. Specially, microstructure-based evaluation techniques for fatigue crack growth have succeeded in the past two decades. Laboratory experiments could be conducted to determine fatigue related parameters, however it is more expensive and time consuming. Hence, the FEA could be considered a good alternative to overcome such barriers, however it requires a vast knowledge about the finite element modelling technique. This study utilized ABAQUS 6.14 version for FEM and simulation was carried out using the J-integral technique under the direct cyclic mode.

Performance of CSH technique depends on a vast number of internal and external parameters which affects fatigue life of such structures. These parameters could be classified as geometrical parameters, loading parameters and material characteristics. Geometric parameters were further classified into the size of the CSH, location of the CSH, thickness of the member and length of the crack. Loading parameters could be

classified as magnitude of loads, loading frequency and the stress ratio. The material characteristic of the CFRP includes the module of elasticity, the length of the CFRP layer and the effects of the fiber angle which were critically evaluated in this study.

### **1.1 Significance of the study**

Many of fatigue experiment are concerned with axial tensile fatigue or rotational fatigue. Nevertheless, flexural fatigue is closer to structural related applications rather than axial fatigue or rotational fatigue. Therefore, this study focuses on investigating LCF behavior of the CSH under flexural cyclic loadings and evaluates potential of the utilized CFRP to overcome limitations of the CSH method.

### **1.2 Research background**

Fatigue is critical for structural engineering related infrastructure such as roads and railway bridges. The action of fatigue plays a main role where nearly 90 percent of material failures occur due to repetitive stress action (Ye et al., 2014). According to previous investigations 80 % to 90 % of structural failures have been dealing with fatigue fractures (ASCE Committee on Fatigue and Fracture Reliability, 1982). In fact, a wide range of steel structures suffer due to the effect of fatigue during its service life which includes bridges, offshore marine flat forms, and any kind of structures. Fatigue failure causes the loss of lives and properties, because material weakens due to repetitive actions. On the other hand, nearly 50 % of existing steel bridges in the world have reached the end of their service lives and needs to be replaced in some instances. Meanwhile service demands of such structures also rapidly increase due to the present socio economic needs such as traffic demand on bridges. This situation causes the existing issue to become more complicated. However, replacement of all degraded structures at the same time is impossible due to lack of finances. Therefore, many authorities continue utilizing the same structures while using appropriate repairing techniques. However, lack of finances and administrative issues delay the repairing of the damaged structures. As a result, micro cracks grow up to critical levels during a short period. Also, the demand for new structures is considerably high which has led to the search of new possibilities.

### **1.3 Problem identification and the research gap**

According to the literature review the research needs were identified under three main categories related to fatigue on steel structures. There are identified potential drawbacks relating to the CSH technique which includes the, lack of fatigue testing apparatus at laboratories and non-availability of an effective numerical model to predict fatigue behavior of a material.

The crack stop hole (CSH) technique is a solution for crack growth stopping as well as changing the direction of the crack that protects the critical area of a structural member. However, CSH starts re-cracking due to continuous service loads as well as average strength decline of the cross section due to material removal of the CSH. Therefore, there should be a solution to improve the performance of the CSH technique. In addition, the performance of this technique highly depends on a large number of parameters including the size of the CSH. The size of CSH is a main debate in this technique and needs an appropriate design guide line to decide the size of the CSH as the effects of such parameters influence fatigue performance.

The available fatigue test apparatus is not cost affordable and is limited to a selected geometrical shape and size. Therefore, there should be a design cost effective fatigue loading apparatus to be used in the laboratory in a higher education institute. Structural engineering related applications are closely connected to flexural loads than tensile loads or rotations. Therefore, a flexural based investigation is essential to estimate the fatigue behavior of structural related applications.

Most laboratory tests are related to fatigue durability which are based on the geometry of the element and it is very hard due to varieties of such sections in the same structure. On the other hand, fatigue deals with material properties. Therefore, a numerical model is essential to assess fatigue behavior based on material properties.

### **1.4 Objectives**

The objective of this study is to investigate the behavior of the CSH under fatigue loading and to introduce design guide lines to select the size of the CSH.

#### **1.4.1 Primary objectives**

1. To provide a detailed investigation of the state-of-the-art fatigue performance in CFRP strengthened steel structures.
2. To design and fabricate a fatigue loading apparatus which can apply cyclic flexural loads on test specimens
3. To introduce design guide lines to decide the appropriate size of the CSH for crack control
4. To evaluate the potential of re-cracking controlling and stiffness enhancement of the CSH by CFRP material
5. To develop an efficient and effective numerical model to simulate the fatigue behavior of the CSH
6. To investigate effects of critical parameters on the CSH under flexural cyclic loading

#### **1.4.2 Secondary objectives**

1. To determine the fatigue bearing capacity by re-installation of CFRP material with respect to the non-strengthened condition.
2. To develop a theoretical model based on the Paris law and improve the Power law with new coefficients based on material properties
3. To compare the loss of fatigue capacity as well as capacity enhancement by the CFRP material with respect to conditioned specimens in the range of LCF

#### **1.5 Methodology**

1. A literature review was conducted to summarize existing investigations related to crack repair as well as CFRP strengthened techniques and identified gap of research
2. A fatigue loading apparatus was designed and fabricated based on electro-hydraulic controls with a 10 kN load capacity.
3. An experimental test program was performed with seven test series to investigate fatigue related measurements of the CSH.

4. The FEM was developed using ABAQUS 6.14, commercially available FE software with a similar test setup with laboratory tests.
5. The model was used to compare laboratory test results for the purpose of validation.
6. A theoretical model was developed based on the Paris law to predict the required number of cycles for re-cracking of the CSH.
7. Model results were utilized to conduct a parametric study to estimate unknown parameter effects on the performance of the CSH.
8. Test results were concluded and FEM results were presented with design guidelines and recommendations for the CSH technique.

### **1.6 Outline of the Thesis**

This thesis is divided into eight chapters and organized as follows:

Chapter 1-The introduction of this research study including the significance of study, background, problem identification and identification of research gap, research objectives and methodology are described in this chapter.

Chapter 2 – The aim of this chapter is to discuss the CFRP strengthened techniques, influencing factors, and test results of the past research efforts related to the CFRP strengthened, crack stop hole method, crack initiation, and CFRP uses for steel strengthening under fatigue loading. Uses of the CSH to accommodate the CSH and the factors influencing the performance of the CSH technique were also included in this chapter. In addition, different techniques utilized to enhance performance of the CSH are discussed in detail. Also, understanding of fatigue failure mechanism with leading explanations is another main aspect of this chapter. Theory related hardening and softening effects on material due to fatigue was also discussed with a leading crack growth model and compared with the present study. In addition, it attempts to understand the steps of fatigue failure, and attention with total life.

Chapter 3- The aim is to design and fabricate a low cost fatigue loading apparatus which is discussed in detail in this chapter. It also focuses on understanding the history of the development of fatigue test apparatus, analyzing operating mechanisms of

existing apparatus, following design steps, selecting load apply mechanism for new apparatus, and selecting load and frequency controlling techniques. There are a few critical components such as loading frame, power supply unit, load apply mechanism and monitoring devices included in this section with concerns regarding the safety, accuracy of reading, maintenance, cost effectiveness of the apparatus and environmental related issues. The ultimate aim in this chapter is explain in detail the design and fabrication of the fatigue loading apparatus to apply the desired loads effectively on the specimens.

Chapter 4– The main target of this chapter is to determine the fatigue behavior of the non-strengthened CSH and compare the test results with the CFRP strengthened technique. In addition, the strain distribution of non-strengthened and CFRP strengthened CSH are also compared in this chapter. It includes the investigation of position of CSH with respect to loading point. Furthermore, describe the influences of bond length on the CSH subjected to cyclic flexural loading. A total of seven test series with 162 test specimens were prepared and tested in this background. Eventually, strength losses due to fatigue and the strength gains by the CFRP were compared and discussed. Consequently, test results are reconciled with the non-strengthened CSH to determine whether this technology shows any significant gain by CFRP.

Chapter 5 –This chapter aims to develop a numerical model to predict fatigue related parameters which support in taking decisions about structural elements using ABAQUS. The result of FEM was compared with the laboratory test results to validate the model. In addition, it aims to discuss the replacement of conventional techniques utilized in predicting crack related parameters due to their restrictions. Numerical modeling was based on cyclic J-integral technique under direct cyclic mode and attention was given to utilize the concept of the Power law.

Chapter 6 – This chapter presents the theoretical approach of the fatigue behavior of CSH. The Paris law and model results are utilized to moderate Power law which is constant due to material properties changing because of fatigue. Specially this chapter investigates the prediction of required number of cycles for re-cracking of CSH as a fatigue related parameter due to the effects of the LCF.

Chapter 7 – In this investigation, the effects of the most critical parameters were considered in the selected domain. This analysis aims to understand and estimate the influences of geometrical parameters such as location, diameter, crack length and thickness of the CSH. The loading parameters considered in this chapter were the magnitude of load, loading frequency and the stress ratio. The CFRP related parameters were also considered in this study with the length of the CFRP material, effects of hybrid composite fiber direction angle with respect to crack direction.

Chapter 8 – The final chapter summarizes conclusions and observations, Engineering implications of findings of the present investigation and provides design guidelines and recommendations to improve the CSH technique. In addition, potential research areas were identified for the future as an extension of the present work.



## ***Chapter – 2***

---

### ***Literature Review***

## **2. LITERATURE REVIEW**

### **2.1 Introduction**

The aim of this chapter is to provide a detail review of the past investigations related to the CFRP uses for steel structures strengthening under fatigue loading. Uses of CSH to accommodate the crack and the factors influencing on performance are also review in this chapter. In addition, different techniques utilized to enhance performance of the CSH are discussed in detail. Furthermore, factors which influence the performance and durability of the steel/CFRP bond, such as surface preparation and selection of the adhesive are also discussed in this section. It discusses mechanical properties of CFRP material and geometric parameter effects on bond performance. Furthermore, it elaborates on structural related test methods and possible failure mechanisms. In addition, this chapter focuses on evaluating the effects of the external factors on bond performance, durability and strength of CFRP/steel composition. Consequently, it would introduce relevant field application to confirm the potential to use this technique as a real world application. A review of other relevant research studies is also provided in this section. A considerable amount of literature has been studied on CFRP embedded technique, however only a minimal amount of research has been carried out on the crack stop hole method, and fatigue life prediction on the crack stop hole. The survey is detailed, add to the present body of study as well as to justify the direction and scope of present study.

#### **2.1.1 Historical development of fatigue investigations**

The first study on metal fatigue was performed by Albert in 1826. This study was based on mine –hoist chain failure due to fatigue. In fact, Poncelet introduced the term of fatigue relating to metal failure in 1839. The term “fatigue” was described firstly in the 1840s to understand failures which occurred due to repeated loads. The first detailed study into fatigue was reported in 1842 based on the Versailles railway accident in France (Suresh, 1991). The first investigation of fatigue was conducted by August Wohler in 1850s while W.J.M. Rankine recognized the characteristics of fatigue fractures as well as emphasized dangers of stress concentration in machine components in 1843. In the 19<sup>th</sup> century, fatigue was considered an enigmatic

phenomenon due to the nature of failure (Ye et al., 2014). Such failure was sudden and unrecoverable which was known as a catastrophic failure. Interestingly, in the 20<sup>th</sup> century, the reason behind fatigue failure was understood as repetitive loads on structures.

Wohler introduced the concept of the endurance limit for fatigue in 1860 (Chandran, 2016). In the second part of the nineteenth century, Gerber in 1874 and Goodman in 1899 individually explain methods for fatigue design. Furthermore, Bauschinger in 1886 reported the variation in the elastic limit of materials due to reverse loading. Theory of micro-structural crystallization was remained un-challenged until to investigation of Ewing and Humphrey in 1903. Authors emphasized the development of slip bands and successive fatigue cracks in poly-crystalline materials (Ewing and Humphrey, 1903). In 1910, the behavior of stress-strain response due to fatigue were examined by Bairstow, et al. and authors reported softening and hardening characteristic of metals. In another instance Basquin (1910), Suresh (1991), Krupp (2007) and Schijve (2009) have proposed empirical laws to characterize the fatigue endurance limit of the material. Also, an energy concept was proposed by Inglis in 1913 and it was confirmed by Griffith in 1926. Similarly, a damage accumulation theory for fatigue were introduced by Palmgren in 1924 while Miner developed a damage accumulation model for fatigue failure in 1945. In addition, Neuber, in 1946, investigated the influences of notches on fatigue deformation, while Langer in 1937 attention with variable amplitude fatigue load. In 1954 Coffin and Manson discovered that independently plastic strain was responsible for cyclic damage. The authors suggested empirical relations between the number of cycles and the plastic strain amplitudes. Paris in 1965 has introduced the relationship between rate of crack growth and stress intensity range and it is known as Paris law. However, Elber showed the fatigue cracks closer concept under cyclic tensile load in 1970. Interestingly, most of fatigue related investigations focused on short crack. Concept related with short crack was explained by Pearson in 1975.

In the past decade high performance computing technique have been introduced as well as advanced experimental methods to estimate the fatigue life under cyclic

loading. Such methods are related to understanding of material degradation, numerical modeling and deformation mechanisms of fatigue. Thus, Barbe and Decker (2001), Devincre (2006), Forest (2007), Saai and Louche (2010) and Schwartz (2010) developed microstructure-sensitive computational methods for fatigue crack formation.

## **2.2 Fatigue failure**

Failure due to fatigue is quite a sudden action. When a service load is applied on structural member, a crack initiate in a microscopic level. This kind of crack gradually develops until to the component separates. The whole process involves an invisible crack initiation at micro scale to a macro scale level. However, fatigue is not an engineering problem since it is related to phenomenon of material. This chapter aims to present material properties and their characteristics effects on fatigue behavior on steel. It classifies all possible types of fatigue and their extensions. In addition, it attempts to understand the steps of fatigue failure, and attention with total life. Further more understanding of fatigue failure mechanism with leading explanations is another main aspect of this chapter. Theory related hardening and softening effects on material due to fatigue is also discussed with the leading crack growth model and compared with the present study. Finally, the chapter includes the discussion of the critical parameter effects on fatigue performance of structures.

Three conditions should be satisfied for fatigue failure, which includes tensile stress, sufficient variation and number of stress cycles. Fatigue loads applied on a structural member could be classified as axial, flexural and torsion stresses (Fatemi & Socie, 1988). Cyclic stresses are usually sinusoidal in a pattern which determines different stress values. Different methods have been used to determine cyclic load spectrum on ductile material such as range of stress and peak stress. All of these techniques shows different results with slight deviations and ultimately which stress is most critical depends on the load spectrum.

### **2.2.1 Sequence of fatigue failure**

Fatigue failure is the phenomena of progressive action of structural damage. It occurs when a material is subjected to repetitive stress due to service loads. The maximum

stress values applied to structural elements should be below the ultimate tensile stress limit of the material. The whole process of failure could be described in three major steps as shown in Figure and there are cracks initiation, propagation, and failure. However, there is no clear guidance to separately identify each stage. It does not have a clear boundary especially between steps of crack initiation and propagation. As these boundaries depend on the number of variables such as, material properties, geometrical parameters, loading characteristics and environmental factors, failure of a material subjected to fatigue can be classified as follows:

- 1) Crack Initiation - The crack start at this stage at the micro-structural level and grows up to the surface. On the tensile surface, it can be visually observed. Reasons for crack initiation are slip bands or dislocations intersecting the surface due to the impact of the work hardening or repetitive loading
- 2) Crack Propagation –crack is rapid growth in this stage due to the continuous repetitive stresses in the material
- 3) Failure - Separation occurs due to the continue cyclic stress because the remaining cross-section is not sufficient to withstand the applied stress. The ultimate results of material separation which occurs rapidly. Such failure is known as an unrecoverable or catastrophic failure

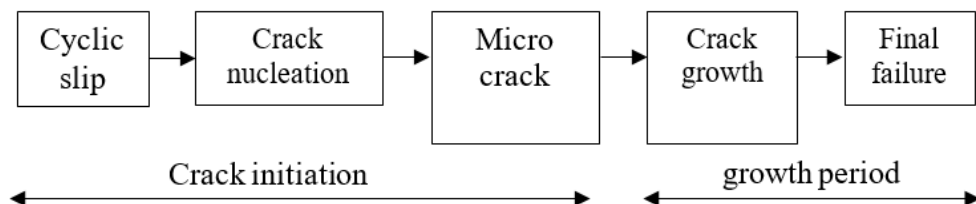


Figure 2-1: Main steps of fatigue (Azeez 2013)

### 2.2.2 The microscopic explanation of fatigue failure

Fatigue failures typically start at the surface of a structural element. The test utilizes a rotating beam test machine which creates a maximum stress level at the surface. The fatigue failure initiate as a microscopic crack and such cracks are very sensitive. Therefore, for better performance the metal surface of the test specimen should be free from defects. As the mechanisms of fatigue failure occurs due to the effects of the reversed plastic flow. There are several reasons for plastic flow, which includes

imperfections in the crystal lattice of a metal, forward and backward motions of dislocations and plastic deformation along the slip planes of material crystals as shown in Figure 2-2. Especially due to cyclic stress, the direction of the strain is reversed repeatedly.

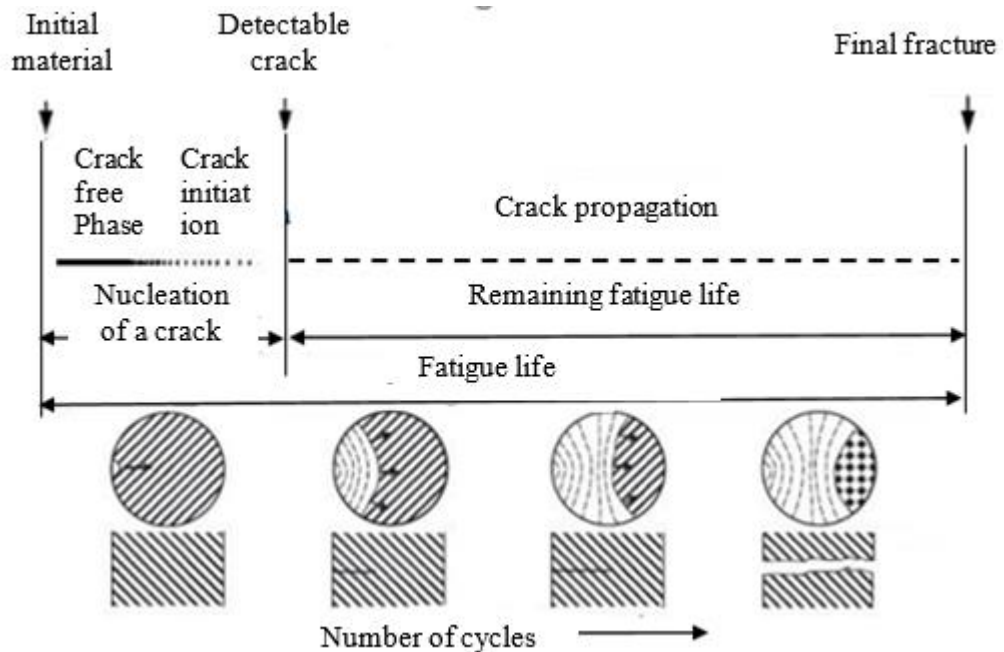


Figure 2-2: Crack growth with number of cycles (Hojjati Talemi, 2014)

### 2.2.3 Material behavior with fatigue loads

Fatigue is the continuous degradation of a ductile material which is subjected to repetitive loads. In the process of fatigue, a structural member is subjected to constant or variable amplitude stress. The applied service load may change from an equal or an unequal positive or negative value which ranges from zero to a maximum value. In most structural related applications, the service life has been governed by several factors. They are the characteristic of the material used in manufacturing, external loads and loading frequency, service environment, surface condition, design details and method of fabrication. The commonly used material in construction industries for the design fatigue capacity is explained below with their primary characteristics. Fatigue behavior of ferrous, non-ferrous and plastic material shows the following material characteristics.

### **1) Ferrous material**

- a) Steel is commonly used as a structural material for fatigue related application. It has a high fatigue capacity and excellent processability.
- b) The optimum microstructure of the ductile material for fatigue is tempered marten site due to it shows maximum homogeneity.
- c) Steel has a high strength, high harden ability, and less residual stresses, which is critical in fatigue related applications.

### **2) Non-ferrous material**

- a) No clear endurance limit for non-ferrous alloys except Titanium.
- b) Aluminum alloys exhibit reasonable fatigue resistance and additionally it shows corrosion resistance and light weight.

### **3) Plastic materials**

- a) The visco-elasticity of plastics shows more complex fatigue behavior than ductile metals.
- b) The fatigue properties of plastics depend on type of loads, changes in temperature and the environmental condition.
- c) The amount of heat generation increases due to the increase of stress and loading frequency.
- d) The failure modes of fatigue in reinforced materials are more complicated and it depend on fabrication process.
- e) Due to practical experiences, some fiber reinforced plastics shows better results in fatigue performance than metal.
- f) Fiber-reinforced plastics have less density.

#### **2.2.4 Characteristics of fatigue**

Characteristic of fatigue could be considered as follows:

- 1) Metal alloys do not contain macroscopic or microscopic discontinuities at the crystalline grain scale.
- 2) Stress concentration locations such as holes, keyways, sharps are usual locations which the fatigue process starts.
- 3) The high stress range of structural elements, the lower life of fatigue.

- 4) Fatigue associated with tensile stresses and fatigue cracks deal with compressive loads.
- 5) The fatigue crack start due to dislocation movements at the microscopic level, which is ultimately the nucleus for short cracks.
- 6) Fatigue could be considered as a process of randomness as there are considerable scatters available in an identical sample under controlled environment.
- 7) The damage is cumulative as the materials do not recover when rested.
- 8) Fatigue life depends on surface finish, temperature, presence of oxidizing, metallurgical microstructure, inert chemicals and residual stresses.

### **2.3 Classification of fatigue**

Fatigue could be divided as high cycle fatigue and low cycle fatigue. The difference between high cycle fatigue and low cycle fatigue deals with a deformation of materials. The HCF is dealing with elastic deformation while the LCF is characterized as a repeated plastic deformation during each cycle. The phenomena of low cycle to high cycle transformation is depends on the stress level as shown in Figure 2-3 (Miannay, 2001). However, fixed transformation life cannot be identified in the real world applications as shown in Figure 2-3, because it is governed by the ductility of the material. The transition point of the curve in Figure 2-3 shows the conversion from LCF to HCF. Usually, an irreversible deformation does not exhibit in the region of high cycle fatigue at the macroscopic level. The low cycle shows significant macroscopic deformation. However, the first micro-cracks appear on structural elements regardless on the fatigue.



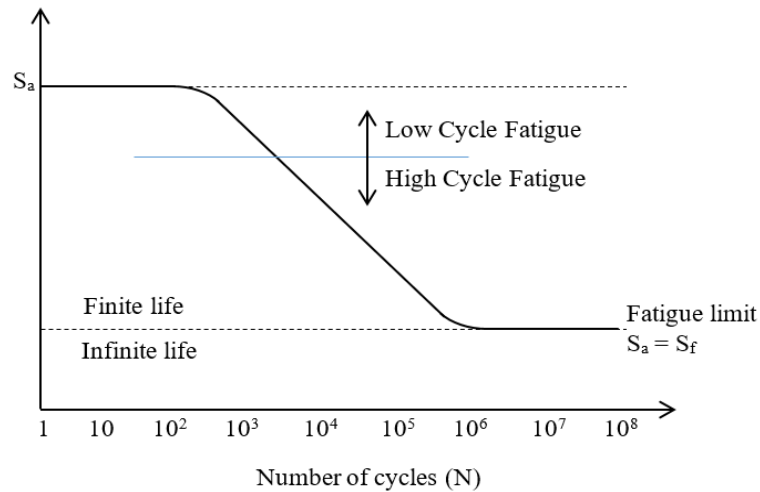


Figure 2-3: HCF to LCF transition (Miannay, 2001)

### 2.3.1 Low cycle fatigue and high cycle fatigue

Fatigue could be classified as low cycle fatigue and high cycle fatigue. There are several types of life prediction techniques which are available in this context. The Palmgren-Miner rule is usually obtained to calculate the cumulative damage. The method developed by Aeran, et al. (2017) were used as a full range S-N curve. Furthermore, this can be applied to both of HCF and LCF failure. The  $\epsilon$ -N curve is developed to evaluate LCF which utilizes the Manson – Coffin relationship which includes an elastic Figure 2-4 shows behavior of load bearing capacity under fatigue load. As shown in Figure 2-4 the number of load cycles are inversely proportional to the load bearing capacity.

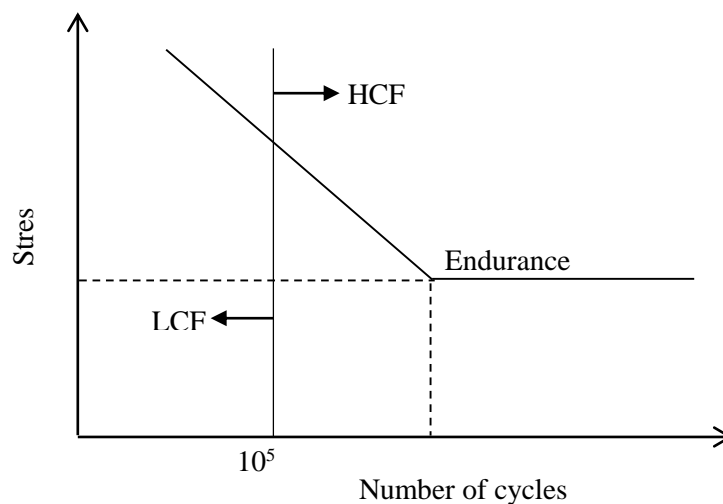


Figure 2-4: Fatigue bearing capacity variation with number of cycles (<https://www.test-and-measurement-world.com/Terminology/Low-cycle-fatigue-vs-High-cycle-fatigue.html>)

The turbine blade of the modern aircraft is a good application of fatigue. It is usually applied to mechanical loads due to vibration, flexural stresses, centrifugal force, and thermal stresses. Therefore, such a fatigue could be explained not only mechanical fatigue but also thermal fatigue. In addition, it can be explained under the creep, corrosion, oxidation and damage due to any foreign objects. Such reasons contribute to significant reductions of the fatigue strength of a structural element. Especially, when the magnitude of the stress is small (below the endurance limit) result is a HCF. On the other hand, low-frequency of high stress loads causes to LCF failure. Ultimately, both of LCF and HCF contribute to failure of structures and it is called 'combined cycle fatigue' (CCF).

The fatigue phenomenon under combined cyclic fatigue (CCF) loadings were reported by Fuchs et al (1977) as well as Namjoshi et al (2001). Authors, estimated the damage from HCF, LCF and a combined cyclic loadings (Zhu et al., 2017). Oakley and Nowell (2007) explained a life prediction method under CCF conditions (Zhu et al., 2017). Schweizer et al.(2011) introduced a mechanism to explain the micro-cracks response on combined cycle fatigue (CCF) loadings (Zhu et al., 2017). The authors emphasized that growth were accelerated between from HCF to LCF transition (Zhu et al., 2017). Stanzl et al.(2016) examined behavior of variable amplitude fatigue loads with high-frequency. Thus, the experimental result recorded that fatigue life was very short under combined variable amplitude loading.

Meanwhile, different types of models have been proposed for the CCF life prediction. Zheng et al.(2013) proposed a combined cycle fatigue (CCF) life estimation model. Karunananda et al.(2010) proposed a combined fatigue life model based on strain-life fatigue curve.

According to practical experience, the linear damage rule or Miner's rule has been generally utilized to evaluate CCF damage due to its simplicity (Miner, 1945). However, this technique has not considered the influences of load interactions on combine cycle fatigue damage. The HCF to LCF interaction is not utilized in most of CCF prediction techniques. However, interactions of load significantly affect the CCF life. Therefore, a CCF life estimation model should consider the damage as well as the

effects of load conditions. Fatigue could be further classified as follows and this investigation is mechanical fatigue applied on the CSH as a cyclic flexural loading.

- 1) Fluctuations in externally applied stresses or strains (mechanical fatigue).
- 2) Fluctuations in temperature as well as stresses and strains (thermo-mechanical fatigue).
- 3) Cyclic loads at high temperatures (creep fatigue).
- 4) Cyclic loads combined with frictional sliding (fretting fatigue).
- 5) Cyclic loads in a chemically aggressive environment (corrosion fatigue).

#### **2.4 Prediction of fatigue life**

The fatigue life estimation methods can be classified into two main groups. The first group is based on the estimation of crack initiation, using a combination of damage estimation rule based on stress/strain of structural element (Depiver et al., 2020). The advantage of this approach is independence from specimen geometry and loading being the fatigue life prediction only by a stress/strain criterion (Depiver et al., 2020). The approach of the second method is based on continuum damage mechanics (CDM), in which fatigue life is predicted estimating a damage parameter cycle by cycle. Inputs and outputs which relating to fatigue life estimation have been summarized in Figure 2-5 as follow.

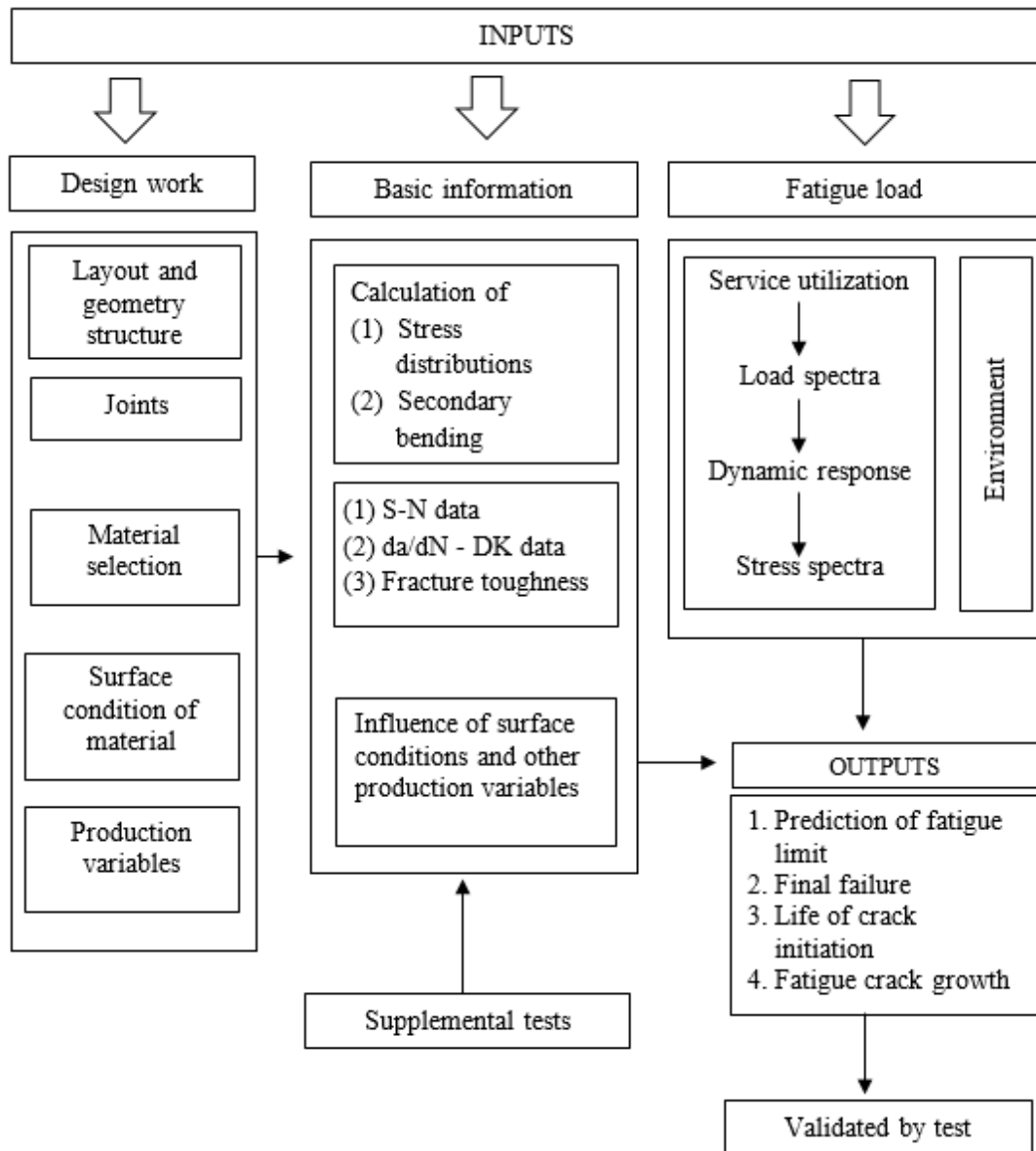


Figure 2-5: Various aspects of fatigue life prediction of steel structures (Schijve, 2003)

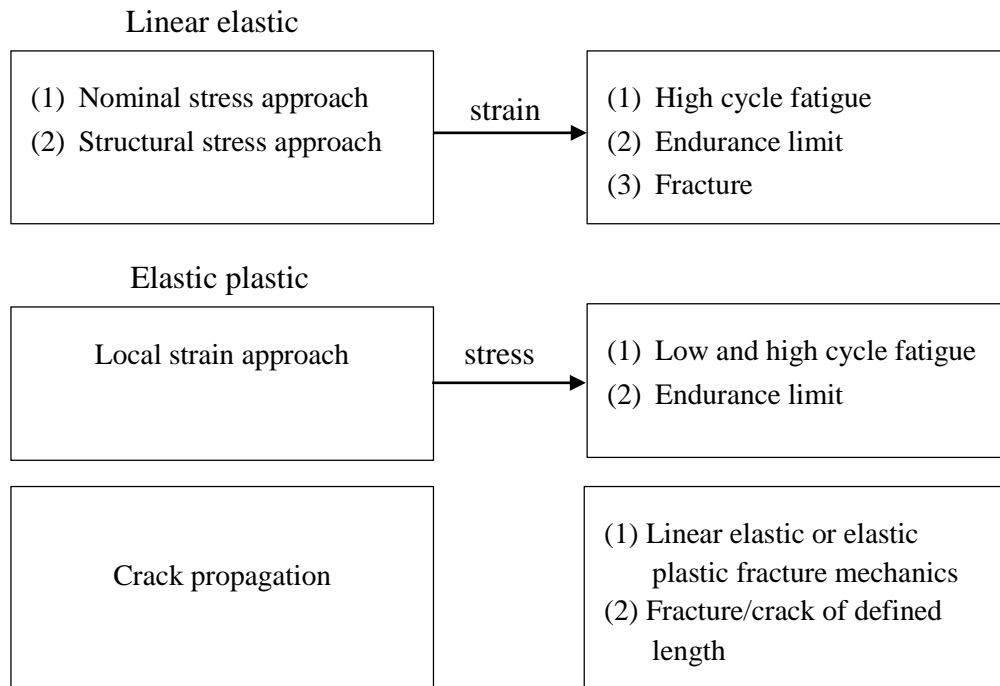


Figure 2-6: Methods of fatigue life evaluation (Dubina, 2013)

#### 2.4.1 Classification of fatigue life prediction techniques

Fatigue is mainly classified according to the load applying method – i.e. constant amplitude load and the variable amplitude load. Constant amplitude load is the simplest fatigue stress where amplitude of the stress always constant. Different samples need different stress levels at the constant amplitude test. Specially this type of loads could be applied on machinery components. Variable amplitudes loads are more complicated and stress varies by cycle to cycle. Most of civil engineering structures encounter variable load stress during their services which includes bridges. When considering the function of bridges in road networks, different types of vehicles move in different speeds and this is good example for variable amplitude (non-harmonic) loads on structures. Variable-amplitude related tests could be further classified as cumulative damage test and service simulating tests. However, limitation of variable amplitude tests has not been developed up to testing standards. Variable amplitude loads are shown in Figure 2-7.



Figure 2-7: Stress variations with time linked to variable amplitude loads

### 2.4.2 Minor rules

Fatigue damage accumulation could be predicted using the Palmgren-Miner's rule and it is considered as the simplest model for fatigue damage. Crack initiation is usually measured on cycle ratio and fractional damage per cycles estimated by  $D = \frac{1}{N}$ . According to Minor's rules failure occurs at  $\sum(\frac{n}{N}) = 1$  and its based on S-N curve with constant amplitude fatigue load. The Minor's rule is mathematically expressed in equation 2.1.

$$\sum_{i=1}^n \frac{n_i}{N_i} = \frac{n_1}{N_1} + \frac{n_2}{N_2} = 1 \dots\dots\dots (2.1)$$

where  $n_i$  is the number of cycles applied on specimen and  $N_i$  is the lifetime of the sample at the same stress. Stress behavior with number of cycles to failure is expressed in Figure 2-8.

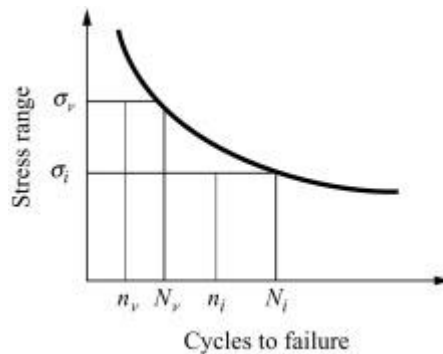


Figure 2-8: Stress variation with number of cycles

Miner's rule has two main limitations. There are no exact S-N data due to its scatter, this rule does not account for high stress or low stress order. In addition, this rule could be applied only for expected values and does not pay attention to the variations of each test unit. Furthermore, there is no attention given to the probabilistic nature of fatigue. On the other hand, this method assumes simple liner life stress relationship. Therefore, Minor rules does not reflect real world applications and it can be identified as a simple and easier way to understand fatigue failure of ductile material. Minor's rule has been introduced to avoid any drawbacks of the probabilistic models. This model has two key features such as fixed value for failure due to Minor rules which are replaced by the special patterns of distribution. In this method, damage does not accumulate in a linear manner. Therefore, this model could be considered as an extension of the Miner's rules.

Invers power law is considered as a function of a stress and its represented in equation 2.2

$$L(S) = \frac{1}{KS^n} \dots\dots\dots (2.2)$$

Where L(S) average fatigue life at stress S, K and n are model parameters. The Minor's law could be considered as a special version of the Invers power law. This model could be further extended to evaluate fatigue damage by using the Weibull distribution.

**2.4.3 Rain flow counting algorithm**

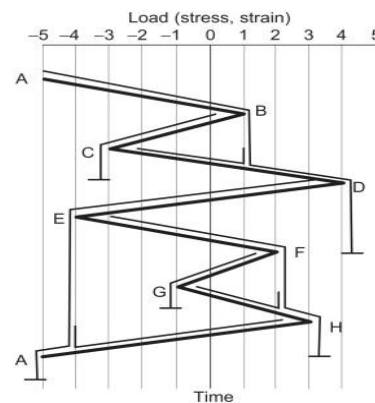
Rain flow counting algorithm was introduced in 1968 by Matsuishi and Endo to estimate fatigue life. This analytical method was developed using a rain fall pattern from the edge of a multi-step roof or a Pagoda roof as shown in Figure 2-9. Therefore, this method was known as Pagoda roofing method. Rain flow algorithm could be considered as a time domain function and fluctuates with amplitude of loads. This method is very close to the actual fatigue stress pattern on real structures. When vehicles pass over bridges its speed and weights are different from each other. As a result, applied stress on structures randomly vary and it is difficult to estimate fatigue life, as stress is fluctuates randomly and it cannot be converted to a unique value of amplitude. Random loading amplitudes are different from each other. In this rain flow method, the stress amplitude transfers to corresponding mean stress. Downing and

Socie presented a rain flow counting method with modifications in 1982. ASTM E 1049-85(2005) standard was practiced for fatigue analysis with rainfall techniques. In addition, the following features of Rain flow counting method are highlighted:

- Identification of history peaks and valleys with the stress time
- Identification of effective stress ranges
- Classification of counting techniques as peak counting, range counting, level crossing counting and rain flow counting (Specially for fatigue damage evaluation)
- Commencing rain flows inside every peak and valley
- Dropping of peaks until it reaches the opposite peak
- Halting of rain flow when it meets the rain flow roof
- Terminating the rain flow at the end of the time series
- Counting the horizontal length of each rain flow as half cycles with selected stress ranges



(a)



(b)

Figure 2-9: Rain-flow counting methods related to (a) Pagoda roof (b) stress history

## 2.5 CSH method as a repairing technique

Most of the materials fail below their yield point due to cyclic stress. This phenomenon is called fatigue failure which explains the theory of fracture mechanics. Fatigue cracks in structural components are very common due to various reasons such as stress, geometrical discontinuities and environmental effects etc. Conventionally crack filling by welding, replacement of components and plate connection with pre-tensioned bolts



are utilized in normal conditions. The Crack stop hole method is another technique utilized for crack repairing purposes. A proper size drilled hole is placed at the crack end in this method. The purpose of such holes is to arrest the crack, the result of which is a control crack propagation. This method is named as a crack stop hole technique. When the crack stop hole is placed on the crack tip it helps to re-distribute stress. However, continuously applying service load on the structure would result in forming a new crack on CSH. This process is introduced as a re-cracking procedure. Therefore, it could be utilized only as a temporary treatment for delaying the crack growth for a significant period of time. The advantages of this technique are simple, easy and low cost in order to arrest the crack. After placing a drilled hole at the crack end, the prediction of time delay is a very important factor for repairing purposes.

Fatigue phenomenon is directly related to fracture theory which deals with cyclic stress. Generally, fatigue failure occurs below the yield point of the material. The three main steps which explain total fatigue life is crack initiation, propagation and failure. However, the appropriate estimation of crack initiation is not an easy task, because of an enormous number of parameters: geometric, material, environment and loading which influences the fatigue life. Those parameters which influence on CSH can be elaborated as follows. The key material properties are elastic modules, Poisson's ratio, yield strength and ultimate strength while the geometric parameters are the shape of the element, aspect ratio, the shape of the hole, crack length, hole diameter and location of the hole. The others are load related variables –i.e. loading pattern, loading type, stress ratio, amplitude of load and loading frequency. The environmental factors which are mainly considered in this context include humidity, salinity, UV effect, range of temperature and temperature fluctuation. In addition, the residual stress around the crack stop hole border also critically influences for crack initiation. Therefore, few or all of them may jointly influence the crack initiation process at the CSH. However, evaluation of the influence of all of them at the same time is an impossible task. It could be highlighted that, few of them were focused on many studies available in the existing literature. Even numerical modeling techniques were also modeled under boundary conditions. Interestingly, the interconnectivity of these factors is still on the topic of extensive research.

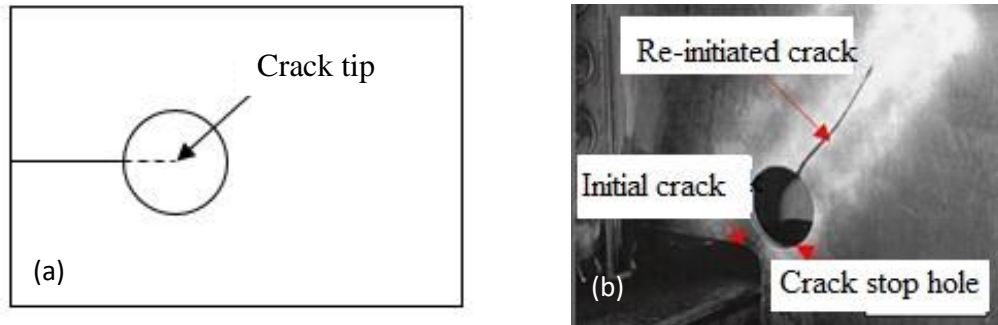


Figure 2-10: CSH placed at the crack tip (a) schematic view of crack stop hole  
 (b) re-cracking of crack stop hole (Dexter and Ocel, 2013)

### 2.5.1 Arrest the crack

The Crack stop hole (CSH) could be introduced as a simple, quick and an economical repair technique which is used to maintain structural elements. Cracks are usually initiated and extended in a perpendicular direction of the loads such as the traffic flow on structural element of steel bridges. This could be considered as another important aspect of fatigue, which is governed by additional stresses. However, this stress does not account for the design and it is concerned about the process of crack.

The bulk of the structural element behaves elastically even through cyclic loading. There have been many research investigations conducted for LCF condition since 1950. The prime objectives of such investigations were to develop an appropriate theory to predict the fatigue life of ductile materials which are used in structural engineering. Those investigations have been extended to different loading and environmental conditions. Also, various types of laboratory test were conducted on different materials by individual researchers. This literature summarizes some of the key studies which predict fatigue life.

This investigation also focuses on the crack initiation life prediction of structural steel. Initially plain specimens were tested with fatigue loads. Consequently, fatigue life prediction was expanded to a plain specimen with a CSH. Furthermore, it was extended to estimate fatigue life enhancement by CFRP materials. Incorporating a CSH in the specimen leads to multi-axial loading and this is similar to the condition created by welds, notches, or other stress concentrations present in the structural

elements. Different investigations have focused on different materials in similar studies and it can be further classified as follows:

First, the micro-crack initiation deals with theory of local strains. In this phenomenon, the material surface is deformed at plane stress conditions. The strain distributions of the specimen surface developed as a fully plastic deformation under plane stress. Similarly, Nebure (2003) proposed an analytical model of theoretical stress/strain concentration to estimate the local plastic strain amplitude. Such a hole causes to generate plane stress and it could be utilized to predict strain profiles. This strain distribution is isolated by the CSH location on the material surface. The local strain amplitudes around the crack stop holes can be evaluated as a function with distance from the CSH and number of cycles. Furthermore, it can be utilized to understand a plastic strain-life analysis which predicts initiation of crack.

The second aspect is the prediction of plastic strain behavior due to cyclic loads. This method is utilized to predict the required number of loading cycles which causes to failure. Prediction is governed by the theory of maximum local strain. In this case it utilizes the Manson-Coffin relationship.

The third aspect considers a theory of cumulative damage to predict the fatigue life. This technique is incorporated with low cycle fatigue predictions after each cycle. This scenario requires a variation of macroscopic plastic strain amplitude during the cyclic loads. It becomes the cause for the behavior of the cyclic hardening as well as cyclic softening.

The strain profiles could be estimated by using a concept of plastic strain distributions. In this case Neuber's analysis was utilized. The behavior of the load-time graph is considered an important indicator relating with low cycle fatigue. Stresses are formed in materials due to various reasons; they are loaded possesses, geometrical discontinuity, corrosion and fluctuation of temperature in a material. The stress concentration factor is another parameter and it was defined as the ratio of the fatigue capacity of un-notched specimen to notched specimen. However, the stress concentration related parameters could be only estimated through a laboratory

experiment. A number of investigations have focused on determining the effects of stress concentrations factor related with fatigue. Reported investigations have been limited to theoretical analysis which is based on effective stress concentration factors. The yield stress deals with stress concentration and it depends on the average stress, the ratio of the maximum stress, and the geometry of the notch. Furthermore, work hardening can be introduced in the vicinity of the CSH. Therefore, stress concentration factor of a notch plays a vital role when, considering the material yields. On the other hand, the concept of stress concentration is important in case of comparison.

Optimum hole size as well as smooth edge of CSH causes to long-term performance of the crack repair method of a damage element. The appropriate size of the CSH diameter should not be less than 25 mm, however a larger hole size could be recommended with details of crack lengths. Larger hole diameter causes to reduce stress concentration as well as the stress range. However, the large size of CSH causes to reduce the cross-section and results in decreased strength of a structural element.

### **2.5.2 Crack stop hole methods for crack control**

The method of the crack stop hole (CSH) requires to place a hole at the proper location and results is slowing crack growth or completely prevents it. According to Anderson (2005), the stress concentration effect on a notch (CSH) is reduce when the diameter of the CSH increases. Theoretically, when the diameter of the CSH approaches zero, the stress concentration should be infinity. However, it is impossible because, any materials do not capable to withstand infinite stresses in real world applications. Therefore, concept of an infinitely stress concentration can be considered as only a theoretical phenomenon. This is because, plastic deformation at the crack end of ductile materials causes to overcome an actual infinite stress concentration. The result of the CSH at the crack end contributes to increases the blunting effect and it causes a significant, dropping in the stress concentration. The effectiveness of CSH has been emphasized in the real world applications over many decades. The CSH not only prevents fatigue cracking, but also provides an effective arrest for a running fracture. When considering a crack repair, proper CSH was an effective method for long-term durability of the repair. The meaning of proper installation of CSH is account location

of hole placement, hole edge condition and diameter of CSH. The equipment recommended to make a CSH includes a magnetic-based drill or annular cutter. However, hand drills also have been accepted as an appropriate tool for effectively hole drilling purposes, even for larger diameter holes. The magnetic-based drilling technique offer excellent speed control ability and precision in a wide range of hole size in narrow space and location of the crack stop.

### **2.5.3 Crack detection and placement of CSH**

The CSH technique is not difficult when arresting cracks and it should follow certain important steps to an effective retrofit. The common mistake is the lack of training and missing the correct crack end when placing the CSH. This results in such an inappropriate location that would possibly disrupt the service as well as repeated repair attempts and further reduction of the cross section of the structural element. Tri-axial restraint through the thickness of the structural element is accelerating slightly cracked growth rates. An extreme example of crack tunneling is where a CSH is installed due to an impact load.

However, some of surface inspection techniques such as liquid penetrant testing (PT) and magnetic particle testing (MT) do not allow the detection of the crack tip of the through thickness. The UT can be utilized in detecting a similar effect of the crack transitions to a through-thickness. Therefore, non-destructive examination (NDE) can suggest the performance on any surface of the cracked plate to confirm the detection of crack. In most cases the crack length is possibly mis-characterized and results in the crack tip not being removed during hole drilling. Precision location of crack stop hole placement deals with the crack tip; hence it is the most prominent factor for the effectiveness of this technique.

The investigation conducted by Fisher et al. in 1980 a proposed a hole placement technique for crack controlling (Fisher et al., 1980). The crack tip is entirely missed in this technique; thus the crack has been continuously growing. However, if the crack stop hole is placed in the correct position it could adequately capture the crack. When the CSH is located at the edge of the cutter it might be intercept the crack end. Therefore, this approach can be considered as a better safeguard. When crack stop hole

is offset from the crack end, the crack allows to grow until it intercepts and then arrested.

The radius of the CSH could also influence on efficiency of this repair technique. Larger size holes contributed to further decreases any stress. A review of the literature suggested that different CSH diameters are required for levels of success. The result of the insufficient hole size is the “Swiss cheese” effect that could occur due to offset crack tip and insufficient edge conditions. The minimum hole size should be less than 25 mm for typical highway bridges (Fisher et al., 1980). Dextor and Ocel (2013) have also confirmed that a minimum size of CSH at least 25 mm diameter for acceptable level of performance. Fish et al.(2015) recommended the hole size from 50 mm to 100 mm for better performance, when target to overcome crack growth on out-of-plane.

Edge condition of the crack stop hole could be identified as another important parameter. Edge condition is very important for fatigue than the diameter of the CSH. Therefore, quality of tools (drill bit) and speed of drilling are critically influences on the overall performance. Brown et al. (2007) suggested that the CSH placed using dull bits would result in fatigue life similar to punch holes. The drilling process makes a rough edge that causes to generate stresses which results in crack initiation. A sand blasting method or an angle grinder can be utilized to finish edges of the CSH. When drilling starts, the magnetic base is possible to offset from the annular cutter due to insufficient magnetic connection.

## **2.6 Mechanical treatments for CSH subjected to fatigue**

There are four different mechanical treatments that can be identified to strengthen the crack stop hole. They are bolted, pinned, cold expanded and ancillary holes. Each strengthening method has reported fatigue life enhancement as well as drawbacks.

### **2.6.1 The bolted CSH**

When the tensile loads are applied on a crack stop hole, as shown in Figure 2-11 the result is that the crack faces close together. Bolt tension loads contribute to reduce the effectiveness of the stress range of compression regime. The result of the bolt tension is delayed crack growth. However; various kinds of parameters could be utilized to

change the stress on the crack stop hole. Such variables are mainly the magnitude of the bolt tension and the method of anchorage. The tightening of the nut results in the tensile loads applied on CSH. Special attention should be made to proper corrosion protection solutions in this method because, specimen material and bolt material may be a different electromotive force and results in accelerating the rate of corrosion near the CSH. The cracked flange always faces compression due to cyclic load. However, the limited amount of research has verified the validity of this technique. Some investigations confirmed that the bolted stop hole technique has high potential to delay re-cracking behavior. In addition, observations have reported that the hardened washer significantly contributes to delay crack re-initiation on a crack stop hole.

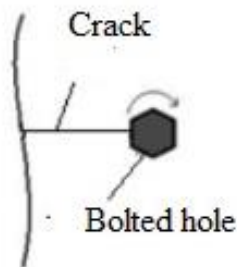


Figure 2-11: Bolted crack stop hole (Makabe et al., 2012)

### 2.6.2 The pinned CSH

In this technique the CSH is placed on a structural element and a pin was inserted into the crack stop hole as shown in Figure 2-12. The pin material and CSH materials are selected as same in this technique, as the pin material, should overcome issues relating to fluctuation of environmental temperature and corrosion effects. However, non-metallic materials such as wood or rubber pin also can be introduced as an alternative. The diameter of the pin selected was 4 % higher than the CSH diameter and the length of the pin and thickness of the member should equal to hole thickness (Recho, 2012). This method is one of the most effective ways to control re-cracking behavior as compressive stress is provided around the crack closure that reduces the stress in the vicinity of the crack stop hole. On the other hand, a pin is inserted into a hole that introduces a residual compressive stress around the hole. Stress reduction causes delay crack initiation effectively, as the pin is inserted to the hole where compressive residual stress is created. Comparatively, this technique reduces stress near the CSH. However,

this method could be considered as a positive visual indication technique, because observers may be visually uncomfortable observing a series of holes on the structures. Furthermore, pin treatments are supported to prevent the activities of birds and other animals in the interior of hollow structural elements.

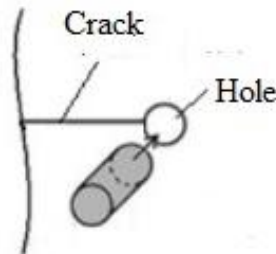


Figure 2-12: Pinned crack stop hole (Makabe et al., 2012)

### 2.6.3 The cold expanded CSH

In the cold expanded stop hole method, the sleeve was inserted into the hole as shown in Figure 2-13. In this method, a metal sleeve or a tapered mandrel was inserted to the hole. Outer radius of the sleeve was slightly higher than the radius of the CSH and the thickness was equal to the specimen thickness. The result created a compressive stress near the CSH. In fact, a cyclic residual stress contributes to crack initiation, however the cold expansion technique reduces the stress around the CSH. Permanent compressive stresses are made surrounding the CSH and the result is delaying of re-cracking. In addition, the cold work around a crack stop hole produces residual stress while both radial and circumferential directions around the CSH. Cold-expansion not only imposes circumferential tensile stresses but also radial compressive stresses around the CSH. These stresses are causes to strain hardening of the material around CSH. Strain hardening contributes to enhanced tensile and yield strength of the material surrounding the CSH. Therefore, it improves the effectiveness of the crack-stop hole.



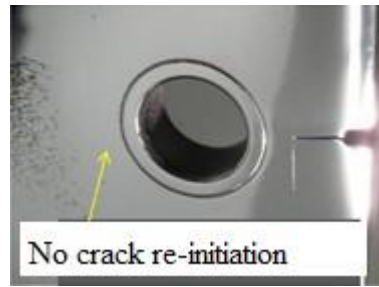


Figure 2-13: Cold expanded CSH (Len and Reid, 2011)

The inner diameter of the sleeve and sleeve materials are major parameters in this technique. However, uniform radial expansion of the crack stop hole should be ensured in this technique. Therefore, the same material is used for making a sleeve, although if there is a different expansion co-efficient it may create unwanted issues due to fluctuation of environmental temperature. In addition, if different materials for sleeves are selected, due to the changed properties of the materials, corrosion effects may accelerate at the crack stop hole. Application of the cold expansion technology has been utilized in repairing of fighters and commercial aircraft (Leitao et al., 1998). Investigations conducted by Champoux (1986), Chandawanich et al.(1979) and Landy et al.(1986) confirmed the effectiveness of compressive residual stresses in enhancing fatigue life under conditions of cyclic loading. Stefanescu et al.(2003) experimentally confirmed the effectively change of residual stresses under static compressive loads.

#### **2.6.4 Ancillary holes in added CSH**

Two or more small holes were placed around the CSH in this method as shown in Figure 2-14 and such holes were called ancillary holes. Additional holes are usually placed near crack stop holes. Ancillary holes support to further minimize stress near the edges of the CSH (Wang et al., 2017). The effectiveness of the overall arrangement of the holes contribute to retarded crack initiation at the CSH. The overall effectiveness of this technique depends on stress concentration and the diameter of ancillary holes. A minimum gap between the crack stop hole and the ancillary holes contribute to reduce stress concentration. This stress concentration is significantly reduced by the large size of ancillary holes (Wang et al., 2017). However, the diameter of the ancillary holes being larger than the crack stop holes is unrealistic. Therefore, the overall effectiveness of this technology depends on the location, number of holes and diameter

of the hole. Furthermore, drilling techniques and the speed of drilling, has an influence on the result due to changed residual stress.

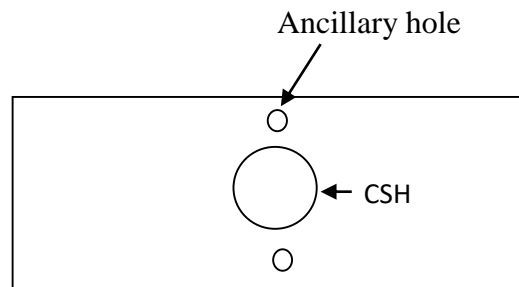


Figure 2-14: Schematic diagram of the ancillary holes added CSH

In general, four different techniques could be identified to strengthen a crack stop hole. They include bolted, pinned, cold expanded and ancillary holes with CSH. According to the investigation of Abeygunasekara et al.(2019) each of these methods were numerically analyzed and the results were compared with CFRP strengthened method. The authors have highlighted the potential of the CFRP strengthened technique compared to each other methods.

### 2.6.5 Comparison of different methods utilized in CSH strengthening

There are four different techniques for enhanced performance of CSH. These methods are bolted hole, pinned hole, cold expansion, and ancillary hole method. Bolted CSH method provides an additional crack control force. Due to tension it could be enhance using a washer with bolts. Performance depends on applied torque on bolts and geometry of CSH however it is difficult to apply at narrow locations. The pinned stop method introduces compressive stress surrounding CSH to control further crack growth. Materials are different and it may change during expansion with temperature. However, it may cause to accelerate corrosion due to galvanic effects. The tolerance between CSH and the pinned should be precise and it would be very difficult to maintain such tolerances without advanced manufacturing technology such as computer numerical control (CNC). However, this technique may be expensive as well and not simple too. The cold expansion technique also supports to enhance stress surrounding CSH with additional circumference tensile stress on CSH. Dimension of sleeves are critical on CSH and it is not easy task. On the other hand, before selecting

material, attention should be given to corrosion effects and expansion due to environment temperature. However, this technique is not much simple than bolted or pinned method. The Ancillary hole method is another technique and in this method additional holes support to stress distribute further. It is causes to lose strength rapidly because overall cross section reduction is heavily effects on strengthen of structures. This method is very simple compared to each of above discussed methods as well as being cost effective and there is no need for any skilled labour. All of these techniques compared as shown in Table 2.1.

Table 2.1: Summary of results of different crack stop hole treatment methods

<b>CSH strengthening methods</b>	<b>Reasons for delayed crack initiation</b>	<b>Parameters governed by performance</b>
Bolted CSH	Due to bolt tension loads the effective stress range of the compression regime is reduced	Applied torque with or without washers
Pined CSH	Introduce residual compressive stresses around crack stop holes, Compressive stress is provided around crack closure	Material properties of the pin
Cold expanded CSH	Imposes circumferential tensile stresses and radial compressive stresses near the CSH Enhanced compressive residual stress around the crack stop hole	Diameter of the sleeve, sleeve materials
Ancillary holes added CSH	Ancillary hole lowers the stress concentration at the CSH edge	Distance between holes, ancillary hole diameter, Number of ancillary holes

### **2.7 CFRP material as a crack repairing technique**

Deterioration of steel structures has become a critical issue in civil engineering applications. Corrosion, fatigue sensitive details and lack of proper maintenance, were reported as major factors relating to durability of steel structures. In addition, lack of information at the time of construction, aging of structural elements, environmental

related parameters, and selection of materials are also considered as effective factors (Gholami et al., 2013). However, due to such reasons, structural health level reduces day by day and a maintenance budget keeps increasing. As a result, researchers have overcome such difficulties by adopting CFRP base technology, as the strengthening of steel structures with CFRP have the potential to substantially extend their service life. However, most of field applications use conventional retrofitting techniques even today. There is steel plate or profile connected to a damage position using welding and steel plates connected through bolting to fastening. These conventional methods also contributed to achieve a desired level and strength gain of a structural element. However, conventional retrofitting techniques have reported many limitations and shortage. Such drawbacks lead to increasing dead loads of the structure and susceptibility to the corrosion. In fact, welding techniques causes changes in the micro structure and the bolted method causes cross section decreases of the structural element. In addition, these conventional techniques are more time consuming, need skilled labour and it is difficult to handle without heavy lifting equipment. Furthermore, welding techniques are not fatigued resistive. However, bolted connections have been reported to have a better fatigue life than welding technique (Gholami et al., 2013).

Considering the above drawbacks, most of research investigations have directed on alternative technologies. Therefore, the CFRP strengthening technique was considered and became rapidly popular as a one of best retrofitting techniques in civil engineering applications. This technology has exhibits to capability of strength concrete, steel, wooden and masonry structures. Most CFRP based studies and field applications have been proven to be of significant strength as opposed to conventional methods.

Investigations conducted by Bocciarelli et al.(2009) have proven that CFRP exhibits better fatigue performance than welded cover plates methods. Yuana et al.(2004), Liu et al.(2005) and Jao et al.(2005) have also confirmed the fatigue performance of CFRP based strengthening technique through their research studies. In addition, number of laboratory investigations also conducted by several authors and all of them have confirmed the effectiveness of CFRP bonded reinforcement technique. Tang, (2013)

and Kalavagunta et al.(2014) have affirmed CFRP's ability to enhance the service life and increase fatigue capacity of structural members. Research studies done by Sreedhar et al. (2014) and Kalavagunta et al.(2014) have also investigated the steel sections ability to gain strength with CFRP. Authors have confirmed resistivity of higher load capacity, high potential to extend fatigue life and less probability of crack propagation with CFRP. According to Cadei et al. (2004) CFRP sheets and strips could be effectively used in renewal the lost capacity of a material. Due to the special characteristics of CFRP materials and compatibility to use with steel were the main reasons for the popularity of this technology. CFRP materials display a high tensile strength, low thermal expansion and low weight, no corrosion effects, high stiffness, high chemical resistance, and high temperature tolerance. Gite et al. (2013) have shown that CFRP capable to reduce one third of the weight and strengthen gain by five times with respect to steel. Therefore, CFRP is introduced as a revolutionary initiative of the retrofitting material in the world. The CFRP technology encourages a sustainable future and is recommended for the strengthening of existing structural members as an excellent alternative solution.

However, this technology has also shown few difficulties: there is bond performance, durability, effects of environmental conditions and cost effectiveness. On the other hand, a majority of CFRP based studies have focused on concrete structures and limited literature which is available relating to steel structures. This literature aims to understand bond performance governing parameters, resistivity under different loading techniques and the effects of different geometrical shape of sections. Ultimately, it strives to understand how load is transferred effectively and effectiveness of strength of composite is reviewed under different scenarios.

CFRP materials show unique characteristics: low weight, high temperature tolerance and low thermal expansion, high tensile strength, high stiffness, high chemical resistance. Therefore, it has become popular as a composite material in civil engineering applications. Module of CFRP material is most important characteristic to decide the strength of CFRP strengthened technique. In general, they have been classified using terms like "ultra-high modulus", "high modulus", and "normal

modulus". However, at present there no standard method for classifying CFRP materials.

Material characteristic of CFRP are critical for structural related applications, as strength gain depends on characteristics of the material. Yield strength, stiffness and module of elasticity critical in structural related applications. These are based on modules of the CFRP material.

### **2.7.1 Modules of CFRP material**

High modulus CFRP material reported a high elastic modulus compare to steel. These properties are important to achieve effective load transfer in steel section below the yield point of material. Schnerch et al.(2007) and Zhao and Zhang (2007) recorded the failure mode of high modulus material is rupture. Dawood et al. (2006) have investigated behavior of full scale beam with ultra-high modulus CFRP and outcomes reported as stiffness increased, significant service level enhancement and service load increased. Schnerch and Rizkalla (2008) also confirmed these results. The research studies conducted by Wu et al.(2012) highlighted the following regarding high module (HM) CFRP material.

- 1) The bond strength was significantly gained even with a higher stress ratio
- 2) The common failure mode has been reported from cohesive de-bonding
- 3) De-lamination was reported after fatigue loading

State university of North Carolina, conducted experimental programs about the CFRP strengthened concrete-steel composite bridge girders under fatigue loads (Massimiliano et al., 2009). Two different retrofitting methods were selected, including the use of HM-CFRP. The strength gain was reported as a 20 % enhancement with respect to non-strengthened specimen.

A considerable amount of research had successfully been undertaken on normal modulus CFRP to strengthen with steel and concrete girders. Lenwari et al. (2006), Aly and El-Hacha (2009) highlighted the effectiveness of normal module CFRP material. Similarly, Zhao and Zhang (2007) reported failure modes with respect to normal modulus of CFRP strengthened steel. The authors identified four types of

failures which include cohesive failure of the adhesive, de-lamination of CFRP, adhesive interface failure, and rupture of CFRP. Wu et al.(2012) reported failure mode as an interfacial de-bonding after fatigue loading. Bond strength was decreased by 10 % due to fatigue loads. Normal module of CFRP material is cost-effective than the other module and significant strength gain.

Due to the investigation of Emrani et al. (2005) stiffness decides the ultimate load bearing capacity and the fracture mode. Furthermore, increase of bond strength and reduction of stiffness was reported by Yu et al.(2011). Similarly, El-Hacha and Ragab (2006) have reported less ductile behavior and higher load capacity by high modulus of CFRP material.

The module of elasticity is another key character governed by the failure modes of CFRP/Steel composite. The type of adhesive and adhesive layer thickens is critical for deciding a module of elasticity (Wang et al., 2018). Properties of CFRP materials and steel are summarized in Table 2.2 and Table 2.3.

Table 2.2: Properties of CFRP material

<b>Module of CFRP material</b>	<b>Tensile strength (MPa)</b>	<b>Tensile modulus (GPa)</b>	<b>Ultimate tensile strain</b>
Normal modulus	2979	187	0.01808
Ultra high modulus	1923	514	0.00332

Source: (Peiris, 2011)

Table 2.3: Characteristics of steel & CFRP

<b>Description</b>	<b>Steel</b>	<b>MBrace 130 CFRP(NM)</b>	<b>MBrace 530 CFRP(HM)</b>
Mean elastic module (GPa)	195	240	640
Yield stress (MPa)	359	NA	NA
Tensile strength (MPa)	484	3800	2650
Ultimate tensile elongation %	NA	1.55	0.4

Source: (Liu et al., 2005)

### **2.7.2 Flexural strength**

Flexural strength also could be identified as one of the most critical characteristic of steel. Kambize et al.(2011) have selected I-section of grade A36 due to ASTM codes and strengthened with CFRP plates to investigate this characteristic where the four-points bending method has been used. The test resulting the CFRP strength gain changed from 11 % to 38 %. The maximum gain was reported with four layers of CFRP. It was observed that the brittle behavior of CFRP plates and de-bonding occurred at the premature end. Furthermore, test results have proven that 36 % elastic stiffness and 45 % flexural strength enhancement (Dawood et al., 2007a). Fatigue strength was increased by the live load level of 20 % compared to non-strengthened beam.

### **2.7.3 Shear strength**

The bond slip and shear stress are important factors when considered the overall performance of CFRP strengthens. Fawzia and Karim (2009) have explained the correlation between slip and shear stress through analytical models. The results were reviewed as a linear relationship and have a high possibility of stress concentration was noticed at the ends of strengthening plate. In general control of such stress affects the health of structures. However, different methods have been applied to reduce such residual stresses. Studies conducted by Miller et al.(2001) and Dawood and Rizikalla (2006) have introduced a beveled ends or reverse tapering of the CFRP material as an alternative solution to significantly decrease the peeling stress. The experimental tests carried out by Fawzia and Karim (2009) and Davaran (2010) to repaired steel beams. The authors recommended to adding a plate of steel with CFRP material for high stress zones and it can enhance the bonding strength by 50 % (Gholami et al., 2013). Kalavagunta et al.(2014) have reported that the local bond–slip is independent from geometry, and its model appropriate to measure bond performance. Relevant key studies with, results are summarized in Table 2.4 (Appendix A).

## **2.8 Effects of the geometrical dimension of CFRP material**

Geometrical parameters of CFRP material is the most important parameter to bond strength, bond durability and bond performance between steel and CFRP. Number of



CFRP layer, length of CFRP layer and thickness of CFRP layer could be considered as main parameters.

### **2.8.1 Effect of CFRP bond length**

Bond length is also one of key parameters investigated by many researchers to understand its effects on bond performance. Fawzia et al. (2005-2010) and Liu et al.(2005) investigated bond length effects. Authors have reported the load carrying capacity of CFRP strengthened steel is linearly propositional to the bond length. The bond length effect on strength has been extensively studied by Chen and Teng (2001),Dai et al.(2005(a)), Shield et al.(2005(b)), Ishikawa et al.(2006), Yu et al.(2011) and Wu et al.(2012).Their research studies have consisted of experimental and analytical works and all of the authors have individually concluded that an effective bond length is required to achieve excellent performance under various types of static and dynamic loading conditions.

### **2.8.2 Multiple layer of CFRP material**

The number of CFRP layers either affecting or not affecting the bond performance was one of other research focus points. Research series conducted by Fawzia et al. (2005-2010) has highlighted the performance variation with different numbers of CFRP layers for steel plate double strap joints. The authors concluded that the strength increases proportional with the number of CFRP layers.

### **2.8.3 Thickness of CFRP layer effects**

CFRP layer thickness affecting on bond performance investigations is another important research target of the many researchers .The bond strength is proportional to the thickness of the CFRP material and it has been confirmed by Yu et al. (2011) through their investigations.

## **2.9 Surface preparation for CFRP strengthened**

Surface preparation of steel could be considered the main factor for the influencing bond performance, failure mechanisms and the durability of the CFRP strengthen method. Various types of surface preparation techniques can be identified as pre-treatments of metallic materials such as sand blasting, grid blasting and grinding.

Surface preparation techniques can be classified as mechanical, chemical, thermal and electrochemical process. The importance of the surface preparation is to enhance bond performance between the metal surface and the epoxy material. Therefore, all surface treatment techniques should be confirmed as chemically active surfaces before the CFRP laminates and there should be no contaminations. Sand blasting or grid blasting have been recommended by many investigations, however, it is not cost effective in the case of field applications. Even specimen preparation for laboratory experiment is also very expensive. Interestingly, these methods are excellent surface preparing techniques. The main draw backs of such methods are high environmental pollution and noise pollution during the blasting period. This study used the grinding technique while the process of cleaning supports the removal of weak layers, degreasing, re-cleaning and escaped oil or other potential contaminants from the metal surfaces. Due to the investigations of Holloway and Cadei (2002) surface treatments contribute to eliminating contaminants from the metal surface and assists in forming a fresh active surface. Schnerch et al. (2007) have reported pre-treatment of steel surface can enhance the durability of chemical bonds. According to investigation conducted by Schnerch (2007) the grit-blasting is most effective methods for the treatment of the steel surface. The reason is that grit blasting can successfully remove inactive oxides and hydroxide layer from metal surfaces. However, the size of a grit is affected to the profile of metal surface. If selected the finer particle of grit result would produce a smooth surface and higher surface energy. Harris and Beevers (1999) noted that grit blasting technology could remove weak layers from metal surfaces and modified the chemical characteristics of the adherence (metal, CFRP). Grit blasting contributes to avoiding micro cracks in the surface. Furthermore, Baldan (2004) reported that the combination of chemical or electro chemical treatment with grit-blasting a caused to significantly improve the durability of the bond strength. In the case of general applications, a wire brush can be used to remove weak layers and vacuum head uses for cleaning the surface. Also, a solvent is used to remove surface contaminants. According to existing literature, all surface treatment methods have contributed to change a certain degree of bond performance. The grinding method can be easily applied in field applications and it is a cost effective simple method. However, this

method is more time consuming. Therefore, this grinding technology was used because it was a simple and cost effective technique which is utilized in field applications.

### **2.9.1 Surface preparation techniques**

Method of surface preparation critically influences bond performance between steel and CFRP adhesive bonded joints. Various types of techniques could be used to perform surface treatments of metallic materials. Baldan (2004) has classified such techniques as chemical, mechanical, electrochemical, and thermal process. All of surface preparation methods are improve the ability of formation between the metal and epoxy adhesive (Gholami et al., 2013). Therefore, surface treatment technique should confirm the chemically active surface before laminating. On the other hand, it should be noted that the surface is free from contaminants as absence of contamination to enhances ability of formation chemical bonds between metal surface and the adhesives. The purpose of the cleaning process is to remove weak layers, degreasing, re-cleaning and escape oil or other potential contaminants from surfaces. In general, it can be used to wire brush, vacuum head or apply solvent to remove the surface contaminants. Hollaway and Cadei (2002) have confirmed the following outcomes through their study. There are surface treatments causing elimination of contaminant from steel surface. Chemical amendment and forming a fresh active surface are another advantage of surface treatment. CFRP/steel strengthening methods are based on bond performance between steel surface and CFRP material with epoxy adhesives. The main purpose of bond is stress transfer through CFRP to steel surface. The study conducted by Schnerch et al.(2007) have proven that pre-treatment of the steel surface has enhanced durability of chemical bonding. Schnerch et al. (2007) have reported the grit-blasting method is the most effective technique for surface preparation because, this technique successfully removes inactive oxides layer from metal surfaces. However, the size of grit affects the profile of the steel surface. The finer particle of grit produces smooth surface and as a result shows a higher surface energy. Harris and Beevers (1999) have confirmed that grit blasting technology can remove weak layers from the surface of structural element and modified the chemical characteristics of the adherence. Furthermore, grit blasting can avoid micro cracks or any kind of other damage in the behind layer and result of such damage the strength of adhesive bonding

may decrease. Dawood and Rizkalla (2010(a)) have shown that silane coupling method of surface treatment can significantly enhance the bond durability of CFRP/ steel. Baldan (2004) has examined the combine effects of electrochemical and grit blasting technique. Author reported significant bond performance enhancement with combined method. According to existing literature all of the available surface treatment methods are significantly contribute to improve the bond performance between steel and CFRP material. The surface preparation technology related key studies are summarized in Table 2.5 (Appendix A). However, this study used an angle grinder for grinding purposes due to easy operation, the simplicity of it and its cost effectiveness.

### **2.9.2 Steps of surface preparation**

The cleaning process of steel surfaces can be explained in three main steps. The first step is removing grease and chemical contaminates from the metal surface. Secondly, weak layers on steel surface are removed using mechanical treatment. Finally, protective primer is applied on the steel surface to ensure complete bonds, removing all surface contaminants. Grease, dust, dirt, and chemicals are considered as contaminants and it should be removed from steel surfaces. The process of cleaning could be performed by wiping on the surface with an appropriate solvent. Rameshni (2011) has showed that acetone is best solvent for the cleaning purposes of metal surfaces. In fact, excessive solvent helps to prevent redistribution of the contaminants during the wiping.

Removing of weak layers from the metal surface such as rust and paint are another important factor. As adhesive layers are not properly bonded to the steel surface, if they are not removed weak layers, from the steel surface and result is premature debonding (Dawood, 2006). Weak layers could be removed using either mechanical abrasion or grit blasting. The grit blasting exhibits good surface preparing for excellent bond performance. But this technique needs heavy machinery and skilled labour. Therefore, this method is more expensive. Mechanical abrasion is comparatively simple to remove contaminants near the metal surface. Furthermore, the grit blasting

method contributes to chemical activate the coarse surface. The overall result is improved mechanical and chemical bond (Schnerch et al., 2007).

### **2.10 Adhesives and adhesive properties**

Steel and CFRP composites are essential to exhibit an excellent bond performance to gain significant enhances. The adhesive material is another important factor which govern bond performance because forces are transferred through adhesives between steel and CFRP. Therefore, adhesive should be able to transmit the forces efficiently through a bond of composite. However, each adhesive is not fully capable of effectively transferring these forces. Understanding of bonding mechanism may be useful to explain any bond performance. According to the study by Baldan (2004) CFRP/steel bonding mechanism has been classified as:

- 1) Physical bonding
- 2) Chemical bonding
- 3) Theory of inter diffusion
- 4) Theory of mechanical interlock

Meanwhile, Stanford (2012) has explained that the effective bonding between CFRP and steel is formed by mechanical interlocking or absorption mechanism. Characteristics of adhesive are other important factors influencing bond performance. Colombi and Poggi (2006) have reviewed the effect of ductility of adhesives and concluded that once high ductility is achieved it can distribute the stresses within the adhesive layers when loading increases. Adhesive layer thickness is another critical factor effect on the bond performance. Xia and Teng (2005) have explained the correlation between thicknesses of adhesive layer and furthermore authors have observed the failure mode too. According to this investigation the following conclusions were determined:

- 1) When the adhesive layer thickness exceeds 2 mm, failure mode is de-bonding
- 2) When the thickness of adhesive layer increases failure occurs as a brittle failure
- 3) Thin adhesive layer causes de-laminate through the adhesive and a ductile failure process occurs

Due to the decreased thickness of the adhesive the bond strength is increased which has been confirmed by Yu et al. (2011). A thin layer of adhesive cause to de-laminate through the adhesive and ductile failure occurs. However, uniform adhesive thickness exhibits the maximum performance, but maintenance of uniform thickness is more difficult. Most of adhesives show low viscosity properties and as a result thickness control is very poor with reduced bond performance.

The bond strength is inversely proportional with the thickness of the adhesive layer. The effect of the adhesive layer was confirmed by the Yu et al. (2011) due to their study. An application of a thin layer of adhesive would cause de-bonding through adhesive and such causes ductile failure. The effects of the uniform adhesive thickness brings maximum performance. However, maintenance of a uniform thickness is a difficult task. On the other hand, most adhesives show a property of low viscosity. Therefore, thickness control is very important but it is a difficult task in practical applications and results in reducing bond performance.

There has been limited attention on research studies related to influences in epoxy material. However existing literature explain the parametric effects on the bond performance, influencing factors on epoxy adhesives and environmental effects on bonding. Ultimately performance of CFRP/steel bond depends on characteristic of the adhesive and it changes with glass transition temperature viscosity and curing time.

#### **2.10.1 Stress concentration of adhesives**

Another important research area focused on understanding the effect of stress concentration of the adhesive. Wright et al. (2000) have reviewed stress concentration level behavior with adhesive thickness. Test result has reported that the reduction of stress concentration was 21 %. This investigation has proven that 32 % stress concentration is reduced by the addition of a fillet.

#### **2.10.2 Stiffness effect of adhesives**

Stiffness is the most important parameter when considering any CFRP/steel bond. According to finding of Emrani et al. (2005) stiffness is deciding ultimate load bearing capacity and the fracture mode of CFRP composite. The decreases of stiffness

contribute to enhance bond strength. The stiffness property of adhesive has been evaluated by Philip (2009) and concluded a flexible adhesive show lower stresses as it deforms to a greater degree. However, low stress is usually shown as the lower ultimate strength. On the other hand, stiffer adhesive causes to higher stresses but it has been shown as the higher ultimate strength. Key research studies related to adhesives and adhesive properties are summarized in Table 2.6 (Appendix A).

## **2.11 Effects of environmental exposure on CFRP/steel bond performance**

Bond performance, strength and durability not only depends on internal factors, but also on external factors too. There is moisture level, temperature, UV radiation effects and combinations of two or fewer of the above factors which are reviewed in this investigation.

### **2.11.1 Effects of environment moisture level on CFRP/Steel bond performance**

Absorption of moisture to the CFRP/steel bond can be identified as the main issue of governing bond performance and durability because both epoxy adhesive and CFRP materials are allowed to penetrate water molecule into the bonded. As a result of water absorption, attraction between two components of composite becomes weak. On the other hand, moisture absorption of CFRP matrix causes physical changes. Due to physical changes, there may be a tendency to decrease the glass transition temperature of epoxy material. Collings et al. (1993) and Hollaway (2010) have examined the effect of moisture level for the failure of the carbon fiber matrix. In addition, ingress of water molecule causes to un-expected structural distortions during their service life of CFRP composite. Kumar et al. (2008) have reported that water absorption caused decrease the shear strength of the CFRP. Because, swelling leads to plasticization with a softening effect while leading to a significant decrease in its tensile strength. Zhang et al.(2012) have also reported that small amount of moisture (around 1 %) ingress of CFRP material causing an approximately 17 % decrease of bending strength. However, Nguyen et al.(2012) have reported that great bond performance even under high level of relative humidity conditions also.

CFRP materials shows good resistance to corrosion and chemical attack (Gholami et al., 2013). However, salt water affects critical since salt can easily penetrate through a

fiber matrix. Tavakolizadeh et al.(2010) have investigated the behavior of CFRP materials when subjected to chemical solutions. Results have shown that CFRP sheets display excellent durability and authors have reported that reduction of mechanical properties. Nguyen et al.(2012) have examined the behavior of tensile strength of CFRP/steel bond after 12 month immersion in 20 °C salted water. The tensile strength reduction has been recorded at around 17 %. Rege and Lakkad (1983), Hollaway (2010) have conducted similar investigations and reviewed the negative effects of moisture ingress on a fiber matrix. Nguyen et al.(2012) reported that the moisture absorption is very fast at the starting and then reached a stable. The temperature of the moisture has decided the quantity of water absorption. Authors have concluded that water absorption by adhesive is 4 % at 20 °C and 5 % at 50 °C (Gholami et al., 2013).

Humidity level effect on epoxy adhesive has been investigated by and Wu et al.(2004) and Lettieri and Frigione (2012). Authors have reported that when the humidity is above 75 % large amounts of water quantity are absorbed. Furthermore, it was noted that the glass transition temperature of the adhesive material is decrease due to plasticization. Wu et al.(2004) have reported that small quantity of moisture (< 2%) is enhanced bond strength and improved curing rate. Key research investigations related to humidity effects on CFRP/steel bond performance are summarized in Table (Appendix-A). Due to the penetration of moisture through CFRP/ steel bond, cohesive force (Hydrogen bond or other valance bond) of adhesive molecules becomes a weakness due to polymer inflation and it has been observed that de-lamination as a main failure mode of bond (Yong-xin et al., n.d.).

### **2.11.2 Cyclic temperature effects on CFRP/Steel bond performance**

Thermal effects could be described under two scenarios as freezing conditions and thermal cycles. In general, most of the investigations have identified that high temperature has an unfavorable influence on CFRP strengthened steel bonding system. CFRP material shows resistivity against elevated temperatures of the environment. However, epoxy resins usually exhibit a susceptible nature and it is highly sensitive to temperature (Gholami et al., 2013). Due to such behavior the strength and stiffness of CFRP bond can be predicted to decrease rapidly. This occurs at high temperature of



the environment and its exceeds the glass transition temperature ( $T_g$ ) of epoxy materials. Ishikawa et al. (2006) have examined the co-relation between mechanical properties of CFRP material variation with temperature. Authors has proved that mechanical properties of CFRP materials tend to reduce with the increase of temperature. Investigation conducted by Chao et al. (2012) and Wu et al.(2012) have proven that the performance of CFRP/steel bonding. The scientific reason behind such a strength change is controlled by the glass transition temperature of epoxy material (Gholami et al., 2013). The viscosity of epoxy increases which rapidly reduces the strength and stiffness of the bonds.

In general, the glass transition temperature ( $T_g$ ) of adhesives varies from 40 °C to 70 °C (Gholami et al.,2013). However, Stratford and Bisby (2012) have reported that a significant level of bond slip appeared before the glass transition temperature of the adhesive. The result is strength reduction of the composite system before the glass transition temperature. Authors have recorded that a bond slip began at around 40 °C and its peak at 65 °C. The ultimate load capacity reduces when temperature reaches the glass transition temperature ( $T_g$ ). Nguyen et al.(2012) have estimated that the reduction of ultimate load capacity under various temperature conditions and noted values as 15 % at 10 °C ,50 % at 20 °C and 80 % when the temperature reached  $T_g$ . At the failure time, the transition temperature was reported as 40 °C. Much research has shown that the degradation of the bond is dependent on level of stress.

CFRP/steel bond should have capability to excellent temperature tolerability under freezing and elevated conditions. Investigations conducted by Mertz and Gillespie (1996) regarding bridges in North America have reported that the selected adhesive should have good environmental durability. In general, the high temperature causes to reduce the bond performance. Always, ambient temperature should be less than the glass transition temperature of selected adhesive (Hegde et al., 2019). Stratford and Bisby (2012) have evaluated temperature behavior and test results have shown glass transition temperature of the adhesive reported as 65 °C, and bond slip start observed around 40 °C. Further it reached the peak value at the glass transition temperature ( $T_g$ ).

### **2.11.3 Ultraviolet (UV) radiation effects on Steel/CFRP bond performance**

Ultra-violet radiation of sunlight is contribute to splits the bonding molecules in polymers (Gholami et al., 2013). Bond dissociation is started due to absorption of the UV radiation (Gholami et al., 2013). Dissociation action continues as subsequent reactions with environmental oxygen. The damaged area has been identified as a potential stress concentration location. Recent research studies have proven that CFRP materials' exposure to artificial sunlight causes variation in the strength. Test result has shown that tensile strength decreases from 15 % to 20 %. Cromwell et al. (2011) have reported that the lower curing temperatures or presence of moisture causes an increase in the rate of degradation. Ishikawa et al. (2006) and Tavakolizadeh et al. (2010) have highly recommended that the fiber reinforce material should be protected by ultra-violate (UV) radiation as the authors emphasized that exposure to UV radiation makes CFRP material more vulnerable than any other environmental factor.

However, an investigation conducted by Lettieri and Frigione (2012) have reported that UV radiation does not critically affect the change in stiffness and tensile strength of the CFRP. The CFRP/steel lap joint when exposed to UV radiation with at 40 °C has exhibited a 35% reduction of tensile strength. Interestingly, UV radiation without temperature did not effect on tensile strength. Therefore, it could be concluded that the decrease of stiffness is mainly governed by temperature alone. UV radiation does not influence on stiffness change. In addition to this, some researchers have suggested that the adhesive is the critical component of UV exposure in the system. However, to get the final conclusion about UV effects on the CFRP/steel system more investigations are needed.

### **2.11.4 Combined effects of environmental factors on Steel / CFRP bond performance**

In real world applications, most of the above parameters jointly affect bond performance. However, few investigations have investigated the combined environmental factors which affect the CFRP/steel bond performance. The influence of combined environmental factors is more complicated and critical. The existing literature focuses on investigation of the combined effects of moisture and temperature

(hygro-thermal). Aoki et al. (2008) have reviewed that hygro-thermal exposure causes significant reduction in glass transition temperature of adhesive material. Li et al. (2011) have investigated combination effect of temperature and relative humidity (50 °C and 93 % RH) for I-section of steel beam. Ultimate load carrying capacity due to bending were reported as 22 %, 26 %, and 57 % with 15, 45, and 90 days respectively.

However, Kim (2012) has reported that the average tensile load capacity of specimens increased by 31 % under wet/dry conditions. This test has considered double lap shear joints with 100 cycles. 17 % of the capacity improvement has been reported at freeze thaw (8 hours – 20 °C, 16 hours – room temperature) conditions. Thus, additional curing of epoxy may cause these abnormal results. Double strap CFRP/steel joints have been subjected to 5 % salted water at 20 °C and 50 °C for 12 months. A decrease in the strength of bonds has been reported as 15 % and 26 % respectively. In addition Dawood and Rizkalla (2010(a)) have observed rapid degradation in the first 2 to 4 months. Similarly, Nguyen et al.(2012) have examined the combined effect of a severe environmental condition. Authors have considered a high temperature (38 °C), salted water (5 %) and sustained load for double lap shear joints. The above studies have explained combine effects of saline water and elevated temperatures. Results have concluded that such factors highly influence change in the mechanical properties of joints dramatically. Key research investigations related temperature and humidity combine effects on CFRP/steel bond performance are summarized in Table 2.9 (Appendix –A).

Humidity or extreme temperatures causes to reduce the durability of bonding strength. In a normal wet environment, ocean spray and long term exposure to wet environments highly affect this kind of behavior. Main reasons for such behavior includes increasing surface energy and the displacement of the secondary bond between adhesive and substrate. However, a water resistant sealant can be used to overcome moisture ingress to surface. The use of the glass fiber reinforced polymer (GFRP) material act as a protective layer and it may enhance the durability of the bond as moisture ingress is decreased. GFRP has ability to adopt moisture and on the other hand it is capable to leach salt.

## **2.12 Different types of testing method for Steel/CFRP bond performance**

CFRP based external strengthening technology mostly depends on the material behavior of the member. Due to literature most of research investigations have focused on evaluating bond performance characteristics. The strength gain with CFRP has been investigated with the following procedures:

- 1) Compression test.
- 2) Tensile test.
- 3) Bending test.
- 4) Impact test.
- 5) Fatigue test.

### **2.12.1 Tensile load effects related investigations**

Jiao and Zhao (2004), Xiao et al.(2005) and Zhao et al. (2005) have conducted test series to understand the tensile behavior of structural element and all of studies have confirmed tensile strength gain with CFRP materials.

### **2.12.2 Compression load effects related investigations**

Circular hollow sections (CHS) strengthened with CFRP was investigated by Hong et al. (2000) and Teng and Hu (2007). Authors have investigated axial compression behavior of CFRP strengthened CHS and the results have concluded significant improvement with CFRP.

### **2.12.3 Combined effects of bending and compression loads**

Doi et al. (2003) and Haedir et al. (2006) have evaluated compression and bending behavior respectively. Authors have confirmed considerable strength gain with CFRP materials.

### **2.12.4 Impact load related investigations**

Haider et al. (2012), Sreedhar et.al. (2013) and Kalavagunta et al. (2014) have investigated bond behavior under impact loads. Authors have confirmed a significant strength gain by CFRP material due to test results.

### **2.12.5 Fatigue load related investigations**

The influence of several factors has investigated thoroughly by authors, but the conclusions of similar studies also given different results. For example Zheng et al.(2006) have found out that steel structure with fatigue strength gain range vary from 155 % to 580%. Jones et al.(2003) have been reported that there is a fatigue life enhancement by 115 % in comparison to non-strengthened specimen. Furthermore, Tavakkolizadeh et al. (2003(b)) have confirmed that there is almost 3 times fatigue strength gain with CFRP technology. Schnerch et al. (2007) have reported the strength gain happens by 20 % and at the North Carolina state university this result was confirmed with similar test series. Täljsten et al. (2009(a)) also described fatigue strength gain after the series of research and recorded a changing from strength gain 2 to 4 times. Mosallarn et al.(1998) have examined the effects of fatigue loading. The result has noted as 15 % fatigue strength gain. These researchers in 1998 have investigated the effect of strengthening with CFRP. They have reported the strength gain as 1.25 times enhanced with comparatively control sample Mosallarn et al. (1998) and Deng and Marcus (2007) have reported that the strength gain was increased by 30 % of fatigue life .However, Wu et al.(2013) have reported 10 % that of bond strength decreased for normal module and no significant gain report for high module (HM). According to the study of Liu et al. (2005) fatigue enhancement was insignificant with CFRP. Therefore, each study results have no uniformity in conclusions regarding the gain of fatigue strength. Results are different from authors to authors. The reason is that strength gain is not dependent on unique parameter. It depends on multiple parameters and their effects are difficult to understand with simple correlation. Such parameters can be identified as properties of materials, Module type of CFRP (NM, HM), Physical dimensions of the sample, environmental conditions such as temperature, salt environment, humidity level, freeze/thaw condition etc. Furthermore, characteristics of epoxy adhesive such as curing time, glass transition temperature, and viscosity also affect the final result. Installation procedures, thickness of adhesive layer, surface preparation, and air bubble removing methods are other critical factors. Condition of structure, pre-stress, corrosion and stress distribution patterns also affects on performance. Loading condition, bond characteristics such as bond length, number of CFRP layers, whether single side or double side lamination also highly influences

bond performance. Type of sample, side notched beam/plate, center hole plate, real sections or small sample affect the final result. Loading patterns such as constant amplitude, variable amplitude or cyclic with impact or none impact rate of loading are other influencing factors. Performance depends on the type of joint – i.e. single lap joint, double lap joint etc. Ultimately, real environmental conditions are beyond human control. Most of the test results have been taken under the one or more parameter controlling situation. Eventually, results may deviate under laboratory conditions. It can be concluded that more than one parameter affects the final result and the combination of many parameters is involved with final outcomes. As a result, prediction is more complicated and results vary in a very wide range.

Different studies have proven that fatigue failure mechanism is dependent on the level of stress. Jones et al. (2003) have observed the cracks propagated behind the CFRP strips and the failure mode have been identified as de-bonding. The investigations of Zheng et al. (2006) have recorded premature de-bonding from the steel surface. Pipinato et al.(2012) have reported that the failure mode is dependent on parameters as type of adhesive, modulus of elasticity of the CFRP, and adhesive layer thickness. Massimiliano et al.(2009) have been shown failure mechanisms start as de-bonding and propagated along the interfaces. Finally, failure mechanism is not uniform and most of studies have observed combination of failure mode as interface de-bonding and CFRP de-lamination. However, this technology helps to delay crack propagation. Tavakkolidazeh and Saadatmanesh (2003(b)) have observed decreases in the crack growth rate. Jones et al. (2003) also had proven that the delayed onset of fatigue cracks propagation. Tavakkolizadeh et al. (2003(a)) have quantified crack growth rates by a decrease of an average of 65 % with CFRP. Deng et al. (2007) again have confirmed that crack initiation showed a delay with CFRP strengthened specimen. However, Pipinato et al.(2012) have proven that the weakest point of the system is the interface between steel and adhesive.

In general, structures subjected to stress fluctuation and such a cyclic action causes to fatigue failure. It can contribute to either partial or complete separate of CFRP composite. Domazet (1996), Bassetti et al.(1998), Okura et al.(2000), Suzuki (2002),

Suzuki and Okamoto (2003), Tavakkolizadeh and Sadatmanesh (2003(b)), Jones and Civjan (2003), Matta (2003) and Liu et al.(2005) have investigated potential to use CFRP material to enhanced fatigue life of structures. Authors have confirmed significant improved by CFRP material. The range of stress, bond length, effect of multiple layers and pre-stressing are critically influences on fatigue life of CFRP/steel composite (Batuwitage et al., 2017).

Al-Zubaidy et al.(2012) investigated influence of loading rate on steel joint. This study considered range of loading rates vary from 2 mm/min to 5 mm/min .Due to this study test result has been reported as a maximum performance occurring at the rate of 3.35 mm/min.

Another research area focused on the evaluation of the hysteretic behavior of axial compression under cyclic lateral load. Zhen et al. (2013) have been reported the result of the experiment. The authors have observed a slowdown in the occurrence of local buckling and as improvement in the ductility of steel columns. The strength gain change from 39 % to 50 %, at the 20 °C and room temperature was identified respectively. When axial compression ratio was 0.2, the changes were 54 % and 62 % at 20 °C and room temperature respectively.

### **2.13 Testing standards**

Crack initiation is a crucial issue relating to steel structures due to fatigue loads. However, even today there are no specific testing standards or modeling procedure or prediction the crack initiation on structural elements. However, invaluable hints have been given by many testing standards relating to fatigue. ASTM D-790 and ISO 178 gives valuable guidance for the three-point bending test setup. In addition, ASTM D 6272 provided guidelines for test setup on unreinforced and reinforced materials. ASTM D 7774 is the standard for uni-axial loading and it has been recommended that the test frequency should be less than 5 Hz to reduce the chances of heat generation. Both ASTM D 7791 and ISO 13003 are explained in the test procedure of flexural fatigue of plastic materials. This method recommends the loading pattern as a sinusoidal pattern. ASTM D 7791 is allowed to perform either a four-point or three-point flexural cyclic loads. ISO 15850 and ASTM D 6115 can be utilized specifically

for the estimate of fracture energy in the inter-laminar region of a composite. However, there is no clear guidance or standards to evaluate crack initiation under fatigue states.

#### **2.14 Behavior of fatigue**

The fatigue effect on the bonds is very important for estimate the service life of CFRP technique. In general, 90 % of failures of metallic structures happen due to fatigue stress. However, most steel structures i.e. bridges, aircraft, and machine components are mainly subjected to cyclic stress during their service life. Structural failure can happen below the tensile or yield strengths of the material due to cyclic stresses. Generally, fatigue failure displays catastrophic features and it occurs suddenly. Such failures are known as engineering disasters. Fatigue failure proceeds with three steps. They are crack initiation, propagation and failure. Crack initiation happens due to cyclic stresses. Cyclic stresses classified as maximum stress, minimum stress and mean stress. The stress range, stress ratio, amplitude of stress, pre-stressing technique and crack arrest hole are major factors influencing on the performance of CFRP/steel bonds. According to Zheng et al.(2006) and Yu et al.(2005) the available research work regarding fatigue strengthening is limited.

Due to research investigations of Bassetti et al.(2000), Colombi et al.(2003(b)) reported strength gain in fatigue life with CFRP increase up to three times. Research series developed by Jones et al.(2003), Colombi et al.(2003(b)), Deng and Marcus.(2007), Nozaka et al.(2005(b)), Monfared et al. (2008(a)) and Täljsten et al.(2009(b)) have examined the behavior of CSH specimens with a constant amplitude sine wave and results have been reported as follows:

- 1) Enhancement of the fatigue strength by CFRP up to 115 %.
- 2) The crack propagation is mainly governed by tension.
- 3) Surface preparation and properties of adhesive critically influence on bond behavior of CFRP/steel bond.
- 4) Sand blasting was recommended as a good surface treatment method.
- 5) Applying CFRP strips to damaged steel specimens enhanced fatigue durability and delayed of crack growth.



Retrofitting of steel structures using a CFRP patch has been conducted by Zheng et al. (2006). A study has been concerned with strengthening method, stress range and stiffness of CFRP. The following findings were noted as test results:

- 1) CFRP strips dramatically increase the fatigue life and strength gain were reported from 155 % to 580 % over non-strengthened specimens.
- 2) Premature de-bonding of the CFRP layer from the metal surface has been reported with low elastic modulus CFRP.

Bassetti et al. (2000) have been investigated various factors effects on bond performance. Pre-stressing level, thickness of CFRP layer and the adhesive material properties have been focused on this study. In all the scenarios it has been shown that there is a significant fatigue life improvement in CFRP material (Bassetti et al., 2000). Jones and Civjan (2003) have experimentally and numerically investigated on the fatigue behavior under several variations. There is a type of CFRP material, thickness and surface preparation technique has identified as key factors. Effective factors have been further described as a series of fatigue test conducted by Domazet (1996), Bassetti et al.(1998), Okura et al.(2000), Suzuki (2002), Jones and Civjan (2003), Matta (2003), Suzuki and Okamoto (2003) and Tavakkolizadeh and Saadatmanesh (2003). All of the above studies have confirmed the enhancement of fatigue life with CFRP materials. Liu et al. (2005) conducted an investigation regarding bond performance under fatigue. The following key findings have been noted by the researcher:

- 1) No fatigue failure occurred until the applied load was below 40 % of the static strength of the specimens.
- 2) Stiffness reduction.

The behavior of steel frame strengthened with CFRP were investigated by Mosallam et al.(1998).The authors reported that test results achieved acceptable ductility ranges. The authors concluded that the CFRP repair technique provides comparatively more than 1.25 times strength gain with control specimen. Tavakkolidazeh and Saadatmanesh (2003(b)) have tested CFRP strengthened notched beams under the fatigue loads. These experimental observations, CFRP extend the fatigue lifetime and as well as decrease the crack growth rate (Tavakkolizadeh et al. 2003(a)). Furthermore,

Tavakkolizadeh et al.(2003(a)) have reported that CFRP extend the fatigue life and as well as decreases the rate of crack growth. The test results proved that there is a strength gain more than three times and rate of crack growth decrease by 62 %. Monfared et al.(2008(b)) investigated CFRP embedded with single side or both sides of a notched specimen and the authors concluded double side patch is more effective.

#### **2.14.1 Pre-stressed and non- pre-stressed behavior of Steel/CFRP bond under fatigue load**

Another bond performance depending parameter is the Pre-stressed of CFRP material. Due to the corrosion or cyclic load such stresses may be built on structural element also. Colombi et al.(2003(a)) have investigated the effectiveness of pre-stressed CFRP bonded strips. Maximum fatigue life improvement due to pre-stressed CFRP specimen was reported about sixteen. Täljsten et al. (2009(a)) have investigated the influence of pre-stressed CFRP and it was estimated that fatigue life increased by 2 to 4 times. In addition, this test series has been identified as pre-stressing the CFRP strip because it reduces the crack propagation and the ability to increase the fatigue life. The authors have concluded that fatigue life and crack propagation rate were dependent on the strip stiffness and pre-stressing force. According to observations of above test series pre-stressing effects increase when the stress ratio (R) decreases. Finally, authors have reported that any violation of fabrication tolerance may cause unpredictable changes.

#### **2.14.2 Failure mechanism of Steel/CFRP bond under fatigue**

Fatigue failure mechanism can be identified under two main stages; an crack nucleation and propagation (Gowhari, 2003). Nucleation of fatigue failure occurs at the microscopic level. This dealing with micro cracks, grain dislocations and slip bands. However, microscopic level failures cannot be visually observed. Surface flaws accelerate the initiation of fatigue crack (Kramberger, 2004). Bannantine, et al. (1990) have conducted test series to understand the correlation between crack length and the rate of propagations .Test results have confirmed rate of crack growth linearly proportional with the length of crack. The fatigue behavior of steel structures retrofitted with CFRP materials have been investigated by Massimiliano (2008) and Colombi et al.(2009). The authors have observed failure mechanisms and it had started

with, initially de-bonded at the plate ends. Furthermore, propagation of failure along the element in the interfaces was noted. Due to cyclic load steel-adhesive interface become a weak and the failure mechanism was identified as de-bonding. Colombi et al. (2003(a)) and Colombi et al.(2003(b)) have conducted the test series to understand the behavior of pre-stressed CFRP plates' effect of cracked steel sections. The authors have recommended complete stop growth of crack or retardation which can be done by following three ways (Massimiliano et al., 2009):

- 1) Reduced crack opening displacements behind the crack front and the result is decrease the stress intensity at the crack tip.
- 2) Produced a crack closure effect on CSH by pre-stressed patches.
- 3) Stiffness increases of the cracked steel sections.

Mosallam (2005) has reviewed the effects of fatigue loading on two different CFRP strengthening systems for steel beams, and it was reported that there was 15 % of the capacity improvement of the control beam. In addition, the authors have observed local buckling failure of the top flange and lateral buckling of the beam. Furthermore, it has been reported that the hybrid panel beam achieved a peak load with 297 kN and 28 % capacity enhancement. However, the bonds after failure have been visually identified as a weakest point of the steel-adhesive interface (Massimiliano et al., 2009). Furthermore, the results have been reported that the excellent fatigue capacity with CFRP material (Massimiliano et al., 2009).

### **2.14.3 Co-relation between geometry specimens' and fatigue**

Most research studies have been based on small scale specimens due to practical limitations of the actual size of test specimens. Small scale specimens have been selected by Colombi. (2006), Liu et al. (2009), Nakamura et al. (2009) and for the laboratory tests. Full scale specimens have been based on research conducted by Dawood et al (2007), Jones and Civijan (2003), Nozaka et al. (2005) and Tavakkolizadeh and Saadatmanesh (2003(a)). All these authors extended the capability of fatigue capacity by CFRP material of steel structures.

## **2.15 Field applications of CFRP strengthened material**

Hollow sections are one of the popular applications of structural design. CFRP based strengthening of such a section is a new trend in the design industries. Therefore, more research has been undertaken targeting the evaluation of the bond performance of CFRP bonded hollow sections. Hollow sections can be mainly classified as a circular hollow section (CHS) and rectangular hollow section.

### **2.15.1 Rectangular Hollow Section (RHS)**

RHS is the most popular section of steel structures. A few of research investigations have been conducted to estimate end bearing capacity of a rectangular hollow section (RHS). Most of them have shown significant strength gain of such sections with CFRP material. Fernando et al.(2008) have calculated the ultimate load for RHS and enhancement was reported as an average value range from 48 % to 103 %. Moreover, this experiment series has been linked with four different possible failure modes which are as follows:

- 1) Failure of adhesion (interfaces between the adhesive and adherents).
- 2) Cohesive failure (failure of adhesive).
- 3) Combined adhesion.
- 4) Cohesive failure and inter laminar failure of CFRP (Zhao, 2013).

In general, cohesive failure depends on the properties of the adhesive. But adhesion failure is controlled by the characteristics of metal surface. The key characteristics are the textures, roughness and chemical composition of the surface. Another research area available in the literature is determined of the crippling behavior of CFRP bonded rectangular hollow section (RHS). According to literature interfacial stress, external corner radius, loading position and depth to thickness ratio of web significantly contribute to reduce the web crippling capacity. According to the study conducted by Mustafy and Asha (2010) the distance between the edges and loading point should be less than 1.5 times of distance. The Strength gain of CFRP strengthened square hollow sections was determined by Shaat and Fam (2007) and reported that significant strength enhancement with CFRP materials. When considering failure modes, it was noted that there were two basic crippling failure modes as web buckling and web yielding.

### **2.15.2 Circular hollow section (CHS)**

Another popular hollow section can be identified as circular hollow section (CHS) as shown in Figure 2-15. These sections are widely used as application of columns. The CFRP jacketing technology can extend with any kind of circular cylindrical structure applications. Steel bridges, liquid storage tanks and steel silos storage tanks can be identified as popular applications in industry. The major advantage of such sections is grate buckling (axial compression) resisting. There are two possible ways of buckling which are inward and outward buckling. Literature has explained that inward buckling can be controlled by using concrete core. However, issues were reported as a prevention of outward buckling. Most of the research investigations have identified CFRP jacketing technique is successful solution for outward buckling. However, CFRP jacketing does not show significant resistance of inward buckling. As a solution researchers have been investigating potential of multiply layers and noted little additional benefits. In addition, CFRP external lamination has been identified as benefited method for the enhancement of ductility. Furthermore, this technology has been reported as seismic retrofitting techniques of such columns. For example, liquid storage tanks are suffering from a combination of internal pressure and axial compression. As a result, such circular structures suffer the elephant's foot buckling failure as shown in 2-15. This kind of failure accelerates due to earthquakes or any other reasons. According to Teng and Hu (2007) ultimate load of the steel tube enhancement was reported between 5 % to 10 % by the CFRP jackets with different thicknesses. Furthermore, it has confirmed the axial shortening at peak load (Energy absorption capacity) which has been enhanced approximately 10 times by the CFRP materials.

According to literature strengthening of circular hollow sections (CHS) with CFRP has been reviewed by Hong et al. (2000) and Teng et al. (2007) under compression and noted for its significant strength gain with CFRP materials. These test series were based on an investigation of thin-walled steel structures. Haedir et al. (2006) have investigated performance bending while Doi et al. (2003) have examined compression and bending behavior of CHS. Jiao and Zhao (2004) have investigated tensile behavior while Xiao et al. (2005) and Zhao et al. (2005) have reviewed strength gain on concrete

filled CHS. Bocciarelli et al. (2009) and Zhao and Zhang (2005) have evaluated the propagation of fatigue crack of CHS. Tavakkolizadeh and Saadatmanesh (2003(b)), Lenwari et al.(2006) and Schnerch and Rizkalla (2007) have investigated flexural performance. All these researches have confirmed that a considerable amount of strength and stiffness gain in steel when CFRP bonded with external. In addition, research has been done on hollow structures by Haedir et al.(2007) and Zhao and Al-Mahaidi (2009). Authors have reported considerable improvement of web buckling. Ghafoori et al. (2012) have investigated the fatigue behavior and reported the significant strength gain. Nuno et al.(2008) and Haider.et al.(2012) have investigated compression behavior and noted significant improvement in strength as well as stiffness of hollow structures with CFRP material.



Figure 2-15: Elephant's foot buckling failure of hollow sections (Haroun, 2005)

### **2.15.3 Bridge repair related applications**

CFRP laminating technology is popular in the case of strengthening bridge girders made by concrete since more than two decades. However, real world applications of CFRP strengthened steel girders are relatively limited. However, few of real world CFRP strengthened applications have been reported. Design guidelines of CFRP strengthened steel have been published by the United Kingdom, United State and Italy (CNR-DT202/2005) have introduced valuable design guidelines. Hollaway and Cadei (2002) have investigated commercial uses of CFRP in the United Kingdom. Bridge related investigations have focused on the several bridges: Bow road bridge in east London, Slattocks canal bridge in Rochdale, Bid bridge in Kent and Hythe bridge over the Thames river in Oxfordshire. CFRP with a normal modulus of laminating

application has been reported in a bridge on state highway 92 in Pottawattamie county. The first high modulus CFRP application was reported on Acton railway bridge in London. The second one was reported to the King street cast iron railway bridge. Both cases have exhibited an enhancement of the fatigue resistance. The Takiguchi bridge in Tokyo is used ultra-high modulus CFRP for strengthening purposes. The bridge girders have been strengthened with 4 mm thick ultra- high modulus CFRP and reported significant fatigue enhancement. The reported bridge repair applications with CFRP materials are summarized in Table 2.10 (Appendix –A).

### **2.16 Theory of material hardening**

The material hardens or softens due to the effects of the cyclic stress and this behavior mainly depends on properties of materials. When repetitive stress cycles are applied on materials it usually shows a stable hysteresis loop. The meaning of stable hysteresis loop which presents the stress and strain response under the cyclic load. Endurance curve (S-N curve) is most commonly used for the estimate of fatigue life. In this method, considered the logarithmic value of stress magnitude (S) variation with relevant stress cycles (N) until to fail (Recho, 2012).

When applying any uni-axial load on the material, it will deform to the yield and result in a hardening of materials as shown in Figure 2-16. In the case of hardening, perfect, plastic stress will reach the yield point (A) of the material. Plastic deformation is ensured, so long as the cyclic load is applied at the yield point. However, when the stress is reduced, elastic unloading may occur. When a material is subjected to elastic response, it can be fully reversed to its original physical shape dealing with the unloading. However, most of the practical applications are experienced beyond the elastic limit of the material. Plasticity is explained as the material response beyond the yield point of the material. The result of plastic behavior of material is an unrecoverable strain even at the end of the unloading. The common characteristic of plastic behavior is rate-independent plasticity at low temperature and low strain rates. These characteristics are very important for the estimation of fatigue life, because it is incorporated with small strain load cycles. The hardening rule describes how the yield surfaces change in shape and size due to the plastic deformation of the material. Kelly

(2012) have presented two basic hardening rules, namely kinematic hardening and isotropic hardening.

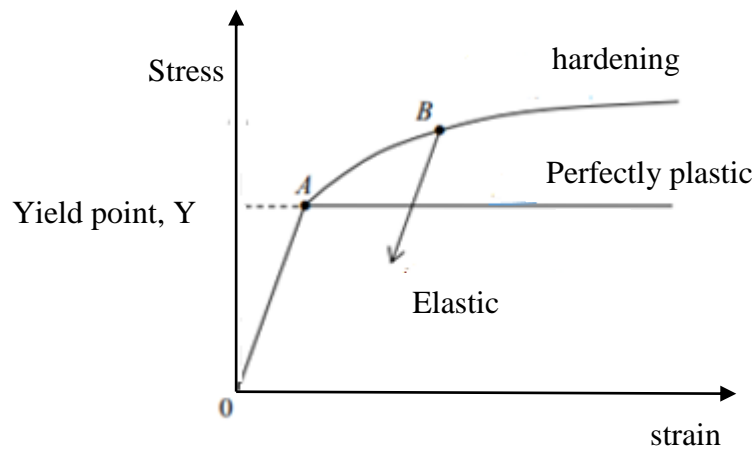


Figure 2-16: Uni-axial stress-strain curve (Chatterjee & Sahoo, 2012)

### 2.16.1 Kinematic hardening

Kinematic hardening is dealing with small strain, fatigue loading simulations. In general, the kinematic hardening rule is used for the simulation of crack propagation. According to kinematic hardening, the yield surface remains constant in size and translates in the direction of yields. A typical uni-axial kinematic hardening curve is shown in Figure 2-17.

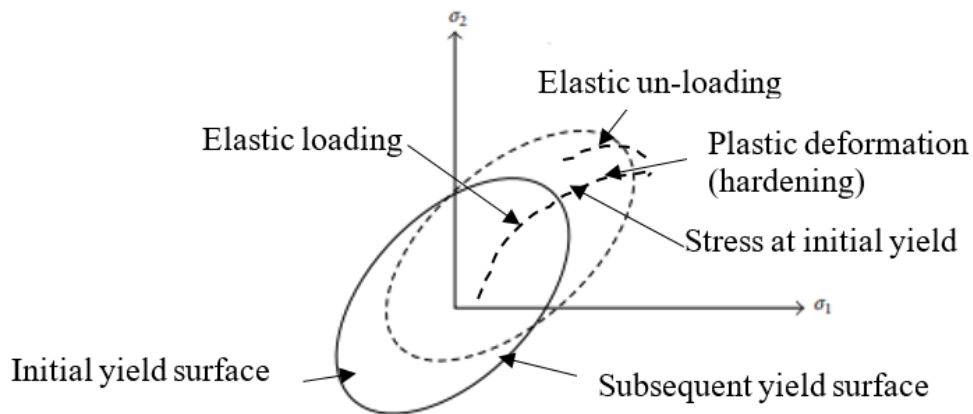


Figure 2-17: Kinematic hardening curve (Chatterjee and Sshoo,2012)



### 2.16.2 Isotropic hardening

Yield strength in tension and compression are initially the same in the typical isotropic material. In case of isotropic hardening, the yield surface remains the same shape. Hardening in tension lead to a softening in a subsequent compression isotropic hardening can be used to evaluate the large strain or proportional loads. Therefore, it cannot be recommended for cyclic load simulation. However, it could be utilized to evaluate the contour integral with stationary crack. A typical uni-axial isotropic hardening curve is shown in Figure 2-18.

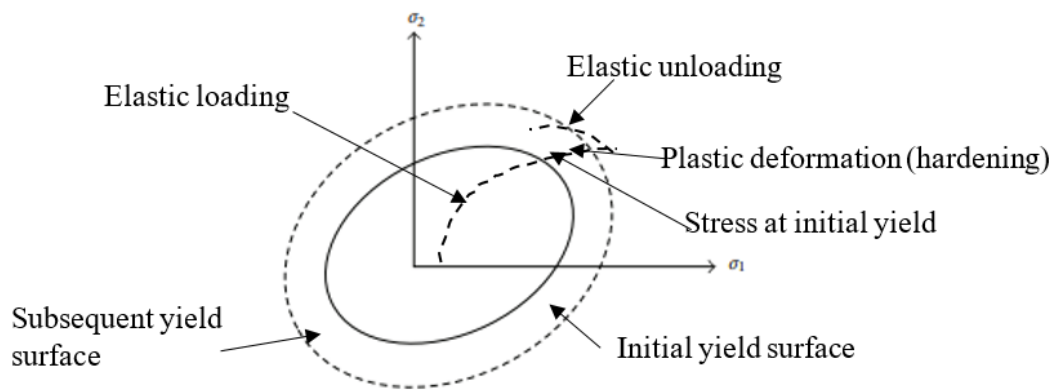


Figure 2-18: Isotropic hardening curve (Chatterjee and Sshoo,2012)

### 2.17 Fatigue related parameter effects on structural elements

Factors affecting fatigue life of structural elements are considered as fatigue parameters. Generally, fatigue parameters are classified as geometric parameters, material properties, environmental factors and loading parameters. These are not individually influenced by a real application of fatigue and two or more variables are combined effects for the final results. This study did not consider variations of material properties and environmental factors. These were kept as constants during the process of analysis. Geometrical and loading parameters mainly focused on this investigation. Therefore, geometric parameters and characteristics of loads were considered as variables in this study. Any structures are possible subject to either variable or constant amplitude cyclic loads during their service life. Variable amplitude is close to reality; however, predictions of such loads are complicated. The loading frequency and stress ratio cannot be expected as constant behavior. In laboratory tests and numerical

analysis methods the variables are normally transferred to the constant behavior due to field data or testing standards. In this investigation it was considered as a constant amplitude cyclic load which is commonly used to conduct fatigue tests.

### **2.17.1 Stress intensity factor**

Irwin (1957) introduced the concept of stress intensity factor (SIF) and it was based on fracture mechanics theory. SIF can be considered as an extension of Griffith's work on the brittle fracture of ductile materials. The author explained the strain energy release rate, which deals with the linear elastic fracture mechanics (LEFM) concept. This is a main concept in most of the crack propagation analysis. This stress intensity factor is used to design and analysis material. Therefore, stress intensity factor can be considered as a critical indicator of material toughness. The failure stress ' $\sigma_f$ ' is function of the crack length 'a' as well as the fracture toughness (Miannay, 2001).

### **2.17.2 Stress concentration**

A majority of the structural elements contain holes, cracks and other irregularities. These geometrical irregularities act as stress raisers and its causes to reduce the fatigue strength significantly. Hence, minimization of irregularities is critically considered in case of design. On the other hand, surface roughness also influences any stress concentration. Furthermore, when considering the metallurgical stress raisers, it heavily influences decarburization, inclusion, and local overheat.

### **2.17.3 Crack tip opening displacement (CTOD)**

Wells suggested that the failure of a cracked component of the structure can be characterized technique using crack tip opening displacement (CTOD) which was based on the fracture theory. The author explained that the degree of crack blunting is in proportion to the material ductility. It is defined that the opening of the crack faces in the vicinity of a sharp crack tip. Bozic et al.(2011) analytically showed a relationship between crack tip opening displacement and J-integral for a given material. Authors concluded that these two quantities are equally valid crack tip characterizing parameters for the elastic-plastic materials.

#### **2.17.4 Rate of energy release (G)**

The rate of energy release (G) can be considered as an amount of work associated with a crack opening or closing. Numbers of criteria have been introduced to specify the crack opening direction. Mainly three methods are explained as maximum energy release rate method, the normal to maximum principal stress method and maximum tangential (circumferential) stress method (Miannay, 2001). All of these methods are based on the numerical calculations of the stress intensity factor and energy release rate.

#### **2.17.5 Crack growth direction**

Crack growth direction is another important factor when considering the fracture mechanics analysis. When the crack is subjected to a mixed-mode loading; the propagating path is decided by least resistance. However, the number of methods has been proposed by the different authors to decide the crack propagation path. These methods are the criteria of maximum tangential stress method, maximum energy release rate method and minimum strain energy density method. Li et al. (2012) have shown that the above mentioned criteria performed a similar crack growth trajectory for a brittle material. In addition, maximum dilatational strain energy density method and the minimum accumulated strain energy method can be utilized to decide the crack propagation path. However, there is no clear way to decide which criteria should be used for a given material. The criteria of maximum tangential stress method are generally applied to FEM simulation of fatigue crack growth, because it is simple to implement and in addition it can approximately explicit solution for the crack growth direction.

#### **2.18 Summary of literature review**

The aim of this chapter was to provide a review of past studies related with structures, related in strengthened of CFRP, specially attention with the crack stop hole method, crack initiation, and CFRP uses for steel strengthening under fatigue loading. Related uses of the CSH to accommodate cracks and the factors which affect that is also considered in this chapter. Furthermore, the potential technique applied to enhance the performance of the CSH and CFRP strengthened methods are discussed while

highlighting it as an optimum method for strengthening. Furthermore, factors influencing performance and durability of the steel/CFRP bond, such as surface preparation and selection of adhesive related investigations have been compared and highlighted with their recommendations for this study. In this review the mechanical characteristics of the CFRP material as well as testing methods relating to structural testing is explained in detail. In addition, results of existing investigations related to the effects of external factors are compiled and compared for bond performance, durability and strength of CFRP/steel composition. The relevant field applications are discussed to confirm the ability to use CFRP in case of real world applications. However, only a few investigations were available relating to the crack stop hole method, and fatigue life prediction on crack stop holes. According to available literature, most of the parameters effect on bond performance and durability of the CFRP applications. The CFRP/steel bond performance governing factors are summarized in Table 2.4.

Table 2.4: Factors affecting the CFRP/ steel bond performance

No	Parameter	Research investigations
1	Properties of the CFRP material	Type of CFRP (NM, HM), physical dimensions, module of elasticity, Poisson's ratio, Young's modules, yield strength, elongation %
2	Characteristic of epoxy	Type of adhesive, curing time, glass transition temperature, viscosity and Poisson's ratio
3	Environmental condition	Temperature, salt environment, humidity level, freeze/thaw and UV effect
4	Sample type	Beam, plate, actual size, small size, geometry of coupon, etc.
5	Loading pattern	Constant amplitude, variable amplitude or cyclic with impact or non-impact rate of loading, etc.
6	Load applying method	Tensile, compression, bending, flexure, 3 point bending, four point bending and fatigue load range
7	Sample shape	Side notched beam/plate and center hole plate
8	Bonding characteristics	Bond length, effective bond length, number of CFRP layers, whether single side or double side lamination.
9	Installation procedure	Thickness of the adhesive layer, surface preparation, air bubble removing methods and method of adhesive applying
10	Condition of structure	Pre-stress, Without stress, corrosion and stress distribution pattern
11	Stress conditions	Stress ratio, stress range and pre stress
12	Joint type	Single lap, double lap, bridging effect by the adhesive
13	Specimen preparation	Sand blasting, grinding, degreasing and vacuum techniques

The critical behavior of elevated temperature decreases viscosity of adhesive. It rapidly leads to strength and stiffness reduction. Another most important parameter is the glass transition temperature ( $T_g$ ) because it plays a key role, as load transfer capacity reduces significantly the temperatures overpass it. In addition, temperature variation near  $T_g$  have also influenced the behavior of CFRP/steel bond. Furthermore, load intensity, bonding length, curing time and moisture ingress also affects bond

performance. The time duration of failure depending on the load related parameters such as number of cycles and magnitude of load. However, this context is not yet fully understood and requires further investigations.

Available literature regarding cyclic load related CFRP/steel performance research activities are very limited. The influences of environmental related parameters such as, relative humidity, temperature and UV effect, etc are not yet simulated. Especially fatigue behavior under the tropical environmental condition, long term bond performance, the method of strength enhancement during temperature fluctuation are still un-solved. The fatigue behavior of the adhesive interface and long term performance of the adhesive interface are also not available in existing literature. The effect of pre-stressing of steel structure also should be investigated. Lack of comprehensive design guidelines is another important research area for future work. Different type of bonding methods introduces to minimized cost of CFRP system and provide sufficient data and develop design guidelines which are critical. Finally, quality controlling guidelines is also needed under installation phase.

However, fatigue related CFRP strengthening composite material has several advantages as it can apply in the field, minimize the traffic disruption, reduce the deadweight increment and reported good durability. Long service life, minimized interruption, impact resistance, good durability and ease of installation are competitive advantages of this technology .However, these advantages are surpassed by higher material costs associated with CFRP materials (Pierluigi et al, 2012.).

In addition, this chapter discusses material properties and their characteristic effects on fatigue behavior of material specially focused on steel. All possible type of fatigue is introduced and discussed with differences of LCF and HCF behavior on structure. This chapter details the steps of fatigue as crack initiation, growth and failure as well as emphasizing the importance of crack initiation at the micro level. In addition, attention to the total life time of the fatigue and dealing with yield stress of the material is also detailed in this chapter. The mechanisms of fatigue failure with different explanation such as slip band theory, fracture mechanics approach and effects of the reversed plastic flow are identified here with detailed explanations. The theory of

fracture mechanics is a very famous concept to explain fatigue and it has been classified in this chapter as LEFM and EPFM while the most practical applications are closer to EPFM. In addition, the hardening and softening effects on material due to fatigue under kinematic hardening as well as isotropic hardening behavior of material is discussed in detail in this chapter. Furthermore, crack growth rate estimation model that is elaborated in Paris law and Power law are compared in this chapter and the Power law is selected due to advantages over Paris law and compatibility with real world applications. Finally, the effective parameters on fatigue which critically influences the performance is explained in detail in this chapter.

## ***Chapter – 3***

---

# ***Designing and Fabricating a Fatigue Loading Apparatus***



### **3. DESIGNING AND FABRICATING A FATIGUE LOADING APPARATUS**

#### **3.1 Introduction of design and fabricated fatigue loading apparatus**

Purchasing a commercially available fatigue testing apparatus has become non-feasible in the current background. In fact, the fatigue testing apparatus which are available in the market vary in price with the loading capacity, speed and level of accuracy of the measurements. Also, the test apparatus available in university laboratories and other research institutions is mostly limited to small specimens. Accordingly, there is no test apparatus available for cyclic flexural testing of medium scale structural elements. Therefore, the aim is to design and fabricate a low cost fatigue loading apparatus which is discussed in detail in this chapter. It also focuses on understanding the history of the development of fatigue test apparatus, analyzing operating mechanisms of existing apparatus, following design steps, selecting load apply mechanism for new apparatus, and selecting load and frequency controlling techniques. There are a few critical components such as loading frame, power supply unit, load apply mechanism and monitoring devices included in this section with concerns regarding the safety, accuracy of reading, maintenance, cost effectiveness of the apparatus and environmental related issues. The ultimate aim in this chapter is explain in detail the design and fabrication of the fatigue loading apparatus to apply the desired loads effectively on the specimens.

##### **3.1.1 History of fatigue test apparatus**

The first fatigue testing apparatus was introduced to the world by the German mining administrator Wilhelm Albert in 1830. Since the same scientist in 1829 had reported the failure of iron mine hoist chains due to repeated loads. This machine was built using a hydro dynamically driven paddle wheel that cyclically applied load to a chain as shown in Figure 3.1. In this arrangement, the repeated load was applied to a chain using a dead weight, which moved up and down reciprocally. The first modern fatigue loading apparatus was designed by August Wöhler in 1860 as a result of investigating the fatigue failures of rail road axles. Lee et al. (2005) developed a structural fatigue testing apparatus with the capabilities of torsional and bending loads where a hydraulic

power was utilized to apply loads. Furthermore, Vincent et al. (2016) and Bhatkar et al. (2017) introduced testing apparatus with loads ranging from 88 N to 300 N which can be used to test small specimens of length less than 150 mm. Similarly, Pach et al. (2012) explained a method for applying axial loads to test specimens by using a “seesaw” motion where the loads were limited to 10 kN. Also, the Cooper Technology in United Kingdom introduce a servo-hydraulic mechanism and it is capable of applying bi-directional loading with a maximum load of  $\pm 10$  kN (McAlorum et al., 2018). This type of servo-hydraulic machine is approximately USD 40,000.



Figure 3.1: The picture of first fatigue testing machine (Sik et,al., 2018)

### 3.1.2 Types of fatigue loading

Fatigue test helps to determine the ability to withstand a cyclic load for particular material. The concept behind the fatigue is cyclic loading and unloading as a tension, compression, torsion, bending or combinations of such stresses. The fatigue loads are usually applied as tension–tension, compression-compression, or tension into compression and reverse.

In a fatigue test a specimen is loaded as a pre-determined test stress while it is unloaded as an opposite load or zero load. This kind of repeated action until to failure occurs. There may be an indication of a crack, however it depends on the relevant parameters of the test or pre-determined number of cycles. Generally, the target of a fatigue test determines the lifespan of the material under cyclic loads. Furthermore, the fatigue strength is reflected by the crack resistance while the fatigue durability of a material is indicated as a total number of load cycles. On the other hand, the fatigue test is used to estimate the maximum load that can withstand. These characteristics are vital in any structure or structural elements where a material is subject to cyclic forces. There are

many kind of fatigue testing methods which can be identified. They can be mainly classified as follows:

- 1) Low cycle fatigue test under strain controlled
- 2) High cycle fatigue test under load controlled

The common objectives of a fatigue tests are to predict the fatigue life, assessment of the risk area and identify the location of failure of a component due to the stress amplitude. The test conditions vary because of a few factors, which influence the fatigue life. In spite of all these conditions fulfilled, there may a number of unidentified and uncontrollable factors which causes fatigue. Therefore, fatigue testing methods are always conducted under controlled conditions.

### **3.2 Classification of existing fatigue loading apparatus**

A fatigue testing apparatus could be categorized from different viewpoints according to the aim of the test, type of load applied, operation method, loading modes, type of load etc. The target of the investigation is most critical in this context. Consequently, fatigue testing machines could be categorized as follows:

- 1) Types loads applied on the test specimen
  - a) Axial loads
  - b) Flexural loads
  - c) Torsion loads
  - d) Rotating flexural loads
  - e) Combined torsion and bending loads
  - f) Bi-axial and tri-axial loads
- 2) Load transmission of the test specimen
  - a) The load applied as a mechanical deflection (It may be combined as reciprocating masses with spring forces)
  - b) Force produced due to spring loads with constant amplitude
  - c) Load applied as an electro-magnetic forces
  - d) Load applied as centrifugal forces
  - e) Load applied by a hydraulic power
  - f) Load applied as thermal energy

- g) Load produced as pneumatic forces
- 3) Types of control systems
  - a) Stress-control
  - b) Strain-control

In addition, fatigue test apparatus can be classified in accordance with the purpose:

- 1) General purpose fatigue testing apparatus
- 2) Testing apparatus for small-scale parts
- 3) Testing apparatus for full-size structures
- 4) Special purpose fatigue testing apparatus

General purpose test apparatus could be further expanded as follows due to stresses applied on test specimens:

- 1) Rotating bending test apparatus
- 2) Cantilever bending test apparatus
- 3) Axial loading (push-pull) type fatigue tester
- 4) Other types of testing machines
- 5) The modern fatigue testing machine

### **3.2.1 Rotating- bending type fatigue testing apparatus**

Since the development of the first rotating bending fatigue testing apparatus, there has been several changes and developments in this context. While Wöhlers' introduced fatigue testing machine subjected on uniform bending loads. The rotating bending load apparatus is used to construct an S-N curve. In this test machine, the motor is turned at a constant speed (r.p.m, or frequency) until to failure of the specimen, while applying a constant-amplitude load as shown in Figure 3-2.

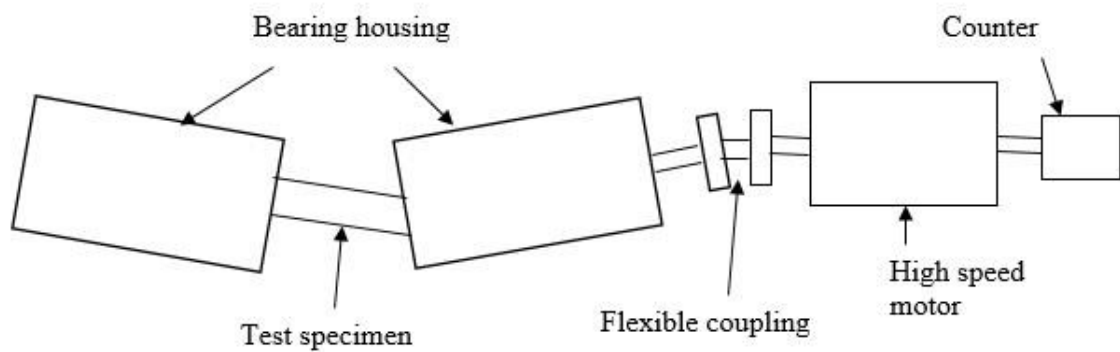


Figure 3-2: Rotating Bending Testing Machine (Azeez, 2013)

The S-N curve indicated a tension-compression variation under the strain controlled fatigue curve. This kind of test machine is capable to apply zero mean cyclic stresses. In this context the specimen is clamped with the mean displacement position of the moving mechanism. However, the rotating bending fatigue test apparatus was the first machine which was utilized to generate fatigue load.

### 3.2.2 Constant deflection amplitude cantilever bending type fatigue testing apparatus

The rotating cantilever bending fatigue testing apparatus was used for specimens under non-uniform bending moment. When the fatigue testing apparatus is fitted with an eccentric crank it can also be used as a rotating bending with a mean deflection. The torsion and bending combined loading is similar to the rotating cantilever bending. It can be subjected to uniform torque as well as non-uniform bending. Constant amplitude deflection cantilever bending fatigue testing machine is shown in Figure 3-3. In this machine, one end of the specimen is connected with an eccentric crank and it is loaded by using an electrical motor.

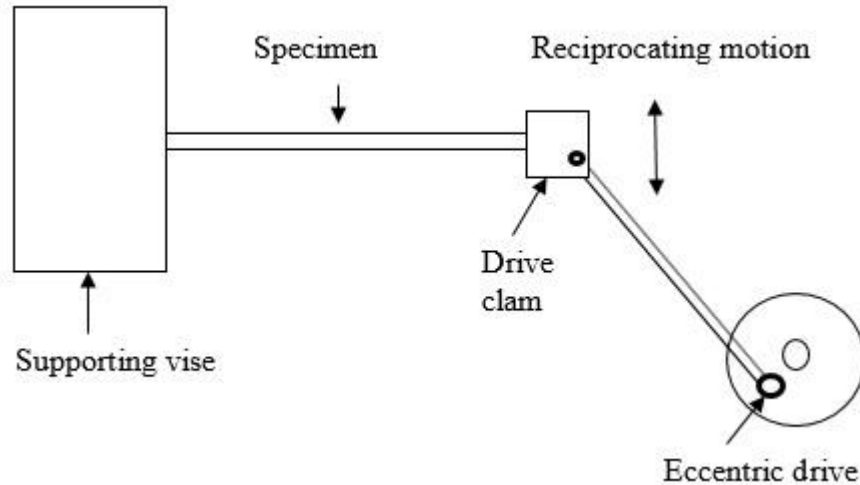


Figure 3-3: Cantilever bending testing machine (Azeez, 2013)

### 3.2.3 Axial loading fatigue testing apparatus

Axial loading type specimen is not exposed to bending loads. It is applied for pure axial (tensile or compression) loads. The axial stress test machine can be used to apply tension, compression as well as a combination of all these (Fatemi and Socie, 1988). The specimen is fixed at two ends and the cyclic load is applied between two ends. An axial loaded fatigue testing machine is shown in Figure 3-4 and in this mechanism the axial mean stresses applies separately as a form of tension, compression and later combinations of both. In this arrangement a test specimen is placed between the top and bottom grip. According to Campbell (2008) the modern fatigue testing machine has facility to collect data from tension and compression loading at high-cycle and low-cycle fatigue ranges. A typical modern axial loaded fatigue testing machine has a facility with sensors and alignment (Campbell, 2008).

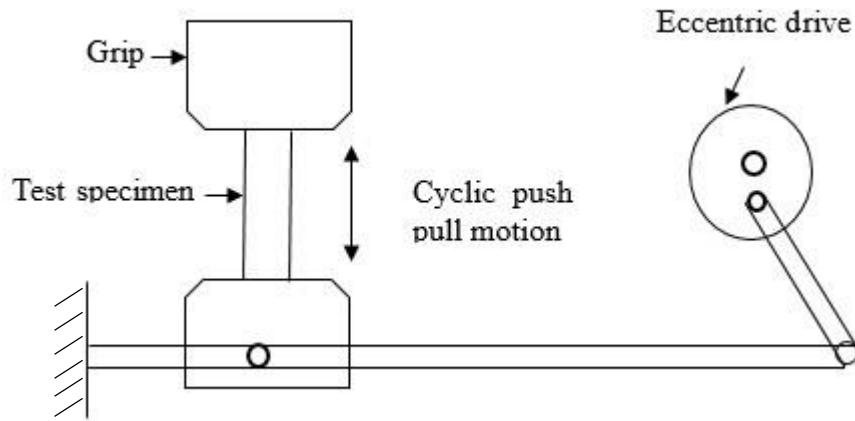
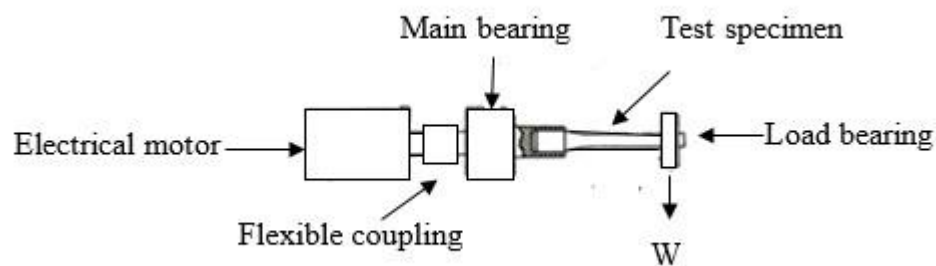


Figure 3-4: Axial loading fatigue testing machine (Azeez, 2013)

### 3.2.4 Other types of fatigue testing apparatus

The other types of fatigue test machines are as follows even though the majority of them are not commonly used for fatigue tests: The rotating cantilever bending fatigue testing apparatus was designed and developed by Wöhlers and the sketch is shown in Figure 3-5 (a). This machine can be utilized to measure non-uniform bending moment on the specimen, due to the arrangement of the loading mechanism. This arrangement was based on the concept of mean stresses. Furthermore, the S-N curve and fatigue limit theory also have been applied in this design. According to architecture of two main bearings at each end, it supports to evenly distribute the loads. The electrical motor and the main bearing have been connected using a flexible coupling for appropriate load transmission. When the axle starts to rotate, it subjected to both tensile and compressive stresses and it could be considered as a fully reversed load. The schematic diagram of rotating bending fatigue loading apparatus is shown in Figure 3-5 (b).



(a)

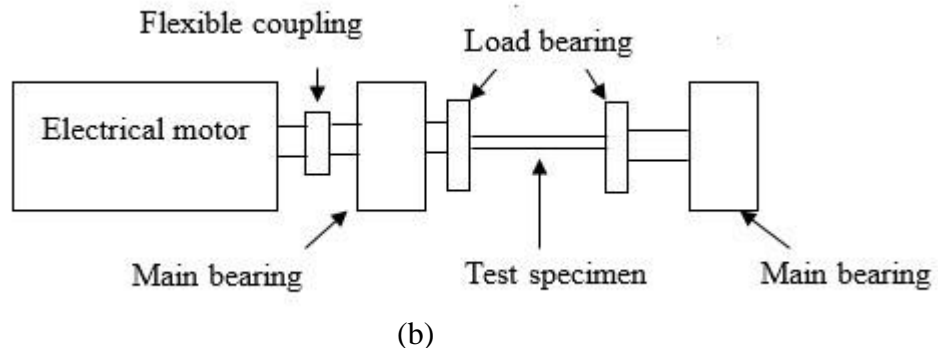


Figure 3-5: Conventional fatigue testing apparatus  
 (a) rotating cantilever bending fatigue testing apparatus (Ali et al., 2019)  
 (b) rotating bending fatigue testing apparatus (Jyothi et al., 2017)

### 3.2.5 The modern fatigue testing machine

The modern testing machine have a closed-loop servo-hydraulic controlled mechanism (Ninomi et al., 1996). The Servo-hydraulic controlled technique is the most popular one and it can apply cyclic loads with a mechanically controlled or automated fatigue load. These kind of test machines perform with fatigue durability from small scale laboratory specimens to large scale complex structures (Fatemi and Socie, 1988).The modern fatigue testing machine contained function generator such as a signal of load, strain, or displacement The common features of such machine are load cells and a linear variable differential transformer (LVDT). A typical modern axial loading fatigue test machine has a facility with sensors and data saving (memory) devices as shown in Figure 3-6.

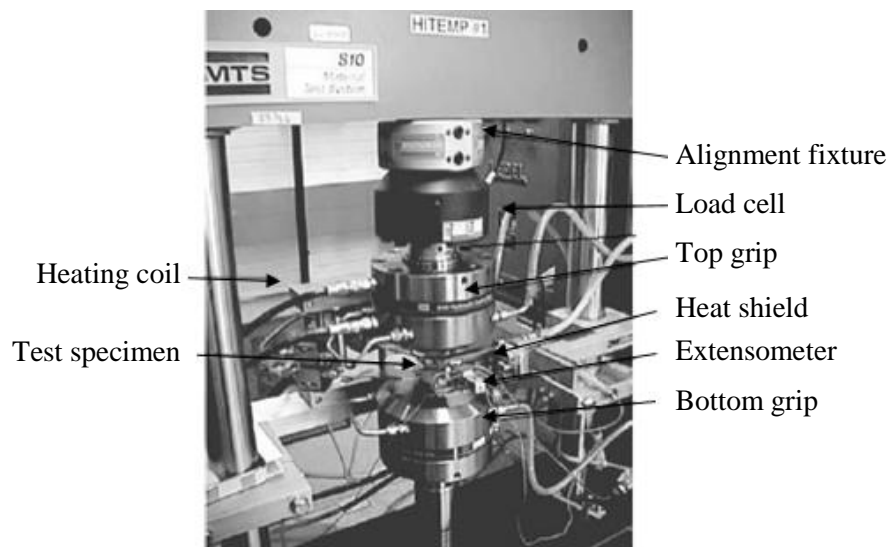


Figure 3-6: Modern fatigue testing machines (Campbell,2008)



### 3.3 Design and detailing of fatigue loading apparatus

There are few main components in this test apparatus which include the loading frame, the load-transmitting element, control devices and measuring devices as shown in Figure 3-7. The loading frame supports the attached accessories of the test apparatus and it should be able to restrain vibration during testing. The load transmitted through a spring return single acting hydraulic actuator attached to the loading frame using a 8 mm diameter loading nose at the end of the hydraulic actuator. Different types of energy conversion in each step as shown in Figure 3-7Figure . The two supportive rollers assist in distributing the desired stress within the test specimen while the controlling devices permit the setting-off of the load and, loading frequency during the test period. However, the load should be periodically scrutinized using load cells. To obtain reliable results from the cyclic flexural test apparatus, a precision calibration technique needs to be introduced. In fact, the calibration of testing machine was done using the load cells to ensure accuracy of readings.

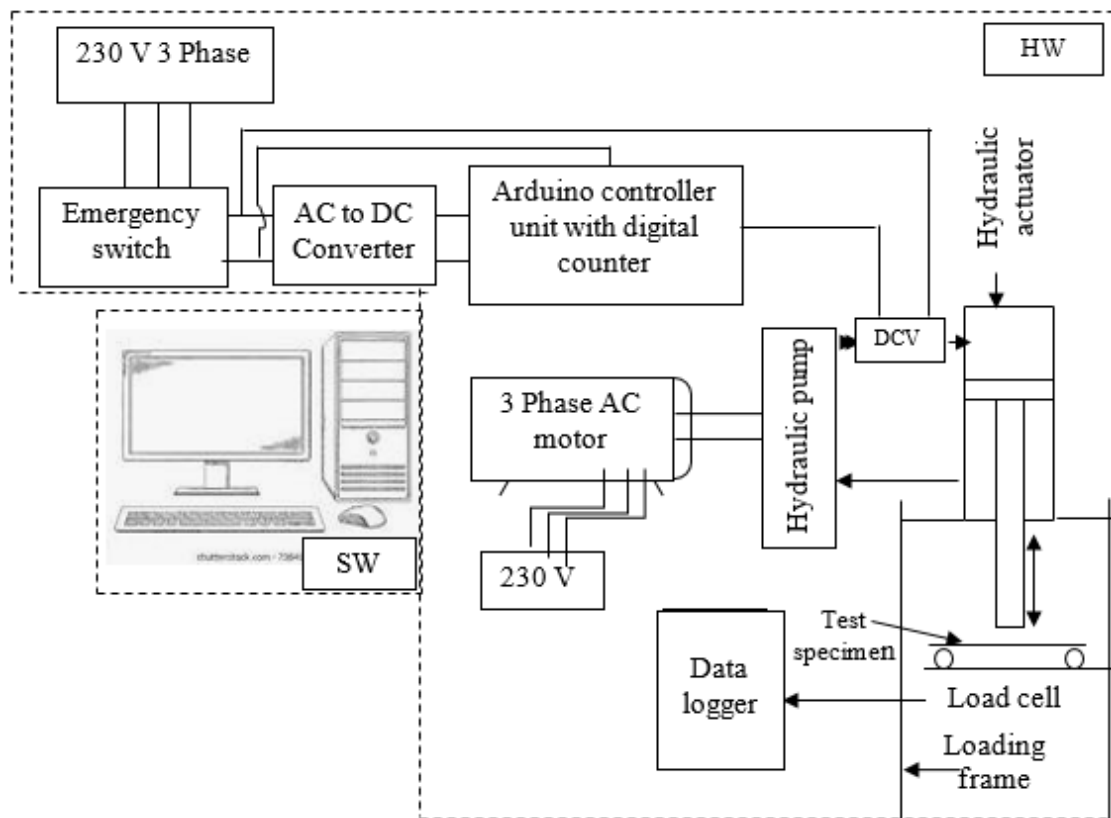


Figure 3-7: The layout of developed fatigue test apparatus

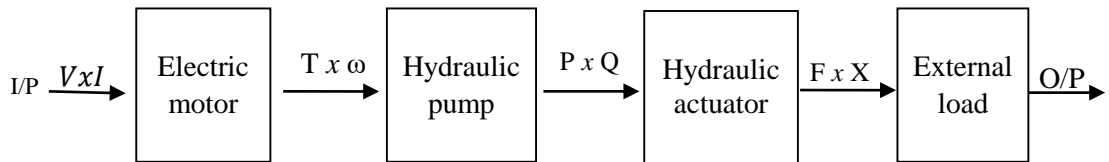


Figure 3-8: Different types of energy conversion in each step.

### 3.3.1 Considering factors for design fatigue loading apparatus

This test machine is designed to fulfill the objectives mentioned below:

- 1) Facility to operate in a simple manner
- 2) Capability for withstanding the required load
- 3) Transmission of energy with minimum losses
- 4) Ease of repairing
- 5) Ease of assembling and disassembling
- 6) Capability to operate for longer periods without frequent start and stop
- 7) Possessing a minimum operating cost
- 8) Reasonable cost of the test apparatus

### 3.3.2 Essential components of any fatigue loading apparatus

The main components of any fatigue testing machine are listed below:

- 1) A load-generating mechanism
- 2) A load transmitting unit
- 3) Monitoring devices
- 4) Control devices
- 5) A shutdown device of apparatus
- 6) A counter (digital or mechanical)
- 7) Framework (loading frame)

### 3.4 Designing steps of fatigue loading apparatus

The design and development process of the cyclic flexural loading apparatus are as follows;

- 1) Calculate the required load to produce a sufficient flexural stress in a pre-determined test specimen. In the present design, this was calculated as 10 kN.
- 2) Design a suitable loading frame and its model by using a Computer Aided

Design (CAD) Program.

- 3) Develop a numerical model using finite element analysis program to predict the load transfer behavior and joint performance.
- 4) Fabricate and assemble the test apparatus, and components, including electrical connections.
- 5) Use the Arduino programming technique for frequency control and monitoring any cracks using a digital display unit.

#### **3.4.1 Designing a loading frame**

Two supporting column structures with a top and bottom cross beams with lateral branching is the main structure of the loading frame. It possesses sufficient strength to withstand the maximum load applied to the frame structure with the vibrations during the testing process. In addition to that, it has the facility to mount other accessories and clamping systems to the loading frame. Nut and bolts were used for fastening each of the structural components together. This cyclic flexural test apparatus can conduct a three-point bending test and also apply uniformly distributed loads on the test specimen.

The hydraulic loading frame (HLF) is flexible for adjusting to required dimensions. One of the frames was fixed to the top of the structure and a hydraulic actuator was mounted on the top cross beam for the application of axial loads in the range of 0-10 kN. The other cross beams have flexibility to move vertically and it has a facility to adjust to the height of the test specimen. The test specimen attachment was fixed with a moving plate on the cross beam.

The loading frame is the heaviest component of this test apparatus and all the other accessories are attached to it. In addition, the applied load of the test specimen and self-weight of the apparatus also should be able to withstand the loading frame. Therefore, the loading frame and joints should have the capability to withstand relevant stresses. The numerical model developed in finite element analysis indicated the weaker regions and maximum stresses at ultimate capacity of the frame. Then the sections and joints were re-designed till it satisfied the safe loading requirements. The

stress concentration at the ultimate load level, including that factor of safety of loading frame is shown in Figure 3-9 (a) and Figure 3-9 (b).

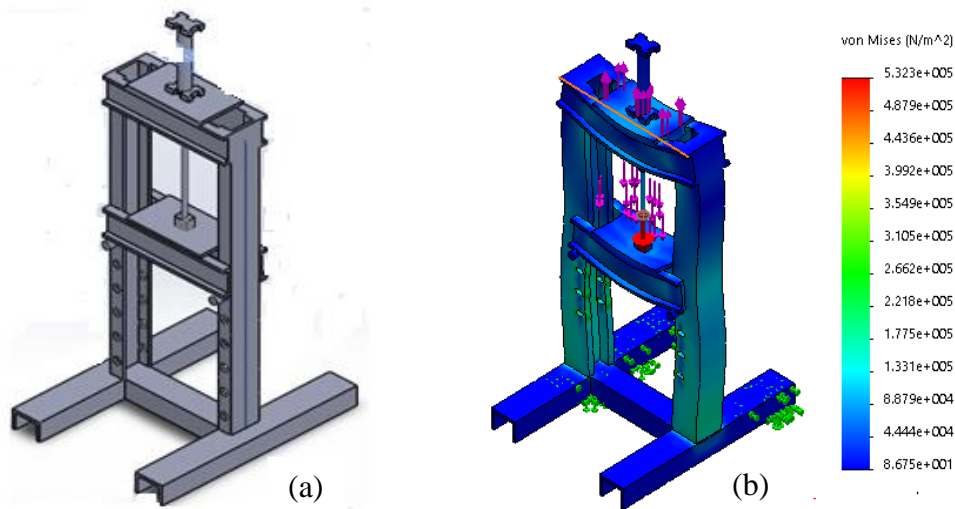


Figure 3-9: Finite element mesh and stress concentration of loading frame  
(a) before FEA (b) After FEA

### 3.4.2 Loads on the loading frame

Various types of loads are possible to be applied to a loading frame during the testing of structural elements. These are compression and tension loads due to hydraulic force, impact loads and vibration due to cyclic load testing and inertia resulted from the reciprocal reaction of the hydraulic actuator. A cross head mounted hydraulic actuator has a maximum force capacity up to 10 kN with a safety factor of 2.5. This test apparatus allows a maximum of 1700 mm vertical clamp space to accommodate full scaled column specimens while the loading frame was flexible to be adjusted to the required height of the sample design for the standard test conditions. In addition, this system has the flexibility to clamp with different gripping systems.

### 3.4.3 The machining process and assembling of testing apparatus

Metal cutting, drilling and grinding were the processes considered in this context. The lathe and milling operations were also used to make a clamping mechanism and the loading nose, which were major machining processes used in this task. Then the fabricated and ready-made parts were assembled together according to the setup as shown in Figure 3-10. The hydraulic circuit, the power supply, the controller and

display units and other accessories are included. All of the above components were attached to a single unit called the cyclic flexural test apparatus. The channel sections were connected using nuts and bolts to provide a three dimensional degree of freedom. The locations of accessories attached to the loading frame were based on the operation, ergonomics and the safety requirements. In this design, the loading frame was kept on a flat horizontal floor to avoid tilt during testing.

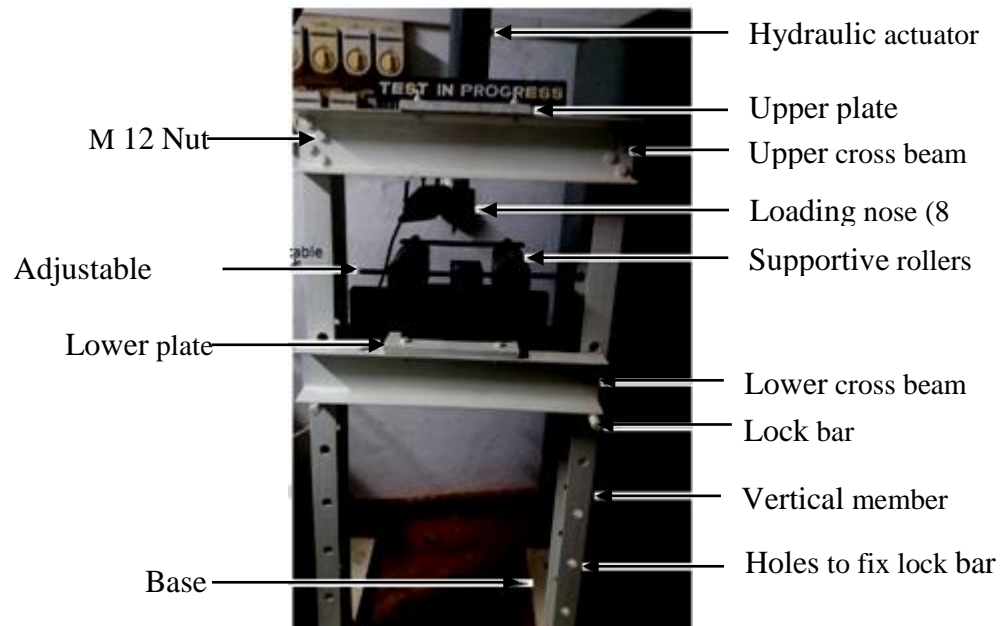


Figure 3-10: Cyclic flexural test apparatus and loading frame

The test specimen holding mechanisms were based on the geometry of the specimen and it was flexible with fixed circular, rectangular or any other geometrical shape of cross section. In addition, the machine has the flexibility to clamp different gripping systems.

#### 3.4.4 Selection of load applying mechanism

Two main mechanisms, hydraulic ramp and mechanical cam were taken into consideration and the relevant features were compared before selecting the most feasible technique. The accuracy, flexibility, cost of product, facility of assembling, availability of standard parts in the open market were mainly considered in this comparison summarized in Table 3.1.

Table 3.1: Comparison of the hydraulic ramp and the cam mechanism

Item no	Hydraulic Ramp Mechanism	Mechanical cam Mechanism
1	Variable load control is simple and easy.	Variable load application is complicated.
2	The load could be applied smoothly.	Shock loading
3	High durability	High durability
4	Easy to load control	Difficult to load control
5	Relatively expensive	Less expensive
6	All components are available in the open market as standard parts	Some components have to be designed and manufactured (e.g.: cam)
7	Less noise level	Relatively high noise level
8	Temperature is critical	No temperature effect
9	Easy to operate	Relatively difficult to operate
10	No gear reduction	Gear reduction is essential




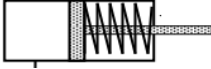

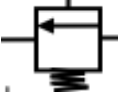
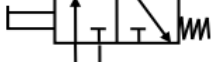

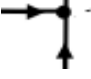
When comparing the above features in both mechanisms, the hydraulic ramp mechanism was selected as the most suitable technique for the design fatigue loading apparatus. Furthermore, implementing the cam mechanism is comparatively difficult in the present context.

#### 3.4.5 Designing the hydraulic circuit of fatigue loading apparatus

Standard hydraulic symbols were used to identify the hydraulic circuit for this test apparatus. Those symbols have supported in providing a unique representation of various components as shown in Figure 3-11(a). These symbols are useful for technical communication and it represents the function of each individual component. The Power unit consists of the reservoir, pump, electric motor, coupling, entry and exit hydraulic lines, with a return filter. The purpose of the reservoir is to provide storage facilities to the working fluid and collecting returns during operation. The hydraulic

pump is driven using a three phase electrical motor with a 3.5 kW capacity. The coupling is used to connect electrical motor and hydraulic pump. Entry pipe was connected to the inlet port of the hydraulic actuator. In addition, several accessories were attached to the circuit to ensure the proper operation. They were the pressure relief valve, pressure gauge, directional control valve and flow control valve. The inlet of the pressure relief valve is connected to the outlet port of the pump and the outlet of the relief valve connected to the reservoir. The main purpose of the pressure relief valve is protecting the system from over pressure due to any possible pressure increases of the system. This can be introduced as a safety device of the hydraulic circuit as well as operator. The mechanical pressure gauge was attached with the outlet of the hydraulic pump to measure the working pressure of the system. It has the capability to measure the pressure level up to 10 bar. The directional control valve was fixed on the inlet line of the circuit and it is positioned between the hydraulic actuator and the pressure gauge. The main purpose of the directional control valve is to govern the moving direction of the hydraulic actuator with the desired pressure. It operates with a 230 V AC power supplied solenoid valve and the input current is controlled by an electronic circuit. This electronic circuit was programmed using the Arduino programming technique. The outlet port of the hydraulic actuator was connected to the reservoir through return filter using a flexible hose while all the accessories were connected to each other using a proper connector or a flexible hose as shown in Figure 3-11(b). A hydraulics simulation software (Fluid SIM) was used to design and simulate the hydraulic circuit before installing the actual accessories. Standard hydraulic symbols were used to identify the hydraulic circuit for this test apparatus. Those symbols have supported in providing a unique representation of various components listed in Table 3.2. These symbols are useful for technical communication and it represents the function of each individual component.

Table 3.2: List of accessories of hydraulic system

Item No	Symbol	Description	Qty
1		A hydraulic pump	01
2		Hydraulic reservoir	01
3		Filter	01
4		Single acting spring return hydraulic actuator	01
5		Flow control valve	01
6		Pressure relief valve	01
7		Solenoid operated 3-position 4-ways DCV (Direction Control Valve)	01
8		Pressure gauge	01
9		Hydraulic hose	02



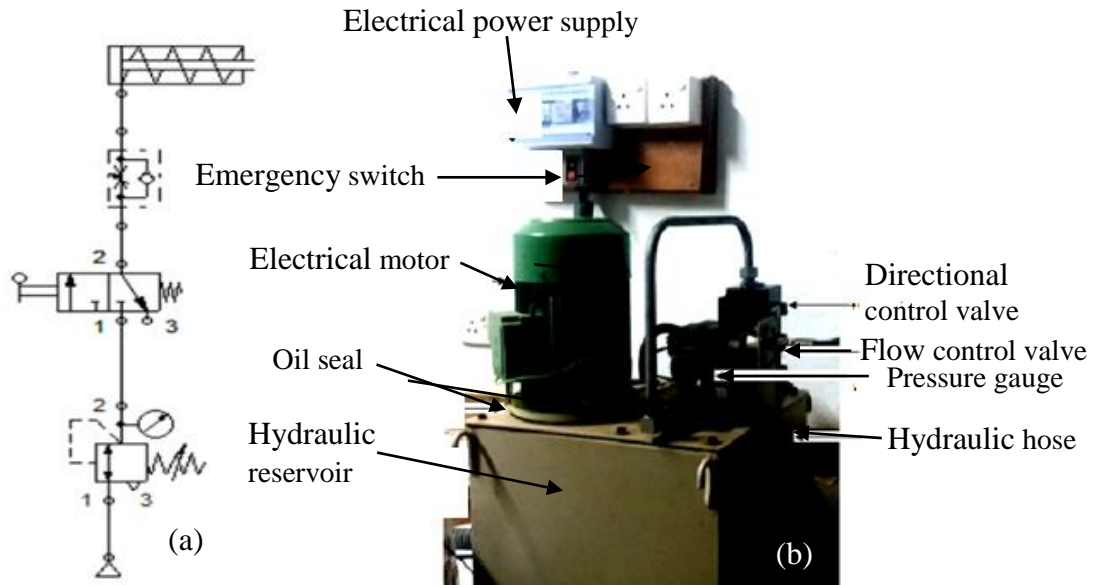


Figure 3-11: Cyclic flexural load circuit (a) simulation circuit  
(b) actual hydraulic circuit

The hydraulic cylinder is mounted on the upper cross head of the loading frame. A hydraulic cylinder is chosen due to the required load and stroke length of the fatigue tests. This hydraulic cylinder should exceed 50 mm in a usual condition to perform a fatigue test. The maximum load of the fatigue test is governed by the diameter of the piston. If need a high power, it should require a high oil flow with large cross section cylinder. However, a lower hydraulic pressure could also submit a desired force. Another aspect of the cylinder selection is the load applying frequency of the fatigue test. However, if the test runs with a high frequency within a short time it performs in a satisfactory manner.

The Extension action is relatively slower when compared to the action and retractions. Also, the forward velocity control is critical in this cylinder as it avoids a shock load. If the impact load is applied on the specimen it causes to shock load. This design helps to reduce a total cycle time of the test procedure. As a result, the overall testing periods could be reduced and it affects the performance of testing. The load application for extensions is governed by the hydraulic pressure. However, the extension speed should not be higher for high speed operating conditions which allow shock loads only as it causes an impact on the load. Therefore, a regenerative circuit is not selected in this

loading mechanism. A single-acting cylinder is the simplest which could be used in this design and is shown schematically in Figure 3-12.

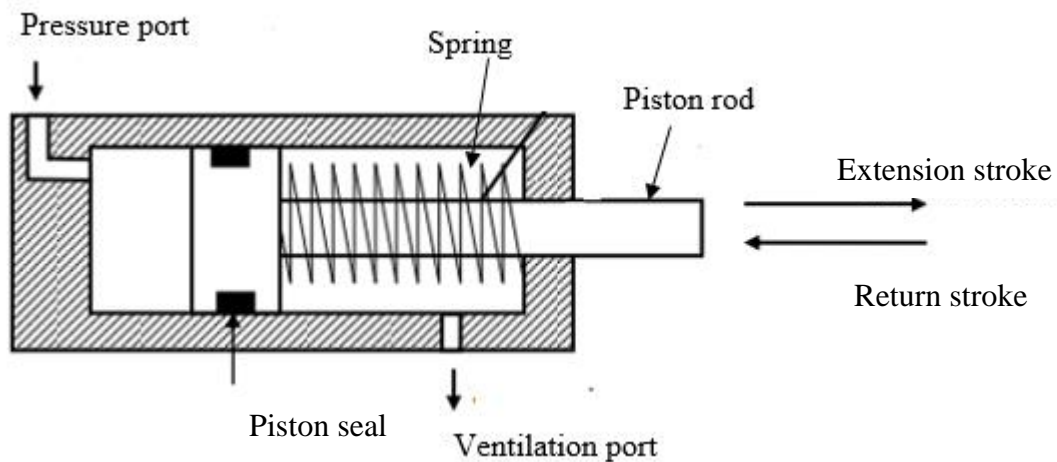


Figure 3-12: Schematic diagram of spring return single acting cylinder (<https://nptel.ac.in/courses/112106175/Module%202/Lecture%2012.pdf>)

### 3.4.6 The controlling system of the lading apparatus

The purpose of this test apparatus was to apply three points, cyclic flexural loads on the test specimen as a repeated load. Hence, this design consists of a number of controlling units; a load control, a directional control, a speed control, a flow control for fluid and a motor control. Some of the parameters were manually controlled and only special parameters were automated due to financial constraints. This test setup was exposed to cyclic flexural load for a long period due to a large number of cycles applied to the test specimen. A single test setup continued for 2-3 hours and it depend on the frequency of the load and required number of cycles. A directional control valve (DCV) was used with a solenoid operated control mechanism. Another important control parameter was the flow control. Due to the required load, the flow rate was adjusted and it was done manually. The pressure limits were manually controlled as a safety requirement of the applied load. The other important parameter of this testing apparatus was the power control and there was a possibility to cut off power due to the rated power of the hydraulic pump by using a miniature circuit breaker (MCB). ARDUINO UNO, open-source electronics circuit used for frequency control as shown in Figure 3-13.



Figure 3-13: ARDUINO UNO, open-source electronics circuit used for fatigue test controller (a) development board (b) circuit

### 3.5 The test setup and the instrumentation of loading apparatus

Structural steel plates were selected as a material. The cross-section was 40 mm width and 5 mm thickness. The length of the plate was selected to be 280 mm and the effective span was selected 240 mm. The diameter of the CSH varied from 4 mm to 25 mm in 4mm steps according to the test plan. A 8 mm radius loading nose attached hydraulic actuator was used for loads applied and mid-vertical span was limited to 5 mm. The constant amplitude load was applied to the specimen. During the testing 5 Hz frequency was maintained according to the ASTM D7774. The number of cycles were counted using a digital counter. Crack initiation was observed with a magnified digital camera as shown in Figure 3-14 (c) it was confirmed through resistivity variation by using an electronic potential meter.

#### 3.5.1 Measuring procedure of test apparatus

The load applied onto the test specimen was measured using a load cell which was attached to the bottom surface of the specimen. Readings of the load cell were made available through a digital indicator attached to a data logger. A mechanical pressure gauge was fixed to measure the applied load. Number of cycles for crack initiation (re-cracking) was predicted using potential drop techniques. In this technique digital voltmeter were fixed between CSH and observed drop of potential. When the potential was dropped at the same time indicate number of cycles applied on the specimen using digital counter attached with controlling unit. A thermocouple was fixed to the oil reservoir to monitor the temperature of hydraulic oil to see whether a considerable heat

gain had occurred during testing. This test apparatus utilizes three variables which includes loads, frequency and, the number of cycles.

### **3.5.2 Calibration of load**

Hydraulic pressure applied on the piston of a single acting cylinder is the load applying mechanism in this apparatus. Hydraulic pressure is applied on the piston with a load applied on the test specimen. The magnitude of the load on the test specimen depends on the applied pressure and a pre-determined load could be applied when adjusting the pressure of the hydraulic circuit. On the other hand, when pressure is released on the piston, the stress is released on the specimen and it moves in a backward direction (Bottom to top) due to the spring tension of the single acting cylinder. At the opposite end, there are two ports – i.e. the inlet and the exit for the hydraulic oil. (Single-acting cylinders can exert a force in the extending direction only.) The return of the piston is not done hydraulically but with a single acting cylinder the retraction is controlled by a spring. This action is repeated during the fatigue test and the number of load cycles applied on test specimens. The number of loads applied on test specimens can be counted using an electronic counter. Theoretically the load applied on the test specimen can be calculated by using a hydraulic pressure and a cross sectional area of the piston with SI units. The piston consists of a cylindrical housing (barrel) with the end of the piston that can reciprocate.

Therefore, hydraulic pressure could be considered as a variable which changes the amplitude of loads on the test specimen. The pressure gauge was attached to the hydraulic circuit of test apparatus to indicate the working pressure. To avoid pressure drops due to other accessories of the hydraulic circuit, the pressure gage was attached to the nearest position of the input port of the hydraulic cylinder. Flow control valve has a screw to change the flow rate of the hydraulic oil and it is adjusted to set a predetermined working pressure for the desired loads applied on the specimen. This test apparatus has the capacity to apply loads up to 10 kN and relevant pressure values were measured for each loads with 1 kN steps. A chart is constructed for pressure variation with respect to applied loads on specimen. However, any mechanical pressure gauge would consist of error factors and it should be calibrated for more accurate results. In this regard, a load cell was used to measure load on the specimen

and the mechanical pressure gauge reading was recorded with respect to the applied load. A load was monitored using a data logger with a digital display as shown in Figure 3-14. According to the load cell readings, the hydraulic pressure was adjusted until it achieved a pre-determined amplitude of the load. The pressure gauge reading should be observed and if there are any deviations, they should be rectified with load cell readings attached to the data logger.

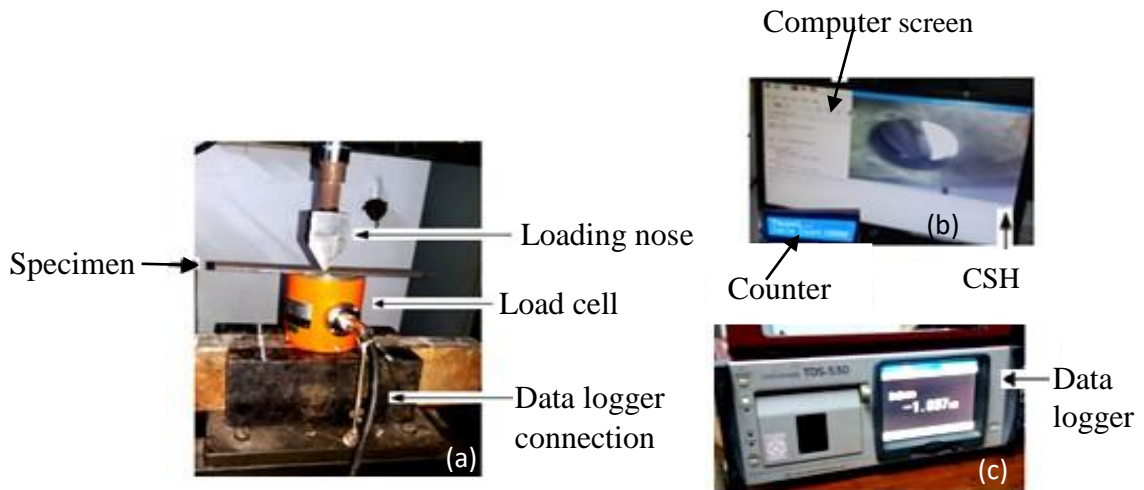


Figure 3-14: Calibration of test apparatus (a) load measured using load cell (b) magnifying CSH (c) data logger with digital display

### 3.5.3 Calibration of loading frequency

The frequency of the applied load on the test specimen is one major parameter in this study and it controls by an electronic circuit programmed by ARDUINO. The frequency control mechanism of this test apparatus allows to disconnect the power supply of the solenoid which is connected to the directional control valve. This power supply is controlled by an electronic signal.

The output signal can be controlled through the Arduino program according to the desired frequency and it can vary from 1 Hz to 8 Hz. Hydraulic pressure is applied and released on the piston according to the operation of directional control valve of single acting cylinder. Predetermined frequency related data can be fed to program using a key board which is attached to the electronic circuit. However, the measurement of the electronic circuit output is important for the accuracy of the loading frequency. An Oscilloscope is used to measure the output signal of the electronic circuit. According

to output signal, the electronic circuit program was adjusted to calibrate the test apparatus to produce more accurate results

### **3.6 Features and benefits of the fatigue loading apparatus**

This fatigue loading apparatus has the following features and those features assist its proper operation:

- 1) A maximum load capacity of 10 kN.
- 2) Ability to test different materials such as steel, aluminum, plastic and their composite with CFRP.
- 3) The test apparatus has the facility to change the frequencies from 1 Hz to 8 Hz.
- 4) Side entry design with full access for easy specimen insertion.
- 5) The test allows various geometries of material either rectangle, square, circular or any other shape of cross sections.
- 6) Ease of conduct three points or four points cyclic tests by changing the loading nose only.
- 7) A wide range of specimen thicknesses can be tested.
- 8) Dimensions of loading frame are ergonomically sound.
- 9) High safety and low operating cost.
- 10) The range of operating temperature is +20 °C to +65 °C (due to the flash point of the hydraulic oil).

Complete test setup before and during testing are shown in Figure 3-15.



Figure 3-15: Completed test setup

### **3.6.1 Cost estimation of the fatigue loading apparatus**

The cost was one of the key factors in the planning stage of this design. In this design, the cost was estimated for several components, including the material cost, equipment and accessories cost and the labour cost. The hydraulic circuit consists of a hydraulic pump, a hydraulic actuator, valves and connecting accessories of the hydraulic circuit. In addition, this hydraulic circuit had different types of accessories. There is a pressure gauge, a safety valve and control valves. As there was minimal labour involvement, the cost was only for the equipment needed in this situation. The electrical circuit required basic electrical accessories; a main switch, a trip switch with electric circuit breakers and an emergency stop switch. Furthermore, a panel board and a panel box with a sufficient length of electrical wire to withstand the three phase electrical load were also needed in this application. This testing apparatus had an electronic control unit which included an electronic display unit. A digital camera was utilized to observe the crack initiation at the crack stop hole (CSH). All accessories and equipment cost were estimated with the current market price which was approximately 1200 USD. The hydraulic circuit and the indicator of their accessories took 62.5 % of the total cost. In addition, an assembling, cost, the machining and the transport cost were also included in this estimation. However, all these expenditures were less than 5 % of the overall cost and 20 % of expenditure were allocated for fabrication as, in fact, a similar test machine on the market costs nearly 40,000 USD without tax, transport and other administration expenditure. This clearly indicates the unavailability of cyclic flexural testing apparatus with adjustable features for medium scale testing in the open market for such a low cost. Detail expenditure of the required components and service costs are given in Table 3.3.

Table 3.3: Expenditure for the fabricate cyclic flexural load test apparatus

Description	Item	Cost (USD)
Hydraulic circuit	Hydraulic Pump	185
	Reservoir and accessories	220
	Hydraulic actuator	150
	Hydraulic Oil	70
An electrical circuit	Electrical accessories and wiring	80
Electronic circuit	Electronic accessories	90
Material cost for loading Frame	C-channel, nut and bolts, plates	90
Labour cost/ Machining cost	Labour and machine cost for fabrication	40
Other expenditures		75
Total material cost		1000
20 % fabrication cost		200
Total cost (Without tax and VAT)		1200

### 3.6.2 Limitations and operating range of fatigue loading apparatus

The main restriction is the limited capacity up to 10 kN. However, this is a good limit when compared with the capacities of available test machines in the market. The accuracy of load readings cannot be expected to be perfect at the extreme end, as the non-linear behavior of hydraulic oil influences. In addition, a load cell has a tolerance limit of  $\pm 0.001$  kN. However, this test apparatus is not recommended to run more than one hour continuously because the temperature of the hydraulic oil could increase and it affects the change of viscosity of the working fluid as well as the properties of packing materials.

### 3.6.3 Safety aspects of the fatigue loading apparatus

A hydraulic actuator was used to generate the mechanical loads. Therefore, the moving parts of the hydraulic cylinder should be covered with a transparent material. For the



stability of the overall system in this apparatus, the center of gravity point was moved down from the upper cross beam to a maximum possible distance. The vertical columns of the test apparatus were connected with long horizontal C-channel with a length of 1700 mm to avoid tilting due to torsion during testing. A 3.5 kW three phase electric motor was utilized to drive the hydraulic pump. Thus, a special attention was given to the insulation of the power connection. In addition, all the accessories were attached considering the ergonomic aspects. The position of the test specimen, the location of the control panel and the monitor were located by considering the safety and the ergonomic factors. The safety of the user as well as the test apparatus was paid high attention in this design. Hence, an emergency switch was fitted for shutdown in case of emergencies.

#### **3.6.4 Environmental impact assessment of the fatigue loading apparatus**

This cyclic flexural test apparatus uses hydraulic oil as a working fluid. This working fluid is only the pollutant, however it hardly impacts the lives of humans as well as the environment since the hydraulic oil is contained in a sealed oil reservoir. Also, the noise level during the testing is 20 dB, which is within the acceptable range.

#### **3.6.5 The maintenance procedure**

Regular maintenance of this testing apparatus is required for proper working conditions and durability. All parts and accessories of the test apparatus should be kept clean in a moisture free environment, as the contaminants and the moisture level of the environment highly contributes to damaging the electronic circuit. When considering the hydraulic lines and connectors of the circuit, it should be cleaned periodically, as the contaminants may cause a leakage of hydraulic oil from the system. Before adding hydraulic oil to the reservoir (Oil Tank), it should be filtered using a 5-micron filter to overcome the effects of possible contaminants. In addition, the following maintenance steps are recommended for better performance while assuring the safety and durability of the test apparatus:

- Check the hydraulic oil level periodically and adding oil if necessary
- Inspect the hydraulic hose, connectors and pipe lines for any possible leakage
- Replace any damaged items immediately

- Check the working temperature of the system as any heat affects to change the properties of the working fluid
- Maintain the range of the working temperature between 40 °C -60 °C
- Inspect the samples of fluid for colour, thickness, contamination particles, etc.
- Drain hydraulic oil from the reservoir when the oil colour is changed
- Replace or clean the filter elements for every 20 million cycles
- Restart and check the systems for proper operation
- Listen to any unusual sounds of the pump to identify any cavitation problems.
- Check the electrical wiring circuit and the trip switch periodically
- Replace the packing of the hydraulic actuator after 20 million cycles
- Calibrate the instrument every year or after testing of 1000 samples which ever lesser

Consequently, the provision of proper maintenance enables to reduce the overall cost of repair in this testing machine.

### **3.6.6 Modification for variable loads**

Actual loads on structures are variable loads such as vehicles passing on bridges, wind effects on structures and wave effects on offshore marine platforms. Therefore, investigating variable loads effects on structures has become critical and this test apparatus has a facility to apply variable amplitude loads with selected time intervals. To apply variable loads on test specimens the pressure should be changed and it could be accomplished by adjusting the position of the flow control valve of the hydraulic circuit. With a constant frequency, the magnitude of the load could be set to desired amplitudes at the end of a particular time interval or number of loading cycles while changing the amplitude of loads with desired values. For this purpose, there is no need to modify the apparatus. However, if need the amplitude of loads needs to be changed from cycle to cycle an additional flow control valve controlling mechanism can be used and it should be controlled according to the desired loading pattern. When attaching the flow control valve controller with the hydraulic circuit, the fluid pressure of the hydraulic circuit changes according to the operation of the flow control valve and simultaneously changes the magnitudes of loads on test specimens. This kind of

loading pattern could be used to evaluate the rain flow counting algorithm or Pagoda roofing technique.

### **3.7 Summary of design and fabricated fatigue loading apparatus**

This chapter focuses on understanding the historical contribution to develop fatigue test apparatus up to the present capacity. The design done in this study was selected comparing an appropriate load application mechanism with respect to other possible methods. Few critical components and accessories were fabricated which includes a loading frame, a power supply unit, a load apply mechanism and a gripping mechanism. In addition, concerns about safety, environment, accuracy of reading, the maintenance procedure and cost effectiveness of the apparatus are discussed in detail. The main objective was to design and fabricate a fatigue load test apparatus while applying and measuring the desired load effectively within the budget. The Loading frame will be designed while the FEM can predict the load bearing capacity using a solid work FEM software. The Hydraulic circuit in this machine was simulated using a Fluid SIM software before assembling the components. An Arduino program was utilized to control the hydraulic actuator due to the desired frequency. In addition, aspects of the design that includes its safety, the environment, the accuracy of reading, calibration method maintenance procedure and cost of the apparatus are also discussed in detail. The following features were obtained at the end of the design and fabrication:

- 1) This apparatus has flexibility to test specimen with any kind of geometrical shaped cross section.
- 2) The test setup has the potential to apply a desired load range up to 10 kN with different frequencies in the range of 1 Hz to 8 Hz
- 3) The testing is not only limited to steel tests but it has potential to apply fatigue loads on any material such as concrete, wood and plastic
- 4) Due to its low cost, high safety and reliability, this can be mainly recommended for research institutions for an affordable price

Cyclic flexural testing apparatus could be possibly extended as a cyclic tension, compression or impact load testing while changing an Arduino program, loading nose and a gripping mechanism. In addition, a micro digital camera or a high sensitive

voltage measurement technique could also be adopted to detect the crack initiation and propagation on test specimens.

## ***Chapter – 4***

---

# ***Experimental Investigations***

## 4 EXPERIMENTAL INVESTIGATIONS

### 4.1 Introduction of experimental investigation relating with CSH/CFRP hybrid system

Placing a CSH at the crack tip is one solution for delaying or permanently stopping crack growth on structural element as well as changing the direction of crack growth to protect the critical element. The main target of this chapter is to determine the cyclic flexural behavior of the CSH and to compare the results with the CFRP strengthened technique. In addition, the strain variation of non-strengthened and CFRP strengthened CSH was estimated in this chapter. A total of seven test series with hundred and sixty-two test specimens were prepared and tested in this background. The stress and strain based test program includes both test series with different sizes of diameter to width ratio of the CSH varies from 0.1 to 0.6 in 0.1 steps. In addition, this chapter aims to describe the experimental program which examined the effects of CSH position and the CFRP length on the CSH subjected to cyclic flexural loading. It includes the investigation of position change with respect to the loading point which is an important parameter because the actual load applying point and the location of the CSH may offset with respect to the loading point. As in real world applications of the CSH it is possible to offset from the loading point. The fatigue bearing capacity enhancement with the variation of CFRP length is another key parameter included in this chapter to evaluate the test set up.

The tensile test was carried out on the stress measured specimen only. In these test series strength losses due to fatigue loads on specimen was discussed and the estimates strength gains by the CFRP. Eventually, strength losses due to fatigue and the strength gains by the CFRP are compared and discussed in this chapter. The strain based test specimens includes non-strengthened and CFRP strengthened CSH. Strain measured non-strengthened specimen is prepared in the usual manner and the strain gauge was attached closer to the CSH while the fatigue test is performed to estimate the strain distribution during fatigue. The CFRP strengthened CSH is conducted in a similar way for the strain measure. Consequently, the results are compared with the non-

strengthened CSH to determine whether this technology shows any significant gain by CFRP.

Three different materials are selected in this investigation and there is steel, CFRP material and epoxy materials. In the present experimental program, MBrace fibre CF130 was chosen as a normal modulus CFRP and its with a 175 MPa modulus of elasticity. Araldite 420 and MBrace saturant were chosen as bonding adhesives. Mild steel plates were used in the experimental program.

## **4.2 Material selection and specimen preparation**

### **4.2.1 Selection of steel**

Concrete and steel are major construction materials in the world. However due to rapid development of the construction industry steel has become more prominent due to competitive advantages. It consumes less material, less time while reducing the weight of the structures and ultimately becoming cost effective. The Elastic module of concrete is in the range of 20 GPa to 40 GPa and steel its around 200 GPa. Therefore, steel shows high stiffness than concrete. Steel is a ductile material and it can withstand fatigue load than concrete. Toughness is another key parameter indicating energy absorption capacity to prevent crack growth which is higher in steel (Wei and He, 2014).

Mild steel is a most popular grade of steel in engineering related applications Generally mild steel has a low carbon content (from 0.16 % to 0.29%). Therefore, it shows excellent ductile characteristics and suitable for metal fabricate such as cutting, drilling, forging and welding. However mild steel not resistive to corrosion and surface protection is required to durability of element of structures. This steel grade is cost effective and high in strength. Therefore, it is used in various types of industrial applications and could be considered as an ideal construction material. Main applications are steel bridges, buildings, machinery parts and pipeline for transportation oil and gas. Most popular steel sections are flat section, hollow sections (Circular, square and rectangular) and channel sections (C-Chanel, I-channel and H-channel). Applications of steel plates are stadium, buildings, bridges, heavy

machineries, general constructions, reinforcing activities and ship building. Sample of steel plate use in this test program shown in Figure 4-1.

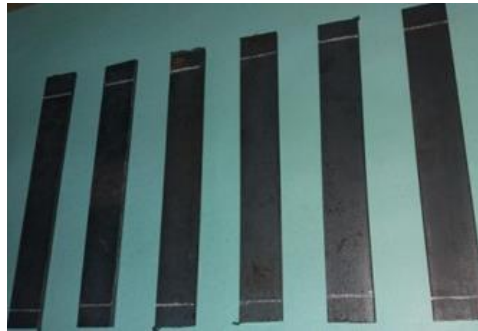


Figure 4-1: Test specimen

This study used the grinding technique while the process of cleaning supports the removal of weak layers, degreasing, re-cleaning and escaped oil or other potential contaminants from the metal surfaces. The purpose of applying primer coats on the cleaning surface is to protect the clean surface. However, the primer does not improve the bond strength. But the primer layer contributes to improve the durability of bonds exposed to the atmosphere (Dawood, 2005). However, the primer protection should be applied carefully, because the result of the improper primer application causes premature de-bonding. The primer has potential to protect the chemically active cleaned steel surface. Resulted in steel surface of specimen used in this study is shown in Figure 4-2.

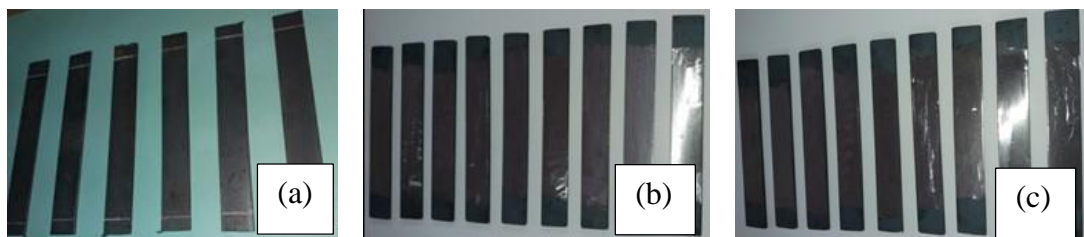


Figure 4-2: Specimen preparation for testing (a) Bare steel plate  
(b) Grinded steel surface (c) Primer coated steel surface

#### 4.2.2 Selection of the adhesive material

Epoxy adhesive plays a very important role on the steel/CFRP bond performance. Epoxy not only governs bond performance but it affects the durability of the steel/



CFRP bond as well as the failure mode. Therefore, epoxy adhesive material is a key parameters influencing on overall bond performance, as external forces are applied on structural element and it is transferred through epoxy layer utilized to attached steel and CFRP. Thus, the adhesive should have the capability of effective load transmitting through a composite bond. However, each adhesive is not fully capable of effectively transferring such a loads. A common phenomenon of load transferring is stress transfer from CFRP to steel surface. The bonding mechanism is one of the key concepts of understanding the bond performance.

The effects of the uniform adhesive thickness bring maximum performance, However, maintenance of a uniform thickness is a difficult task. In addition, most adhesives show a property of low viscosity. Therefore, thickness control is very difficult task in practical applications and results in reducing bond performance.

There has been limited attention on research studies related to influences in epoxy material. However, existing literature explain the parametric effects on the bond performance, influencing factors on epoxy adhesives and environmental effects on bonding. Ultimately performance of CFRP/steel bond depends on characteristic of the adhesive and it changes with glass transition temperature viscosity and curing time and detail explained in chapter 2. A two-part epoxy adhesive (Araldite 420) was selected in this study and mixed in 1:2 ratios by volume and applied to pre-treated metal surface during its pot life according to the guidelines provided by the manufacturer. Two-part epoxy adhesive material is shown in Figure 4-3.

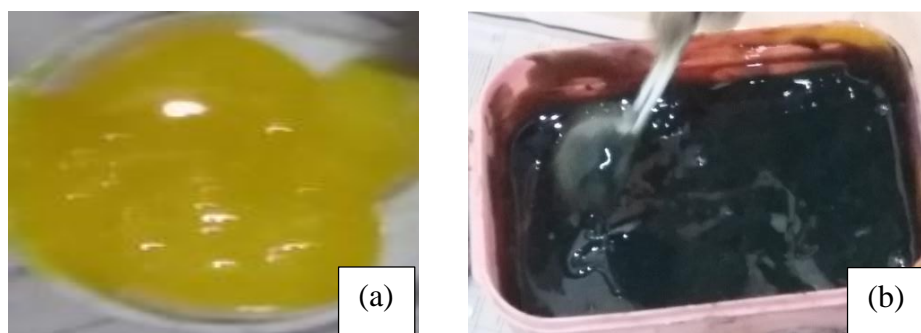


Figure 4-3: Two-part epoxy adhesive (Araldite 420) (a) before mixing (b) after mixing with hardener

### 4.2.3 Selection of the CFRP material

Conventional repairing technique have been replaced by the CFRP material, due to their superior characteristics. Therefore, it has become the most popular composite material in the world. The module of the CFRP material is one of the critically influencing parameters that affect CFRP/steel bond performance. Generally, the CFRP material can be classified as ultra-high modulus (UHM), high modulus (HM) and normal modulus (NM). However, at present it is difficult to find a general classification method for CFRP material. Normal module of CFRP material shows average elastic module, high tensile strength and high tensile elongation. Much research investigations have been focused on the normal modulus of CFRP sheets used to strengthen wooden, concrete, masonry or steel structures.

A Normal module (Mbrace CF 130) was selected in this study as shown in Figure 4-4 and the sheets were manufactured by master builders technology in USA. Pyrolizing poly acrylonitrile (PAN) based fiber process at 1500 °C and result is aligned carbon fiber chain. The modulus of elasticity and the ultimate tensile strength are 228 GPa, and 4275 MPa respectively reported by manufacturer and thickness of the sheet is 0.165 mm. The tensile strength and modulus of elasticity of CFRP were taken from the experimental data in similar research investigation conducted at the computational mechanics' laboratory. The properties of material are listed in table 4.1.



Figure 4-4: Normal module of CFRP material (Mbrace CF 130)

### 4.2.4 Procedure of CFRP installation with steel

This testing program included different geometrical dimensions and cross sections according to the requirement. In each test series, the bottom side surface of the steel section was prepared by using an angle grinder. After that, sandpaper with grit P240

was used to modify the surface quality which maximized the bond performance. Acetone was used to clean the grease, weak layers and dust particles. Then a primer was applied with a brush on acetone cleaned surface prior to applying selected epoxy adhesive and it was allowed to dry for approximately 5 to 8 hours. The two components epoxy adhesive were dosed 1:2 ratio by volume, according to the manufacturer's guidelines and mixed until a homogeneous light gray paste was obtained and applied to pre-treated steel surface during its pot life according to manufacturer guidelines. Firstly, the CFRP sheets were cut to the proper size using a saw cut the epoxy adhesive was then distributed evenly on treated steel surface and about 1 mm thickness. The schematic view of CFRP attached specimen shown in Figure 4-5. Finally, the CFRP layer was attached to the treated surface as shown in Figure 4-6. Rib roller used to remove air bubble between CFRP layer and adhesive to confirm best bonding.

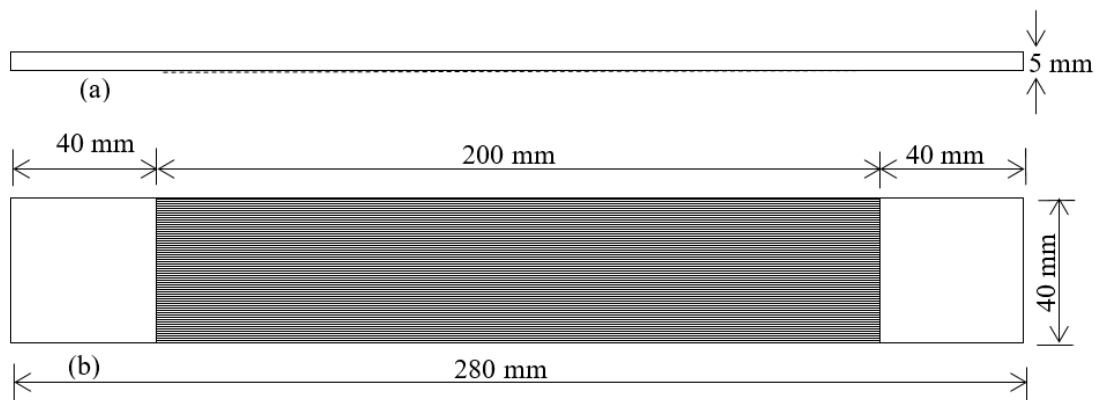


Figure 4-5: CFRP strengthened specimen schematic view



Figure 4-6: Typical test specimen

#### 4.2.5 Material properties

The modulus of elasticity and tensile strength of steel and CFRP material were determined experimentally by a coupon test in similar investigation conducted at the computational mechanics' laboratory. Also, the tensile strength and elastic modulus of the steel were measured according to the ASTM D 3039 standards. In fact, a tensile strength of 583 MPa and an average elastic modulus of 200 GPa were reported. Tensile strength of and an average elastic modulus of CFRP material were reported 175 MPa and 1575 MPa respectively. The poison's ratio value assumed as a 0.3. The measured material properties of steel and CFRP materials are listed in table 4.1.

Table 4.1: Measured and manufactures provided material properties

Material property	Measured data			Manufacturers provide data		
	Steel	Epoxy adhesive	CFRP	Steel	Epoxy adhesive	CFRP
Average tensile strength (MPa)	583	25	1575	350	27	550
Average elastic modulus (GPa)	200	0.579	175	210	1.85	240
Average Poisson's ratio	-	-	-	0.3	0.3	0.2

Source: (Chandrathilaka, 2019)

#### 4.3 Test program

This test program presents a detailed investigation on CFRP embedded steel elements with CSH under low cycle fatigue. A total of seven test series were performed to evaluate the effects of critical parameters on performance of CSH technique. A total of hundred and sixty-two specimens were tested (Table 4.2) while two series of them ( $S_1$  and  $S_2$ ) were performed to investigate the behavior of strengthened and non-strengthened steel plate specimens with conditioning under fatigue load as a control measure. Other two test series ( $S_3$  and  $S_4$ ) were performed to determine the characteristics of CFRP strengthened and non-strengthened CSH specimens subjected to low cycle fatigue load. The series  $S_5$  and  $S_6$  were planned to examine the effects of location of CSH on service performance. The series,  $S_7$  was conducted to estimate the effect of extended length of CFRP (bond length) beyond the CSH on low cycle fatigue

performance. Detailed test procedures were presented in this chapter.

Table 4.2: Summary of test programs

<b>Series</b>	<b>Geometry of specimen</b>	<b>Conditioning type</b>	<b>Monitored effect</b>	<b>Strengthens</b>	<b>Number of sample</b>
S <sub>1</sub>	steel plates with and without CSH	2000 cycles(step) (Max 10,000)	strength	non-strengthened	24
S <sub>2</sub>	steel plates with and without CSH	2000 cycles(step) (Max 10,000)	strength	Strengthened	24
S <sub>3</sub>	steel plates with CSH	Non conditioned (control samples)	strength	strengthened and non-strengthened	24
S <sub>4</sub>	steel plates with CSH	10,000 cycles	strength and strain	strengthened and non-strengthened	36
S <sub>5</sub>	steel plates with CSH with change in position (location of CSH varied from 20 mm to 100 mm in 20 mm steps)	10,000 cycles	strength and strain	non-strengthened	18
S <sub>6</sub>	steel plates with CSH with change in position (location of CSH varied from 20 mm to 100 mm in 20 mm steps)	10,000 cycles	strength and strain	strengthened	18
S <sub>7</sub>	steel plates with and without CSH (bond length vary from 20 mm to 120 mm with 20 mm steps)	10,000 cycles	strength	strengthened	24

### 4.3.1 Test setup and instrumentation

The loading frequency for the application of cyclic flexural load was selected in accordance with ASTM D7774. The test specimen was kept on two cylindrical shaped, supportive rollers with 25 mm diameter each and the span was fixed at 240 mm between centers of the rollers as shown in Figure 4-7. These specimens were conditioned following the pre-defined flexural cyclic load, intensity and period of load application. The strain variation at CSH of the specimen during conditioning was measured. At the end of conditioning period, a transient tensile load was applied to determine the retained average strength as shown in Figure 4-8.

### 4.3.2 Cyclic flexural loading setup for applying fatigue load on specimen

Specimens were kept on two supportive rollers with 25 mm diameter and the span length was fixed at 240 mm between centers of the rollers as shown in Figure 4-7. The specimen was conditioned up to pre-determined cycles (10,000 cycles) using developed fatigue test apparatus operating with hydraulic actuator. This procedure was repeated up to pre-determined cycles with 2 kN amplitude and 5 Hz loading frequency as shown in Figure 4-7.

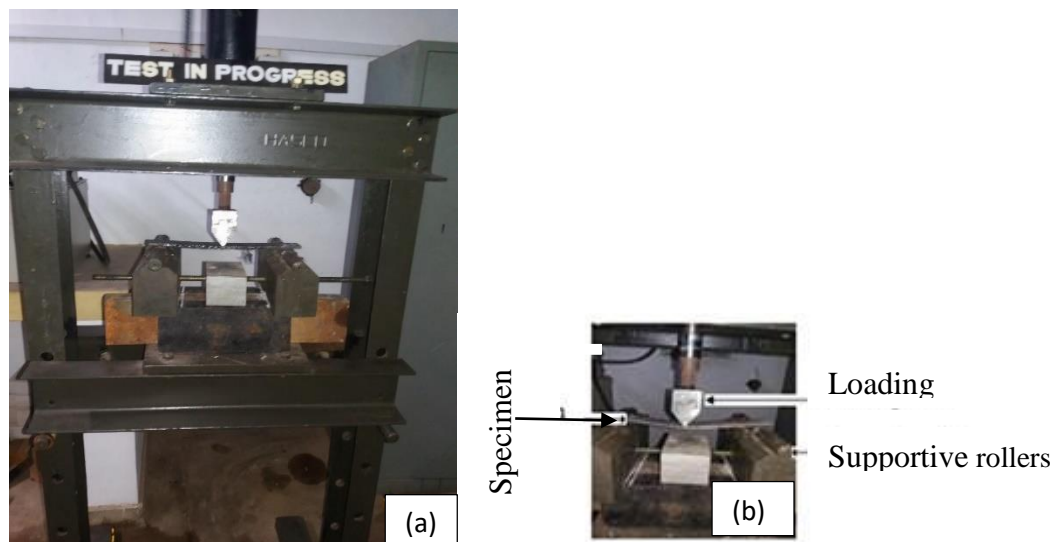


Figure 4-7: Cyclic flexural test setup for conditioning (a) loading frame  
(b) specimen fixture

### 4.3.3 Tensile test setup for measuring the retained average strength on specimens

After conditioning with pre-determined number of cycles the sample was removed from the cyclic flexural testing machine and it was fixed to the universal tensile testing machine (UTM) with 100 kN capacity (Figure 4-8). Transient tensile load was applied as shown in Figure 4-8 to determine the retained average strength. This procedure was repeated and the average value of the load was measured for each specimen.

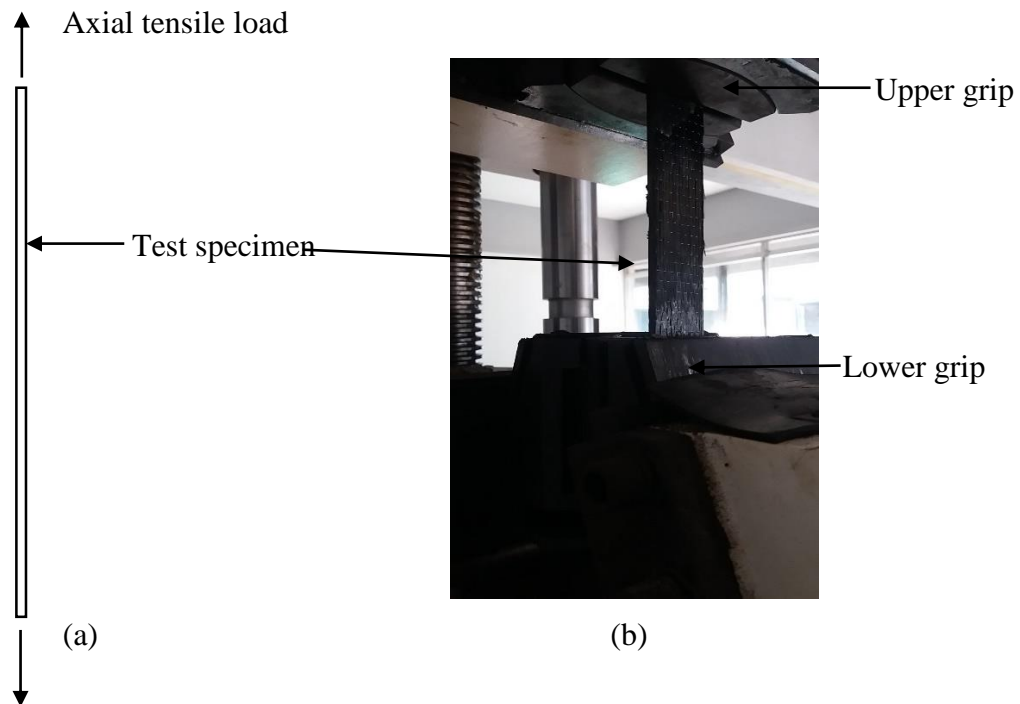


Figure 4-8: Tensile test setup (a) schematic test layout (scale 1:4)  
(b) typical test fixture

### 4.4 Behavior of the steel element with respect to loading cycles

A total of forty-eight specimens were conditioned up to 10,000 flexural load cycles with 2 kN amplitude and 5 Hz frequency ( $S_1$  and  $S_2$ ). The tensile surface of twenty-four samples ( $S_2$ ) were retrofitted with a CFRP patch contains the same length of 200 mm and twelve of them had CSH with 16 mm diameter at the midpoint. The remaining twenty-four samples ( $S_1$ ) were not strengthened and out of twelve were fabricated introducing a CSH with 16 mm diameter at the midpoint of main axis and considered as control specimens. In these two test series, the number of cycles was considered as

a main variable and it varied from 0 to 10,000 in 2,000 steps.

#### 4.4.1 Behavior of non-strengthened steel element without CSH under fatigue load

The specimens were designed in accordance with ASTM D 790 with the use of steel plates with a cross-section of 40 mm (width) x 5 mm (thickness) (Figure 4-1). The length of the plate member was chosen to be 280 mm and the effective span was considered as 240 mm due to a restriction in the flexural cyclic loading apparatus (Figure 4-7). A total of twelve specimens were tested to determine the characteristics of non-strengthened steel plate specimens without CSH subjected to low cycle fatigue load. The schematic diagram of non-strengthened specimens and typical test specimen shown in Figure 4-9.

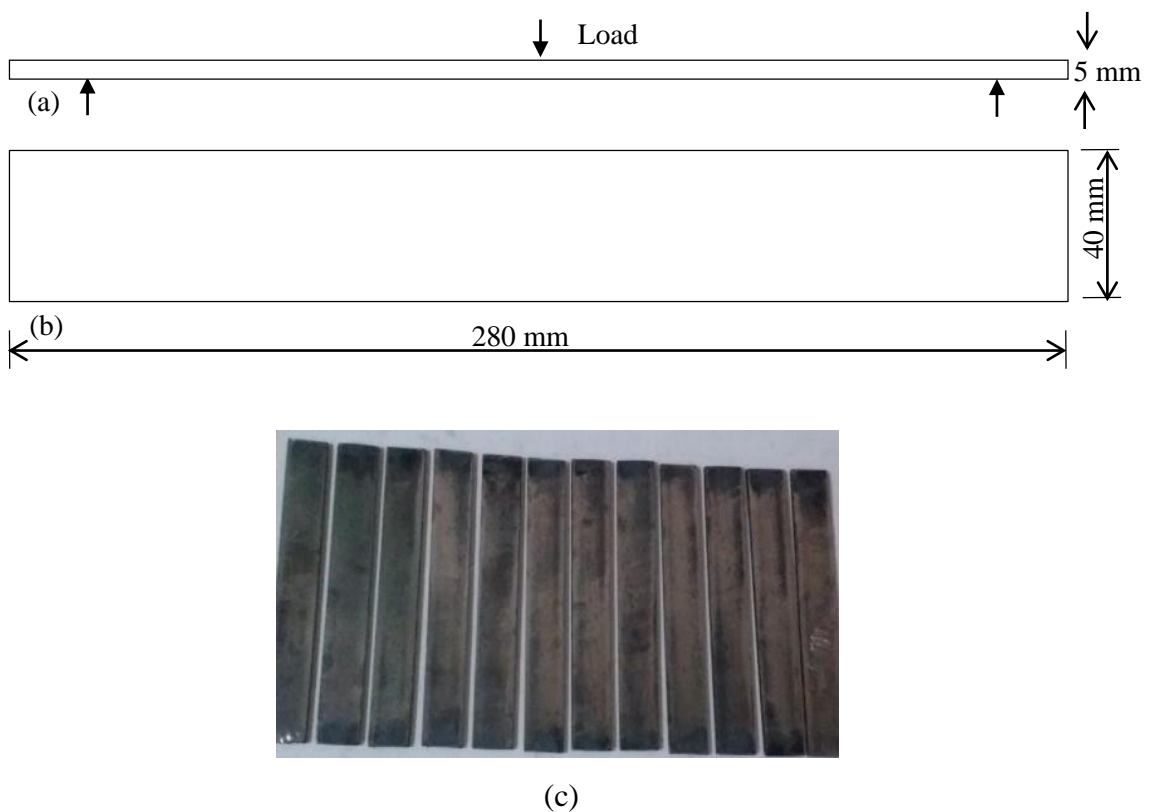


Figure 4-9: Schematic diagram (a) elevation (b) Plane view  
(c) typical specimens of non-strengthened plates without CSH

In this test, the number of cycles was considered as a main variable and it varied from 0 to 10000 in 2000 steps. Table 4.3 summarizes the retained average strength together with the variation of different number of load cycles of the test results.



Table 4.3: Retained average strength of non-strengthened steel element with the number of cycles

Number of flexural load cycles	Average tensile load (kN)	Average strength (MPa)
0	68.4	342.0
2000	68.3	341.7
4000	67.5	337.3
6000	64.0	320.0
8000	62.6	313.0
10000	61.5	307.3

Figure 4-10 indicates the retained average strength variation with exposure duration. As shown in Figure 4-10, when the number of load cycles is increased, the average tensile strength decreases. Failure modes are shown in Figure 4-11.

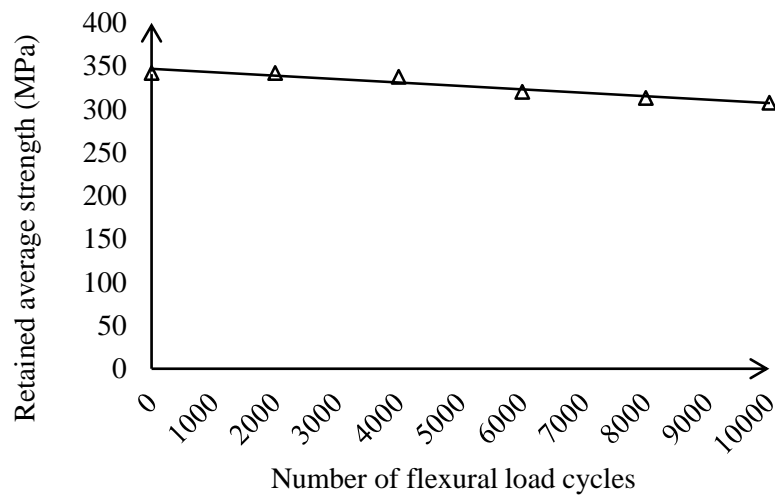


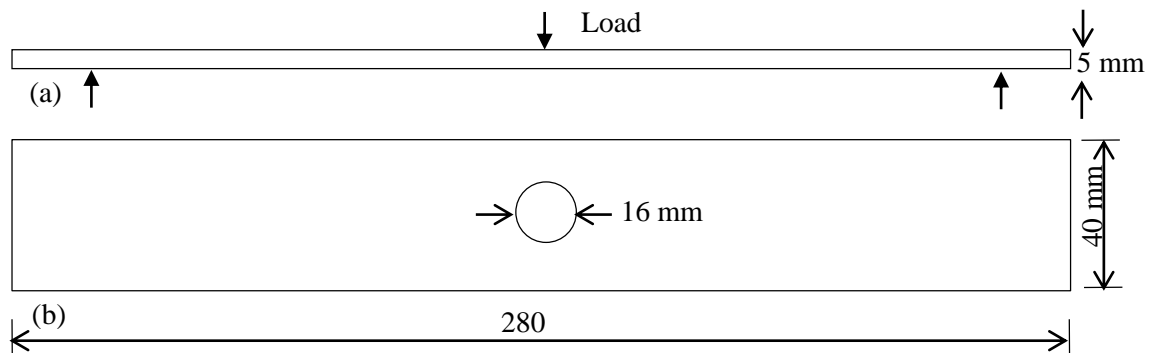
Figure 4-10: Variation of retained average strength with exposure cycles for non-strengthened plate specimen

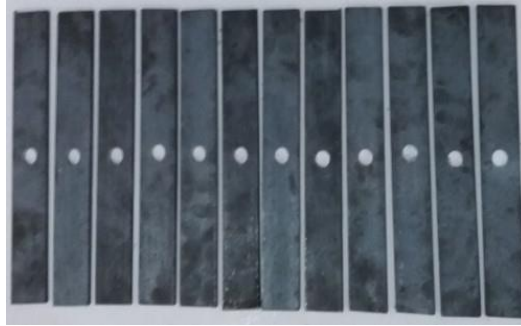


Figure 4-11: Failure mode of plane specimens non-strengthened plates without CSH

#### 4.4.2 Behavior of non-strengthened steel element with CSH under fatigue load

The specimens were designed in accordance with ASTM D 790 with the use of steel plates with a cross-section of 40 mm (width) x 5 mm (thickness) (Figure 4-1). The length of the plate member was chosen to be 280 mm and the effective span was considered as 240 mm due to a restriction in the flexural cyclic loading apparatus (Figure 4-7). CSH was fabricated at the midpoint of main axis with 16 mm diameter and considered as control specimens. A total of twelve specimens were tested to determine the characteristics of non-strengthened steel plate specimens with CSH subjected to low cycle fatigue load. The schematic diagram of non-strengthened specimens and typical test specimen are presented in Figure 4-12.





(c)

Figure 4-12: Schematic diagram (a) elevation (b) plane view  
(c) typical specimens of non-strengthened plates with CSH

In this test, the number of cycles was considered as a main variable and it varied from 0 to 10000 in 2000 steps. Table 4.4 summarizes the retained average tensile strength together with the variation of different number of load cycles of the test results.

Table 4.4: Retained average strength of non-strengthened steel element with CSH

<b>Number of flexural load cycles</b>	<b>Average tensile load (kN)</b>	<b>Average strength (MPa)</b>
0	56.5	282.5
2000	55.9	279.3
4000	54.6	273.0
6000	53.0	264.8
8000	52.2	261.0
10000	50.8	254.0

Figure 4-13 indicates the residual strength variation with exposure duration. As shown in Figure 4-13, when the number of load cycles is increased, the average strength decreases. Failure modes are shown in Figure 4-14.

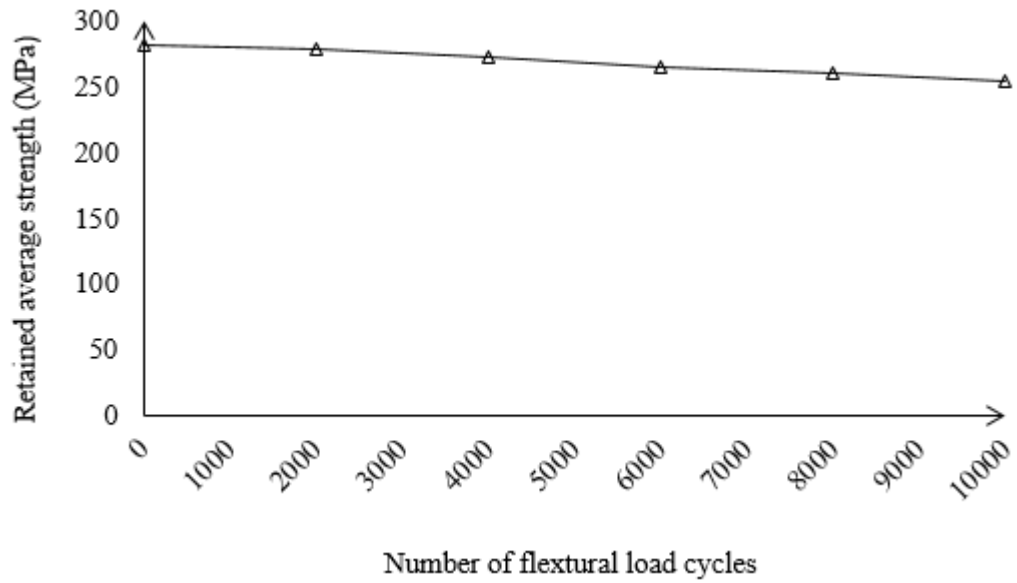


Figure 4-13: Variation of retained strength with exposure cycles for non-strengthened plate specimen with CSH



Figure 4-14: Failure mode of plane specimens non-strengthened plates with the CSH

#### 4.4.3 Behavior of CFRP-strengthened steel element without CSH under fatigue load

The specimens were designed in accordance with ASTM D 790 with the use of steel plates with a cross-section of 40 mm (width) x 5 mm (thickness) (Figure 4-1). The length of the plate member was chosen to be 280 mm and the effective span was considered as 240 mm due to a restriction in the flexural cyclic loading apparatus (Figure 4-7). The tensile surface of samples was retrofitted with a CFRP patch contains the same length of 200 mm. A total of twelve specimens were tested to determine the characteristics of CFRP-strengthened steel plate specimens without CSH subjected to

low cycle fatigue load. The schematic diagram of non-strengthened specimens and typical test specimen shown in Figure 4-15.

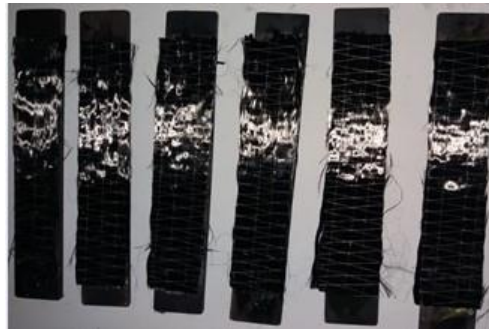
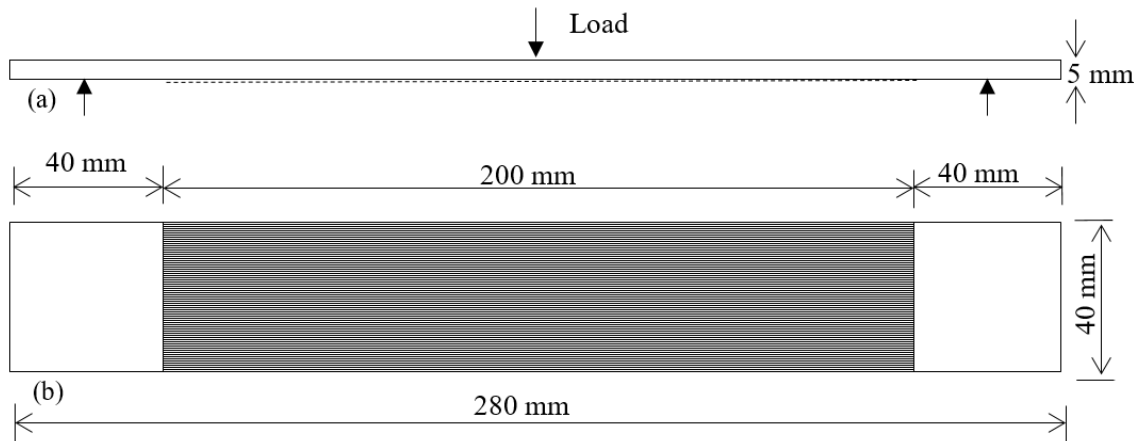


Figure 4-15: Schematic diagram (a) elevation (b) Plane view (c) typical specimens of CFRP strengthened plates without CSH

In this test, the number of cycles was considered as a main variable and it varied from 0 to 10000 in 2000 steps. Table 4.5 summarizes the retained average tensile strength together with the variation of different number of load cycles of the test results.

Table 4.5: Retained average strength of CFRP – strengthened steel element without CSH

Number of flexural load cycles	Average tensile load (kN)	Average strength (MPa)
0	88.5	442.3
2000	86.8	433.8
4000	86.3	431.7
6000	85.9	429.7
8000	85.3	426.7
10000	83.9	419.6

Figure 4-16 indicates the residual strength variation with exposure duration. As shown in Figure 4-16, when the number of load cycles is increased, the average tensile strength decreases. Failure modes are shown in Figure 4-17.

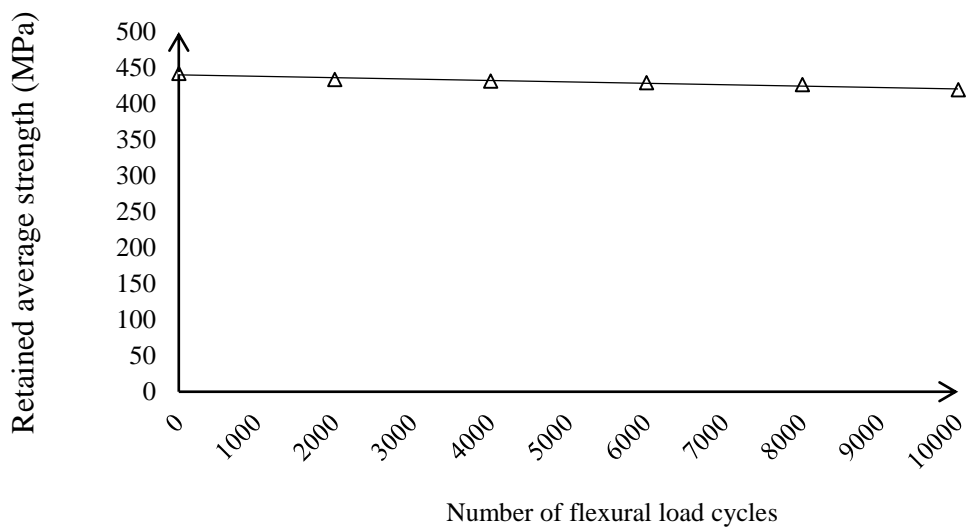


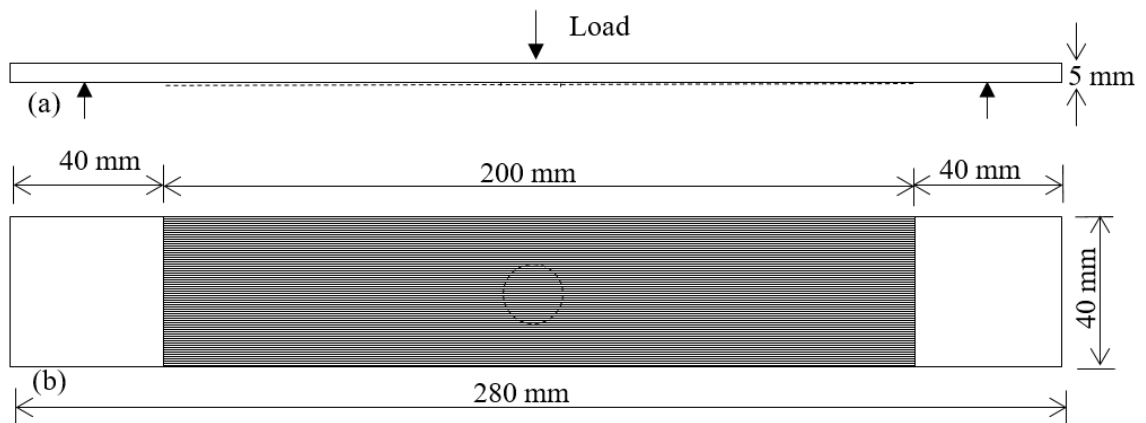
Figure 4-16: Variation of retained average strength with exposure cycles for CFRP-strengthened plane specimen



Figure 4-17: Failure mode of CFRP strengthened plane specimens without CSH

#### 4.4.4 Behavior of CFRP-strengthened steel element with CSH under fatigue load

The specimens were designed in accordance with ASTM D 790 with the use of steel plates with a cross-section of 40 mm (width) x 5 mm (thickness) (Figure 4-1). The length of the plate member was chosen to be 280 mm and the effective span was considered as 240 mm due to a restriction in the flexural cyclic loading apparatus (Figure 4-7). CSH was fabricated at the midpoint of main axis with 16 mm diameter and considered as control specimens. The tensile surface of samples was retrofitted with a CFRP patch contains the same length of 200 mm. A total of twelve specimens were tested to determine the characteristics of CFRP-strengthened steel plate specimens with CSH subjected to low cycle fatigue load. The schematic diagram of non-strengthened specimens and typical test specimen presented in Figure 4-18.





(c)

Figure 4-18: Schematic diagram (a) elevation (b) Plane view (c) typical specimens of CFRP strengthened plates with CSH

In this test, the number of cycles was considered as a main variable and it varied from 0 to 10000 in 2000 steps. Table 4.6 summarizes the retained average strength together with the variation of different number of load cycles of the test results.

Table 4.6: Retained average strength of CFRP-strengthened plane specimen with CSH

<b>Number of flexural load cycles</b>	<b>Average tensile load (kN)</b>	<b>Average strength (MPa)</b>
0	73.4	366.8
2000	72.9	364.3
4000	71.6	357.8
6000	70.0	350.0
8000	67.9	339.5
10000	65.8	329.0

Figure 4-19 indicates the average strength variation with exposure duration. As shown in Figure 4-19, when the number of load cycles is increased, the average strength decreases. Failure modes are shown in Figure 4-20.



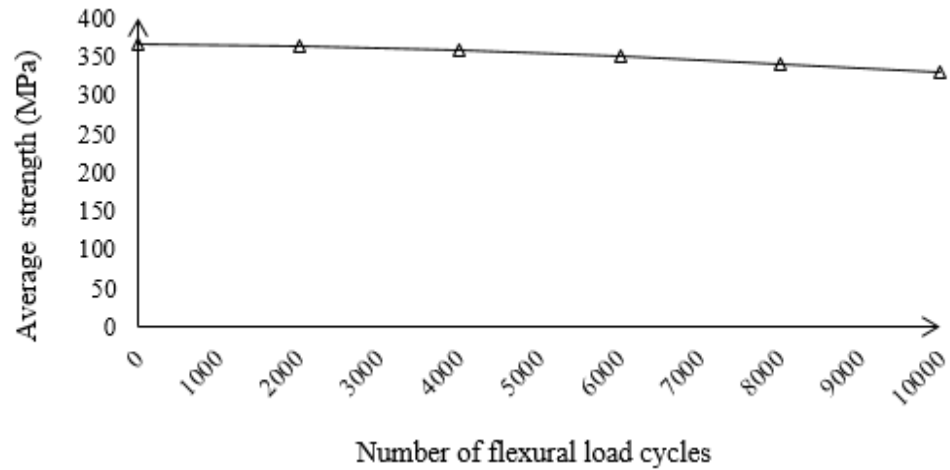


Figure 4-19: Average strength variation with number of cycles for CFRP-strengthened steel element with CSH



Figure 4-20: Failure mode of CFRP-strengthened steel element with CSH

#### 4.4.5 Comparison of fatigue behavior with respect to load cycles

A summary of the laboratory test results for non-strengthened and CFRP strengthened steel specimens is presented in Table 4.7. The table lists the number of cycles applied on specimen, average yield load for all test specimen and strength gain by CFRP strengthened steel specimen. It summarizes the tensile load values together with the variation of different number of loading cycles from the range of 0 to 10,000. Number of cycles varied in the range of 2000 cycles. The average tensile strength due to the number of stress cycles compared with non-strengthened and CFRP strengthened steel plate.

Table 4.7: Comparison of strength gain by CFRP

No. of test	Number of flexural load cycles	Retained average strength (MPa)				Strength gain by CFRP (%)	
		Non-strengthened steel plate without CSH	CFRP strengthened steel plate without CSH	Non-strengthened steel plate with CSH	CFRP strengthened steel plate with CSH	Without CSH	With CSH
2	0	342.0	442.3	282.5	366.8	29.3	29.8
2	2000	341.7	433.8	279.3	364.3	26.9	30.4
2	4000	337.3	431.7	273.0	357.8	28.0	31.0
2	6000	320.0	429.7	264.8	350.0	34.3	32.2
2	8000	313.0	426.7	261.0	339.5	36.3	30.1
2	10000	307.3	419.6	254.0	329.0	36.5	29.5

Figure 4-21 shows the average retained tensile strength variation of CFRP strengthened and non-strengthened conditioning steel element with and without CSH. The number of applied cycles subjected to cyclic flexural loading.

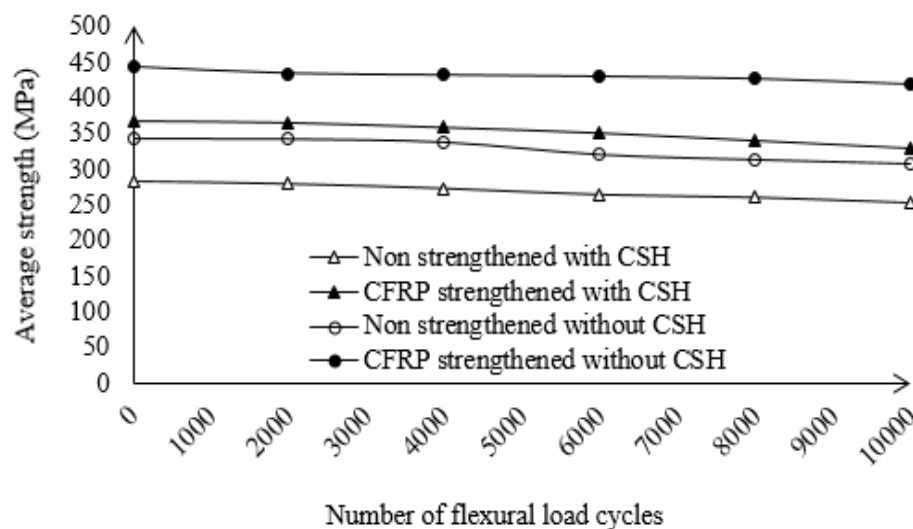


Figure 4-21: Variation of retained average strength with exposure cycles

When the material is conditioned up to 10,000 flexural load cycles, the average retained strength decreases indicating a similar trend irrespective from the sample characteristics. Therefore, strength variation is inversely proportionate to the number of flexural load cycles as shown in Figure 4.21. According to the graph, both non-strengthened and CFRP strengthened specimens show a similar pattern with a similar trend of stress variation with the exposure period. However, the retrofitted specimens without CSH reported a strength enhancement in the range between 26 % and 36 %. A negligible strength reduction was noted in the low cycle fatigue range from CFRP strengthened specimens. Strength gained by CFRP was compared with the CSH as shown in Figure 4-21 and exhibit a significant fatigue enhancement in the range from 29 % to 32 %, as the CFRP layer added an extra tensile capacity for steel/CFRP composite. This additional tensile strength causes to redistributing the stresses concentration at the bottom surface of CSH and results in enhancing the yield capacity of the material. These results show that the CFRP installation has significantly affected on the strength recovery of material to delay the crack initiation at the CSH. The cracks initiate at the highest stress concentration point of the element and it was near the region of the loading point which is the potential critical region. However, there was no failure reported in the adhesive, steel, or in the CFRP layer under the flexural cyclic load. The cracks initiated closer to the loading point and the propagation direction was perpendicular to the direction of the tensile load as shown in Figure 4-11. In destructive testing done after conditioning, the interface de-bonding of CFRP layer was noted from CSH specimens. Figure 4-22(a) and Figure 4-22 (b) shows the percentage of strength gain by CFRP/steel composite with and without a CSH respectively.

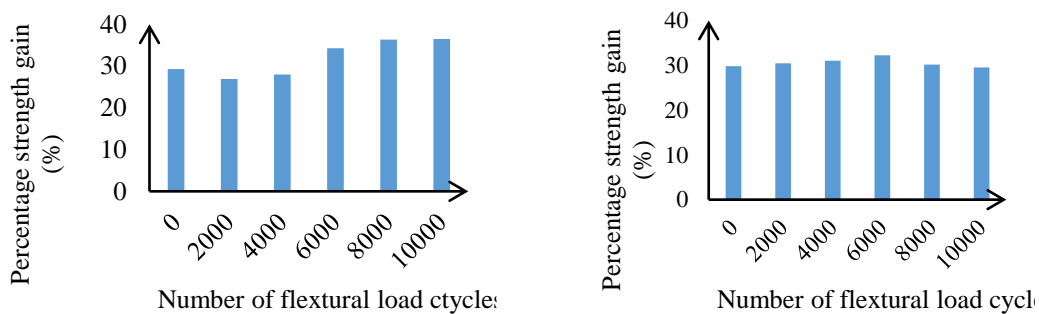


Figure 4-22: Percentage of strength gain by CFRP with respect to loading cycles  
 (a) without CSH (b) with CSH

#### 4.5 Effects of CSH diameter on LCF

A total of thirty-six specimens were conditioned up to 10,000 flexural load cycles with 2 kN amplitude and 5 Hz frequency (Series S<sub>3</sub> and S<sub>4</sub>). The tensile surface of thirty samples (Series S<sub>2</sub>) were retrofitted with a CFRP patch contains the same length of 200 mm. The remaining thirty samples (S<sub>1</sub>) were not strengthened and considered as control specimens. In these two test series, the diameter to width ratio ( $d/b$ ) was considered as a main variable and it varied from 0.1 to 0.6 in 0.1 steps.

##### 4.5.1 Behavior of non-strengthened steel element with CSH under non conditioned

The specimens were designed in accordance with ASTM D 790 with the use of steel plates with a cross-section of 40 mm (width) x 5 mm (thickness) (Figure 4-1). The length of the plate member was chosen to be 280 mm and the effective span was considered as 240 mm (Figure 4-7). The CSH was placed at the center-point of the specimen with a diameter to width ratio range from 0.1 to 0.6 with 0.1 step. A total of twelve specimens were tested to determine the characteristics of non-strengthened steel plate specimens with CSH. The schematic diagram of non-strengthened specimens and typical test specimen shown in Figure 4-23.

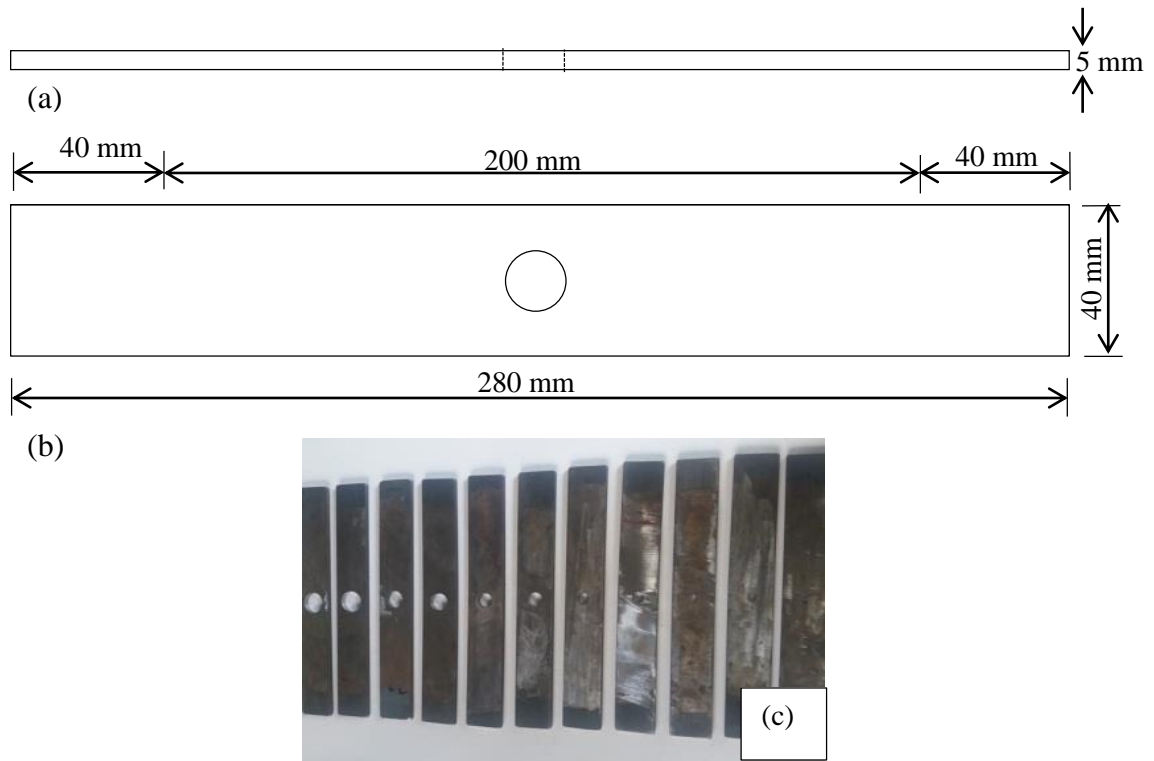


Figure 4-23: Schematic view of the non-conditioned and non-strengthened specimen (Scale 1:2) (a) elevation (b) plane view (c) typical specimen

In this test, the diameter to width ratio was considered as a main variable and it varied from 0.1 to 0.6 in 0.1 steps. Table 4.8 summarizes the retained average yield strength together with the variation of different number of load cycles of the test results.

Table 4.8: Retained average strength of non-strengthened steel element with the number of cycles

<b>Diameter to width ratio (d/b)</b>	<b>Average tensile load (kN)</b>	<b>Average strength (MPa)</b>
0.1	86.6	433.1
0.2	82.4	412.1
0.3	78.2	393.1
0.4	73.6	368.3
0.5	63.4	317.2
0.6	49.7	248.5

Figure 4-24 indicates the residual strength variation with exposure duration. As shown in Figure 4-24, when the diameter to width ratio is increased, the average strength decreases. Failure modes are shown in Figure 4-25.

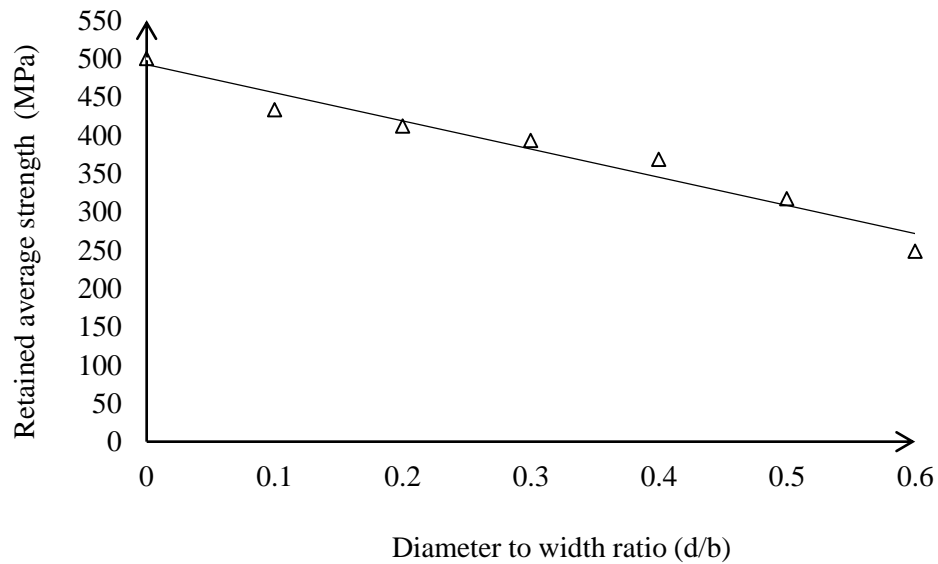


Figure 4-24: Retained average strength variation with diameter to width ratio



Figure 4-25: Failure mode of non-conditioned non-strengthened CSH

#### 4.5.2 Behavior of CFRP-strengthened steel element with CSH under a non-conditioned situation

The specimens were designed in accordance with ASTM D 790 with the use of steel plates with a cross-section of 40 mm (width) x 5 mm (thickness). The length of the plate member was chosen to be 280 mm and the effective span was considered as 240 mm. The CSH was placed at the center-point of the specimen with a diameter to width ratio range from 0.1 to 0.6 with 0.1 step. A 200 mm long unidirectional normal modulus CFRP fabric was used to strengthened the CSH. A total of twelve specimens were tested to determine the characteristics of CFRP-strengthened non-conditioned steel plate specimens with CSH. The schematic diagram of non-strengthened specimens and typical test specimen shown in Figure 4-26.

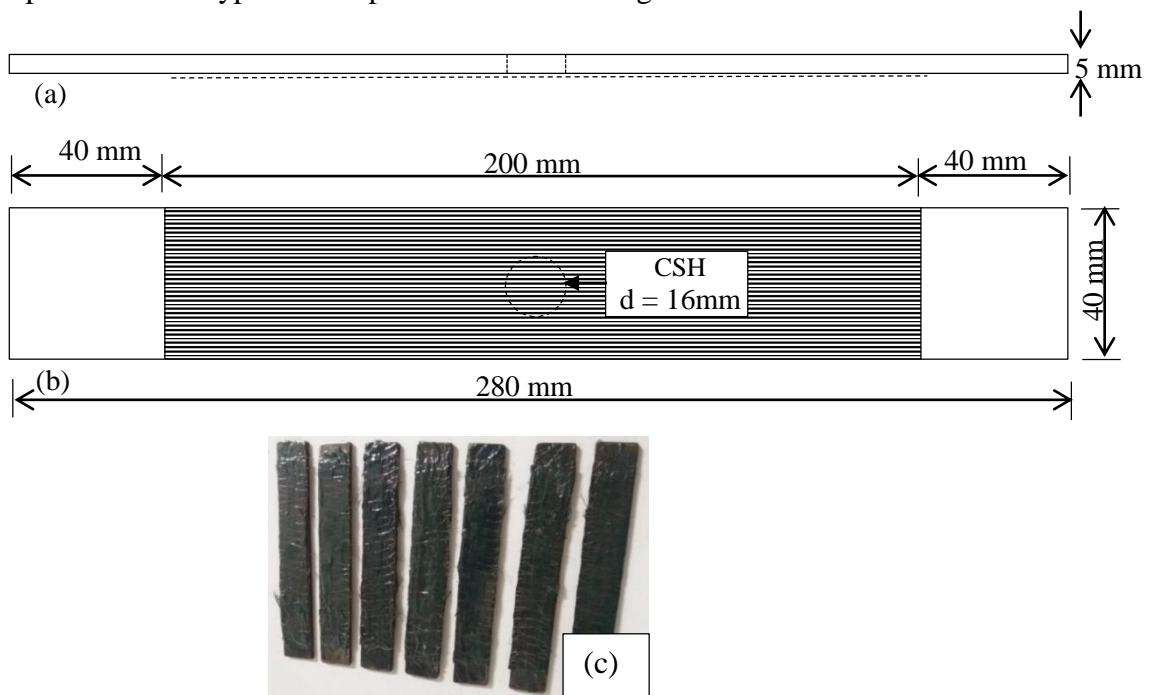


Figure 4-26: Schematic view of the non-conditioned CFRP-strengthened specimen (Scale 1:2) (a) elevation (b) plane view (c) typical specimen

In this test, the diameter to width ratio was considered as a main variable and it varied from 0.1 to 0.6 in 0.1 steps. Table 4.9 summarizes the retained average yield strength together with the variation of different number of load cycles of the test results.

Table 4.9: Retained average strength of bare steel varies with the number of cycles

Diameter to width ratio (d/b)	Retained average tensile load (kN)	Average strength (MPa)
0.1	108.5	542.3
0.2	103.2	516.0
0.3	92.9	464.3
0.4	84.0	420.0
0.5	74.0	370.0
0.6	56.0	280.0

Figure 4-27 indicates the residual strength variation with exposure duration. As shown in Figure 4-27, when the diameter to width ratio is increased, the average yield strength decreases. Failure modes are shown in Figure 4-28.

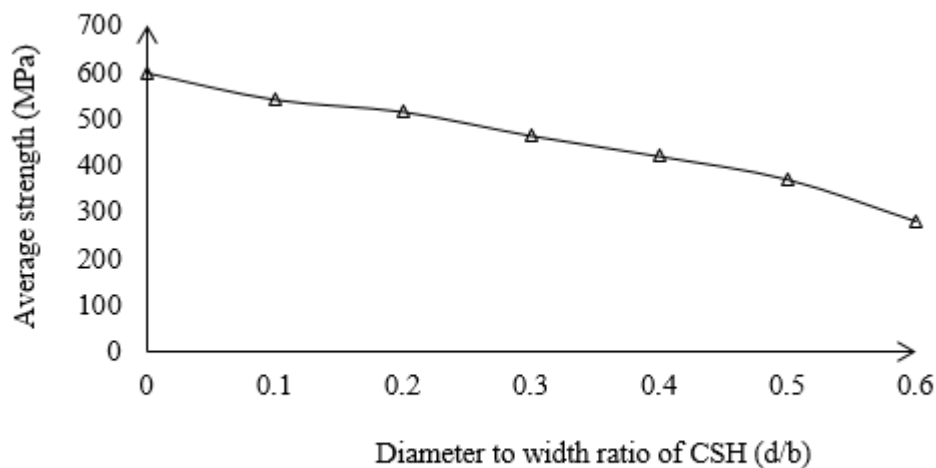


Figure 4-27: Retained average strength variation with number of cycles for CFRP - strengthened steel element with CSH



Figure 4-28: Failure mode of non-conditioned CFRP strengthened specimen

#### 4.5.3 Behavior of non-strengthened steel element with CSH under fatigue load

The specimens were designed in accordance with ASTM D 790 with the use of steel plates with a cross-section of 40 mm (width) x 5 mm (thickness) (Figure 4-1). The length of the plate member was chosen to be 280 mm and the effective span was considered as 240 mm due to a restriction in the flexural cyclic loading apparatus (Figure 4-7). A total of twelve specimens were tested to determine the characteristics of non-strengthened steel plate specimens with CSH subjected to low cycle fatigue load. The schematic diagram of non-strengthened specimens and typical test specimen shown in Figure 4-29.

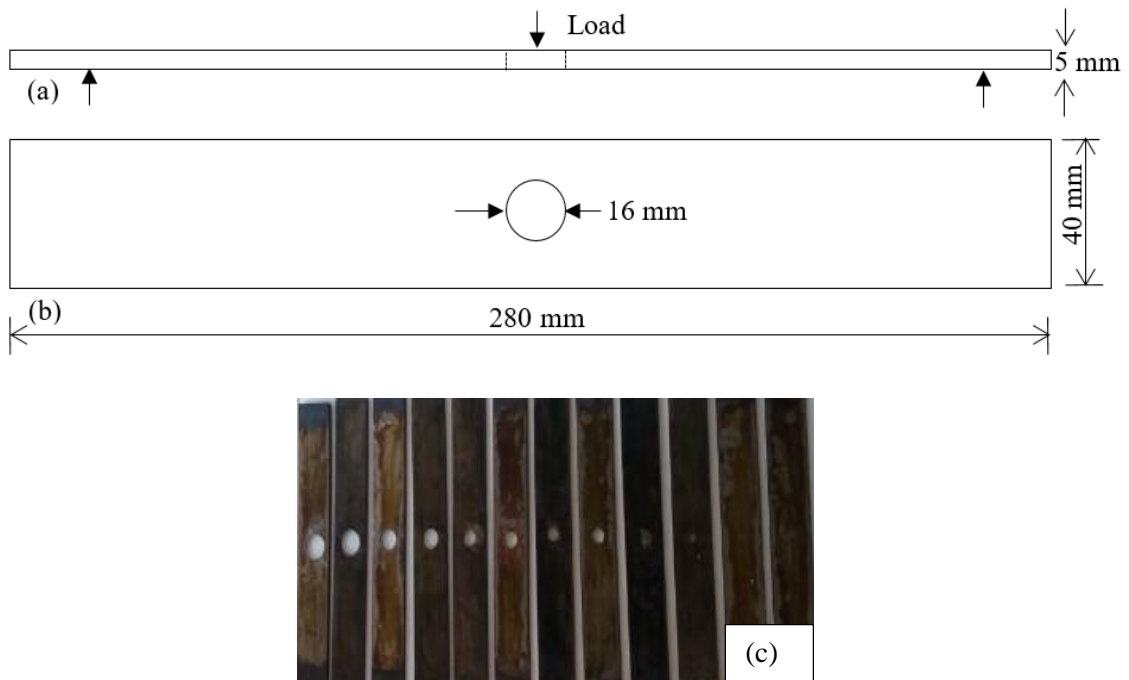


Figure 4-29: Schematic view of the conditioning steel element with non-strengthened CSH specimen (scale 1:2) (a) elevation (b) plane view (c) typical test specimen



In this test, the diameter to width ratio was considered as a main variable and it varied from 0.1 to 0.6 in 0.1 steps. Table 4.10 summarizes the retained average tensile strength together with the variation of different diameter to width ratio of the test results.

Table 4.10: Retained average strength of non- strengthened steel varies with the number of cycles

Diameter to width ratio (d/b)	Average tensile load (kN)	Average strength (MPa)
0.1	75.0	375.1
0.2	71.1	355.6
0.3	67.1	335.6
0.4	60.0	300.1
0.5	49.2	245.8
0.6	37.2	185.8

Figure 4-30 indicates the residual strength variation with exposure duration. As shown in Figure 4-30 when the diameter to width ratio is increased, the average strength decreases. Failure mode are shown in Figure 4-31.

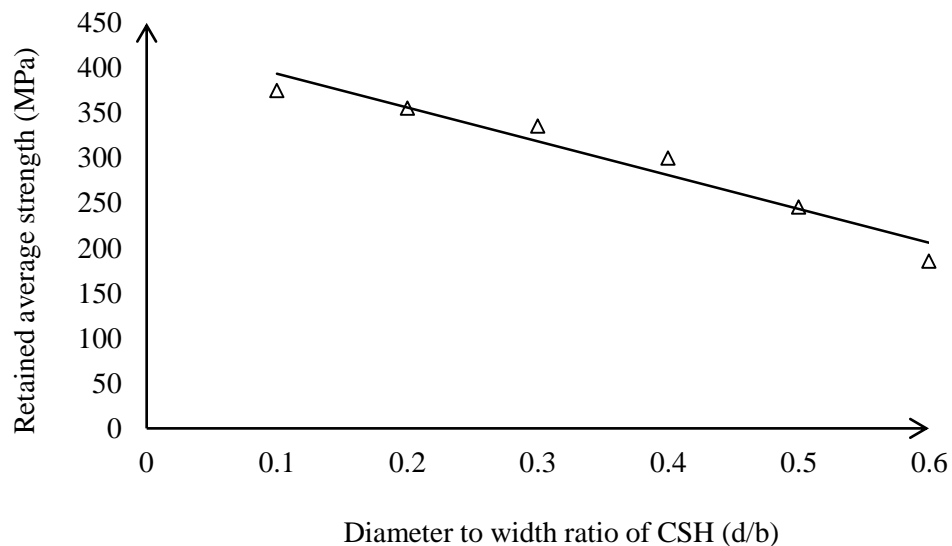


Figure 4-30: Retained average strength variations with the diameter to width ratio of conditioned non strengthened CSH

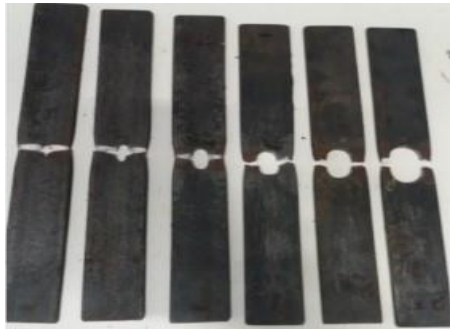


Figure 4-31: Failure mode of conditioned non strengthened steel element with CSH

#### 4.5.4 Behavior of CFRP strengthened steel element with CSH under fatigue load

The specimens were designed in accordance with ASTM D 790 with the use of steel plates with a cross-section of 40 mm (width) x 5 mm (thickness) (Figure 4-1). The length of the plate member was chosen to be 280 mm and the effective span was considered as 240 mm due to a restriction in the flexural cyclic loading apparatus (Figure 4-7). A 200 mm long unidirectional normal modulus CFRP fabric was used to strengthened the CSH. A total of twelve specimens were tested to determine the characteristics of CFRP-strengthened steel plate specimens with CSH subjected to low cycle fatigue load. The schematic diagram of CFRP - strengthened specimens and typical test specimen shown in Figure 4-32.

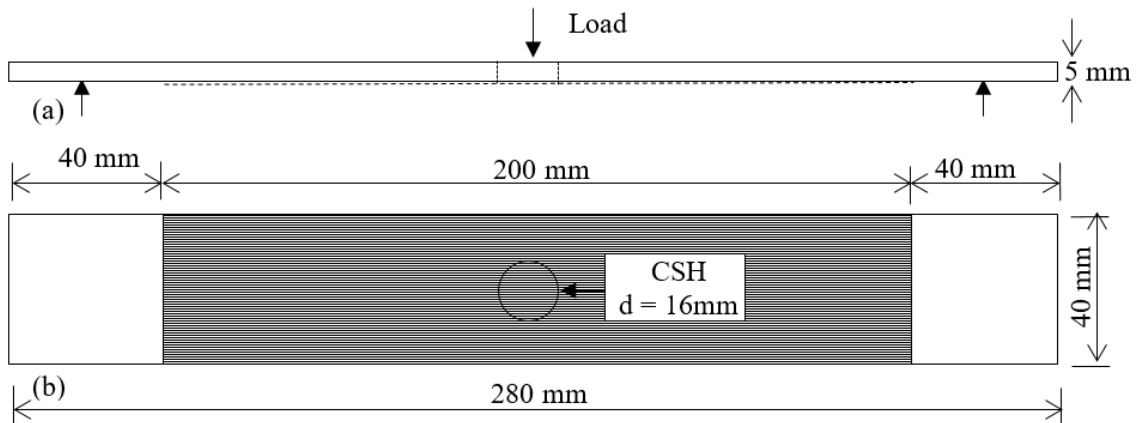


Figure 4-32: Schematic diagram of the conditioning steel element with CFRP strengthened CSH (a) elevation (b) plane view (c) typical test specimen

In this test, the diameter to width ratio was considered as a main variable and it varied from 0.1 to 0.6 in 0.1 steps. Table 4.11 summarizes the retained average yield strength together with the variation of different diameter to width ratio of the test results.

Table 4.11: Retained average strength of CFRP strengthened conditioned CSH varies with the diameter to width ratio

<b>Diameter to width ratio of CSH (d/b)</b>	<b>Average tensile strength (kN)</b>	<b>Average strength (MPa)</b>
0.1	99.6	498.0
0.2	94.0	470.0
0.3	89.1	445.5
0.4	81.0	405.0
0.5	71.2	356.0
0.6	54.0	270.0

Figure 4-33 indicates the residual strength variation with exposure duration. As shown in Figure 4-33, when the diameter to width ratio is increased, the average strength decreases. Failure mode are shown in Figure 4-34.

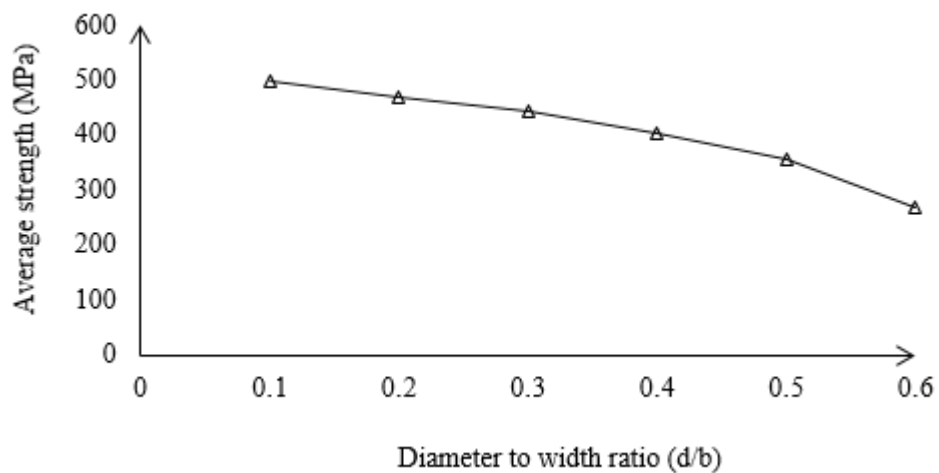


Figure 4-1: Retained average strength variation of CFRP strengthened conditioned CSH with respect to diameter to width ratio



Figure 4-34: Failure mode of conditioned CFRP strengthened CSH

#### 4.5.5 Comparison of strength variation of non-strengthened and CFRP strengthened CSH

The test results of the conditioning and non-conditioning steel element for non-strengthened and CFRP strengthened CSH were compared as shown in Table 4-12. It summarizes the tensile load values together with the variation of different CSH diameter to width ratio from the range of 0.1 to 0.6.

Table 4.12: Average strength gained by CFRP material under cyclic flexural loads

Diameter to width Ratio (d/b)	Number of test	Retained average strength (MPa)				Results	
		Non conditioned		Conditioned		Strength losses %	Strength gain by CFRP %
		Non strengthened	CFRP strengthened	Non strengthened	CFRP strengthened		
0.1	2	433	542	375	498	13	33
0.2	2	412	516	355	470	14	32
0.3	2	393	464	335	445	15	33
0.4	2	368	420	300	405	18	35
0.5	2	317	370	245	356	22	44
0.6	2	248	280	185	270	25	45

Figure 4-35 shows the average tensile strength variation with respect to diameter to width ratio under fatigue. As shown in Figure 4-35, when the diameter to width ratio is increased, the average yield strength decreases. The test result of tensile strength

shows significant decreases with the diameter to width ratio in the range from 0.1 to 0.6. in 0.1 steps.

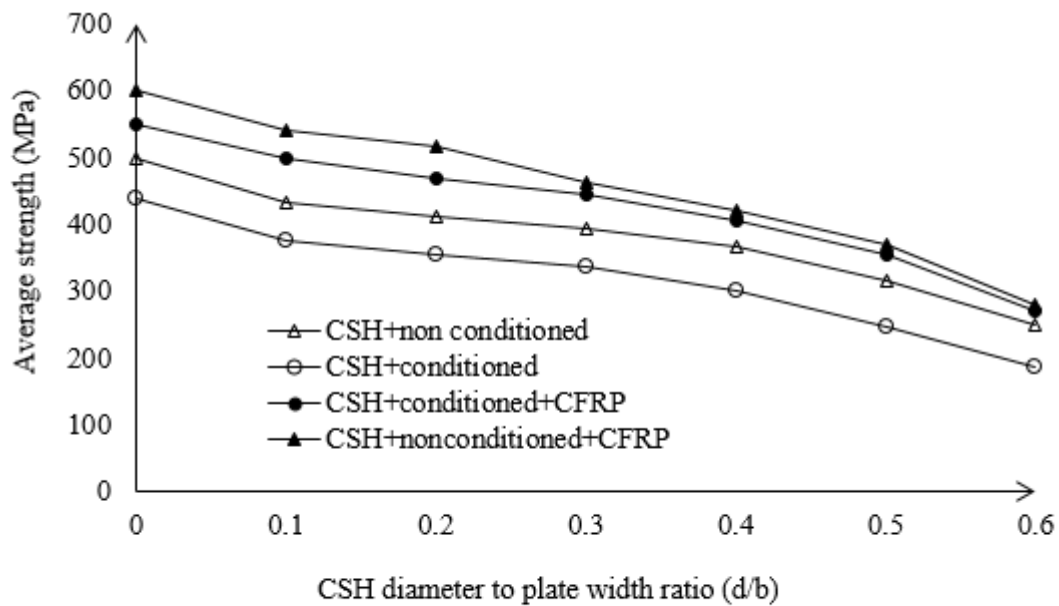


Figure 4-35: Comparison of strength gains for non-strengthened and CFRP strengthened CSH

CSH causes the reduction in stiffness due to the removal of materials from the specimen. In addition, fatigue stress near the hole significantly influences to change the material properties. According to the Figure 4-35, the retained tensile strength shows a non-linear behavior with respect to the diameter to width ratio ( $d/b$ ) of CSH, as material becomes weak due to fatigue and stiffness changes. When a CSH is placed at the crack tip, an average of 13 % to 25 % loss in yield stress is recorded compared to the non-conditioned situation. This is mainly due to the material failure resulted from repetitive loading. When the CSH covered with CFRP which laid in the tensile direction, the strength gain was reported up to 31% while recovering the strength losses due to the cyclic load exposure. This reduction can be considered as the stiffness lost due to material removal for the CSH while the strength losses are due to fatigue. Therefore, it has a potential to enhance stiffness as well as the restoration of fatigue bearing capacity of the material at the same time. Therefore, CFRP laminate had caused to reduce the stress concentrations and had enhanced overall stiffness of the composite material. However, the number of fiber layers, the module of the material, fiber direction, the

bond length and environmental conditions at the installation phase would significantly influence the overall performance of the strengthened system (Abeygunasekara et al., 2019). In case of conditioned CFRP strengthened specimens, there was no failure reported in steel, adhesive and the CFRP layer. However, steel starts to crack near the CSH and the failure modes are shown in Figure 4-34. The crack appears in perpendicular direction to the applied tensile load since both sides of the CSH are weakest regions of the specimen due to fatigue. Figure 4-36 (a) and Figure 4-36 (b) shows the percentage of strength gain by CFRP/steel and percentage of strength reduction on the CSH due to fatigue.

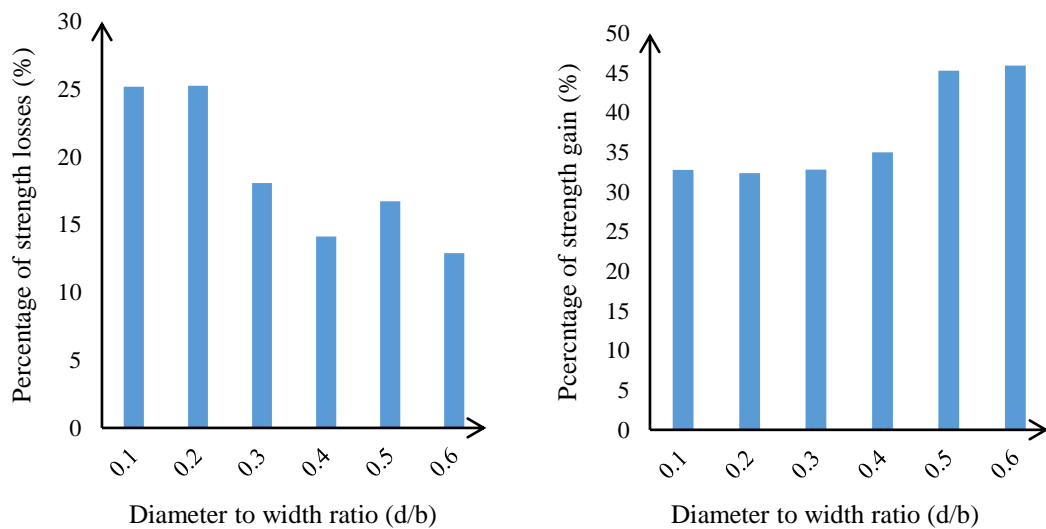


Figure 4-36: Average strength with respect to diameter to width ratio  
(a) losses due to fatigue (b) gain by CFRP

#### 4.5.6 Strain variation of non-strengthened CSH under fatigue load

The specimens were designed in accordance with ASTM D 790 with the use of steel plates with a cross-section of 40 mm (width) x 5 mm (thickness) (Figure 4-1). The length of the plate member was chosen to be 280 mm and the effective span was considered as 240 mm due to a restriction in the flexural cyclic loading apparatus (Figure 4-7). A total of six specimens were tested to determine the characteristics of non-strengthened steel plate specimens with CSH subjected to low cycle fatigue load. A strain gauge was fixed near the CSH and the schematic diagram of non-strengthened specimens and typical test specimen shown in Figure 4-37.

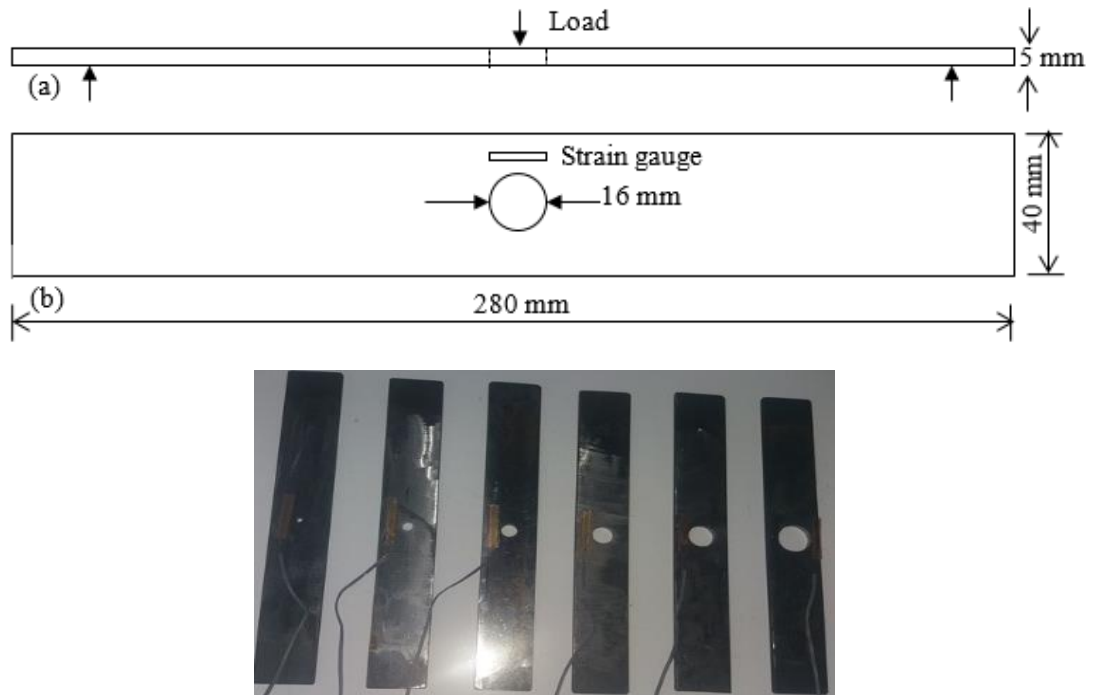
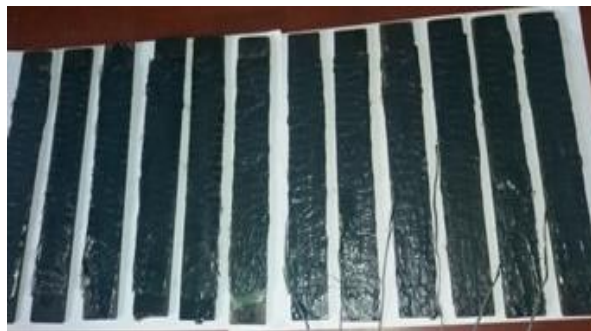
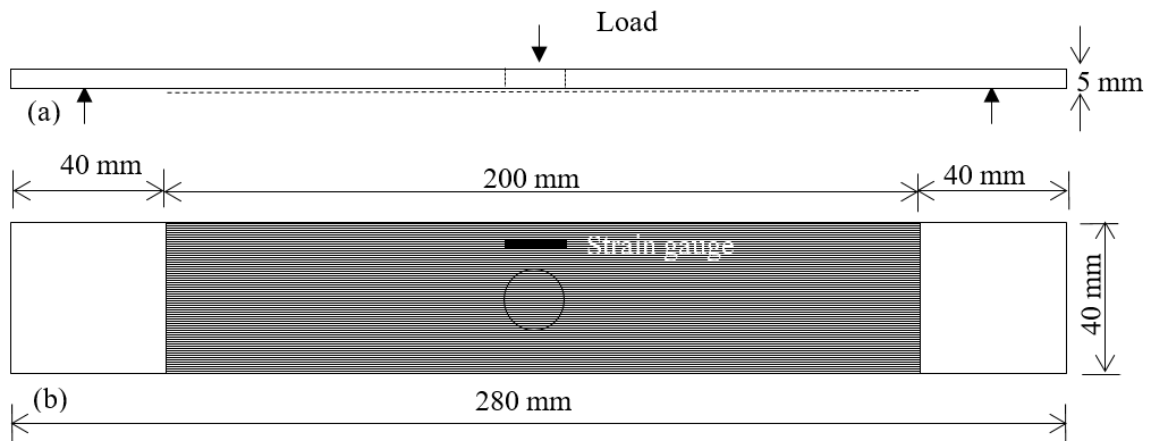


Figure 4-37: Schematic view of the non-strengthened strain gauge attached CSH specimen (a) elevation (b) plane view (c) typical test specimen

#### 4.5.7 The strain variation of CFRP strengthened CSH under fatigue load

The specimens were designed in accordance with ASTM D 790 with the use of steel plates with a cross-section of 40 mm (width) x 5 mm (thickness) (Figure 4-1). The length of the plate member was chosen to be 280 mm and the effective span was considered as 240 mm due to a restriction in the flexural cyclic loading apparatus (Figure 4-1). A 200 mm long unidirectional normal modulus CFRP fabric was used to strengthened the CSH. A total of six specimens were tested to determine the characteristics of CFRP-strengthened steel plate specimens with CSH subjected to lowcycle fatigue load. A strain gauge was fixed near the CSH and the schematic diagram of CFRP- strengthened specimens and typical test specimen shown in Figure 4-38.



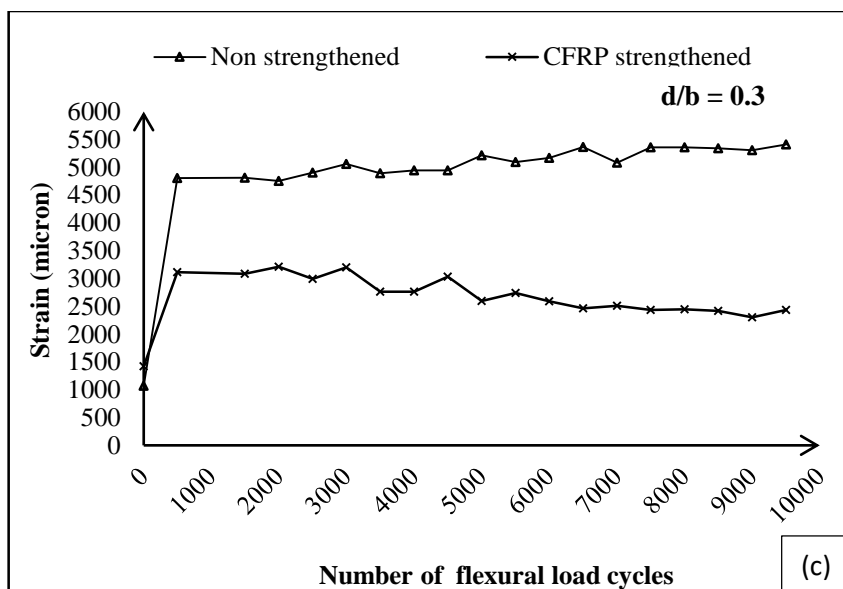
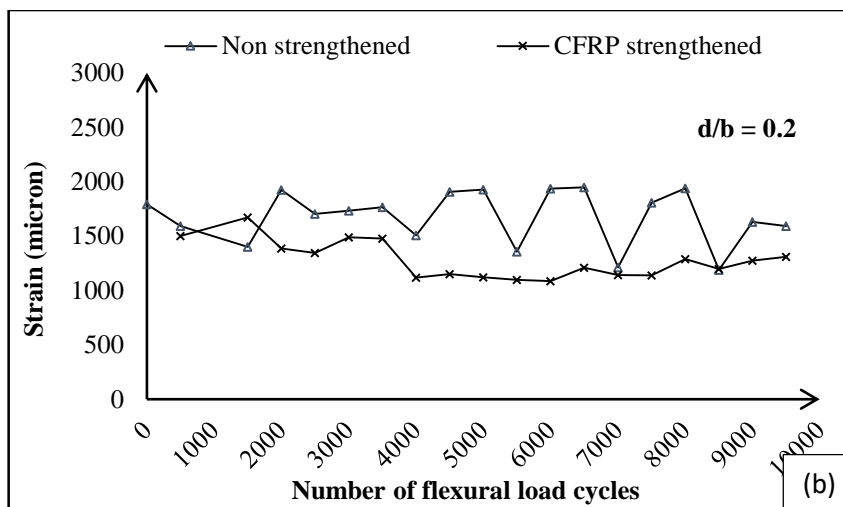
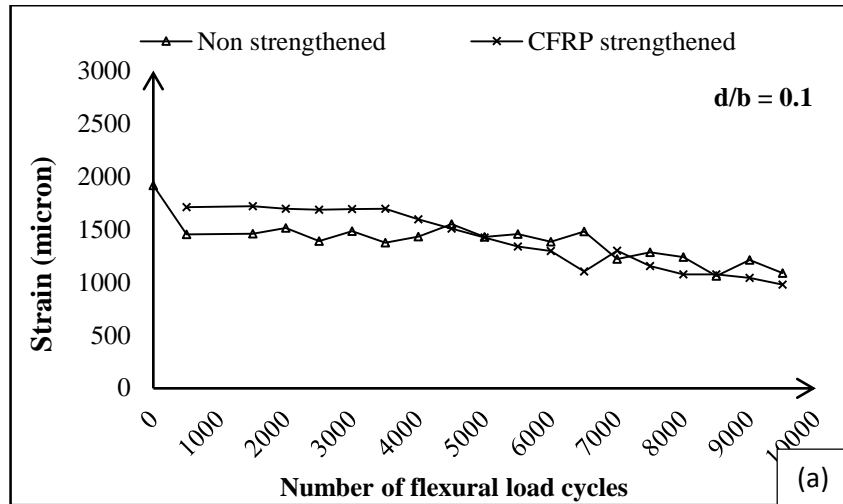
(c)

Figure 4-38: Schematic view of the CFRP strengthened strain gauge attached CSH specimen (a) elevation (b) plane view (c) typical specimen

#### 4.5.8 Comparison of strain behavior of non-strengthened and CFRP strengthened CSH

Figure 4-39 shows the strain distributions of the conditioning steel element with non-strengthened and CFRP strengthened CSH. All specimens show similar pattern of strain distributions; that, increases with number of load cycles. It can be seen from all figures that the strain level reaches an almost constant after the number of cycles exceeds a certain value as shown in Figure 4-39.





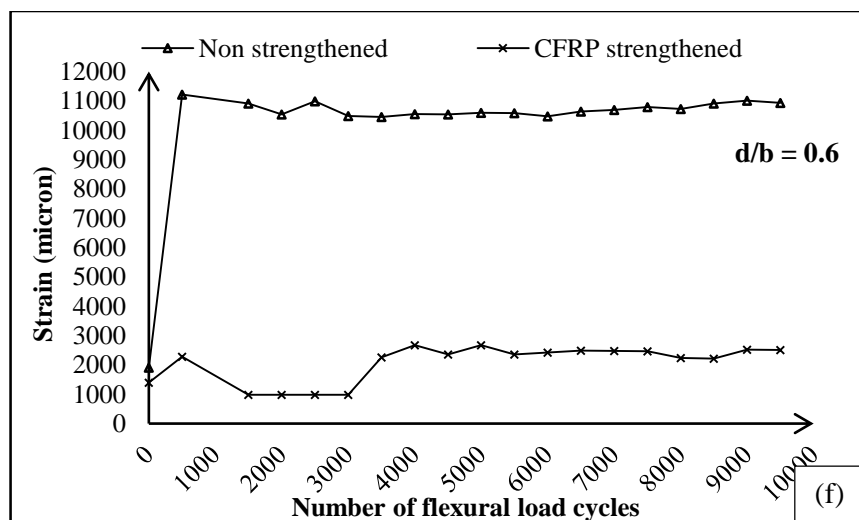
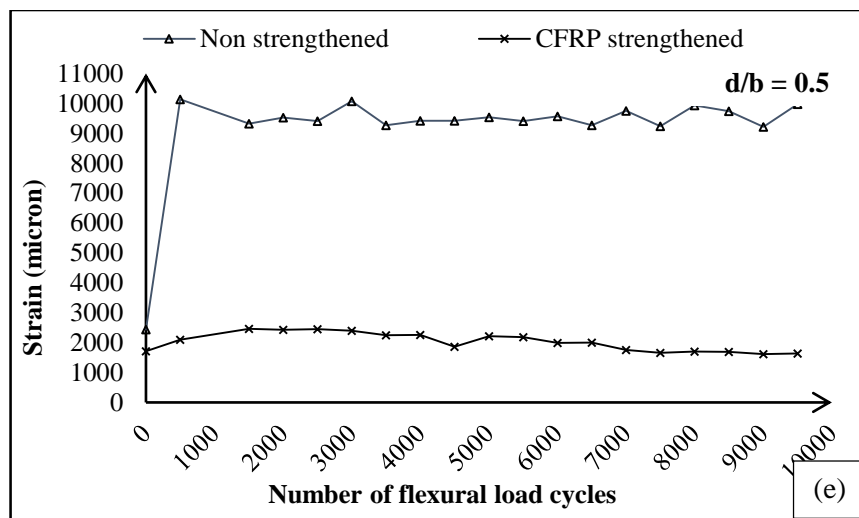
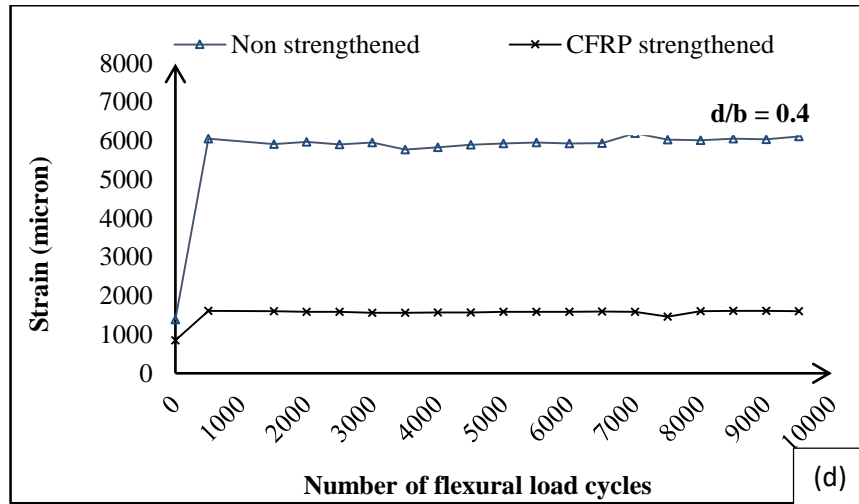


Figure 4-39: Strain variations with number of flexural cycles when  $d/b$  is: (a) 0.1 (b) 0.2 (c) 0.3 (d) 0.4 (e) 0.5 (f) 0.6

Figure 4-39 shows the strain variation with number of flexural load cycles. According to the Figure 4-39 (a) and Figure 4-39 (b), no significant deviation was noted in strain variation of both strengthened and non-strengthened samples for the applied load intensity. This shows that the bond effects of CFRP application in CSH is negligible due to the smallest diameter to width ratios of 0.1 and 0.2 because steel substance can bear the strain itself without using the composite action. However, when the diameter to width ratio increases from 0.3 to 0.6, the strain variation with CFRP strengthened CSH exhibits a significant reduction with respect to non-strengthened CSH as shown in Figure 4-39 (c) to Figure 4-39 (f) indicating the effective stress transfer and load sharing ability of the CFRP sheet.

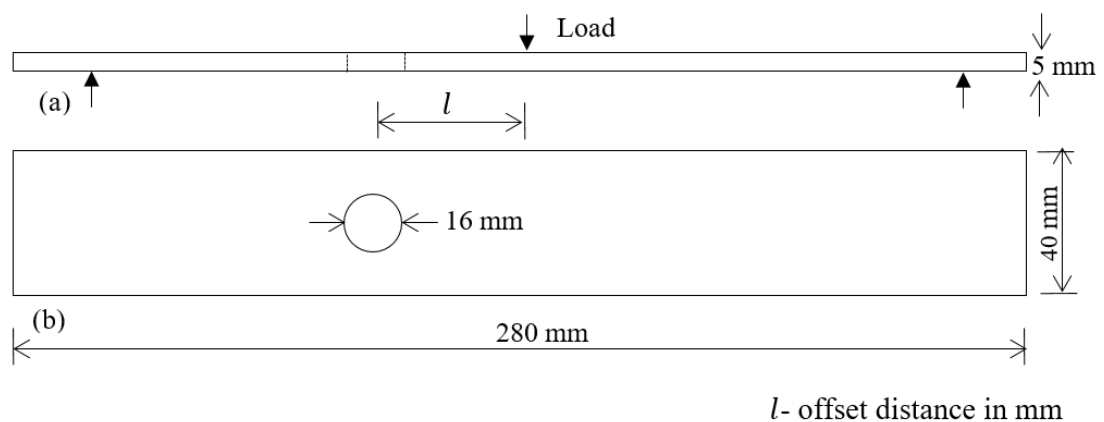
#### **4.6 Effects due to distance from mid-point to CSH**

A total of thirty-six steel specimens with change in position of the CSH were conditioned up to 10,000 flexural load cycles with 2 kN amplitude and 5 Hz frequency (Series S<sub>5</sub> and S<sub>6</sub>). Eighteen of them were strengthened with 200 mm long CFRP layer. The remaining samples were non-strengthened and considered as controlled specimens. In these two test series, the distance from loading point to CSH was considered as the main variable and a CSH with 16 mm diameter was placed at the different locations on the main axis of the specimen. Location of CSH varied from 20 mm to 100 mm in 20 mm steps. At the end of exposure, the retained yield strength of samples was noted. The strain variation was measured using data logger during conditioning.

A total of eighteen samples were tested and all of them were conditioned control samples (Series, S<sub>5</sub>). Only non-strengthened samples were test in this series. Each samples conditioned up to 10,000 flexural load cycles with 2 kN amplitude and 5 Hz frequency. In this test series, the distance from loading point to CSH was considered as the main variable and 16 mm diameter CSH was placed at the different locations on the main axis of the specimen. Location of CSH varied from 20 mm to 100 mm in 20 mm steps. The strain variation was measured using data logger during conditioning and the average tensile load was determined using universal tensile test apparatus end of the conditioning (Figure 4-8).

#### 4.6.1 Fatigue behavior of non-strengthened CSH with respect to distance from the mid - point

The specimens were designed in accordance with ASTM D 790 with the use of steel plates with a cross-section of 40 mm (width) x 5 mm (thickness) (Figure 4-1). The length of the plate member was chosen to be 280 mm and the effective span was considered as 240 mm due to a restriction in the flexural cyclic loading apparatus (Figure 4-7). CSH with 16 mm diameter was placed at the different locations on the main axis of the specimen. Location of CSH varied from 20 mm to 100 mm in 20 mm steps. At the end of exposure, the retained average strength of samples was noted. The schematic diagram and typical test specimens indicated in Figure 4-40



(c)

Figure 4-40: Schematic view of the non-strengthened offset CSH specimen  
(a) elevation (b) plane view (c) typical test specimen

In this test, the distance from loading point to CSH was considered as the main variable and location of CSH varied from 20 mm to 100 mm in 20 mm steps. Table 4.13 summarizes the retained average strength together with the variation of offset distances from the mid-point along longitudinal axis of specimen.

Table 4.13: Retained average strength variation with the location of the non-strengthened CSH

CSH offset distance from the mid-point (mm)	Average load (kN)	Average strength (MPa)
0	33.6	167.8
20	45.7	228.3
40	47.0	234.8
60	56.9	284.5
80	77.6	388.0

Figure 4-41 indicates the average strength variation with exposure duration. As shown in Figure 4-41, when the number of flexural load cycles is increased, the average retained average strength increases. Failure modes are shown in Figure 4-42.

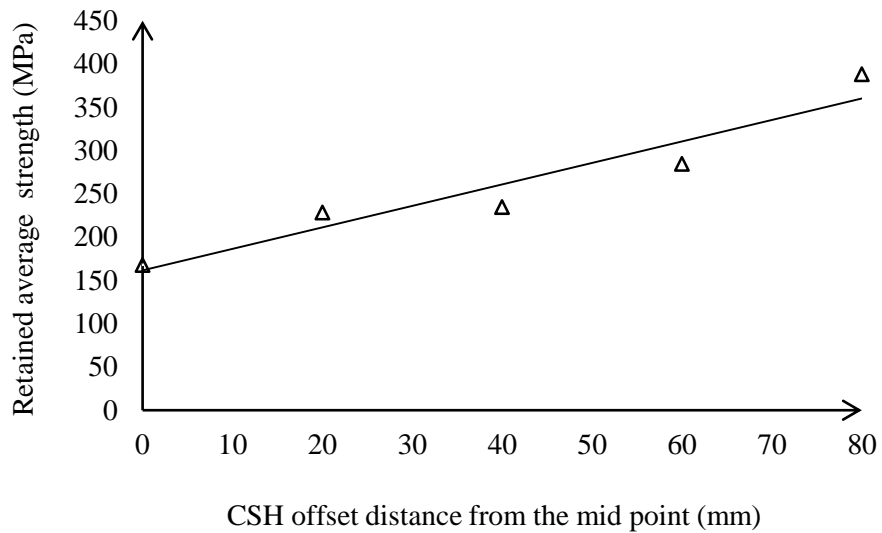


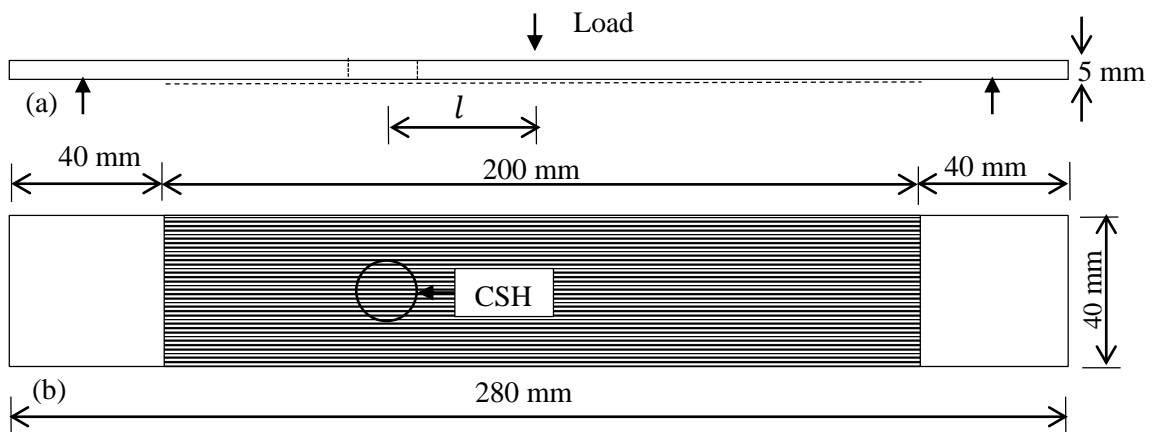
Figure 4-41: Variation of retained average strength with offset distance for strengthened samples



Figure 4-42: Failure mechanisms with offset distance for non-strengthened samples

#### 4.6.2 Fatigue behavior of CFRP-strengthened CSH with respect to distance from the mid point

A total of eighteen samples were tested and all of them were conditioned control samples (Series S-6). Each samples conditioned up to 10,000 flexural load cycles with 2 kN amplitude and 5 Hz frequency. In this test series, the distance from loading point to CSH was considered as the main variable and 16 mm diameter CSH was placed at the different locations on the main axis of the specimen. Location of CSH varied from 20 mm to 100 mm in 20 mm steps. Each of them were strengthened with 200 mm long CFRP layer. The average tensile load was determined using universal tensile test apparatus end of the conditioning (Figure 4-8). The schematic diagram and typical test specimens are indicated in Figure 4-43.





(c)

Figure 4-43: Schematic view of the CFRP strengthened offset CSH specimen  
(a) elevation (b) plane view (c) typical test specimen

In this test, the distance from loading point to CSH was considered as the main variable and location of CSH varied from 20 mm to 100 mm in 20 mm steps. Table 4.14 summarizes the retained average strength together with the variation of offset distances from the mid-point along longitudinal axis of specimen.

Table 4.14: Retained average strength variation with the location of the CFRP strengthened CSH

<b>CSH offset distance from the mid-point (mm)</b>	<b>Average load (kN)</b>	<b>Average strength (MPa)</b>
0	58.0	290.0
20	62.5	312.5
40	63.7	318.5
60	70.5	352.5
80	77.6	388.0

Figure 4-44 indicates the residual strength variation with exposure duration. As shown in Figure 4-44, when the offset distance is increased, the average retaining strength also increases.

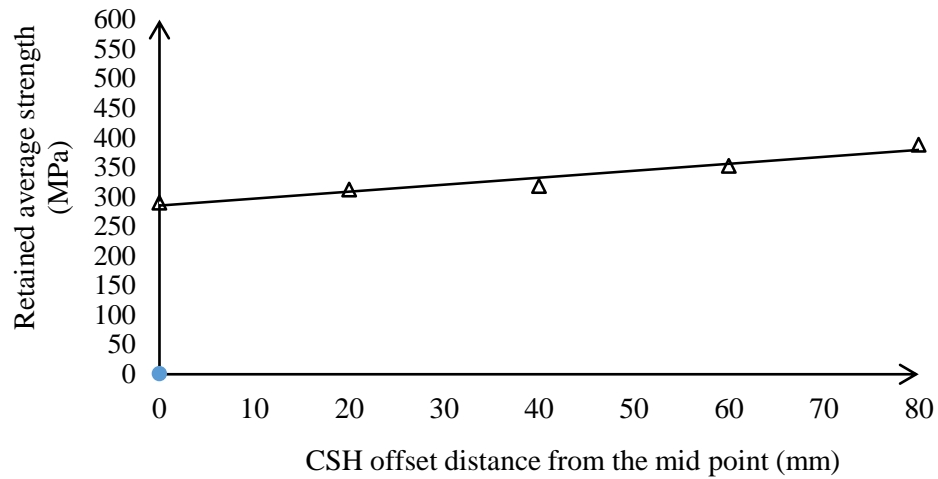


Figure 4-44: The average strength variation with the location of the CSH



Figure 4-45: Failure mode of CFRP strengthened offset CSH

#### 4.6.3 Comparison of fatigue behavior of CSH with respect to distance

A summary of the laboratory test results for non-strengthened and CFRP strengthened steel specimens with the position of CSH is presented in Table 4.15. The table lists the offset distance from the midpoint of specimen, average retained tensile load for all test specimen and strength gain by CFRP strengthened steel specimen. It summarizes the tensile load values together with the variation of location of CSH from the range of 20 mm to 100 mm. Offset distance varied in the range of 20 mm steps. The average tensile strength due to the location compared with non-strengthened and CFRP strengthened steel plate.



Table 4.15: Retained average strength, gain with CFRP strengthened offset CSH

CSH offset distance from the mid point (mm)	Number of test	Non strengthened CSH	CFRP strengthened CSH	Strength gain by CFRP (%)
0	2	167.8	290.0	42
20	2	228.3	312.5	27
40	2	234.8	318.5	26
60	2	284.5	352.5	19
80	2	328.5	388.0	15

Figure 4-46 shows the retained average strength variation of CFRP strengthened and non-strengthened conditioning steel element with CSH position. The number of applied cycles subjected to cyclic flexural loading.

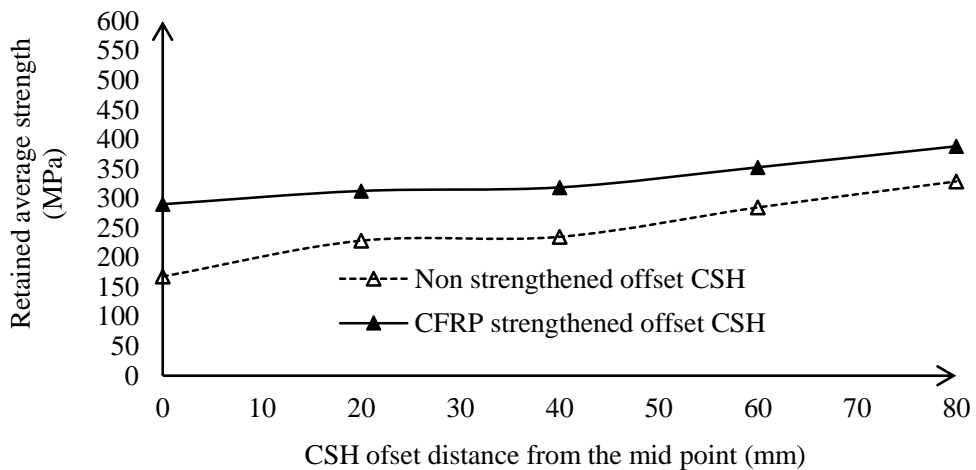


Figure 4-46: Variation of retained average strength gain with offset distance for non-strengthened and CFRP strengthened samples

A similar trend of stress variation with respect to ratio between offset distance of CSH to the span of plate was noted from both strengthened and non-strengthened samples. The main purpose of these test series were to compare the retained tensile stress after exposure to the maximum low cycle flexural fatigue cycles to quantify the effectiveness of CFRP application depending on the location of CSH. The fatigue sensitive zone is near the loading point and this region can be considered as a high stress area of the specimen because the flexural cyclic load helps to increase the

stresses intensity near the mid-point. When the offset distance increases reference to the loading point (midpoint of the specimen), the stress concentrations near CSH reduces. The graphs provide convincing evidence on such behaviour. CFRP supports to reduce the stress concentration as well as to enhance the tensile strength of the specimen. As a result, the CFRP strengthened specimens show a significant yield strength gain compared to the non-strengthened specimen. Covering the CSH at any location using a CFRP patch will enhance the strength and fatigue performance with eliminating negative effects resulted from drilling the member to form a CSH. When performing the tensile test on conditioned specimens, a crack initiation was noted near the CSH and started to propagate in transverse direction with a slight inclination resulting delamination of CFRP sheet as shown in Figure 4-45. Gope et al.,(2013) have investigated the effects of offset distance of crack tip of CSH of non conditioned and non strengthened steel element and they reported a similar failure mode in this study. Figure 4-47 shows the percentage of strength gain by CFRP strengthened CSH with respect to the position of CSH.

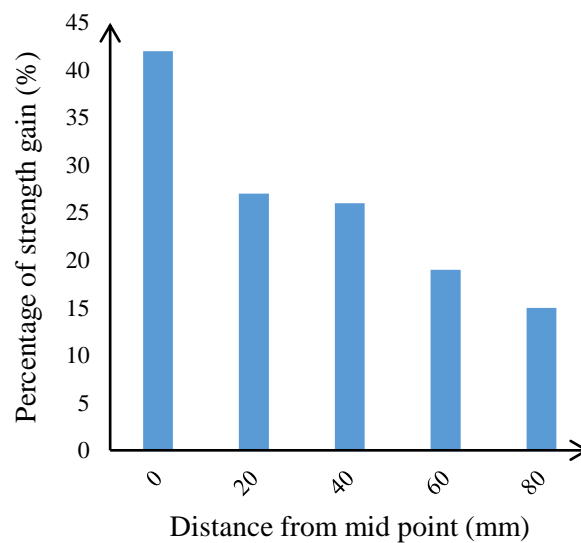


Figure 4-47: Percentage strength gain by CFRP strengthened with respect to CSH position

#### 4.6.4 Strain variation of non-strengthened CSH with respect to offset distance

The purpose of the experimental activity was to estimate the strain variation of steel element with position variation of CSH. A total of six rectangular cross sectionals flat

steel plates were prepared for this investigation. Dimensions of specimens are 40 mm x 5 mm cross section with 280 mm length was used for this. In this test series, the distance from loading point to CSH was considered as the main variable and 16 mm diameter CSH was placed at the different locations on the main axis of the specimen. Position of CSH from the midpoint of specimen varied from 20 mm to 100 mm in 20 mm steps. A Strain gauge was fixed near the CSH and the schematic view is shown in Figure 4-48 and typical test specimens are indicated in Figure 4-49.

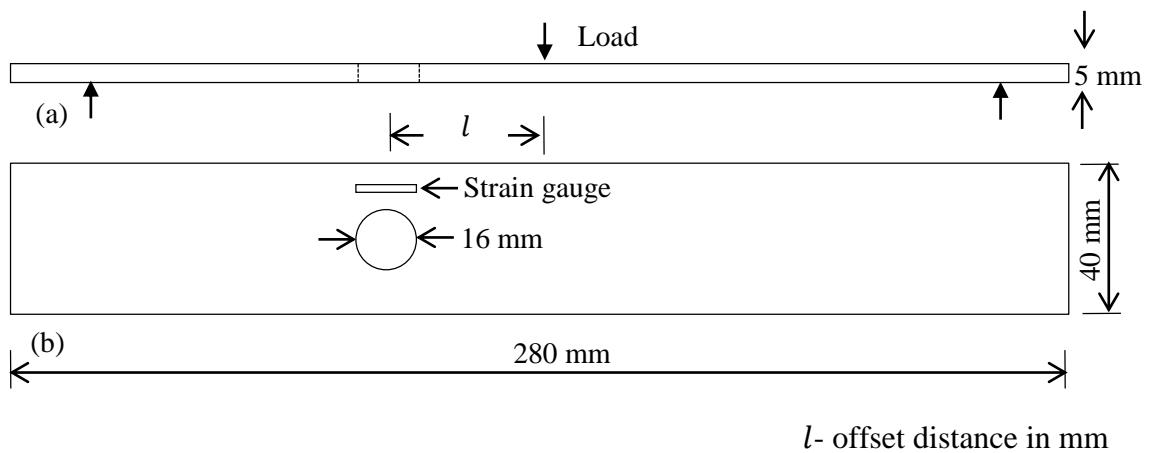
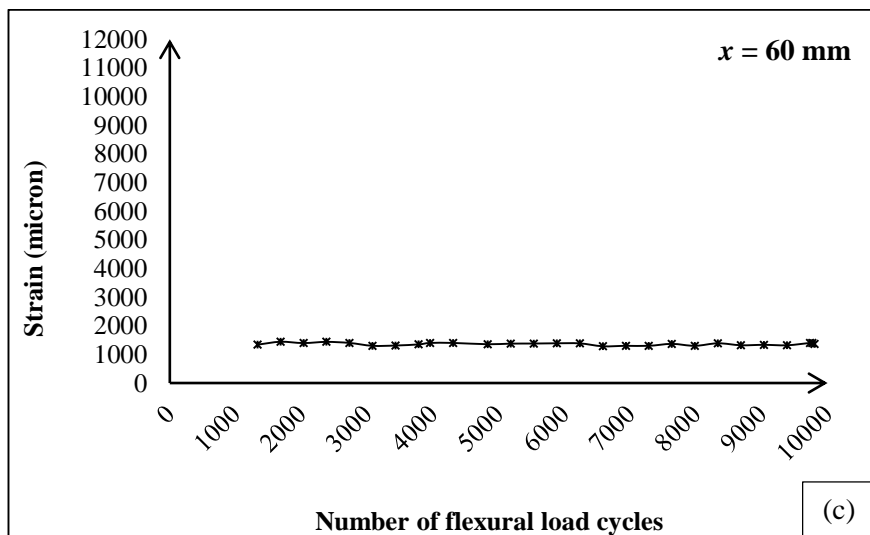
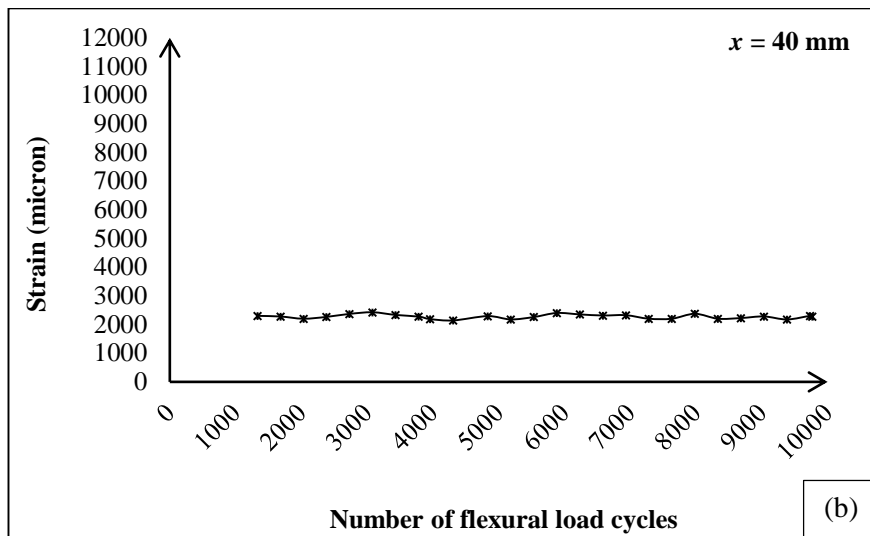
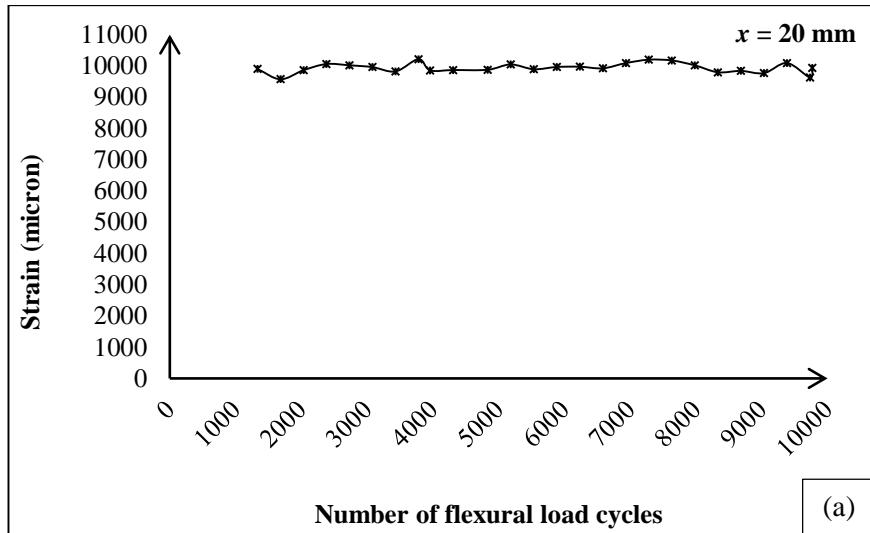


Figure 4-48: Schematic view of the non-strengthened strain gauge attached offset CSH specimen (a) elevation (b) plane view



Figure 4-49: Typical specimen of non-strengthened strain gauge attached offset CSH

The average strain near the CSH in steel substance noted at the end of each pre-determined exposure cycles is plotted in Figure 4-50 based on the position of CSH.



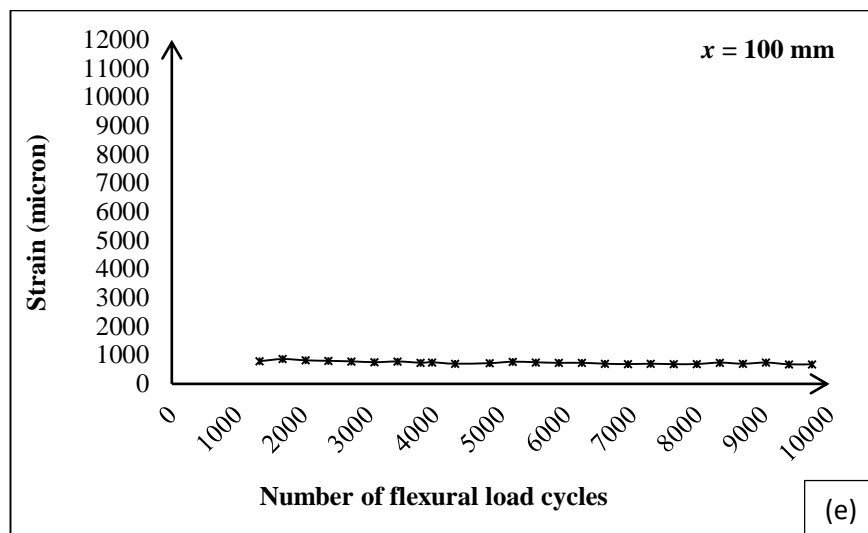
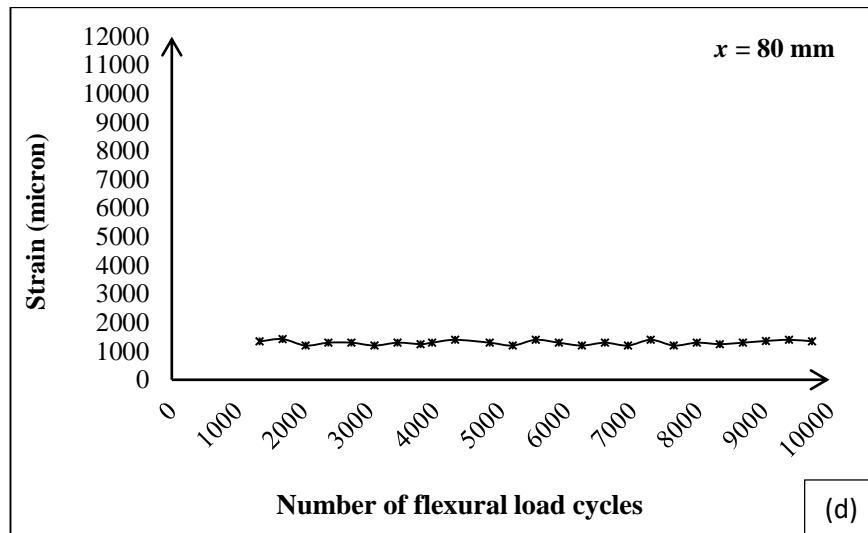


Figure 4-50: Strain variations with offset distance of non-strengthened CSH  
When  $x$  is ; (a) 20 mm (b) 40 mm (c) 60 mm (d) 80 mm (e) 100 mm

The strain distribution for non-strengthened CSH in different positions was conditioned up to 10,000 flexural load cycles are shown in Figure 4-50. According to the graph, a considerable amount of strain variation can be observed up to 100 mm distance from the mid-point. However, beyond the 60 mm from mid-point it did not give significant deviation on the CSH.

#### 4.6.5 Strain variation of CFRP strengthened CSH with respect to offset distance

The purpose of the experimental activity was to estimate the strain variation of steel element with CFRP strengthened offset CSH. A total of six rectangular cross sectional flat steel plates were prepared for this investigation. Dimensions of specimens are 40 mm x 5 mm cross section with 280 mm length was used for this. In this test series, the distance from loading point to CSH was considered as the main variable and 16 mm diameter CSH was placed at the different locations on the main axis of the specimen. Location of CSH varied from 20 mm to 100 mm in 20 mm steps. A Strain gauge was fixed near the CSH and 200 mm long CFRP layer was attached to the bottom of the specimen. The schematic view and typical test specimens are indicated in Figure 4-51.

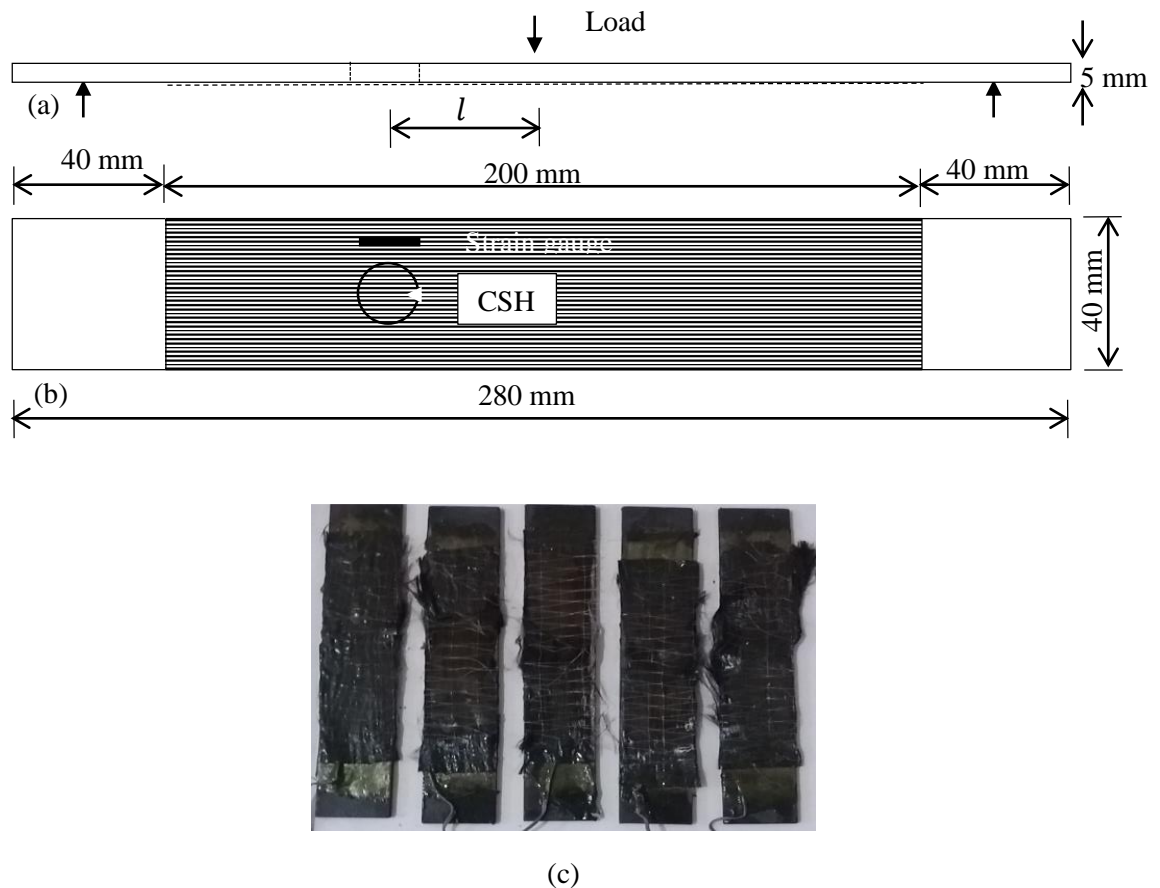
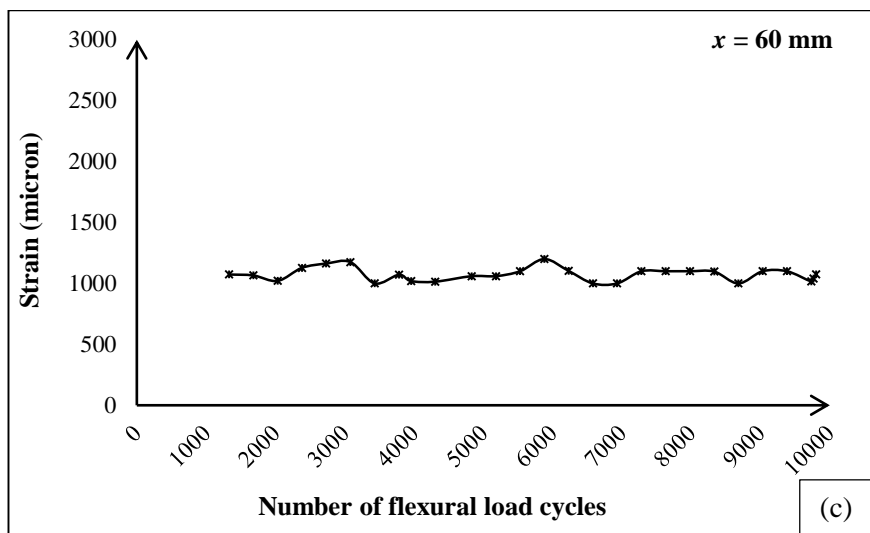
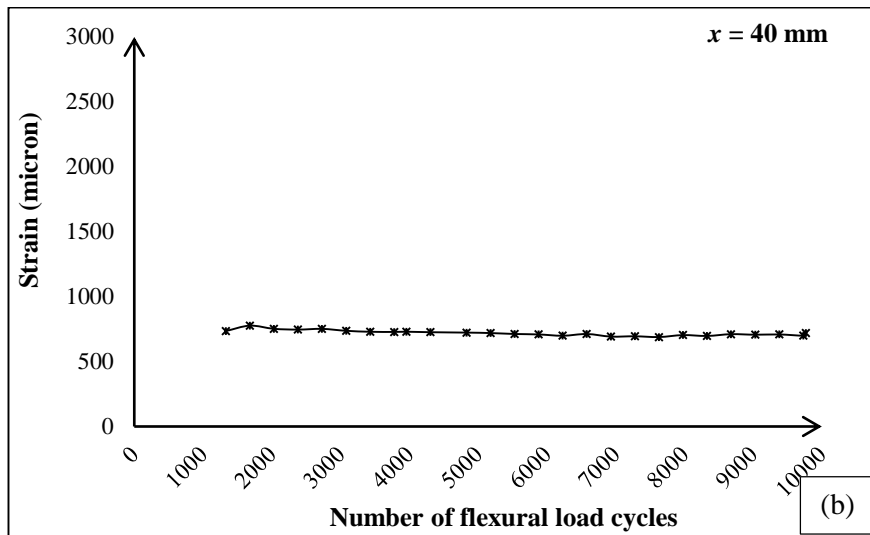
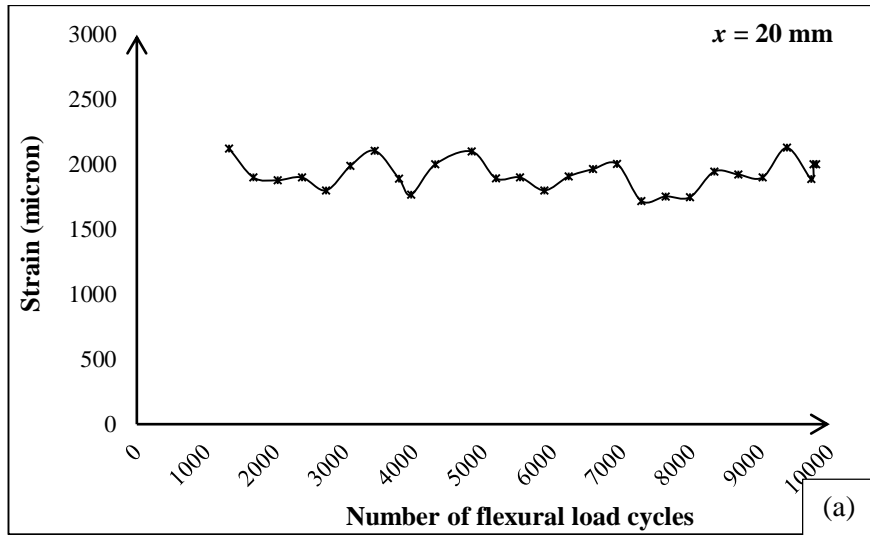


Figure 4-51: Schematic view of CFRP-strengthened strain gauge attached offset CSH  
(a) elevation (b) plane view (c) typical specimen

The average strain near the CSH in steel substance noted at the end of each pre-determined exposure cycles is plotted in Figure 4-52 based on the position of CSH.



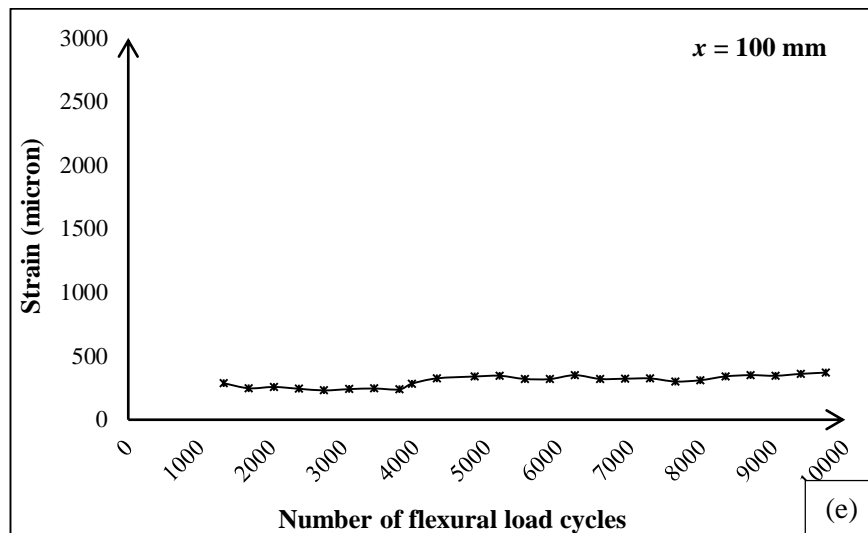
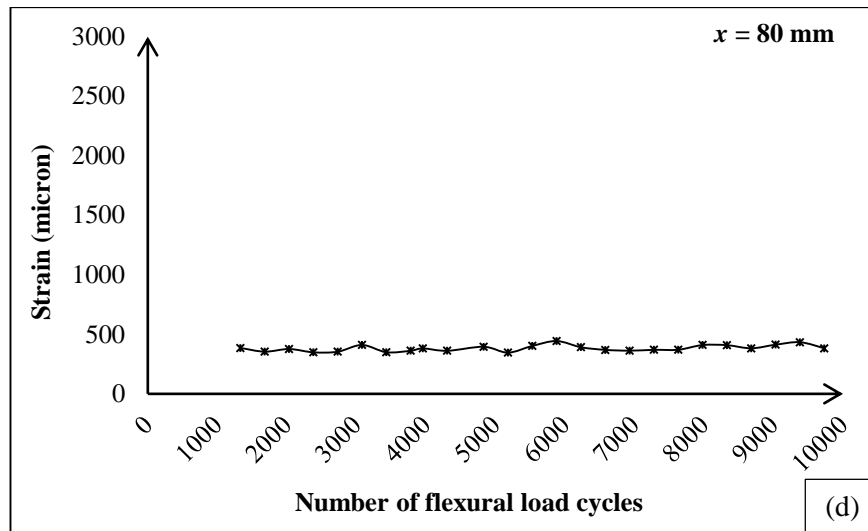


Figure 4-52: Strain variations with offset distance of CFRP-strengthened CSH when  $x$  is; (a) 20 mm (b) 40 mm (c) 60 mm (d) 80 mm (e) 100 mm

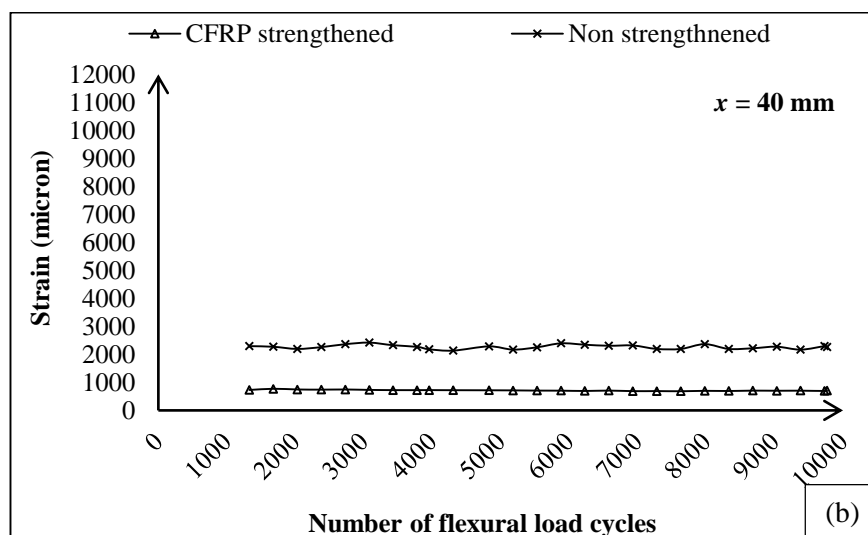
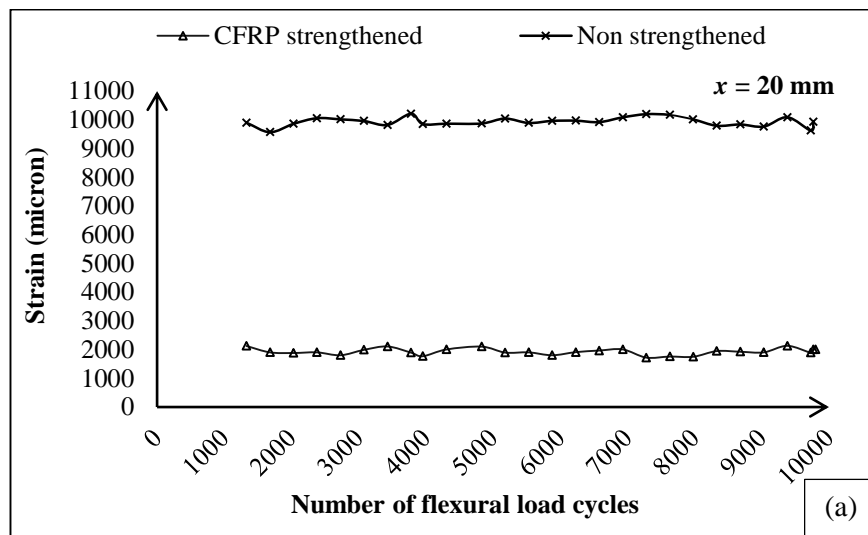
The strain distribution for CFRP strengthened CSH in different positions were conditioned up to 10,000 flexural load cycles and compared Figure 4-49. According to the graph, a considerable amount of strain was controlled by the CFRP and it can be observed up to 60 mm distance from the mid-point. However, beyond the 60 mm from mid-point it did not give significant effects on the CSH. This clearly indicates the strain control ability of CFRP layer. Hence, the CFRP patches can be successfully applied to dissipate the strain when the member with offset CSH subjects to cyclic fatigue load. This well helps to accommodate the tensile load on the specimen resulting



to delay the re-cracking of the CSH as well as to enhance the fatigue durability which helps to expand the service life of member.

#### 4.6.6 Comparison of strain behavior of non-strengthened and CFRP strengthened CSH

Figure 4-53 shows the strain distributions of the conditioning steel element with non-strengthened and CFRP strengthened CSH. All specimens show similar pattern of strain distributions; that, increases with number of load cycles. It can be seen from all figures that the strain level reaches an almost constant after the number of cycles exceeds a certain value as shown in Figure 4-53.



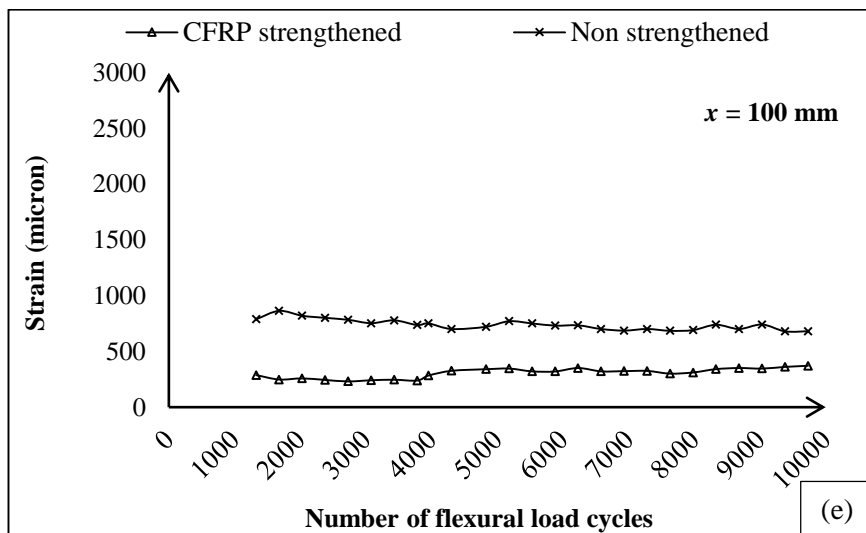
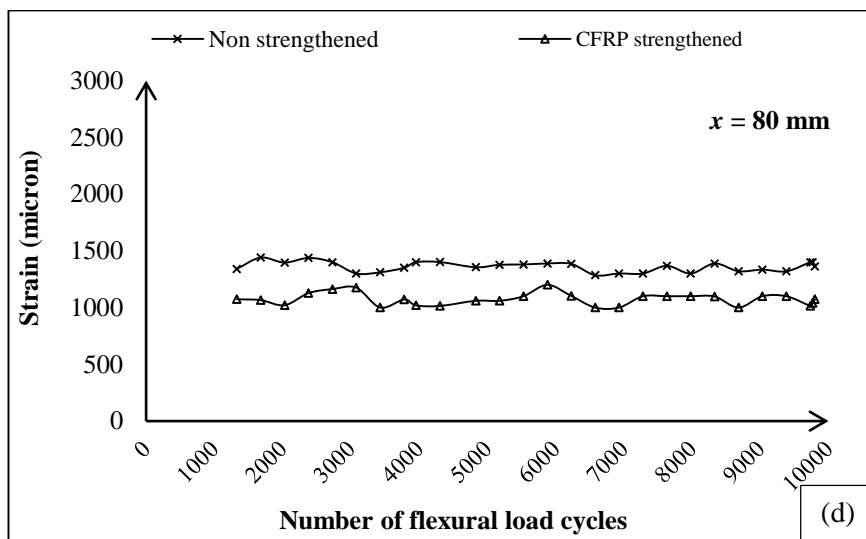
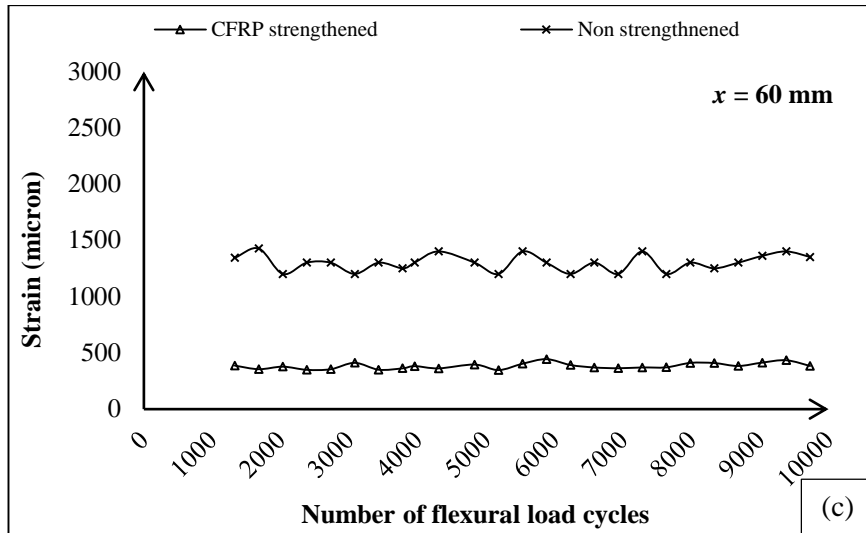


Figure 4-53: Comparison of strain variations with offset distance for non-strengthened and CFRP strengthened CSH when  $x$  is : (a) 20 mm (b) 40 mm (c) 60 mm (d) 80 mm (e) 100 mm

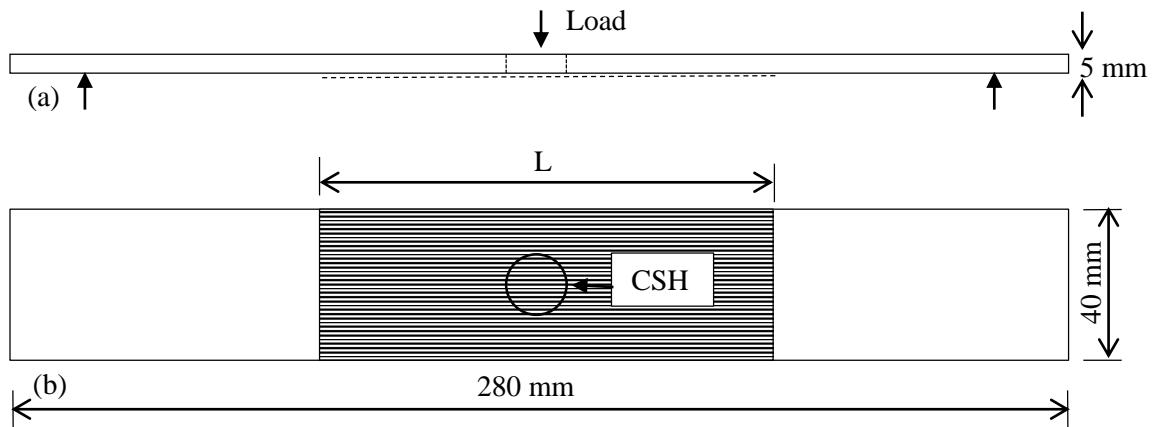
The strain distribution for non-strengthened and CFRP strengthened CSH in different positions were conditioned up to 10,000 flexural load cycles and compared in Figure 4-53. According to the graph, a considerable amount of strain was controlled by the CFRP and it can be observed up to 60 mm distance from the mid-point. However, beyond the 60 mm from mid-point it did not give significant effects on the CSH. This clearly indicates the strain control ability of CFRP layer. Hence, the CFRP patches can be successfully applied to dissipate the strain when the member with offset CSH subjects to cyclic fatigue load. This will help to accommodate the tensile load on the specimen resulting to delay the re-cracking of the CSH as well as to enhance the fatigue durability which helps to expand the service life of member.

#### **4.7 Fatigue behavior of CFRP strengthened steel element with respect to bond length**

A total of twenty-four steel specimens with and without CSH were conditioned up to 10,000 flexural load cycles with 2 kN constant amplitude and 5 Hz frequency (Series S7). In these two test series the length of CFRP was considered as the main variable and it varied from 40 mm to 240 mm in 40 mm step. At the end of exposure, the retained tensile strength of samples was noted (Figure 4-8).

##### **4.7.1 Fatigue behavior of CFRP strengthened CSH with respect to bond length**

The specimens were designed in accordance with ASTM D 790 with the use of steel plates with a cross-section of 40 mm (width)  $\times$  5 mm (thickness) (Figure 4-1). The length of the plate member was chosen to be 280 mm and the effective span was considered as 240 mm due to a restriction in the flexural cyclic loading apparatus (Figure 4-7). A 16 mm diameter CSH was placed at the mid-span of specimens. A total of twelve specimens were tested to determine the characteristics of bond length effects on steel plate specimens with CSH subjected to low cycle fatigue load. The schematic diagram of CFRP - strengthened specimens and typical test specimen shown in Figure 4-54.



L- Bond length in mm



Figure 4-54: Schematic view of the CFRP strengthened specimen with different bond length (Scale 1:2) (a) elevation (b) Plane view (c) typical specimen

In this test, the CFRP bond length was considered as the main variable and it varied from 20 mm to 120 mm in 20 mm steps. Table 4-16 summarizes the retained average tensile strength together with the variation of CFRP bond length from the mid-point along longitudinal axis of specimen.

Table 4.16: Retained average strength varies with the length of CFRP

Length of CFRP layer (mm)	Diameter to bond length ratio (d/L)	Average tensile load (kN)	Average strength (MPa)
20	0.8	22.3	111.5
40	0.4	42.3	211.3
60	0.26	51.7	258.5
80	0.2	65.5	327.3

100	0.16	72.2	361.0
120	0.13	72.9	364.5

Figure 4-55 indicates the residual strength variation with exposure duration. As shown in Figure 4-55, when the CFRP bond length is increased, the average strength increases. Failure mode are indicated in Figure 4 -56.

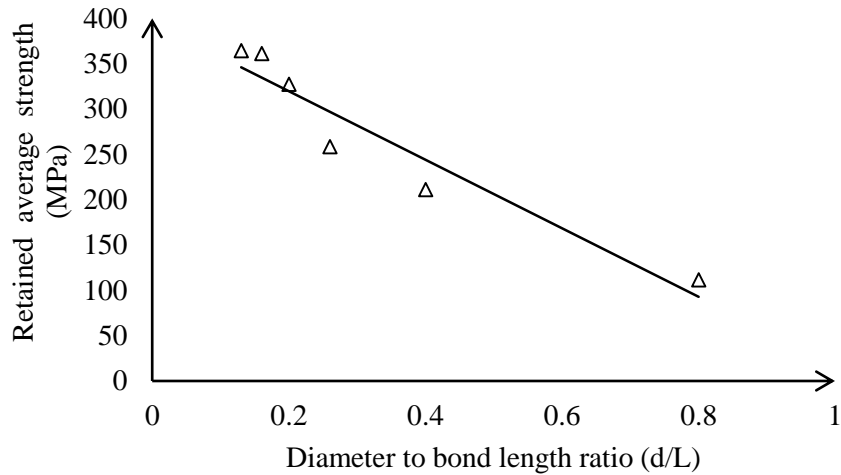


Figure 4-2: Retained average strength varies with the length of CFRP

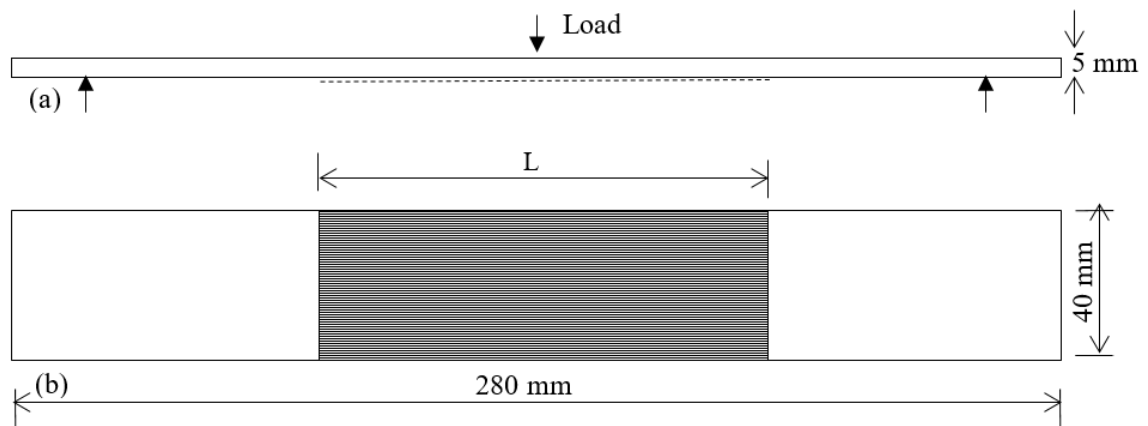


Figure 4-56: Failure mode of CSH due to bond length variation

#### 4.7.2 Fatigue behavior of CFRP strengthened steel plate with respect to bond length

The specimens were designed in accordance with ASTM D 790 with the use of steel plates with a cross-section of 40 mm (width)  $\times$  5 mm (thickness). The length of the plate member was chosen to be 280 mm and the effective span was considered as 240 mm due to a restriction in the flexural cyclic loading apparatus (Figure 4-7) A total of twelve specimens were tested to determine the characteristics of bond length effects on steel plate specimens without CSH subjected to low cycle fatigue load. The

schematic diagram of CFRP - strengthened specimens and typical test specimen shown in Figure 4-57.



L- Bond length in mm



(c)

Figure 4-57: Schematic view of the CFRP strengthen specimen (Scale 1:2)  
 (a) elevation (b) plane view (c) typical specimen

In this test, the CFRP bond length was considered as the main variable and it varied from 20 mm to 120 mm in 20 mm steps. Table 4.17 summarizes the retained average tensile strength together with the variation of CFRP bond length from the mid-point along longitudinal axis of specimen.

Table 4.17: Retained average strength varies with the length of CFRP

Length of CFRP layer (mm)	Average tensile load (kN)	Average strength (MPa)
20	76.3	381.5
40	77.9	389.5
60	79.2	396
80	80.4	402
100	84.6	412
120	85.2	426

Figure 4-58 indicates the residual strength variation with exposure duration. As shown in Figure 4-58, when the CFRP bond length is increased, the average tensile strength increases. Failure mode indicated in Figure 4-59.

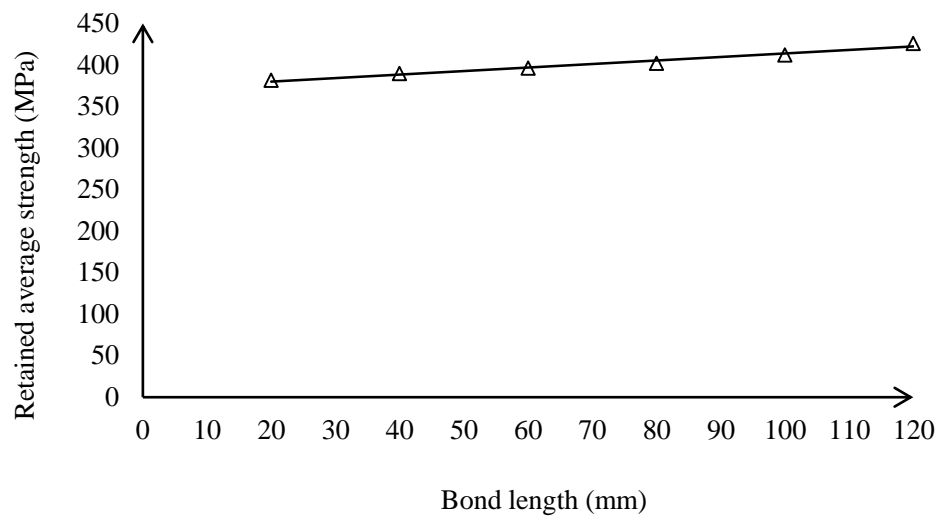


Figure 4-58: Retained average strength varies with the length of CFRP



Figure 4-59: Failure mode of steel member without CSH variation with bond length

### 4.7.3 Comparison of CFRP length effects

The test results of the conditioning CFRP strengthened steel element with and without CSH were compared as shown in Table 4-18. It summarizes the yield load values together with the variation of different bond length from the range of 40 mm to 240 mm.

Table 4.18: Comparison of retained average strength, variation with bond length

Length of CFRP layer (mm)	Number of test	Average strength (MPa)		Strength variation %
		Without CSH	With CSH	
20	2	381.5	111.5	70.8
40	2	389.5	211.3	45.8
60	2	396	258.5	28.3
80	2	402	327.3	18.6
100	2	412	361.0	12.4
120	2	426	364.5	14.4



Figure 4-60 shows the average retained strength variation of CFRP strengthened conditioning steel element with and without CSH. The number of applied cycles subjected to cyclic flexural loading.

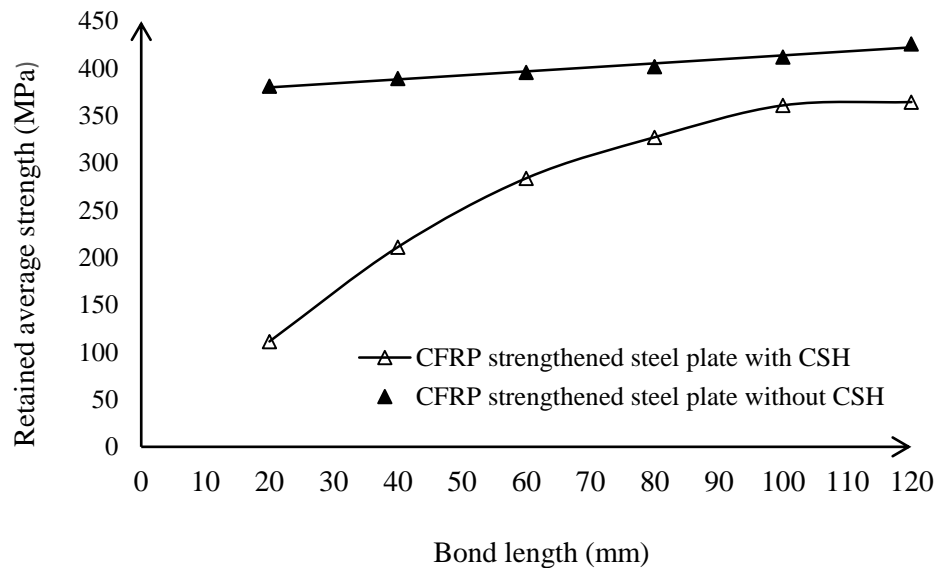


Figure 4-60: Comparison of strength variation by CFRP bond length

Figure 4-60 indicates that the average variation of tensile stress with CFRP bond length of steel specimens with and without a CSH. Steel plates without a CSH shows a linear relationship and a nonlinear behavior for steel plates with the CSH, since the steel plates without a CSH only adds an additional tensile strength. Specimen with CSH is material remove for place the hole and result is reduction of stiffness. Flexural cyclic loads had contributed to change material properties due to the increase of stress near the loading point (mid-point) and the resulting material becomes weak. Therefore, the specimen with the CSH is more complex than a plane specimen absence of a CSH. When the length of the CFRP layer is increased up to 100 mm the average yield strength is also proportionally increased in this context. After that it becomes constant with respect to the length of the CFRP layer. Therefore, there is no need to further extend the CFRP layer in this context, as when increasing the coverage area, the cost of the material will also increase resulting changes to the installation cost. According to test results, a 100 mm length from mid-point can be considered as an optimum bond length. Generally, fatigue cracks start from the tensile surface and it penetrates through thickness. The cracks propagate along the weakest path of the material until it fails as

shown in Figure 4-59. However, steel failure does not occur during the period of conditioning. When performing the tensile test on the conditioned specimen, it starts to propagate cracks in a perpendicular direction of the CSH as shown in Figure 4-59.

#### 4.8 Bond stress variation

Bond stress plays vital role in CFRP/steel strengthened technology and it can be considered as a characteristics of the adhesive as the failure of CFRP composite is governed by the adhesive layer. Bond stress is based on amplitude of loads and the area of the bond. This study estimated the bond stress variation with number of loading cycles, the size of CSH and the CFRP bond length of the CSH. Results are shown in Figure 4-61.

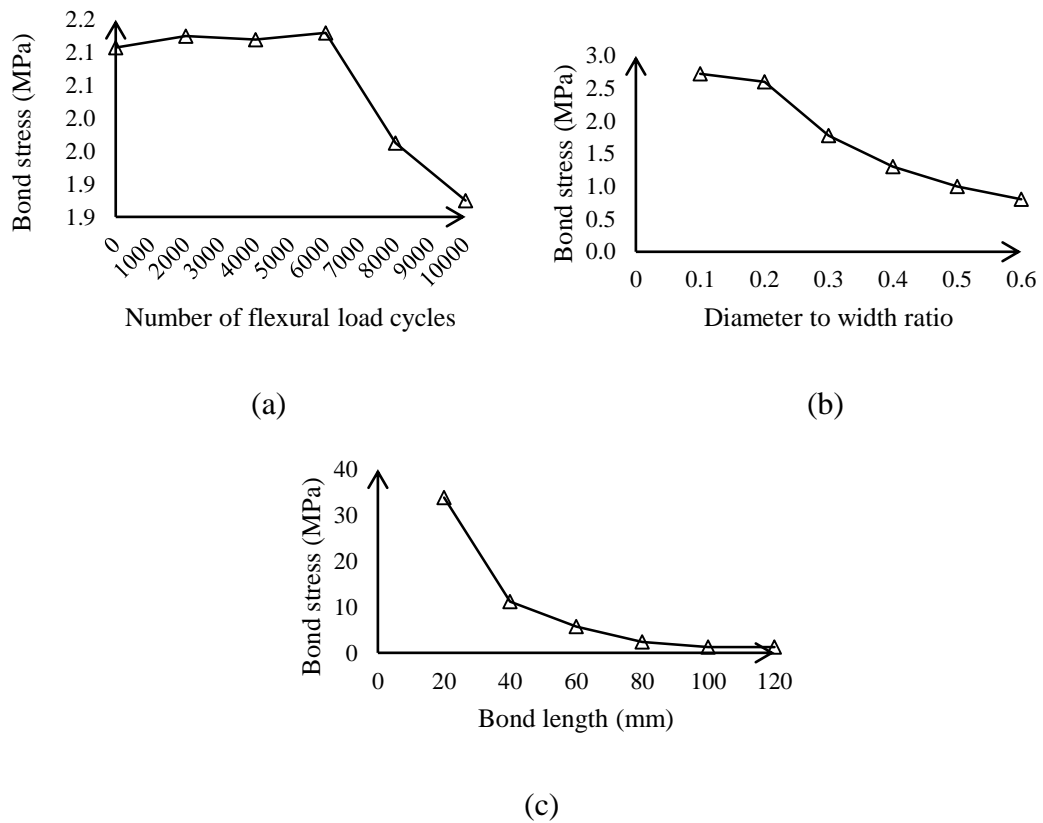


Figure 4-61: Bond stress variation with respect to (a) number of cycles (b) diameter to width ratio (c) bond length

#### **4.9 Summary of experimental investigation related to the CSH/CFRP hybrid system**

This test program is based on stress and strain variations of the CSH due to fatigue. The stress based test is further divided into non-strengthened controlled, CFRP strengthened control and conditioned with non-strengthened and CFRP strengthened. According to test results, a considerable amount of strength loss is shown due to fatigue with significant strength gain by the CFRP. In addition, the strain based test setup exhibited excellent strain control by the CFRP material when compared to non-strengthened CSH. CFRP strengthened steel plate were performing under cyclic flexural loads to determine the fatigue bearing capacity of CFRP/steel composites with respect to number of cycles. In this investigation, a position of CSH was investigated under cyclic flexural loading and test results were compared with CFRP strengthened technique. Test results confirmed that CFRP significantly enhanced the strength of offset CSH. Furthermore, the effects of the CFRP length was also investigated with the significant strength gained by CFRP. Therefore, CFRP strengthened technique could be successfully utilized to re-install the loss fatigue strength on CSH using the CFRP material.

In fact, CSH under fatigue loading in stress intensity region has a high tendency for crack initiations. In this investigation, the fatigue sensitive zone is surrounded by the CSH. Crack starts at this zone depending on the level of stress. Cyclic flexural load causes to increase the stresses at the CSH and the effect of yield stress was significant losses and it is mainly governed by the size of CSH, as cyclic effects causes to convert hardening properties of material to soften. Furthermore, residual stress also significantly contributes to stress, which occurs due to drilling and other mechanical processes done on CSH such as drilling and grinding. However, magnitude of loads, loading frequency, rate of loads and material properties also affect the performance. The test results were used to draw the following conclusions and recommendations.

- 1) This CFRP strengthened method recorded the performance; which is in the range of 27 % to 36 % strength gain compared to the non-strengthened

specimen with the number of cycle change from 0 to 10,000 in 2000 cycle step

- 2) Test results agreed with the Coffin-Manson theoretical model
- 3) This investigation reported the strength losses which were in the range of 13 % to 25 % compared to the non-conditioned CSH with the diameter ranging from 4 mm to 25 mm
- 4) This investigation reported the tensile strength enhancement with CFRP which is in the range of 32 % to 45 % compared to the non-strengthened CSH with the diameter range change from 4 mm to 25 mm
- 5) This investigation reported strain, controlled by the CFRP strengthened CSH compared to the non- strengthened CSH showing significant gain
- 6) There was no failure observed during fatigue, however a de-lamination failure was observed with a tensile load
- 7) The fatigue resistivity of CSH with offset distance had significantly enhanced with respect to the mid-point subjected to fatigue load
- 8) This study recorded a strength increase with respect to off-set distance; which in the range of 36 % to 131 % compared to the CSH at the midpoint
- 9) CFRP strengthening offset CSH exhibited significant yield strength variation and its range in variation were recorded as 19 % to 42 % with respect to offset distance
- 10) The optimum length of the CFRP layer for the purposes of strengthened CSH was recorded as 200 mm
- 11) Failure mode was observed as de-lamination of the CFRP layer with the fatigue load as well as the tensile load

## ***Chapter – 5***

---

### ***Finite Element Modeling of Fatigue Behavior of CSH Subjected to Cyclic Flexural Loading***

## **5 FINITE ELEMENT MODELLING OF FATIGUE BEHAVIOR OF CSH SUBJECTED TO CYCLIC FLEXURAL LOADING**

### **5.1 Introduction of finite element modelling related to CSH/CFRP hybrid system**

Fatigue is a critical issue related with structural failure and cost of fatigue has become very high. Furthermore, structural failures related to fatigue have become very dangerous with loss of lives and properties. This is due to fatigue failure occurring quickly and suddenly without any prior warning and such a failure is called a catastrophic failure. The main reason for catastrophic failure is crack growth up to critical level due to effects of a large number of internal and external parameters. This study has focused that the model of CSH behavior to control any crack growth of a structural element. The main limitations of the CSH technique was identified as reduction of stiffness and re-cracking due to continuous service load. Furthermore, performance of this technology is governed by a range of parameters. These parameters could be classified as geometrical related parameters, load related parameters and material related parameters. The effects of individual parameters could be investigated by laboratory experiments and such procedure is more complicated, expensive and time consuming. The modern world has utilized FEA software to predict any effects of such parameters due to cost effectiveness and time constraints. However, material properties are needed for the precision of results from the FEM. Therefore, mechanical properties of selected materials were tested under the laboratory conditions and relevant values were measured respectively. In this study, the commercially available ABAQUS 6.14 version was used to develop FEM due to its competitive advantage when compared to similar software such as ANSYS. Hardware of the computer is also critical for this FEM and specially for this kind of analysis a high end machine is recommended. In this study FEM was developed using cyclic J-integral technique under direct cyclic mode and model results were validated with experimental results.

### **5.1.1 Background of FEM**

FEM plays a vital role in analysis of structures. Mechanical behavior such as stress and strain of structural elements reflect effects of fatigue due to cyclic loads. However, most of them are invisible and difficult to be measured using a testing apparatus. Furthermore, laboratory investigations are expensive and time consuming. Also, Steel embedded with CFRP has become more complicated due to complicate bond slips and failure modes. When considering the CFRP embedded CSH, performance depends on a range of parameters. Therefore, development of a FEM is a possible way to investigate fatigue behavior of the CSH which critically influences parameters. Such a model helps to investigate hidden things which affects the overall performance of the proposed technique and the proposed model is flexible as it could change mechanical properties of the material of existing structures. In addition, the proposed model has the facility to change geometrical dimensions, loading parameters and boundary conditions according to the available data from real world applications. The ABAQUS could be considered as a leading simulation software which is used for finite element analysis (FEA). It has the capability to simulate linear behavior as well as non-linear behavior of different types of structural material and their composite.

Vicinity of the CSH developed more plastic behavior due to fatigue and the remaining area exhibits elastic behavior during the service loads. Elastic properties of material deals with the linear characteristics and plastic properties are well explained by the nonlinear behavior. However, in this analysis the size of the CSH are very small compared to the balance area of the specimen and assuming overall behavior of material is elastics. On the other hand, overall plastic behavior of the material is impossible during the service period because if the material reaches the plastic level it would fracture and the structural element collapses.

### **5.1.2 Procedure of simulation**

A finite element (FE) model was developed using a commercially available finite element software. A computer with 8 GB RAM, 2 GB VGA and 2 core processor was used for this analysis. First, the geometric modelling was done for steel plates with a CSH, supportive rollers and a loading nose. After that the CFRP layer was introduced

according to requirement of the pre-designed analysis. In this analysis two interactions were introduced between two supportive rollers the specimen. In this case standard type of general contact was utilized with mechanical friction (Lei,2016). The coefficient of the friction value was taken as a 0.15 between each surface. Special options have been used to create the crack while the extension direction was selected using a q vector option as shown in Figure 5-3. The model was with the same configurations as the laboratory test setup shown in Figure 5-1. Each specimen module was loaded with the LCF mode using a direct cyclic option. A 8 mm radius loading nose was used to apply loads at the mid-plane of the specimen.

Frequency of loads was fixed as 5 Hz using an amplitude option of loads. When considering the boundary conditions, two supportive cylinders were fixed to avoid a moving or rotating in direction during an analysis. In this case, encastre options were used for the settings. Loading rates at the mid-plane were kept constant at a fixed rate of 0.2 mm/min throughout the analysis using loading options. The maximum deflection for loading direction (Y-direction) at mid-plane was limited to 2 mm and movement of remaining directions and rotations around all other axis was fixed during analysis. The direct cyclic mode in the software was utilized to determine the response of the fatigue. The steel plate with the CSH was modelled as an elastic–plastic metal with isotropic hardening. Three dimensional 8 node solid brick elements with reduced integration (C3D8R) were used to model the steel plate, supportive rollers and loading nose components as shown in Figure 5-5. All the material properties assigned to the model was the same as in the test procedure explained in chapter 4. The composite lay-up option of the material property model was utilized to embedded CFRP layer in this regards. The conventional shell elements and material type were selected as the lamina type. The Hashin damage option was used to model the CFRP fabric and a tie constraint was used to represent the bond between steel and the CFRP. The assemble mesh model was run for analysis and the results were collected from the ODB file in the visualization module end of the analysis.



## 5.2 Detailed steps of simulation

### 5.2.1 Geometry of the crack model

Firstly, a part module was used to create and edit individual elements of the specimen and the schematic view is shown in Figure 5-1. The length of the specimen was selected as 280 mm with a cross section of 40 mm width and 5 mm thickness. A crack stop hole was introduced with 16 mm diameter at the midpoint of the main axis. The crack and the contour path were introduced with 16 mm diameter at the CSH as shown in Figure 5-1.

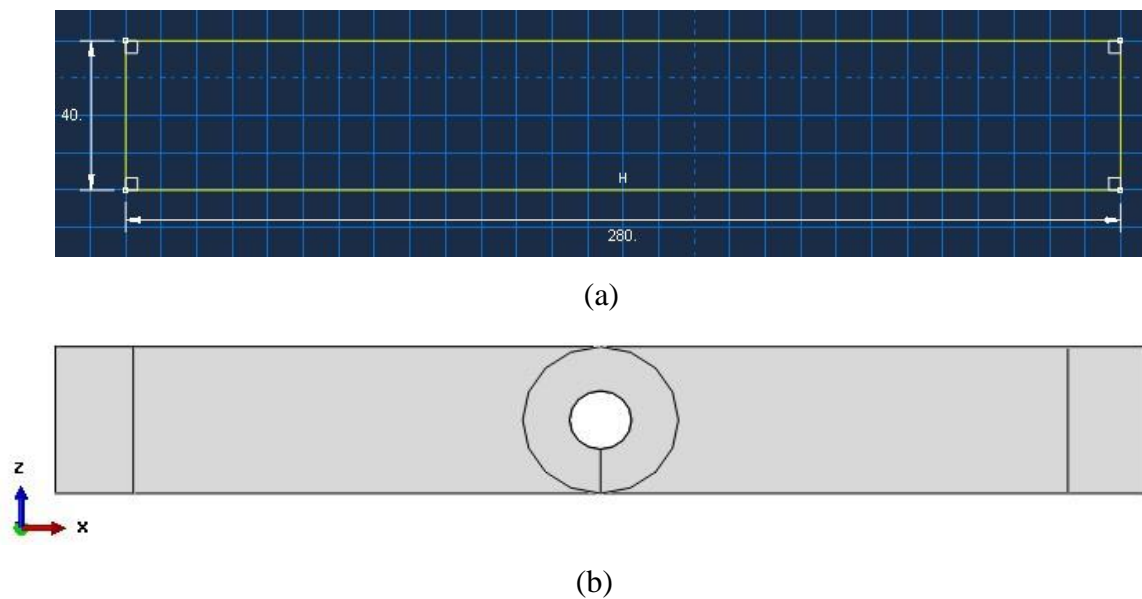


Figure 5-1: A model view of the specimen after introducing contours and crack seems (Schematic diagram)

Cracks could be modeled either by using conventional finite element analysis (FEA) or extended finite element methods (XFEM) (Moës et al., 1999). The pre-defined contour integral crack path is required in this model. In addition, the crack front as well as direction of the crack extension should be specified. A seam crack must also be introduced to allow separate fracture surfaces. The XFEM method applies for model stationary cracks. However, propagation cannot be automatically modeled using this method and the process of crack growth also can be modeled (Beesley et al., 2015). In this technique does not need element boundaries, like conventional FEM (Beesley et al., 2015). Therefore, refinement of mesh in the crack region is not necessary and it is known as mesh-free technique. However, the capability of XFEM method is limited

to determining crack parameters only for stationary cracks. This technique is a simple method for more complicated crack geometries also without any extensive mesh refinement. Contour integral parameters such as the J-Integral and SIF are more precise when the contour is close to the crack tip (Alan and Zehnder, 2012). Therefore, the XFEM modeling method is not recommended to determine contour integrals.

The test specimen prepared for the experimental program consists of a CSH hole placed on a steel specimen without any cracks. This was due to one objective of the test program which was to predict re-cracking behavior of the CSH. Crack length is not considered at the crack initiation stage because initially the crack size is very small and is difficult to visually observe. This usually occurs at the micro structural level of the material. There are two techniques for crack evaluation which includes the extended finite element (XFEM) method and the contour integral technique. XFEM technique does not produce stress intensity factor (SIF) and this method introduce pre-cracks on the specimen to separate material. It is widely used to evaluate stationary cracks. This study selected the contour integral technique which is considered in pre-defined crack direction for crack growth although it was a limitation . Therefore, this FEM has introduced a crack direction as shown in Figure 5.1. However, there are no singularity forms along the pre-determine partition line of FEM to initial flaw. On the other hand, this investigation was focused on short crack (less than 1 mm) estimation only and does not pay attention to large cracks as fatigue life estimation is based on the crack initiation stage in this study. Therefore, introduction of crack direction of FEM does not significantly influence the final results. Furthermore, XFEM methods show competitive advantages such as not defining the crack path or location, the mesh of the crack generating independently and not needing to partition the geometry at the crack location.

### **5.2.2 Material properties**

Material properties were assigned using a property module of ABAQUS. This analysis was assumed isotropic hardening characteristics and elastic behavior of the steel. Numerical values of elastic module of the steel, CFRP and adhesive were experimentally determined as 200 GPa, 175 GPa and 25 respectively. The Poisson's

ratio of each material was assumed as 0.3. Measured material properties in experiment is presented in Table 4.1 which were used for modeling.

### 5.2.3 Assembling of geometrical components

The assembly module was used for assembling relevant substances and positioning the instances according to laboratory test setup as explained in chapter 4. The loading nose and two supportive cylinders were assembled as shown in Figure 5-2.

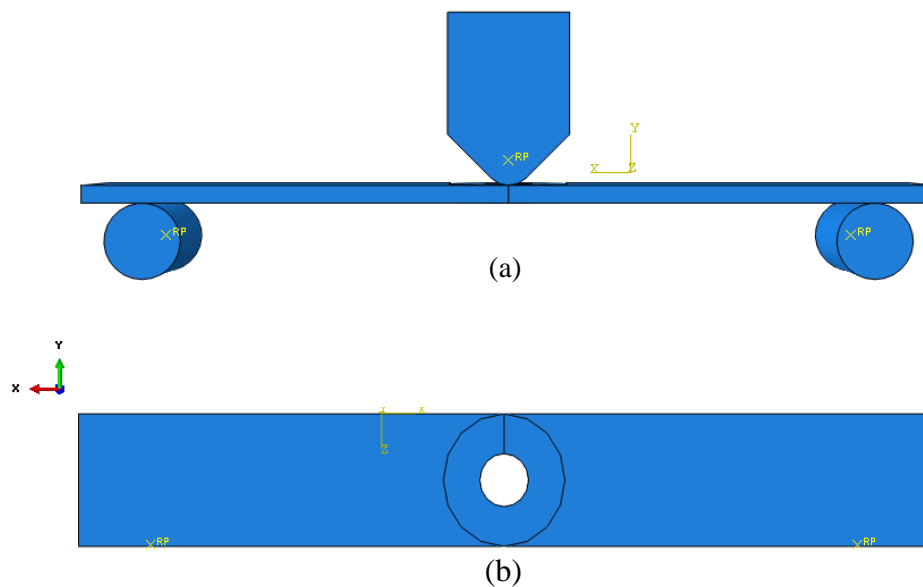


Figure 5-2: The assembly module of the test setup (a) front view (b) plane view

CFRP material attached to the steel plate is very important for strengthening purposes of steel. The FEM has many options when considering how it is to be attached to the composite layers with steel plates using ABAQUS. Tie constrain method is a technique to bond two surfaces, in this case the steel surface was considered the master surface and the CFRP layer was considered the slave surface. Tie region was equal to the surface area of the CFRP layer. Similarly, node to node contact and surface to surface contact in an interaction model are very common methods. The surface to surface approach is the default in the ABAQUS/Standard. It was perfectly contact and displayed excellent bond characteristic due to the mechanical interlocks between the two surfaces. In addition, the composite lay-up option in the property model could also be used for these purposes. However, the surface to surface contact method should be more accurate than the sandwich material method. Therefore,

surface to surface contact method was selected with the tie constraint option to confirm the CFRP/Steel bond in the FEM.

#### 5.2.4 Configuration of the FEM

The step module was utilized for configuring FEA with relevant steps which are associated with output requirements. It has a sequence of options to change in the boundary conditions and loading of each steps. Output requests were also included in this configuration which were named as the history output and the field output. The field output data deals with the entire model and the history output focuses only specific points in the model. In this study, two loading steps were introduced as step 1 and step 2. The static general loading method was applied in step 1 from 0 – 0.02 Sec while the direct cyclic loading method was applied from 0.02 to 0.2 Sec. Crack option in history output was selected for contour integral domain. The number of contours around the crack tip was considered as 10 near the crack tip.

#### 5.2.5 Mechanical interaction between contact surfaces

Controlling interaction between each surface is very important. In this analysis two interactions were available such as interaction between supporting rollers and specimen as well as the loading nose and the specimen. The option of general contact algorithm of the ABAQUS which was utilized for this purpose. The coefficient of the friction value was taken as a 0.15 between each contact surfaces. A special option was used to create the crack while the extension direction was selected using a q vector option as shown in Figure 5-3.

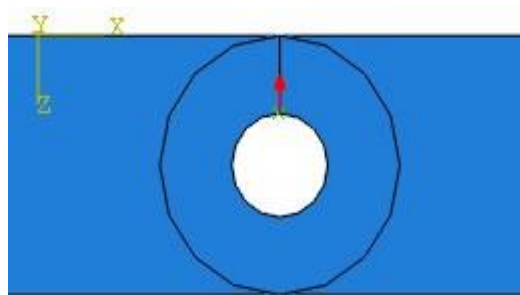


Figure 5-3: The contour path and crack seams

### 5.2.6 Loads and boundary conditions

The load module is specifically used to control loads and boundary conditions of the model. The proposed model was developed with the low cycle fatigue (LCF) mode under direct cyclic option. Loading nose with 8 mm radius was used for cyclic loads applied at the mid-plane of the test specimen. In this analysis, the pressure load was applied using a loading nose as shown in Figure 5-4. The magnitude of pressure was depending on the cross section of the top of the loading nose and it was calculated as a  $1.25 \text{ N/mm}^2$ . It was equivalent with 2 kN amplitude and 5 Hz frequency of loads using an amplitude option of loads. During analysis the stress ratio, R was kept at a constant level and the numerical value of R was 0.1.

When considering the boundary conditions, two cylinders were fixed to avoid a moving or rotating in any directions which using encastre option. The reference point of the loading nose allows moving only at a vertical direction and it was limited up to 2 mm with respect to the horizontal position. Movement of remaining directions except Y axis and rotations around each axis was fixed during analysis. The displacement /rotation option was selected to control the direction of movement. The load module with all boundary conditions are shown in Figure 5-4 similar with laboratory test setup explained in the chapter 4.

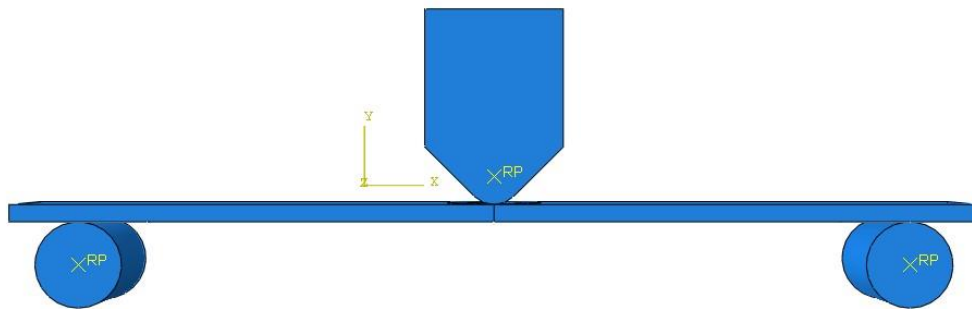


Figure 5-4: A loading mode and boundary conditions

### 5.2.7 Meshing of the model and mesh sensitivity analysis

A mesh module of the ABAQUS was used to control the mesh size as well as the element type in this analysis. A rosette pattern was formed at the crack tip region and a coarser mesh was used for the remaining area as shown in Figure 5-5 (b). Around the crack stop hole, a circular partition was introduced using the “sweep meshing”

technique with medial axis algorithm as shown in Figure 5-5 (b). The remaining part of the model also utilized a “medial axis” meshing algorithm with edge-based tools used to mesh seeding around the crack tip as well as loading nose and supportive rollers. This analysis selected a three dimensional brick element (C3D8R) with 2 mm mesh size.

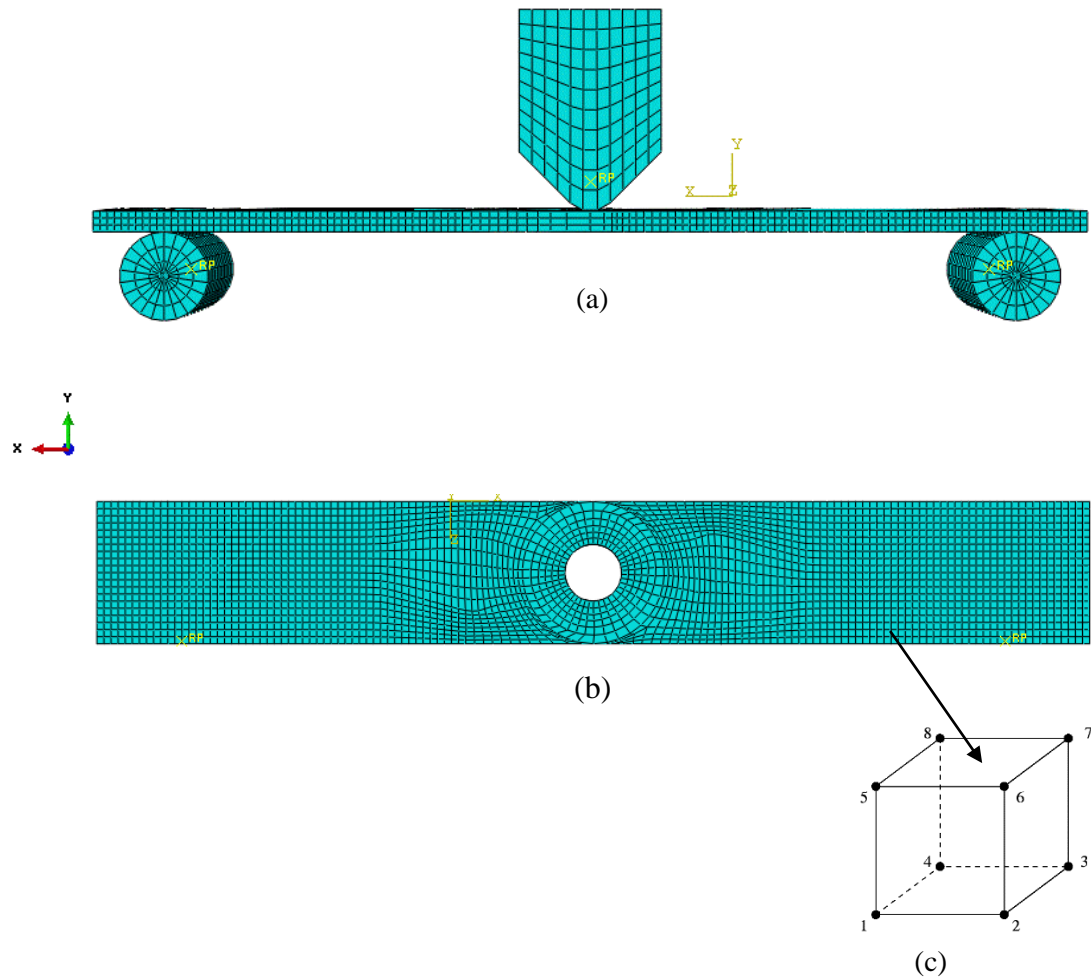
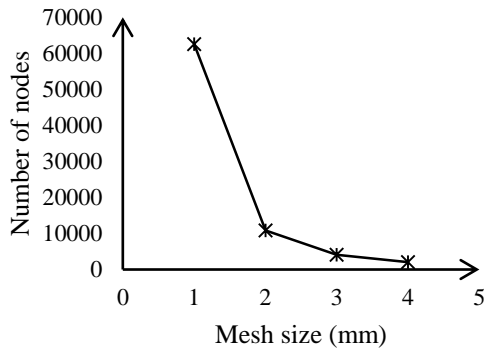


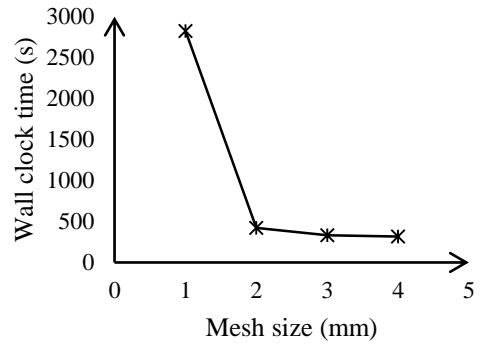
Figure 5-5: Mesh model (a) Front view of the mesh model (b) Bottom view of the mesh model (c) 8 node brick element

The main issue of any FEM technique is deciding the mesh size for analysis, as large element sizes contribute to fast analysis process. However, its less accurate. When selecting small sized elements, there may be a higher degree of accuracy but its take more time for analysis. The reason for this is, iterations time is longer at every stage for fine meshed ones.

Therefore, computing time and improving level of accuracy with mesh size should be optimized in this situation. Mesh refinement is the most vital method of judging the mesh size, and it can be classified as coarse mesh, medium mesh and fine mesh. Reducing the element size is the easiest mesh refinement strategy, with element sizes reduced throughout the modeling domains. This approach is attractive due to its simplicity, but the drawback is there are no preferential mesh refinement in regions where a locally finer mesh may be needed. Therefore, the need to select a fairly good mesh size for proposed FEM with the required level of accuracy becomes important. In industrial practice a fine mesh is introduced only around sensitive regions of high-stress concentrations and the remaining area which has a lesser importance is introduced to a coarser mesh. The convergence test is another way to check whether the size of the mesh is worth or not for the FEM. In this method half of mesh size is selected and compared with the previous analysis and the program is re-run with the new analysis. If the results are insignificant when compared to the previous mesh size it is considered as an appropriate mesh size. This could be repeated until the level of acceptance. However, there are no definitions regarding the mesh size when starting this convergence test and it should be repeated at least three times with different mesh sizes until insignificant variations. High stress near the CSH area displays a higher level of convergence than other areas. During analysis, attention should be on stress singularity because it does not allow to converge. When the size of the mesh is very small it results in generating a singularity point. Stress at the singularity points are theoretically considered as infinity. Therefore, considering all of above factors, an FEM result of 2 mm mesh size was selected as an appropriate size in this analysis. It was confirmed by the mesh sensitivity analysis and results of mesh sensitivity analysis are shown in Figure 5-6. and relevant stress contours are shown in Figure 5-7.

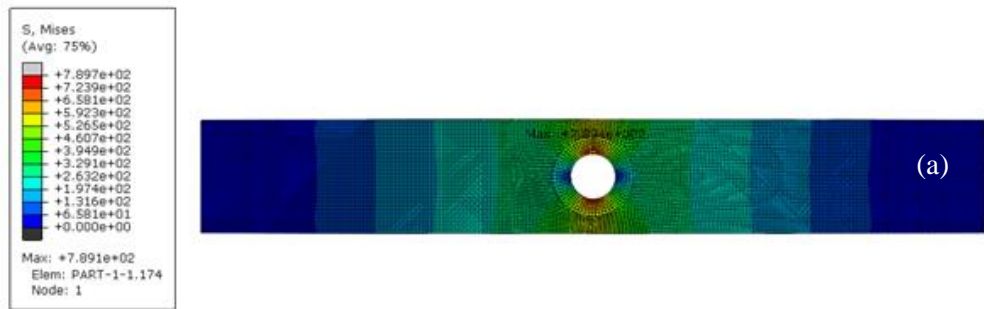


(a)

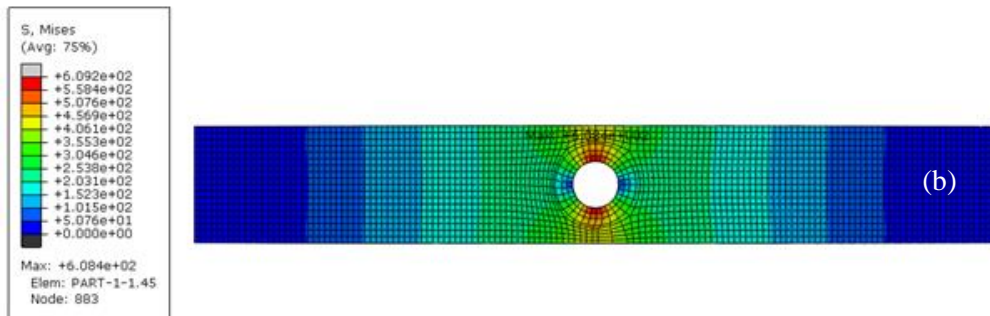


(b)

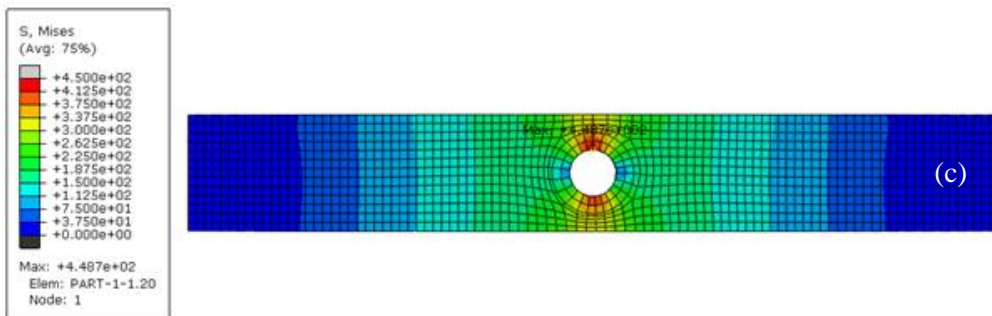
Figure 5-6: Mesh sensitivity analysis with the mesh size (a) number of nodes (b) wall clock time



(a)



(b)



(c)



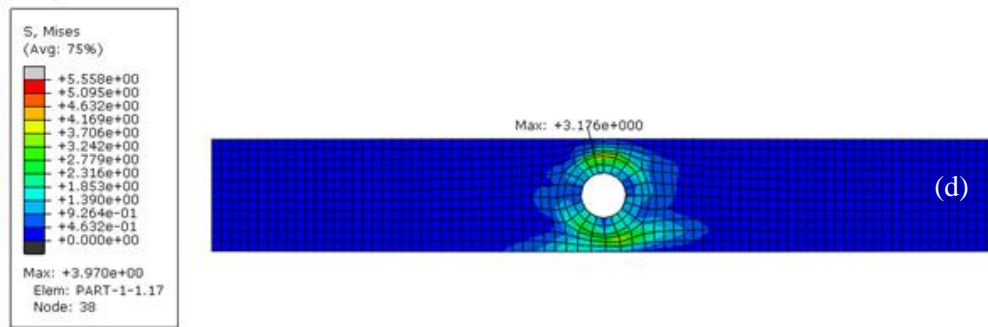


Figure 5-7: Contours with different mesh size (a) 1 mm (b) 2 mm  
(c) 3 mm (d) 4 mm

Mesh sensitivity analysis compared different mesh sizes and it was confirmed that the 2 mm mesh size was the reasonable analysis time as well as the reasonable number of nodes. This FEM results were compared with stress as well as strain variation near the CSH in the laboratory test results. Both stresses and strain scenario has confirmed insignificant deviation between test results and FEM results. However, finer mesh can be introduced at the surrounding of the CSH which has insignificant effects on overall performance of the final results. Therefore, selected mesh size could be considered as an optimum size of the mesh for the proposed FEM.

### 5.2.8 Analysis and model results

Submission of the job for analysis is the final step and the job module was utilized in this stage. The analysis was run and the results were collected from the data file or visualization modulus. At the end of the analysis maximum and minimum value of the J-integral were obtained from the data file of monitor option in the job module. Stress and strain values were obtained from the visualization module using XY data as shown in Figure 5-8.

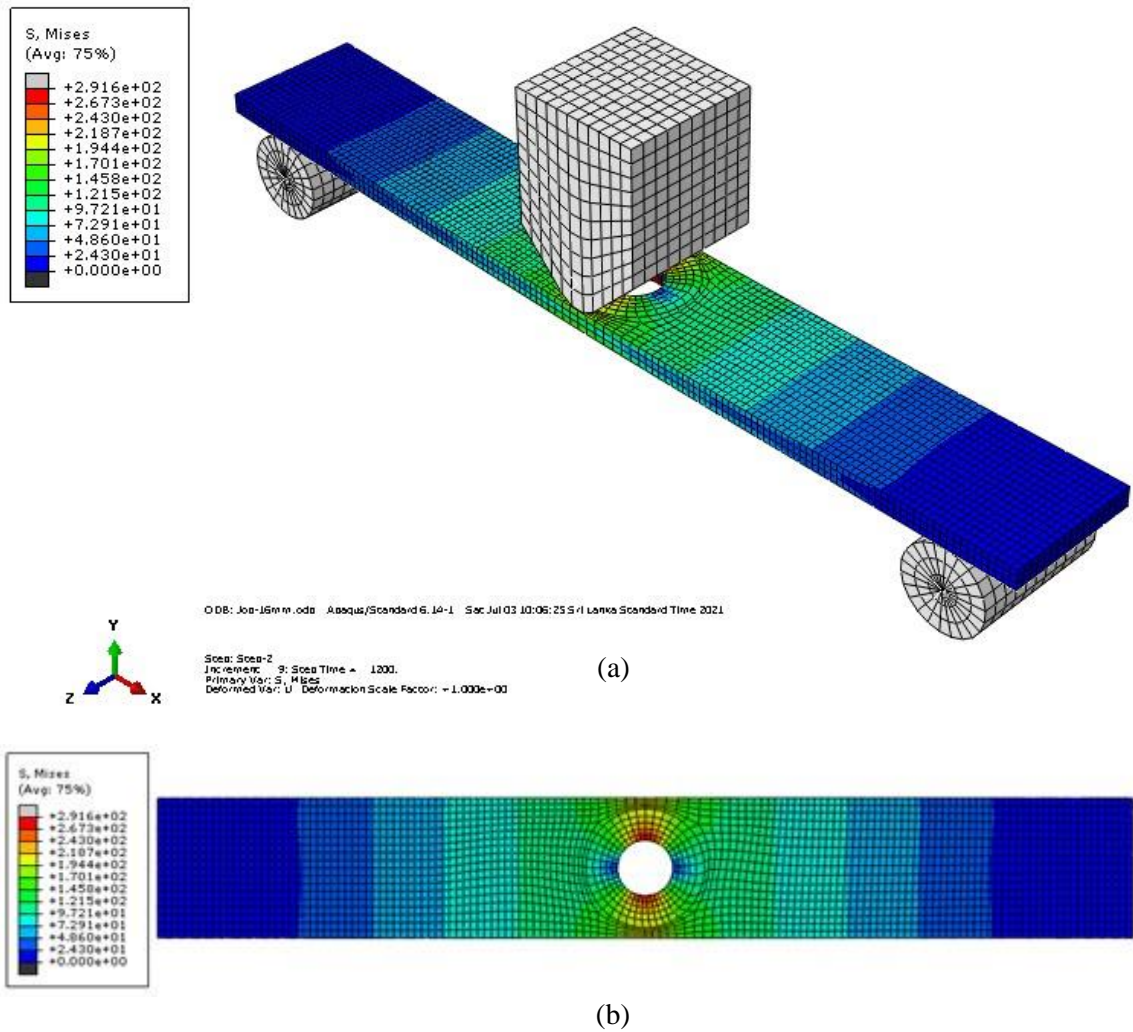


Figure 5-8: The Visualization module of specimen (a) test setup (b) bottom view

During the fatigue testing of CSH/CFRP, the composite did not go through failures considering predetermined load cycles. When a tensile load is applied up to the yield, any bonding or de lamination failures were not observed. When tensile loads on the test specimen is further increased it separates the CFRP layer from the steel surface. Therefore, FE model did not observe any bond failure during analysis too.

### 5.3 Validation of the model

Experimental results obtained in chapter 4 were compared with results obtained from FEA. Basically two tests series were considered in this background as diameter to width ratio and location of CSH variation. Diameter to width ratio was changed from 0.1 to 0.6 and other parameters were kept as a constant during the analysis. In addition,

offset distance vary from 0 to 80 mm with respect to mid-point. Both of these tests, stress and strain were determined as explained in chapter 4. The model was identical with configurations of the laboratory test setup. Results of laboratory test and FEM results were compared to validate the developed model.

Mechanical properties of the material play a vital role when considering fatigue. Yield strength and tensile strength are two main material properties considered in fatigue analysis of ductile material. These material properties are representing resistivity to failure due to deformation and fracture respectively. Yield strength and tensile strength are representing different meaning related to fatigue. Yield strength (yield stress) represent maximum stress just before the permanent deformation and tensile data represents maximum stress prior to material fracture. When considered the ductile material yield value, it is prominent and the brittle material deals with tensile strength. As brittle material does not achieve the yield load, when performing tensile loads, it suddenly recedes to fractures. Hence, this study used a tensile test to determine yield strength (fatigue stress) of the CSH at the end of condition to measure any retained yield strength.

This is one of the critical parameters related to fatigue evaluation due to fatigue effects and strength of material change at the micro structural level. Variation could be quantified using retained yield data of material. In general, yield strength of material should be constant and however it is not constant due to effects of fatigue as cyclic load causes to change the micro structure of material and result is decrease yield strength. This is a main reason for sudden failure of material without any prior warning. This study retained an average yield stress of the material (ratio of yield load to cross section area) which was estimated at the end of fatigue loads as retained yield strength indicates the effects of fatigue on the CSH specimen. Developed FEM also estimated yield strength at the end of fatigue and it was measured using stress at the edge of the CSH. This value is nearly three times the applied load on the specimen as shown in Figure 5.9. This approximation is an extension of theory developed by English in 1913. Author has introduced a stress calculation technique closer to the hole as shown in equation 5.1. In addition, stress-strain curve under visualization model in the field output data could also be utilized to estimate the yield stress. Furthermore,

the yield strength could be estimated using the theoretical equation as shown in equation 5.2.

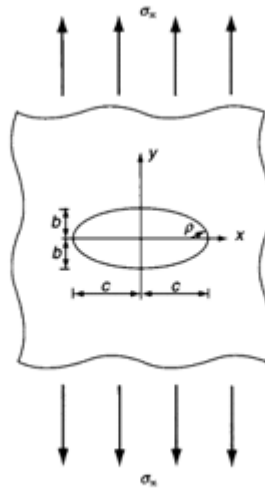


Figure 5-9: Stress distribution near the crack stop hole

$$\frac{\sigma_{max}}{\sigma_0} = \left(1 + \frac{2a}{b}\right) \dots\dots\dots (5.1)$$

*a* -the major radius  
*b* - the minor radius,

Stress variation near the hole of the steel plates was quantified by English in 1913 and it was considered a very important historical milestone for the fracture mechanics theory. Circular holes in the stress plates are uniformly distributed while the CSH stress is significantly higher than average stress and its mathematical expression is as follows (equation 5.2).

$$\frac{\sigma_{max}}{\sigma_0} \approx 3 \dots\dots\dots (5.2)$$

$$\sigma_0 \approx \frac{1}{3} \sigma_{max}$$

### 5.3.1 Non-strengthened and CFRP strengthened CSH

In this FEA, the diameter to width ratio was considered as a main variable and it varied from 0.1 to 0.6 in 0.1 steps. Table 5.1 summarizes the average strength of the non-strengthened and CFRP strengthened CSH from the test results as well as FEM results.

Table 5.1: FEM results compared with test results for CSH

Diameter to width ratio (d/b)	Average strength (MPa)			
	Non strengthened		CFRP strengthened	
	Test	FEM	Test	FEM
0.1	375.1	391.7	498.0	547.7
0.2	355.6	376.3	470.0	507.6
0.3	335.6	347.5	445.5	471.7
0.4	300.1	314.6	405.0	439.5
0.5	245.8	267.4	356.0	387.6
0.6	185.8	203.9	270.0	297.2

The test results of the non-strengthened and CFRP strengthened CSH under cyclic flexural load conditions were compared with relevant FEM results in Figure 5-10. It summarizes the average strength variation of different diameter to width ratio range from 0.1 to 0.6 in the 0.1 step.

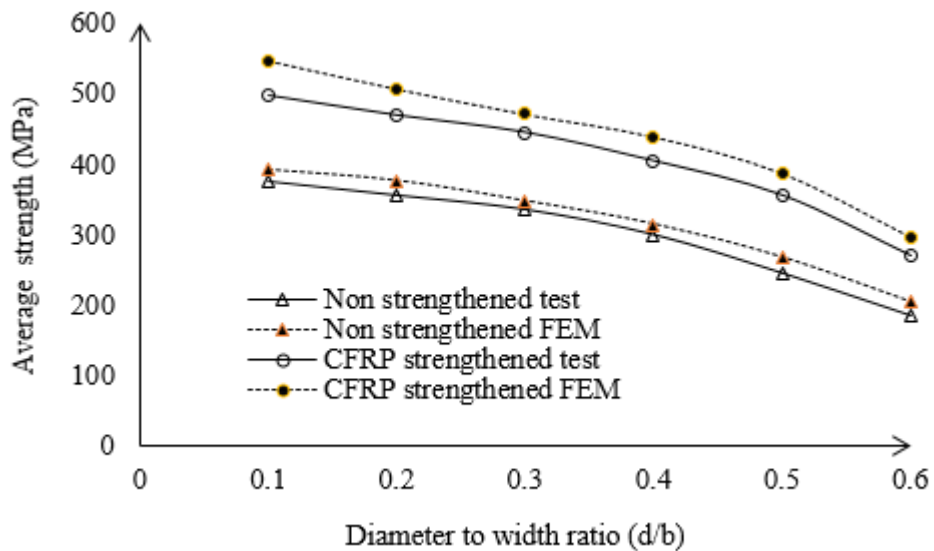
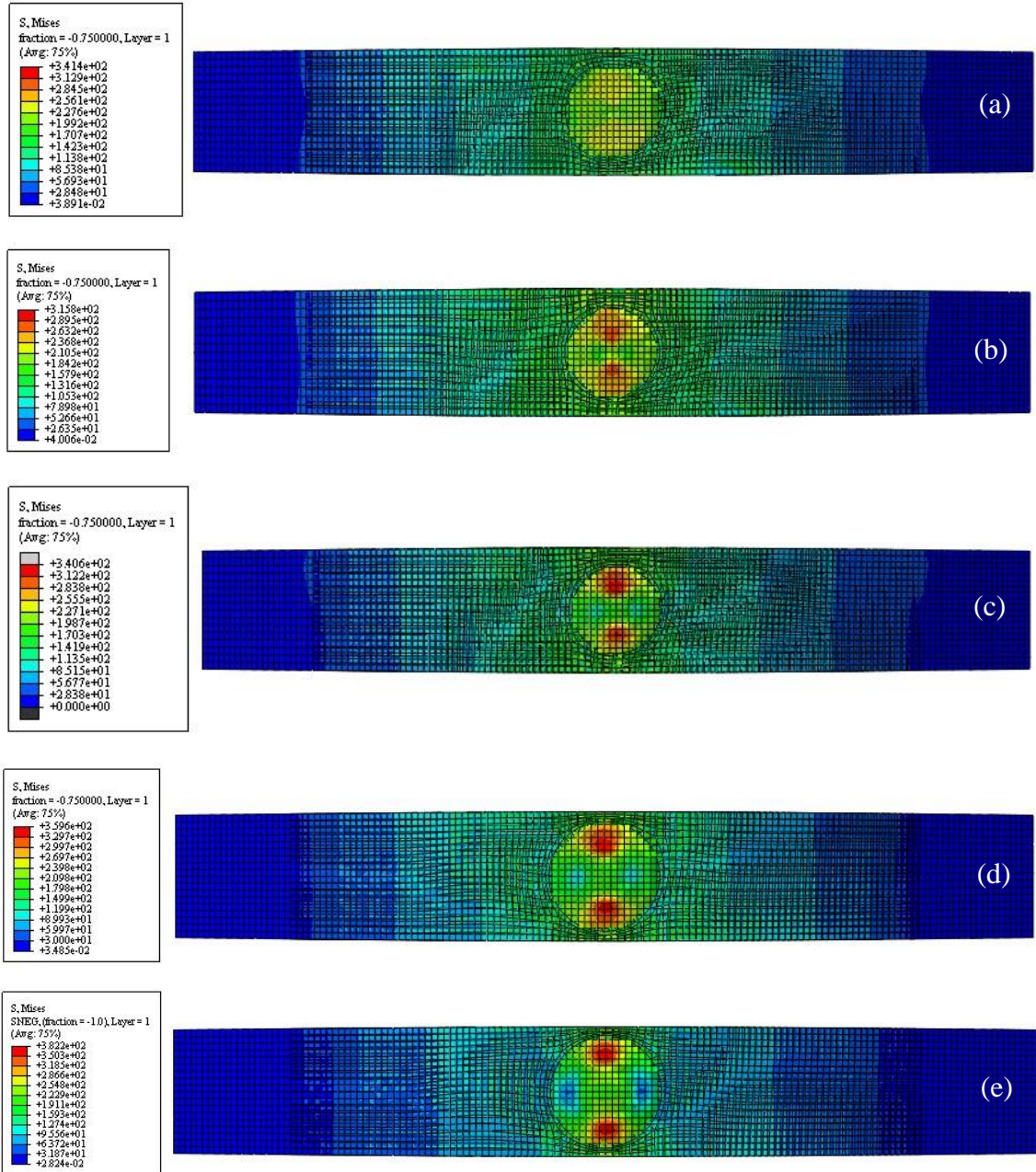


Figure 5-10: Average strength variation with diameter to width ratio of CSH

The average strength variation with diameter to width ratio of non-strengthened and CFRP strengthened CSH under fatigue where the test results agreed with the FEM results as shown in Figure 5-10. Contour of the tensile surface (bottom surface) of the specimen under flexural cyclic load with diameter to width ratio is shown in Figure 5-11.



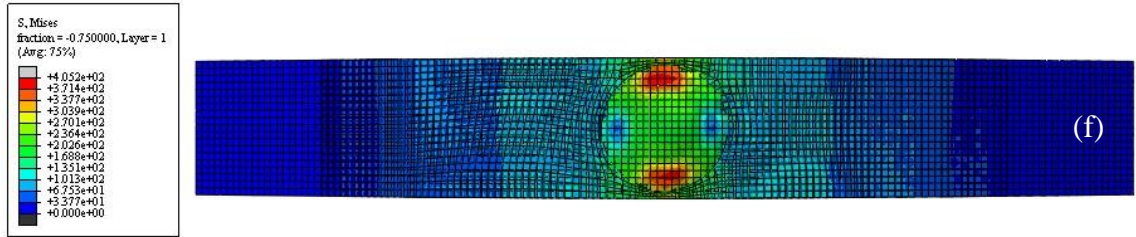
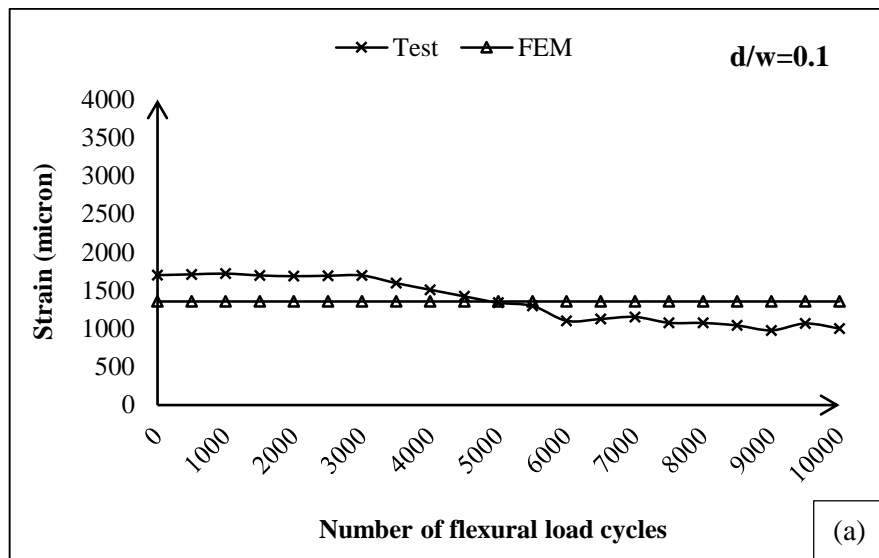
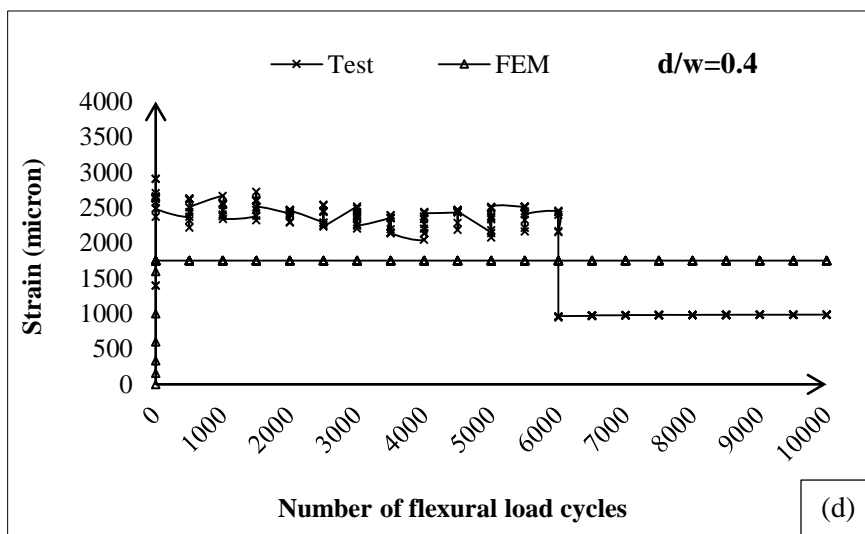
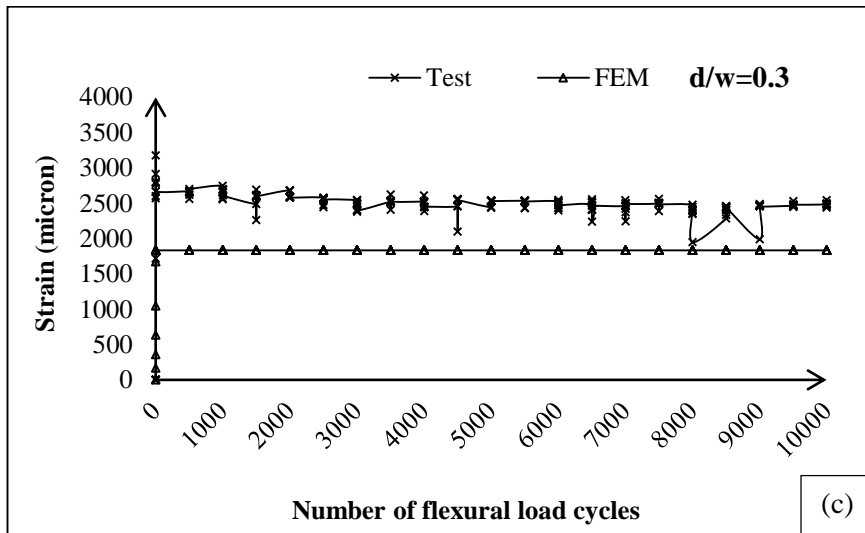
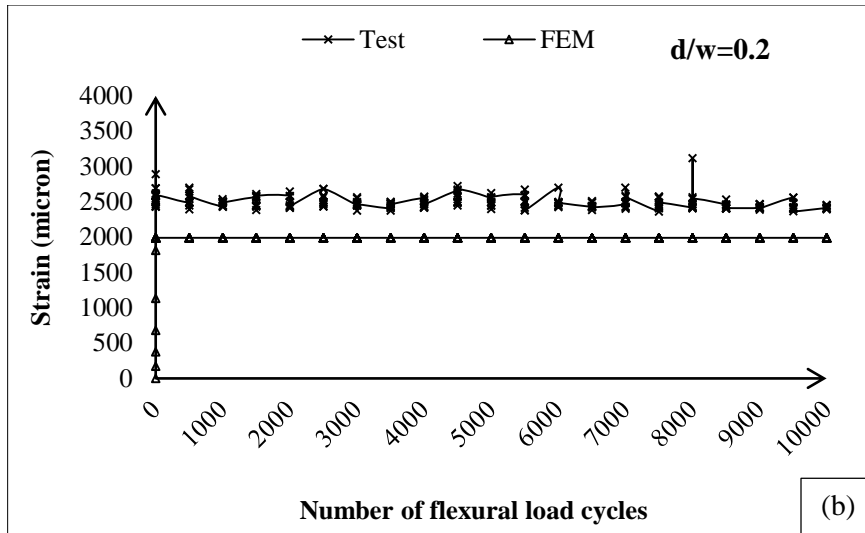


Figure 5-11: Visualization of the bottom view under fatigue load profile with diameter to width ratio of CFRP strengthened CSH specimen (a) 0.1 (b) 0.2 (c) 0.3 (d) 0.4 (e) 0.5 (f) 0.6

### 5.3.2 FEM results compared with experimental results for non-strengthened and CFRP strengthened CSH

The predicted strain from the finite element analysis and laboratory test results were compared as shown in Figure 5-12.







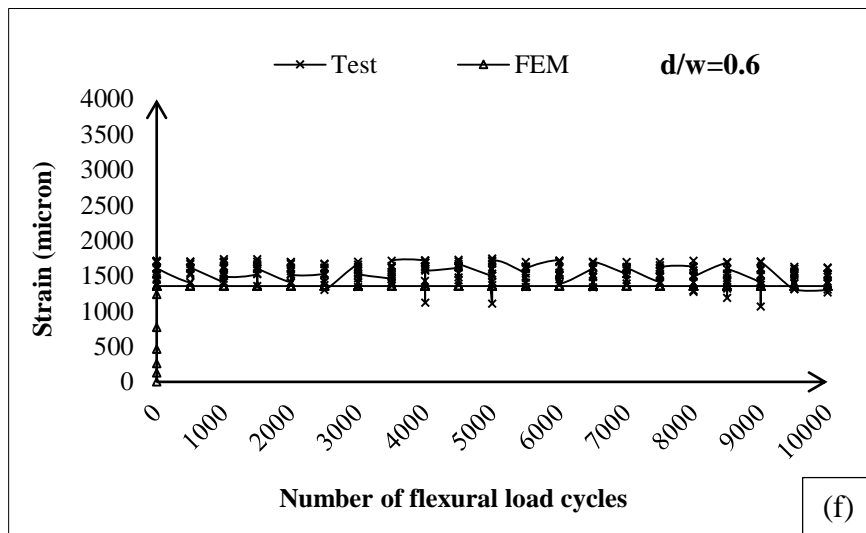
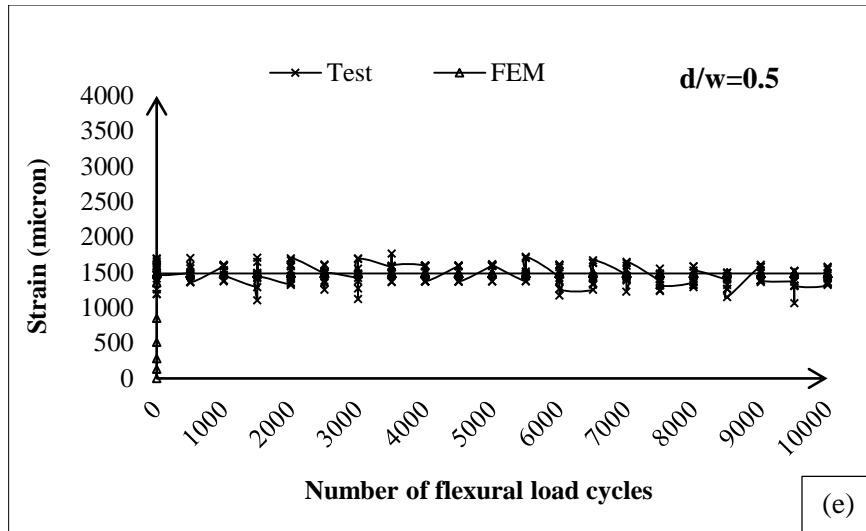


Figure 5-12: Numerical models comparing the experimental results for different diameter to width ratio ( $d/b$ ) under cyclic flexural load (a) 0.1 (b) 0.2 (c) 0.3 (d) 0.4 (e) 0.5 (f) 0.6

The strain distribution near the CSH was measured and compared with FEM results as shown in Figure 5-12. According to graphs the model results and experimental results were reasonable for the selected range of diameter to width ratio of the CSH. However, the strain variation due to the diameter to width ratio of CFRP-strengthened CSH test results agreed well with the FEM results as shown in Figure 5-12.

### 5.3.3 FEM results compared with experimental results for position change of non-strengthened and CFRP strengthened CSH (Stress based)

In this FEA, the position of CSH was considered as a main variable and it varied from 0 to 80 mm in 20 mm steps. Table 5.2 summarizes the strength of the non-strengthened and CFRP strengthened offset CSH from the test results as well as FEM results.

Table 5.2:FEM result and test results compared with position of CSH

Offset distance (mm)	Average strength (MPa)			
	Non-strengthened		CFRP-strengthened	
	Test	FEM	Test	FEM
0	207.9	167.8	235.9	290.0
20	260.2	228.3	267.2	312.5
40	261.2	234.8	322.9	318.5
60	286.4	284.5	308.6	352.5
80	387.6	388.5	410.1	388.0

The test results of CSH with different position were compared with the FEM in Figure 5-13. It summarizes the tensile strength values together with the variation of different location from the midpoint up to 80 mm in the range of 20 mm step. The stress variation due to the position of the CSH agreed with the FEM results shown in the Figure 5-13.

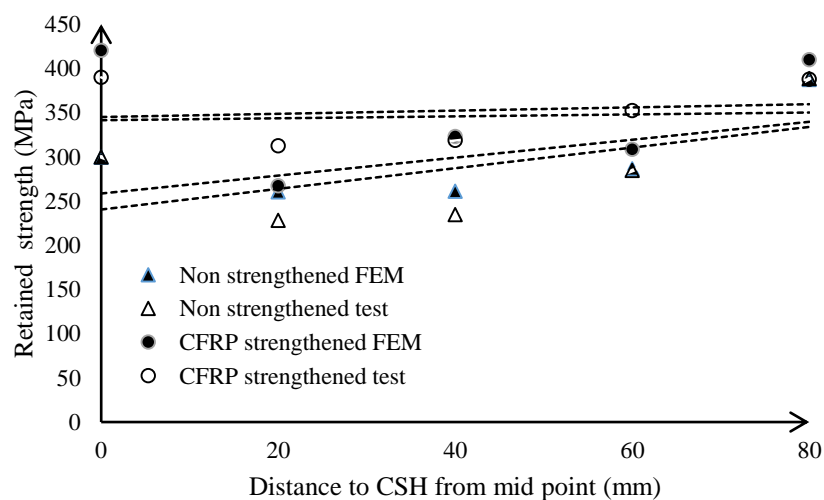


Figure 5-1: Average strength variation with offset distance of CSH

The average strength variation due to the position of CSH agreed with the FEM results as shown in Figure 5-13. The test results of the CFRP strengthened CSH also compared in FEM in Figure 5-13. It summarizes the retained average strength values together with the variation of different diameter to width ratio from the range of 0.1 to 0.6 in the range of 0.1 step. Contour of the tensile surface (bottom surface) of the specimen under flexural cyclic load with offset distance is shown in Figure 5-14.

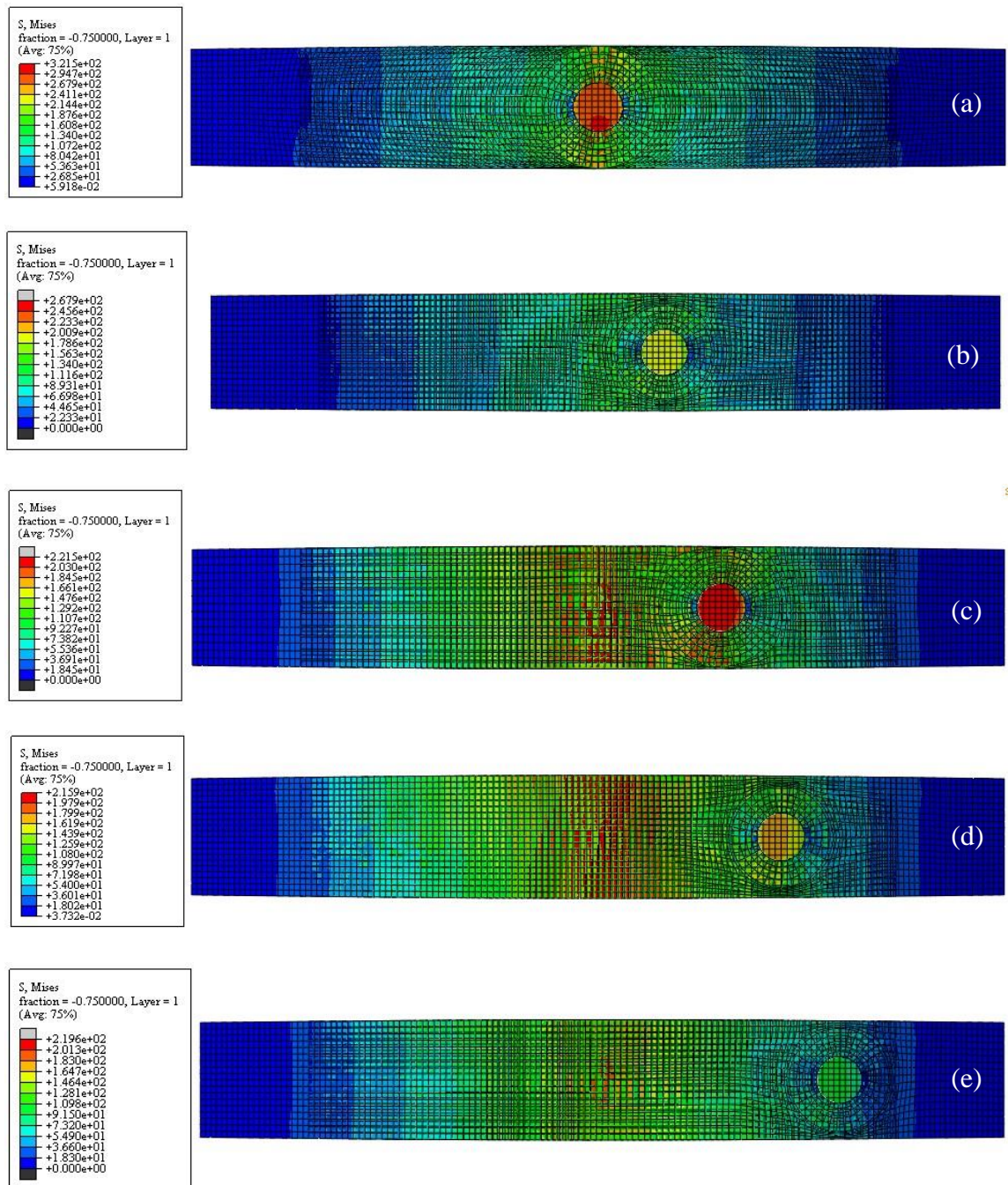


Figure 5-14: Visualization of the bottom view under fatigue load profile with offset distance. (a) 0 (b) 20 mm (c) 40 mm (d) 60 mm (e) 80 mm

#### **5.4 Summary of finite element modelling related with CSH/CFRP hybrid system**

This study focuses on a nonlinear FEA at the CSH under cyclic flexural loads. The model geometry, material properties, boundary conditions and the finite element mesh are described in this chapter. Proposed model was solved with direct cyclic mode while the numerical technique was based on cyclic J-integral method dealing with EPFM approach.

Numerical model results agreed with the laboratory test results too. The part module allows sketching of any shape of geometry and property module allows to the change of material properties in ABAQUS. Also, it has flexibility to use any shape of geometry as well as any material. This model could be easily applied in real world applications to overcome expensive laboratory test procedures. Therefore, the numerical model presented in this chapter could be successfully applied with the CSH model under fatigue conditions of structures.

ABAQUS FEA packages have the capability to estimate the value of J-Integral under monotonic loads. However, they do not have the capacity to automatically available J-Integral value from history outputs or ODB database. In addition, accuracy of results highly depends on mesh size while a very fine mesh size results are more precision. However, high end hardware facilities are needed to run fine mesh analysis. Therefore, these can be considered as major limitations for this evaluation technique and such reasons would significantly tolerate the final results of the analysis. It is interesting to note that, effects of environmental conditions are not allowed to control in this background.

When considering the geometrical parameters like the size of test specimen and actual size of structural members, there are considerable differences. On the other hand, geometrical size of test specimen for the experimental program in the chapter 4 and model size for FEM explained in the chapter 5 are identical. However, this study focuses on investigating variations of mechanical property due to fatigue and diameter to width ratio as a main parameter relating to geometry. Finite element model also focuses to predict mechanical property variation at the end of fatigue. This study is not based on the size of the CSH but it was based on the diameter to width ratio. Therefore, it can be compared with any geometric dimensions as the final outcomes are

independent from the geometry. Hence an experimental and numerical model can be considered as a geometry independent investigation. On the other hand, FEM in this study was based on the J- integral techniques. Most of conventional fatigue related investigations utilizes the Paris law to estimate the rate of the crack growth. However, Paris law constants are highly dependent on geometrical parameters as well as stress ratios and some authors have emphasized this as a major limitation of the Paris law. Thus, this study was based on the Power law, as the constant of the Power law direct deals with material properties and does not deals with geometrical parameters. Eventually the outcome of this investigations could be utilized for any real geometrical size without correction factors. Therefore, it does not affect the final results of the actual structural elements.

## ***Chapter – 6***

---

# ***Theoretical Approach for Evaluate Re-cracking behavior of CSH***

## **6. THEORETICAL APPROACH TO EVALUATE RE-CRACKING BEHAVIOR OF THE CSH**

### **6.1 Theoretical background of the CSH technique**

The crack growth is another important concept when considering fatigue failure analysis of material components. Crack growth further could be classified as stable and unstable crack growth. A stable crack growth process occurs at the micro-level and generally it is perpendicular to the direction of major tensile direction. The unstable crack growth process occurs at the macro-level and usually it contributes to increase size of the crack. The stress generated due to any external or internal reasons have a tendency to initiate cracks on components of structures. When the range of stress intensity factor reaches a critical level, the result shows the start of growing cracks (Recho, 2012). Such crack growth occurs rapidly and as explained as an exponential behavior until the fracture takes place.

According to reported data, nearly 40–50 % of the existing steel bridges in the world should be repaired due to fatigue crack observations. Therefore, prediction methods are essential to estimate crack growth of structures and this can support to determine the inspection intervals for maintenance and repair purposes. If there are any proposed methods, it should be simple and accurate. However, fulfilling all of above requirements is not an easy task, as numerous variables significantly influence the crack propagation process. Also, there is no direct way to estimate the retaining fatigue life of structures. Evaluation of S-N curve, endurance limits and behaviour of strain can be considered as popular methods for fatigue life prediction. In addition, tensile data and micro structural behaviour also provides a good insight. Total fatigue life consists of the two components which is crack initiation and crack propagation. Therefore, prediction of the crack initiation is the most important data to decide the retaining life span of the structure.

The Paris law based on theory of fracture mechanics can be considered a very popular method utilized to estimate crack growth. This co-relation highly depends on geometry and the stress ratio and it is based on linear elastic fracture mechanics theory. Real

world application, changing mechanical properties of material due to fatigue effects and do not account in model related with the Paris law. The Power law is linked with the theory of elastic plastic fracture mechanics. Constants of the Power law depends on material characteristics and it is independent from geometrical, characteristics.

## 6.2 Theory of fracture mechanics

Fracture mechanics theory is one of the leading ways to predict fatigue durability of the material in the presence of cracks. The main reason for crack propagation is the effect of the cyclic stress on structural components. Geometrical discontinuities such as holes, notches and crack zones have a high tendency in the process of crack initiation. The main steps of fatigue failure are the crack initiation, propagation and fractures as explained above. Crack propagation analysis is based on three parameters related to fracture mechanics. These are stress intensity factor (K), J-integral, and energy release rate (G). In 1957 Irwin explained three possible ways in which crack faces move with respect to each other as shown in Figure 6-1. In addition to fracture mechanics, stress analysis and strain analysis also utilized for fatigue life estimation.

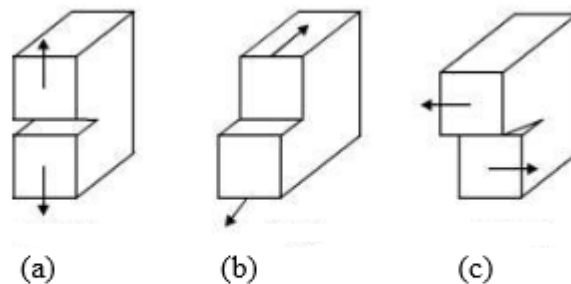


Figure 6-1: Basic modes of crack deformation. (a) opening; (b) In-plane shear  
(c) Out-plane shear (Hashim, 2012)

### 6.2.1 Linear elastic fracture mechanics (LEFM)

The linear elastic fracture mechanics (LEFM) considers that the material is isotropic and has a linear behavior within the elastic region. Stress intensity near the crack tip could be estimated using the theory of elasticity. Hooke's law is applied within the theory of elasticity to determine any stress that exceeds the material fracture toughness value results in start crack growth. This method is only valid for the small-scale yielding processes. In 1957 Irwin introduced this SIF concept for ductile materials. In



addition, Irwin described that the SIF depended on the crack length ‘a’ and mean stress ‘ $\sigma$ ’. The concept of linear elastic analysis, SIF and the concept of energy release rate have a close relationship.

### 6.2.2 Elastic-plastic fracture mechanics (EPFM)

EPFM (Elastic Plastic Fracture Mechanics) could be considered as an alternative fracture mechanics model. This theory is used to analyze fracture caused in large deformations at crack initiation stage and both summarizes in Table 6.1. When the large plastic zone is formed in front of the crack end, the theory of EPFM can be applied which explains the crack tip plasticity (Alan and Zehnder, 2012). In addition, elastic-plastic fracture mechanics implies to time-independent materials and plasticity effect on the crack tip is taken into account in this approach. As a result, this method is highly utilized in the case of analysis fracture behavior of ductile materials. Fracture theory which is based on two methods is introduced for the ductile fracture assessment. These are called J-integral method and crack tip opening displacement (CTOD) method. CTOD is more popular in Europe and J-integral technique is widely used in the United States. Values of CTOD and J- integral are shown as geometry-independent measures dealing with fracture toughness. It exhibits a relatively high plasticity at the crack end and it could be considered as a limitation of both J-integral and CTOD methods.

Table 6.1: Summary of the fracture mechanics theory (Alam et al.)

<b>Description</b>	<b>Material Property</b>	<b>Parameter</b>
Linear Elastic Fracture Mechanics (LEFM)	1) time-independent 2) linear,	1) Energy release rate (G) 2) Stress intensity factor (K)
Elastic-Plastic Fracture Mechanics (EPFM)	1) time-independent 2) non-linear	1) crack tip opening displacement (CTOD), 2) J-integral

The cyclic J-integral ( $\Delta J$ ) could be considered as a crack tip parameter utilized with elastic-plastic fracture mechanics. James Rice in 1968 introduced the path-

independent contour integral analysis technique for crack analysis. Author explained that the J-integral method is usually connected with elastic-plastic fracture mechanics (EPFM). On the other hand,  $\Delta J$  can be considered as a rate of energy released in the independent path contour. Suresh et al. (1984) have confirmed that the J –integral based fatigue crack growth provides a good quality approximation to predict behavior of a short crack. However, the ABAQUS does not provide the facility to directly obtain the value of cyclic J-integral, thus Ochensberger and Kolednik introduced an equation 6.1 to fulfil this gap. Where  $\Delta J$  is the cyclic J- integral value,  $J_{\min}$  is the minimum value available at particular FEA results and  $J_{\max}$  is the maximum value available in the same evaluation.

$$\Delta J = J_{\min} + J_{\max} - \sqrt{J_{\min} + J_{\max}} \quad (6.1)$$

However, there no available standard methods or universally accepted co relations to predict the cyclic J-integral (Ochensberger and Kolednik, 2014). The SIF range is a function of the cyclic J-integral for an elastic module as explained in equation 6.4 (Ochensberger and Kolednik, 2014a). Sumpter (1976) explained J-Integral under both of elastic and plastic phenomena dealing with crack growth. Therefore, the results can be assumed to be cumulate of the elastic and plastic components.

### 6.2.3 The Fatigue mechanism

Different methods have been used to estimate fatigue stresses such as peak stress and stress range. Each of these methods has slightly different results and the result depends on the loading condition. Initiation and propagation of cracks constitute main steps of fatigue mechanisms. Initiation of fatigue crack at smooth surface consumes nearly 90 % of load cycles while crack propagation may need only balance 10 % cycles at the ambient conditions. The common explanation of the fatigue mechanism is based on the theory of dislocation and its deals with the stresses of metals. According to dislocation theory, it explains the atomic structure of the metal crystals with numerous missing atoms. These missing atoms causes to make gaps between crystals and it creates massive stress raisers. This atomic gaps are contributing to crack formed at the microscopic level and it is called a crack nucleation. When the load is increased crack opens and due to the load fluctuation such cracks expand.

Stress due to high cycle fatigue loads proportion to ultimate tensile stress of the material, which effects of failure under a given number of cycles. If level of stresses maintained below a definable stress limit; result is the structural element should exhibit an infinite life. If the stresses are applied below 50 % of the tensile strength it does not fail due to fatigue, which is utilized at the design stage. Either ultimate tensile or yield stress should be considered in design and it varies from 80 to 90 % of tensile stress of the material.

All fatigue failures start from the outer surface of the structural component at stress concentration points. The stress raiser or concentration points are drill holes, grooves, fillets, holes, joints, hinges, bending points, threads, welds, key ways, splines, etc. Hence such a stress concentration should be taken into account in the design steps to confirm the durability of service. However, the effects of a stress concentration is directly proportional of its radius. The micro cracks consist of material which accelerate fatigue failure. However, high ductile material exhibits less stress raisers. The stress concentration variation of a rectangular plate with a hole is shown in location of the imperfection Figure 6-2. Stress levels across the plate with hole increases from the plate edge to hole edge. Furthermore, each type of the stress raiser acts as a stress concentrator at the location of the imperfection.

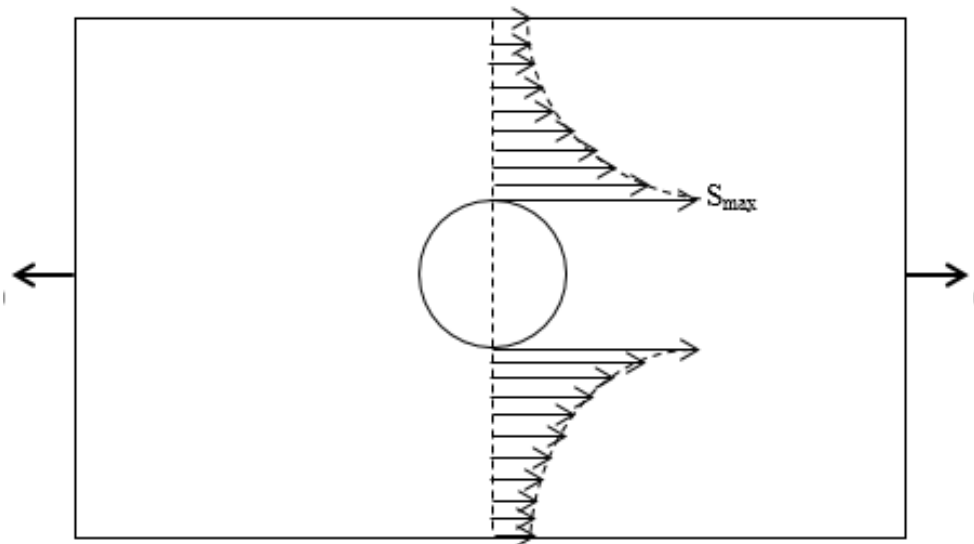


Figure 6-2: Stress distribution at CSH of steel plate (Cassa and Zyl, 2010)

Failure due to fatigue usually starts at the surface of a structural member which service loads or external loads produce maximum stresses. Two parameters greatly influence crack initiation such as microstructure and surface finish of the element. Generally, tensile stresses accelerate and compressive stresses decelerate the fatigue failure, which compressive stresses are caused to increase fatigue load carrying capacity. If the material surface can be kept with compressive stress it has less probability for metal fatigue.

### **6.3 Theoretical model to predict crack growth**

This study mainly focuses on crack initiation and it occurs under the elastic plastic deformation at the crack stop hole. Cyclic plastic deformation usually occurs at stress raiser points of the structure due to effects of continuous repetitive load applied on structures. Any discontinuities on the structural elements have a high motivation to crack initiation even under the small number of loading cycles. This action is called a re-cracking at the crack stop hole. Crack growth at this stage is highly dealing with micro structural characteristics of the material. The main characteristics are grain types, grain size, and grain arrangement. Furthermore, stress intensity factor range, operating temperature and other environmental parameters influence the crack re-initiation of the CSH. Specially, the mean stress is critically influencing at this stage. The largest portion of the total fatigue life is taken by the crack propagation. The propagation stage consists of thousands of millions of stress cycles. Failure occurs when the crack grows up to a critical crack length, because the remaining material is impossible to withstand applying cyclic stress. Therefore, the numerical representation of the total fatigue life contains a number of cycles sustained in crack initiation and propagation.

#### **6.3.1 Total fatigue life**

The total fatigue life of the structural components could be divided into basically two parts such as crack initiation and propagation. The fatigue failure process of a structural material could be classified into two main sections. These are mainly crack initiation and propagation explained by the Paris curve as shown in Figure 6-3 and boundaries between the two sections are not clearly defined. However, the total fatigue

life,  $N_f$  consists of a crack initiation period,  $N_i$  and crack propagation period,  $N_p$  as explained in equation 6.2. A method for resolving crack initiation can be considered as an elastic-plastic fracture mechanics (EPFM) approach. Furthermore, it could be further classified as a micro-structural short crack and a physically small crack. The physically small crack (PSC) growth assumes that micro-cracks due to high-stress concentration. When length of micro crack reaches a depth of 0.3 mm is considered as the threshold for crack initiation due to fatigue load. The time taken to achieve this threshold depth could be estimated using fracture mechanics models. This study was focused on an estimation of fatigue capacity at the crack stop hole. Fatigue life ( $N_f$ ) is defined as the total number of load cycles required to fail as explain in equation 6.2.

$$N_f = N_i + N_p \quad (6.2)$$

### 6.3.2 The Paris law

Paris law is the most popular theory to evaluate crack growth which could be utilized to estimate the simulation of fatigue crack subjected to low cycle fatigue (Paris et al., 1961). This law explains that the crack length per cycle is a function of stress intensity factor range ( $\Delta K$ ) as explain in equation 6.3 which dealing with linear elastic fracture mechanics. 'C' and 'm' constants are called as Paris law coefficient and exponent respectively. The Paris law coefficient and exponent are constant and it highly depends on the geometrical parameters of the structural element. Therefore, it cannot be used commonly to predict fatigue crack growth (FCG) rates with different geometric dimensions. Revankar and Ronznic (2012) suggested that constants are a better way which could be obtained from laboratory experiments, because 'C' and 'm' highly depend on the specimen geometry as well as stress ratio, 'R'. However, in each analysis, such a lengthy procedure is not a practical task. Therefore, most of the studies these values are taken from literature. The Paris law behavior is shown in Figure 6-3.

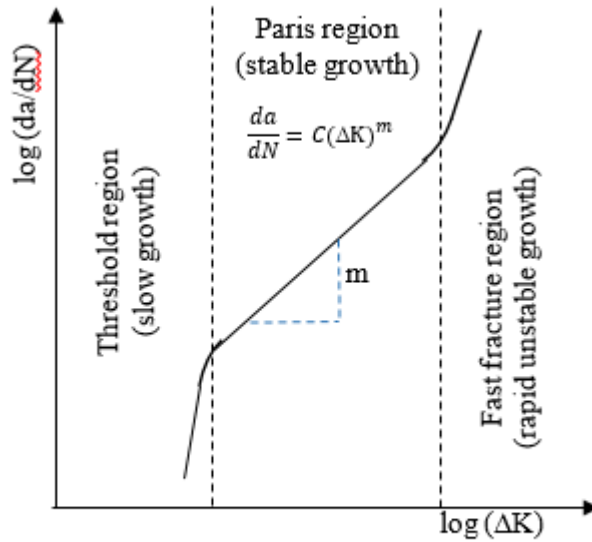


Figure 6-3: Paris law related curve (Butkewitsch, 2006)

$$\frac{da}{dN} = C(\Delta K)^m \quad (6.3)$$

The number of cycles (N) for a crack growth from the initial to final length has been explained by the Paris law given in equation 6.3 (Paris et al., 1961). The number of cycles required to crack initiation at the crack stop hole, depends on stress level of material. Equation 6.3 is utilized to determine the stress intensity factor range,  $\Delta K$ . Dowling et al. (1976) have confirmed that the relationship given in equation 6.3 shows an excellent result of crack behavior under the plane stress conditions. Numerical values of the J-integral can be estimated by using the contour integral technique in FEA. Ochensberger and Kolednik (2014) introduced an equation 6.4 to estimate cyclic J-integral value,  $\Delta J$ .

$$\Delta J = \frac{(\Delta K)^2}{E} \quad (6.4)$$

Equation 6.4 is used to estimate the cyclic J-integral value,  $\Delta J$  by using 10 contours and the results were substituted into equation 6.4 which determined the value of stress intensity range,  $\Delta K$  and 'E' is an elastic modulus of the material. The number of cycles, 'N' for a crack growth from an initial crack length to the final crack length is given in equation 6.3.

### 6.3.3 The Power law

Fracture mechanics theory is a well-established and commonly applied method to predict crack propagation. An elastic-plastic fracture mechanics approach is more compatible to evaluate more complex and nonlinear context. The cyclic J-integral approach is based on the fracture mechanics. Dowling and Begley (1976) have introduced the J-integral method considering the rate of crack growth, 'da/dN', and cyclic J-integral, 'ΔJ'. This is called as the Power law and is explained in equation 6.5 very similar to the Paris law. This analysis is valid for both linear-elastic and elastic plastic models.

Estimation of a crack growth is important for structural components during their service life, because such estimations help in deciding the remaining service life of the structural elements or whole structures. In addition, it can be used to determine inspection intervals for maintenance and repair purposes. Therefore, accurate and reliable prediction techniques are needed to estimate crack propagation behavior of component. In addition, such a technique should be simple and cost effective. However, fulfilling both requirements at the same time is difficult, because numerous parameters significantly effects on the fatigue process.

$$\frac{da}{dN} = A(\Delta J)^n \quad (6.5)$$

When considering the Power law, it was assumed that the cyclic J –integral, 'ΔJ' includes the summation of elastic and fully plastic solutions. The rate of fatigue crack growth in the Power law depends on constants 'A' and 'n'. These two parameters are called as the Ramberg-Osgood coefficient and strain hardening index respectively (Wu et al., 2009). However, these two parameters do not depend on the geometry and based on material properties. These constants specially indicate the tensile properties of materials.

However, according to Siegmund and Brocks (1999) Power law cannot be applied for reverse or non-proportional loading conditions . Furthermore, authors have explained that material descriptions are based on theory of plasticity (Ochensberger and Kolednik, 2016). Lee (1970), Sih,(1974) and Peralta and Laird (2016) proposed an

alternative methods to characterize the FCG under elastic-plastic conditions. It was based on geometric correlations among the extension of crack, “da” and the crack tip opening displacement, (CTODC). In this context the CTODC method was not a material parameter, but it was considered as a mechanical constraint which is the main advantage of this method. However, Suresh et al. (1984) confirmed that the J–integral based fatigue crack growth provides a good approximation to predict the behavior of a short crack.

#### **6.3.4 Comparison of Paris law and Power law**

The Paris law is a conventional and the most popular correlation which is utilized to estimate the rate of the crack growth. It is related to the geometry of the structure and basically considers the LEFM behavior of material. The coefficient of Paris law varies with geometry of structure and therefore some authors suggested it should take from laboratory testing. However, it is very difficult to applicable in field applications. The Power law also explains the rate of crack growth and it deals with elastic plastic fracture mechanics. There are two coefficients and numerical values which depend on material characteristic. The real world application fatigue not only deals with LEFM but also very close to the EPFM. On the other hand, fatigue always deals with properties of material. Therefore, Power law approximation can be considered as the most suitable method to estimate the crack growth rate of a material. This study focuses on Power law which is utilized to estimate the re-cracking behavior of the CSH and replaces the conventional Paris law (Paris et al., 1961).

#### **6.3.5 Developing a theoretical model to predict the rate of the crack growth**

James Rice in 1968 proposed J-integral technique implies with theory of elastic-plastic fracture mechanics (EPFM). This technique is specially utilized to characterize the crack driving force. J-integral method deals with the strain energy as well as crack tip stress under elastic-plastic condition (Miannay, 2001). Author confirmed the basis of elastic plastic fracture mechanics methodology well beyond the validity limits of linear elastic fracture mechanics. Wang et al. (2019), have shown the J-integral is represent the energy release rate at a crack tip under the condition of non-linear elastic.



Fatigue life under linear elastic fracture mechanics (LEFM) deals with the stress intensity factor (SIF),  $K$ . The range of SIF and Paris law is utilized to predict the fatigue durability of the material (Erdogan, 1963). The results of the Paris law are more accurate with the theory of LEFM than EPFM. However, the Paris law cannot be applied directly to determine fatigue life under EPFM, as the crack growth of material occurs at elastic as well as plastic levels (Santecchia et al., 2016). This limitation could be overcome by introducing a new parameter for elastic plastic properties of material (Recho, 2012). J-Integral technique, can be extended to apply cyclic loads on cracked element. Ochensberger and Kolednik, (2014) introduced an empirical formula to determine cyclic J-integral values as shown in equation 6.1.

Table 6.2 summarizes the range of stress, cyclic J-integral values, and required cycles for crack initiation together with different CSH diameters to width ratio due to the analytical results and their extension obtained in this analysis.

Table 6.2: Number of cycles for crack initiation by the Paris law with respect to diameter to width ratio

<b>Diameter to width ratio of CSH, <math>d</math> (mm)</b>	<b>Cyclic J-integral value (<math>\Delta J</math>)<math>\times 10^{-2}</math></b>	<b>The range of stress, (<math>\Delta K</math>) (MPa<math>\sqrt{mm}</math>)</b>	<b>Fatigue crack growth rate (mm/Cycle) <math>\times 10^{-5}</math></b>	<b>Number of cycles for crack initiation</b>
0.1	1.00	1.41	10.8	9234
0.2	2.14	2.07	15.6	6412
0.3	3.70	2.72	20.3	4931
0.4	4.10	2.86	21.3	4694
0.5	5.53	3.33	24.6	4067
0.6	11.55	4.81	35.0	2857

Table 6.3 summarizes the log value of rate of fatigue crack growth together with the log value of the cyclic J- integral with different diameter to width ratio of CSH from the analytical results. Laird et al.(2016) proposed an alternative method to characterize the FCG under elastic-plastic conditions.

Table 6.3: Log values of the crack growth rate variations with diameter to width ratio of the CSH

Diameter to width ratio (d/b)	Cyclic J-integral value ( $\Delta J$ ) $\times 10^{-2}$	$\ln(\Delta J)$	Fatigue crack growth rate (mm/Cycle) $\times 10^{-5}$	$\ln(da/dN)$
0.1	1.00	-4.61	10.8	-9.13
0.2	2.14	-3.84	15.6	-8.77
0.3	3.70	-3.30	20.3	-8.50
0.4	4.10	-3.19	21.3	-8.45
0.5	5.53	-2.89	24.6	-8.31
0.6	11.55	-2.16	35.0	-7.96

Using the results of the log value of the rate of crack growth range which varies with the log value of cyclic J-integral due to effects on fatigue loads are shown in Figure 6-4.

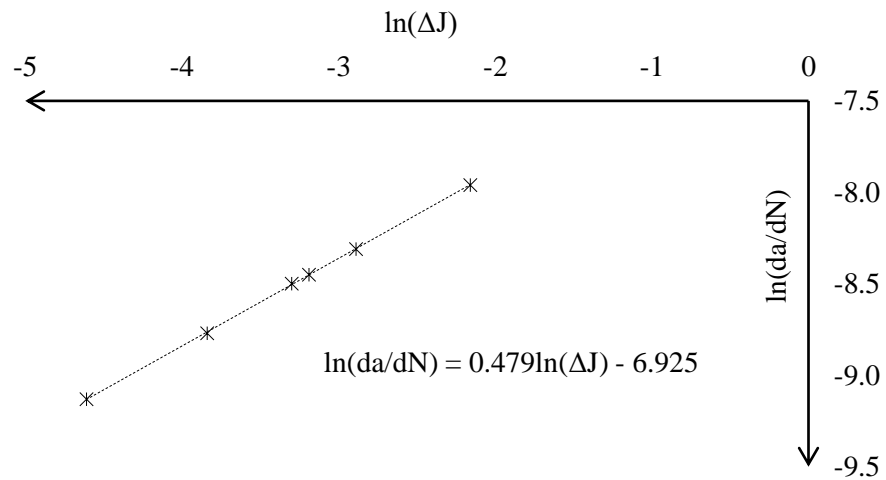


Figure 6-4: Log value of rate of fatigue crack growth with cyclic J-integral

As shown in Figure 6-4 when the log value of cyclic J-integral increases, the log value of the fatigue crack growth rate also increases. The log value taken from equation 6.5 builds a linear co- relation with respect to the cyclic J-integral as shown in equation 6.6.

$$\ln\left(\frac{da}{dN}\right) = n * \ln(\Delta J) + \ln(A) \quad (6.6)$$

The log value of the crack growth rate with respect to the log value of the cyclic J-integral value is represented by Figure 6-4 and the results curve fitted with the linear co-relation as shown in equation 6.6.

$$Y = 0.479x - 6.922 \quad (6.7)$$

Equation 6.6 and equation 6.7 are represents the same co-relations and individual terms considered in the linear function as explained in both of the equations.

$$n = 0.479 \text{ and } \ln(A) = -6.922$$

Then calculated numerical value of 'A' using equation 6.7.

$$A = e^{-6.922} \quad (6.8)$$

$$A=9.858x10^{-4} \quad (6.9)$$

The analytical results taken from Table 6.3 were utilized as shown in Figure 6-5. The power law function related to the relevant J-integral was shown in equation 6.10 as a polynomial function.

$$\frac{da}{dN} = 9.858x10^{-4}(\Delta J)^{0.479} \quad (6.10)$$

The crack growth rate was approximate using the equation 6.8 which deal with J-integral. The maximum and minimum values of J-integral were taken from ODB database of FEM and these values utilized in equation 6.1. The value obtained from equation 6.1 substitutes for equation 6.10 and obtained the rate of crack growth. The estimated number of cycles for re-cracking was up to 1 mm length of the crack. Potential drop technique was used to measured re-cracking and relevant number of cycles were recorded using digital counter attached to developed fatigue loading apparatus explain in Chapter 3. Table 6.4 summarizes the required cycles for re-cracking together with different diameter to width ratio of the CSH due to the Power law approximation and laboratory test results.

Table 6.4: Test results comparison with the Power law approximation

Diameter to width ratio of CSH (d/b)	Required number of cycles for re-cracking	
	According to Power law	Experimental investigation
0.1	9209	10066
0.2	6397	6990
0.3	4921	5372
0.4	4685	5115
0.5	4059	4431
0.6	2853	3113

Figure 6-5 shows number of load cycles; N for re-cracking varies with the diameter to width ratio of CSH due to effects on cyclic flexural load with constant amplitude load. As shown in Figure 6-5 the number of load cycles are inversely proportional with the diameter to width ratio. The required number of load cycles for re-cracking shows a significant decrease with the increase of the diameter to width ratio of the CSH from one-hole diameter to another. Consequently, the test results agreed with the theoretical approximation.

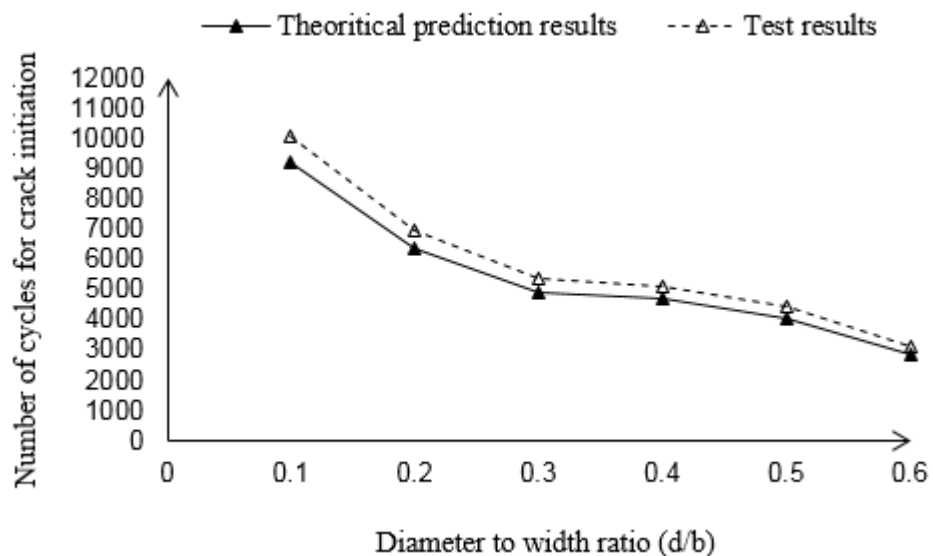


Figure 6-5: Comparison of Power law with laboratory test results

ABAQUS as well as most of FEA packages have the capability to estimate the value of J-Integral under monotonic loads. FEA, results highly depended on mesh size while a very fine mesh size results would be precise but more time consuming. In addition, high end hardware facilities are needed to run the fine mesh analysis. Therefore, these could be considered as major limitations for this evaluation technique and such reasons would significantly affect the final results of the analysis.

## 6.4 Factors that affect re-cracking of the CSH

### 6.4.1 Effects of the CSH diameter

In this theoretical prediction, the diameter to width ratio was considered as a main variable and it varied from 0.1 to 0.6 in 0.1 steps. All of other parameters were kept constant during the analysis and the procedure used for the analysis is explained in chapter 5. Table 6.5 in Appendix B summarizes the results with respect to the diameter to width ratio. The required number of cycles for re-cracking variation with diameter to width ratio are shown in Figure 6-6.

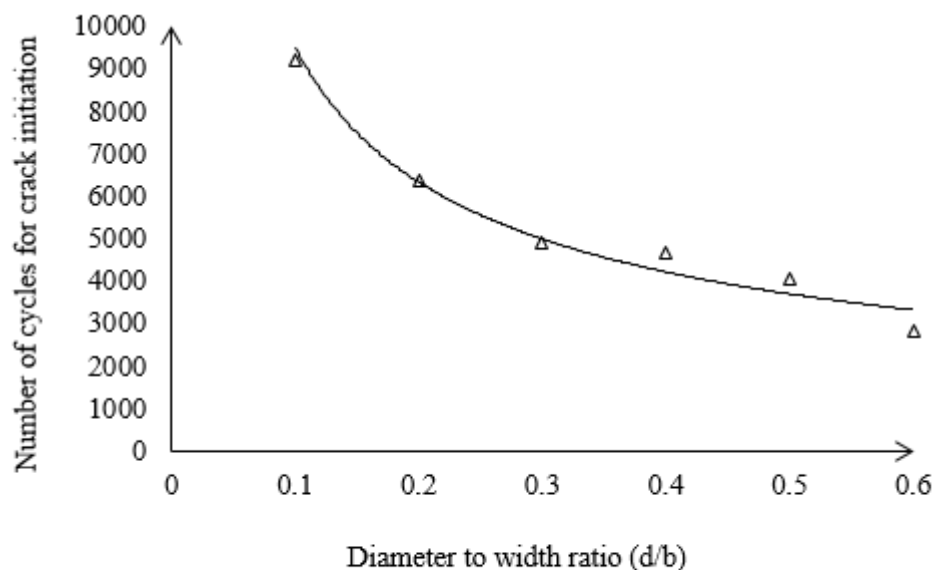


Figure 6-6: Number of cycles for crack initiation with the CSH diameter

As shown in Figure 6-6, when the diameter to width ratio increases, the number of cycles for crack initiation decrease. The predicted result of number of cycles shows significant decreases with the diameter to width ratio in the range from 0.1 to 0.6. in 0.1 steps (4 mm to 25 mm). Reasons for such behavior would be the reduction of the

stiffness at the crack stop hole which increases the diameter to width ratio of the CSH. On the other hand, the micro structure of the material changes due to the effect of cyclic load. As a result, the required number of cycles for crack initiation decreases with respect to diameter to width ratio (CSH diameter). Ishikawa et al. (2013) also recommended CSH diameter range from 6 mm to 24.5 mm for crack arrest. Rolfe and Barsom (1977) and by Fisher et al (1980, 1990) independently formulated the correlation for the CSH diameter for any crack initiation delay.

#### 6.4.2 Effects of member thickness

In this theoretical prediction, the thickness to diameter ratio was considered as a main variable and it varied from 0.1 to 0.5 in 0.1 steps. All of other parameters were kept constant during the analysis and procedure used of analysis as explained in chapter 5. Table 6.6 in Appendix B summarizes the results with respect to the thickness to diameter ratio. The required number of cycles for re-cracking variation with diameter to width ratio is shown in Figure 6-7.

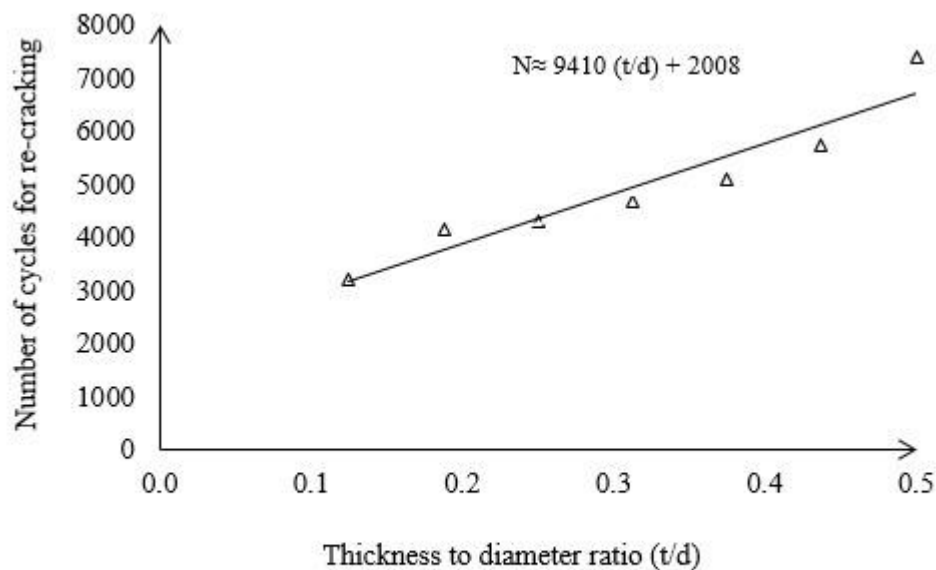


Figure 6-7: Number of cycles for crack initiation varies with the thickness to diameter ratio of the specimen

As shown in Figure 6-7, when the thickness to diameter ratio increases, the number of cycles for crack initiation non linearly increase as explained in equation 6.1. The predicted result of number of cycles shows significant decreases with the diameter to

width ratio in the range from 0.1 to 0.6. in 0.1 steps. Reason for such behavior is capability to withstand residual stress applied at the midpoint of the specimen due to the increase crack growth resistance. When the thickness of CSH increase, residual stresses and notch stress also decreases (Cotterell, 2010). The net effect contributes to the increase of the number of load cycles for re-cracking.

### 6.4.3 Effects of the crack length

In this theoretical prediction, the diameter to crack length ratio was considered as a main variable and it varied from 0.2 to 0.8 in 0.2 steps. All of other parameters were kept as constant during the analysis and procedure used of analysis as explained in chapter 5. Table 6.7 in Appendix B summarizes the results with respect to the diameter to crack length ratio. Figure 6.7 indicates the required number of cycles for re-cracking variation with diameter to crack length ratio.

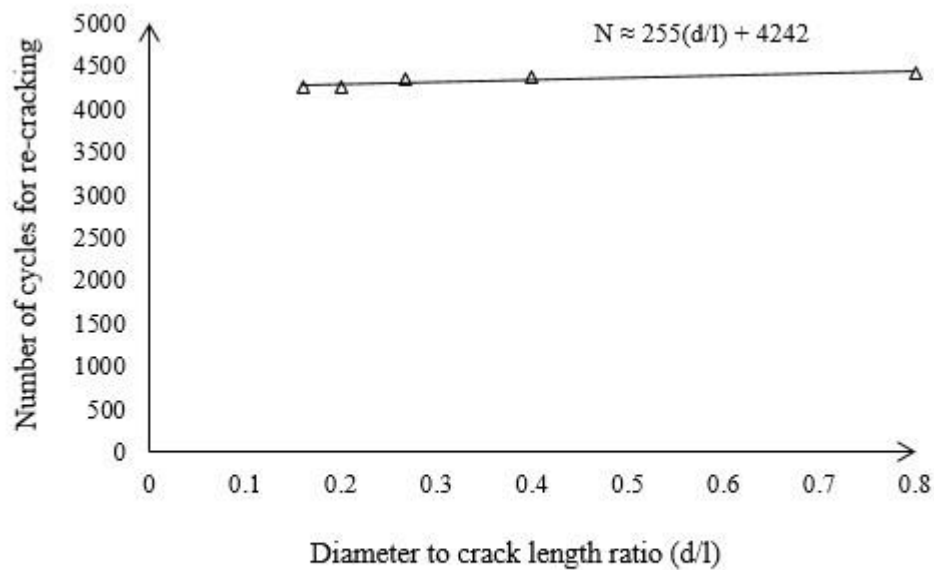


Figure 6-8: Number of cycles for crack initiation vary with the crack length of the specimen

As shown in Figure 6-8, when the diameter to crack length ratio increases, the number of cycles for re-cracking increase non-linearly. The predicted result of number of cycles shows significant variations with the diameter to crack length ratio in the range from 0.2 to 0.8. in 0.2 steps. Number of cycles for crack initiation of the CSH is lower at highest diameter to crack length ratio, as just before crack initiation the highest stress

is built on the surface near the crack stop hole due to surface energy which is utilized for crack growth. In addition, materials surrounding the CSH are weaker than the CSH and it affects the rapid growth of the crack. When the crack grows up to a certain level, material becomes harder than the surrounding CSH and then slows down the crack growth. In addition, the compressive residual stress applied on the CSH at the midpoint of the specimen had critically affected here. When the crack length increases from the midpoint, the residual stresses also increase and the notch stress is almost constant due to a constant diameter of the CSH.

#### 6.4.4 Position of the CSH

In this theoretical prediction, the diameter to offset distance ratio was considered as a main variable and it varied from 0.2 to 0.8 in 0.2 steps. All of other parameters were kept as constant during the analysis and procedure used for the analysis is explained in chapter 5. Table 6.8 in Appendix B summarizes the results with respect to the diameter to offset distance ratio. Figure 6-9 indicates the required number of cycles for re-cracking variation with diameter to offset distance ratio.

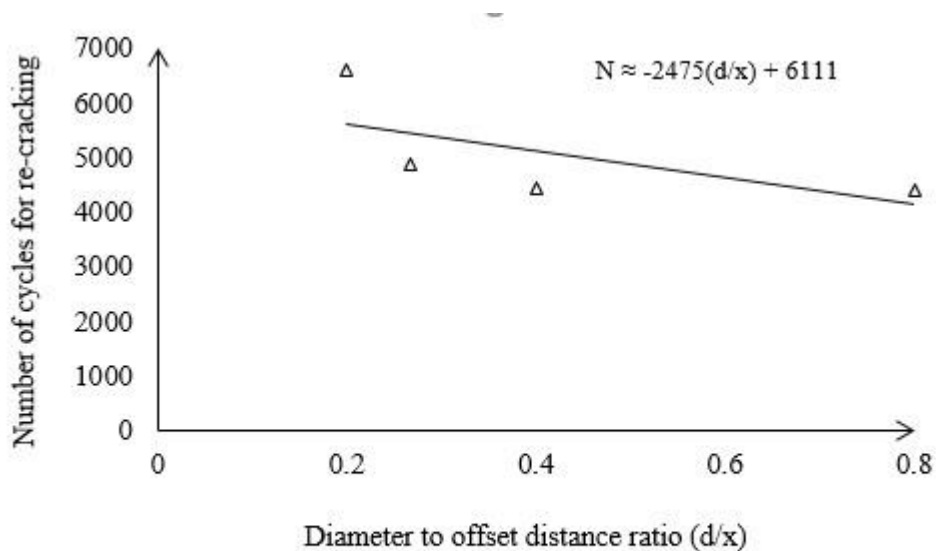


Figure 6-8: Number of cycles for crack initiation varies with diameter to offset distance ratio



As shown in Figure 6-9, when the diameter to offset distance ratio is increased, the number of cycles for re-cracking decreases non-linearly. The predicted result of number of cycles shows significant variation with the diameter to offset distance ratio. When the offset distance with respect to the mid-point increases, the required number of cycles rapidly decrease as stress at the midpoint is high and there is weak material around the CSH. When the offset distance from the loading point decreases, the required number of cycles for crack initiation slightly decreases as shown in Figure 6-9. The main reason is that the, stress intensity at the CSH of the specimen varies according to the influences of stress concentration. When the CSH is offset from the midpoint, residual stress decreases and notch stress is almost constant. Therefore, the ultimate result is the increase of the required number of cycles for re-cracking with respect to the offset distance. When the stress is further increased the required number of cycles for re-cracking also increases as shown in Figure 6-9.

#### 6.4.5 Amplitude of the load

In this theoretical prediction, the diameter to load ratio was considered as a main variable and it varied from 1 to 8. All other parameters were kept constant during the analysis and procedure used of analysis as explained in chapter 5. Table 6.9 in Appendix B summarizes the predicted results with respect to the diameter to load ratio. Figure 6-10 indicates the required number of cycles for re-cracking variation with diameter to load ratio.

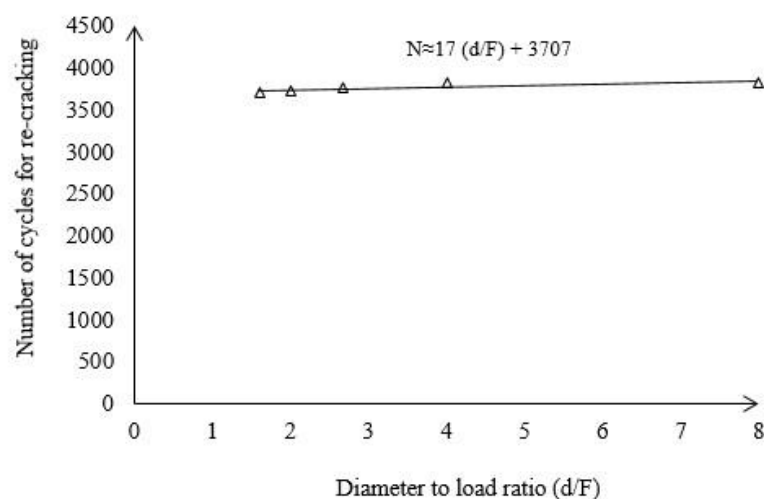


Figure 6-10: Number of cycles for crack initiation with respect to diameter to ratio

As shown in Figure 6-10, when the diameter to load ratio increases, the number of cycles for re-cracking increases non-linearly. The predicted result of number of cycles shows significant variation with the diameter to load ratio in the range from 1 to 8. The number of cycles for re-cracking varies with the loading magnitudes of the structural element. In this theoretical model, the loading magnitude is inversely proportional with number of load cycles as shown in Figure 6-10. The reason is that the, stress intensity at the midpoint of the specimen due to the effects of the loading amplitude. When the loading amplitude increases at the CSH, the notch stress is almost constant. On the other hand, surface energy increases due to the increase of the loading amplitude. The result is the reduction of the required number of cycles for re-cracking, as shown in Figure 6-10.

#### 6.4.6 Loading frequency

In this theoretical prediction, the diameter to loading frequency ratio was considered as a main variable and it varied from 1 to 8 in 1 steps. All of other parameters were kept constant during the analysis and procedure used of analysis are explained in chapter 5. Table 6.10 in Appendix B summarizes the predicted results with respect to the diameter to load ratio. Figure 6-11 indicates the required number of cycles for re-cracking variation with diameter to loading frequency ratio.

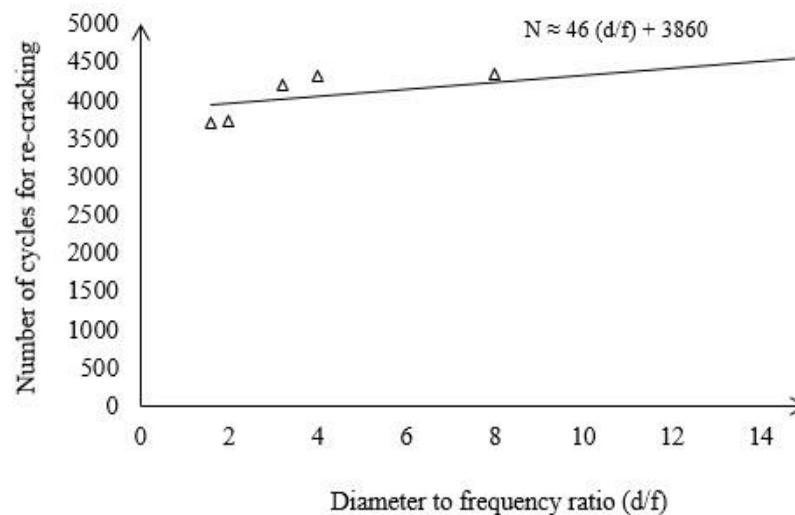


Figure 6-11: Required number of cycle for crack initiation variations with respect to diameter to loading frequency ratio

As shown in Figure 6-11, when the diameter to frequency ratio increases, the number of cycles for re-cracking increases non-linearly. The predicted result of number of cycles shows significant variation with the diameter to frequency ratio in the range from 1 to 8. The reason is that the changing rate of stress applied at the midpoint of the specimen effects on material softening which enhances re-cracking. When the loading frequency increases from 5 Hz to 10 Hz, the rate of change hardening rapidly changes.

#### 6.4.7 Stress ratio effects

In this theoretical prediction, the ratio of diameter to stress ratio was considered as a main variable and it varied from 32 to 160 in 40 steps. All of other parameters were kept constant during the analysis and procedure used for analysis is explained in chapter 5. Table 6.11 in Appendix B summarizes the predicted results with respect to the diameter to load ratio. Figure 6-12 indicates the required number of cycles for re-cracking variation with the ratio of diameter to stress ratio.

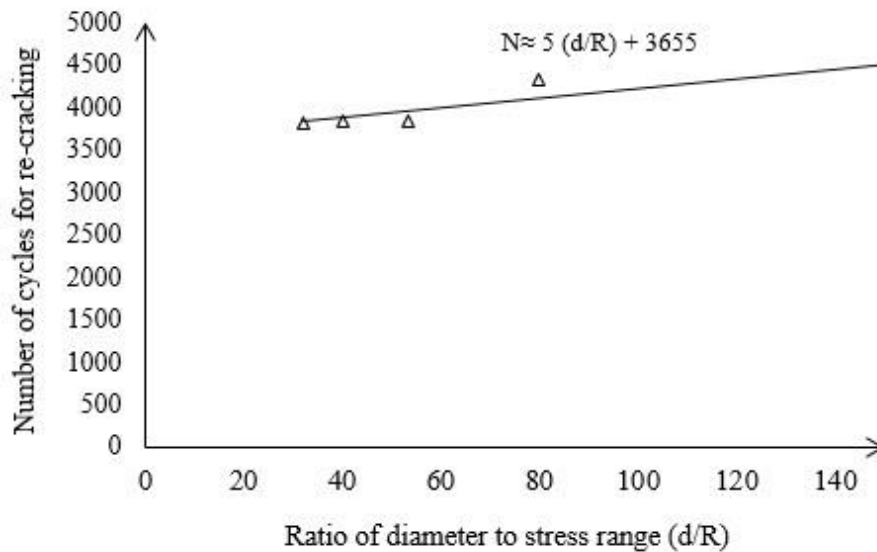


Figure 6-12: Number of cycles for crack initiation with respect to ratio of diameter to stress ratio

As shown in Figure 6-12, when the ratio of diameter to stress ratio increases, the number of cycles for re-cracking increase non-linearly. The predicted result of number of cycles shows significant variation with the diameter to frequency ratio in the range

from 1 to 8. The number of cycles for re-cracking varies with the stress ratio of loads applied to the structural element. In this analysis, the stress ratio of the crack stop hole was changed without altering other variables. The stress ratio varies at the loading point while the required number of cycles for re-cracking was calculated using the modified Power law approximation. The behavior of the stress ratio with number of cycles is shown in Figure 6-12 with the stress intensity applied at the midpoint of the specimen according to the influences of stress ratio (Singh and Sharma, 2021). When the stress ratio increases at the midpoint, residual stress increases and notch stress are almost constant. The result is the reduction of required number of cycles for re-cracking. When the stress ratio is further increased the required number of cycles decrease rapidly as shown in Figure 6-12.

#### 6.4.8 Effects of fiber direction of the CFRP

In this theoretical prediction, the fiber direction angle was considered as a main variable and it varied from 0 to 90 degrees in 30 steps. All of other parameters were kept constant during the analysis and procedure used for the analysis is explained in chapter 5. Table 6.12 in Appendix B summarizes the predicted results with respect to the diameter to load ratio. The required number of cycles for re-cracking variation with ratio of diameter to stress ratio are shown in Figure 6-13.

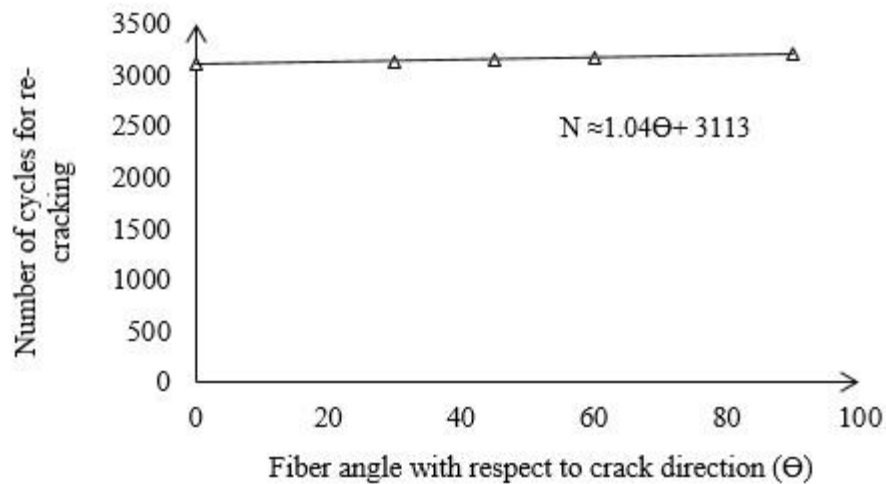


Figure 6-13: Fiber direction with respect to the crack direction

As shown in Figure 6-13, when the fiber angle increases, the number of cycles for re-cracking increases in a linear manner. The predicted result of number of cycles shows

significant variation with the fiber direction angle in the range from 0 to 90 degrees in 30 degree steps. CFRP laminate had caused to reduce the stress concentrations and had enhanced overall stiffness of the composite material. However, the fibre direction significantly influences the overall performance of the CFRP strengthened system. Theoretical prediction results have exhibited slight variations with respect to fiber direction. The reason is the stress intensity controlled by the CFRP layer attached to the bottom surface of the specimen ( Zhao et al., 2004). When the fiber direction angle is perpendicular with direction of crack driving force shows maximum performance. In addition, residual stresses are controlled by the CFRP layer and notch stress is almost constant. The result is the increase of the required number of cycles for re-cracking with respect to fiber direction as shown Figure 6-13.

#### 6.4.9 Effects of the CFRP length.

In this theoretical prediction, the CFRP bond length was considered as a main variable and it varied from 40 mm to 240 mm in 40 mm steps. All of other parameters were kept as constant during the analysis and procedure used of analysis as explained in chapter 5. Table 6.13 in Appendix B summarizes the predicted results with respect to the diameter to load ratio. Figure 6-14 indicates the required number of cycles for re-cracking variation with ratio of diameter to bond length.

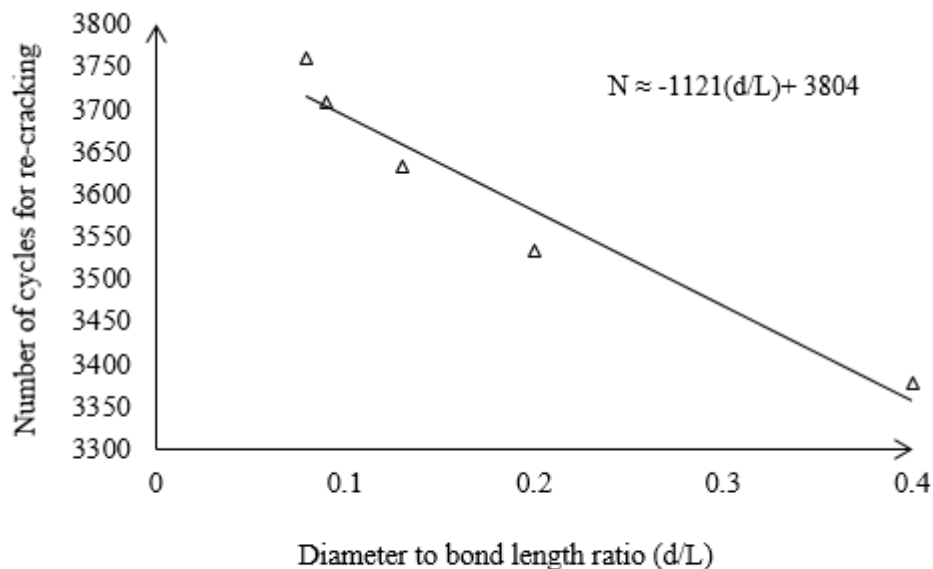


Figure 6-14: Number of cycles for crack initiation with respect to diameter to bond length ratio

As shown in Figure 6-14, when the diameter to bond length ratio increases, the number of cycles for re-cracking decrease non-linearly. The predicted result of the number of cycles show significant variations with the diameter to bond length ratio in the range from 0.1 to 0.4 in 0.1 steps. When the length of the CFRP layer is changed from the tensile direction, the required number of cycles for re-cracking increases as the residual stress due to the compressive load at the midpoint of the specimen is controlled by the length of CFRP layer attached with the tensile flange of the specimen. The bond length increases from the tensile direction, stress intensity is controlled by the CFRP length (Wang et al., 2017). However, notch stress is almost constant due to the un-changed of the dimension of the CSH in this analysis.

### **6.5 Summary of theoretical model relating with the CSH**

In this study, the CSH was theoretically estimated using the Paris law. The required number of cycles for re-cracking for the CSH were estimated by using J-integral technique. Results of the Paris law were utilized to modified Power law approximations and its validated using laboratory test results. The laboratory test results agreed well with the modified Power law approximation. The coefficient ‘A’ and ‘n’ of the Power law were estimated as  $9.858 \times 10^{-4}$  and 0.479 respectively. Thus, the power law seems to be more efficient than the conventional Paris law, as the Power law directly deals with the cyclic J-integral, less time consumption and more convenience than the Paris law. Furthermore, this method does not dependent on the geometry of the specimen and highly depends on material properties. These correlations are simple and easy to use in field applications. On the other hand, it has flexibility to be used in any geometrical shape as well as any material. Therefore, this model could be easily applied in the real world applications. This proposed theoretical model provides a unique solution for all of the above drawbacks at the same time and potential to replace laboratory tests. However, effects of environmental conditions do not allow control and there are no facilities to directly determine the cyclic J-integral from ABAQUS. Ultimately, Remberg-Osgood coefficient was modified to predict re-cracking behaviour of CSH in steel structures and replaced conventional Paris law. In practice, a number of variables have an effect on re-cracking. They are residual stress, local plastic deformation, environmental temperature and material properties.

Homogeneous and isotropic material characteristics were main assumptions in this analysis.

In addition, the load related variables such as the loading pattern, the loading type, the stress ratio, amplitudes of the load and the loading frequency effects on re-cracking. All these factors may individually or jointly influence the process of re-cracking of the CSH. However, the evaluation of all influencing parameters simultaneously is impossible. Thus, the following conclusions were obtained:

- 1) The required number of cycles for re-cracking was largely reduced in different stress levels due to the increase of the diameter to width ratio of the CSH.
- 2) The constant values of the Power law (A and n) were estimated as  $9.858 \times 10^{-4}$  and 0.479 respectively.
- 3) The Power law approximation is highly recommended for predict re-cracking behaviour of CSH.
- 4) Power law is simple than the Paris law to predict re-cracking of the CSH.
- 5) This predicted value of re-cracking of CSH is independent of the geometry of the specimen.
- 6) Co-relations of the Power law is simple and easy to use in the field.

## ***Chapter – 7***

---

### ***Parametric Study***



## **7 PARAMETRIC STUDY**

### **7.1 Introduction of parametric study**

Fatigue performance of the CFRP strengthened crack stop hole depends on many parameters. Such parameters could be classified as geometric related parameters, load related parameters and CFRP related parameters. In this investigation, the effects of most critical parameters were considered in the selected domain. Geometry related parameters were considered which included the diameter to width ratio of the CSH, the crack length, location of the CSH with respect to the loading point and thickness of the CSH. The loading parameters which were considered in this chapter are the magnitude of load, loading frequency and the stress ratio. The CFRP related parameters are also considered in this study with the length of the CFRP material and fiber direction angle with respect to crack direction. All other variables were kept as constant during the process of analysis except the considered variable. This parametric study was performed with using FEA software in ABAQUS (version 6.14) as explain detail procedure in chapter 5.

### **7.2 Fatigue Performance of CSH varying with geometry related parameters**

Steel structures have various types of geometrical sections such as rectangular, I – section and C-channel. Also, the thickness of such sections are different to each other. When considering the ageing structures several cracks could be observed that ranges from micro level to macro level crack lengths due to various reasons such as stress and corrosion effects. The CSH techniques propose different diameters by different authors, therefore, these parameters are critical for any structures. This parametric study focused on the effects of the thickness of the CSH and crack length effects were also considered.

#### **7.2.1 Member thickness**

In this parametric study, thickness to diameter ratio was considered as a main variable and it varied from 0.1 to 0.5 in 0.1 steps and procedure followed as explained in chapter 5. Table 7.1 summarizes the analytical results with respect to the thickness to diameter ratio.

Table 7.1: Strength with respect to thickness to diameter ratio

Thickness to diameter ratio of specimen (t/d)	Strength (MPa)
0.13	192.2
0.19	246.4
0.25	290.8
0.31	311.5
0.38	356.4
0.44	425.0
0.50	525.1

When thickness is increased, the tensile strength variation could be illustrated as shown in Figure 7-1. The reason for such behavior is that stiffness increases with thickness and less residual stress due to the CSH. When the thickness of the CSH increase, residual stresses and notch stress also decreases (Cotterell, 2010). The net effect is the increase of strength with respect to thickness to diameter ratio.

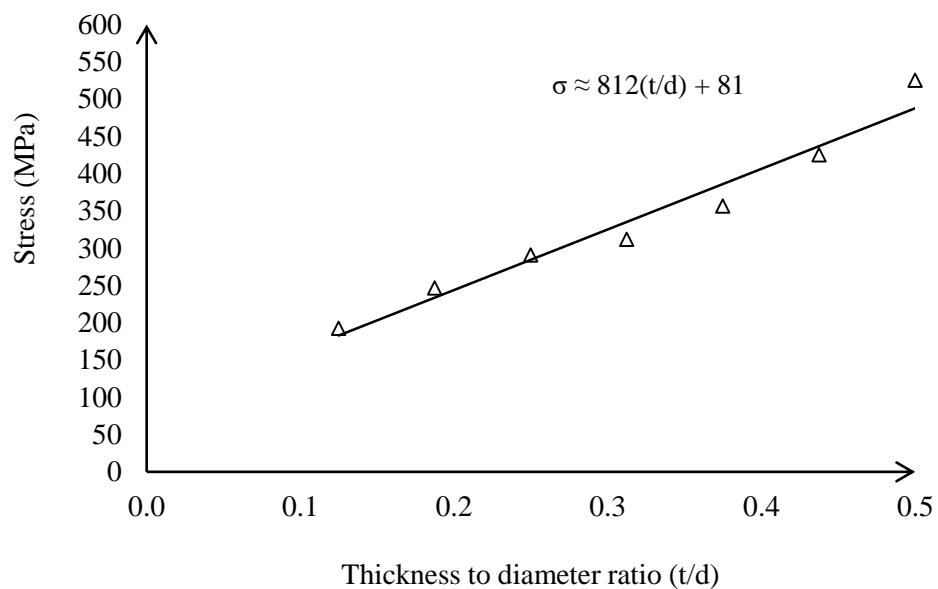


Figure 7-1: Strength variation with thickness to diameter ratio of member

Due to effects of fatigue, the material becomes weak. In addition, the yield strength of any material is governed by the residual stress, notch stress, stiffness and hardening effects it. Therefore, yield strength is directly proportional to the thickness of the CSH. When the thickness of specimen gradually increases the residual stress also increases. However, the notch stress effects on the CSH could be ignored in this analysis as the selected diameter is constant. Contour of the tensile surface (bottom surface) of the specimen under flexural cyclic load with member thickness is shown in Figure 7-2.

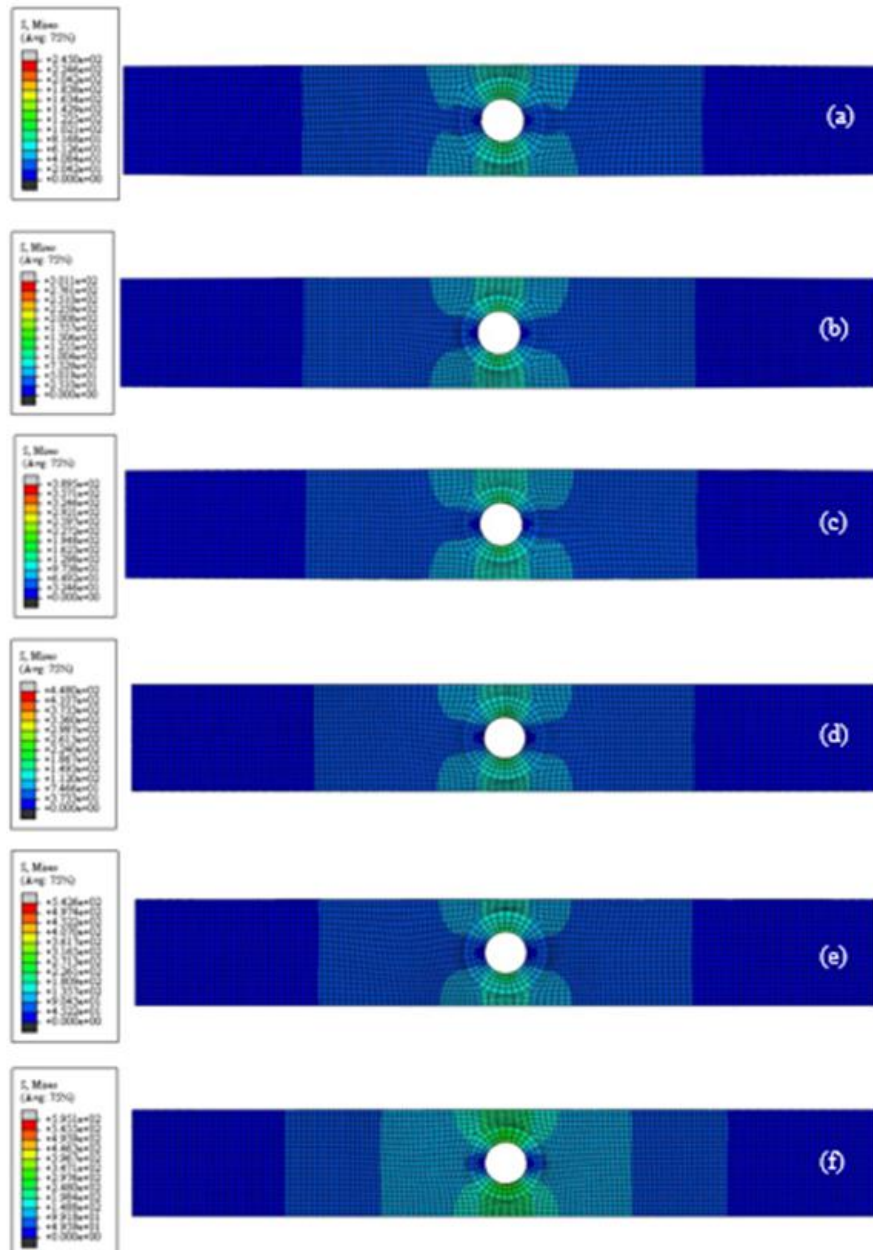


Figure 7 2: Visualization of the bottom view under fatigue load profile with thick specimen. (a) 5 mm (b) 6 mm (c) 7 mm (d) 8 mm (e) 9 mm (f) 10 mm

### 7.2.2 Crack length

In this analysis, the diameter to crack length ratio was considered as a main variable and it varied from 0.1 to 0.8 in 0.1 steps. All of other parameters were kept constant during the analysis and procedure followed in this analysis is explained in chapter 5. Table 7.2 summarizes the FEM results with respect to the diameter to crack length ratio.

Table 7.2: Strength variation with respect to the diameter to crack length ratio

<b>Diameter to crack length ratio (d/l)</b>	<b>Strength (MPa)</b>
0.80	304.4
0.40	287.2
0.27	282.5
0.20	269.9
0.16	254.9

In this analysis, the length of the crack was changed without altering other variables. Tensile strength was determined with respect to the crack length and its variation with respect to the crack length which is shown in Figure 7-3. The reason is that the micro structure of the material change due to cyclic loads effects and weak material surrounding the CSH. Especially the elastic properties of the material are converted to plastic. In addition, the discontinuity of the material due to cracks causes to reduce stiffness and then resulting the tensile load capacity of the material being inversely proportional to the length of crack. However, notch stress is almost constant due to constant diameter of the CSH.

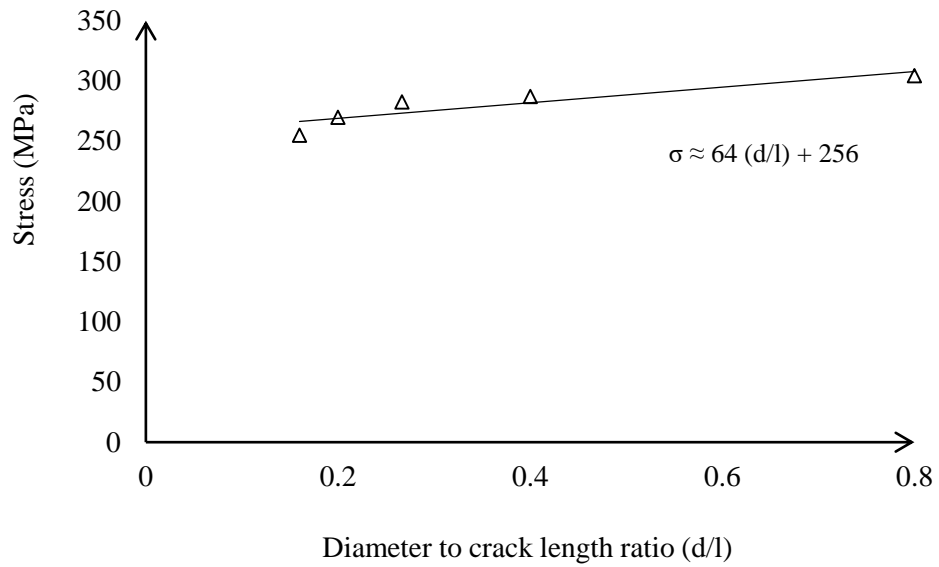
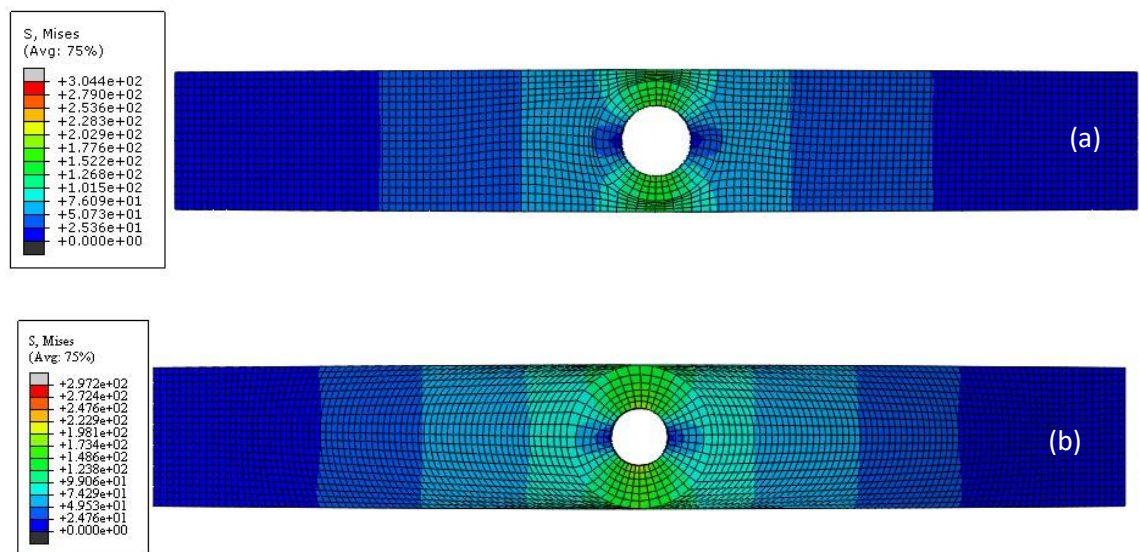


Figure 7-3: Strength variation with diameter to crack length ratio

Stress concentration is reflected by overall effects of fatigue, residual stress and notch stress. At the initial stage of the crack reported highest yield load due to toughness of the material. When increasing the crack length, it shows an inversely proportional behavior the diameter to crack length up to 0.3 and after that exhibits a rapid reduction of yield strength with a long crack as shown in Figure 7-3. However, notch stress can be considered as constant due to constant diameter of each case. Contour of the tensile surface (bottom surface) of the specimen under flexural cyclic load due to crack length effect is shown in Figure7-4.



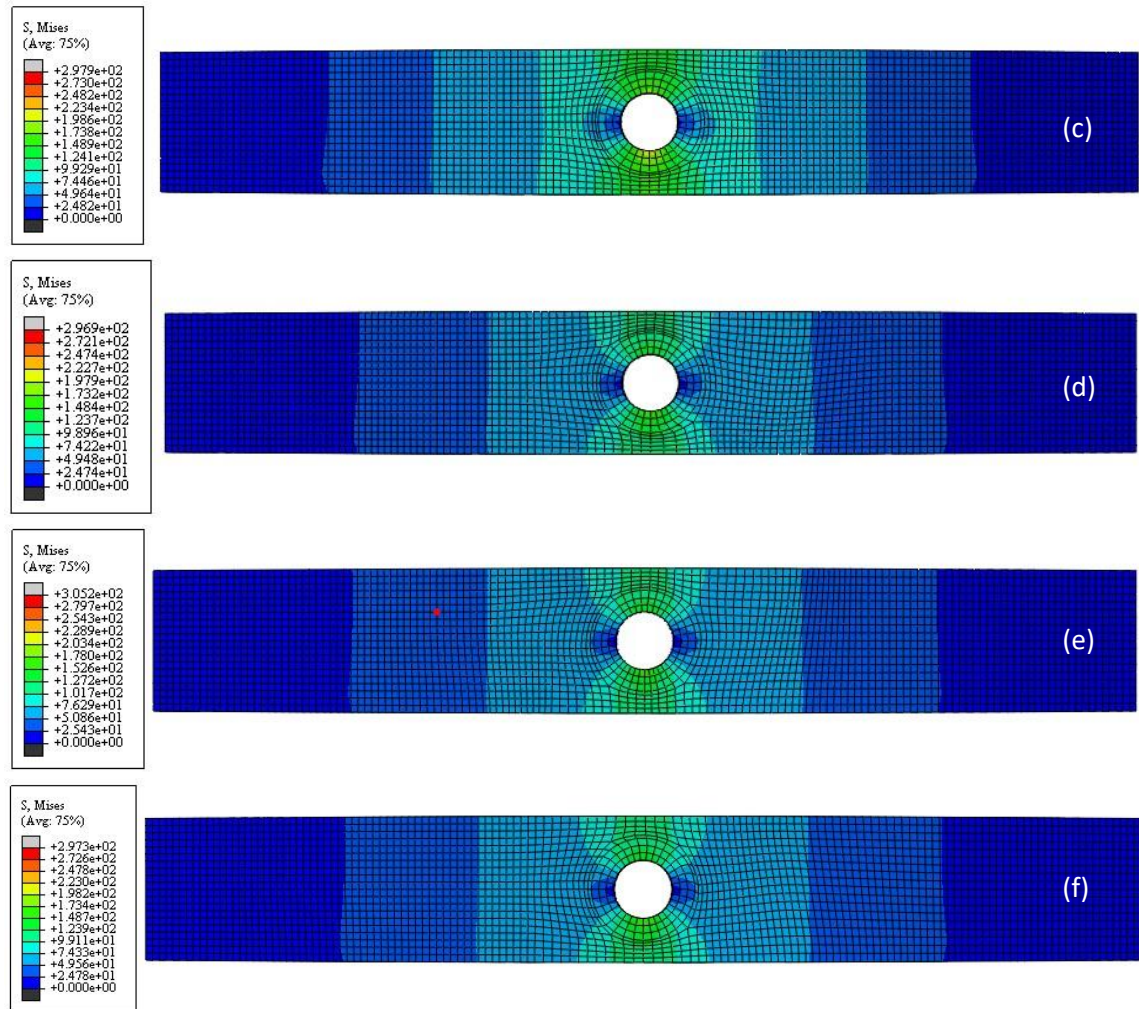


Figure 7-4: Visualization of the bottom view under fatigue load profile with crack length from the mid- point (a) 0 (b) 20 mm (c) 40 mm (d) 60 mm (e) 80 mm (f) 100 mm

### 7.3 Load related parameters

Steel structures suffer from effects of various types of loading parameters such as amplitude of loads, loading frequency and stress ratio. According to the service requirement, amplitude of load varies on existing structures. In addition, loading frequency also varies with service demand and it may fluctuate during peak to off peak times. The other important factor is stress ratio due to fluctuation of loads on structures. All of these factors are external factors and these could be controlled. However, due to deterioration of the existing structures these could be limits to those parameters for the safety and the durability of them.

### 7.3.1 Amplitude of load

In this FEA, the amplitude of applied load on CSH was considered as a main variable and it varied from 2 kN to 10 kN in 2 kN steps. All of other factors were kept constant during the analysis and procedure followed for analysis as explained in chapter 5. Table 7.3 summarizes the FEM results with respect to the amplitude of load.

Table 7.3: Strength variation with respect to the diameter to loading amplitude ratio

Amplitude of load (kN)	Strength (MPa)
8.0	264.6
4.0	253.9
2.6	247.9
2.0	235.7
1.6	225.4

According to numerical model results strength varies with the loading magnitudes as shown in Figure 7-5. In this numerical model, the loading magnitudes were changed without altering other variables. The strength variation is directly proportional to the diameter to load ratio with different gradients as shown in Figure 7-5. When increasing the amplitude of the load, stress increases and stress intensity also increases in this case. However, the residual stress and notch stress are almost constant.

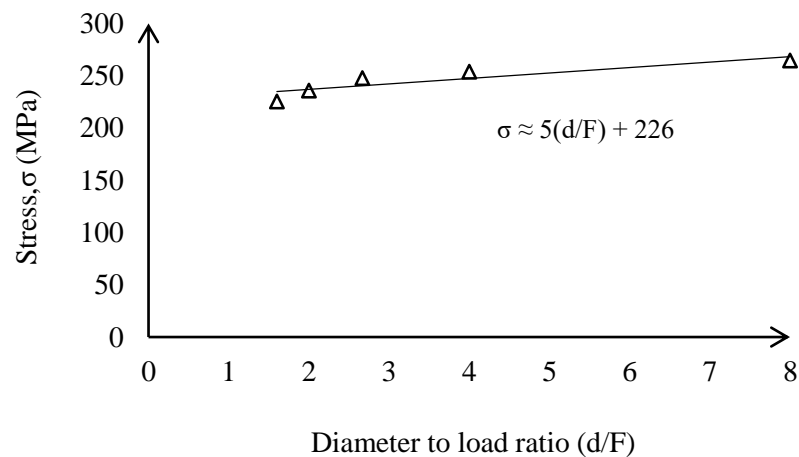


Figure 7-5: Strength variation of CSH with load

Stress concentration is the main reason for the decline in strength and it is governed by stress due to the fatigue load. In this analysis stress is applied on the CSH due to

the cyclic load. The magnitude of load is inversely proportional to the strength and Plasticity of material also effects on final results. Contour of the tensile surface (bottom surface) of the specimen under flexural cyclic load due to amplitude of load is shown in Figure 7-6.

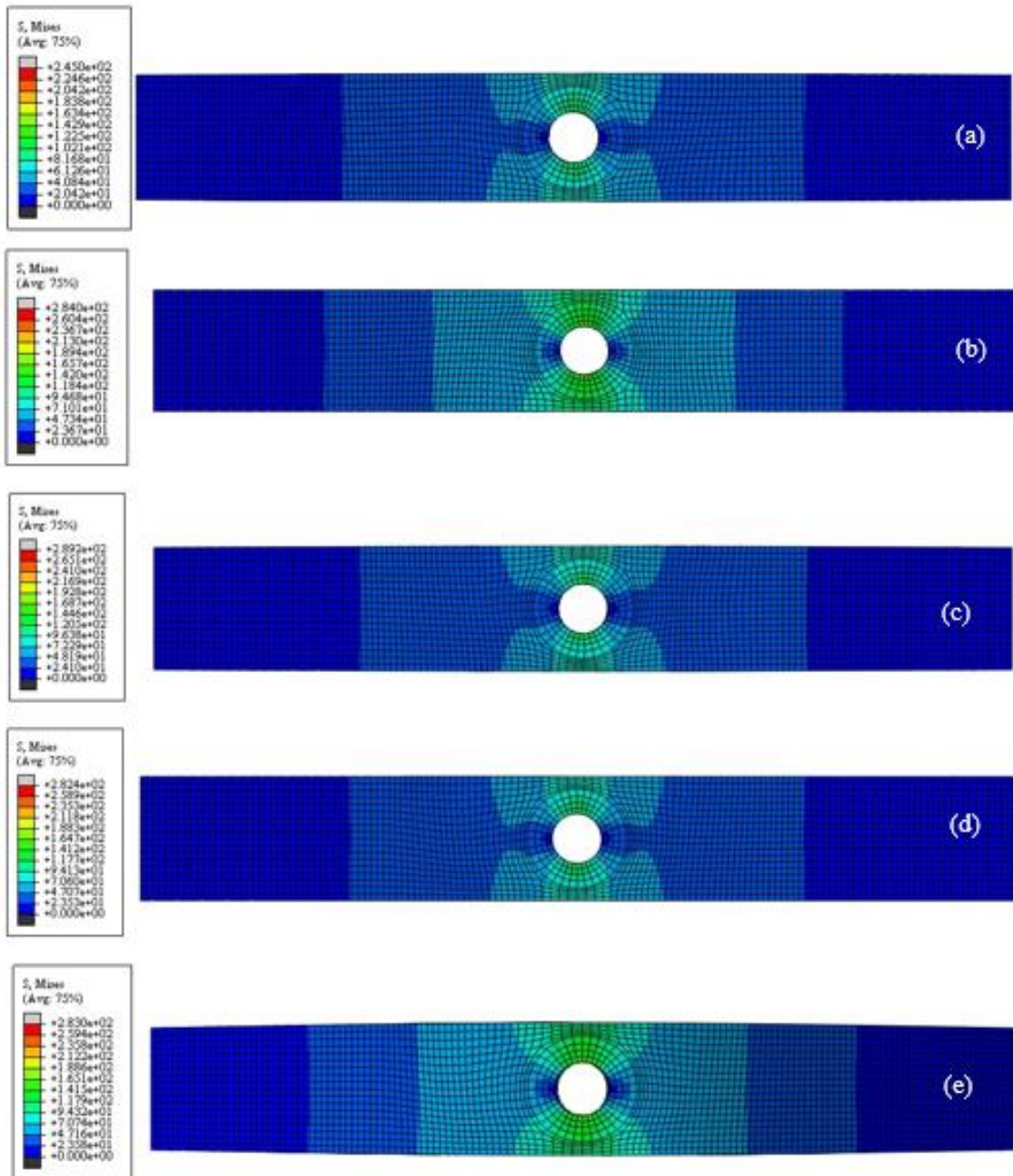


Figure 7-6: Visualization of the bottom view under fatigue load profile with loaded specimen. (a) 2 kN (b) 4 kN (c) 6 kN (d) 8 kN (e) 10 kN



### 7.3.2 Loading frequency

In this analysis, frequency of applied load on CSH was considered as a main variable and it varied from 1 Hz to 10 Hz. All of other parameters were kept constant during the analysis and procedure followed for analysis is explained in chapter 5. Table 7.4 summarizes the FEM results.

Table 7.4: Stress variation with respect to the diameter to loading frequency ratio

Loading Frequency (Hz)	Diameter to frequency ratio (d/f)	Stress (MPa)
1	16	321.3
2	8	309.6
4	4	307.9
5	3.2	299.4
8	2	266.3
10	1.6	264.2

When considering steel structures, loading frequency varies due to applications. The best example is the speed of the vehicle through steel bridges. According to the results of this analysis, the strength of the crack stop hole had rapidly changed with a high frequency and slightly changed with a lower frequency. Stress variation with loading frequency is shown in Figure 7-7.

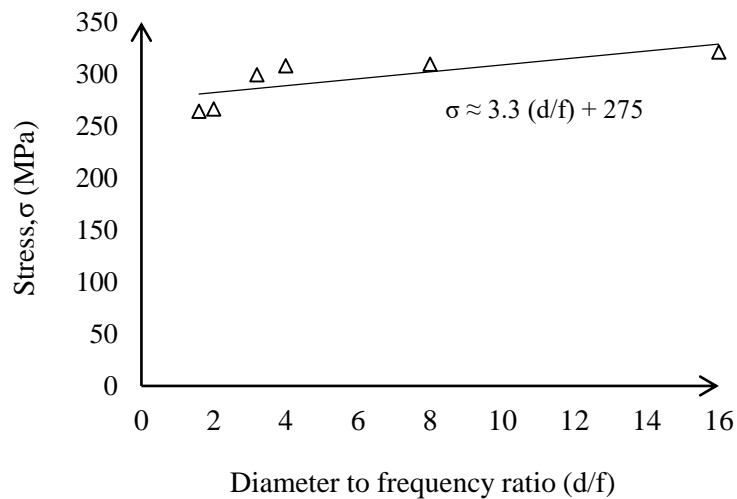
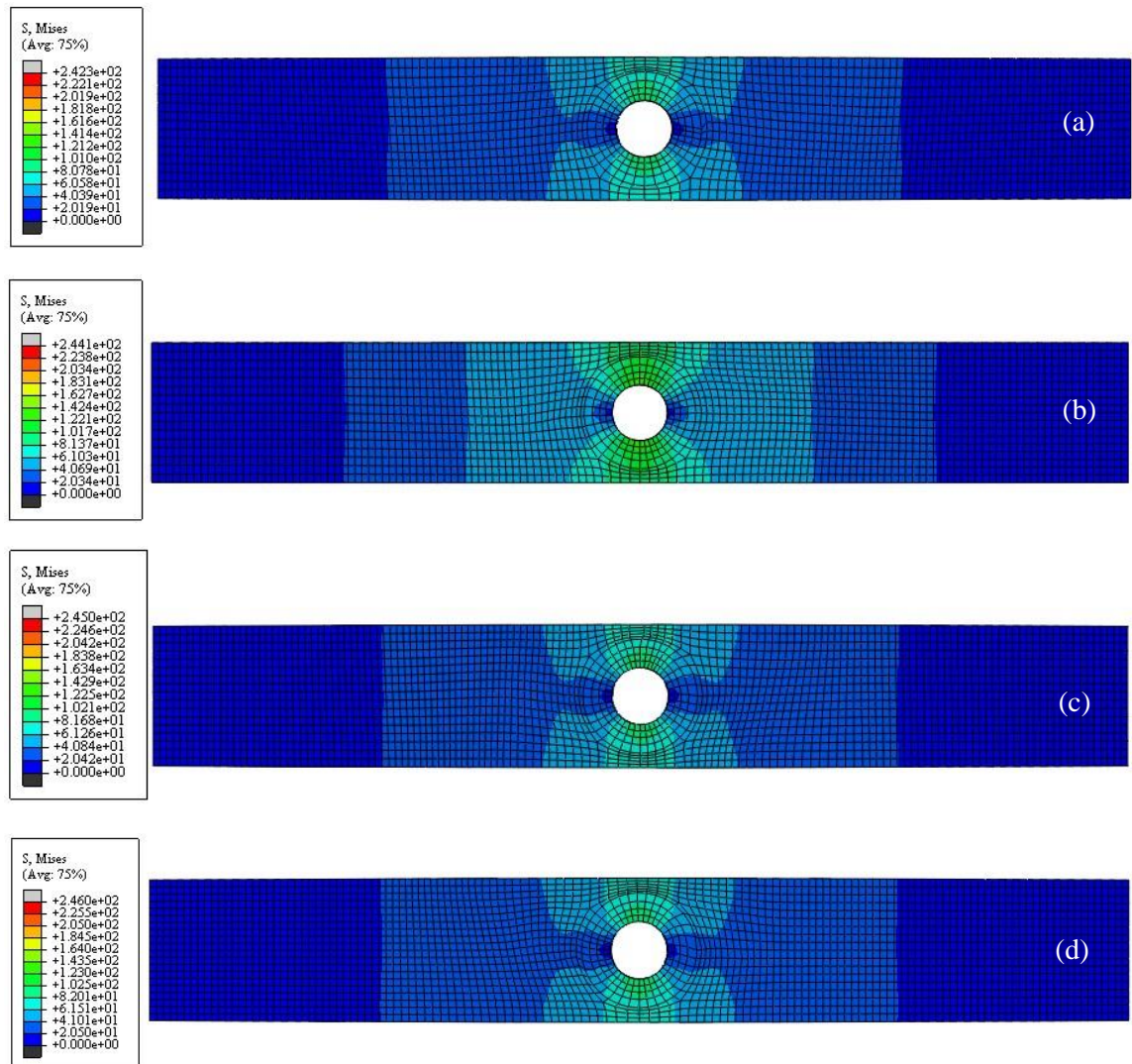


Figure 7-7: Strength variation with diameter to frequency ratio

In this case cyclic flexural stress is applied at the loading point and residual stress generates due to placing of the CSH. However, notch stress could be considered constant because of geometrical dimensions of the hole is constant for each case. Fatigue stress applied strongly contributes to increase the plasticity of the material at the stress concentration point. As a result, when each of the above actions happens, material becomes weak and the strength declines. Contour of the tensile surface (bottom surface) of the specimen under flexural cyclic load due to frequency of load is shown in Figure 7-8.



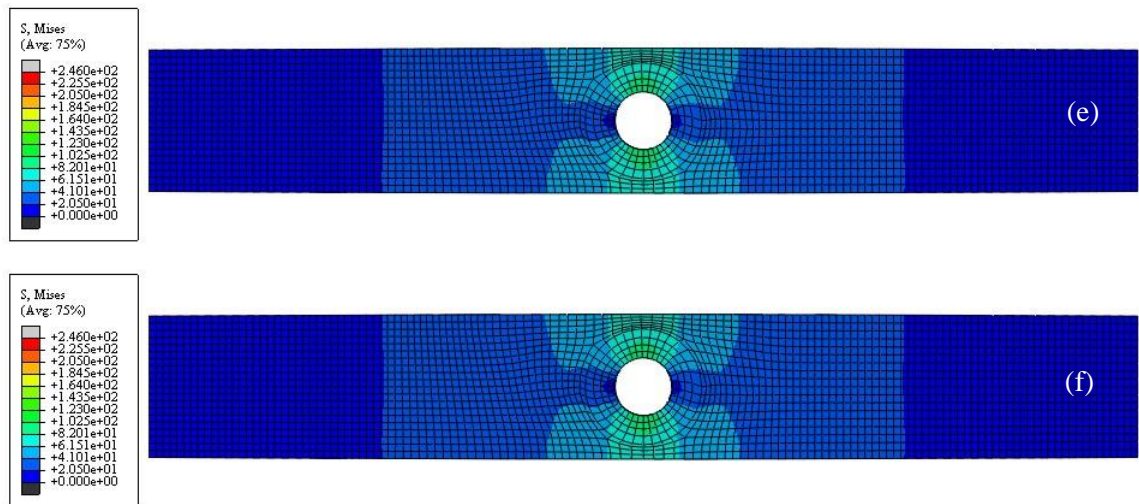


Figure 7-8: Visualization of the bottom view under fatigue load profile with loading frequency at the midpoint (a) 1 Hz (b) 2 Hz (c) 4 Hz (d) 5 Hz (e) 8 Hz (f) 10 Hz

### 7.3.3 The stress ratio

In this analysis, the stress ratio of applied load on the CSH was considered a main variable and it varied from 0.1 to 0.5 in 0.1 steps and the procedure followed for analysis is explained in chapter 5. Table 7.5 summarizes the FEM results with respect to the ratio of diameter to stress ratio.

Table 7.5: Strength variation with respect to the ratio of diameter to stress ratio

Stress ratio (R)	Ratio of diameter to stress ratio (d/R)	Strength (MPa)
0.1	160	299.5
0.2	80	288.9
0.3	53	274.9
0.4	40	264.5
0.5	32	255.1

During service period of steel structures stress fluctuates and such a variation was represented by the mechanical parameters like stress ratio. In this analysis the focus was to investigate the effects of the stress ratio on yield stress and results are presented in Figure 7-9. When stress ratio increases the stress drastically dropped and with a

lower range of stress ratio, a maximum yield load capacity was shown. During the analysis, residual stress and notch stress are almost constant, as the diameter of the crack stop hole is the same for each case.

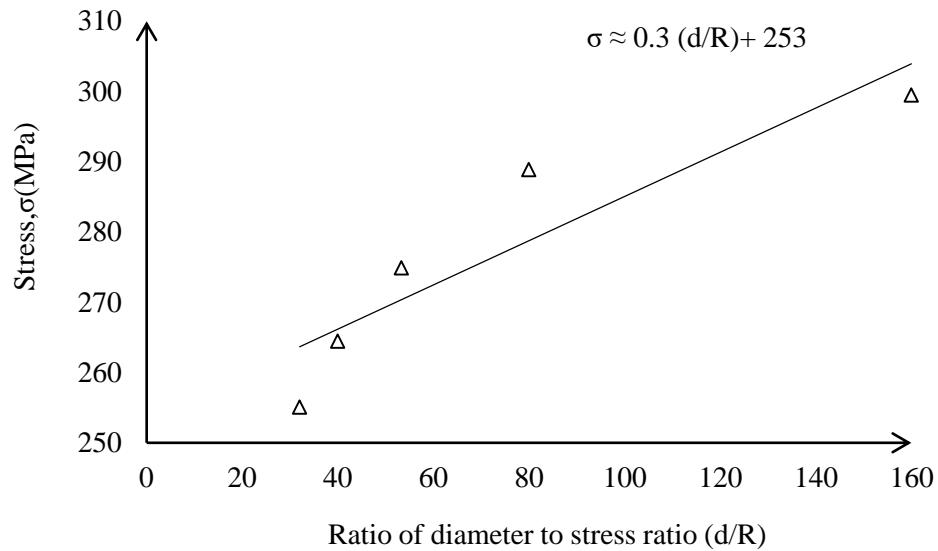


Figure 7-9: Strength variation with stress ratio

In this analysis mechanical stress was applied at the CSH due to the fatigue load. However, residual stress and notch stress are constant in this case because geometrical parameters of the hole are constant. Contour of the tensile surface (bottom surface) of the specimen under flexural cyclic load due to stress ratio of load is shown in Figure 7-10.

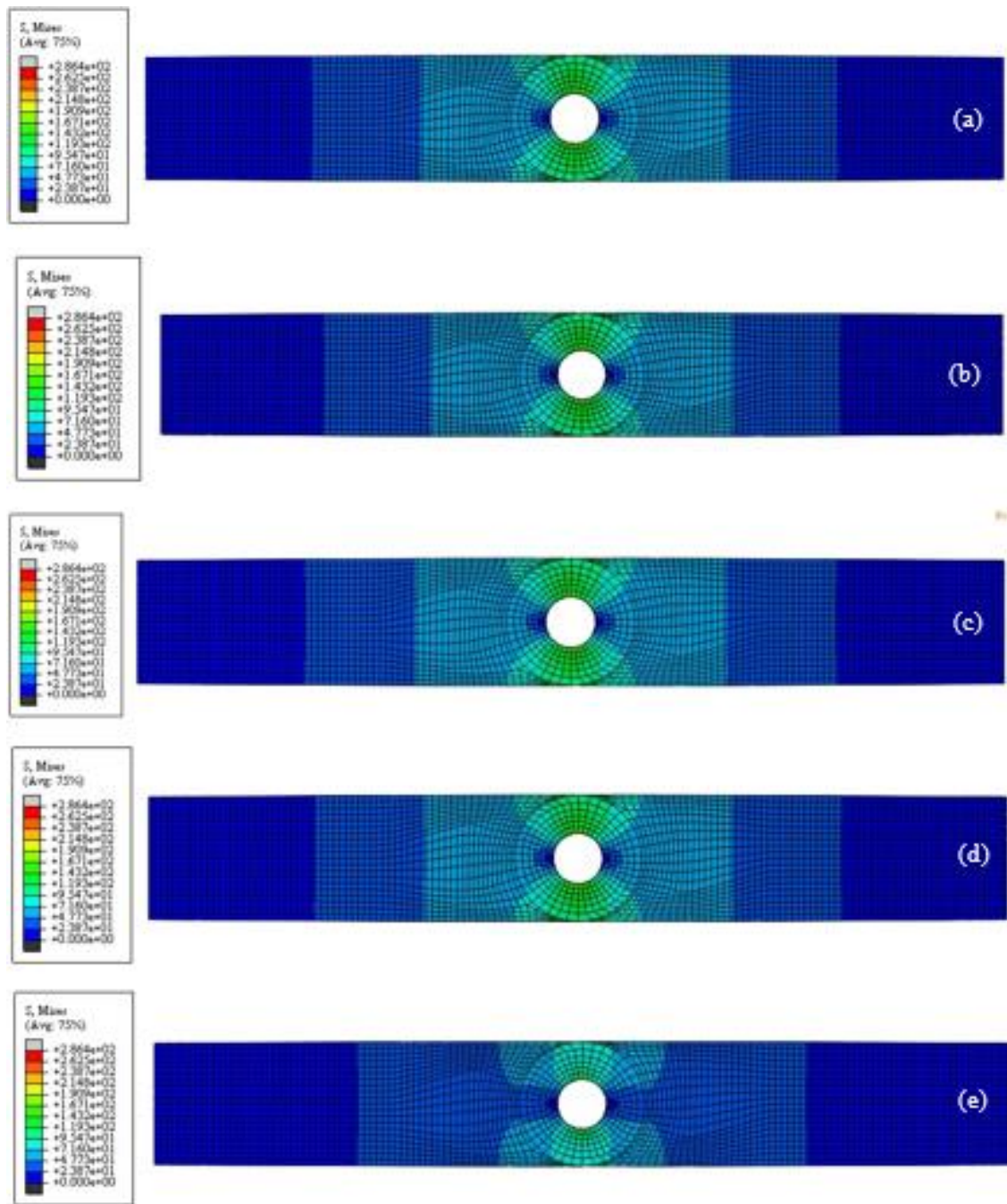


Figure 7-10: Visualization of the bottom view under fatigue load profile with stress ratio at the mid-point (a) 0.1 (b) 0.2 (c) 0.3 (d) 0.4 (e) 0.5

#### 7.4 Fatigue behavior of CSH varying with polymer material related parameters

In this analysis attention with the characteristic of polymer material affects the composite and is linked to fiber direction with respect to crack direction as main parameters. Cyclic flexural loads were applied at the midpoint when selecting parameters which varied during the analysis and all other parameters were kept constant.

##### 7.4.1 Fiber direction angle of the CFRP

In this analysis, the effect of fiber direction on CSH was considered as a main variable and it varied from 0 to 90 degrees in 30 degrees steps. All of other parameters were kept as constant during the analysis and procedure followed for analysis as explained in chapter 5. Table 7.6 summarizes the FEM results variation with fiber direction angle.

Table 7.8: Stress variation with respect to the fiber direction

Fiber direction angle with respect to crack direction	Stress (MPa)
0	195.3
30	208.9
45	217.3
60	227.0
90	238.0

In this analysis the fiber direction angle was changed with respect to crack direction of the crack stop hole without altering other variables. Strength variation with fiber direction is shown in Figure 7-11. Stress varies as a linear function with the fiber direction angle. The reason for this is the stress intensity which is controlled by the CFRP material (Zhao et al., 2004). When the fiber direction angle increases from the crack direction, residual stresses and notch stress are almost constant.

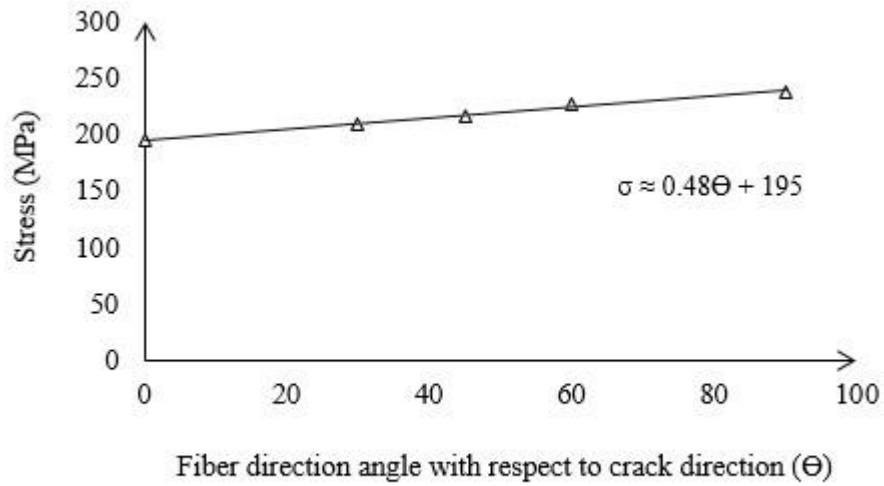
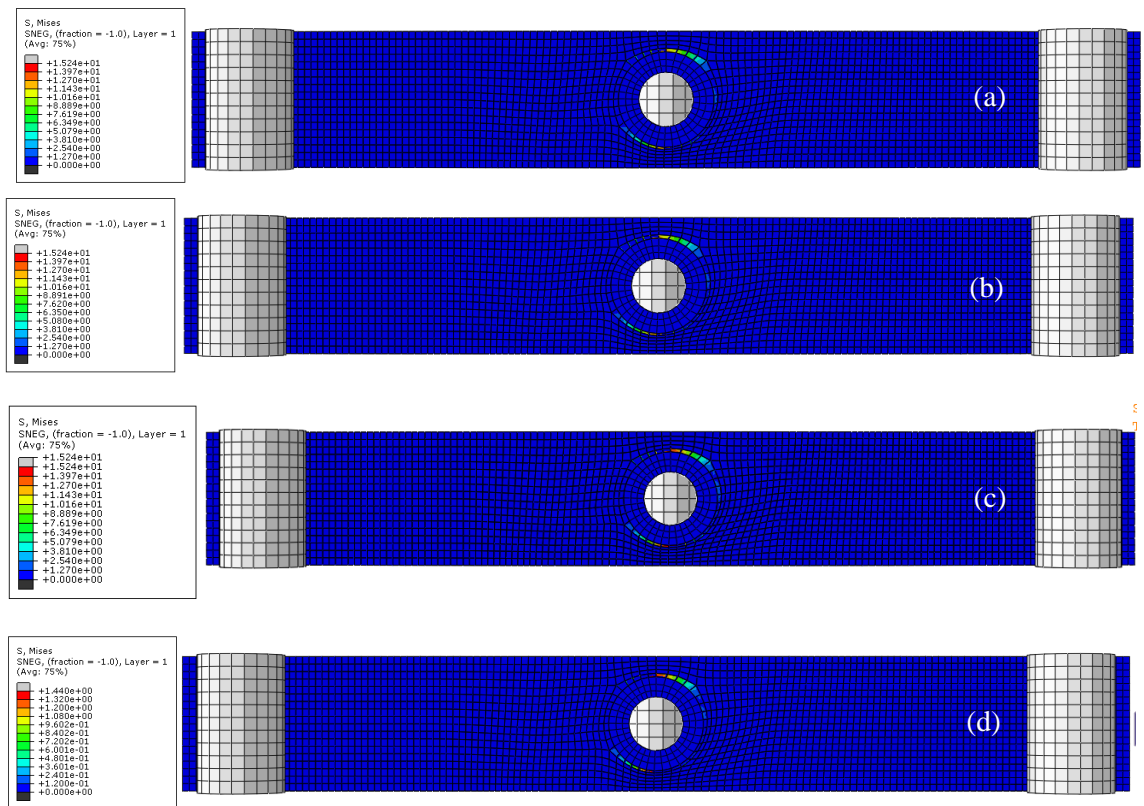


Figure 7-11: Stress variation with respect to fiber direction

The main reason is that the, effect of the tensile resistivity at the bottom surface due to the effect of fiber direction of the CFRP layer. Contour of the tensile surface (bottom surface) of the specimen under flexural cyclic load due to fiber direction angle is shown in Figure 7-12.



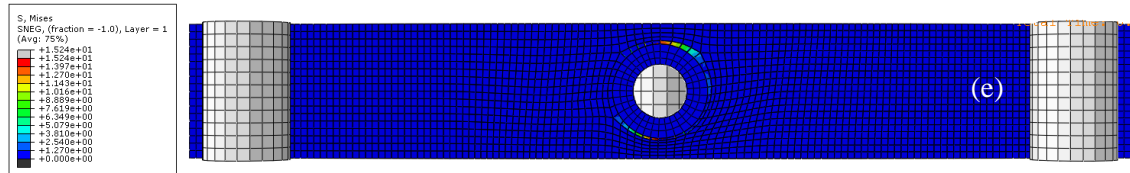


Figure 7-12: Visualization of the bottom view under fatigue load profile with fiber angle with respect to crack direction (a) zero (b) 30° (c) 45° (d) 60° (e) 90°

## 7.5 Summary of the parametric study relating to CSH/CFRP hybrid system

The Fatigue life of structural elements depends on a large number of internal and external factors. Such parameters could be broadly classified as geometry related, load related, Fiber material property related and environmental related factors. In this study a few parameters were evaluated using experimental process as explained in chapter 04. However, it was impossible to evaluate all possible parameters through experimental results due to testing costs and time consumption. Therefore, the FEM was introduced as explained in chapter 05 to determine the effect of other possible parameters. According to laboratory test results as well as FEM results, several parameters were selected to estimate effects on final results. However, all these parameters show huge variations among them. Some parameters were critical influences and some others were not critical for the final results. All considered results were utilized to developed design guidelines as shown in Table 7.7 to estimate the appropriate size of the CSH within the available parameters in the range considered with individual effects.

This parametric study was conducted to predict the effects of selected parameters on the CSH and it is utilized to introduce design guidelines to decide the size of the CSH. According to literature there are no universally accepted methods to decide the size of the CSH. Different authors have suggested different sizes for the CSH as explained in chapter 2. According to different views of authors can be identified huge gap of research about the CSH dimensions. One of primary objectives of this study was to introduce a design guideline to estimate the appropriate diameter of the CSH considering the most critically influencing parameter effects on the CSH.



A numerical model was utilized to investigate parametric influences on the CSH. This study member thickness, amplitude of loads, stress ratio, crack length and fiber direction angle were selected as a critically influencing parameters in the range considered. However, the loading frequency insignificantly contributes to the final results within the range selected. According to the experimental program as explained in chapter 4 the diameter of the CSH, the position of the CSH and bond length effects were experimentally investigated and test results have confirmed significant effects for those parameters. Experimental and parametric study results were utilized to introduce design guidelines to estimate the appropriate size of the CSH and guidelines are shown in Table 7.7.

Table 7.7: Fatigue related design guidelines for CSH

Category	Parameter	Range of Operation
Geometry	Diameter to width ratio (d/b)	$\frac{d}{b} \leq 0.2$
	Thickness to diameter ratio (t/b)	$\frac{t}{d} \leq 0.5$
	Diameter to crack length ratio (d/l)	$\frac{d}{l} \geq 0.4$
	Diameter to offset distance ratio (d/x)	$\frac{d}{x} \leq 0.2$
Load	Ratio of diameter to stress ratio (d/R)	$\frac{d}{R} \geq 80$
	Diameter to frequency ratio (d/f)	$\frac{d}{f} \geq 3$
	Diameter to load ratio (d/F)	$\frac{d}{F} \geq 3$
CFRP	Diameter to bond length ratio (d/L)	$\frac{d}{L} \leq 0.1$

## ***Chapter – 8***

---

# ***Conclusions and Recommendations***

## 8 CONCLUSIONS AND RECOMENDATIONS

### 8.1 Conclusions

This research investigated fatigue behavior of the CSH under flexural cyclic loads and estimated strength gains by the CFRP material. Experimental test results were compared with the FEM results. The performance of the CSH technology was estimated and it provided design guide lines to decide the diameter of the CSH with respect to critical parameters. The most effective parameters were compared with the CFRP strengthened technique. According to this investigation the fatigue capacity enhancement of the CSH was confirmed with the CFRP material while delaying re-cracking. Thus, the findings of this study provide design guide lines an insight to future research related to fatigue performance. In addition, flexural fatigue loading apparatus were designed and fabricated to apply cyclic loads of experiment investigations. This apparatus was cost effective and affordable for higher education institutions. Furthermore, a FEM was developed using a cyclic J-integral technique to predict fatigue behavior of the CSH and strength gains by the CFRP. In addition, a theoretical model was developed to predict re-cracking and effects of parameters related to fatigue. The detailed experimental and numerical simulations conducted on the novel hybrid technique to control cracks of steel elements in civil engineering infrastructures yield the following conclusions:

1. Carried out comprehensive literature review to evaluate the existing knowledge regarding fatigue, CFRP related applications, crack repairing methods, CSH techniques and other related theories, analysis as well as key research findings. Available data was critically analyzed to identified the gap of the research and successfully utilized it to implement the CFRP strengthened CSH system to delay fractures in steel infrastructures to enhance the service life of such structures under fatigue effects.
2. Availability of fatigue test apparatus was the major challenge to continue fatigue related experimental program in many of higher education institutions and this study planned to build a test apparatus in house to fulfil this requirement. Learning of the historical development of the existing

apparatus was up to date the study compared the mechanism of loads applied on test specimens before designing and fabrication. Apparatus was successfully utilized to perform cyclic flexure loads on test specimens in this experimental program. Furthermore, this apparatus is strongly recommended for carrying out fatigue related experiments in higher education institutions with or without minor modifications according to customer requirements.

3. Diameter of the CSH was a one main argument in available literature and there are no clear guidelines to decide if it considers the effects of critical parameters. In this study effects of several parameters were experimentally and numerically estimated while the critical effects on final results were based on geometry with loading and CFRP material characteristics. Using those results this study has introduced design guide lines to decide the appropriate size of the CSH for crack control to delay fracture failures on steel structures due to fatigue.
4. CSH technique is a proven technology for fracture control in steel infrastructures and stiffness is reduced due to material removal for the CSH. Average strength reductions in the range between 13% to 25% was measured subjected to low cycle fatigue exposure. On the other hand, re-cracking occurs due to continuous service load on the CSH. However, re cracking is controlled by appropriate CSH sizes as well as effects of the CFRP material. This is due to the CSH effectively recovering the strength losses while enhancing the strength in the range between 32% to 45% with respect to the non-strengthened non conditioned material features. Therefore, a novel CSH/CFRP hybrid system in this study could be utilized successfully to eliminate the main drawbacks related to the CSH technique. This method exhibits a significant capacity enhancement for crack controls and is strongly recommended to improve the service life of steel infrastructures under fatigue load.
5. Fatigue is a more complicated process and its depends on a large number of internal and external parameters. The proposed numerical model in this study

validates well as it uses the measured data during the experiment. Hence, this developed numerical model can be effectively utilized to estimate effects of unknown parameter as well as to predict re-cracking behaviour of the CSH under fatigue response.

6. A numerical model can be utilized to investigate invisible characteristics by the experiment and the developed numerical model was prognosticating the range of stress intensity variation, stress variation along crack direction, prediction of the direction of maximum tangential stress which was compared for CFRP strengthened CSH with respect to non-strengthened CSH. Numerical results have confirmed the potential of CFRP utilized ones that enhances the fatigue life of structure.

## **8.2 Contributions**

This investigation focused on evaluating fatigue behavior of the CSH with the CFRP strengthening technique. The contributions from this study could be summarized as follows:

1. Summarized detailed explanations into how fatigue loading influenced non-strengthened and CFRP strengthened CSH
2. The design and fabrication of the fatigue loading apparatus was cost effective and affordable for academic and higher education institutions
3. A sound numerical model was developed based on material properties which is capable to simulate fatigue behavior of the CSH subjected to cyclic flexural loading
4. A modified theoretical model based on material properties which was predict re-cracking behavior of CSH
5. Design guidelines for the CSH technique summarized

### **8.3 Future research works**

CSH technology has a potential to control crack arrest in structures and this study confirmed that conventional drawbacks of the CSH could be eliminated with a CFRP material. However, fatigue is one of the critical study areas linked to engineering as well as materials. Therefore, it could be suggested that in future work fatigue related repaired techniques could be improved in a feasible manner. Fatigue life of structures depends on a large number of internal and external parameters. This study paid attention to the effects of internal parameters only. However, internal and external parameters jointly affect the final results. Therefore, in future investigations the combined effects of two or more parameters such as environmental factors with fatigue loads could also be considered as well.

This study does not account for effects of residual stress of material, however during the fabrication process such as rolling, bending, hole drilling, surface grinding, or welding process build a residual stress. Quantify of this residual stress may greatly contribute to the better performance of fatigue analysis technique.

Majority of fatigue related studies are focused on surface cracks as general cracks start from the surface. Therefore, the condition of surfaces is critically influenced by the process of crack initiation and a limited number of investigations are available in literature regarding the effects of surface roughness. This study did not pay much attention to this factor. Therefore, a future investigation could pay attention to the effects of surface roughness on fatigue performance of CSH. In addition, identification of the exact point of the crack tip is very important to place the CSH. Non-destructive tests and magnetic tests are popular methods to identify crack tips on a surface, however detection of cracks growth from the middle of the through thickness is very a difficult task and there is a need to develop an appropriate method to decide the exact crack tip for cracks start from the through thickness.

Fatigue is governed by the micro structure of a material due to external or internal stress. Therefore, there should be a microscopic analysis regarding grain arrangement, dislocation, and information regarding missing atoms of the material with critical parameters. Crack nucleation and fracture process deals with energy transfer due to

stress. There is a knowledge gap between different types of energy, energy transfer mechanism and micro structural behavior under fatigue loads. To better understand the fatigue behavior of the CSH at the micro structural level the gaps have to be filled in the future. Fatigue related applications in the real world are variable amplitudes and impact loads on structures. Therefore, there should be an experimental and numerical analysis regarding non harmonic fatigue response on the CSH under variable amplitude loads. In addition, the present study should emphasize future investigations on seismic capacity of CSH/ CFRP systems.

Stress fluctuation occur regularly on the structures and the effects of the sequence are relatively negligible and when load history changes, different frequencies are caused which drastically accelerate or decelerate the level of the crack opening. Future research should focus on evaluating how this behavior affects the crack rate growth. The CFRP layer is combined with glass fiber reinforced materials (GFRP) and natural fiber (treated bamboo) materials which should be investigated, as the cost of the CFRP material is main barrier for the growth of this technology.

The finite element model does not have a facility to model the effects of environmental factors on bond performance. This can be considered as a significant gap of FEM techniques. Furthermore, evaluating the long term bond performance relating investigations of the CSH/CFRP hybrid system to confirm durability of this technique could also be carried out in the future.

Due to the placing of the CSH on structural element, the crack growth delaying time period or required number of cycles until re-cracking should be quantified in future research. Furthermore, results should be compared with the results before placing a CSH at the same element.

#### **8.4 Engineering implications**

1. According to results from the laboratory test, the FEM results cumulated the design guidelines for the CSH technique. This method could replace the conventional fatigue repairing techniques and re-install strength losses of aging structures. Ultimately it may contribute to the delay of repairing or replacing as well as inspection intervals. In addition, this may overcome drawbacks

related with conventional repair methods. As a result it contributes to save money with continuous service demands according to the present demand.

2. Fatigue related tests are limited to laboratories and in most cases pay attention to axial or rotational loads due to mechanical applications. However, structural related specific fatigue investigations are limited and available fatigue tests apparatus are very expensive. This apparatus is designed and fabricated by considering the cost, accuracy, durability flexibility to change any geometry and its environment friendly feature. It can be recommended as a fatigue loading apparatus. Therefore, as an alternative, a cost-effective fatigue loading apparatus was introduced for universities and high educations institutes.
3. The numerical model results based on material properties of structures and replaced conventional method based on geometry, as fatigue is concerned with material characteristics.



## *References*

---

## REFERENCES

- ABAQUS, H. (2014). ABAQUS standard user's manual, version 6.14. Providence, RI, USA: Dassault Systems.
- Abeygunasekera, S., Gamage, J. C. P. H., & Fawzia, S. (2017). Effects of environmental humidity at installation phase on performance of CFRP strengthen steel I-beam. In Proceedings of the 8th International Conference on Structural Engineering and Construction Management 2017 (pp. 18-22). University of Peradeniya.
- Abeygunasekera, S., Gamage, J. C. P. H., & Fawzia, S. (2019). Numerical modeling on re-cracking behaviour of strengthened crack stop holes in steel structures. 10th International Conference on Structural Engineering and Construction Management (ICSECM) 12th – 14th December 2019 1 Earl's Regency Hotel 1 Kandy 1 Sri Lanka, 335–344.
- Abeygunasekera, S., Gamage, J. C. P. H., & S, F. (2020). Numerical Modelling of Re-cracking Behaviour in Retrofitted Crack Stop Holes in Steel Structures. Springer Science and Business Media LLC.
- Abeygunasekera, S., Gamage, J. C.P.H., & Fawzia, S. (2022) Investigating the Effects of Offset Distance in CSH on Steel Plates Under Three-Point Flexural Cyclic Loads in the LCF Range. ICSBE 2020: Proceedings of the 11th International Conference on Sustainable Built Environment. Springer, Singapore, pp. 331-346.
- Aeran, A., Siriwardane, S. C., Mikkelsen, O., & Langen, I. (2017). A new nonlinear fatigue damage model based only on SN curve parameters. *International Journal of Fatigue*, 103, 327-341.
- Albert, W. A. J. (1837). *Uber Treibseile am Harz*. *Archiv fur Mineralogie, Geognosie. Bergbau und Huttenkunde*, 10, 215.
- Al-Emrani, M., Linghoff, D., & Kliger, R. (2005, December). Bonding strength and fracture mechanisms in composite steel-CFRP elements. In *International Symposium on Bond Behaviour of FRP in Structures (BBFS 2005)*, International Institute for FRP in Construction. Hong Kong, China.
- Ali, S., Tahir, M. H., Saeed, M. A., Khan, M. K., & Zaffar, N. (2019). Design and Development of Fatigue Machine: Rotating Bending Fatigue Testing on different Materials. *Int. J. Adv. Eng. Manag*, 4(2), 8. <https://doi.org/10.13140/RG.2.2.32181.32484>

- Aly, M. Y. E., & El-Hacha, R. (2009). Strength evaluation of steel-concrete composite girders strengthened with prestressed FRP laminates. *Group*, 1, B1-30.
- Al-Zubaidy, H., Al-Mahaidi, R., & Zhao, X. L. (2012). Experimental investigation of bond characteristics between CFRP fabrics and steel plate joints under impact tensile loads. *Composite Structures*, 94(2), 510-518.
- Aoki, Y., Yamada, K., & Ishikawa, T. (2008). Effect of hygrothermal condition on compression after impact strength of CFRP laminates. *Composites science and technology*, 68(6), 1376-1383.
- ASTM International. (2012). ASTM D7774-12-Standard Test Method for Flexural Fatigue Properties of Plastics.
- ASTM, E. (2005). 1049-85, "Standard practices for cycle counting in fatigue analysis". *Annual book of ASTM standards*, 3(01), 614-620.
- Ayatollahi, M. R., Razavi, S. M. J., & Chamani, H. R. (2014). Fatigue life extension by crack repair using stop-hole technique under pure mode-I and pure mode-II loading conditions. *Procedia Engineering*, 74, 18-21.
- Azeez, A. A. (2013). Fatigue failure and testing methods. *University of Applied Sciences HAMK*, 1, 32.
- Baldan, A. (2004). Adhesively-bonded joints and repairs in metallic alloys, polymers and composite materials: Adhesives, adhesion theories and surface pretreatment. *Journal of materials science*, 39(1), 1-49.
- Bannantine, J., Comer, J., & Handrock, J. (1990). *Fundamentals of metal fatigue analysis*(Book). Research supported by the University of Illinois. Englewood Cliffs, NJ, Prentice Hall, 1990, 286.
- Barbe, F., Decker, L., Jeulin, D., & Cailletaud, G. (2001). Intergranular and intragranular behavior of polycrystalline aggregates. Part 1: FE model. *International journal of plasticity*, 17(4), 513-536.
- Basquin, O. H. (1910). The exponential law of endurance tests. In *Proc Am Soc Test Mater* (Vol. 10, pp. 625-630).
- Bassetti, A., Liechti, P., & Nussbaumer, A. (1998). Fatigue resistance and repairs of riveted bridge members (No. CONF, pp. 535-546).

- Bassetti, A., Nussbaumer, A., & Hirt, M. A. (2000). Crack repair and fatigue life extension of riveted bridge members using composite materials. In Proceedings of Bridge Engineering Conference (No. CONF, pp. 227-238). The Egyptian Society of Engineers.
- Batuwitage, C., Fawzia, S., Thambiratnam, D., & Al-Mahaidi, R. (2017). Durability of CFRP strengthened steel plate double-strap joints in accelerated corrosion environments. *Composite Structures*, 160, 1287-1298.
- Beesley, R., Chen, H., & Hughes, M. (2015). On the modified monotonic loading concept for the calculation of the cyclic j-integral. *Journal of Pressure Vessel Technology*, 137(5).
- Bhatkar, O. P., Mhatre, S. Y., Pilankar, A. S., Desai, V. S., & Katlikar, M. J. (2017). Design and fabrication of combined fatigue testing machine. *Int. Adv. Res. J. Sci. Eng. Technol*, 4.
- Bocciarelli, M., Colombi, P., Fava, G., & Poggi, C. (2009). Fatigue performance of tensile steel members strengthened with CFRP plates. *Composite Structures*, 87(4), 334-343.
- Božić, Ž., Mlikota, M., & Schmauder, S. (2011). Application of the  $\Delta K$ ,  $\Delta J$  and  $\Delta CTOD$  parameters in fatigue crack growth modelling. *Tehnički vjesnik*, 18(3), 459-466.
- Brown, J. D., Lubitz, D. J., Cekov, Y. C., Frank, K. H., & Keating, P. B. (2007). Evaluation of influence of hole making upon the performance of structural steel plates and connections (No. FHWA/TX-07/0-4624-1).
- Butkewitsch, S. (2006). Dynamical modelling, stochastic simulation and optimization in the context of damage tolerant design. *Shock and Vibration*, 13(4-5), 445-458.
- Buyukozturk, O., Gunes, O., & Karaca, E. (2004). Progress on understanding debonding problems in reinforced concrete and steel members strengthened using FRP composites. *Construction and Building Materials*, 18(1), 9-19.
- Cadei, J. C., Stratford, T. J., Duckett, W. G., & Hollaway, L. C. (2004). Strengthening metallic structures using externally bonded fibre-reinforced polymers. *Ciria*.
- Campbell, F. C. (Ed.). (2008). *Elements of metallurgy and engineering alloys*. ASM International.

- Cassa, A. M., Van Zyl, J. E., & Laubscher, R. F. (2010). A numerical investigation into the effect of pressure on holes and cracks in water supply pipes. *Urban Water Journal*, 7(2), 109-120. <https://doi.org/10.1080/15730620903447613>
- Champoux, R. L. (1986). An overview of hole cold expansion methods. *Engineering Materials Advisory Services Ltd.*, 35-52.
- Chandawanich, N., & Sharpe Jr, W. N. (1979). An experimental study of fatigue crack initiation and growth from coldworked holes. *Engineering Fracture Mechanics*, 11(4), 609-620.
- Chandran, K. R. (2016). A physical model and constitutive equations for complete characterization of SN fatigue behavior of metals. *Acta Materialia*, 121, 85-103.
- Chandrathilaka, E. R. K. (2019). Bond performance of CFRP/Steel composite at elevated temperatures (Doctoral dissertation).
- Chandrathilaka, E. R. K., Gamage, J. C. P. H., & Fawzia, S. (2019). Numerical modelling of bond shear stress slip behavior of CFRP/steel composites cured and tested at elevated temperature. *Composite Structures*, 212, 1-10.
- Chatterjee, B., & Sahoo, P. (2012). Research Article Effect of Strain Hardening on Elastic-Plastic Contact of a Deformable Sphere against a Rigid Flat under Full Stick Contact Condition. <https://doi.org/10.1155/2012/472794>
- Chen, J. F., & Teng, J. G. (2001). Anchorage strength models for FRP and steel plates bonded to concrete. *Journal of structural engineering*, 127(7), 784-791.
- Coffin, L.F. (1954) A study of the effects of cyclic thermal stresses on a ductile metal. *Transactions of the American Society of Mechanical Engineers* 76, 931- 950.
- Collings, T. A., Harvey, R. J., & Dalziel, A. W. (1993). The use of elevated temperature in the structural testing of FRP components for simulating the effects of hot and wet environmental exposure. *Composites*, 24(8), 625-634.
- Colombi, P. (2005). Plasticity induced fatigue crack growth retardation model for steel elements reinforced by composite patch. *Theoretical and Applied Fracture Mechanics*, 43(1), 63-76.
- Colombi, P., & Fava, G. (2012). Fatigue behaviour of tensile steel/CFRP joints. *Composite Structures*, 94(8), 2407-2417. <https://doi.org/10.1016/j.compstruct.2012.03.001>

- Colombi, P., & Poggi, C. (2006). Strengthening of tensile steel members and bolted joints using adhesively bonded CFRP plates. *Construction and Building Materials*, 20(1-2), 22-33.
- Colombi, P., Bassetti, A., & Nussbaumer, A. (2003). Analysis of cracked steel members reinforced by pre-stress composite patch. *Fatigue & Fracture of Engineering Materials & Structures*, 26(1), 59-66.
- Colombi, P., Bassetti, A., & Nussbaumer, A. (2003). Crack growth induced delamination on steel members reinforced by prestressed composite patch. *Fatigue & Fracture of Engineering Materials & Structures*, 26(5), 429-438.
- Committee on Fatigue and Fracture Reliability of the Committee on Structural Safety and Reliability of the Structural Division, American Society of Civil Engineers. (1982). Fatigue reliability: Development of criteria for design. *Journal of the Structural Division*, 108(1), 71-88.
- Cotterell, B. (2010). *Fracture and life*. World Scientific.
- Crain, J. S., Simmons, G. G., Bennett, C. R., Barrett-Gonzalez, R., Matamoros, A. B., & Rolfe, S. T. (2010). Development of a technique to improve fatigue lives of crack-stop holes in steel bridges. *Transportation research record*, 2200(1), 69-77.
- Cromwell, J. R., Harries, K. A., & Shahrooz, B. M. (2011). Environmental durability of externally bonded FRP materials intended for repair of concrete structures. *Construction and Building Materials*, 25(5), 2528-2539.
- Dai, J., Ueda, T., & Sato, Y. (2005). Development of the nonlinear bond stress-slip model of fiber reinforced plastics sheet-concrete interfaces with a simple method. *Journal of composites for construction*, 9(1), 52-62.
- Davaran, A. (2010). *Experimental Study on Bonding Improvement of CFRPSTRIPS Used for Strengthening of Steel Beams*.
- Dawood, M., & Rizkalla, S. (2006, December). Bond and splice behavior of high modulus CFRP materials bonded to steel structures. In *Proceedings of the 3rd International Conference on FRP Composites in Civil Engineering Miami*.
- Dawood, M., & Rizkalla, S. (2010). Environmental durability of a CFRP system for strengthening steel structures. *Construction and Building Materials*, 24(9), 1682-1689.

- Dawood, M., Rizkalla, S., & Sumner, E. (2007). Fatigue and overloading behavior of steel–concrete composite flexural members strengthened with high modulus CFRP materials. *Journal of Composites for Construction*, 11(6), 659-669.
- Deng, J., & Lee, M. M. (2007). Fatigue performance of metallic beam strengthened with a bonded CFRP plate. *Composite Structures*, 78(2), 222-231.
- Deng, J., Lee, M. M., & Moy, S. S. (2004). Stress analysis of steel beams reinforced with a bonded CFRP plate. *Composite structures*, 65(2), 205-215.
- Depiver, J. A., Mallik, S., & Harmanto, D. (2021). Solder joint failures under thermo-mechanical loading conditions–A review. *Advances in Materials and Processing Technologies*, 7(1), 1-26.
- Devincre, B., Kubin, L., & Hoc, T. (2006). Physical analyses of crystal plasticity by DD simulations. *Scripta materialia*, 54(5), 741-746.
- Dexter, R. J., & Ocel, J. M. (2013). Manual for repair and retrofit of fatigue cracks in steel bridges (No. FHWA-IF-13-020). United States. Federal Highway Administration.
- Doi, H. (2003). Deformation capacity of circular tubular beam-columns reinforced with CFRP subjected to monotonic loading. *Journal of Constructional Steel*, 11, 431-438.
- Domazet, Ž. (1996). Comparison of fatigue crack retardation methods. *Engineering Failure Analysis*, 3(2), 137-147.
- Dowling, N. E., & Begley, J. A. (1976). Fatigue crack growth during gross plasticity and the J-integral.
- Downing, S. D., & Socie, D. F. (1982). Simple rainflow counting algorithms. *International journal of fatigue*, 4(1), 31-40.
- Dubina, D., Dinu, F., Marginean, I., & Petran, I. (2013, June). Collapse prevention design criteria for moment connections in multi-story steel frames under extreme actions. In 4th Int. Conf. on Integrity, Reliability and Failure, Funchal, Portugal (pp. 23-27).
- El-Hacha, R., & Ragab, N. (2006, December). Flexural strengthening of composite steel-concrete girders using advanced composite materials. In Proceedings of the 3rd International Conference on FRP composites in Civil Engineering (CICE 2006) (pp. 13-15).

- Erdogan, P. P. and F. (1963). A critical analysis of crack propagation laws. *Journal of Basic Engineering, Transactions of the American Society of Mechanical Engineers*, December, 528–534.
- Ewing, J.A. and Humfrey, J.C. (1903) The fracture of metals under rapid alterations of stress. *Philosophical Transactions of the Royal Society, London A200*, 241-250.
- Fatemi, A., & Socie, D. F. (1988). A critical plane approach to multiaxial fatigue damage including out-of-phase loading. *Fatigue & Fracture of Engineering Materials & Structures*, 11(3), 149-165.
- Fawzia, S., & Karim, M. A. (2009). Investigation into the Bond between CFRP and Steel Plates. *International Journal of Civil and Environmental Engineering*, 3(5), 223-227.
- Fernando, D., Yu, T., Teng, J. G., & Zhao, X. L. (2008, January). CFRP strengthening of rectangular steel tubes subjected to end bearing loads: effect of adhesive properties. In *4th International Conference on FRP Composites in Civil Engineering, CICE 2008*. Empa-Akademie.
- Fiber, J., & Epoxy, R. (2015). Method of arresting crack growth for application at a narrow working space. June. <https://doi.org/10.1299/mej.2014smm0058>
- Fish, P., Schroeder, C., Connor, R. J., & Sauser, P. (2015). *Fatigue and Fracture Library for the Inspection, Evaluation, and Repair of Vehicular Steel Bridges*.
- Fisher, J. W. (1990). *Distortion-induced fatigue cracking in steel bridges (Vol. 336)*. Transportation Research Board.
- Fisher, J. W., Barthelemy, B. M., Mertz, D. R., & Edinger, J. A. (1980). *Fatigue behavior of full-scale welded bridge attachments*. NCHRP Report 227. Transportation Research Board, National Research Council, USA.
- Fuchs, H. O., Nelson, D. V., & Toomay, T. L. (1977). *Fatigue under complex loading*. Warrendale, PA, Ed.
- Gerber, H., & Burton, R. F. (1874). Geographical Notes on the Province of Minas Geraes. *The Journal of the Royal Geographical Society of London*, 44, 262-300.
- Ghafoori, E., Motavalli, M., Botsis, J., Herwig, A., & Galli, M. (2012). Fatigue strengthening of damaged metallic beams using prestressed unbonded and bonded CFRP plates. *International Journal of Fatigue*, 44, 303-315.



- Gholami, M., Sam, A. R. M., Yatim, J. M., & Tahir, M. M. (2013). A review on steel/CFRP strengthening systems focusing environmental performance. *Construction and Building Materials*, 47, 301-310.
- Gite, B. E., & Margaj, M. S. R. (2013). Carbon fibre as a recent material use in construction. *Civil Engineering Portal*. Retrieved from <http://www.engineeringcivil.com/carbon-fibre-as-a-recent-material-use-in-construction.html>.
- Goodman, J. (1899) *Mechanics Applied to Engineering*, Longmans Green, London.
- Gope, D., Gope, P. C., & Thakur, A. (2013). Influence of crack tip and crack offset distance on crack interaction and growth direction in multiple cracks. *International Journal of Structural Integrity*. <https://doi.org/10.1108/IJSI-05-2012-0013>
- Gowhari-Anaraki, A. R., Hardy, S. J., & Adibi-Asl, R. (2003). Mixed-mode fatigue crack propagation in thin T-sections under plane stress. *The Journal of Strain Analysis for Engineering Design*, 38(6), 557-575.
- Griffith, A. A. (1921). VI. The phenomena of rupture and flow in solids. *Philosophical transactions of the royal society of london. Series A, containing papers of a mathematical or physical character*, 221(582-593), 163-198.
- Haedir, J., Bambach, M. R., Zhao, X. L., & Grzebieta, R. H. (2006). Bending strength of CFRP-strengthened circular hollow steel sections. In *International Conference on FRP Composites in Civil Engineering (CICE) 2006* (pp. 701-704). Florida International University.
- Haedir, J., Bambach, M. R., Zhao, X. L., & Grzebieta, R. H. (2008). Behaviour of thin-walled CHS beams reinforced by CFRP sheets. In *4th International Structural Engineering and Construction Conference, ISEC-4-Innovations in Structural Engineering and Construction* (pp. 701-706).
- Haroun, M. A. (2005). Mitigation of elephant-foot bulge formation in seismically-excited steel storage tanks.
- Harris, A. F., & Beevers, A. (1999). The effects of grit-blasting on surface properties for adhesion. *International journal of adhesion and adhesives*, 19(6), 445-452.
- Hashim, S. (2012). Investigate the Effectiveness of Stop Drill Hole in Delaying Crack from Crack Initiation (Doctoral dissertation, UMP).
- Hashin, Z. (1980). Failure criteria for unidirectional fiber composites.

- Hashin, Z., & Rotem, A. (1973). A fatigue failure criterion for fiber reinforced materials. *Journal of composite materials*, 7(4), 448-464.
- Hegde, S., Shenoy, B. S., & Chethan, K. N. (2019). Review on carbon fiber reinforced polymer (CFRP) and their mechanical performance. *Materials Today: Proceedings*, 19, 658-662.
- Hojjati Talemi, R. (2014). Numerical Modelling Techniques for Fretting Fatigue Crack Initiation and Propagation.
- Hollaway, L. C. (2010). A review of the present and future utilisation of FRP composites in the civil infrastructure with reference to their important in-service properties. *Construction and building materials*, 24(12), 2419-2445.
- Hollaway, L. C., & Cadei, J. (2002). Progress in the technique of upgrading metallic structures with advanced polymer composites. *Progress in Structural Engineering and Materials*, 4(2), 131-148.
- Inglis, C. E. (1913). Stresses in a plate due to the presence of cracks and sharp corners. *Trans Inst Naval Archit*, 55, 219-241.
- Irwin, G. R. (1957). Analysis of stresses and strains near the end of a crack traversing a plate. *Journal of Applied Mechanics*, 24, 361–364.
- Isaac, P. M. (2009). Effect of Adhesive Stiffness on FRP Anchorage Strengthening of Steel. Department of Architecture and Civil Engineering.
- Ishikawa, T., Okura, I., & Kita, N. (2006). Debonding shear stress in steel plates with a fiber sheet inserted under a CFRP plate. *JSCE, Journal of Structural Engineering*, 52, 1317-26.
- Jiao, H., & Zhao, X. L. (2004). CFRP strengthened butt-welded very high strength (VHS) circular steel tubes. *Thin-walled structures*, 42(7), 963-978.
- Jones, S. C., & Civjan, S. A. (2003). Application of fiber reinforced polymer overlays to extend steel fatigue life. *Journal of Composites for Construction*, 7(4), 331-338.
- Jyothi Prakash, K., Vidhyasagar, Suhas, R., & Shashank. (2017). Design and Fabrication of Fatigue Testing Machine of Cantilever. *IARJSET*, 4(7).
- Kabir, M. H., Fawzia, S., & Chan, T. H. T. (2016). Durability of CFRP strengthened circular hollow steel members under cold weather: Experimental and numerical investigation. *Construction and Building Materials*, 123, 372-383.

- Kalavagunta, S., Naganathan, S., & Mustapha, K. N. B. (2014). Axially loaded steel columns strengthened with CFRP. *Jordan Journal of Civil Engineering*, 8(1), 58-69.
- Kamal, K., Mitao, O., Ranjith, D., & Sudath, S. (2010). A combined high and low cycle fatigue model to estimate life of steel bridges. *Journal of Engineering and Technology Research*, 2(8), 144-160.
- Kelly, P. (2012). *Engineering Solid Mechanics*. University of Auckland.
- Kim, Y. J., Hossain, M., & Yoshitake, I. (2012). Cold region durability of a two-part epoxy adhesive in double-lap shear joints: Experiment and model development. *Construction and Building Materials*, 36, 295-304.
- Kitagawa, H. (1976). Applicability of fracture mechanics to very small cracks or the cracks in the early stage. *Proc. of 2nd ICM, Cleveland, 1976*, 627-631.
- Kramberger, J., Šraml, M., Glodež, S., Flašker, J., & Potrč, I. (2004). Computational model for the analysis of bending fatigue in gears. *Computers & structures*, 82(23-26), 2261-2269.
- Krupp, U. (2007). *Fatigue crack propagation in metals and alloys: microstructural aspects and modelling concepts*. John Wiley & Sons.
- Kumar, S. B., Sridhar, I., & Sivashanker, S. (2008). Influence of humid environment on the performance of high strength structural carbon fiber composites. *Materials Science and Engineering: A*, 498(1-2), 174-178.
- Landy, M. A., Armen Jr, H., & Eidinoff, H. L. (1986). Enhanced stop-drill repair procedure for cracked structures. *Fatigue in mechanically fastened composite and metallic joints, ASTM STP, 927*, 190-220.
- Langer, B. F. (1937). *Fatigue failure from stress cycles of varying amplitude*.
- Lee, E. H. (1970). Thermo-elastic-plastic analysis at finite strain. In *Thermo inelasticity* (pp. 156-169). Springer, Vienna.
- Lee, Y. L., Pan, J., Hathaway, R., & Barkey, M. (2005). *Fatigue testing and analysis: theory and practice* (Vol. 13). Butterworth-Heinemann.
- Lei, Y. (2016). Validation of contour integral functions (J and C (t)) in ABAQUS v6. 11-v6. 14 for combined mechanical and residual stresses. *Procedia Structural Integrity*, 2, 2566-2574.

- Leitao, V. M. A., Aliabadi, M. H., Rooke, D. P., & Cook, R. (1998). Boundary element methods for the analysis of crack growth in the presence of residual stress fields. *Journal of materials engineering and performance*, 7(3), 352-360.
- Lenwari, A., Thepchatri, T., & Albrecht, P. (2006). Debonding strength of steel beams strengthened with CFRP plates. *JOURNAL of composites for construction*, 10(1), 69-78.
- Lettieri, M., & Frigione, M. (2012). Effects of humid environment on thermal and mechanical properties of a cold-curing structural epoxy adhesive. *Construction and Building Materials*, 30, 753-760.
- Li, J., Tian, X. X., & Abdelmoula, R. (2012). A damage model for crack prediction in brittle and quasi-brittle materials solved by the FFT method. *International journal of fracture*, 173(2), 135-146.
- Li, S., Ren, H. T., Lu, Y. Y., & Shi, M. H. (2011). Environmental degradation of carbon fiber reinforced polymer (CFRP) and steel bond subjected to hygrothermal aging and loading. In *Materials science forum* (Vol. 675, pp. 559-562). Trans Tech Publications Ltd.
- Li, Z. G., & Yi-Heng, L. I. (2012). Hysteretic behavior of steel column strengthened with CFRP in thermal environment. *telkomnika Indonesian J. Electr. Eng*, 10(5), 919-924.
- Liu, H. B., Zhao, X. L., & Al-Mahaidi, R. (2005, December). The effect of fatigue loading on bond strength of CFRP bonded steel plate joints. In *Proceedings of the international symposium on bond behaviour of FRP in structures* (pp. 459-64).
- Makabe, C., Miyazaki, T., & Hattori, N. (2012). Improvement of fatigue life of a holed specimen of aluminum-alloy 2024-t3 by indentation and hole expansion. 6, 336–342. <https://doi.org/10.1142/S2010194512003406>
- Manson, S.S. (1954) *Behaviour of Materials Under Conditions of Thermal Stress*. National Advisory Commission on Aeronautics: Report 1170, Lewis Flight. ' Propulsion Laboratory, Cleveland.
- Matsuishi, M., & Endo, T. (1968). Fatigue of metals subjected to varying stress. *Japan Society of Mechanical Engineers*, Fukuoka, Japan, 68(2), 37-40.
- Matta, F. (2003). Bond between steel and CFRP laminates for rehabilitation of metallic bridges. Faculty of Engineering, University of Padua: Padua, Italy.

- McAlorum, J., Rubert, T., Fusiek, G., Niewczas, P., & Zorzi, G. (2018). Design and demonstration of a low-cost small-scale fatigue testing machine for multi-purpose testing of materials, sensors and structures. *Machines*, 6(3), 30.
- McDowell, D. L., & Dunne, F. P. E. (2010). Microstructure-sensitive computational modeling of fatigue crack formation. *International journal of fatigue*, 32(9), 1521-1542.
- Mertz, D. R., & Gillespie Jr, J. W. (1996). Rehabilitation of steel bridge girders through the application of advanced composite materials (No. NCHRP-IDEA Project 011).
- Miannay, D. P. (2001). *Time-dependent fracture mechanics*. Springer Science & Business Media.
- Miller, T. C., Chajes, M. J., Mertz, D. R., & Hastings, J. N. (2001). Strengthening of a steel bridge girder using CFRP plates. *Journal of bridge engineering*, 6(6), 514-522.
- Miner MA (1945) Cumulative damage in fatigue. *Journal of Applied Mechanics* 12: 159–164.
- Moës, N., Dolbow, J., & Belytschko, T. (1999). A finite element method for crack growth without remeshing. *International journal for numerical methods in engineering*, 46(1), 131-150.
- Monfared, A., Soudki, K., & Walbridge, S. (2008, July). CFRP reinforcing to extend the fatigue lives of steel structures. In *Proceedings of the Fourth International Conference on FRP Composites in Civil Engineering (CICE'08)*.
- Mosallam, A. S., Chakrabarti, P. R., & Spencer, E. (1998). Experimental investigation on the use of advanced composites & high-strength adhesives in repair of steel structures. In *international sampe symposium and exhibition (pp. 1826-1837)*. sampe society for the advancement of material.
- Mustafy, T., & Ahsan, R. (2010, August). FE modeling and experimental verification of a CFRP strengthened steel section subjected to transverse end bearing force. In *IABSE-JSCE Joint Conference on Advances in Bridge Engineering-II, August (pp. 8-10)*.
- Nakamura, H., Jiang, W., Suzuki, H., Maeda, K. I., & Irube, T. (2009). Experimental study on repair of fatigue cracks at welded web gusset joint using CFRP strips. *Thin-Walled Structures*, 47(10), 1059-1068.

- Namjoshi, S. A., & Mall, S. (2001). Fretting behavior of Ti-6Al-4V under combined high cycle and low cycle fatigue loading. *International Journal of Fatigue*, 23, 455-461.
- Narmashiri, K., Ramli Sulong, N. H., & Jumaat, M. Z. (2011). Flexural strengthening of steel I-beams by using CFRP strips. *International Journal of the Physical Sciences*, 6(7), 1620-1627.
- Neuber, H. (1946). *Theory of notch stresses: Principles for exact stress calculation* (Vol. 74). JW Edwards.
- Nguyen, T. C., Bai, Y., Zhao, X. L., & Al-Mahaidi, R. (2012). Durability of steel/CFRP double strap joints exposed to sea water, cyclic temperature and humidity. *Composite Structures*, 94(5), 1834-1845.
- Niinomi, M., Kobayashi, T., Toriyama, O., Kawakami, N., Ishida, Y., & Matsuyama, Y. (1996). Fracture characteristics, microstructure, and tissue reaction of Ti-5Al-2.5 Fe for orthopedic surgery. *Metallurgical and Materials Transactions A*, 27(12), 3925-3935.
- Nozaka, K., Shield, C. K., & Hajjar, J. F. (2005). Effective bond length of carbon-fiber-reinforced polymer strips bonded to fatigued steel bridge I-girders. *Journal of bridge Engineering*, 10(2), 195-205.
- Oakley, S. Y., & Nowell, D. (2007). Prediction of the combined high-and low-cycle fatigue performance of gas turbine blades after foreign object damage. *International journal of fatigue*, 29(1), 69-80.
- Ochensberger, W., & Kolednik, O. (2014). A new basis for the application of the  $J$  integral for cyclically loaded cracks in elastic-plastic materials. *International Journal of Fracture*, 189(1), 77-101.
- Ochensberger, W., & Kolednik, O. (2015). Physically appropriate characterization of fatigue crack propagation rate in elastic-plastic materials using the  $J$  -  $J$ -integral concept. *International Journal of Fracture*, 192(1), 25-45.
- Ochensberger, W., & Kolednik, O. (2016). Overload effect revisited— Investigation by use of configurational forces. *International journal of fatigue*, 83, 161-173.
- Okura, I., Fukui, T., Nakamura, K., Matsugami, T., & Iwai, Y. (2000). Application of CFRP sheets to repair of fatigue cracks in steel plates. *Journal of Construction Steel, Japan*, 8, 689-696.

- Pach, E., Korin, I., & Ipina, J. P. (2012). Simple fatigue testing machine for fiber-reinforced polymer composite. *Experimental Techniques*, 36(2), 76-82.
- Palmgren, A. (1924). Die lebensdauer von kugellagern. *Zeitschrift des Vereines Duetsher Ingenieure*, 68(4), 339.
- Paris, P. C. (1961). A rational analytic theory of fatigue. *Trends Engin*, 13, 9-14.
- Paris, P. C. (1964). The fracture mechanics approach to fatigue. *Fatigue-an interdisciplinary approach*.
- Pearson, S. (1975). Initiation of fatigue cracks in commercial aluminium alloys and the subsequent propagation of very short cracks. *Engineering Fracture Mechanics*, 7(2), 235-247.
- Peiris, N. A. (2011). Steel beams strengthened with ultra high modulus CFRP laminates. University of Kentucky.
- Peralta, P., & Laird, C. (2016). Cyclic plasticity and dislocation structures. Reference Module in Materials Science and Materials Engineering; Elsevier: Amsterdam, The Netherlands.
- Pipinato, A., Pellegrino, C., & Modena, C. (2012). Fatigue behaviour of steel bridge joints strenghtened with FRP laminates. *Modern Applied Science*, 6(10), 1.
- Poncelet, J. V. (1839). *Introduction à la mécanique industrielle, physique ou expérimentale*. Thiel.
- Rameshni, R. (2011). Innovative hybrid FRP/steel splice details for modular bridge expansion joints. Queen's University (Canada).
- Rankine, W. J. M. (1843). On the causes of the unexpected breakage of the journals of railway axles; and on the mean of preventing such accidents by observing the law of continuity in their construction. *Journal of the Franklin Institute*, 36(3), 178-180.
- Recho, N. (2012). *Fracture mechanics and crack growth*. John Wiley & Sons.
- Rege, S. K., & Lakkad, S. C. (1983). Effect of salt water on mechanical properties of fibre reinforced plastics. *Fibre Science and Technology*, 19(4), 317-324.
- Reid, L. (2011, July). Mitigating Bridge Structural Fatigue Cracking Using Aerospace Derived Technology. In *New York Bridge Conference*. New York, New York (pp. 25-26).

- Revankar, S. T., Wolf, B., & Roznic, J. R. (2012). Metal Fatigue Crack Growth Models. *International Journal of Advanced Engineering Applications*, Volume1, 4, 85-91.
- Rice, J.R. (1968) A path independent integral and the approximate analysis of strain concentrations by notches and crack. *J. Applied Mech* 35, 379-86
- Ritchie, R. O. (1999). Mechanisms of fatigue-crack propagation in ductile and brittle solids. *International journal of Fracture*, 100(1), 55-83.
- Rolfe, S. T., & Barsom, J. M. (1977). *Fracture and fatigue control in structures: Applications of fracture mechanics*. ASTM International.
- Saadatmanesh, H., Tavakkolizadeh, M., & Mostofinejad, D. (2010). Environmental effects on mechanical properties of wet lay-up fiber-reinforced polymer. *ACI materials journal*, 107(3), 267.
- Saai, A., Louche, H., Tabourot, L., & Chang, H. J. (2010). Experimental and numerical study of the thermo-mechanical behavior of Al bi-crystal in tension using full field measurements and micromechanical modeling. *Mechanics of Materials*, 42(3), 275-292.
- Santecchia, E., Hamouda, A. M. S., Musharavati, F., Zalnezhad, E., Cabibbo, M., El Mehtedi, M., & Spigarelli, S. (2016). A review on fatigue life prediction methods for metals. *Advances in Materials Science and Engineering*, 2016.
- Schijve, J. (2003). Fatigue of structures and materials in the 20th century and the state of the art. *International Journal of fatigue*, 25(8), 679-702.
- Schnerch, D., & Rizkalla, S. (2008). Flexural strengthening of steel bridges with high modulus CFRP strips. *Journal of Bridge Engineering*, 13(2), 192.
- Schnerch, D., Dawood, M., Rizkalla, S., & Sumner, E. (2007). Proposed design guidelines for strengthening of steel bridges with FRP materials. *Construction and building materials*, 21(5), 1001-1010.
- Schwartz, J., Fandeur, O., & Rey, C. (2010). Fatigue crack initiation modeling of 316LN steel based on non local plasticity theory. *Procedia Engineering*, 2(1), 1353-1362.
- Schweizer, C., Seifert, T., Nieweg, B., Von Hartrott, P., & Riedel, H. (2011). Mechanisms and modelling of fatigue crack growth under combined low and high cycle fatigue loading. *International journal of fatigue*, 33(2), 194-202. <https://doi.org/10.1016/j.ijfatigue.2010.08.008>



- Selvaratnam, A., Arachchi, K. K., Gamage, J. C. P. H., & Attanayake, V. (2021). Investigation on an effective bond arrangement of insulated CFRP-strengthened flexural members for improved thermo-mechanical performance. *Case Studies in Construction Materials*, 14, e00544. <https://doi.org/10.1016/j.cscm.2021.e00544>
- Shaat, A., & Fam, A. (2007, December). Control of overall buckling of HSS slender steel columns using CFRP plates. In *Proceedings of the First Asia Pacific conference FRP Structures (APFIS2007)*, Hong Kong, China (pp. 12-14).
- Sharpe, N. C. and W. N. (1979). N. Chandawanich and W.N. Sharpe Jr. *Eng. Fract. Mech.*, 11.
- Siegmund, T., & Brocks, W. (1999). Prediction of the work of separation and implications to modeling. *International Journal of Fracture*, 99(1), 97-116.
- Sih, G. C. (1974). Elastic-plastic fracture mechanics. *Prospects of Fracture Mechanics*, 613-621.
- Şik, A., Atak, A., Yavuz, C., & Özdemir, V. (2018). The Design of Fatigue Strength Machine Being One of the Methods for Determining the Mechanical Properties of the Materials Used in the Industry. *Journal of Science PART A: ENGINEERING AND INNOVATION*, 5(2), 79–88. <http://dergipark.gov.tr/gujsa>
- Silvestre, N., Young, B., & Camotim, D. (2008). Non-linear behaviour and load-carrying capacity of CFRP-strengthened lipped channel steel columns. *Engineering structures*, 30(10), 2613-2630.
- Singh, R., & Sharma, V. (2021). Numerical modelling of residual stresses during orthogonal cutting of Ti6Al4V using internally cooled cutting inserts. *Journal of Manufacturing Processes*, 65, 502-511.
- Smallman, R. E., & Bishop, R. J. (1999). *Modern physical metallurgy and materials engineering*. Butterworth-Heinemann.
- Song, H. W., Wan, Z. M., Xie, Z. M., & Du, X. W. (2000). Axial impact behavior and energy absorption efficiency of composite wrapped metal tubes. *International Journal of Impact Engineering*, 24(4), 385-401.
- Stanzl-Tschegg, S. E., Meischel, M., Arcari, A., Iyyer, N., Apetre, N., & Phan, N. (2016). Combined cycle fatigue of 7075 aluminum alloy–Fracture surface characterization and short crack propagation. *International Journal of Fatigue*, 91, 352-362.

- Stefanescu, D., Dutta, M., Wang, D. Q., Edwards, L., & Fitzpatrick, M. E. (2003). The effect of high compressive loading on residual stresses and fatigue crack growth at cold expanded holes. *The Journal of Strain Analysis for Engineering Design*, 38(5), 419-427.
- Stratford, T. J., & Bisby, L. A. (2012). Effect of warm temperatures on externally bonded FRP strengthening. *Journal of Composites for Construction*, 16(3), 235.
- Sumpter, J. D. G., & Turner, C. E. (1976). Method for laboratory determination of  $J_c$  (pp. 3-18). ASTM International.
- Suresh, S. (1998). *Fatigue of materials*. Cambridge university press.
- Suzuki, H. (2002, July). Strengthening of a steel beam with carbon fiber reinforced polymer strip. In *Proceedings of the First International Conference on Bridge Maintenance, Safety and Management IABMAS*.
- Suzuki, H., & Okamoto, Y. (2003). Repair of steel members with a fatigue crack using the carbon fiber reinforced polymer strip. *Journal of Constructional Steel, Japan*, 11, 465-472.
- Täljsten, B., Hansen, C. S., & Schmidt, J. W. (2009). Strengthening of old metallic structures in fatigue with prestressed and non-prestressed CFRP laminates. *Construction and Building Materials*, 23(4), 1665-1677.
- Tang, J. H., Sridhar, I., & Srikanth, N. (2013). Static and fatigue failure analysis of adhesively bonded thick composite single lap joints. *Composites Science and Technology*, 86, 18-25.
- Tavakkolizadeh, M., & Saadatmanesh, H. (2003). Fatigue strength of steel girders strengthened with carbon fiber reinforced polymer patch. *Journal of structural engineering*, 129(2), 186-196.
- Teng, J. G., & Hu, Y. M. (2007). Behaviour of FRP-jacketed circular steel tubes and cylindrical shells under axial compression. *Construction and Building Materials*, 21(4), 827-838.
- Vincent, M. K., Varghese, V., & Sukumaran, S. (2016). Fabrication and analysis of fatigue testing machine. *Int. J. Eng. Sci*, 5, 2319-1813.
- Wang, J., Jiang, W., Li, Y., Wang, Q., & Xu, Q. (2019). Numerical assessment of cyclic  $J$ -integral  $\Delta J$  for predicting fatigue crack growth rate. *Engineering Fracture Mechanics*, 205, 455-469.

- Wang, Y., Li, J., Deng, J., & Li, S. (2018). Bond behaviour of CFRP/steel strap joints exposed to overloading fatigue and wetting/drying cycles. *Engineering Structures*, 172, 1-12.
- Wang, Z. Y., Wang, Q. Y., Li, L., & Zhang, N. (2017). Fatigue behaviour of CFRP strengthened open-hole steel plates. *Thin-Walled Structures*, 115, 176-187.
- Wei, X., & He, X. (2014, June). The Application of Steel Structure in Civil Engineering. In 2014 International Conference on Education, Management and Computing Technology (ICEMCT-14) (pp. 253-256). Atlantis Press.
- Wöhler, A. (1860). Tests to determine the forces acting on railway wagon axles, and the capacity of resistance of the axles. *Z Bauw*, 10, 583-616.
- Wohler, A. (1867) Versuche über die Festigkeit der Eisenbahnwagenachsen (English summary) *Engineering* 4,160-1.
- Wolf, E. (1970). Fatigue crack closure under cyclic tension. *Engineering fracture mechanics*, 2(1), 37-45.
- Wright, P. N. H., Wu, Y., & Gibson, A. G. (2000). Fibre reinforced composite–steel connections for transverse ship bulkheads. *Plastics, Rubber and Composites*, 29(10), 549-557.
- Wu, C., Zhao, X. L., Chiu, W. K., Al-Mahaidi, R., & Duan, W. H. (2013). Effect of fatigue loading on the bond behaviour between UHM CFRP plates and steel plates. *Composites Part B: Engineering*, 50, 344-353.
- Wu, C., Zhao, X., Duan, W. H., & Al-Mahaidi, R. (2012). Bond characteristics between ultra high modulus CFRP laminates and steel. *Thin-Walled Structures*, 51, 147-157.
- Wu, H., Imad, A., Nourredine, B., de Castro, J. T. P., & Meggiolaro, M. A. (2009). On the modeling of the stop-hole crack repair method. In *Technical Contribution to 64th ABM Annual Congress*.
- Wu, L., Hoa, S. V., & Ton-That, M. T. (2004). Effects of water on the curing and properties of epoxy adhesive used for bonding FRP composite sheet to concrete. *Journal of applied polymer science*, 92(4), 2261-2268.
- Xia, S. H., & Teng, J. G. (2005, December). Behaviour of FRP-to-steel bonded joints. In *Proceedings of the international symposium on bond behaviour of FRP in structures* (pp. 419-26). International Institute for FRP in Construction.

- Xiao, Y., He, W., & Choi, K. K. (2005). Confined concrete-filled tubular columns. *Journal of structural engineering*, 131(3), 488-497.
- Yao, J., Teng, J. G., & Chen, J. F. (2005). Experimental study on FRP-to-concrete bonded joints. *Composites Part B: Engineering*, 36(2), 99-113.
- Ye, X. W., Su, Y. H., & Han, J. P. (2014). A state-of-the-art review on fatigue life assessment of steel bridges. *Mathematical Problems in Engineering*, 2014.
- Yong-xin, Y., Qing-rui, Y., & Fu-ming, P. (2005). Experimental research on bond behavior of CFRP to steel. In *Int. Symp. Bond Behav. FRP Struct.(BBFS 2005)* (pp. 419-24).
- Yu, Y., Chiew, S. P., & Lee, C. K. (2011). Bond failure of steel beams strengthened with FRP laminates—Part 2: Verification. *Composites Part B: Engineering*, 42(5), 1122-1134.
- Yuan, H., Teng, J. G., Seracino, R., Wu, Z. S., & Yao, J. (2004). Full-range behavior of FRP-to-concrete bonded joints. *Engineering structures*, 26(5), 553-565.
- Yun, Z., Lieping, Y., & Qingrui, Y. (2005). Research progress of FRP reinforcement steel structure. *Industrial Construction*, 35(8), 20-26.
- Zeghadi, A., Forest, S., Gourgues, A. F., & Bouaziz, O. (2007). Ensemble averaging stress–strain fields in polycrystalline aggregates with a constrained surface microstructure—Part 2: Crystal plasticity. *Philosophical Magazine*, 87(8-9), 1425-1446.
- Zeghadi, A., N'guyen, F., Forest, S., Gourgues, A. F., & Bouaziz, O. (2007). Ensemble averaging stress–strain fields in polycrystalline aggregates with a constrained surface microstructure—Part 1: Anisotropic elastic behaviour. *Philosophical Magazine*, 87(8-9), 1401-1424.
- Zehnder, A. T. (2012). Elastic Plastic Fracture: Crack Tip Fields. In *Fracture Mechanics* (pp. 137-183). Springer, Dordrecht.
- Zhang, A. Y., Li, D. H., & Zhang, D. X. (2012). Effect of moisture absorption on the bending strength of CFRP. In *Advanced Materials Research* (Vol. 450, pp. 482-485). Trans Tech Publications Ltd.
- Zhao, L. G., Tong, J., & Byrne, J. (2004). The evolution of the stress–strain fields near a fatigue crack tip and plasticity-induced crack closure revisited. *Fatigue & Fracture of Engineering Materials & Structures*, 27(1), 19-29.

- Zhao, X. L. (2013). FRP-strengthened metallic structures. Crc Press.
- Zhao, X. L., & Zhang, L. (2007). State-of-the-art review on FRP strengthened steel structures. *Engineering structures*, 29(8), 1808-1823.
- Zhao, Y., Gu, W., Xu, J., & Zhang, H. (2005, June). The strength of concrete filled CFRP-steel tubes under axial compression. In the Fifteenth International Offshore and Polar Engineering Conference. OnePetro.
- Zheng, X., Engler-Pinto Jr, C. C., Su, X., Cui, H., & Wen, W. (2013). Modeling of fatigue damage under superimposed high-cycle and low-cycle fatigue loading for a cast aluminum alloy. *Materials Science and Engineering: A*, 560, 792-801.
- Zheng, Y., Ye, L., Lu, X., & Yue, Q. (2006, December). Experimental study on fatigue behavior of tensile steel plates strengthened with CFRP plates. In Third international conference on FRP in composites in civil engineering (CICE 2006).
- Zhu, S. P., Yue, P., Yu, Z. Y., & Wang, Q. (2017). A combined high and low cycle fatigue model for life prediction of turbine blades. *Materials*, 10(7), 698

## *Appendices*

---

## ***Appendix-A***

---

**APPENDIX-A**

Table 2.5: Summary of bond performance characteristics related studies

No	Research Area	Method	Results	Reference
1	Bond performance characteristics	Evaluated bond behavior between steel plate strengthened with CFRP subjected to impact tensile loads	Effective bonding length is insensitive with the rate of loads	Haideret al.( 2012)
2	Thin-walled steel members	Web buckling Fatigue behavior Compression	Improved capacity bearing load  Strength and stiffness improvement	Haedir et al. (2007),Zhao and Al-Mahaidi (2009) and Haedir <i>et al.</i> (2010)  Nuno <i>et al.</i> (2008) and Jimmy and Xiao-Ling (2011)



Table 2.6: Summary of surface preparation technology related key studies

No	Methods / Procedure	Result / Observations	References
1	chemical, mechanical, electrochemical, and thermal procedures	Significantly enhanced the bond performance	Baldan (2004)
2	Any surface preparation	(a) form an active surface (b) chemical rectification of the surface (c) remove of contaminant materials from surface	Hollaway and Cadei (2002)
3	Grit Blasting	(a) grit-blasting method is most effective technique (b) Grit blasting method can be avoid micro cracks	Schnerch et al.(2007)
4	Grit blasting	(a) improve the chemical characteristics of the adherents (b) remove weak layers from metal surface	Harris and Beevers (1999)
5	grit-blasting with electrochemical treatments	improved bond strength	Baldan (2004)
6	Silane coupling agent method for surface treatment	Significantly improved the bond durability	Dawood and Rizkalla (2010(a))

Table 2.7: Key research studies related to adhesives and adhesive properties

No	Investigation	Results	References
1	Evaluating the capability of effective load transfer through the bond	Each adhesive is not fully capable of transferring forces, effectively and some investigators have suggested possibility to used additional fasteners	Sen and Liby (1994)
2	Investigate bond performance effects	Significant improvement	Hildebrand (1994), Täljsten (1997), Deng et al.(2004) and Fawzia et al.(2006)
3	Investigating the relationship of local bond–slip with geometrical parameters.	Local bond slip is not dependent on geometric related parameters	Sreedhar et al. (2014)
4	Investigating bond strength	Considerable Strength gain was reported	Chen et al. (2001), Nozaka et al. (2005(a)), Ishikawa et al. (2006)
5	Investigate effects of bond length and different numbers of CFRP layers	The load carrying capacity is linearly propositional to the bond length	Fawzia et al. (2005-2010)
6	Understanding durability of adhesive under elevated and freezing conditions of temperature.	Adhesive that has reported good durability under elevated and freezing conditions of temperature	Mertz and Gillespie(1996)
7	Investigating the stress concentration level behavior with adhesive thickness	The stress concentration level was reduced by 21 %	Wright et al. (2009) and Wright et al.(2000)
8	Examine effects of adding a fillet at the end of the bond line	32 % stress concentration, reduced	Unknown
9	Understanding adhesive stiffness effects of bond performance	(a)A flexible adhesive will cause lower stresses as it deforms to a greater degree but lower ultimate strength (b) Stiffer adhesive will cause higher stress, but it shows a higher ultimate strength	Philip (2009)

Table 2.8: Summary of bonding mechanisms related to key research investigations

No	Research area	Results	References
1	Understanding an efficient bonding mechanism a) theory of mechanical interlock b) physical bond c) chemical bond d) theory of diffusion	absorption mechanism and mechanical interlocking methods are highlighted as effective bonding mechanism	Baldan(2004),Stanford (2009)
2	Investigating the effect of adhesive layer thickness to failure mode	a) an increase the thickness of adhesive layer failure occurs as a brittle failure b) de-bonding occurs when thickness of adhesive layer exceeded 2 mm c) de-bonding occurs through the adhesive due to effect of thin adhesive layer d) when increase thickness of adhesive ductile failure occurs	Xia and Teng (2005)
3	Evaluating the effect of high ductility	ductility of adhesive contribute to successfully distribute the stresses	Nozaka et al.(2005), Colombi and Poggi (2006), Shield et al.(2005(b))
4	Understanding the effect of the thickness of CFRP plate	The bond strength is proportional to thickness of CFRP plate	Yu et al.(2011)

No	Research area	Results	References
5	Evaluating the behavior of stiffness of CFRP	fracture mode and ultimate load bearing capacity governed by the stiffness of CFRP material	Al-Emrani et al. (2005)
6	Correlation between bond strength and stiffness	reduction of stiffness increases in bond strength substantially	Yu et al.(2011)
7	Using the result of HM CFRP material	(a) higher load capacity (b) less ductile behavior	El-Hacha and Ragab (2006)
8	Investigate co relation between slip and shear stress	shear stress and slip show linear relationship (b) stress concentration high at the ends of strengthening plate	Fawzia and Karim (2009)
9	stress concentration reducing methods	beveled ending and reverse tapering methods are significantly reduces stress concentration	Miller et al. (2001), Dawood and Rizikalla(2006)
10	bond strength increasing techniques	steel plate adding with CFRP at high stress region strength enhanced up to 50 %	Shervani and Davaran (2010)

Table 2.9: Key research studies related to humidity effects on CFRP/steel bond performance

No	Research area	Result/ Observations/Conclusions	References
1	Investigating effects of moisture ingress	a) weak attraction between adhesive and CFRP b) change physical characteristic of material c) decrease the glass transition temperature  a) unexpected structural distortions  a) reduces the shear strength of the polymer b) decrease bending strength approximately 17 % by 1 % of moisture	Collings et al.(1993), Kumar et al. (2008)  Kumar et al.(2008) and Hollaway (2010)  Zhang et al.(2012)
2	Investigating effects of CFRP material	Exhibit excellent durability under sever environmental condition Rate of moisture absorption very fast at the starting and after that reached a constant level	Nguyen et al.( 2012)
3	Investigating the effect of the humidity level	relative humidity level exceeds 75 %, rate of moisture absorption is very fast	Lettieri and Frigione. (2012)
4	Investigating exposure to a small amount of moisture (<2 %)	Improves the curing rate and enhances bonding strength	Wu et al.( 2004)

Table 2.10: Summary of key research investigations related temperature and humidity combination effects on CFRP/steel bond performance

No	Methods/ Procedure	Result/ Observations	References
1	Investigation of the effect of moisture and temperature (hygro-thermal) combination.	Significant reduction has been reported in glass transition temperature of CFRP.	Aoki et al.(2008)
2	Temperature and relative humidity (50 °C – 93% RH) the I-steel beams tested for bending after 15, 45, and 90 days	ultimate load carrying capacity reduction reported by 22 %, 26 %, and 57 % with respect to time.	Shan et al.(2011)
3	Investigation of the effect of hygro-thermal condition for double lap joints	reduction of stiffness and tensile strength lower than 10%.	Nguyen et al.( 2012)
4	Investigation of double lap shears joint behavior subjected to 100 cycles	tensile strength improved 31%	Kim(2012)
5	Evaluation of double strap CFRP/steel joints	strength of joints decreased was observed 15% and 26 % respectively	Dawood and Rizkalla (2010(b))
6	Temperature behavior evaluation	the peak value at Tg . was 65 °C, and joint slip start around 40 °C	Stratford and Bisby (2012)
7	Examine the effects of a severe environmental condition	Sustained load for double lap shear joints. combination of saline water and elevated temperatures are highly influenced on mechanical properties of joints.	Nguyen et al.( 2012)

Table 2.11: Summary of reported bridge retrofitted with CFRP (Nisal Abeetha, 2011)

No	Bridge	Location	Laminate Type (Modulus)	Year
1	Takiguchi bridge	Tokyo (Japan)	Ultra High modulus CFRP plate (Modulus 450 GPa)	2008
2	Acton bridge	London Underground (England)	High modulus CFRP plates (Modulus 310 GPa)	2000
3	King street bridge	Mold, Flintshire (England)	High modulus CFRP + GFRP plates (Modulus 360 GPa)	2000
4	1-704 bridge on I-95 over Christina creek	Newark, Delaware (USA)	CFRP plate (Modulus 112 GPa)	2000
5	Ashland bridge on state Rt. 82 over Red Clay Creek	Northern Delaware (USA)	CFRP plate (Modulus 112 GPa)	2002
6	7838.5S092 Bridge on state highway 92	Pottawattamie county, Iowa (USA)	CFRP plates (Modulus 138 GPa)	2003
7	Hythe bridge over the Thames river	Oxfordshire (England)	CFRP plates (Modulus 160 GPa)	1999
8	Slattocks canal bridge	Rochdale (England)	CFRP plates (Modulus unknown)	2000
9	Bow road bridge	East London (England)	CFRP plates (Modulus unknown)	unknown
10	Bid bridge	Kent (England)	CFRP plates (Modulus unknown)	unknown

Source: (Peiris, 2011)

## ***Appendix-B***

---



**APPENDIX -B**

Table 6.5: Number of cycles for crack initiation with respect to the diameter to width ratio

Diameter of CSH (mm)	Diameter to width ratio of CSH (mm)	Minimum J-integral (Jmin) $\times 10^{-3}$	Maximum J-integral (Jmax) $\times 10^{-3}$	Cyclic J-integral ( $\Delta J$ ) $\times 10^{-2}$	Number of load cycles for crack initiation
4	0.1	3.58	6.16	8.90	9209
8	0.2	0.24	0.66	2.91	6397
12	0.3	1.42	1.71	5.28	4921
16	0.4	3.39	5.91	8.71	4685
20	0.5	0.11	0.2	1.73	4059
25	0.6	2.87	4.21	7.71	2853

Table 6.6: Number of cycles for crack initiation with respect to the thickness to diameter ratio

Thickness to diameter ratio of Specimen (mm)	Minimum J integral (Jmin $\times 10^{-3}$ )	Maximum J integral (Jmax $\times 10^{-3}$ )	Cyclic J-integral ( $\Delta J$ ) $\times 10^{-2}$	Number of cycles for crack initiation
0.13	0.01	0.02	0.54	3229
0.19	1.12	1.52	4.87	4159
0.25	0.16	4.88	4.15	4312
0.31	0.82	0.98	4.06	4704
0.38	0.18	3.28	2.69	5097
0.44	0.24	0.52	2.68	5738
0.50	1.16	1.27	1.22	7404

Table 6.7: Number of cycles for crack initiation with respect to the diameter to crack length ratio

<b>Diameter to crack length ratio</b>	<b>Minimum J- integral (J min <math>\times 10^{-3}</math>)</b>	<b>Maximum J- integral (J max <math>\times 10^{-3}</math>)</b>	<b>Cyclic J- integral (<math>\Delta J</math>) <math>\times 10^{-2}</math></b>	<b>Load cycles for crack initiation</b>
0.80	0.92	1.58	4.75	4427
0.40	0.85	1.5	4.61	4385
0.27	1.11	1.66	4.99	4353
0.20	1.16	1.65	5.02	4265
0.16	1.00	1.53	4.78	4251

Table 6.8: Number of cycles for crack initiation with respect to the diameter to offset distance ratio

<b>Diameter to offset distance ratio</b>	<b>Minimum J integral (J min <math>\times 10^{-3}</math>)</b>	<b>Maximum J integral (J max <math>\times 10^{-3}</math>)</b>	<b>Cyclic J integral (<math>\Delta J</math>) <math>\times 10^{-2}</math></b>	<b>Number of cycles for crack initiation</b>
0	1.48	2.16	5.67	4011
0.8	0.93	1.43	4.62	4423
0.4	0.94	1.38	4.58	4440
0.27	0.67	0.88	3.78	4868
0.2	0.1	0.32	2.01	6589

Table 6.9: Number of cycles for crack initiation with respect to the diameter to load ratio

<b>Amplitude of Load (kN)</b>	<b>Diameter to load ratio</b>	<b>Minimum J- integral (J min<math>\times 10^{-3}</math>)</b>	<b>Maximum J-integral (J max<math>\times 10^{-3}</math>)</b>	<b>Cyclic J-integral (<math>\Delta J</math>) <math>\times 10^{-2}</math></b>	<b>Number of cycles for crack initiation</b>
2	8	2.43	3.09	6.70	3832
4	4	2.35	3.04	6.59	3818
6	2.7	2.15	2.82	6.55	3743
8	2	1.45	2.78	6.28	3733
10	1.6	1.43	2.68	6.24	3704

Table 6.10: Number of cycles for crack initiation with respect to the diameter to loading frequency

<b>Diameter to frequency ratio</b>	<b>Minimum J-integral (J min <math>\times 10^{-3}</math>)</b>	<b>Maximum J- integral (J max <math>\times 10^{-3}</math>)</b>	<b>Cyclic J integral (<math>\Delta J</math>) <math>\times 10^{-2}</math></b>	<b>Number of cycles for crack initiation</b>
16	1.05	1.53	4.82	4498
8	2.35	2.83	6.68	4334
4	0.97	1.51	4.73	4311
3.2	1.07	1.57	4.87	4198
2	2.34	2.72	6.61	3728
1.6	1.28	1.69	5.15	3709

Table 6.11: Number of cycles for crack initiation with respect to the ratio of diameter to stress ratio

<b>Stress Ratio(R)</b>	<b>Diameter to stress range ratio</b>	<b>Minimum J- integral (J min <math>\times 10^{-3}</math>)</b>	<b>Maximum J-integral (J max <math>\times 10^{-3}</math>)</b>	<b>Cyclic J-integral (<math>\Delta J</math>) <math>\times 10^{-2}</math></b>	<b>Number of cycles for crack initiation</b>
0.1	160	0.72	1.48	4.47	4493
0.2	80	1.05	1.53	4.82	4334
0.3	53	1.8	2.58	6.18	3849
0.4	40	1.38	3.07	6.23	3835
0.5	32	1.4	3.1	6.26	3826

Table 6.12: Number of cycles for crack initiation with respect to the angle of fiber direction

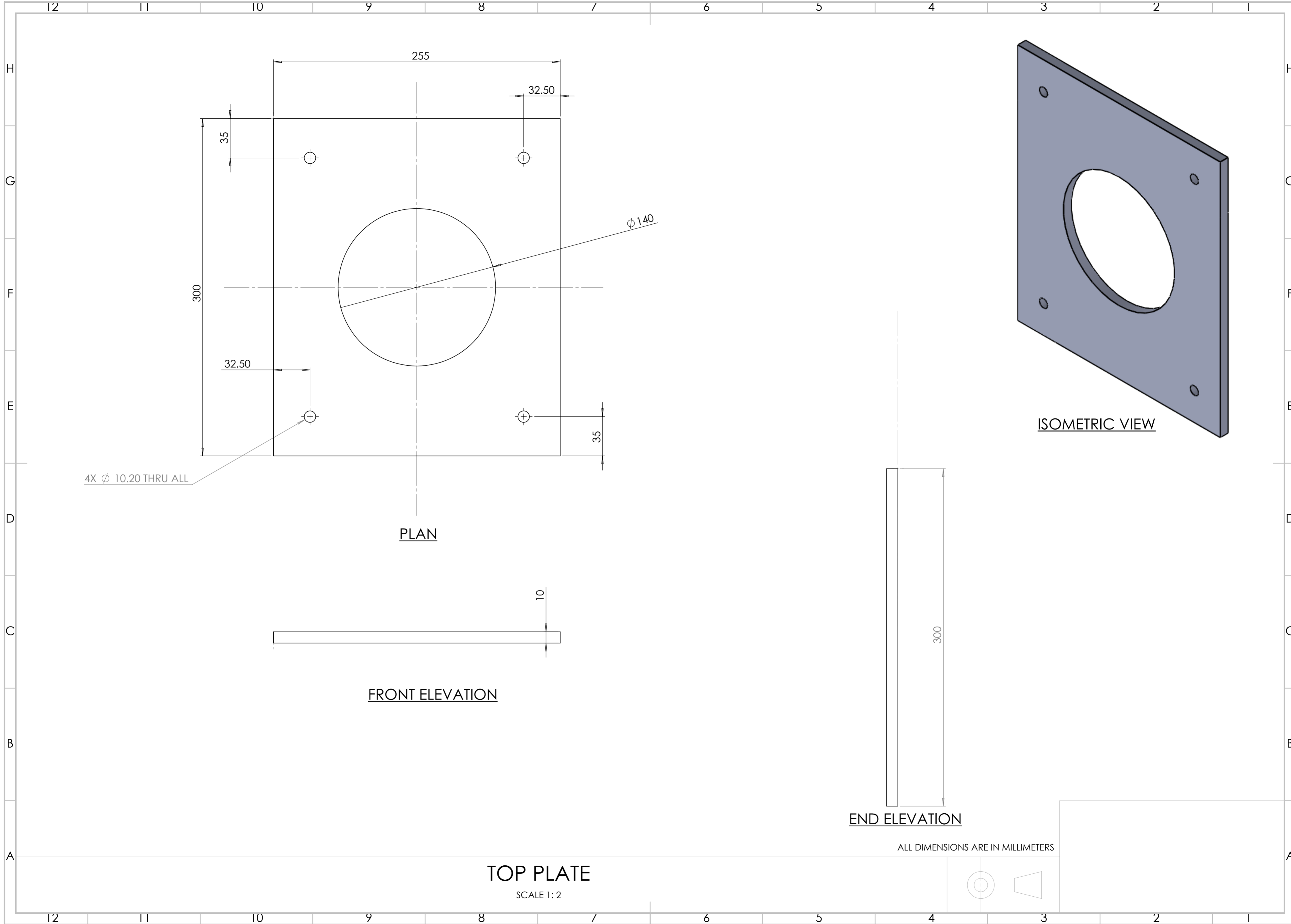
<b>Fiber direction of CFRP layer with respect to crack direction</b>	<b>Minimum J- integral (J min <math>\times 10^{-3}</math>)</b>	<b>Maximum J- integral (J max <math>\times 10^{-3}</math>)</b>	<b>Cyclic J-integral (<math>\Delta J</math>) <math>\times 10^{-2}</math></b>	<b>Number of cycles for crack initiation</b>
0	4.87	6.61	9.57	3124
30	4.79	6.53	9.51	3133
45	4.65	6.37	9.40	3151
60	4.45	6.13	9.23	3178
90	4.21	5.84	9.02	3213

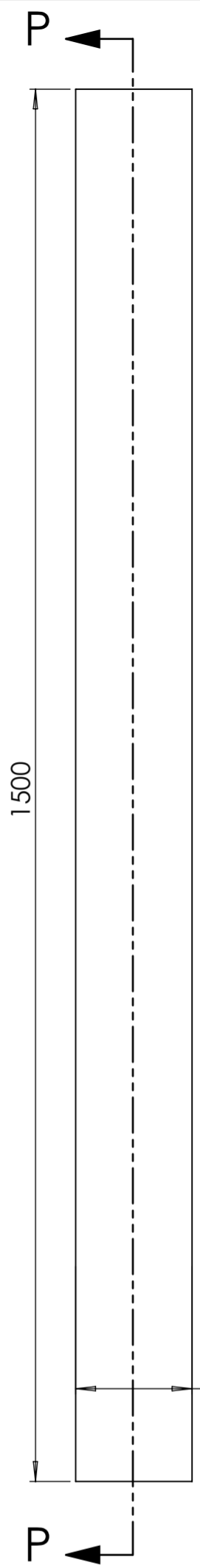
Table 6.13: Number of cycles for crack initiation with respect to the diameter to bond length ratio

<b>Diameter to bond length ratio</b>	<b>Minimum J integral (J min<math>\times 10^{-3}</math>)</b>	<b>Maximum J integral (J max<math>\times 10^{-3}</math>)</b>	<b>Cyclic J-integral (<math>\Delta J</math>) <math>\times 10^{-2}</math></b>	<b>Number of cycles for crack initiation</b>
0.40	2.78	5.18	8.13	3377
0.20	2.84	3.62	7.39	3534
0.13	2.7	2.99	6.97	3633
0.09	2.3	2.88	6.68	3709
0.08	2.18	2.69	6.49	3760

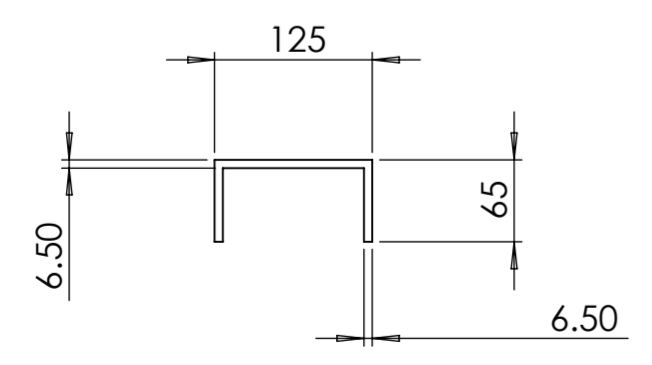
## ***Appendix-C***

---

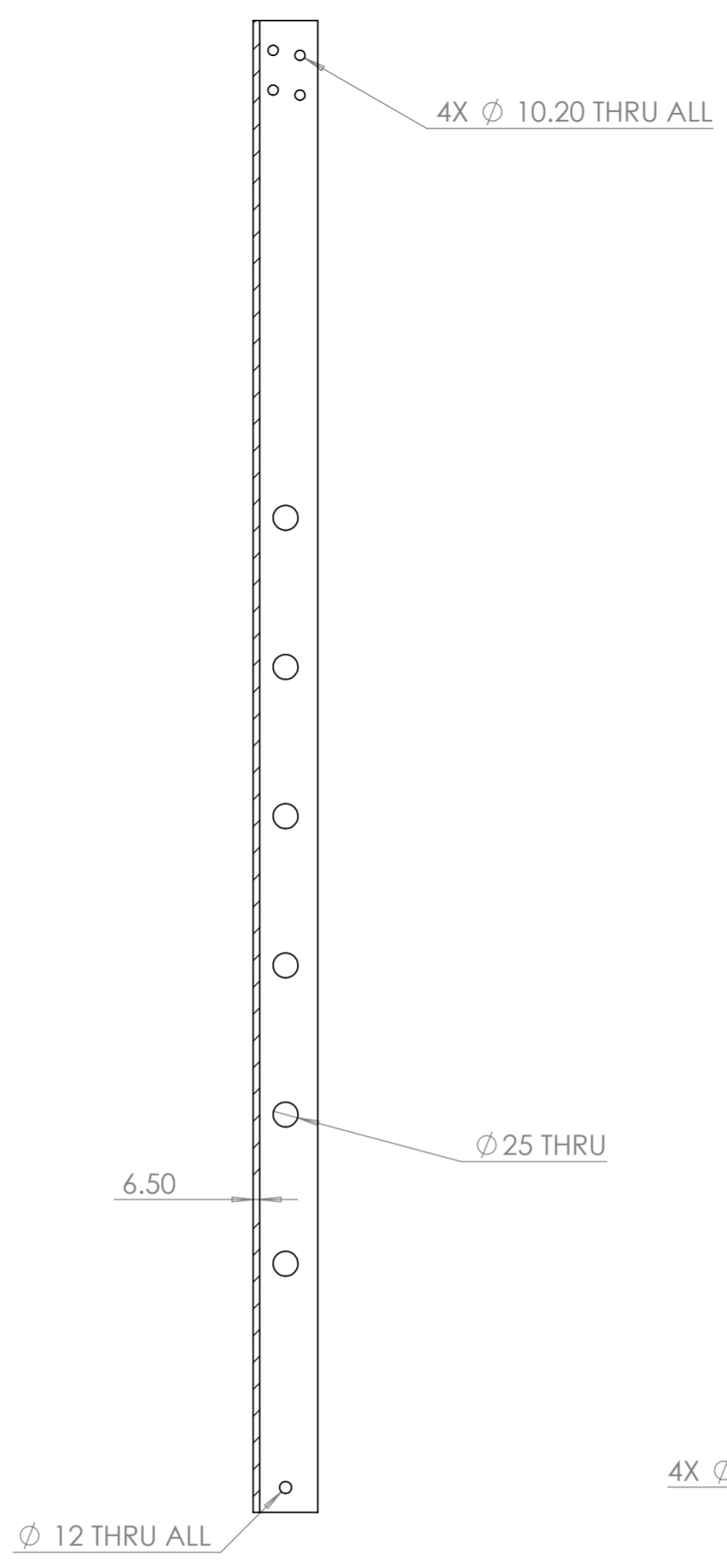




PLAN

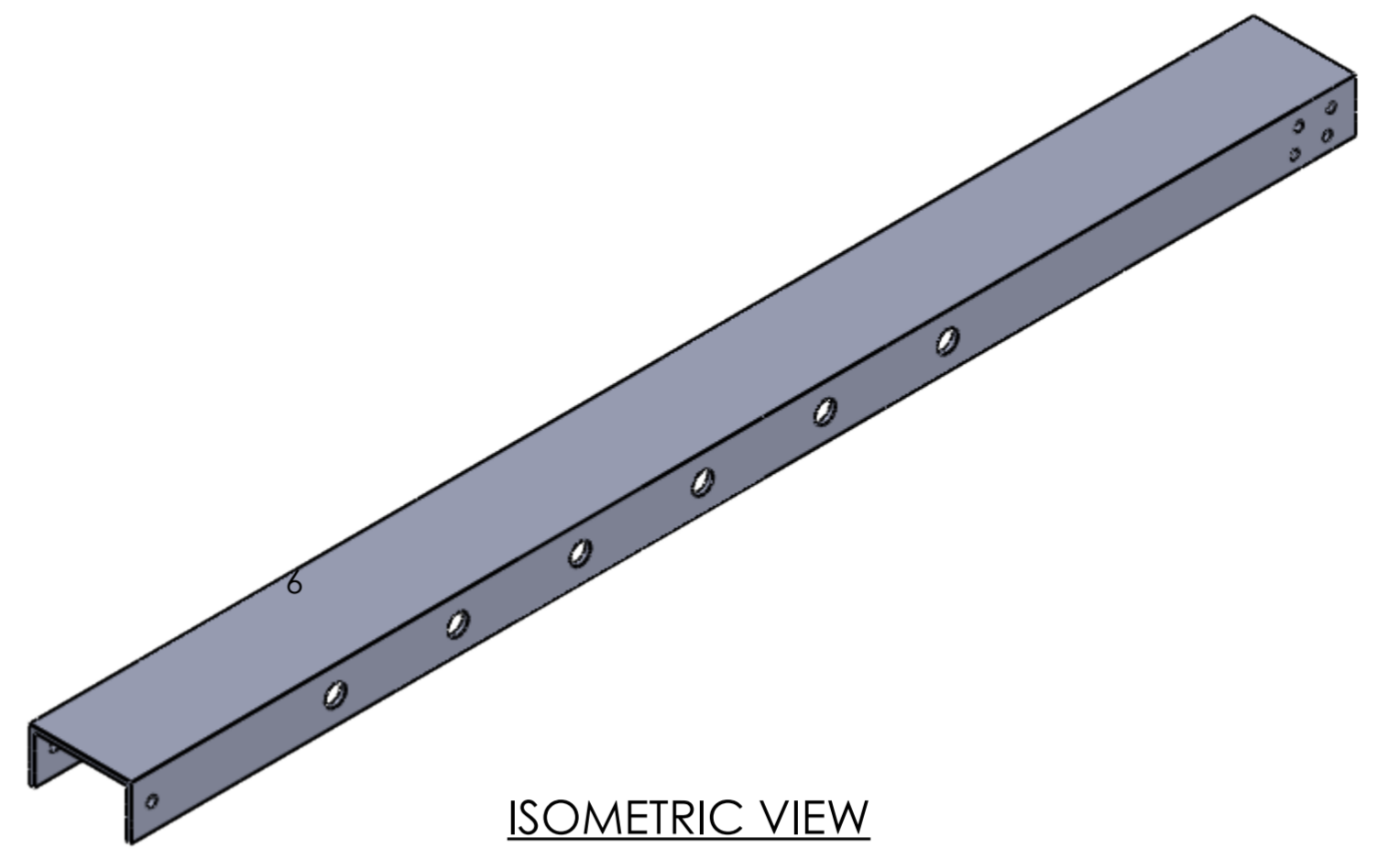


FRONT ELEVATION

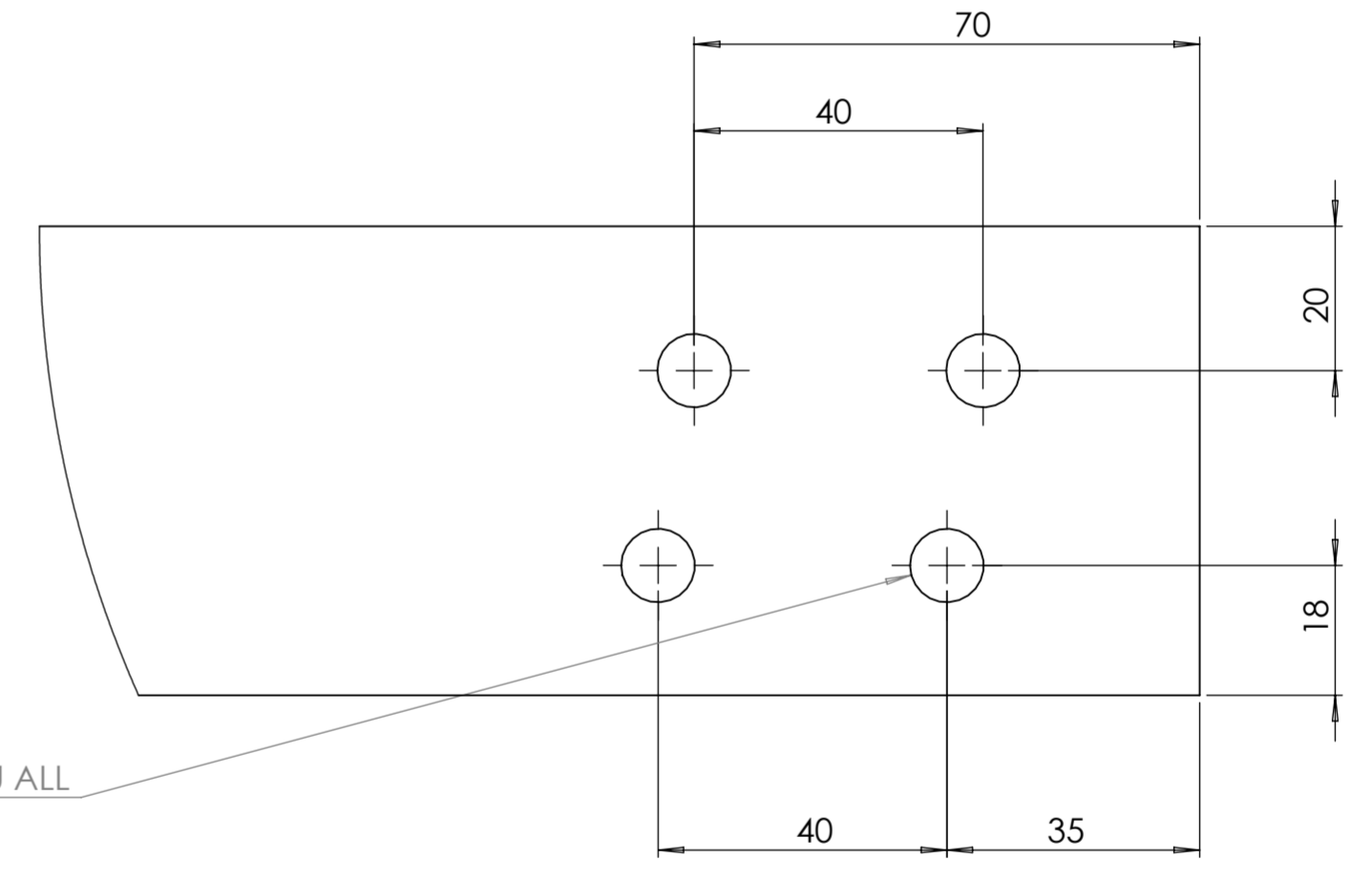


SECTION P-P

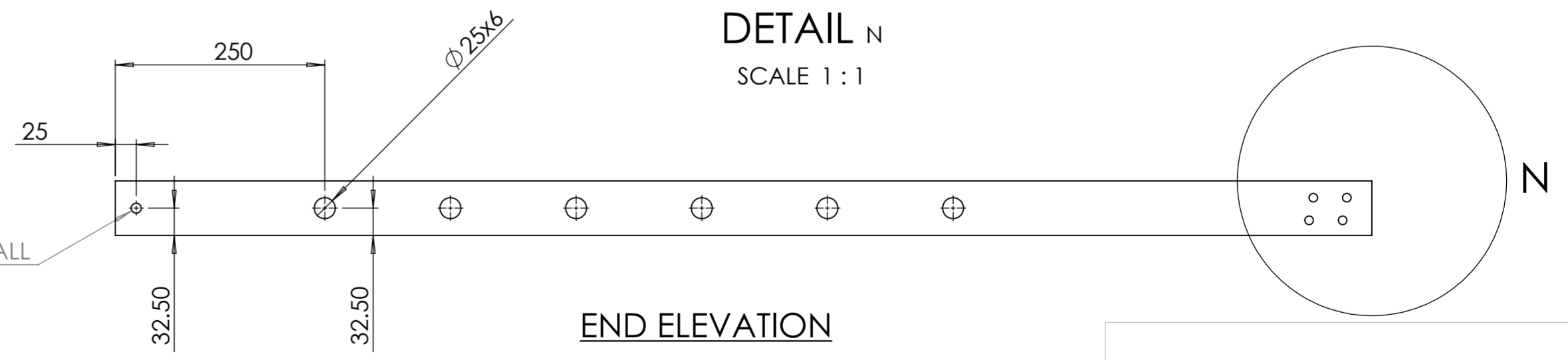
VERTICAL C CHANNEL  
SCALE 1:6



ISOMETRIC VIEW

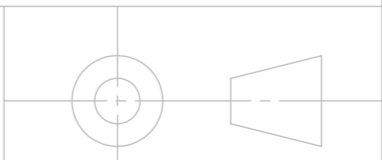


DETAIL N  
SCALE 1:1

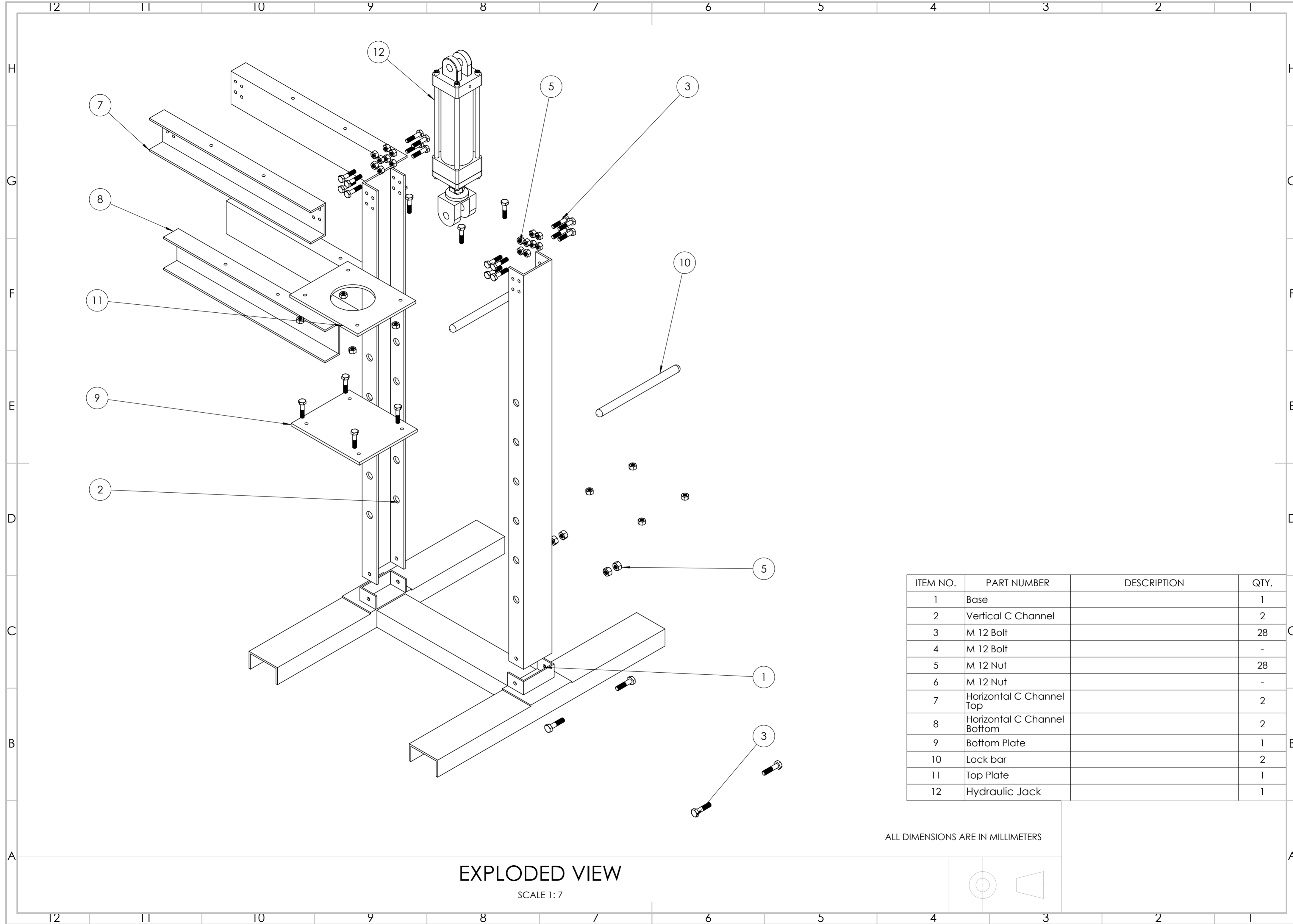


END ELEVATION

ALL DIMENSIONS ARE IN MILLIMETERS



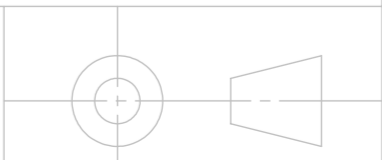


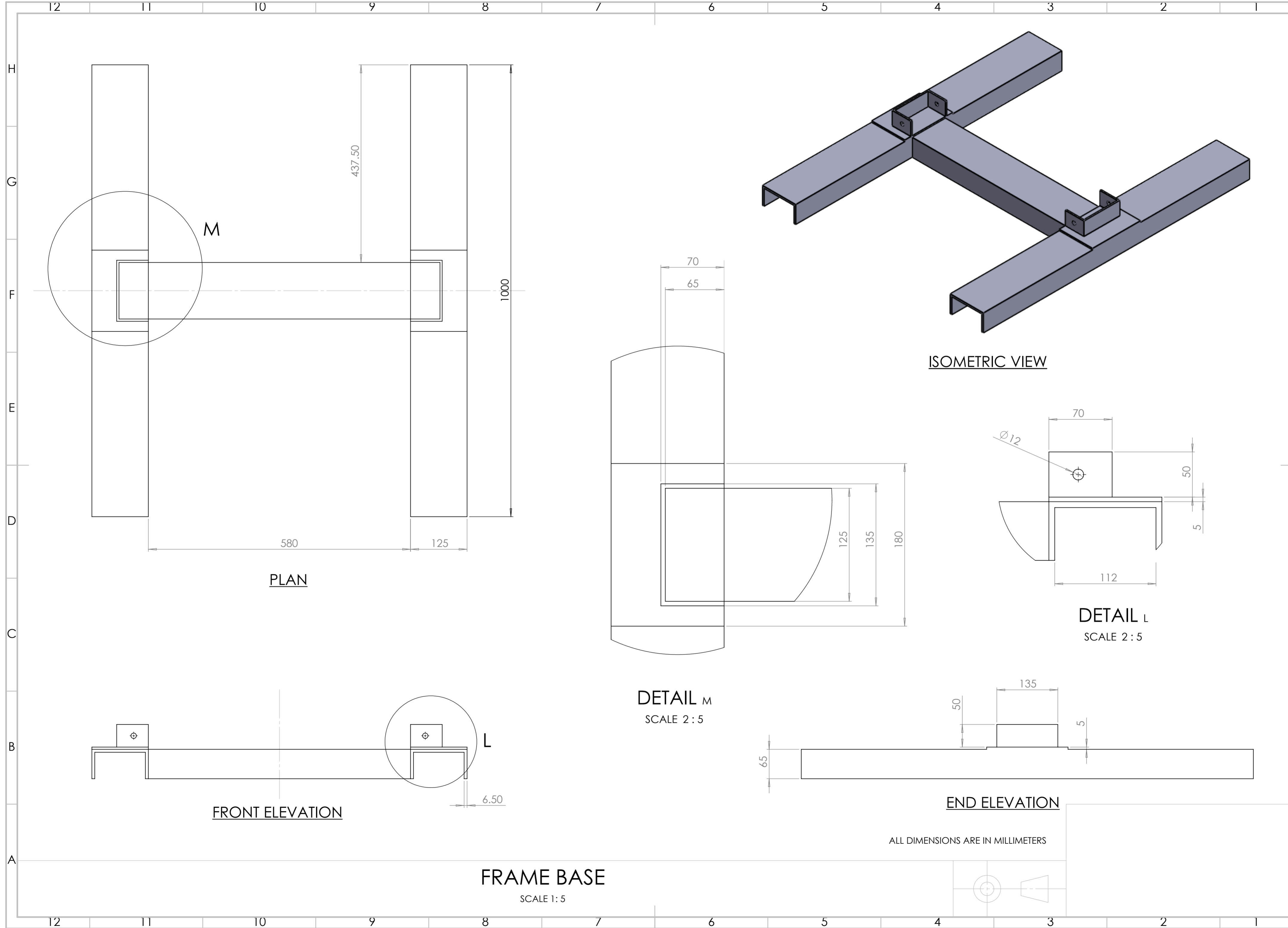


ITEM NO.	PART NUMBER	DESCRIPTION	QTY.
1	Base		1
2	Vertical C Channel		2
3	M 12 Bolt		28
4	M 12 Bolt		-
5	M 12 Nut		28
6	M 12 Nut		-
7	Horizontal C Channel Top		2
8	Horizontal C Channel Bottom		2
9	Bottom Plate		1
10	Lock bar		2
11	Top Plate		1
12	Hydraulic Jack		1

ALL DIMENSIONS ARE IN MILLIMETERS

EXPLODED VIEW  
SCALE 1:7





PLAN

ISOMETRIC VIEW

DETAIL M  
SCALE 2 : 5

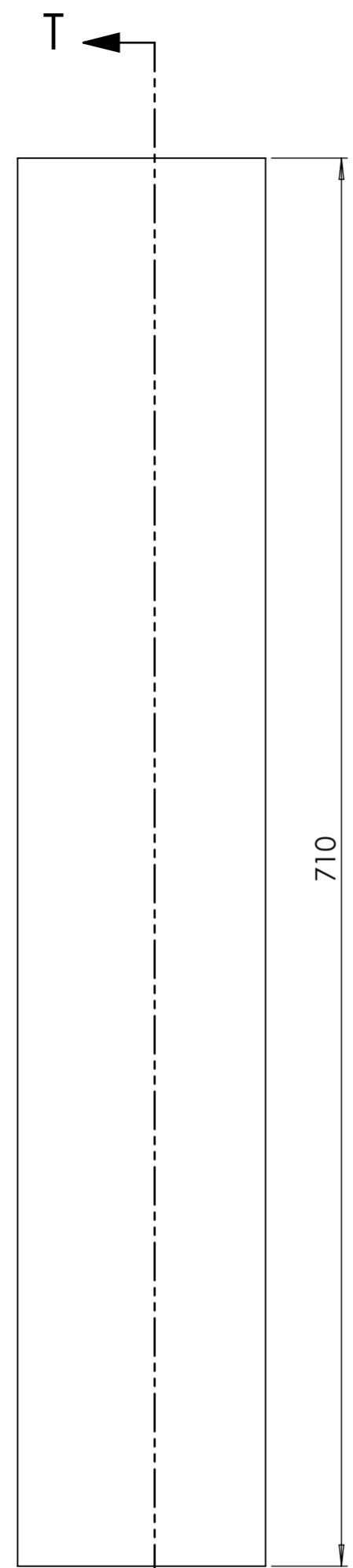
DETAIL L  
SCALE 2 : 5

FRONT ELEVATION

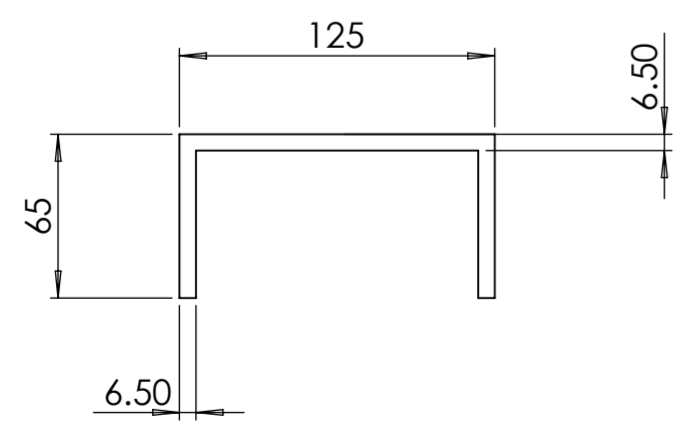
END ELEVATION

FRAME BASE  
SCALE 1 : 5

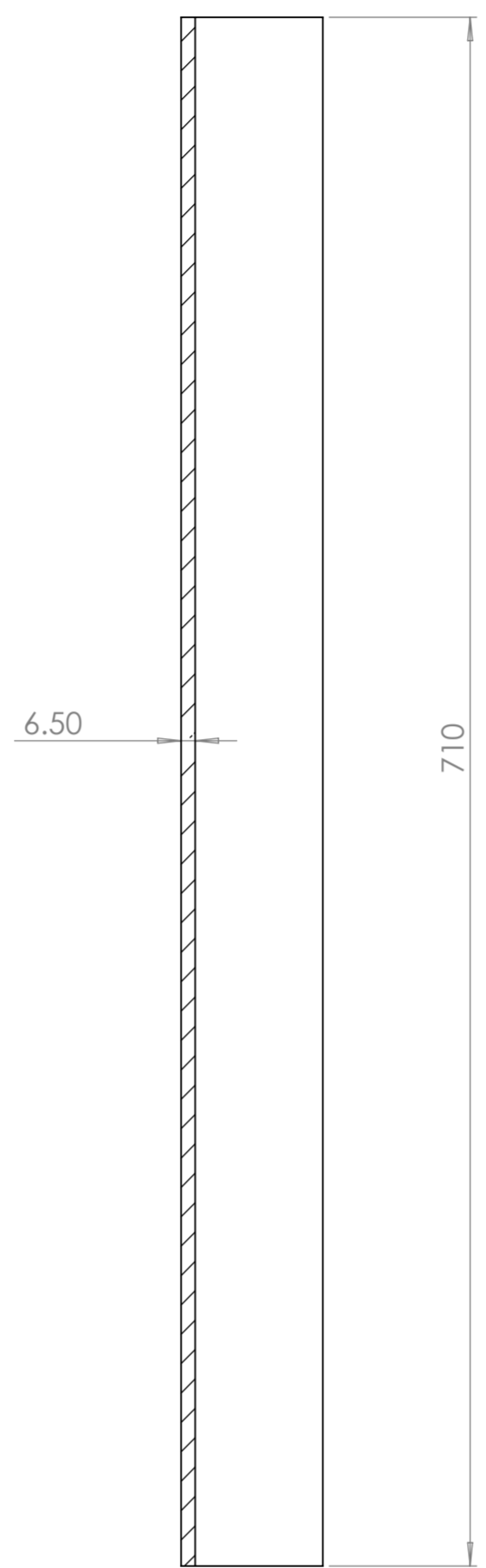
ALL DIMENSIONS ARE IN MILLIMETERS



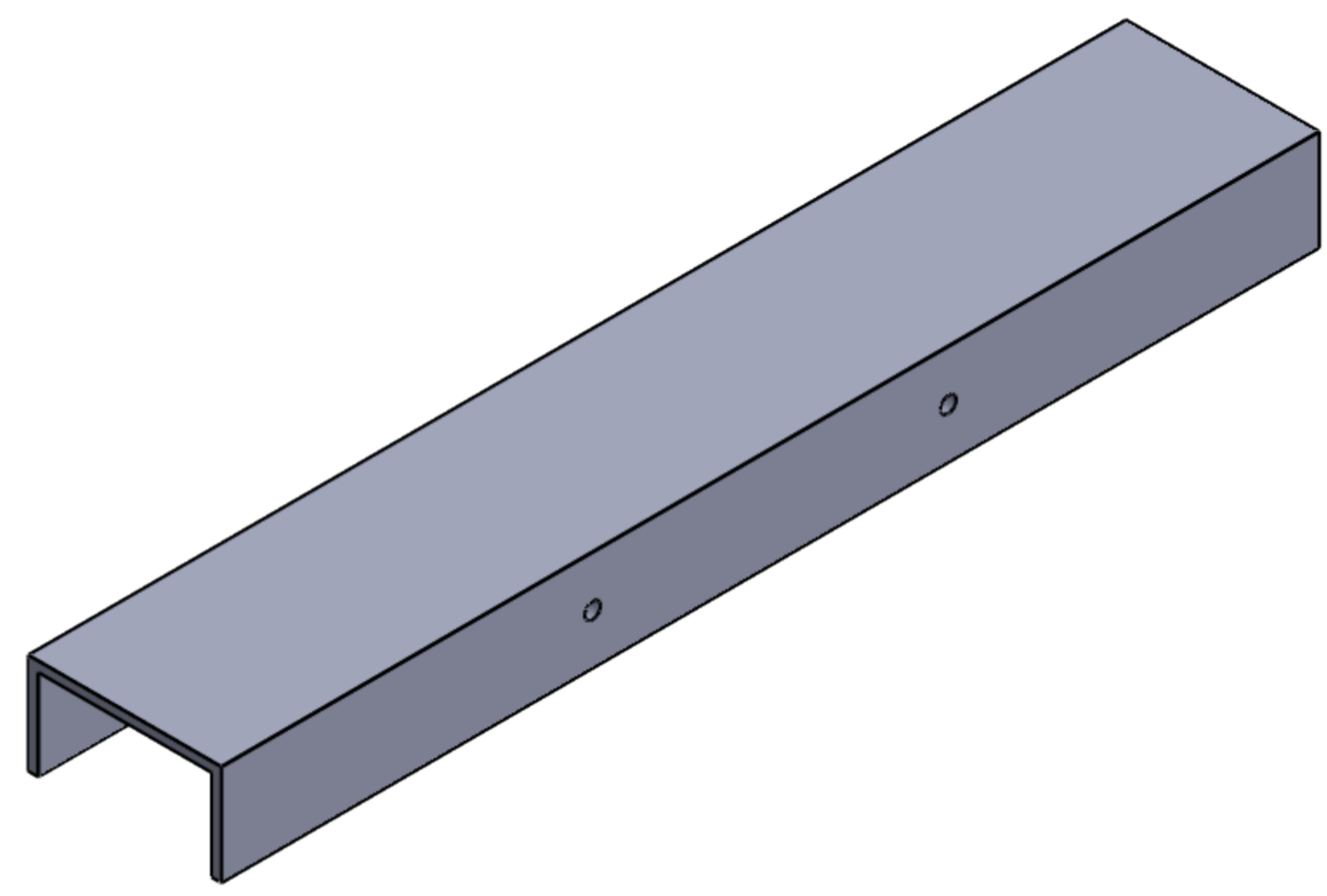
PLAN



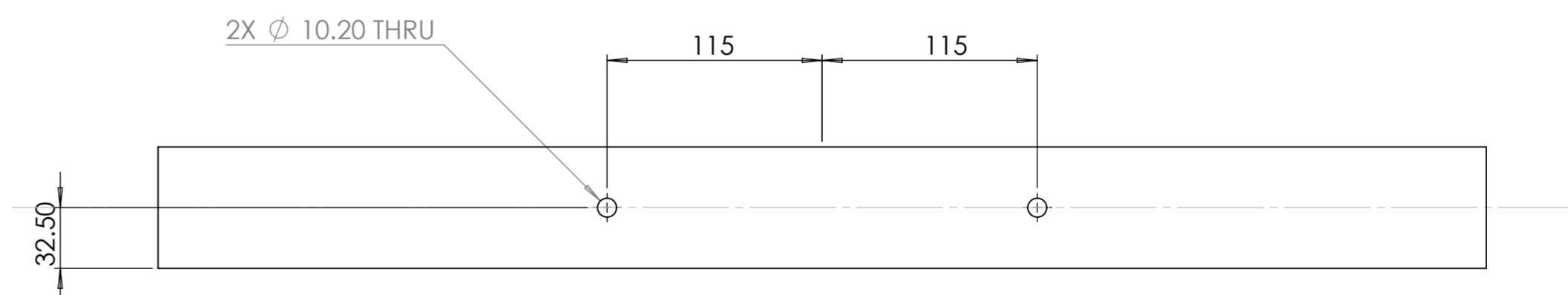
FRONT ELEVATION



SECTION T-T



ISOMETRIC VIEW

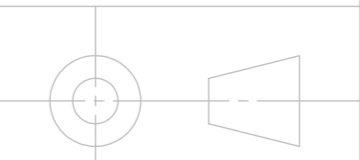


END ELEVATION

ALL DIMENSIONS ARE IN MILLIMETERS

HORIZONTAL C CHANNEL

SCALE 1:3



## ***Appendix-D***

---

# Investigating the Effects of Offset Distance in CSH on Steel Plates Under Three-Point Flexural Cyclic Loads in the LCF Range



S. Abeygunasekera, J. C. P. H. Gamage, and S. Fawzia

**Abstract** This paper aims to investigate the effects of offset distance of crack stop hole (CSH) on steel plate with respect to its loading point. Laboratory tests and finite element simulations were performed to estimate the effect of offset distance from the midpoint of the specimens. The experimental study was performed in segments of rectangular plate stresses with a cyclic flexural load which applied through a mid-plane of the top surface of the specimen. 5 Hz frequency and 2 kN constant amplitude fatigue test were performed in the low cycle fatigue (LCF) range up to 10,000 cycles. Also, crack stop holes of 16 mm diameter were placed at the different offset distance from midpoint up to 100 mm in the range of 20 mm, and their effectiveness in Yield strength was evaluated by using laboratory test and test results were validated using a cyclic J-integral option using the ABAQUS FEM technique. The results of laboratory test as well as numerical analysis were synonymous. The offset distance of the CSH indicated a significant variation in the yield strength which in the range of 26.5–56.8% compared to the CSH at midpoint. This investigation reported a significant yield strength variation in the range of 19.3–42.1% with respect to CSH placed at mid-point of the specimen.

**Keywords** Location of CSH · Yield strength · 3-point flexural cyclic load · LCF · J-integral

## 1 Introduction

A considerable amount of research studies in the past decade highlighted the capability of delaying crack initiation by any CSH technique. However, this technique could be considered as a temporary solution and there are limitations due to the geometric constrain and the location of the crack tip. The reason is, in some cases it is impossible to drill a hole with a desired diameter as obtained from designed, due

---

S. Abeygunasekera (✉) · J. C. P. H. Gamage  
University of Moratuwa, Katubedda, Moratuwa, Sri Lanka

S. Fawzia  
Queensland University of Technology, Brisbane, Australia

to the limited space in a structural member. In such situations, may be placed as an undersized CSH as a temporary solution. However, results of such an approach lead to a re-initiation of a crack (Re-cracking) from the CSH after few loading cycles. Therefore, the CSH technique is fully effective only if the diameter of the hole satisfies design requirements. However, if an appropriate CSH is placed on a particular crack tip, it would reduce cross section of the structural member.

The usual practice is attaching additional plates to the cracked member, using a welding technique. However, it was observed that in most cases cracks were re-initiated from the edges of these attached plates. Furthermore, the CSH tightened with bolts and insert pinned or mandrel is another method of controlling the re-cracking process due to continuous service loads on structural members. However, such methods are not a solution for strength losses due to discontinuity of material. CSH strengthened with CFRP material is a good alternative to overcome both issues at the same time. The aim of this work is to investigate the performance of a re-cracking of CSH with respect to offset distance from the loading point.

A limited number of research investigations related to CSH are available in literature. Lin et al. [8] explained regarding the externally bonded CFRP strips greatly reduced strain concentration of the drilled hole. Also, experimental studies conducted by Fisher et al. [6] discussed a repair technique-i.e. drilling a crack stop hole (CSH) ahead of a crack tip while authors emphasized the effectiveness of this technique to control the crack growth. The theory behind the placed CSH at the crack tip is to convert the sharp crack into a blunt notch. The size of the CSH to be drilled is governed by applying loads and material property. However, the success of this technique depends on a large number of parameters such as the length of the crack, location of CSH, type of the loads and loading frequency etc. Furthermore, Nakamura et al. showed a CFRP patching technique is an excellent first-aid technique for prolonging the fatigue life [11]. According to investigations of Miller et al. [10] Carbon Fiber Reinforced Polymer have been successfully used to replace such steel plates due to their excellent material characteristic such as light weight and better fatigue performance [10]. The combined effect of drilling holes and adhesive patches CFRP techniques should be developed as a new technique. Interestingly, the crack repairing guidelines were introduced by Indian railways manual for Indian railway bridges in 1998. The authors recommended a 7 mm diameter CSH place ahead of crack tip and welding a plate over the crack is a permanent solution to retard the crack growth. Fisher et al. [9] conducted a series of fatigue tests on steel plates strengthen by using CFRP strips. The results showed that the fatigue resistance of the joints was at least comparable with welded cover plates. Miller et al. [10] conducted two different research programs and no de-bonding was reported and the retrofit was then regarded to have good fatigue performance. Liu et al. [7] conducted a series of fatigue tests using high and medium modulus CFRP strips bonded steel plates. After the fatigue loading, tensile tests were performed to evaluate the residual bond strength capacity. The influence of the fatigue loading on bond strength was marginal and bond slip stiffness reduction was reported. Furthermore, interfacial de-bonding was observed for medium modulus CFRP and fiber breakage reported for high modulus CFRP. Similarly, Deng et al. [5] conducted an experimental program on small-scale

steel beams strengthened with CFRP strips. They reported that bonded joints crack nucleates and grows firstly in mode-I [5]. Also, Moy studied the effect of cyclic loading on epoxy curing and test results indicated a progressive stiffness, increase of the CFRP strengthen specimen as the epoxy cured. Interestingly, beams subject to higher loads during curing did not fully develop the adhesive bond. Similarly, Zhang et al. [14] beam specimens were exposed to loads varying between an upper and a lower limit throughout the curing period. Bocciarelli et al. [4] conducted fatigue tests on strengthened steel plates using CFRP strips at different loading conditions and authors recorded the stiffness degradation of the CFRP strengthened member.

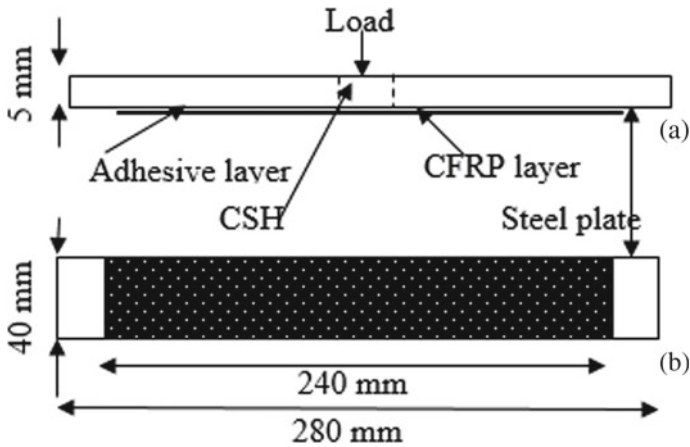
However existing literature has not reported sufficient data on the repair effect achieved by combined crack stop holes with externally bonded CFRP strips [8]. For example, it has been proven that in comparison with drilled holes, the fatigue strength was greatly increased when using both drilled holes and CFRP strips on small coupon specimens of flat steel plate [13]. Therefore, in this study, the effect of repair using both drilled holes and externally bonded CFRP strips is examined experimentally using a CSH rectangular plates.

## 2 Specimen Preparation and Material

### 2.1 Overview

The specimens were designed according to the guidelines of ASTM D 790 standards [3]. The steel plates with a cross-section 40 mm (width) and 5 mm (thickness) were used for sample preparation. Also, the length of the plate member was chosen as 280 mm and the effective span was considered 240 mm. A total of twenty-four rectangular cross sectionals flat steel plates were prepared for this study. The schematic diagram of each test specimens bonded with CFRP is shown in Fig. 1.

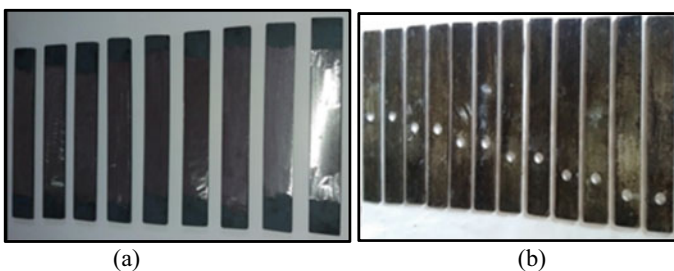
Prior the application of the CFRP, surface preparation of the steel plate is very important to ensure effective load transfer between steel plate and the CFRP sheet. Therefore, surface preparation could be considered as the main factor when influencing bond performance; failure mechanism and the durability of the CFRP strengthening method. Various types of surface preparation techniques could be identified for pre-treatments of metallic materials. According to an investigation conducted by Baldan such techniques could be classified as chemical, mechanical, electrochemical, and thermal process [1]. The theory behind surface preparation of steel is the enhancement of the formation of chemical bonds between the metal surface and the epoxy adhesive. Therefore, when selecting a treatment method, the chemically active surface should be confirmed before the CFRP laminates while the surface should be free of any kind of contamination. In addition, the process of cleaning supports to remove weak layers, degreasing, re-cleaning and escape oil or other potential contaminants from the metal surfaces. However, the selected surface preparation technique should have the facility for practical applications and



**Fig. 1** Schematic diagram of CSH: **a** Side view, **b** plan view

should also be environmentally safe. The most effective way for surface preparation is recommended to be grit blasting [12]. However, the grit blasting method is not available at University of Moratuwa laboratories. Therefore, an angle grinder was used for surface preparation of samples and resulted surface is shown in Fig. 2a. Dust particles were removed using an acetone. The primer consist of two parts (base and the primer) which was mixed into weight ratios. A thin layer of primer coat was applied on the cleaned steel surface according to the manufacturer's guidelines as shown in Fig. 2b and the samples were kept for about an hour before bonding applications.

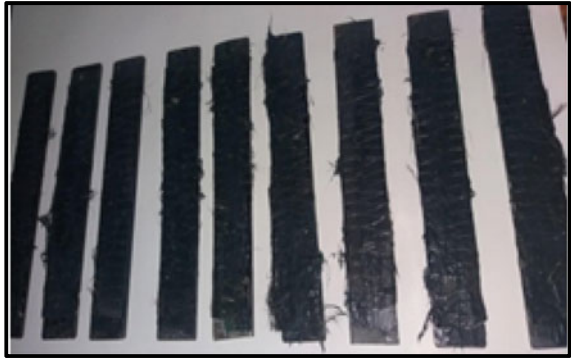
Normal modulus MBrace CF130 and Arelidite 420 epoxy were selected in this strengthening process. A two-part epoxy adhesive (Araldite 420) was properly dosed with 1:2 ratios by volume and mixed until a homogeneous light gray paste was obtained. This paste was applied to the pre-treated steel surface during its pot life according to the manufacturer guidelines. Then a thin layer of adhesive was uniformly applied on top of the primed steel surfaces.



**Fig. 2** Specimen preparation for laboratory test: **a** Grinded steel surface, **b** Primer coated steel surface



**Fig. 3** The CFRP strengthened specimen



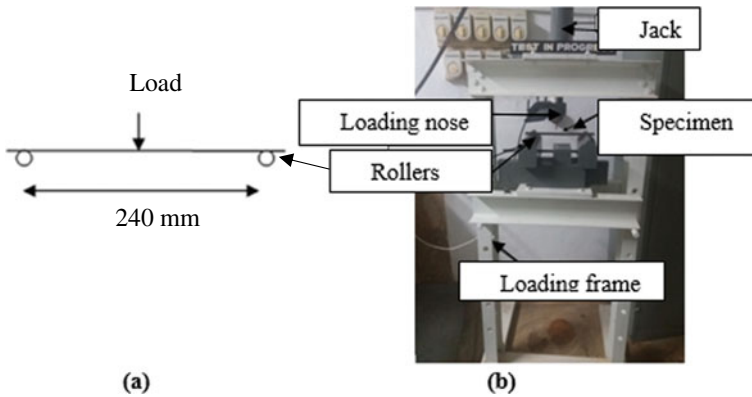
A fibre layer of CFRP fabrics (Mbrace CF 130) were cut to the explained dimensions ( $200\text{ mm} \times 40\text{ mm}$ ) and it was placed on top of the adhesive layer. The test specimens are shown in Fig. 3. The excess epoxy and air bubbles were removed using a ribbed roller moving in the direction of fibres. Finally, samples were kept for 72 h according to manufacturer provided guidelines.

### 3 The Experimental Program

The experimental program was performed at the structural testing Laboratory of the Department of Civil Engineering of the University of Moratuwa. The aim of the testing activity was to investigate the cyclic flexural behaviour of the adhesive bond offset CSH with CFRP under LCF. This test setup included two consecutive testing steps called the flexural test and axial tensile test for the same specimen. Firstly, a cyclic flexural load was applied on the specimen, then the tensile test was performed for each specimen.

#### 3.1 Flexural Test Setup

The three-point cyclic flexural tests were conducted using a self-developed 10-kN electro-hydraulic cyclic flexural testing apparatus (see Fig. 4). The testing apparatus has the capability to control load and frequency. Specimens were kept on two cylindrical shaped, supportive rollers with 25 mm diameter each and the span length was fixed at 240 mm between centers of the rollers as shown in Fig. 4a. Each specimen was loaded up to a 10,000 cycle range of low cycle fatigue (LCF) using the developed 3-point cyclic flexural loading apparatus by actuating a spring return hydraulic actuator. The 3-point flexural cyclic load was applied on the specimen at the mid-plane using a loading nose with 8 mm radius as shown in Fig. 4b. The maximum



**Fig. 4** Cyclic flexural load testing machine: **a** Schematic view, **b** Test setup and instrumentation

deflection in the load direction (Y-direction) at mid-plane was limited to 5 mm. The magnitude of the load and frequency were selected according to the ASTM D7774 standards. A constant amplitude 2 kN load was applied and during the testing period 5 Hz frequency was maintained. The number of cycles counted by using the digital display unit attached with an electro controller and load variation were monitored by using a load cell fixed at the midpoint of the bottom surface of the specimen.

### 3.2 Tensile Test Setup

After applying the 10,000 load cycles, the sample was removed from the cyclic load testing apparatus and it was attached to the tensile testing machine as shown in Fig. 5. Tensile loads were applied on specimen with 2 mm/min rate of load and measured yield value of each specimen. This procedure was repeated for each specimen within the limits of LCF. Average value of the yield load was recorded for similar specimens too.

## 4 Test Results

This tests series focus on estimating the average yield strength variation due to cyclic flexural effects on the offset of the CSH. Twenty four specimens were tested with control specimens as shown in Figs. 2b and 3. The yield load, crack initiation, number of cycles and failure mode were monitored during and after testing. The mechanical behaviour of the material is reflected by the yield strength of the material. The average yield strength due to the offset distance is compared with the CFRP strengthened CSH which is shown in Table 1.

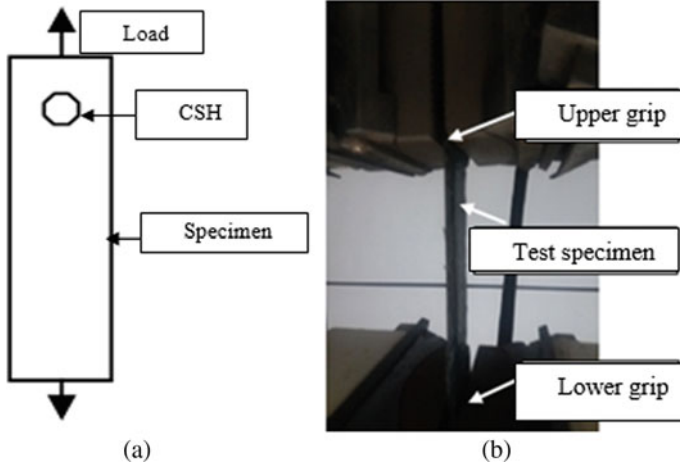


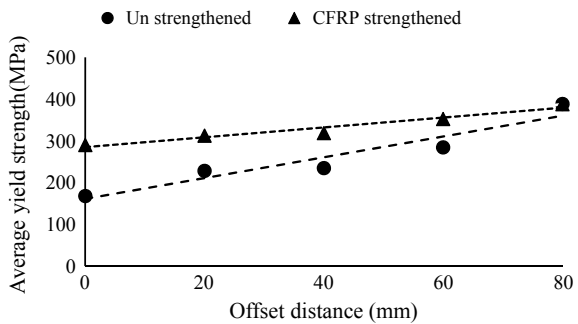
Fig. 5 Axial tensile load testing machine: a Schematic view, b Test setup and instrumentation

Table 1 Comparison of yield strength variation of unstrengthened and CFRP strengthened CSH

Offset distance (mm)	Number of specimens	Yield strength (MPa)		Strength gain by CFRP (%)
		Un strengthen CSH	CFRP strengthen CSH	
0	2	167.8	290.0	42.1
20	2	228.3	312.5	26.9
40	2	234.8	318.5	26.3
60	2	284.5	352.5	19.3
80	2	388.5	388.0	Insignificant

The comparisons of the CFRP strengthened and un-strengthened CSH shown in the Fig. 6. The common behaviour of both graphs is linear with a slightly different gradient.

Fig. 6 Comparison of strength gains for CFRP strengthened and un-strengthened offset CSH



### 5 Finite Element Model

Finite element (FE) models were developed using the commercially available finite element package ABAQUS version 6.14. The models were with the same configurations of the tested plates as given in Fig. 7. The direct cyclic mode under LCF analysis method was used to determine the response of the specimens. Also, the steel plate was modeled as an elastic–plastic metal with isotropic hardening. The Young’s modulus and possions ratio were considered as 200 GPa and 0.3 respectively J-integral value of the composite were adopted in FE model to represent the material behaviour.

Each specimen module was loaded with an LCF mode using the direct cyclic option. A 8 mm radius loading nose was used for loads applied and the mid-vertical span was limited to 5 mm. Furthermore, a fatigue load was applied to the specimens at the mid-plane with 5 Hz frequency as shown in Fig. 7. The static general loading method was applied from 0 to 0.02 s and the direct cyclic loading method was applied from 0.02 to 0.2 s. Then, while maintaining the fatigue load under the 2 kN constant amplitude with 5 Hz frequency. The numerical models were run several times until the best validation was achieved. Also, the required number of cycles for crack initiation ( $N_i$ ) was obtained by using the results of analytical methods and the development of the Power law equation.

In this numerical analysis location of CSH were changed from 0 to 80 mm, and according to the results of the numerical analysis the minimum and maximum J-integral values were obtained. The maximum and minimum values of J integral were taken from data file of the analysis results. The cyclic J-integral value is calculated according to Eq. 1[2]. By using the Power law in Eq. 2 the required number of cycles of re cracking at the CSH is obtained [2]. The result of the CSH offsets from the center of major axis as shown in Table 2. It summarizes the maximum and minimum J-integral values together with the variation of different location from the analytical results.

$$\Delta J = J_{\min} + J_{\max} - \sqrt{J_{\min} + J_{\max}} \tag{1}$$

$$\frac{da}{dN} = 9.85 \times 10^{-4} (\Delta J)^{0.479} \tag{2}$$

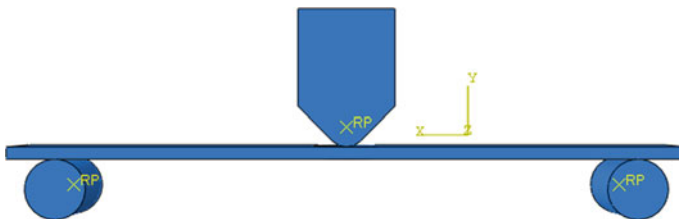


Fig. 7 The geometry for the specimen for FE model

**Table 2** Properties of material

Material	Testing standards	Tensile strength (MPa)	Elastic modulus (MPa)	Poisson's ratio
Steel	ASTM A 370-02	583	200	0.3
Araldite -420	ASTM D638-02(a)	29	0.977	0.3
CFRP	ASTM D3039/D3039M	1575	175	0.3

In this analysis, offset distance of the CSH was considered as a main variable. It was changed from 20 to 80 mm and numerical modeled under the cyclic flexural loads. All other parameters except the distance of CSH with respect to the midpoint of the specimen were kept as constant during the analysis. Diameter of 16 mm CSH was placed at the relevant offset distance as explained above. The 3D model visualization of un-strengthened and CFRP strengthened is shown in Fig. 8a and b respectively.

### 5.1 Element Types and Mesh Density

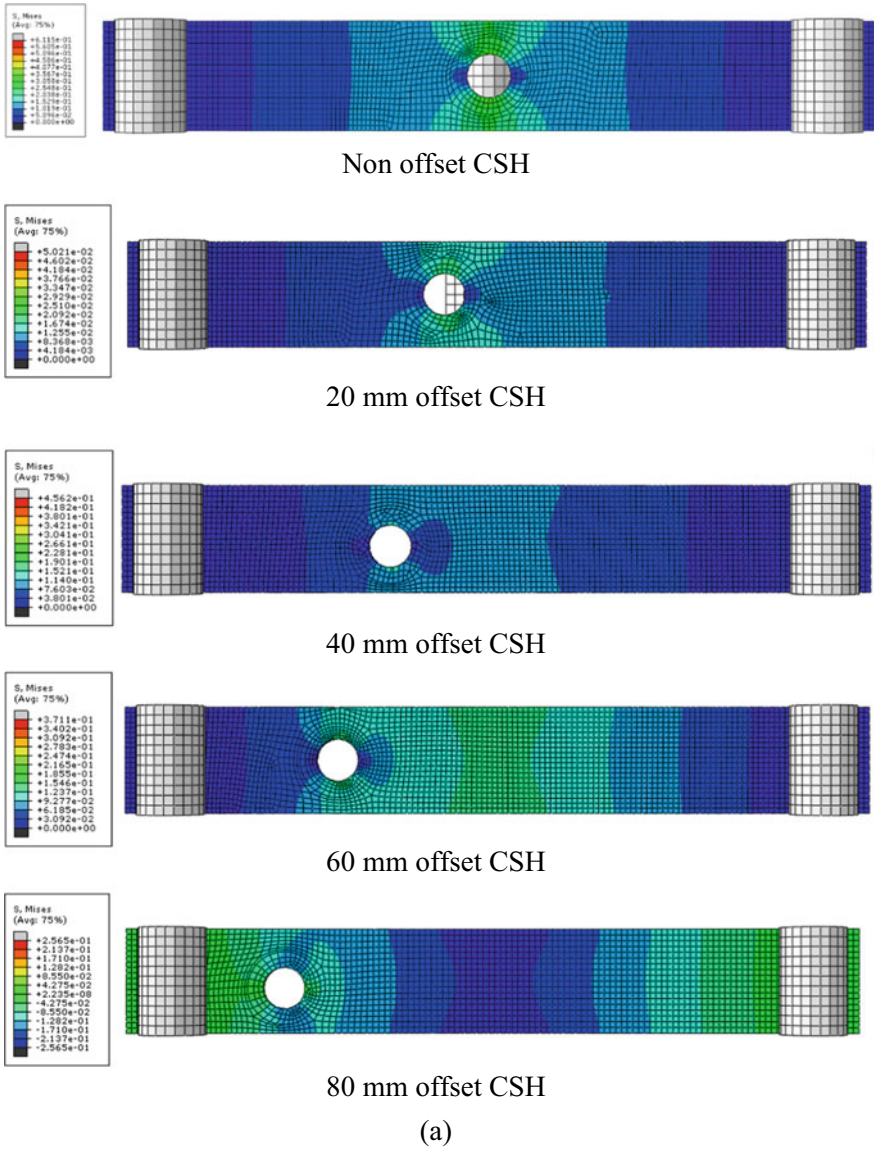
Different types of elements are available in the finite element package, ABAQUS 6.14 software. The steel plates are modeled using 8-node 3-D solid element (C3D8H), as the three dimensional thick solid geometry leads to improve accuracy in resolving contact problems. Also, the computational time was reduced by introducing 2 mm mesh for the steel plate.

### 5.2 Material Properties in FE Analysis

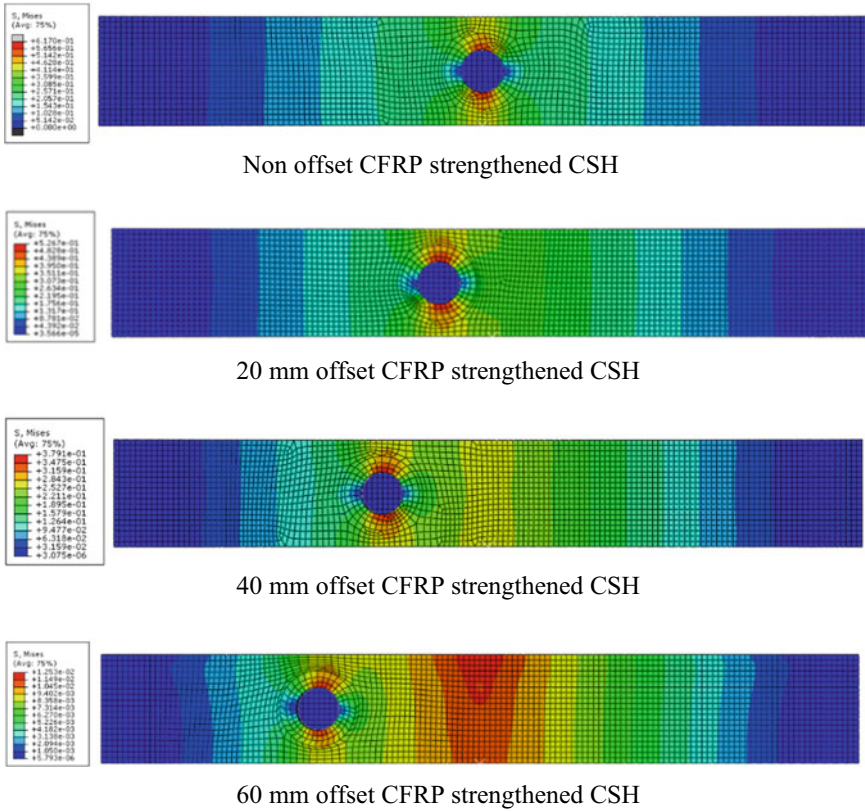
The tensile strength and the modulus of elasticity of steel are taken from the experimental data. The steel plates had an average yield strength of 583 MPa, and the modulus of elasticity was 200 GP were reported by a coupon test. Possion's ratio value was assumed as a 0.3. The properties of three materials are listed in Table 2.

### 5.3 Result of FE Modeling

In this numerical analysis the location of the CSH was considered as a main variable and it varied from 0 to 80 mm respectively at the loading point. The cyclic loads were applied at the midpoint when all other parameters were kept at a constant level except the location of the CSH. Numerically modeled results have exhibited influences of



**Fig. 8** Visualization of the bottom view under 3 points cyclic flexural load with different offset distance: **a** un-strengthened CSH, **b** CFRP strengthened CSH



(b)

Fig. 8 (continued)

the location of the CSH with respect to the loading point. The results are tabulated in Table 3.

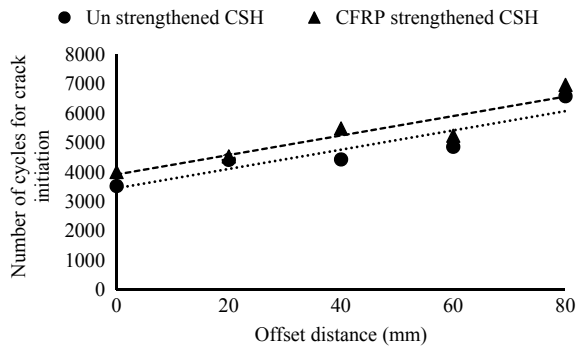
Figure 9 shows required number of cycle variation of each test series with the CSH diameter due to the effects on 3 points flexural cyclic loads with 2 kN constant amplitude load. As shown in Fig. 9, when the offset distance is increased, the number of cycles also increases in both test series. For a given load and frequency, the best-fit curves could be characterized by similar slopes.

In this numerical analysis, the location of the CSH was considered as a main variable and it varied from 0 to 100 mm respectively at the loading point. The cyclic loads were applied at the midpoint when all other parameters were kept as un-strengthened and CFRP strengthened CSH. Numerically, the modeled results agreed well with the laboratory test results with respect to the location of the CSH. The FEM results are tabulated in Table 4.

**Table 3** Cyclic J-Integrals and number of cycles for crack initiation

Offset distance from mid-point (mm)	Cyclic J integral value $\times 10^{-2}$		No. of cycles for crack initiation	
	Un strengthened	CFRP strengthened	Un strengthened	CFRP strengthened
0	5.67	7.39	4011	3534
20	4.62	4.37	4423	4542
40	4.58	2.94	4440	5490
60	3.78	3.23	4868	5246
80	2.01	1.78	6589	6972

**Fig. 9** No of cycles for crack initiation variation with offset distance



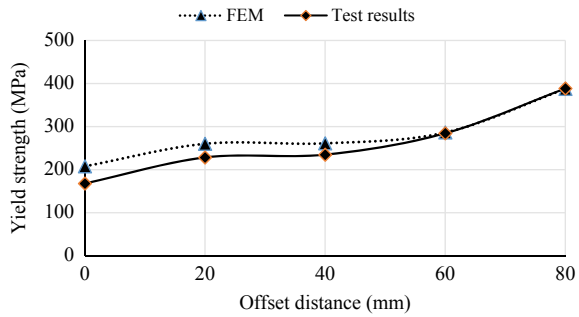
**Table 4** Yield strength variation with offset distance according to numerical modelling results

Offset distance from mid point (mm)	Non-strengthened CSH		CFRP strengthened CSH	
	Yield load (kN)	Yield strength (Yield load $\times$ cross section) (MPa)	Yield load (kN)	Yield strength (Yield load $\times$ cross section)(MPa)
0	41.6	207.9	47.2	235.9
20	52.0	260.2	53.4	267.2
40	52.2	261.2	64.6	322.9
60	57.3	286.4	61.7	308.6
80	77.5	387.6	82.0	410.1

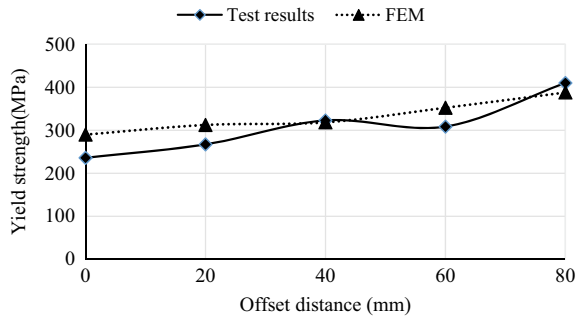
When offset distance is increased the Yield strength also increases as shown in Fig. 10. Reason for such behaviour is the stress concentration effect at the CSH location. On the other hand, when the offset distance of CSH increase, residual stresses and notch stress also decreases. The net effect is the increase of the yield strength. FEM results agreed well with the laboratory test results as shown in Fig. 10.



**Fig. 10** Comparison of FEM and laboratory test results for un-strengthened CSH



**Fig. 11** Comparison of FEM and laboratory test results for CFRP strengthened CSH



When offset distance is increased the yield strength also increases as shown in Fig. 11. The reason for such behaviour is the stress concentration effect at the CSH location. On the other hand, the CFRP material added additional tensile strength and it contributes to re-distribute stress at the CSH. As a result, the overall yield strength increased when compared to non-strengthened CSH. The FEM results agreed well with the laboratory test results as shown in Fig. 11.

## 6 Discussion

The main purpose of this investigation was to estimate the re-cracking behaviour and yield strength variation of CSH by variation of offset distance. CSH under cyclic loading stress concentration zones are usually exposed to crack initiation. In the present case, the fatigue sensitive zone is surrounded by the CSH. Re-cracking starts at these stress concentration zones depending on the relevant stress level. However, the 3-point flexural cyclic load helps to increase the stresses at the CSH. The effect of yield stress was significant losses and it is mainly governed by the distance of the CSH, as cyclic effects convert hardening properties of material to soften. Furthermore, residual stress also significantly contributes to stress, which occurs due to the drilling and other mechanical process done on the CSH. However, magnitude of loads,

**Fig. 12** Failure mode of offset hole



loading frequency; rate of loads and material properties of the parent metal also significantly effects on the results. The tendency of crack initiation is higher at the bottom surface rather than the upper side of the specimen. When offset distance increase with respect to loading point, the stress concentration reduces. As a results average yield load increases. The offset CSH strengthened with CFRP supports to reduce the stress concentration and enhances the tensile strength of the CSH specimen.

### ***6.1 Mode of Failure and Crack Patterns***

Since these specimens were prepared by using steel plates, the crack failure occurred at both side of the CSH and was perpendicular to the tensile direction which is the weakest part of the specimen. The cyclic flexural cracks started near the CSH and it appeared at the perpendicular direction of the tensile load as shown in Fig. 12. The failure mode was observed as an interface de-lamination and de-bonding of the CFRP strengthened CSH. Consequently, cyclic load causes to weaken any bond between the metal and the adhesive as well as the adhesive and CFRP sheets.

## **7 Conclusions**

In this study, the flexural behaviour of steel fibre-reinforced CSH under cyclic loading was investigated. From the test results, the following conclusions were obtained:

- (1) The fatigue resistivity of CSH with offset distance from midpoint was significantly enhanced with respect to the mid-point, even after the 3 point flexural cyclic loads.

- (2) This study recorded yield load increase due to the effects of off-set distance; in the range of 26.5% to 56.8% compared to the CSH at the midpoint.
- (3) The yield capacity enhancement of the offset CSH by CFRP material was in the range of 19.3–42.1% with respect to un strengthened CSH.
- (4) The result of the FE model agreed well with the laboratory test results in case of un-strengthened as well as CFRP strengthened CSH.

### Future Work

Further work should be performed in order to provide a larger data set of cyclic loads and then to provide a more accurate estimation of the yield strength gained by the CSH. Moreover, a parametric study should be conducted in order to investigate their effect on the overall performance while the effects of the CFRP strengthened should be compared with the results of this investigation.

**Acknowledgements** The authors would like to thank, University of Moratuwa (UOM) for providing support to carry out the work reported in this paper. The authors gratefully acknowledge the staff in the structural engineering and IT laboratory of the Department of Civil Engineering at the University of Moratuwa for their support in carrying out this investigation.

### References

1. Baldan A (2004) Adhesively-bonded joints and repairs in metallic alloys, polymers and composite materials: adhesives, adhesion theories and surface pretreatment. *J Mater Sci* 39:1–49
2. Abeygunasekera S, Gamage JCPH, Fawzia S (2019) Theoretical approach to evaluate the rate of crack growth in crack stop holes using j-integral technique. ICSEM, Kandy, Sri Lanka
3. ASTM D790–10, Standard test methods for flexural properties of unreinforced and reinforced plastics and electrical insulating materials. (2011). D20 10, Ed, ASTM International, West Conshohocken, PA
4. Bocciarelli M, Colombi P, Fava G, Poggi C (2009) Fatigue performance of tensile steel members strengthened with CFRP plates. *Compos Struct* 87(4):334–343
5. Deng J, Lee MMK, Moy SSJ (2004) Stress analysis of steel beams reinforced with a bonded CFRP plate. *Compos Struct* 65:205–215
6. Fisher JW, Barthelemy BM, Mertz DR, Edinger JA (1980) Fatigue behavior of full-scale welded bridge attachments (NCHRP Report 227). Transportation Research Board, Washington, DC
7. Liu HB, Zhao XL, Al-Mahaidi R (2005) The effect of fatigue loading on bond strength of CFRP bonded steel plate joints. International Institute for FRP in Construction (BBFS)
8. Lin F, Sun JG, Nakamura H, Maeda K (2012) Fatigue crack repair using drilled holes and externally bonded CFRP strips. In: *Bridge maintenance, safety, management, resilience and sustainability*, Taylor & Francis, London
9. Matta F (2003) Bond between steel and CFRP laminates for rehabilitation of metallic bridges. University of Padua, Padua, Ph.D Thesi
10. Miller CT, Chajes MJ, Mertz DR, Hastings JN (2001) *ASCE J Bridge Eng* 6(6, November-December):514–522
11. Nakamura H, Jiang W, Suzuki H, Maeda K, Irube T (2009) Experimental study on repair of fatigue cracks at welded web gus-set joint using CFRP strips. *Thin-Walled Struct* 47(10):1059–1068

12. Schnerch D, Dawood MR (2006) Proposed design guidelines for strengthening of steel bridges with FRP materials. *J Constr Build Mater* 21:1001–1110
13. Suzuki H, Okamoto Y (2003) Repair of steel members with a fatigue crack using the carbon fiber reinforced polymer strip. *J Constr Steel, JSSC* 11:465–472 (in Japanese)
14. Zhang Z, Liu Y, Huang Y, Liu L, Bao J (2002) The effect of carbon-fiber surface properties on the electron-beam curing of epoxy-resin composites. *Compos Sci Technol*



# Numerical Modelling of Re-cracking Behaviour in Retrofitted Crack Stop Holes in Steel Structures

S. Abeygunasekera<sup>1</sup>(✉), J. C. P. H. Gamage<sup>1</sup>, and S. Fawzia<sup>2</sup>

<sup>1</sup> University of Moratuwa, Katubedda, Moratuwa, Sri Lanka  
abeygunasekarasampath@gmail.com

<sup>2</sup> Queensland University of Technology, Brisbane, Australia

**Abstract.** This paper focuses on the delaying of crack initiation process in a crack stop hole (CSH) in steel structures. The cyclic J-Integral ( $\Delta J$ ) numerical model was adopted to develop this study. Also, the Power law was applied to estimate the required number of cycles for crack initiation at the crack stop hole with the effects of carbon fiber reinforced polymer (CFRP) strengthening CSH improvement techniques. CFRP strengthened CSH indicated a significant improvement in the CSH. This retrofitting technique reported an optimal performance; in the range between 17.7% and 163.6% delay in required cycles for the crack initiation when compared to an un-strengthened CSH.

## 1 Introduction

Crack stop hole (CSH) technique is a widespread method in the steel industry as a crack repairing method. In this method, a drilled hole is fabricated at the crack tips to crack transfer into a notch. The main purpose of the crack stop hole is the redistribution of the stresses which reduces stress concentrations at the crack tip. The result is delay in crack propagation and changes in the direction of crack propagation. The crack stop hole technique has been verified as enhancing the fatigue service life of a structure [1, 2]. This technique is a simple and non-expensive method [3]. As a result, this crack stop hole technique is widely applied in the maintenance of metallic structures [4]. This technique is especially used in the aerospace industry.

Due to the removal of material to prepare CSH, the load is redistributed throughout the structure. Hence, the stress is maximum at the edge of the crack stop hole. Therefore, the maximum stress concentration occurs around the CSH. Stress concentration in ductile materials is higher when compared with the yield strength of material. Such behaviour causes the redistribution and deformation of the local plastic stresses. However, stress intensity factor (SIF) could be considered as a good indicator representing the stress at the vicinity of the crack tip as it could be used to predict stress and fracture behaviour of the CSH. The simulation of the crack is important for predicting the fatigue life with different techniques which could be used for this purpose. Thus, the J-Integral technique could be considered as one of the best alternatives, as an extension of SIF.

The potential of fatigue damage occurring at the crack stop hole is maximum with respect to the remaining areas, since such a crack stop hole acts as a structural discontinuity. When the CSH is continuously subjected to cyclic loads, it results in the stress concentration increase near the CSH. Due to the increase in the stress concentration, crack initiation restarts from the CSH and this action is called a crack re-cracking on CSH. In fact, only a few numerical investigations are available in the literature to estimate delaying crack incubation and growth at the CSH. According to Tanaka and Mura (1981), the reason for crack initiation originates at the slip bands, without accounting for the effect of cyclic hardening of the material. Also, Bozek et al. (2008) suggested a probabilistic simulation technique to understand the re-cracking behaviour in members. Similarly, Fine and Bhat (2007); Mura and Nakasone (1990); Bobylev et al. (2010) and Xie et al. (2016) have emphasized the ability of delay in crack initiation due to energy barrier techniques.

## 2 Background

Computerized finite element analysis techniques are more popular due to the practical difficulties of laboratory testing. This study also utilized the J-integral technique in ABAQUS for analysis. The Paris law was used to estimate the rate of crack propagation at the CSH and its regression curve was fitted to obtain the power law approximation. In fact, the rate of crack growth could be estimated accurately by using the results of the power law approximation. When comparing the results of Paris law, the proposed power law approximation showed negligible differences (less than 3%). The Paris law behaviour was based on characteristic of material such as homogeneity, isotropy, and elasticity.

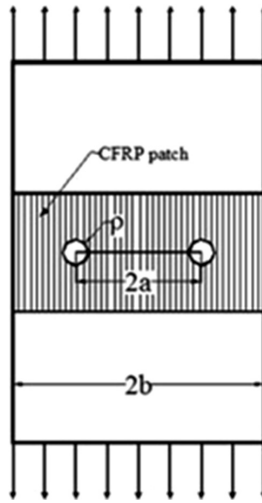
The main problem in CSH is the initiation of re-cracking at the tip of the hole. There are some techniques already applied in this field to understand the delay in this crack propagation. The main objective of this investigation is the analysis of the re-cracking behavior of CSH. In addition, the behaviour of retrofitted CSH was also explored in this context.

Carbon Fiber Reinforce (CFRP) materials show excellent fatigue resistance in strengthened steel structures. Furthermore, CFRP materials exhibit exceptional characteristics; few of them being lightweight, high strength, corrosion resistance, and ease of installation. Field applications also confirmed the usefulness of the CFRP related strengthened steel structures. Therefore, this investigation focuses on the numerical modelling of CFRP strengthened CSH as an alternative solution to delaying re-cracking in a CSH.

## 3 Methodology

In this method, a single layer of CFRP was attached to the CSH at the bottom surface of the member which is shown in Fig. 1. A tensile load was applied on the bottom surface of the member. Thus, the tendency of crack initiation is high at the bottom surface rather than the upper side of the specimen. Crack stop hole strengthened with CFRP

assist in reducing the stress at the edge of the hole. Thus, the dimensions of the CFRP layer were selected as 100 mm length and 40 mm width. Also, uni-directional CFRP material was selected which is commercially denoted as CF 130. Thickness of the CFRP layer was taken as 0.167 mm according to the data sheet provided by the manufacturer. Young's modulus and Poisons ratio of the material was taken as 240 GPa and 0.28 respectively. Interaction mode in the ABAQUS was utilized for modelling of the CFRP layer under vicinity of the crack stop hole in the structural member. Steel plates were considered as the master surface and the CFRP layer was considered as the slave surface.

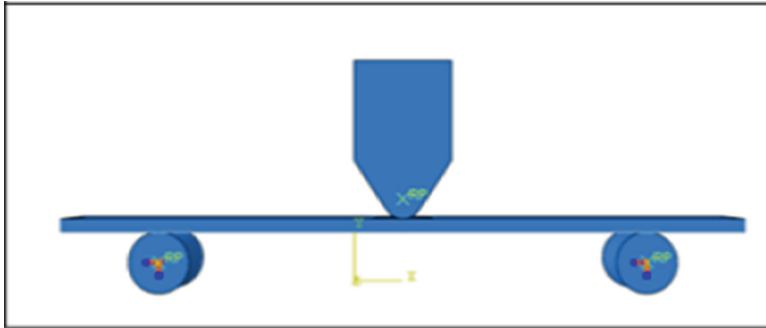


**Fig. 1.** Schematic view of the CFRP patched with CSH.

CFRP strengthened CSH specimens were kept on two cylindrical shaped, supportive rollers with each having a 25 mm diameter and the span length was fixed at 240 mm between centers of the rollers as shown in Fig. 2. The specimen module was loaded with a low cycle fatigue (LCF) mode using the direct cyclic option in ABAQUS. A Cyclic load was applied on the specimen at the mid-plane using the loading nose and 8 mm radius loading nose was used as shown in Fig. 2. The load was applied at the mid-plane of the specimen. The maximum deflection in the load direction (Y direction) at mid-plane was limited to 5 mm. The magnitude of the frequency was selected according to the ASTM D7774 standards [5]. A constant amplitude load was applied to the model while during the analysis, 5 Hz frequency and 0.05 stress ratio were maintained. Parametric study was conducted by varying the diameter of CSH and alternative bonding techniques of CFRP. The procedure followed is listed below:

1. The geometry of the model using the part modulus of ABAQUS was created.
2. A pre-defined crack profile using a partition cell extrude/sweep edges option of the part modulus was assigned.

3. The material properties, boundary conditions, interaction properties and loads for both the static general step and the cyclic step were utilized in this module. (Static general step for the applying step 1 load, direct cyclic step 2 for fatigue load)
4. Mesh of the model using CPE4R elements was utilized.
5. A special enrichment function called “seams” using contour integral, under interaction modulus were performed to this procedure.
6. The analysis was created and the results were taken from the data file of visualization modulus.



**Fig. 2.** 3D object with 240 mm span length under the 3 points cyclic flexure load

In this numerical analysis, the diameter of CSH varied from 8 mm to 24 mm. According to the model of the numerical analysis, the minimum and maximum J-integral values were obtained while the cyclic J-integral value was calculated according to Eq. 1. The required number of cycles for crack initiation was calculated by using the power law approximation.

## 4 Theory

### 4.1 Theory of Fracture Mechanics

At present, two main fracture mechanics approaches are used for predicting the fatigue life. They are the S-N curve approach method and fracture mechanics approach method. The fracture mechanics approach is utilized in this study where the concept of fracture mechanics was introduced by Leonardo da Vinci several centuries earlier [6]. Theory of fracture mechanics is based on the initiation and propagation of the cracks. Since, fracture mechanics are based on the mechanical behaviour of steel structures, the ultimate effect of the fracture is the catastrophic (Unrecoverable) failure of the structure. Therefore, understanding of fracture and its control is important in the real-world application to assure safety. The best way to estimate fatigue life is a prediction of crack initiation. Studies of Griffith (1921), Irwin(1957), and Rice (1968) have greatly contributed to develop the theory on fracture mechanics [7]. Similarly, Irwin in 1948



has extended the Griffith approach to metals [8]. This extension was utilized as energy dissipates due to local plastic flow. During the same period, Orowan [10] independently proposed similar modifications as the Griffith theory [9, 10]. In 1948 Mott extended the Griffith theory considering the rapid propagation of the crack [11]. In 1956, Irwin developed the concept of strain energy release rate [12]. This concept showed a direct relation with the Griffith's theory.

## 4.2 J-integral Technique

Dr. James Rice in 1968 introduced a path-independent contour integral analysis technique for crack analysis [13]. Rice explained the J-integral method with elastic-plastic fracture mechanics (EPFM). The cyclic  $J$ -integral ( $\Delta J$ -integral) could be considered as a crack tip parameter. The cyclic J-integral ( $\Delta J$ ) value can be obtained by using finite element analysis. The result of crack driving force is propagation of a short fatigue crack. In fact, the crack driving force can be alternatively named as a crack tip stress or as the strain energy release rate during the crack growth under elastic-plastic condition. Therefore, the J-integral technique could be viewed as an energy related parameter as well as a stress intensity parameter for non-linear materials. Hutchinson, Rice, and Rosengren have confirmed that the J-integral technique is unique for non-linear materials. Rice has confirmed the basis of EPFM methodology well beyond the validity limits of LEFM. The estimation of cyclic J-integral values from using minimum and maximum values of the J-integral could be explained as follows.

$$\Delta J = J_{\min} + J_{\max} - (J_{\min} + J_{\max})^{1/2} \quad (1)$$

Where  $\Delta J$  is the cyclic J-integral value,  $J_{\min}$  is the minimum value of the J-integral taken from FEA and  $J_{\max}$  is the maximum J-integral value available from the same analysis.

## 4.3 The Power Law

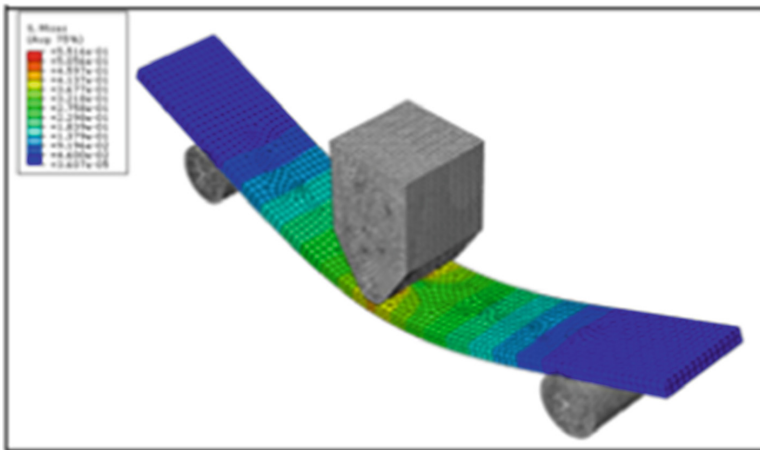
Prediction of crack growth is important for structural elements during their service life, as such predictions helps the estimation of the remaining service life of any structural element. In addition, such a prediction supports to estimate the inspection intervals of structures for maintenance. Therefore, accurate and reliable approximation is required to predict the behaviour of crack propagation in structures. On the other hand, the method of prediction should not be complicated. However, to satisfy all these conditions at the same time is not an easy task as, numerous variables significantly influence the process of crack initiation. The cyclic J-integral technique is based on the theory of fracture mechanics. Dowling and Begley [8] have proposed and implemented the J-integral technique considering the relations of crack growth rate ( $da/dN$ ), and cyclic J-integral ( $\Delta J$ ) [14]. The power law approximation is similar to the Paris law. The Power law and fatigue crack growth rate of structures exposed to cyclic loading can be calculated as follows:

$$da/dN = A(\Delta J)^n \quad (2)$$

In the Power law application, it is assumed that the cyclic J-integral ( $\Delta J$ ) includes the sum of elastic and fully plastic solutions. The rate of fatigue crack growth in the Power law depends on constants **A** and **n**. These two parameters are called the **Ramberg-Osgood coefficient and strain hardening index**, respectively. These constants specially represent the tensile data of materials. However, these two parameters do not depend on the geometry and it is based-on material properties. In this analysis, these power law constants, A and n were considered as 0.95 and 0.47 respectively, using the Paris law results approximation with the Power law. The cyclic J-integral values were obtained from numerical analysis.

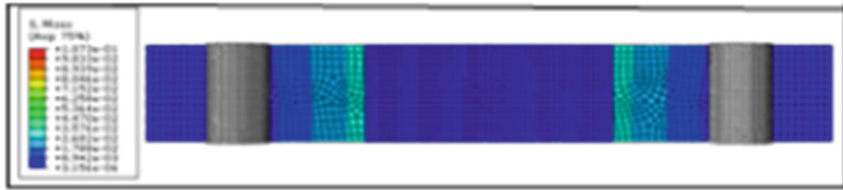
## 5 Model Results

In this study, CFRP strengthened and un-strengthened CSH were modelled to compare the results. All other parameters which critically affected crack behaviour was kept as a constant during the process of numerical analysis. The boundary conditions, properties of materials, loading rates, frequency, stress ratio and aspect ratio were kept as constants throughout the analysis (Fig. 3).



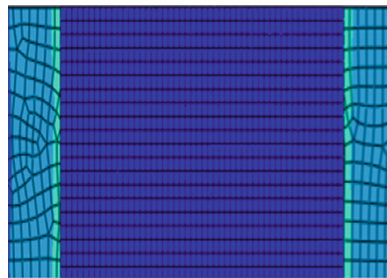
**Fig. 3.** Visualization of the 3D view under 3 - points flexural cyclic load with an adhesive CFRP strengthen CSH.

The stress concentration at CFRP strengthened CSH contours is shown in Fig. 4.



**Fig. 4.** Visualization of the bottom view under 3 - points flexural cyclic load with CFRP strengthened CSH.

When the three points cyclic flexural loads are applied on a CFRP strengthened crack stop hole, the change of stress distribution pattern is shown in Fig. 5. In this case, the stress variation around the CSH is not clearly visible as the elastic plastic zone is controlled by the CFRP layer. This is the main reason for the delay in crack initiation at the CSH compared to unstrengthened CSH.



**Fig. 5.** Stress distributions at CFRP strengthen CSH.

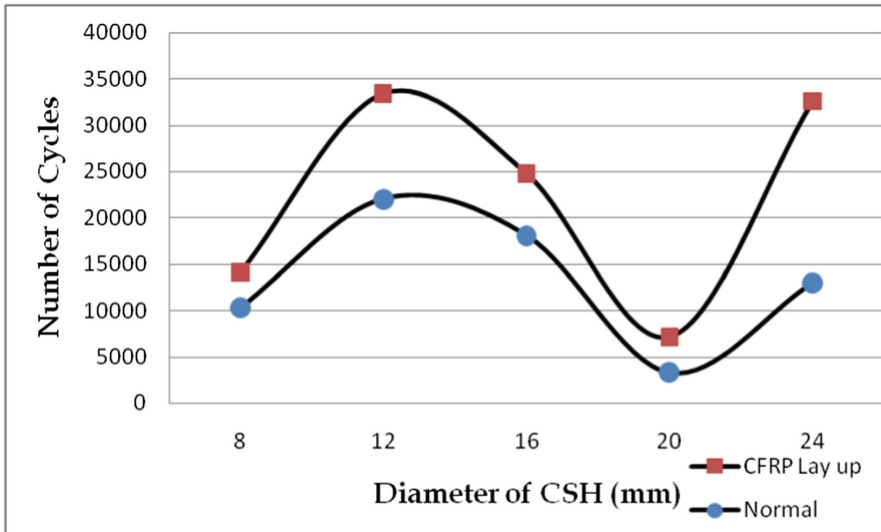
## 6 Results and Discussion

The analytical results of the CFRP strengthened CSH and un-strengthened CSH were compared as shown in Table 1. It summarizes the maximum and minimum J-integral values together with the variation of different CSH diameters from the range of 8 mm to 24 mm. Interestingly, the number of cycles for crack initiation varied with the hole size. The number of cycles for crack initiation compared with un-strengthened and CFRP layer attached CSH is shown in Fig. 6.

**Table 1.** J-integral values and cyclic J-integral of CFRP strengthened CSH.

Diameter of the CSH (mm)	$J_{Min}$	$J_{Max}$	Cyclic J integral ( $\Delta J$ )
8	1.44E-04	8.54E-04	0.0006473207
12	1.24E-04	1.40E-04	0.0001322426
16	1.71E-04	2.25E-04	0.0001998495
20	4.54E-03	8.90E-03	0.0070834286

The variation of the number of cycles for crack initiation with respect to the diameter of the CSH is shown in Fig. 6. The comparison of the un-strengthened CSH and the CFRP strengthened CSH are shown in the same graph. The common behavior of both graphs is sinusoidal wave patterns, which can be observed. According to the investigations conducted by Kormay and Disnig [15], Ack et al. (1988) it was confirmed that theoretical stress concentration factor for a plate with a hole under bending loads were a response to a sinusoidal stress pattern [8, 15]. When the diameter is changed from 8 mm to 24 mm it showed significant delaying of the crack initiation when compared to un-strengthened CSH.



**Fig. 6.** Comparison of number of cycles for crack initiation with un-strengthened and CFRP strengthened crack stop hole with a hole diameter.

According to this study, the CFRP material exhibited a significant crack initiation delay and its range in variation were recorded as 17.7% to 163.6% with respect to an untreated crack stop hole. This technique is performed with 8 mm to 24 mm range of the diameter of the CSH. However, up to medium size of the CSH diameter, significant improvements were exhibited with respect to the untreated crack stop hole (Table 2).

**Table 2.** Delaying of crack initiation due to CFRP strengthened

Diameter of CSH (mm)	Percentage of delaying crack initiation compare to un-strengthened CSH (%)
8	162.5
12	90.6
16	163.6
20	17.7
24	50.3

## 6.1 Discussion

CSH method shows a high potential in successfully delaying crack initiation at the crack stop hole. When the CFRP layer was attached to the bottom surface of the specimen, the effects of the tension load on bottom surface was controlled by the CFRP, since the tension plunge shows a high tendency of crack initiation rather than the compression surface (upper side) of the specimen. The CFRP laminate also helps to reduce the stresses at the edge of the CSH. Thus, a number of fiber layers, the module of CFRP material, lay-up angles and bond length could be considered as the main variables which affect the process of crack initiation.

Stress concentration at the CSH is the main reason for crack initiation and it is governed by the residual stress and notch stress. When the CSH diameter is small, the required number of cycles is less. The residual stress is high due to the mechanical stress on the process of manufacturing such as cold forming and rolling. When the hole diameter gradually increases in the notch, the stress decreases and the residual stress, increases due to the process of drilling. According to the net effects of both stresses, the required number of cycles for crack initiation increases as, a comparatively less stress concentration is shown at the CSH. When the hole size was further increased, the required number of cycles for crack initiation decreased again, because residual stress increases due to the drilling process. Net effects of both actions contribute to create high stress concentration at the CSH. When the hole diameter becomes larger, the required number of cycles for crack initiation had drastically increased. This is due to the reduction of notch stress when compared to the residual stress at the CSH. The bottom surface is retrofitted with CFRP and the required number of cycles for crack initiation was increased because the CFRP layer contributed to reduce the stress at the edge of the holes.

## 7 Conclusions

In this study, CSH was strengthened with externally bonded CFRP sheets which were numerically studied with the required number of cycles and crack initiation for CSH were estimated using J-integral technique. The following conclusions were obtained:

1. Stress concentration at the crack stop hole edges effectively decreased with the CFRP material.
2. The plastic zone of the vicinity of crack stop hole edges can be reduced by the externally bonded CFRP sheets.
3. This retrofitting technique reported the performance; which is in the range of a 17.7% to 163.6% delay in crack initiation compared to the un-strengthened CSH with the diameters changed from 8 mm to 16 mm.

**Acknowledgments.** The authors gratefully acknowledge the support of the staff in computer laboratory, the Department of Civil Engineering at the University of Moratuwa for their valuable support.

## References

1. Wu H, Imad A, Benseddiq N, Castro JTPD, Meggiolaro MA (2010) On the prediction of the residual fatigue life of cracked structures repaired by the stop-hole method. *Int J Fatigue* 32 (4):670–677
2. Crain JS, Smmons GG, Bennett CR, Barrettgonzalez R, Matamoros AB, Rolfe ST (2010) Development of a technique to improve fatigue lives of crack-stop holes in steel bridges. *Transp Res Rec: J Transp Res Board* 2200:69–77
3. Wang Y, Pan Q, Wei L, Li B, Wang Y (2014) Fracture toughness and fatigue crack growth analysis of 7050-T7451 alloy thick plate with different thicknesses. *J Central South Univ* 21 (8):2977–2983
4. Makabe C, Kaito N, Ferdous MS (2014) Method of arresting crack growth for application at a narrow working space. *Mech Eng J* 1(6):1–12
5. Lin F, Sun JG, Nakamura H, Maeda K (2012) Fatigue crack repair using drilled holes and externally bonded CFRP strips. In: *Bridge maintenance, safety, management, resilience and sustainability*. Taylor & Francis Group, London
6. ASTM D7774-12 (2013) Standard test method for flexural fatigue properties of plastics, D20.10.24, Ed. West Conshohocken, PA: ASTM International
7. Anderson TL (1991) *Fracture mechanics: fundamentals and applications*. CRC Press Inc., Florida
8. Rice R (1968) A path independent integral and the approximate analysis of strain concentration by notches and cracks. *J Appl Mech* 35:379–386
9. Irwin GR (1948) Analysis of stresses and strains near the end of a crack traversing a plate. *J Appl Mech* 24:361–364
10. Orowan E (1948) Fracture and strength of solids. *Rep Progress Phys* XII:185
11. Griffith AA (1920) The phenomena of rupture and flow in solids. *Philos Trans Ser A* 221:163–198
12. Mott NF (1948) Fracture of metals: theoretical considerations. *Engineering* 165:16–18
13. Irwin GR (1956) Onset of fast crack propagation in high strength steel and aluminum alloys. In: *Sagamore research conference proceedings, vol 2*, pp 289–305
14. Begley JA, Landes JD (1972) The J-integral as a fracture criterion. *ASTM STP* 514. American Society for Testing and Materials, Philadelphia, pp 1–20
15. Kormay K, Disnig W (1991) pp 66–69

# THEORETICAL MODEL FOR PREDICTING RE-CRACKING BEHAVIOR OF CRACK STOP HOLES USING J-INTEGRAL TECHNIQUE

S. Abeygunasekera<sup>1\*</sup>, J. C. P. H. Gamage<sup>2</sup>, S. Fawzia<sup>3</sup>

<sup>1</sup> Postgraduate, University of Moratuwa, Katubedda, Moratuwa, Sri Lanka.

<sup>2</sup> Professor, University of Moratuwa, Katubedda, Moratuwa, Sri Lanka.

<sup>3</sup> Senior Lecturer, Queensland University of Technology, Australia.

\* E-mail: abeygunasekarasampath@gmail.com, TP: +94712227790

**Abstract:** Re-cracking of the crack stop hole due to fatigue loads on structures has become a key issue relating to the durability of the CSH technique. In fact, many of theoretical model can be introduced to estimate the required number of cycles for re-cracking of the CSH while the Paris law has become most popular theoretical model utilized in estimating the rate of the fatigue crack growth. In this study the Power law and the Paris law was combined together and replaced Paris law which based on geometrical characteristics. Consequently, the Rumberg Osgood coefficient and the hardness index of the Power law were re-estimated as  $9.858 \times 10^{-4}$  and 0.479 respectively. These constants are independent of geometric characteristics and depends on material properties. Therefore, this model can be applied in any shape of structural element with different structural materials to predict re -cracking behavior of the CSH. This investigation was based on the cyclic J-integral technique of ABAQUS which is dealing with material characteristics. In this study the range from 0.1 to 0.6 CSH diameter to width ratio in 0.1 step were performed under laboratory tests with non-strengthened and CFRP strengthened. FEM results are well agreed with laboratory test results for the considered range of the CSH diameter.

**Keywords:** CSH, re-cracking, cyclic J-integral, Paris law, Power law

## 1. Introduction

Prediction of any crack growth is important for structural components during their service life, because such predictions help in deciding the calculation of the remaining service life of any structural component or whole structure (Jun HK, Seo JW, Jeon I-S, Lee SH, 2016). In addition, it can be supported to determine inspection intervals for maintenance and repair purposes. Therefore, a more accurate and reliable numerical approach is needed to estimate crack propagation behavior on structures. On the other hand, such a method should be simple. However, fulfilling both requirements at the same time is not an easy task, as numerous variables significantly influence the crack propagation process (Song, P. S. and Shieh, 2004).

The crack stop hole (CSH) method is the most popular emergency repairing technique to extend the fatigue life of cracked components in steel structures (WU et al., 2010). This method can be introduced as the quickest, simplest and most economical repairing technique (Buxbaum O, 1987). The process of the CSH technique commences by fabricating a drill hole at the crack tip to transfer the crack into a notch (Ghfiri R et al., 2000). When the drilled hole is placed on the crack tip, it helps to re-distribute stresses (Crain J.S et al., 2010). Originally this technique was successfully applied to the aerospace industry (Abeygunasekara S et al., 2018). In fact, the CSH method can enhance the residual fatigue life of the cracked structure compared to members with untreated crack components (Shin C. S., Wang, C. M., and Song, 1996). The CSH technique is a simple and a cost effective way to enhance fatigue durability of steel structures such as railways and road network bridges (Makabe C, Kaito N, 2014) (Wang Yi-lin, Pan Qing-lin, Weili-li, LI Bo, 2014). Furthermore, this method can be introduced as an emergency repairing technique to control crack growth as well as to change crack direction to avoid critical areas of the structures (ASCE Committee on Fatigue and Fracture Reliability, 1982). However, even after placing the crack stop hole at the crack tip with the continuous application of service loads on structures there is a gradual increase on service loads due to the current traffic demand (Miller, C., Chajes. J., Mertz, D. R., and Hastings, 2001). Fatigue causes catastrophic failure in these structures and need appropriate treatment to avoid re-cracking of the CSH (Crain J S, Smmons G, Bennett C R, Barrettgonzalez R, Matamoros A B, 2010). As it is an initial step of fatigue to start crack growth up to a critical level and finally fail catastrophically. Therefore, prediction of crack initiation would be the most important data to decide any suitable maintenance action related to fatigue control while deciding the retaining life span of the structure.



The fatigue phenomenon is directly related to the theory of fracture mechanics which is linked to cyclic stresses (Fish et al., 2015). Fatigue failure usually occurs below the yield point of a material. There are three main steps which explain the total fatigue life as crack initiation, propagation and failure (Crain, 2010). The key material properties that affect the crack initiation process are the elastic modulus, Poisson's ratio, yield strength and the ultimate strength of steel member (Crain J S, Smmons G, Bennett C R, Barrett Gonzalez R, Matamoros A B, 2010). In addition, geometric parameters such as shape of the element, aspect ratio, the shape of the CSH, crack length, hole diameter and the location of hole are also critically influenced. Furthermore, the load-related variables such as the loading pattern, the loading type, the stress ratio, amplitudes of the load and the loading frequency affect the behavior. All these factors may individually or jointly influence the process of re-cracking of the CSH. Hence, the evaluation of all influencing parameters at the same time is impossible (Ayatollahi, M. R., Razavi, S. M. J. and Chamani, 2014). There is no standard method to estimate the rate of crack growth and the required number of cycles for crack initiation. Only limited research studies have been found on crack stop holes. Due to the influence of many parameters on re-cracking behaviour, the identification of effects of all these parameters are practically not feasible (Santecchia et al., 2016). Hence, the development of a numerical model may yield proper approximations on re-cracking. The objective of this investigation is to develop a simulation technique to estimate the re-cracking behaviour of the CSH using finite element analysis.

## 2.1 Experimental test program

### 2.1.1 specimen preparation

A total of 24 steel plates with the CSH, with different sizes in the range from 4 mm to 25 mm were tested in this context. The steel plate dimensions had rectangular cross-sections of 40 mm width and 5 mm thickness. Also, the length of the plate member was chosen to be 280 mm and the effective span was 240 mm which depended on workability, test facility at laboratory and testing standards for a three-point flexural cyclic test. The schematic views and typical test specimens shown in Figure 1.

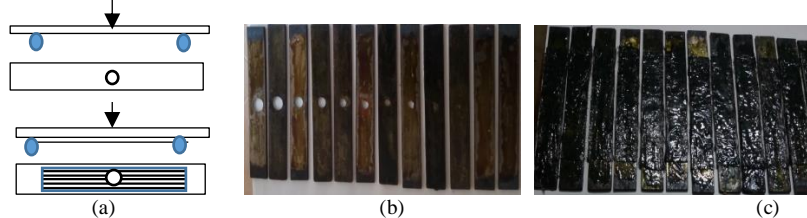


Figure 1. The test specimen with CSH (a) schematic view of (i) non strengthened (ii) CFRP strengthened (b) non strengthened (c) CFRP strengthened

## *2.2 Test setup and instrumentation*

### *2.2.1 The fatigue loading setup*

Fatigue loading was conducted using a self-developed 10 kN capacity electro-hydraulic control fatigue loading apparatus (Figure 2 (a)). The loading apparatus has the capability to control the amplitude and frequency of the applied load. All the CSH specimens were conditioned up to 10,000 load cycles. Arduino programmed digital counter was used to count number of load cycles applied on the specimen and the magnitude of the load was measured using a load cell. Maximum deflection in the load direction (vertical direction or Y-direction) at mid-plane was limited to 2 mm. The applied load was adjusted by using a flow control valve in a hydraulic circuit. Test specimens were kept on two cylindrical shaped, supportive rollers with 25 mm diameter each and the span was fixed at 240 mm between centers of the rollers as shown in Figure 2(a). A constant amplitude 2 kN magnitude load with 5 Hz frequency was applied on the mid of the specimen as shown in Figure 2(a).

### *2.2.2 Tensile test setup*

After applying the fatigue loads, the sample was removed from the fatigue loading apparatus and it was attached to the tensile test with the universal tensile testing machine as shown in Figure 2(b). Tensile loads were applied on specimen with 0.5 mm/min rate of load and yield value of each specimen was measured too. This procedure was repeated for different diameter to width ratio of the CSH from 0.1 to 0.6 range in steps of 0.1. Test results are shown in Table 4.

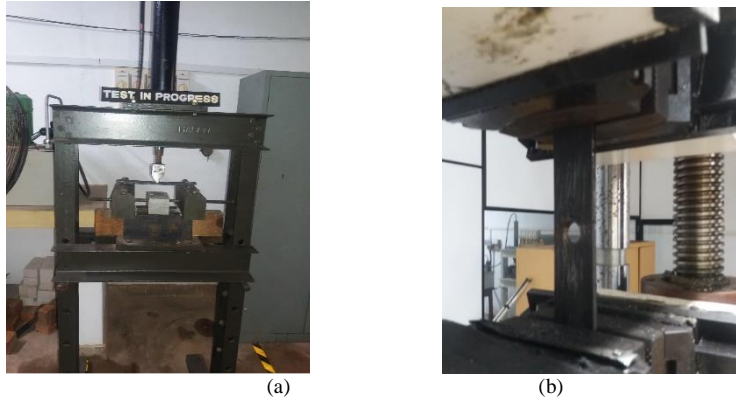


Figure 2. Test setup and instrumentation for applying load on specimen  
 (a) cyclic flexural test setup (b) Tensile test setup

Fatigue under flexural mode was performed, in this investigation, as it exhibits a number of advantages over conventional axial fatigue test which are very close to “real world” loading conditions. The overall test procedure involved two testing steps, namely, a fatigue loading and an axial tensile. There are no exact test standards to measure the flexural fatigue. However, the test setup and loading frequency was selected according to the ASTM D7774 (*ASTM D7774-12, Standard Test Method for Flexural Fatigue Properties of Plastics*, 2013).

### 3 FE modelling and analysis

#### 3.1 Modelling description

ABAQUS is a leading structural analysis software based on the finite element method (FEM). It is able to solve problems ranging from relatively simple linear analyses to the most challenging non-linear context. This software is flexible to analysis various type of engineering materials including metal, rubber, polymer, composites and reinforced concrete. This FEA package was developed by Habbitt, Karlson and Sorensenin 1978. Consequently, ABAQUS version 6.14 is used for all the modeling in this study. ABAQUS included several functional units called modules (Example & Manual, n.d.). Each module contains only the relevant tools. For example, the Part module contains only the tools needed to create a new part, while the Mesh module contains the tools for meshing the model. The order of the modules in the menu is in a logical sequence therefore when creating the

model, following the logical sequence is required. Before submitting the particular model for analyze, the geometry and other physical properties of the model must be defined step by step.

### *3.2 Procedure of simulation*

For the FEM simulation, the J-integral technique was utilized in this pre-crack analytical method and the procedure for FEM is given below.

1. Created the geometry of the model using the part module of ABAQUS and developed pre-defined crack profile using partition cells extrude/sweep edges option of the part module
2. Installed material properties for individual component prepared in part module and numerical values taken from the laboratory test or existing literature
3. The module of assemble was used to assemble each of components prepared in part module according to typical test setup
4. The step module used to select required history outputs and field outputs according to requirement and introduced domain of analysis with 10 number of contours for model of test specimen with CSH
5. In the load module introduced loads with 2 kN, sinusoid loading pattern, 5 Hz loading frequency and 0.1 stress ratio as well as all of relevant boundary conditions for assembling module similar with test setup
6. Individual part of the assembly module was meshed using C3D8R mesh and 2 mm mesh size in mesh module
7. Run the assemble mesh model for analysis and collect the J-integral values from the ODB file and stress values taken from X-Y data from field output option in the visualization module at the end of the analysis

## **3.3 Steps of model**

### *3.3.1 Part module*

The Part module allows creating and editing individual parts by sketching their geometry directly in ABAQUS. The dimensions of specimen 280 mm in length, 40 mm in width and 5 mm in thickness. Also , crack and contour paths were introduced at the hole as shown in Figure 3.

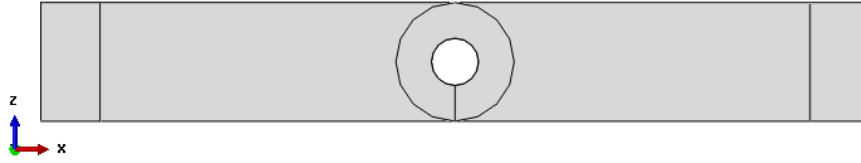


Figure 3.A model view of the specimen after introducing contours and crack seems (not to scale)

### 3.3.2 Material properties

Material properties of each region are assigned in the property module in ABAQUS. This analysis concerns two materials as steel and CFRP. Steel is considered as an elastic material with isotropic hardening characteristics, and the CFRP material model uses the Hashine option of a composite material. The modulus of elasticity and tensile strength of steel and CFRP material were determined experimentally by a coupon test in a similar investigation conducted at the computational mechanics laboratory. Also, the tensile strength and elastic modulus of the steel were measured according to the ASTM D 3039. In fact, a tensile strength of 583 MPa and an average elastic modulus of 200 GPa were reported. Tensile strength and an average elastic modulus of CFRP material were reported as 175 MPa and 1575 MPa, respectively. The Poisson's ratio value is assumed as 0.3. Numerical values of material properties are taken from laboratory experiments as shown in Table 1. (Hiroomi & Nakazawa, 1984)(Kubota et al., 2017).

Table 1: Material properties (Ralalage & Chandrathilaka, 2019)

Material property	Steel	Araldite 420	CFRP (130)
Average tensile strength (MPa)	583	25	1575
Average elastic modulus (GPa)	200	0.579	175
Average Poisson's ratio	0.3	0.3	0.3

### 3.3.3 Load and boundary conditions

A Load module is used to specify loads and boundary conditions of the model. Each specimen module was loaded with the LCF mode using the direct cyclic option. Thus, the magnitude of pressure was due to the cross section of the top of the loading nose and frequency of loads was fixed as 5 Hz using an amplitude option of loads. Also, the movement of the remaining directions and rotations around all other axis were fixed during the analysis. The applied pressure load using a loading nose and all boundary conditions are shown in Figure 4. similar with laboratory test setup according to the ASTM D 790.

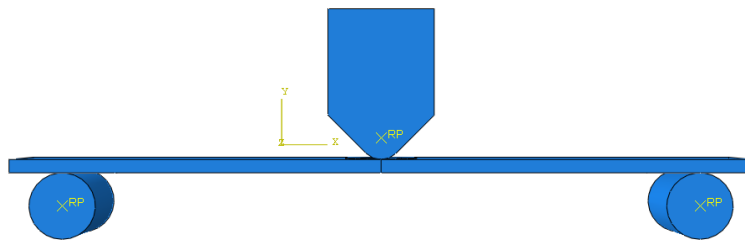


Figure 4: A loading mode and boundary conditions

#### 3.3.4 Interaction module and crack

The Interaction module is used to specify mechanical interactions between regions of a model, connections between two points, connections between two edges or connections between point and a surface. In this analysis two interactions were available between two supportive rollers and the bottom surface of the plate. Special options were used to create the crack while the extension direction was selected using a q vector option as shown in Figure 5.

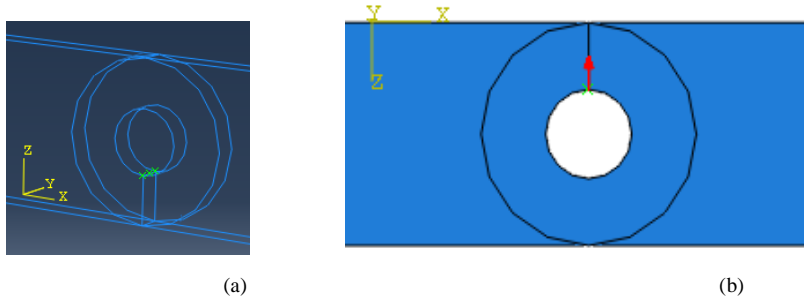
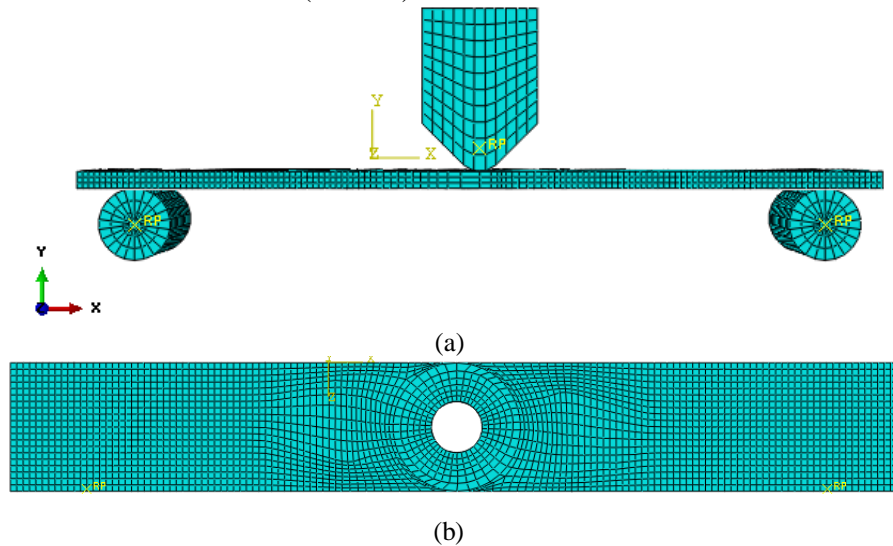


Figure 5. Crack model on CSH (a) Contour path (b) Crack seams

### 3.3.5 Mesh module

The mesh module plays a vital role in the contour integral analysis method. A special mesh pattern was introduced around the crack initiation region to avoid stress singularity occurring at the crack stop hole, due to the recommendations of the ABAQUS user manual (User, n.d.). A Rosette pattern was formed at the crack tip region and the coarser mesh was used for the remaining area as shown in Figure 6. Around the crack stop hole (CSH) a circular partitioned area was introduced using the “swept meshing” technique as shown in Figure 6. This technique helped to regulate and focus on the mesh. The remaining part of the model was utilized using a “medial axis” meshing technique with edge-based tools used to mesh seeding around the crack tip as well as the loading nose and supportive rollers. In this analysis three dimensional brick element (C3D8R) was selected with 2 mm mesh size.







gral ( $\Delta J$ ) is determined as an analytical approximation of numerical methods. However, the ABAQUS does not provide the facility to directly obtain the value of cyclic J-integral, thus Ochensberger and Kolednik introduced an Eq 1 to fulfil this gap (Ochensberger & Kolednik, 2014). Where  $\Delta J$  is the cyclic J-integral value,  $J_{min}$  is the minimum value available at particular FEA results and  $J_{max}$  is the maximum value available in the same evaluation.  $\Delta J$  can be considered as a rate of elastic energy released in the independent path contour. The advantage of the J-integral technique is the ability to remotely evaluate the stress, strain, and displacement parameters at the crack tip.

$$\Delta J = J_{min} + J_{max} - \sqrt{J_{min} + J_{max}} \quad (1)$$

### 3.3.2. The Paris law

The Paris law is the most popular theory to evaluate crack propagation which can be utilized to predict the fatigue life (Paris et al., 1961). This law explains that the crack length per cycle ( $da/dN$ ) is related to the change of stress intensity factor range ( $\Delta K$ ). The number of cycles ( $N$ ) for a crack to propagate from an initial crack length to the final crack length is explained by the Paris law relationship given in Equation 2. “C” represents the Paris law coefficient and “m” is an exponent. Revankar, Wolf, and Ronznic suggested that parameters are a better way to be obtained from laboratory experiments. Because, “C” and “m” are highly depends on the specimen geometry as well as stress ratio, R (Wijesuriya, 2018). However, in each analysis such a lengthy procedure is not a viable task. The Paris law constants were taken from the literature and values of “C” and “m” were taken as  $7.77 \times 10^{-5}$  and 0.959 respectively (Hiroomi & Nakazawa, 1984) (Kubota et al., 2017). The cyclic J-integral is linked to  $\Delta K$  according to Equation 3 whereas the cyclic J-integral value,  $\Delta K$  is the stress intensity factor range and E is an elastic modulus value of the material.

$$\frac{da}{dN} = C(\Delta K)^m \quad (2)$$

$$\Delta J = \frac{(\Delta K)^2}{E} \quad (3)$$

The calculated value of cyclic J-integral were substituted into Eq 3, which determines the value of the stress intensity factor range, ( $\Delta K$ ). Table 2 summarizes

the cyclic J-integral, the range of stress and the required cycles for crack initiation together with different CSH diameters due to the analytical results and their extension obtained in this analysis.

Table 2: FEM results variation with CSH diameter

Diameter of CSH, d(mm)	Cyclic J-integral value ( $\Delta J$ ) $\times 10^{-2}$	The range of stress, ( $\Delta K$ ) (MPa $\sqrt{mm}$ )	Fatigue crack growth rate (mm/Cycle) $\times 10^{-5}$	Number of cycles for re-cracking
4	1.00	1.41	10.80	9234
8	2.14	2.07	15.60	6412
12	3.70	2.72	20.30	4931
16	4.10	2.86	21.30	4694
20	5.53	3.33	24.60	4067
25	11.55	4.81	35.00	2857

### 3.3.3. The Power law

Fracture mechanics theory is a well-established and commonly applied method to predict crack propagation. An elastic-plastic fracture mechanics approach is more compatible to evaluate more complex and nonlinear context. The cyclic J-integral technique is based on the fracture mechanics. Dowling and Begley have proposed and implemented the J-integral technique considering relations of crack growth rate,  $da/dN$ , and cyclic J-integral,  $\Delta J$  (Dowling, N. & Begley, 1976). This is called the Power law, explained in Eq 4 and it is very similar to the Paris law. In the Power law application, it was assumed that the cyclic J-integral,  $\Delta J$  includes the summation of elastic and fully plastic solutions. The rate of fatigue crack growth in the Power law depends on constants 'A' and 'n'. These two parameters are called as the Ramberg-Osgood coefficient and strain hardening index respectively (Ramberg & Osgood, 1943). These two parameters do not depend on geometry and are based on material properties. Also, these constants especially represent the tensile data of materials.

$$\frac{da}{dN} = A(\Delta J)^n \quad (4)$$

Laird, Pelloux and Sih, also proposed an alternative method to characterize the FCG under elastic-plastic conditions (Peralta & Laird, 2016)(Sih, 1974).Table 3 summarizes the log value of fatigue crack growth rate together with the log value of the cyclic J- integral with different CSH diameters from the analytical results.

Table 3:Log values of crack growth rate and cyclic J-integral variation with the CSH diameter

Diameter (mm)	Cyclic J- integral value ( $\Delta J$ )x10 <sup>-2</sup>	ln( $\Delta J$ )	Fatigue crack growth rate (mm/Cycle) x 10 <sup>-5</sup>	ln(da/dN)
4	1.00	-4.61	10.8	-9.13
8	2.14	-3.84	15.6	-8.77
12	3.70	-3.30	20.3	-8.50
16	4.10	-3.19	21.3	-8.45
20	5.53	-2.89	24.6	-8.31
25	11.55	-2.16	35.0	-7.96

Using the results of the log value of the fatigue crack growth rate and the cyclic J-integral , a graph was constructed as shown in Figure 8. The rate of the crack growth variation with the cyclic J-integral variation with various CSH diameters were considered from one-hole diameter to another. Figure 8 shows the log value of the fatigue crack growth rate range which varied with the log value of cyclic J-integral due to effects on fatigue load.

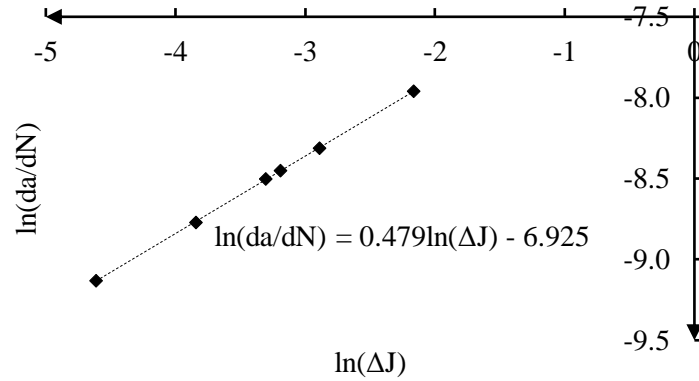


Figure 8. Log value of crack growth rate variation with cyclic J-integral

As shown in Figure 8 when the log value of cyclic J-integral is increased, the log value of the fatigue crack growth rate also increases. The log value taken from Equation 4 builds a linear co- relation between the rate of crack growth with respect to the cyclic J-integral as shown in Eq 5.

$$\ln \left( \frac{da}{dN} \right) = n * \ln(\Delta J) + \ln(A) \quad (5)$$

The log value of the crack growth rate with respect to the log value of the cyclic J-integral value is represented by

Figure 8 and the results curve fitted with the linear co-relation as shown in Eq 6.

$$Y = 0.479x - 6.922 \quad (6)$$

Eq 5 and Eq 6 are represent the same co-relations and individual terms considered in the linear function as explained in both of the equations .

n=0.479 and

$$\ln(A) = -6.922$$

Then calculated numerical value of 'A' using Eq7.

$$A = e^{-6.922} \quad (7)$$

$$A = 9.858 \times 10^{-4}$$

The analytical results taken from Table 3 were utilized to construct the fitted curve as shown in Figure 8. The power law function related to the relevant J-integral was shown in Eq 8 as a polynomial function.

$$\frac{da}{dN} = 9.858 \times 10^{-4} (\Delta J)^{0.479} \quad (8)$$

The visualization of the bottom view under the fatigue load profile with the CSH diameter shown in Figure 9 and Figure 10.

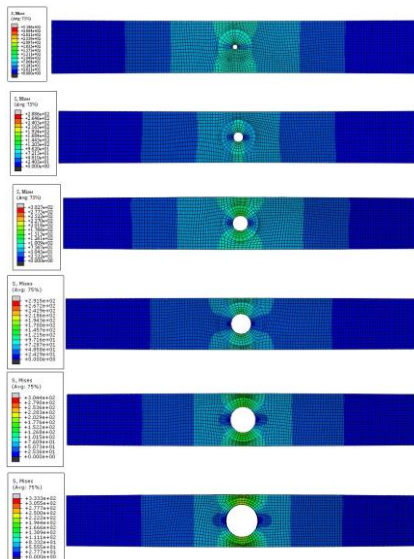


Figure 9

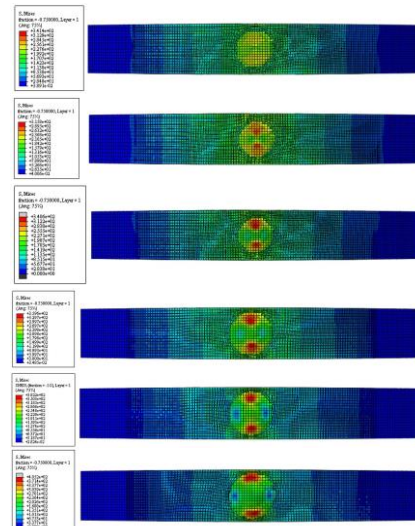


Figure 10

Figure 9. The Visualization of the bottom view under fatigue load profile with the diameter of the non-strengthened CSH specimen (a) 4 mm (b) 8 mm (c) 12 mm (d) 16 mm (e) 20 mm (f) 25 mm

#### 4. Model results and validation

##### 4.1. Comparison of test results and FEM

Table 4 summarizes the average yield stress together with the variation of different diameters of CSH from the test results as well as the FEM results. Stress values for FEM are taken from XY data from field out put option in the visualization module.

Table 4.FEM results compared with laboratory test results for the CSH

Diameter to width ratio	Yield stress(MPa)			
	Non strengthened		CFRP strengthened	
	Test	FEM	Test	FEM
0.1	375.1	441.7	498.0	557.7
0.2	355.6	376.3	470.0	507.6
0.3	335.6	289.5	445.5	471.7
0.4	300.1	275.6	405.0	449.5
0.5	245.8	238.8	356.0	324.0
0.6	185.8	167.8	270.0	297.0

The test results and FEM results of the CSH under flexural cyclic load were compared in Figure 10. It represent the yield stress values together with the variation of different diameter from the range of 4 mm to 25 mm in the range of 4 mm steps ( diameter to width ratio from the range of 0.1 to 0.6 in the range of 0.1 step).

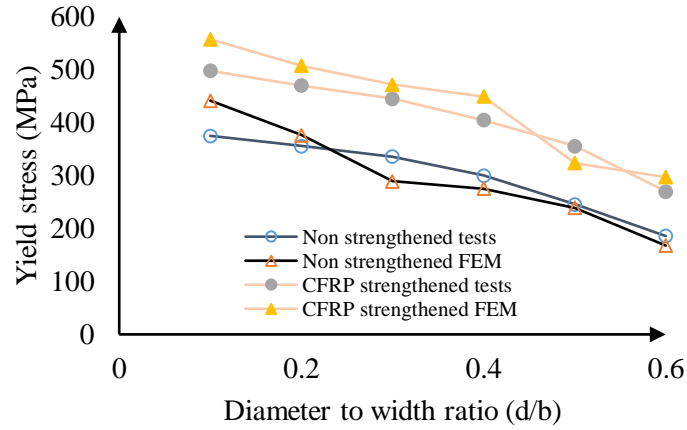


Figure 10. Yield stress variation with diameter to width ratio of CSH

Measuring number of cycles for crack initiation is not an easy task as it originates from the surface and it is very small. In this test setup a digital camera was attached to observe and magnify crack initiation in the CSH. In addition, a digital voltmeter was attached between the CSH. When monitoring the CSH through a digital screen with a magnifying scale, a sudden change of resistivity was observed in this context. Because when start to crack conductivity of material loos and at the same time noted number of cycles using digital counter and repeat this procedure to take average value of number of cycles. Table 5 summarizes the number of cycles together with the variation of different diameters of CSH from the test results as well as the FEM results.

Table 5. Results comparison of Power law and laboratory test results

Diameter of CSH(mm)	Results based on the Power law	Laboratory test results	Diameter of CSH(mm)	Results based on the Power law	Laboratory test results
4	9209	10066	16	4685	5115
8	6397	6990	20	4059	4431
12	4921	5372	25	2853	3113

Figure 11 shows the number of cycles for crack initiation,  $N$  variation with the CSH diameter due to effects on cyclic flexural load with a constant amplitude load. As shown in Figure 11 when the CSH diameter is increased, the number of cycles decreases in this context. The analytical results which include the Power law approximation illustrated in Eq 8 and the laboratory test results were compared as shown in Figure 11.

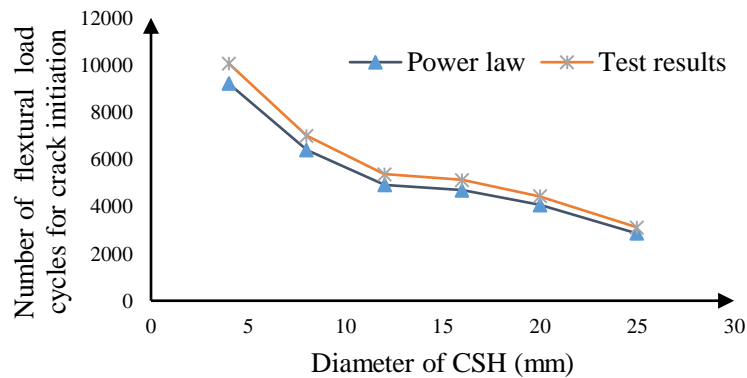


Figure 11. Comparison of Power law and Paris law with laboratory test results

ABAQUS as well as most of the FEA packages have the capability to estimate the value of the J-Integral under monotonic loads. However, all of them do not have the capacity to automatically determine the cyclic J-Integral from history outputs or ODB database. Manual calculation of the cyclic J-Integral is a more time-consuming process. On the other hand, results would highly depend on the mesh size while a very fine mesh size result would be highly accurate but more time consuming. Furthermore, high end hardware facilities are needed to run fine mesh analysis. In addition, performance of CFRP strengthened technology is highly depending on environmental factors such as humidity level and temperature. However, ABAQUS not provided facility to control such factors in this analysis. Therefore, these can be considered as major limitations for this evaluation technique and such reasons would significantly tolerate the final results of the analysis.

## 5. Conclusions

In this study, the CSH was numerically analyzed using the Paris law. The required number of cycles for crack initiation for the CSH were estimated



by using J-integral technique. Results of the Paris law were utilized to modified Power law approximations and its validated using laboratory test results. The laboratory test results were well agreed with the modified Power law approximation. Thus, the following conclusions were obtained:

1. The required number of cycles for crack initiation was largely reduced in different stress levels due to the increase of the crack stop hole diameter with a constant cross section
2. The constant values of power law (A and n) were estimated as  $9.858 \times 10^{-4}$  and 0.479 respectively
3. Comparatively, the power law approximation is highly recommended for fatigue related analysis
4. Power law is less time consuming than the Paris law to estimate the number of cycles for crack initiation and determine the FCGR in the CSH
5. This modified method is independent of the geometry of the specimen
6. Co-relations of the Power law is simple and easy to use in the field

#### **Declaration of Competing Interest**

The authors declare that they have no known competing or financial interests or personal relationships that can have appeared to influence the work reported in this paper.

#### **Conflict of interest**

The authors declare that they have no conflicts of interest.

#### **Acknowledgements**

The authors gratefully acknowledge the support of the staff in computer laboratory, as well as the staff of the structural testing laboratory, Department of Civil Engineering, University of Moratuwa, Sri Lanka for their valuable support.

#### **References**

- Abeygunasekara.S, Gamage, J. C. P. H., & Fawzia.S. (2018). Numerical modelling of re-cracking behavior in retrofitted crack stop holes in steel structures.

- ICSBE-2018 ,Earl's Regency Hotel, Kandy, Sri Lanka., 481.
- ASCE Committee on Fatigue and Fracture Reliability. (1982). Fatigue reliability: development of criteria for design. *ASCE Journal of the Structural Division*, 108(1), 71–88.
- ASTM D7774-12, *Standard Test Method for Flexural Fatigue Properties of Plastics*. (2013). D20.10,24, West Conshohocken, PA: ASTM International.
- Ayatollahi, M. R., Razavi, S. M. J. and Chamani, H. R. (2014). Fatigue life extension by crack repair using stop-hole technique under pure mode-I and pure mode-II loading conditions. *Procedia Engineering*, 74, 18–21.
- Buxbaum O, H. H. (1987). Expansion of cracked fastener holes as a measure for extension of lifetime to repair. *Engng Fract Mech*, 28(.5/6), 689–98.
- Crain.J.S, Smmons.G.G, Bennett.C.R, Barrettgonzalez.R, Matamoros.A.B, & .S., R. . (2010). Development of a technique to improve fatigue lives of crack-stop holes in steel bridges. *Journal of the Transportation Research Board*, 2200, 69–77.
- Crain, J. (2010). *Fatigue Enhancement of Undersized, Drilled Crack-Stop Holes*. [Http://Kuscholarworks.Ku.Edu/Handle/1808/6288](http://Kuscholarworks.Ku.Edu/Handle/1808/6288).
- Crain J S, Smmons g G, Bennett C R, Barrettgonzalez R, Matamoros A B, R. S. T. (2010). Development of a technique to improve fatigue lives of crack-stop holes in steel bridges. *Journal of the Transportation Research Board*, 2200, 69-77.
- Dowling, N. & Begley, J. (1976). Fatigue Crack Growth During Gross Plasticity and the J- Integral. *Mechanics of Crack Growth ASTM-STP W1.*, 82–103.
- Example, A., & Manual, P. (n.d.). *Abaqus 6.1 2. 1*.
- Fish, P., Schroeder, C., Connor, R. J., & Sauser, P. (2015). Fatigue and fracture library for the inspection, evaluation, and repair of vehicular steel bridges. *Purdue University. West Lafayette, Indiana*.
- Ghfiri.R, Amrouche.A, Imad.A, & Mesmacque.G. (2000). Fatigue life estimation after crack repair in 6005 A-T6 aluminium alloy using the colding expansion hole technique. *Fatigue Fract Engng Mater Struct*, 23:911, 6.
- Hiroomi, H., & Nakazawa, H. (1984). Numerical Analysis of Fatigue Striation. *J. Mech. Phys. Solids*, 32(3), 213–226.
- Jun HK, Seo JW, JeoniI-S, Lee SH, C. Y. (2016). Fracture and Fatigue crack growth analyses on a weld-repaired railway rail. *Engi Fract Anal*, 59, 478–492.
- Kubota, M., Kataoka, S., Takazaki, D., & Kondo, Y. (2017). A quantitative approach to evaluate fretting fatigue limit using a pre-cracked specimen. *Tribol. Int*, 108, 48–56.
- Makabe C, Kaito N, F. M. S. (2014). Method of arresting crack growth for application at a narrow working space. *Mechanical Engineering Journal*, 1(6), 1–12.
- Miller, C., Chajes. J., Mertz, D. R., and Hastings, J. N. (2001). Strengthening of a Steel Bridge Girder Using CFRP Plates. *Journal of Bridge Engineering*, 6(6), 514–522.
- Ochensberger, W., & Kolednik, O. (2014). Physically appropriate characterization of fatigue crack propagation rate in elastic-plastic materials using the J - integral concept. *International Journal of Fracture*, 192(1), 25–45.

- Paris, P. C., Gomez, R. E., & Anderson, W. E. (1961). A rational analytic theory of fatigue. *Trend Eng*, 13(1), 9–14.
- Peralta, P., & Laird, C. (2016). Cyclic Plasticity and Dislocation Structures. *Reference Module in Materials Science and Materials Engineering*.
- Ralalage, E., & Chandrathilaka, K. (2019). *BOND PERFORMANCE OF CFRP / STEEL COMPOSITE BOND PERFORMANCE OF CFRP / STEEL COMPOSITE*. February.
- Ramberg, W., & Osgood, W. R. (1943). Description of Stress-Strain Curves by Three Parameters. *NCAA TN 902*.
- Rice, J. R. (1968). A Path Independent Integral and the Approximate Analysis of Strain Concentration by Notches and Cracks. *Journal of Applied Mechanics*, 35, 379–386.
- Santecchia, E., Hamouda, A. M. S., Musharavati, F., Zalnezhad, E., Cabibbo, M., El Mehtedi, M., & Spigarelli, S. (2016). A Review on Fatigue Life Prediction Methods for Metals. *Advances in Materials Science and Engineering*, 2016. <https://doi.org/10.1155/2016/9573524>
- Shin C. S., Wang, C. M., and Song, P. S. (1996). Fatigue damage repair: a comparison of some possible methods. *International Journal of Fatigue*, 18(8), 535–546.
- Sih, G. C. (1974). Elastic-Plastic Fracture Mechanics. *Prospects of Fracture Mechanics*, 613–621.
- Song, P. S. and Shieh, Y. L. (2004). Stop drilling procedure for fatigue life improvement. *Fatigue International Journal of Fatigue*, 26,(No.12), 1333–1339.
- User, A. A. (n.d.). *Abaqus 6.1 2. V*.
- Wang Yi-lin, Pan Qing-lin, Weili-li, LI Bo, W. Y. (2014). Fracture toughness and fatigue crack growth analysis of 7050-T7451 alloy thick plate with different thicknesses. *Journal of Central South University*, 21(8), 2977–2983.
- Wijesuriya, H. S. (2018). *predicting fretting fatigue crack propagation using finite element analysis predicting fretting fatigue crack*.
- WU, H., Imad, A., Benseddiq, N., Castro J T P, D., & Meggiolaro M, A. (2010). On the prediction of the residual fatigue life of cracked structures repaired by the stop-hole method. *International Journal of Fatigue*, 32(4), 670–677.

## INFLUENCE OF SURFACE PREPARATION ON CFRP/STEEL BOND PERFORMANCE

S. Abeygunasekera<sup>1\*</sup>, J. C. P. H. Gamage<sup>2</sup>, S. Fawzia<sup>3</sup>

<sup>1</sup> Postgraduate, University of Moratuwa, Katubedda, Moratuwa, Sri Lanka.

<sup>2</sup> Professor, University of Moratuwa, Katubedda, Moratuwa, Sri Lanka.

<sup>3</sup> Senior Lecturer, Queensland University of Technology, Australia.

\* E-mail: [abeygunasekarasampath@gmail.com](mailto:abeygunasekarasampath@gmail.com), TP: +94712227790

**Abstract:** CFRP strengthened technique was a potential method to strengthen steel structures and their elements. However, de-bonding is one of the main barriers to popularize this technique. The performance of the CFRP/steel bonds is depending on the surface condition of steel. Because the load transfers through the CFRP /steel bonds. The main purpose of the bond is stress transfer through CFRP to the steel or steel to CFRP surface. In addition, the failure mechanism of the composite and failure modes such as de-lamination and de-bonding is also depending on bond performance. Because the durability of bonds depends on the attraction force between steel and epoxy as well as epoxy and CFRP. This paper presents a state-of-the-art review of the effects of surface preparation methods on the durability of CFRP/steel bond strength. For steel surfaces, three-step approach was recommended removal of grease and chemical contaminants, removal of weak layers on steel surfaces, and application of protective primer. Surface preparation techniques can be classified as chemical, mechanical, electrochemical, and thermal processes. The theory behind the surface preparation of steel is enhancing the formation of chemical bonds between the metal surface and epoxy adhesive. Therefore, any surface treatment technique should be confirmed absence of contaminations. In addition, the process of any cleaning techniques should be supported to remove weak layers, degreasing, re-cleaning and escape oil or other potential contaminants from the metal surface. This study compared existing surface preparation techniques and discuss the merits and de-merits of each method and provided broad insight for select appropriate surface preparation techniques according to application in industry.

**Keywords:** *surface treatment; sand blasting; grit blasting; De-bonding; de-lamination*

## **1. Introduction**

Due to the significant advantages of CFRP material it has popular as an external reinforcement technique of strengthening steel structures. Comprehensive research has been carried out focusing on their bond performance, durability and failure mechanism. Most of available literature were discussed the factors affecting on bond performance due to, characteristic of CFRP materials, properties of epoxy and surface preparation techniques.

Furthermore, existing literature was attention to the effect of environmental conditions on bond performance. Majority of experimental studies over the last two decades have targeted on short term performance under tensile, compressive or bending loads. However, a little amount of investigations has targeted at understanding of the CFRP/Steel bond performance under cyclic loads also. In addition, field applications also review by a few authors and confirmed the suitability of CFRP applications in steel sections.

Several issues arising with deterioration of steel structures. They are corrosion, fatigue sensitivity, cracking, load bearing capacity with future demand. Therefore, proper maintenance and retrofitting are very crucial in such structures to the safe of lives and properties. However, lack of proper maintenance, environmental related deterioration, aging of structural components, insufficient detailing at the period of construction and use of standard materials were reported as major issues in durability of steel structures. Due to such reasons, structural health levels reducing day by day as well as maintenance budget increasing. However, strengthening of steel structure has potential to continue their services. Most of real-world retrofitting applications of structures are using conventional techniques as follows.

1. Steel plate or profile connected with damage position using welding
2. Steel plates connected through bolting to fastening

This conventional method contributes to re-install the capacity losses of structures. However, the conventional method has many limitations and shortage. There are increasing dead loads of structure, tendency to the corrosion, increase stress concentration and a change in a micro structure. In addition, the conventional retrofitting methods are more time consuming and difficult to handle without heavy lifting equipment and required skill labours and tools. On the other hand, welding technique is not fatigue resistive. Researchers have introduced CFRP base technology as a solution of such drawbacks.

The one of main limitation of CFRP/steel composite is a de-bonding which is dealing with characteristic of metal surface. This study summarizes the experimental studies of various research programs, the aim of which is to understand the behavior of the CFRP/steel bond performance with various types of surface preparation technique

## **2. Surface preparation**

CFRP/steel strengthening method is based on bonding of CFRP to steel surface with epoxy adhesives. Shulley et al. (1994), Karbhari et al.(1995) and Liu et al.(2005) have confirmed proper installation of CFRP with steel contribute to betterment of bond performance and durability of the strengthened member. The purpose of the surface preparation is to enhance the formation of a chemical bond between the adherent (CFRP, steel) and adhesive. In this case, the active steel surface is must because surface must be free from contaminants. On the other hand, weak layers should be removed from the surface. Sand blasting method is more popular because it can successfully utilize to remove any weak exterior layers from the parent metal. On the other hand, sand blasting causes to increase surface roughness. If there remains any dust on the metal surfaces, it can be removed by vacuuming and wiping. Some solvents also can be recommended to remove contaminants. Acetone is highly recommended by many of studies to remove all possible contaminants from the metal surface.

### **2.1 Preparation Techniques**

Surface preparation can be considered as the main factor of influencing bond performance, failure mechanism and durability of the CFRP strengthen method. Various types of surface preparation techniques can be identified for pre-treatments of metallic materials. According to investigation conducted by Aldan (2004) such techniques can be classified as chemical, mechanical, electrochemical, and thermal process. Theory behind surface preparation of steel is enhancing the formation of chemical bonds between the metal surface and epoxy adhesive. Therefore, in any case of treatment should confirmed chemically active surface before the CFRP laminates. On the other hand, it should be confirmed that the surface is the absence of any contaminations. In addition, the process of cleaning is supporting to remove weak layers, degreasing, re-cleaning and escape oil or other potential contaminants from the metal surfaces Due to the investigations of Hollaway and Cadei (2002), surface treatments contribute to eliminating contaminant from metal surface and forming a fresh active surface. According to a study conducted by Schnerch et al. (2007) proved that pre-treatment of steel surface can enhance the durability of chemical bonds. Schnerch (2007) reported that the grit-blasting is one of the most effective methods for the preparation

of the steel surface. The reason is grit blasting can successfully remove inactive oxides and hydroxide layer from metal surfaces. However, the size of a grit is affected to the profile of metal surface. If select the finer particle of grit result produces smooth surface and higher surface energy. Harris and Beevers (1999) noted that grit blasting technology can remove the weak layers from metal surfaces and modified the chemical characteristics of the adherence (steel and CFRP). Grit blasting contributes to avoiding micro cracks in the surface. Baldan (2004) explained combination of grit-blasting with a chemical or electrochemical treatments cause to significantly improve the durability of bond strength. In the case of general applications, wire brush can be used to remove weak layers and vacuum head uses for cleaning the surface. Solvent uses to remove surface contaminants. According to existing literature, all surface treatment methods are contributing to change a certain degree of bond performance.

Table 01: Key studies related to surface preparation techniques

Methods/Procedure	Result/Observations	References
chemical, mechanical, electrochemical, and thermal procedures	Significantly enhanced the bond performance	Baldan. (2004)
Any surface preparation	(a)elimination of contaminant materials, (b)forming a fresh active surface (c)chemical amendment of the surface	Hollaway and Cadei (2002)
Grit Blasting	(a) grit-blasting is one of the most effective techniques. (b)Can be avoid micro cracks	Schnerch (2007)
Grit Blasting	(a)removes weak layers of structures (b)modifies the chemical characteristics of the adherents	Harris and Beevers(1999)

Combination of grit-blasting with chemical or electrochemical treatments	increase the durability of bond strength	Baldan (2004)
Silane coupling agent for surface treatment	Enhanced the bond durability	Dawood and Rizkalla (2010)

The cleaning process of steel surfaces can be explained under three main steps. The first step is removing grease and chemical contaminants from the metal surface. Secondly, remove weak layers on steel surface using mechanical treatment. Finally, apply protective primer on steel surface. Because, to ensure complete bonds, removing all surface contaminants. Grease, dust, dirt, and chemicals are considered as contaminants and it should be removed from steel surfaces. The process of cleaning can perform by wiping on the surface with an appropriate solvent. Howard(2006) and Rameshni(2011) have confirmed acetone is best solvent for the cleaning purposes of steel surfaces. Excessive solvent usage helps to prevent redistribution of the contaminants during the wiping

Removing of weak layers from the steel surface such as paint and rust are another important factor. Because CFRP layers are loosely attached to the steel surface if they are not properly removed, from the steel surface and result is premature de-bonding (Dawood, 2005). Weak layers can be removed using either mechanical abrasion or grit blasting. However, grit blasting showed excellent bond performance. But this method is more expensive. Mechanical abrasion is comparatively simple to remove contaminants near the metal surface. Furthermore, grit blasting method is contributing to chemical activate the coarse surface. The overall result is improved chemical and mechanical bond (Schnerch et al., 2007).

Chemically active surface is exposure to atmosphere steel surface can oxidize. The purpose of applying primer coats on cleaning surface is protected on the clean surface. However, the primer does not increase the static strength of the bond. But prime layer is contributing to improving durability of bonds under exposed to the atmosphere (Dawood, 2005). In case of primer protection should be applied carefully, because the result of the improper primer application is causes to premature de-bonding failure. The primer has potential to protect the cleaned, chemically active steel surface.



However, CFRP should be bonded to the steel very soon after complete surface preparation. According to Dawood(2005) and Schnerch et al.(2007) chemically active surface helps to minimize the chance of any re-contamination or oxidation of the steel surface. The result of improper bonding is de-bonding, which is an undesirable failure mode.

Surface preparation is very important when considered the performance and durability of the adhesive bond. Therefore, rehabilitation takes place on site, surface treatment must environmentally friendly. In addition, it should easily accomplish in field conditions. Brockmann (2004) reported that CFRP material can attached up to 150 hours after completing of surface preparation. Surface grinding or sandblasting method is very popular in case of remove rust, paint, and primer from the steel surface.

## **2.2 Surface treatment**

Reliability of the bonds is highly depending on surface treatment processes.<sup>i</sup> Various types of studies have conducted to investigate the effects of surface preparation. In this review commonly discussed such methods and merits and demerits of each considered surface preparation method. The objective of any surface preparation technique is to obtain a clean, rough, and chemically active surface. Monfared et al. (2008) have emphasized surface preparation is significantly affected by fatigue performance. Jiao et al. (2012) have recommended a grinding method to remove the corrosion of the welded area on a steel beam. Wu et al.(2012) recommended grinding method as a treating technique of the tension flange surface. In addition, the authors have suggested, surfaces of the tension flange cleaning with acetone before the reinforcing with CFRP for the fatigue test. Tavakkolizadeh and Saadatmanesh (2003) suggested a sand blasting is excellent for the surface preparation. Teng et al.(2011) also reported that sand blasting is more effective surface treatment method of bonding the CFRP strips to the beams. Kim and Harries (2011) used a 1500 sfpm (surface feet per minute) belt sander and a 40-grit zirconia alumina belt for the surface preparation. Authors have ensured the effectiveness of this method.

Deng and Lee (2007) recommended the types of the CFRP plates also must be finished smoothly by using sandpaper. However, according to Schnerch et al.(2007) such smooth surface is causing to reduce the bonding ability of the surface. In addition, chemically active steel surface should be free from contaminants. Because, contaminant free surface is essential to confirm the chemical bonds between the adhesive and the metallic surface. Brushing, ultrasonic, or vapour degreasing systems are another technique identified as most efficient way to remove the surface contaminants. In addition, solvents

also can be used for the purposes of surface cleaning. According to Hollaway (2002) high-energy surface should be form on steel surface and it can be considered as most efficient way to treating (Hollaway and Cadei, 2002). Grit blasting with angular grit helps to remove inactive oxide and hydroxide deposits of the base material. Grit size critically affects the surface profile of the steel. Harris and Beevers (1999) have observed that fine particles create a smooth surface than abrasive grit particles. Generally, a smooth surface is contributed to effective adhesive-steel surface bonds. Due to investigation of Schnerch et al. (2006) the surface profile of the steel is not influenced on long-term durability. However, after grit blasting, solvents recommended to be used for wash and clean the steel surface.

### **2.3 Installation Steps**

The bonded side of the steel should be sanded to increase the surface roughness. Surface grinding, medium grit sandpaper or a sandblaster method can be used for surface preparation. Then the metal surface should be wiped and cleaned with acetone or any suitable solvent. Next, the pre-treated steps such as adhesive promoter or primer coating are applied to the clean steel surface. Either an adhesive promoter or a primer conditioner, which leaves a thin layer attached to the metal oxide surface. Because, adhesive promoter significantly improves the long-term durability of bonds due to moisture absorption control through such coating. In addition, the hydrolysis of the primary bonds is slowed down by the adhesive promoter. Finally, CFRP bonding either laminates or sheets to the steel surface. The appropriate adhesive layer thickness should be approximately 1 mm. The bonded plates can cure for enough time and it should not be less than 48 hours. Miller et al. (2007) suggested a method of accelerating curing activities. They are using heating blankets or induce heaters to increase the curing rate of the adhesive. The adhesive is typically used as a two-component viscous epoxy. A less viscous epoxy can be utilized for laminates each other. The alkaline solution also helps to overcome oxidation of the metal surface.

### **3 Conclusions**

3. All of the surface preparation methods are contributed to the enhancement of chemical bonds between the metal surface and epoxy adhesive
4. Any type of preparation technique has common objectives as the removal of grease and chemical contaminants, and the removal of weak layers on steel surfaces

5. Before the CFRP bonding should be confirmed chemically active surface and absence of any contaminations
6. The capacity of load transfer through the composite is governing by bond performance
7. Therefore, bond is a critical for performance evaluation. surface conditions are most effective parameter in the case of bond

### **Acknowledgements**

The authors gratefully acknowledge the support of the IT laboratory staff of the Department of Civil Engineering at the University of Moratuwa for their support.

### **References**

- Baldan A. Adhesively-bonded joints and repairs in metallic alloys, polymers and composite materials: adhesives, adhesion theories and surface pretreatment. *J Mater Sci* 2004;39:1–49.
- Hollaway L, Cadei J. Progress in the technique of upgrading metallic structures with advanced polymer composites. *Progr Struct Eng Mater* 2002;4:131–48.
- Schnerch D, Dawood D, Rizkalla S, Sumner E. Proposed design guidelines for strengthening of steel bridges with FRP materials. *Constr Build Mater* 2007;21:1001–10.
- Harris A, Beevers A. The effects of grit-blasting on surface properties for adhesion. *Int J Adhes Adhes* 1999;19:445–52.
- Schnerch D, Stanford K, Sumner E, Rizkalla S. Bond behavior of CFRP strengthened steel bridges and structures. *Proceedings of the International Symposium on Bond Behaviour of FRP in Structures (BBFS '05)*; 2005; International Institute for FRP in Construction;
- Monfared A, Soudki K, Walbridge S. CFRP reinforcing to extend the fatigue lives of steel structures. *Proceedings of the Fourth International Conference on FRP Composites in Civil Engineering (CICE '08)*; 2008; Zurich, Switzerland.

- Jiao H, Mashiri F, Zhao X-L. A comparative study on fatigue behavior of steel beams retrofitted with welding pultruded CFRP plates and wet layup CFRP sheets. *Thin-Walled Structures*. 2012;59:144–152.
- Wu G, Wang H, Wu Z, Liu H, Ren Y. Experimental study on the fatigue behavior of steel beams strengthened with different fiber-reinforced composite plates. *Journal of Composites for Construction*. 2012;16(2):127–137.
- Tavakkolizadeh M, Saadatmanesh H. Fatigue strength of steel girders strengthened with carbon fiber reinforced polymer patch. *Journal of Structural Engineering*. 2003;129(2):186–196.
- Teng J, Fernando D, Yu T, Zhao X. *Advances in FRP Composites in Civil Engineering*. 2011. Treatment of steel surfaces for effective adhesive bonding; pp. 865–868.
- Kim YJ, Harries KA. Fatigue behavior of damaged steel beams repaired with CFRP strips. *Engineering Structures*. 2011;33(5):1491–1502.
- Deng J, Lee MMK. Fatigue performance of metallic beam strengthened with a bonded CFRP plate. *Composite Structures*. 2007;78(2):222–231.
- Schnerch D, Dawood M, Rizkalla S, Sumner E. Proposed design guidelines for strengthening of steel bridges with FRP materials. *Construction and Building Materials*. 2007;21(5):1001–1010.
- Hashim SA. Adhesive bonding of thick steel adherents for marine structures. *Marine Structures*. 1999;12(6):405–423.
- Hollaway L, Cadei J. Progress in the technique of upgrading metallic structures with advanced polymer composites. *Progress in Structural Engineering and Materials*. 2002;4:131–148.
- Harris AF, Beevers A. The effects of grit-blasting on surface properties for adhesion. *International Journal of Adhesion and Adhesives*. 1999;19(6):445–452.

## INFLUENCES OF ENVIRONMENTAL FACTORS IN CFRP-STEEL BONDING: STATE OF THE ART

S. Abeygunasekera<sup>1\*</sup>, J. C. P. H. Gamage<sup>2</sup>, S. Fawzia<sup>3</sup>

<sup>1</sup> Postgraduate, University of Moratuwa, Katubedda, Moratuwa, Sri Lanka.

<sup>2</sup> Senior Lecturer, University of Moratuwa, Katubedda, Moratuwa, Sri Lanka.

<sup>3</sup> Senior Lecturer, Queensland University of Technology, Australia.

\* E-mail: abeygunasekarasampath@gmail.com, TP: +94712227790

**Abstract:** CFRP material has become a super hero material during the past decade, owing to specific characteristics of this material - such as light weight, high strength, fatigue and corrosion resistance, easy to install and excellent strength gained compared with conventional repair techniques. CFRP based retrofitting techniques are utilized with concrete, steel, masonry and wooden structures. However, performance and durability of this technique is depend on several internal and external factors. Internal factors can be identified as properties of material, installation method, number of CFRP layers attached with parent materials and the module of CFRP material. Significantly influencing external factors are magnitudes of loads, loading frequency, stress ratio and environmental factors. Over the past decade, CFRP has been established as an excellent retrofitting material to be used for strengthening steel structures. This paper presents a state-of-the-art review on the effects of environmental factors on bond performance of CFRP/steel strengthen under the influence of critical environmental factors such as humidity, temperature, UV concentration effects and combined effects of two or more factors. This is because all of these structures are frequently exposed to such an environmental condition during their service life.

**Keywords:** *relative humidity; thermal effects; temperature effects; CFRP/steel bond*

## 1. Introduction

CFRP related investigations have been conducted by many researchers throughout the world. The study area has focused on numerous parametric studies. There are bond performance, loading methods, surface preparation, characteristics of material and epoxy and effects of environmental parameters on bond durability as well as failure mechanisms. One of the key research available in the literature is understanding of environmental factors which influenced on CFRP/steel bond performance. This kind of investigations can be further classified as influencing on thermal effects, moisture level and UV effects. However, performance and durability of CFRP related applications depend on a vast number of variables. Evaluation of overall performance and long-term durability under real environmental conditions is not reported in the literature. On the other hand, similar investigations conducted by different authors, have different conclusions.

Jones et al. (2003) has observed the cracks propagated behind the CFRP strips and the failure mode was reported as de-bonding. Y et al. (Y et al., 2006) noted the premature de-bonding of the CFRP strip from the steel surface. Pipinato1 et al (Pipinato1 et al., 2012) has reported that the failure mode depends on modulus of elasticity of the CFRP, type of adhesive and thickness of the adhesive layer. Bocciarelli.M et al.(Bocciarelli.M et al., 2009) has shown that failure mechanisms start with initial de-bonding at the plate end and failure propagates along the element in the interfaces. However, failure mechanism is not uniform, and it is combined with a failure mode as interface de-bonding and CFRP de-lamination.

Therefore, results of each investigation have no uniformity regarding strength gain and fatigue strength owing to varyig results from author to author. The reason behind the different results is because performance does not only depend on a unique parameter. Because, performance is depending on the environmental parameters such as temperature, salt environment, humidity level, freeze/thaw condition. However, most of the laboratory tests are conducted under controlled conditions. Most of the parameters and environmental factors are kept as a constant during the testing. As a result, the actual outcome may deviate from the estimated results. Also, results may change from author to author. On the other hand, the combination of two or multiple parameters is involved with the final outcomes and real environmental conditions are beyond human control. Since analysis of the effects of all parameters simultaneously is practically impossible, prediction is more complicated, and the results vary in a wide range. Most possible influences parameters are summarized in Table 1.

Table 1: Summarizes parameters influence on CFRP/steel bond performance

Parameter	Description
Properties of CFRP material	Type of CFRP (NM, HM), physical dimensions, Module of elasticity, poisson ratio, Young's modules, yield strength, elongation%
Characteristic of epoxy	Type of adhesive, curing time, glass transition temperature, viscosity, poisson ratio,
Environmental condition	Temperature, salt environment, humidity level, freeze/thaw,UV effect,
Sample type	Beam, plate, actual size, small size, geometry of coupon, etc (Basically shape and size effect)
Loading pattern	Constant amplitude, variable amplitude or cyclic with impact or non-impact rate of loading, etc.
Load applying method	Tensile, compression, bending, flexure,3-point bending, four-point bending, fatigue load range
Sample shape	Side Notched beam/plate, center hole plate
Bonding characteristics	Bond length, effective bond length, number of CFRP layers, whether single side or double side lamination
Installation procedure	Thickness of adhesive layer, surface preparation, air bubble removing methods, method of adhesive applying
Condition of structure	pre-stress, without stress, corrosion, stress distribution pattern
Stress conditions	Stress ratio, stress ranges, pre-stresses
Joint type	Single lap, double lap, bridging effect due to the adhesive in the gap
Specimen preparation	Sand blasting, grinding, degreasing and vacuum

## 2. Influences of environment factors

The main objective of this review is to understand environmental factors that influence on bond performance. Effective parameters are humidity level, temperature variation and UV effects or combined effects of two or more factors. Furthermore, to highlight correction factors and design guidelines available in the literature regarding environmental effects.

## **2.1 Effects of moisture level (Relative Humidity)**

Ingress of moisture to the CFRP/steel bonding joint can be considered as a major problem regarding bond performance. The reason is both epoxy adhesive and CFRP materials are allowed to penetrate water molecules into the bonded joint. The result of water absorption attraction between CFRP/steel and epoxy/steel bond becomes a weakness. On the other hand, moisture absorption of CFRP matrix causes changes in the physical shape of CFRP material. Physical changes of epoxy material have a tendency to reduce the glass transition temperature ( $T_g$ ). According to investigations of Collings.T et al.(Collings.T et al., 1993) and Hollaway.L (Hollaway.L, 2010) moisture is effectively responsible for the failure of fiber matrix. Kumar.S et al.(Kumar.S et al., 2008) has found that water absorption contributes to reduce the shear strength of the polymer due to swelling, plasticization and softening effects. Swelling is remarkable in the thickness of the laminates and it causes to significantly decrease the tensile strength. Zhang.A et al.(Zhang.A et al., 2012) reported 1% moisture absorption by the CFRP laminates causes to decrease bending strength around 17% after 14 days curing time. However, Nguyen.T et al (Nguyen.T et al., 2012) demonstrated excellent durability of CFRP materials against severe environmental conditions and that decreases of strength and stiffness is negligible.

### **2.1(a)Moisture absorption**

CFRP materials have shown excellent resistance to corrosion and chemical attacks. However, salt water may affect the material because salt can easily penetrate the fiber matrix. Tavakolizadeh.M et al (Tavakolizadeh.M et al., 2010) examined the effects of various types of CFRP materials' exposure to chemical solutions. Results showed that CFRP sheets display excellent durability. However, the authors concluded that mechanical properties are slightly decreased due to results of moisture absorption. Nguyen.T et al (Nguyen.T et al., 2012) examined the behavior of tensile strength of CFRP/steel joints under a salted environment. The amount of tensile strength reduction was reported as 17%. Rege.S & Lakkad.S,(Rege.S & Lakkad.S, 1983) and Hollaway.L (Hollaway.L, 2010) also conducted similar investigations and reviewed the ingress of moisture affects for the CFRP matrix.

### **2.1(b)Moisture absorption rate at the beginning**

According to the experiments conducted by Nguyen.T et al.(Nguyen.T et al., 2012) the rate of moisture absorption is very fast at the beginning and after that it reached a constant level. However, the ambient temperature controlled the quantity of water absorption by the CFRP material. This research



pointed out that water absorption of bulk adhesive was 4% and 5% at the temperatures 20 °C and 50 °C, respectively.

### **2.2 The humidity effects on epoxy adhesive**

The humidity level is affected on epoxy adhesive and it affects the CFRP/steel bond performance. Lettieri.M & Frigione.M, (Lettieri.M & Frigione.M, 2012) reported that huge amounts of water (above 75%) is absorbed by the epoxy material. In addition, noted, the glass transition temperature (T<sub>g</sub>) of the adhesive is reduced through plasticization. Due to the penetration of water through CFRP/ steel bonds it has become weak. Because cohesive force (Hydrogen bond or other valance bond) of adhesive molecules is weak due to polymer inflaton and the result is de-lamination failure. However, a study of Wu et al. (2004) showed that exposure to a small amount of moisture (<2%) is improved by the curing rate and it contributes to enhance the bonding strength of CFRP/steel.

### **3. Thermal effects**

Thermal energy also critically influenced the CFRP/steel bond performance. It can be described as two way as thermal cycles and freezing conditions. Generally, a vast number of studies have confirmed that high temperature is an unfavourably influence on CFRP/steel bonds. However, a CFRP material shows excellent resistivity against elevated temperatures of the environment. However, epoxy resins cannot tolerate temperature elevation and adhesive layer between CFRP and steel is highly sensitive to temperature. According to the temperature sensitivity, strength and stiffness of CFRP/steel bonds rapidly decrease. Usually this happens when environmental temperature exceeds the glass transition temperature (T<sub>g</sub>) of epoxy materials. Ishikawa et al (Ishikawa et al., 2006) showed co-relation between mechanical properties and temperature. The authors concluded that mechanical properties of CFRP/steel bonds reduce with temperature. Viscosity of epoxy increases due to the effects of temperature; the ultimate result is the rapid reduction of the strength and stiffness of the bonds.

Generally, the glass transition temperature (T<sub>g</sub>) range of epoxy adhesives varies from 40 °C to 70 °C. However, Stratford and Bisby (2012) showed that joint is starting to slip before the glass transition temperature of the adhesive. The overall result is the reduction of strength before the transition temperature. Furthermore, the authors reported that a joint slip starts at around 40 °C and its peak at around T<sub>g</sub> (65 °C). Since, ultimate load bearing capacity is reduced when the temperature reaches T<sub>g</sub>. Nguyen.T et

al.(Nguyen.T et al., 2012) estimated that the reduction of ultimate load bearing capacity varies under different elevated temperature conditions. The results were recorded at 15%, 50%, and 80% strength change when the temperature reached  $T_g$ ,  $10\text{ }^{\circ}\text{C}$  above  $T_g$ , and  $20\text{ }^{\circ}\text{C}$  above  $T_g$ , respectively.

### **3.1 Influence of Temperature**

The CFRP Steel bond must show good temperature tolerability under elevated and freezing conditions of the environment. Investigations conducted by Gillespie J W (Mertz.D.R & Gillespie.J.W, 1996) regarding bridges in North America have reported that the selected adhesive has indicated good environmental durability. In general, high temperature causes to reduce the bond performance. However, it should be lower than the glass transition temperature of the adhesive. Stratford.T & Bisby.L(Stratford.T & Bisby.L, 2012) have investigated temperature behavior and the test result has shown that the glass transition temperature of the adhesive was  $65\text{ }^{\circ}\text{C}$ , and that the joint slip started at around  $40\text{ }^{\circ}\text{C}$ . Further, it reached the peak value at  $T_g$  (Glass Transition Temperature).

### **4. Influence of ultraviolet radiation**

Ultraviolet radiation is a part of sunlight and it causes to split the bond of molecules of the polymers. Bond dissociation is initiated due to absorption of the ultraviolet radiation. Dissociation is continued as a subsequent reaction with oxygen in the atmosphere. However, the depth of degradation is only up to a few microns. The damaged area can be identified as the location of the high stress concentration. Recent research studies proved that when the CFRP materials is exposed to artificial sunlight, it causes to variate the tensile strength. Test result reported that tensile strength decrease range varies from 15% to 20%. (Ishikawa et al., 2006) and (Tavakolizadeh.M et al., 2010) strongly recommended that the composite material should be protected from UV radiation because UV radiation with CFRP material is more vulnerable than any other environmental effect. However, Lettieri.M & Frigione.M,(Lettieri.M & Frigione.M, 2012) suggested that UV radiation does not significantly affect the change in tensile strength and stiffness of CFRP.

CFRP/steel double lap strap joint when exposed to UV radiation with at  $40\text{ }^{\circ}\text{C}$  temperature reported a 35 % of tensile strength reduction. However, radiation without temperature does not affect the change of tensile strength. Therefore, stiffness reduction is mainly governed by the temperature alone. The effects of UV are insignificantly influenced. Some authors suggested

that the adhesive is the crucial component of UV exposure in the CFRP system. However, further investigations regarding the effect of UV on CFRP/steel are required.

### **5. Combined effects of environmental factors on CFRP/steel bond**

In the real-world applications most of the above parameters are jointly affected on bond performance. However, few investigations have been conducted regarding the effects of joint influences of environmental factors. CFRP/steel bonds are available in the literature. The influence of combined environmental factors is more complicated in the process of analysis. Most of the existing literature is focused on investigation of moisture and temperature (hygro-thermal) effects on CFRP/steel bond. Aoki et al (2008) reviewed that hygro-thermal exposure significantly contributes to reduce of the glass transition temperature of epoxy material.

Combination of temperature and relative humidity (50 °C – 93% RH) has been investigated by Shan et al. (2011) for the I- beams. Bending tests were conducted after 15, 45, and 90 days and reported a remarkable reduction of the ultimate load carrying around 22%, 26%, and 57% respectively. Nguyen (2012) investigated the effect of hygro-thermal for double lap shear strap joints under two scenarios. In the first case the constant temperature and humidity (50°C– 90% RH) is taken into consideration. The second case has the thermal cycles (20–50 °C) with constant humidity (90% RH). Both scenarios have showed a reduction of tensile strength. However, the reduction of stiffness was reported as lower than 10 %. According to the investigation of combined effect of hygro-thermal, the glass transition temperature ( $T_g$ ) of the adhesive is changed and result is that the joints fail under lower tensile loads. The authors concluded that the bond performance greatly depends on temperature as well as time. However, Kim, Y. (2012) reported that the average tensile load capacity of specimens increased by 31 % under wet/dry conditions for double lap shear joints. 17 % of capacity improvement has been noted under freeze thaw conditions. However, probably, additional curing of epoxy adhesive may cause such abnormal results. Double strap CFRP/steel joints subjected to 5% salted water at 20 °C and 50 °C during 12 months time period. Strength decreases of the joints has been reported as 15% and 26% respectively. Furthermore, Dawood M (Dawood M, 2010) have observed rapid degradation duration from 2 to 4 months period. Nguyen.T et al (Nguyen.T et al., 2012) examined the combined effect of a severe environmental condition. The authors have considered a high temperature (38 °C), salted water (5%) and sustained load for double lap shear joints. Results concluded that such factors highly influenced to change mechanical properties of joints.

### 6. Correction factors for environmental effects

Environmental factors are always changing and impossible to control as a uniform level. Under the laboratory conditions it can be controlled up to a certain level. However, in field applications, it is impossible to control the effects of moisture, temperature and UV effects individually or combined. Therefore, correction factors have been introduced in literature to minimize the influences of environmental effects on final results. There are three main guidelines that are shown in Table 2, Table 3 and Table 4 as, Italian Guidelines, CIRIA and ICE respectively.

**Table 2:** Environmental Reduction Factors, (Italian Guidelines)(National Research Council Advisory Committee, 2007)

Exposure Conditions	Types of FRP/Resin	$\eta_a$	Loading Mode	Type of FRP/Resin	$\eta_i$
Internal environment	Glass/epoxy	0.75	Continuous (Creep and relaxation)	Glass/epoxy	0.3
	Aramid/epoxy	0.85		Aramid/epoxy	0.5
	Carbon/epoxy	0.95		Carbon/epoxy	0.8
External environment	Glass/epoxy	0.65	Cyclic	All	0.5
	Aramid/epoxy	0.75			
	Carbon/epoxy	0.85			
Aggressive environment	Glass/epoxy	0.5			
	Aramid/epoxy	0.7			
	Carbon/epoxy	0.85			

**Table 3:** Environmental related partial factors, CIRIA guidelines(Cadei G, Stratford T, Hollaway L, 2004)

Partial factor parameter	Parameter value	Partial factor

Environmental factor	Adhesive properties determined for the environmental condition in service	1.0
	Adhesive properties determined for the environmental conditions different from service conditions	2.0

Table 4: Recommended values for partial safety factors for adhesive joint, ICE guidelines(McQuillan, 1999)

Partial factor parameter	Parameter value	Partial factor
Environmental condition	Service conditions Outside conditions	2.0
	Adhesive properties determined for service condition	1.0

Humidity and extreme temperature are causes that reduce the durability of CFRP/steel bond. Generally, long term exposure to wet environment or ocean spray is highly affected for bonds weak. Main reasons for such behavior are increases of the surface energy and displacement of the secondary bond between steel and adhesive. However, a water-resistant sealant can control such behaviour. The combination of a nonconductive barrier also significantly controlled the rate of corrosion. GFRP material is reducing the moisture absorption of the bond. In addition, the use of GFRP material act as a protective layer and it causes to control corrosion of the metal. Temperature is causes to change bond performance because it is effects on glass transition temperature of adhesive material. De bonding and de-lamination of CFRP bond is govern by the temperature of the environment.

## 7. Conclusions

This paper has reviewed some of the influential research papers presented so far in order to understand the bond performance and durability of CFRP strengthened steel joints. This summarizes the effects of relative humidity,

temperature and UV effects. Effects of the environmental factors critically influence on bond performance and durability. In addition, the existing guidelines and correction factors for influences of environment is discussed here in available literature. Furthermore, the following conclusions were obtained:

1. Bond performance, durability and failure mode are critically influenced on environmental factors
2. Humidity and extreme temperature are causes that reduce the durability of CFRP/steel bond
3. Temperature is causes to change bond performance because it is effects on glass transition temperature of adhesive material
4. Combined effects of several factors on bond performance, durability and failure mode
5. Highest influencing factor is moisture level and most critical combination is influences of hygro thermal (Temperature moisture effects)
6. GFRP material is reducing the moisture absorption of the bond and act as a protective layer to control corrosion of the metal

### **Acknowledgements**

The authors gratefully acknowledge the support of the staff in the computer laboratory, the Department of Civil Engineering at the University of Moratuwa for their valuable support.

### **8. Future work**

Future research work is needed to validate accelerated environmental tests so that the actual environmental conditions are simulated. The bond behaviour of the strengthened members subjected to dynamic loading (fatigue and impact) should be thoroughly investigated especially under severe exposure conditions. Long term behaviour of the CFRP/steel bonded joint under different loading and the environmental conditions should be implemented. Further, the factors affecting the bond-slip models should be studied in order to make the relationship more reliable and useful.

### **References**

Bocciarelli.M, Colombi.P, Fava.G, & C, and P. (2009). Fatigue

- performance of tensile steel members strengthened with CFRP plates. *Composite Structures*, 87(4), 334–343.
- Cadei G, Stratford T, Hollaway L, D. W. (2004). Strengthening metallic structures using externally bonded fiber reinforced polymer. *Construction Industry Research and Information Association (CIRIA)*, London, UK.
- Collings.T, Harvey.R, & Dalziel.W. (1993). The use of elevated temperature in the structural testing of FRP components for simulating the effects of hot and wet environmental exposure. *Composites*, 24, 625–34.
- Dawood M, R. S. (2010). Environmental durability of a CFRP system for strengthening steel structures. *Construction Building Materials*, 24, 1682–9.
- Hollaway.L. (2010). A review of the present and future utilization of FRP composites in the civil infrastructure with reference to their important in-service properties. *Construction Building Materials*, 24, 2419–45.
- Ishikawa, T., Okura, I., & Kita, N. (2006). Debonding Shear Stress in Steel Plates with a Fiber Sheet Inserted under a CFRP Plate. *JSCE Journal of Structural Engineering*, 52A, 1317–1326.
- Kumar.S, Sridhar.I, & Sivashanker.S. (2008). Influence of humid environment on the performance of high strength structural carbon fiber composites. *Mater SciEng*, 498, 174–8.
- Lettieri.M, & Frigione.M. (2012). Effects of humid environment on thermal and mechanical properties of a cold-curing structural epoxy adhesive. *Construction Building Materials*, 30, 753–60.
- McQuillan, D. (1999). The structural use of adhesives. *Institution of Structural Engineering*, London, UK.
- Mertz.D.R, & Gillespie.J.W. (1996). Rehabilitation of steel bridge girders through the application of composite materials. *NCHRP Report No. 93-ID11, Transportation Research Board, Washington*, 1–20.
- National Research Council Advisory Committee. (2007). Guidelines for design and construction of externally bonded FRP systems for strengthening existing structures – metallic structures. *National Research Council*, Rome, Italy.
- Nguyen.T, Bai.Y, Zhao.X, & Al-Mahaidi.R. (2012). Durability of steel/CFRP double strap joints exposed to sea water, cyclic

- temperature and humidity. *Composite Structures Struct*, 94, 1834–45.
- Pipinato<sup>1</sup>, A., Pellegrino<sup>1</sup>, C., & Modena, C. (2012). Fatigue Behaviour of Steel Bridge Joints Strengthened with FRP Laminates. *Modern Applied Science*, 6 (10)(ISSN 1913-1844 E-ISSN 1913-1852), Published by Canadian Center of Science and Educat.
- Rege.S, & Lakkad.S. (1983). Effect of salt water on mechanical properties of fi-ber reinforced plastics. *Fiber Sci Technol Ogy*, 19, 317–24.
- Stratford.T, & Bisby.L. (2012). Effect of warm temperatures on externally bonded FRP strengthening. *J Composite Construction*, 16, 235–44.
- Tavakolizadeh.M, Saadatmanesh.H, & Mostofinejad.D. (2010). Environmental effects on mechanical properties of wet lay-up fiber reinforced polymer. *ACI Mater J*, 107, 267–74.
- Y, Z., L, Y., X, L., & Q, Y. (2006). Experimental Study on Fatigue Behaviour of Tensile Steel Plates Strengthened with CFRP Plates. *Third International Conference on FRP Composites in Civil Engineering (CICE 2006)*, December, 13-15 Miami, Florida, USA.
- Zhang.A, Li.D, & Zhang.D. (2012). Effect of moisture absorption on the bending strength of CFRP. *Adv Mater Res*, 450, 482–5.



# LOW CYCLE FATIGUE BEHAVIOUR OF STEEL/CFRP COMPOSITE EXPOSED TO LOADS WITH CONSTANT AMPLITUDE.

S. Abeygunasekera<sup>1</sup>\*, J. C. P. H. Gamage<sup>2</sup>, S. Fawzia<sup>3</sup>

<sup>1</sup>Postgraduate, University of Moratuwa, Katubedda, Moratuwa, Sri Lanka.

<sup>2</sup>Senior Lecturer, University of Moratuwa, Katubedda, Moratuwa, Sri Lanka.

<sup>3</sup>Senior Lecturer, Queensland University of Technology, Australia.

\* E-mail: abeygunasekarasampath@gmail.com, TP: +94712227790

**Abstract:** This paper investigates fatigue strength gain with respect to un-strength steel structures under Low Cycle Fatigue (LCF). Three point flexural cyclic load was applied to the specimens with 5 Hz frequency and 2 kN constant loads amplitudes. The Coffin-Manson relation was used to explain the behaviour of LCF cycles. The effects of Carbon Fiber Reinforced Polymer (CFRP) strengthening of steel subjected to LCF was investigated. CFRP strengthened steel indicated a significant improvement in the fatigue life. This retrofitting technique reported excellent performance; in the range between 26.8 % and 36.52 % .

**Keywords:** CFRP, fatigue, three points flexural cyclic load, LCF.

## 1. Introduction

In general 90% of failures of metallic structures have been reported due to fatigue stress. However, most steel structures such as bridges, aircraft, and machine components were made aware of cyclic stress during their operation. Structural failure could happen below the tensile or yield strengths of the material due to cyclic stresses. Generally, fatigue failure displays catastrophic features and they would be unrecoverable and sudden. These have been named as engineering disasters. Fatigue failure consists of three steps which includes crack initiations, propagation and failure. Cyclic stresses can be classified as maximum, minimum and mean stress. The range of stress, its amplitude, the stress ratio, the stress range, the number of cycles, CFRP bond length, number of CFRP layers, crack stop hole and pre-stressing technique mainly influence performance of CFRP bonds of structures. According to Zheng et al. (2005), the available research work regarding fatigue strengthening is limited. On the other hand, most of the available literature has reported a significant strength gain of CFRP system.

Research series developed by Colombi et al. (2003), Deng et al. (2005), Jones et al. (2003), Monfared et al. 2008, Nozaka et al. (2005), Täljsten et al. (2008) and Jones et al. (2003) have examined the behavior of notched and hole drilled specimens with a constant amplitude sine wave and results have been reported as follows;

- 1) A considerable increase in the fatigue life of the strengthened specimens up to 115%
- 2) The CFRP strips did not fracture. The crack propagation behind the CFRP strips from steel is de-bonding and it does mainly govern by tension.
- 3) Surface preparation, proper use of adhesive, and the method of adhesive application can influence significant change of the behavior of the test specimen. To avoid such a situation sand blasting, vacuuming, and degreasing the steel surface were recommended.
- 4) Applying CFRP strips to damaged steel specimens not only prolonge fatigue life, but also delayed the onset of fatigue crack propagation.

- 5) Covering the center hole resulted in an increase in the fatigue life of the strengthened system about two times that of a specimen with CFRP strips applied on either side of the hole.

Retrofitting of steel structures using a CFRP patch has been investigated by Zheng et al. (2006). A study has been concerned with stress range, strengthening method and stiffness of CFRP. The following findings were noted as test results:

- 1) Externally bonding CFRP strips dramatically increased the fatigue life and strengthen gain range reported 155~580% over un-strengthened specimens.
- 2) Identifying the effectiveness of CFRP strips when higher modulus CFRP strips bonded both sides of the steel plates;
- 3) Premature de-bonding of the CFRP strip from the steel surface has been reported in specimens with low elastic modulus of CFRP.

Bassetti et al. has conducted a series of fatigue tests to understand how various factors affect the bond performance. Pre-stressing level, thickness of CFRP layer and the adhesive material properties has been the focus in this study. In all the scenarios it has been shown that there is a significant fatigue life improvement after apply certain types of CFRP materials. Jones and Civjan have experimentally and numerically investigated the fatigue behavior of under several variables. The type of CFRP material, thickness, surface preparation technique and symmetric or non-symmetric repair have been identified as key factors.

Effective factors have further been described using a series of fatigue testing conducted by Domazet, (1996), Bassetti et al., (1998), Okura et al., (2000), Suzuki, (2002), Suzuki and Okamoto, (2003), Tavakkolizadeh and Saadatmanesh, (2003), Jones & Civjan, (2003) and Matta, (2003). In fact, the above studies have confirmed the enhancement of fatigue life with application of CFRP materials. Furthermore, major factors such as stress range of fatigue cycles, number of CFRP layers, CFRP bond length, crack arrest

hole and pre-stressing technique were identified too. Liu et al. (2005) investigated the fatigue bond behavior of CFRP /steel interfaces. The following key findings have been noted by the researcher;

- 1) No fatigue failure occurred until the load was less than 40% of the static strength of the strengthened specimens
- 2) The influence of fatigue loading on the bond strength was insignificant (less than 10%) if the maximum applied load was less than about 35% of the specimen's static strength
- 3) A reduction in the bond-slip stiffness was observed due to the accumulated damage caused by the fatigue loading

The fatigue failure modes were not significantly affected by the range of applied stresses except for those bonded with high modulus CFRP, where fibres had fractured in several locations. The behavior of steel frames strengthened with CFRP under cyclic load were investigated by Mosallam et al. (1998). The authors reported that test result achieved acceptable ductility ranges. Authors concluded that CFRP repair technique provided comparatively more than 1.25 times strength gain with respect to the control specimen. An experimental program was carried by Tavakkolidazeh & Saadatmanesh (2003) to test the behaviour of retrofitted notched steel beams with CFRP patches for medium cycle fatigue loading. Based on experimental observations, a CFRP patch tends to extend the fatigue lifetime and as well as decreases the crack growth rate. Furthermore, Tavakkolizadeh et al. (2003b) have also reported that CFRP strip overlay not only extend the fatigue life but also decreases significantly the crack growth rate. The test results proved that there is a strength gain more than three times and the stable crack growth rates decrease by an average of 65%. Buyukozturk et al. (2003) conducted an experimental study involving fatigue testing of side notched steel specimens repaired with FRP patches of various widths and lengths. The study has confirmed the effectiveness of the technique by increased their fatigue lives with the width and length at CFRP sheet. Investigations by Bocciarelli et al., (2009) have

proved that CFRP exhibits better fatigue performance than welded cover plates methods . Lua et al.,(2005) Yuan et al., (2004) , Yao, Teng, and Chen, (2005) and Pellegrino, Pipinato, and Modena, (2011) have also confirmed fatigue performance of CFRP based strengthen technique successfully through their research studies. Many laboratory experiments conducted by several researchers have proven the effectiveness of CFRP-bonded reinforcement technique. Sreedhar. K (2013) has affirmed CFRP's ability to improve the load carrying capacity and service life of metallic members. Research studies done by Sreedhar K et. al (2014) have also investigated the steel sections ability to gain strength. Authors have confirmed resistivity of higher load capacity, high potential to extend fatigue life and less probability of crack propagation with CFRP. According to Cadei et al.(2004). CFRP sheets and strips can be effectively used in restoring the lost capacity of a damaged steel section.

Special characteristics of CFRP materials and compatibility with steel are the main reasons for the popularity of this technology. Reinforced polymer materials display a high strength-to weight ratio, a less negative effect due to corrosion, high stiffness, high tensile strength, low weight, high chemical resistance, high temperature tolerance and low thermal expansion. CFRP has also proven to be not only the enhanced of strength but also rigidity of retrofitted member. Strength is caused by resistance to breaking whereas rigidity is caused by bending or stretching.

## 2.0.Test specimens

A total of twenty four steel plates, identical in their dimensions, having rectangular cross-sections of 40 mm width and 5 mm thickness were tested. The length of the plate member was chosen to be 280 mm and the effective span was 240 mm depending on workability , test facility at laboratory and testing standard for a three-point flextural test.

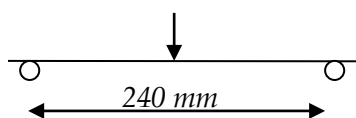


Figure 1:Schematic diagram of the test setup(not to scale)

### 2.1. Specimen preparation

Prior to the application of CFRP, the plate surface was prepared by grinding to a white metal finish to achieve a rough surface for better bonding as shown in Figure 2. At this stage the bottom surface of the steel plate was cleaned. Acetone was used to remove the deposited dust particles ,weak layer, and grease. Primer was applied with a brush on acetone cleaned surface for 12 specimens prior to applying epoxy adhesive as showan in Figure 3 and allowing it to dry for approximately 5 to 8 hour. These 12 specimens were considered as treated surfaces. A two part epoxy adhesive(Arelldite 420) was properly mixed in 1:2 ratio by volume and applied to pre-treated steel surface during its pot life according to manufacturer guidelines[ ]. The CFRP strips were cut to the dimensions with 240 mm length and 40 mm width.The fiber layer of CFRP fabrics (MBRACE CF 130) oriented longitudinally to the length of the plate as shown in Figure 4.A rib roller was used to press the fabric and to remove air bubbles entrapped in the bond. Also, the rib roller was run along the direction of the fiber.CFRP adhesive specimens kept for a period of at least 24 hours for curing.Two specimens were selected as control specimens for both strength and un-strength cases.



Figure2 :Cleaned steel plate



Figure 3 :Primer coted steel plate



**Figure 4 : CFRP patched with steel plate**

## 2.2. Test setup and instrumentation

The test setup and apparatus are shown in Figure 5. A 2 kN constant magnitude load with 5Hz frequency was applied. The load was applied by using a hydraulic actuator which is controlled by an electronic circuit with “Arduino” program. The load was applied as “flexural cyclic load” at a constant rate. The load was continued up to 10,000 cycles with 2000 steps as shown in Table 1.



**Figure 5:Test setup to apply cyclic flexure load**

**Table 1:Average Yield stress of steel vary with number of cycle**

Number of cycles	Number of samples	Average Yield stress(MPa)
0	2	342.00
2000	2	341.75
4000	2	337.35
6000	2	320.00
8000	2	313.00
10000	2	307.35

## 3.0. Test procedure

In this test setup, a single layer of CFRP was attached to the steel plate at the bottom surface as shown in Figure 4 , because the tendency of crack initiation is higher at the bottom surface. A cyclic load is applied on specimens with 2 kN magnitudes and 5 Hz frequency. Dimensions of the CFRP layer were selected as 240 mm length and 40 mm width. Uni- directional CFRP material was selected and it is commercially denoted as CF 130.The thickness of CFRP layer was taken as 0.167 mm according to the data sheet provided by the manufacturer. Young’s modulus and Poisons ratio of the material was taken as 240 GPa and 0.28, respectively.

CFRP strengthen specimens were kept on two cylindrical shaped, supportive rollers with 25 mm diameter each and the span was fixed at 240 mm between centers of the rollers as shown in Figure 5. The specimen was loaded with a range of low cycle fatigue (LCF). A cyclic load was applied to the specimen at the mid-plane using a 8 mm radius loading nose (Figure 5). The load is applied at mid-plane of the specimen. Maximum deflection in the load direction (Y direction) at mid-plane was limited to 5 mm. The magnitude of the frequency was selected according to the ASTM D7774 standards. A constant amplitude 2 kN load was applied to the sample. During the testing period, a 5 Hz frequency was maintained. A parametric study was conducted by varying the number of cycles and without bonding of CFRP.

After applying the cyclic loads , the sample was removed from the cyclic loading machine and was attached to the tensile testing machine as shown in Figure 7.Tensile loads were applied on specimen with 2 mm/min rate of load and measure yield value of each specimen.This procedure was repeated for different stress cycles within the limits of LCF (Up to 10,000 cycles).Average value of yield load was measured for each specimen as shown in Table 1 and Table 2.



Figure 7 :Test setup to apply tensileload

#### 4. Result and Discussion

Stress concentration at the bottom surface is the main reason for crack initiation and it is governed by the residual stress. The residual stress is high due to the mechanical stress on the process of manufacturing such as cold forming and rolling. When the number of applied stress cycles gradually increases in the material, the stress decreases since, a comparatively less stress concentration is shown at the lower number of cycles. The load was continued up to 10,000 cycles with 2000 steps as shown in Table 2. When the number of cycles were increased further , the strength decreased as shown in Figure 8, because stress increases due to the cyclic loads. When the magnitude of the load and frequency of load becomes larger ,the strength gained should be drastically decreased. This is due to the increase of stress when compared to the low frequency. The bottom surface is retrofitted with CFRP and the strength gained by the plate was decreased as shown in Figure 9. because the CFRP layer contributed to reduce the stress at the bottom surface of the specimen.

Table 2: Average Yield stress of CFRP strengthened steel vary with number of cycle

Number of cycles	Number of samples	Average Yield stress(MPa)
0	2	442.35
2000	2	433.85
4000	2	431.75
6000	2	429.75

8000	2	426.75
10000	2	419.60

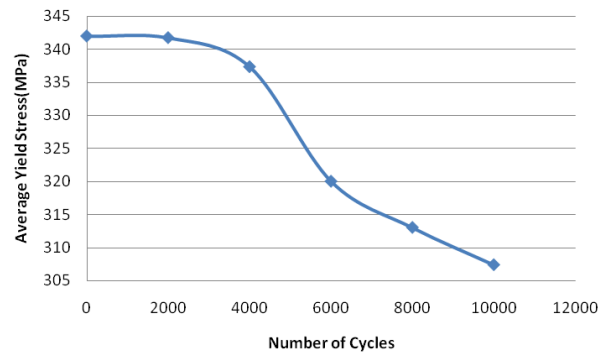


Figure 8:Average Yield stress variation with number of cycle

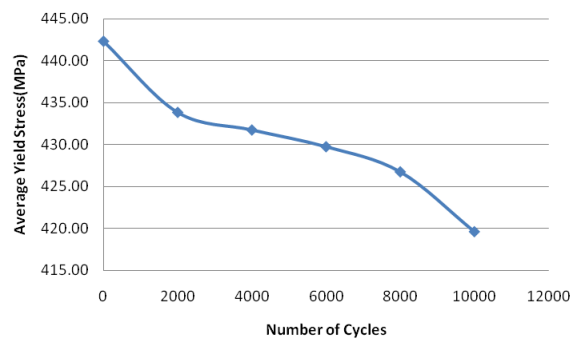


Figure 9:Yield stress of CFRP strengthened steel varies with the number of cycles

The Test results of the CFRP strengthened and un-strengthened plate was compared as shown in Table 03. It summarizes the Yield load values together with the variation of different number of loading cycles from the range of 2000 to 10,000. Strength due to the number of stress cycles compared with un-strengthened and CFRP strengthened steel plate is shown in Figure 10.

Table 3: Yield stress gain with CFRP under cyclic loads.

Number of Cycles	Bear Steel plate	CFRP strengthened steel plate	Gain of Yield stress(%)
0	342.00	442.35	29.3
2000	341.75	433.85	26.9

4000	337.35	431.75	28.0
6000	320.00	429.75	34.3
8000	313.00	426.75	36.3
10000	307.35	419.60	36.5

The variation of the yield strength gain of steel with respect to the number of stress cycles is shown in Figure 10. The comparison of the un-strengthen specimens and the CFRP strengthen specimens are shown in Figure 10. Low cycle fatigue is usually characterized by the Coffin-Manson relation conducted by the L.F.coffin in 1954 [23], S.S.Manson in 1953). When the number of cycles is increased from 0 to 10,000 it showed a similar pattern

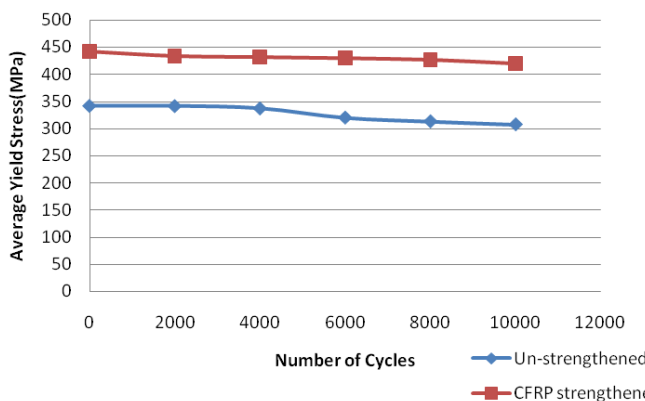


Figure 10: Comparison of strength gain for un-strengthen and CFRP strengthening plate

According to this study CFRP material exhibited a significant fatigue enhancement in percentage between 26.8 % and 36.3% with respect to an untreated specimen. This technique is performed in 0 to 10,000 ranges of the stress cycles of the specimen under 5 Hz frequencies with 2 kN constant amplitude loads.

#### 4.2. Discussion

When the CFRP layer was attached to the bottom surface of the specimen the effects of the tension load on bottom surface was considerably controlled as the tension flange shows a high tendency of fatigue failure rather than compression surface (upper side) of the specimen. CFRP laminate helps to reduce the stresses at the bottom of the surface. However, number of fiber layers, module of CFRP

material; lay-up angles and bond length significantly affects on the process of fatigue gain.

#### 5. Conclusions

In this investigation, steel was strengthened with externally bonded CFRP sheets which was tested under constant amplitude load under 5Hz loading frequency. The strength gained due to cyclic flexural load effects on steel plate were investigated in this study. Strength gained by CFRP was estimated for range of LCF. The following conclusions were obtained:

- 1) Stress concentration at the steel was effectively decreased with the application of CFRP material
- 2) The fatigue resistivity of steel plate could be significantly enhanced by the externally bonded CFRP sheet
- 3) This retrofitting technique reported the performance; which is in the range of 26.8 % to 36.3 % yield strength gain compared to the un-strengthen steel with the cycle range varies from 0 to 10,000.

#### Acknowledgements

The authors gratefully acknowledge the support of the staff in computer laboratory, as well as staff of the structural testing laboratory, Department of Civil Engineering, University of Moratuwa, Sri Lanka for their valuable support.

#### References

- Bocciarelli, M., Colombi, P., Fava, G. and Poggi, C. (2009) 'Fatigue performance of tensile steel members strengthened with CFRP plates', *Composite Structures*, 87(4), pp. 334-343.
- Buyukozturk, O., Gunes, O and Karaca (2003) 'Progress on Understanding De-bonding Problems in Reinforced Steel Members Strengthened Using FRP Composites.', *Proceedings of the Structural Faults and Repair on 10th International Conference & Exhibition*.
- Deng, J. and Lee, M.M.K. (2007) 'Fatigue performance of metallic beam

- strengthened with a bonded CFRP plate', *Composite Structures*, 78(2), pp. 222–231.
- Domazet, Ž. (1996) 'Comparison of fatigue crack retardation methods', *Engineering Failure Analysis*, 3(2), pp. 137–147.
- Cadei, J.M.C., Stratford, T.J., Hollaway, L.C. and Duckett, W.H. (2004) *Strengthening metallic structures using externally bonded fibre-reinforced polymers*. London: Design Guide.
- Jones, S.C. and Civjan, S.A. (2003) 'Application of fiber reinforced polymer overlays to extend steel fatigue life', *Journal of Composites for Construction*, 7(4), pp. 331–338.
- Jones, S.C. and Civjan, S.A. (2003) 'Application of fiber reinforced polymer overlays to extend steel fatigue life', *Journal of Composites for Construction*, 7(4), pp. 331–338.
- Jones, S.C. and Civjan, S.A. (2003) 'Application of fiber reinforced polymer overlays to extend steel fatigue life', *Journal of Composites for Construction*, 7(4), pp. 331–338.
- Matta, F. (2003). Bond Between Steel and CFRP Laminates for Rehabilitation of Metallic Bridges, Ph.D Thesis, University of Padua, Padua.
- Monfared, A., Soudki, K. and Walbridge, S. (2008) 'CFRP Reinforcing to Extend the Fatigue Lives of Steel Structures', *Proceedings of the Fourth International Conference on FRP Composites in Civil Engineering (CICE2008)*. Zurich, Switzerland
- Mosallarn, A.S., Chakrabarti, P.R. and Spencer, E. (1998) 'Experimental Investigation on the Use of Advanced Composites & High-Strength Adhesives in Repair of Steel Structures', *Proceedings of the 43rd International Symposium SAMPE* pp. 1826–1837
- Nozaka, K., Shield, C.K. and Hajjar, J.F. (2005) 'Effective bond length of carbon-fiber-reinforced polymer strips bonded to fatigued steel bridge i-girders', *Journal of Bridge Engineering*, 10(2), pp. 195–205.
- Okura, I., Fukui, T., Nakamura, K., Matsugami, T. and Iwai, Y. (2000) 'Application of CFRP Sheets to Repair of Fatigue Cracks in Steel Plates', *Journal of Construction Steel*, 8, Japan, pp. 689–696
- Pellegrino, C., Pipinato, A. and Modena, C. (2011) 'A simplified management procedure for bridge network maintenance', *Structure and Infrastructure Engineering*, 7(5), pp. 341–351.
- Suzuki, H. (2002) 'Strengthening of a Steel Beam with Carbon Fiber Reinforced Polymer Strip', *Proceedings of the First International Conference on Bridge Maintenance, Safety and Management (IABMAS)*, Barcelona.
- Suzuki, H. and Okamoto, Y. (2003) 'Repair of Steel Members with a Fatigue Crack Using the Carbon Fiber Reinforced Polymer Strip', *Journal of Constructional Steel*, Japan, 11, pp. 465–472.
- Täljsten, B., Hansen, C.S. and Schmidt, J.W. (2009) 'Strengthening of old metallic structures in fatigue with prestressed and non-prestressed CFRP laminates', *Construction and Building Materials*, 23(4), pp. 1665–1677.
- Tavakkolizadeh, M. and Saadatmanesh, H. (2003) 'Fatigue strength of steel girders strengthened with carbon fiber reinforced polymer patch', *Journal of Structural Engineering*, 129(2), pp. 186–196.
- Tavakkolizadeh, M. and Saadatmanesh, H. (2003) 'Fatigue strength of steel girders strengthened with carbon fiber reinforced polymer patch', *Journal of Structural Engineering*, 129(2), pp. 186–196.
- Yao, J., Teng, J.G. and Chen, J.F. (2005) 'Experimental study on FRP-to-concrete bonded joints', *Composites Part B: Engineering*, 36(2), pp. 99–113.
- Yuan, H., Teng, J.G., Seracino, R., Wu, Z.S. and Yao, J. (2004) 'Full-range behavior of FRP-to-concrete bonded joints', *Engineering Structures*, 26(5), pp. 553–565.
- Zheng, Y., Ye, L., Lu, X. and Yue, Q. (2006) 'Experimental Study on Fatigue Behaviour of Tensile Steel Plates Strengthened with CFRP Plates', *Proceedings of the Third International Conference on FRP Composites in Civil Engineering (CICE 2006)*. Miami, Florida, USA.
- Zheng Yun, Ye Lieping and Yue Qingrui (2005). "Progress in research on steel structures

## EVALUATE FLEXTURE BEHAVIOUR OF CFRP LAMINATED STEEL I-SECTIONS UNDER DIFFERENT HUMIDITY LEVEL AT THE INSTALLATION PHASE.

S. Abeygunasekera<sup>1\*</sup>, J. C. P. H. Gamage<sup>2</sup>, S.Fawzia<sup>3</sup>

<sup>1</sup>University of Moratuwa, Katubedda, Moratuwa, Sri Lanka.

<sup>2</sup>University of Moratuwa, Katubedda, Moratuwa, Sri Lanka.

<sup>3</sup>Queensland University of Technology, Australia.

\* E-mail: abeygunasekarasampath@gmail.com, TP: +94712227790

**Abstract:** Steel I section selected as a specimen and it was strengthened with low module CFRP material. Installation process conducted at the different humidity conditions due to selected locations. In this investigation were selected three different locations as Matale, Galle, and Colombo considering humidity level of atmosphere. CFRP 130 selected as a reinforced material and two parts epoxy used as adhesive material. Four point bending test were perform in this test series. The test results have exhibit significant strength variation with humidity level. Maximum strength gain has shown with lowest humidity level and it was recorded as a 52.4 % strength gain respective to control sample at the 68 % RH .

**Keywords:** Four points bending, relative humidity, I sections, CFRP

### 1. Introduction

A large number of steel structures are functioning throughout the world and most of them have becoming a critical age. As a result it has showing a signs of degradation. It may be happened due to numerous reasons. Number of factors is contributing for this behaviour such as life time, current demand, and environmental deterioration and design parameters. In addition affects corrosion, lack of proper maintenance, Design and construction errors, and fatigue sensitive details can be highlighted. Aging of structural components, insufficient detailing at the time of construction or design, and use of standard materials also should be an account at real applications. However fulfil of the current service demand is a more critical. □

Various kind of repairing techniques are used for recovery of service life losses in such structures. CFRP material based strengthen technology has providing substantial solution as repairing technology. It has become a leading due to their competitive advantages than conventional methods. But steel/CFRP bonding performance is critical in this technology. Bond performance and durability are depends on many variables. Such variables can be classified as internal and external factors. Internal factors can be identified as surface preparation techniques, type of epoxy. apply

loads, loading frequency and environmental effects. Environmental parameters are more critical external factor. Such factors are consider as moisture level, temperature and UV effects are critical. □

When consider the effect of moisture level of atmosphere it is crucially influence for the bond performance. Because, epoxy adhesive material and CFRP materials are allow to water molecule penetrate into the bonded joint. As a result of water absorption, the attraction between two components will become a weak. On the other hand moisture absorption is causes to physical changing CFRP matrix. Due to physical changes it has tendency to reduce the glass transition temperature.

### 2. Previous Studies

A numerous investigations have been conducted to understand the influencing of humidity level of CFRP strengthen technology. According to study of Collings, Harvey, Dalziel, (1993) <sup>i</sup> and Hollaway, (2010) <sup>ii</sup> have discussed the effects of moisture level. According to study of authors concluded moisture effects cause for unexpected structural distortions during their service life. Kumar, Sridhar, and Sivashanker, (2008) <sup>iii</sup> has been examined effects of moisture level and reported water absorption is causes to reduce shear strength of the polymers. Zhang et al.(2012)<sup>iv</sup> have reported that the result of 1% moisture



## ICSECM2017-86

absorption of CFRP laminates is causes to 17 % bending strength reduction. According to Nguyen et al., (2012)<sup>v</sup> moisture absorption is very fast at the beginning and then reached a constant level.

### 2.1. The Effect of Humidity on Epoxy Adhesive

The effect of humidity level for epoxy adhesive has been investigated by Lettieri and Frigione (2012)<sup>vi</sup>. Authors have reported that humidity is contribute to water absorb up to 75%. In addition it has observed, the glass transition temperature of the adhesive is reduced through plasticization. However, a study conducted by Wu, Hoa, and Ton-That, (2004)<sup>vii</sup> has showed that exposure to small amount of moisture (<2%) is contribute to improve the curing rate of adhesives and it is causes to enhance bond strength of composite. In generally penetration of water to CFRP/ steel is causes to make a weak bond strength. The reason for the weakness is cohesive force (Hydrogen bond or valence bond) of adhesive molecules is become a weak due to polymer inflaton <sup>viii</sup>

## 3. Details Experimental

### 3.1. Materials and Testing Procedures

Specimens were prepared using structural steel I-sections with dimensions 100 mm height and 50 mm width. Flange thickness and web thicknesses are 5 mm and 4 mm respectively. Each specimen's length was 600 mm. A total of eight specimens were tested in this preliminary test programme. The specimen details are listed in Table 1. □

Table 1: The summary of the test programme

Specimen Series	No of sample	Ambient Temperature(°C)	Relative Humidity (%)
S1	2	29	79
S2	2	27	90
S3	2	33	68
S4	2	NA	NA

In this study CFRP- M130 sheets were used for strengthening of steel I beam. The main characteristics of Carbon fibers are strength and Young's modulus. A two part saturant was selected as adhesive. Material properties of

CFRP sheets and two part epoxy adhesive are listed in Table 2. □

Table 2: Material properties

Properties	CFRP(According to Manufacturer)	Epoxy(According to Manufacturer)
Material Type	MBrace CF130	Araldite 420
Cure time	N/A	7days
Set time	N/A	24hours
Tensile Strength	2600Mpa	27.3MPa
Thickness	0.146mm	NA

### 3.2 Specimen Preparation

450 mm long steel I sections were selected as a specimen and tensile flange planed to strengthen using CFRP sheet. An angle grinder was used for surface preparation of selected samples and grinded surface is shown in Fig.1 (a). Acetone used for the clean bond surface of steel. A thin layer of primer coat was applied on the prepared and cleaned steel surface according to manufacturer's guidelines. Primer consist of two parts (base and the primer) was mixed into 1:1 weight ratios. Samples were kept to cure about 1 hour before bonding applications as shown in Fig. 1(b). Thin layer of adhesive was uniformly applied on top of the primed steel surfaces after cure. CFRP material layer was cut to the explained dimensions (100 mm x 50 mm) and it was placed on top of the adhesive layer. Measure the wet and dry bulb temperatures of surrounding environment when bonding to take a value of relative humidity. The excess epoxy and air bubbles were removed using a ribbed roller moving in the direction of fibers. Followed same procedure and single layer of CFRP sheet was paste on the bottom of the specimen. Repeat this procedure for each specimen and kept 24 hours to cure according to manufacturer provided guidelines.



Figure 1(a)



Figure 1(b)

### 3.3 Test Setup and Procedure

The test was planned to determine the bending capacity of specimens. The specimens were fixed in the CFTM-300D digital control flexure testing machine as shown in Fig 2(a). Typical specimens attached to the test machine as shown in Fig 2(b). Each specimen was loaded in a 300 kN capacity four points bending machine with rate of 0.5 mm/min. Test series  $S_1, S_2$  and  $S_3$  were strengthened using CFRP sheet and bond length was 100mm. Test series  $S_4$  kept as a control test series. The bending load was applied gradually until to specimen fail and repeated same procedure for each test series and individually noted the magnitude of failure load. Figure 2(b) shows the test set up in a compression and flexure testing machine with a dial gauge (0.01-50mm).



Fig 2(a): CFTM 300



Fig 2(b): Sample testing

The summary of test results is shown in Table 3. The maximum strength gain was recorded in test series  $S_3$  and average value was 93 kN and relative humidity level in test series 3 measured as 68 %. Test series,  $S_1$  were strengthened under 79 % humidity level and average failure load was reported as 89 kN. In test series 2 samples was installed at 90 % humidity level. Failure load value was recorded as 86 kN. The lowest failure load in this tested series has noted at the series 3 and it was 93 kN at the lowest selected humidity level.

Therefore the maximum bending load carrying capacity is reported at lowest RH value. In generally, can be conclude as strength and RH values is wise versa. Furthermore, can be concluding the highest bond performance is

available at lower RH value at the installation phase.

Table 3: Failure Load with RH and Temperature

Test Series number	Temperature/ °C	Relative Humidity %	Maximum Average Deflection/m m
S1	29	79	3.82
S2	27	90	4.47
S3	33	68	3.39
S4	Controlled sample (Without CFRP)		5.40

### 4. Results and Discussion

Relative humidity level in Sri Lanka is comparatively high as a tropical climate. According to test result, CFRP material installations under low humidity level can be more benefitting than high moisture level of environment. However moisture level is not an individual factor effecting for bond performance. Because real world application are applying effects of other factors and it may be combine effect for the final results. Specially hygro thermal (Moisture and Temperature combination) effect is critically influencing for the bond performance. Therefore estimated values may have possibility to deviate due to effect of other parameters. However, temperature fluctuation in this test series were occurs around the Glass Transition temperature ( $T_g$ ) of epoxy during the installation process. It has recorded minimum temperature as 29 °C and maximum temperature as 33 °C. Due to measured value the difference of the temperature was 5 °C. Therefore, effect of the temperature fluctuation can be consider as insignificant influencing for the bond performance. On the other hand recorded temperature is not achieved the glass transition temperature of the adhesive material. Because, according to the manufacturer it has recorded as 55°C for the selected epoxy. However UV effects were not considered in this test programme. Because, all of installation were perform at the night time.

#### 4.1. Crack propagation and Failure modes

Furthermore, failure mode also observed in each specimens. It was identified as de lamination and interface de-bonding occurs.□



Figure 3: Crack propagation zone under loading □

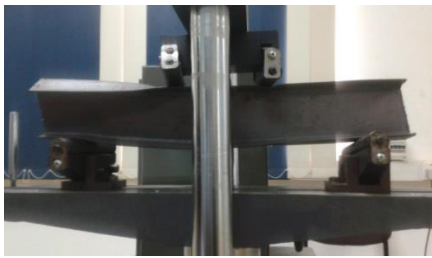


Figure 4: Normal modulus CFRP failure mode (de-laminate / Interface de-bonding)

In Table 4 has shown the average failure load variation with failure modes. The failure modes were noted as a delaminated and de-bonding .De lamination can be observed at the lower and middle RH level.De bonding has reported at highest RH level.GFRP layer can apply to minimize the moisture absorption.

Table 4: The summary of test results

Test Series	RH %	Failure Load(kN)	Strength Change (%)	FM
S1	79	89	45.9	DL
S2	90	86	40.9	ID
S3	68	93	52.4	DL
S4	NA	61	NA	NA

#### 5. Conclusions and Recommendations□

CFRP strengthened steel I sections were perform under four point bending loads to determine the bending load capacity of CFRP/steel composites under different humidity level. The following observations and conclusions are made.

1).Failure load capacity of steel I section was enhanced from 41 % to 52.4% with CFRP material.□

2).Flexural load carrying capacity of steel I section was enhanced from 17.2% to 37.2% □

3).When increases the atmosphere moisture level bond performance has decreased.

4) CFRP strengthen technology can recommend even high humidity environmental condition also. Because even at the 90% moisture level also reported 41 % strength gain.

#### Future works

□

1) Few more test should do by using different humidity level between 20 to 50 %.□

2) Should be investigate the availability hygrothermal effects for bond performance.□

#### Acknowledgements

I would like to express my gratitude towards the workshop and laboratory staff of the University for their Support for this test programme.

#### References

Collings, T.A., Harvey, R.J. and Dalziel, A.W. (1993) 'The use of elevated temperature in the structural testing of FRP components for simulating the effects of hot and wet environmental exposure', *Composites*, 24(8), pp. 625-634.

<sup>1</sup> Hollaway, L.C. (2010) 'A review of the present and future utilization of FRP composites in the civil infrastructure with reference to their important in-service properties', *Construction and Building Materials*, 24(12), pp. 2419-2445.

<sup>1</sup> Kumar, S.B., Sridhar, I. and Sivashanker, S. (2008) 'Influence of humid environment on the performance of high strength structural carbon fiber composites', *Materials Science and Engineering: A*, 498(1-2), pp. 174-178.

<sup>1</sup> Zhang, A. Y., Li, D. H., & Zhang, D. X. (2012). Effect of Moisture Absorption on the Bending

## ICSECM2017-86

Strength of CFRP. *Advanced Materials Research*, 450-451, 482-485.

<sup>1</sup> Nguyen, T.-C., Bai, Y., Zhao, X.-L. and Al-Mahaidi, R. (2012) 'Durability of steel/CFRP double strap joints exposed to sea water, cyclic temperature and humidity', *Composite Structures*, 94(5), pp. 1834-1845.

<sup>1</sup> Lettieri, M. and Frigione, M. (2012) 'Effects of the humid environment on thermal and mechanical properties of a cold-curing structural epoxy adhesive', *Construction and Building Materials*, 30, pp. 753-760.

<sup>1</sup> Wu, L., Hoa, S.V. and Ton-That, M.-T. (2004) 'Effects of water on the curing and properties of epoxy adhesive used for the bonding FRP composite sheet to concrete', *Journal of Applied Polymer Science*, 92(4), pp. 2261-2268.

<sup>1</sup> Yang Yong-xin, Yue Qing-rui, and Peng Fu-ming EXPERIMENTAL RESEARCH ON BOND BEHAVIOR OF CFRP TO STEEL Central Research Institute of Building and Construction, MCC Group, China

J.M.R.S. Appuhamy, M. Ohga, P.B.R. Dissanayake and K.K. Wijesundara [2012], Development of Brisk Finite Element Analytical Method of Predicting Tensile Strength Reduction due to Corrosion, 2<sup>nd</sup> SAIMM Research Symposium on Engineering Advancements (RSEA-2012), Malabe, Sri Lanka.

Mehran Gholami a, Abdul Rahman Mohd Sam a, Jamaludin Mohamad Yatim a, Mahmood Md Tahir b A review on steel/CFRP strengthening systems focusing environmental performance *Construction and Building Materials* 47 (2013) 301-310

Munsinghe, M.G.J. 2011, Study to Recommend a Steel Truss System With Minimum Steel Quantity Usage For Medium Span Bridges, MEng Thesis, University of Moratuwa, Sri Lanka. pp22-23. □

Gillespie, J. W., Mertz, D. R., Edberg, W. M., Ammar, N., Kasai, K., and Hodgson, I. C. Rehabilitation of Steel Bridge

Girders Through Application of Composite Materials. 28<sup>th</sup>. International SAMPETechnical Conference. November 4-7, 1996, pp. 1249-1257.

Sveinsdottir, S.L. 2012. Experimental Research on Strengthening of Concrete Beams by The Use of Epoxy Adhesive And Cement Based Bonding Material, MScience Thesis, Haskolinn, Reykjavik University Iceland.

Schnerch.D.Dawood.M, and Razkalla, S, 2006, 'Proposed Design Guidelines For Strengthening of Steel Bridges With FRP Materials', *Journal of Construction and Building Material* 21 (1001-1110), North Carolina State University, USA. □

Stratford T, Bisby L. Effect of warm temperatures on externally bonded FRP strengthening. *J Compos Constr* 2012;16:235-44.

---

## AFFECT OF ENVIRONMENTAL CONDITIONS DURING INSTALLATION PROCESS ON BOND STRENGTH BETWEEN CFRP AND STEEL.

S. Abeygunasekera<sup>1\*</sup>, J. C. P. H. Gamage<sup>2</sup>, S.Fawzia<sup>3</sup>

<sup>1</sup>University of Moratuwa, Moratuwa, Sri Lanka,

<sup>2</sup>University of Moratuwa, Moratuwa, Sri Lanka

<sup>3</sup>Queensland University of Technology, Australia

\*E-mail: [sampath\\_08@uom.lk](mailto:sampath_08@uom.lk), TP: +94777175042

### Abstract

This paper focuses on the use of externally bonded Carbon Fiber Reinforced Polymer (CFRP) materials to strengthen steel plates with simple but joint subjected to tension. A fully slender steel section was selected in this test programme (50mm x 4mm). CFRP strengthened steel under various humidity levels and tested to fail under axial tensile load. The middle part of the strut bonded with epoxy and externally strengthened using CFRP sheet. The test results showed a significant strength variation from 1.05kN to 1.28kN due to different relative humidity level from 47% at 19<sup>o</sup>C to 90% at 30<sup>o</sup>C failure mode of strengthened members. This study confirms that there is wide range of strength vary due to relative humidity level and ambient temperature cure time and the short term performance of CFRP strengthened steel structure under axial tension.

**Keywords:** Axial Tension, Bond Length, Bond Performance, CFRP/Steel Composites, Relative Humidity

---

### 1.0 Introduction

Carbon Fiber Reinforced Polymers (CFRP) have been used in many field applications and have become the ideal material selection in many industries such as the aerospace, automobile, electricity and telecommunication transmission towers, marine applications, offshore platforms and many other industries. This technology was rapidly growth, due to their light weight, high strength, rigidity, and noncorrosive properties. Therefore FRP materials have successfully appealed to engineers in various fields above mention; however, CFRP composites were recently become a one of main topic of research in the civil engineering industry. Because large numbers of steel structures exist in the world and most of them have become a critical age with rapidly increasing signs of degeneration and reduced functionality. Several factors affect to this kind of signals such as environmental deterioration and level of demand. In addition when Consider steel structures, many factors have been identified such as corrosion, lack of proper maintenance, Design and construction errors, and fatigue sensitive details are major issues.

Aging of structural components, insufficient detailing at the time of construction or design, and use of standard materials are other main effective agents. Mainly engineer and researcher are always trying to give proper answer two questions regarding steel structures. How can repair or extend the life of existing steel structure? How can we avoid corrosion of steel structure in the future? As an answer of this kind of questions welding and bolting connections has been introduced conventionally. However, welding is not a favourable solution due to fatigue problems and mechanical details and bolted connections which have better fatigue life but time consuming and costly [2]. A considerable attention has been given to use Carbon Fiber Reinforced Polymer (CFRP) materials to repair existing steel structures past decay. Because; maintaining steel bridges have been identified as a one of main critical issue in road and railway network system of each country. However maintenance of every aged bridge structure is very difficult and impracticable task for many countries within their bridge budgets [1] Specially this task is heavy burden for economy of under developed countries such as Sri Lanka and Bangladesh. According to Appuhamy[1] in Japan, there are

more than 50,000 steel railway bridges, and half of them have been used over 60 years and some bridges are aged over 100 years. According to Munasinghe [3] Sri Lanka road network have more than 4000 steel bridges. CFRP technology has been successfully used in many countries due to their material properties and cost effectiveness. CFRP laminates weigh less than one fifth of the weight of a similar size steel plate and are also corrosion resistant. The replacement costs were compared with the cost of rehabilitation at an assumed 25 percent section loss. It was concluded that total replacement cost was 3.65 times higher than the cost of rehabilitation [4]. Slattocks Canal Bridge repair in England year 2000, Ashland Bridge on State Rt. 82 over Red Clay Creek in USA year 2002 and Takiguchi Bridge in Tokyo(Japan) year 2008 are examples for successful field applications. However during their entire service life it should be properly function within the safe range.

Strength of steel structures may be deficient due to external factors such as corrosion, increased load and aging. Replacing of structures with new structures is relatively expensive and makes an inconvenience for users of such structures. CFRP is an attractive solution applying in Aerospace industry and Automobile industry for more than 50 years to retrofit metallic members. Since 1980s Civil Engineers have been successfully applied this technique for retrofitting civil engineering structures [5]. Mainly such structures are based on concrete or steel. In addition CFRP can be used for strengthening timber and masonry structures. Considerable amount of researches were focused on strengthening of concrete structures. Nowadays there are many applications in retrofitting steel members in buildings, bridges and towers using Fibre Reinforced Polymer (FRP) materials. Steel bridge girders, pin jointed trusses and steel frames can be taken as examples. Considerable amount of research has been conducted to investigate performance of Carbon Fiber Reinforced Polymer (CFRP) materials for strengthening steel structures in countries such as Australia and UK. However, the relative humidity level of these countries is lower than in Sri Lanka. The humidity at the installation phase may affect on bond performance of polymeric adhesives. In this composite system, two part epoxy adhesive is used to create the bond between CFRP and steel and it is very

sensitive to humidity in the installation phase [8]. The high relative humidity level in Sri Lanka may affect on the composite performance. Therefore, it is important to investigate the short term performance of the system before exploring long term performance such as the composite performance when the system subjected to cyclic loading and environmental changes. There is a high potential to apply this technology in retrofitting deficient railway and road bridges in Sri Lanka because our road networks have more than 4000 steel bridges and most of them are constructed under British colonial periods. Some of these bridges have been constructed about 50 to 100 years ago [3]. No research studies have been conducted in Sri Lanka to evaluate the feasibility of CFRP applications in strengthening steel structures. Therefore, this research is focused on short term performance of CFRP strengthened steel plates subjected to axial tension.

## 2. Experimental Programme

A total of eight specimens were tested in this preliminary test programme. The specimen details are listed in Table 1. Specimens were prepared using structural steel plate with dimensions 50 mm x 4 mm cross section and 450 mm length.

### 2.1 Materials

In this study CFRP sheets were used to strengthen steel plates. The main characteristics of Carbon fibres are their strength and Young's modulus. A two-part saturant (base and hardener) was selected for this test series to examine the feasibility to make bond between CFRP and steel. The manufacturer provided material properties of CFRP sheet and two part epoxy adhesive are listed in Table 2.



Figure 1: CFRP Material

**Table 1:** The summary of test specimens

Specimen Series	Ambient Temperature(°C)	Relative Humidity (%)	No of Specimen
S1 and S2	21	47	2
S3 and S4	19	59	2
S5 and S6	30	75	2
S7 and S8	25	90	2

**Table 2:** Material properties

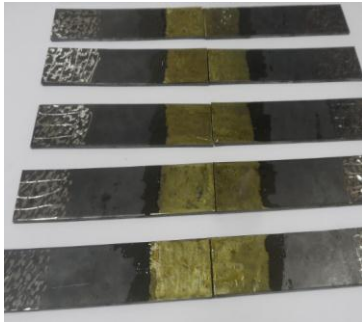
Properties	CFRP(According to Manufacturer )	Epoxy(According to Manufacturer)
Material Type	MBrace CF130	MBrace
Cure time	N/A	7days
Set time	N/A	24hours
Tensile Strength	2600Mpa	27.3MPa
Thickness	0.146mm	1mm

## 2.2. Specimen Preparation

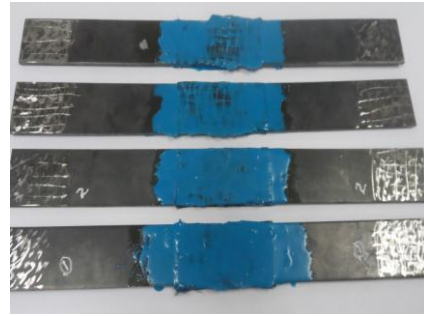
Surface preparation of the steel plate is very important to ensure effective load transfer between steel plate and CFRP sheet. The steel plates with dimensions 450 mm length 50 mm width and 4mm thickness were used for strengthening. The selected surface preparation technique should have facility for practical applications and also environmentally safe. Most effective way for the surface preparation is recommended as grit blasting [6]. However, the grit blasting method is not available in University of Moratuwa laboratories. Therefore an angle grinder was used for surface preparation of samples and resulted surface is shown in Fig.2 (a). In addition cross section area of steel plates were grinded by angle grinder in the area to be bonded to ensure better mechanical interlocking. Dust particles were removed using an acetone. Primer consist of two parts (base and the primer) was mixed in to weight ratios. A thin layer of primer coat was applied on the prepared and cleaned steel surface according to manufacturer's guidelines as shown in Fig. 2(b) and the samples were kept to cure about 1 hour before bonding applications. . A small amount of adhesive was applied on cross-sectional area of both steel plates joining together. Then a thin layer of adhesive was uniformly applied on top of the primed steel surfaces. CFRP material layer was cut to the explained dimensions (100mmx50mm) and it was placed on top of

the adhesive layer. Measure the wet and dry bulb temperatures of surrounding environment when bonding. Because according to the thermo meter readings can be take a value of relative humidity under of different environmental condition. The excess epoxy and air bubbles were removed using a ribbed roller moving in the direction of fibres. Following the same procedures, one layer of CFRP sheet was paste on the other side also. The prepared samples are shown in Fig. 2(c). Finally samples were kept 24 hours to cure according to manufacturer provided guidelines. The schematic diagram of each test specimens bonded with CFRP is shown in Figure 3. However during the bonding duration two bonding component of steel plates should kept horizontally using suitable clamping mechanism before applying adhesives and CFRP.

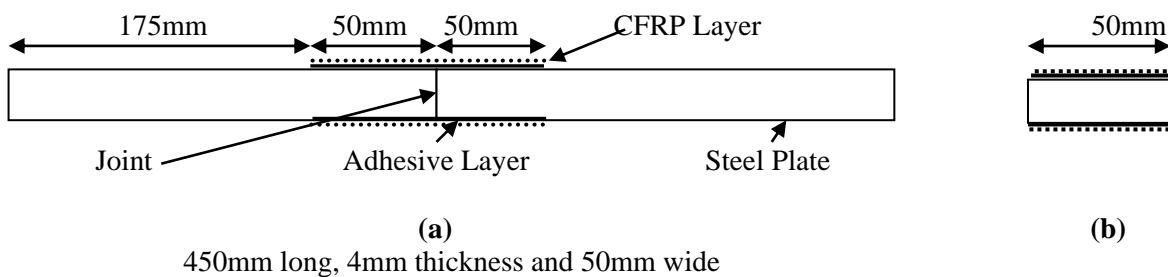
**Fig 2(a):** Grinded Surface



**Fig 2(b):** After Application of Primer



**Fig 2(c):** Prepared Specimens



**Figure 3:** The schematic view of CFRP strengthened specimen, (a) Front Elevation, (b) Cross Section

### 2.3 Test Setup and Procedure

The test was planned to determine the axial tensile load capacity of specimens. The specimens were fixed in the Avery tensile testing machine as shown in Fig 4(a) and shows typical specimens with attached to the test machine. Each specimen was loaded in tension in a 14.5 kN capacity with a loading rate of 0.5 mm/min. Figure 4(b) shows the test set up in a Avery tensile testing machine with dial gauge (0.01-50mm). The tensile load was applied gradually until to fail specimen and repeat same procedure for each specimen and noted magnitude of failure load individually. The schematic diagram of test setup in a universal testing machine with dial gauge is given in Figure 4(a).



**Fig 4(a)**



**Fig 4(b)**

**Fig 4(a):** Schematic diagram of test setup

**Fig4(b):** Test setup in Avery tensile test apparatus

### 3. Experimental Results and Discussion

Each of test series, axial tensile failure of individual specimens was measured. The summary of test results is shown in Table 3. Test specimens S1-S8 were strengthened using CFRP and bond length was 100mm. The maximum strength gain of S7 and S8 specimens was 1.28kN at 90% relative

humidity level. Sample S1 and S2 were strengthened under 47% humidity level and it is 1.14kN of failure value shown of the specimens. Sample S5 and S6 were strengthened under 75% humidity level and it is 1.12kN of failure value shown of the specimens. The minimum failure load noted in S3 and S4 specimens and it was 1.05kN with



respect to other specimens. It was the minimum tensile load carrying capacities that observed in this test series. On the other hand failure loads are varying with ambient temperature also. Due to this test result maximum strength gain shown at 25<sup>0</sup>C. A higher strength gain was noted in the specimens with 90% humidity level. However variation of strength change with RH value was within 10% can be neglect. Otherwise highest average strength gain shown at the 90% humidity level. But in generally strength and RH values behaviour is wise versa. However these kinds of things happened due to the combination of environmental effect. Specially hygro thermal (Moisture and Temperature combination) effect is most critically influenced for bond performance or imperfect bond between CFRP and steel in these specimens. According to this experimental series has been shown highset strength gain with 25<sup>0</sup>C.Ambient temperature

or moisture level effect cannot consider individually. However under the low RH value and low temperature condition is shown maximum bond performance.

Average temperature value is varying in Sri Lanka between 25 -35<sup>0</sup>C and Relative Humidity vary from 50% to 90% .Due to this test result can be recommended CFRP as a solution of strengthened steel structures in Sri Lanka.

The strength variation was noted from these specimens and it is shown in Table 3 and 4. Table 3 indicates that the average tensile load capacity variation with Relative Humidity and ambient temperature. Table 4 shows average failure load variation with failure modes. The failure modes was noted as a delaminated and debonding

**Table 3:Failure Load Behaviour with RH and Temperature**

Specimen Series	Ambient Temperature( <sup>0</sup> C)	Relative Humidity (%)	Average Failure Load(kN)
S1 and S2	21	47	1.14
S3 and S4	19	59	1.05
S5 and S6	30	75	1.12
S7 and S8	25	90	1.28

**Table 4:The Summary of Test Results**

Specimen Series	Relative Humidity (%)	Average Failure Load(kN)	% of Strength change	Failure mode
S1 and S2	47	1.14	NA	Delaminate/Debonding
S3 and S4	59	1.05	7.9	Delaminate/Debonding
S5 and S6	75	1.12	6.3	Delaminate/Debonding
S7 and S8	90	1.28	12.5	Delaminate/Debonding



**Figure 5: Normal Modulus CFRP Failure Mode (Delaminate /Interface Debonding)**

#### 4. Conclusions and Recommendations

CFRP strengthened steel struts were tested under uni-axial tensile load to determine the performance of CFRP/steel composites. The following observations and conclusions are made.

- The tensile load carrying capacity of steel was enhanced considerably with increase of Relative humidity level from 59% to 90%.
- The tensile load carrying capacity of steel was decreased considerably with increase of Relative humidity level from 47% to 59%.
- Lower end or higher end of moisture level is shown good bond performance. However relative humidity value around 60% environmental condition is not recommended to CFRP bonding with steel.
- Adhesive layer between CFRP and steel is sensitive to temperature.
- Stratford & Bisby .2012[7] ; design guidelines recommend that  $T_g$  must be higher than  $15^{\circ}\text{C}$  from operating temperature and it can proven through this test series because glass transition temperature ( $T_g$ ) is  $40^{\circ}\text{C}$  and therefore best operating point should be  $25^{\circ}\text{C}$  .Here maximum performance does show at  $25^{\circ}\text{C}$ .
- CFRP is resistive to moisture and less affects it at higher moisture level
- Moisture level and ambient temperature are difficult to account individually .However hygro thermal effect (Combination of temperature and moisture level) is more severely effect for bond performance.
- The selected two part adhesive showed good performance however the relatively short pot life with high ambient temperature is a critical issue for practical applications.
- Optimum ambient temperature for installation is  $25^{\circ}\text{C}$
- This technology can recommended for Sri Lankan Environment(High humidity environment)
- Few more test should done by using different humidity level between 20 to 50%.
- Should be investigating availability of another temperature moisture combination for maximum bond performance.

#### Acknowledgement

I would like to express my gratitude towards the laboratory staff of University of Moratuwa for their support for this initial test programme.

#### References

1. Ohga, J.M.R.S. M., Dissanayake, P.B.R., Wijesundara, K.K.. Development of Brisk Finite Element Analytical Method of Predicting Tensile Strength Reduction due to Corrosion, the 2<sup>nd</sup> SAITM Research Symposium on Engineering Advancements (RSEA), 2012, Malabe, Sri Lanka.
2. Mehran Gholamia, Abdul Rahman Mohd Sama, Jamaludin Mohamad Yatima, Mahmood Md Tahirb , A review on steel/CFRP strengthening systems focusing environmental performance Construction and Building Materials ,2013 ;Vol47: 301–310.
3. Munsinghe, M.G.J , *Study to Recommend a Steel Truss System With Minimum Steel Quantity Usage For Medium Span Bridges*, M.Eng Thesis ,2011, University of Moratuwa, Sri Lanka. 22-23.
4. Gillespie, J. W., Mertz, D. R., Edberg, W. M., Ammar, N., Kasai, K., Hodgson, I. C. Rehabilitation of Steel Bridge Girders Through Application of Composite Materials, 28<sup>th</sup>. International SAMPETechnical Conference, 1996.
5. Sveinsdottir, S.L., *Experimental Research on Strengthening of Concrete Beams by The Use of Epoxy Adhesive And Cement Based Bonding Material*, MSience Thesis ,Haskolinn, Reykjavik University Iceland, 2012.
6. Schnerch, D., Dawood, M., Razkalla, S., 2006, 'Proposed Design Guidelines For Strengthening of Steel Bridges With FRP Materials', Journal of Construction and Building Material 21 (1001-1110), North Carolina state University, USA.
7. Stratford T, Bisby .L, Effect of warm temperatures on externally bonded FRP strengthening. J Compos Constr 2012.
8. Gamage, J.C.P.H, Al-Mahaidi, R. and Wong, B, "Bond slip models for CFRP-concrete interface under combined effects of cyclic temperature, humidity and stress", International conference on composite structures (ICCS-15), Porto, Portugal, 2009.

# BOND PERFORMANCE OF CFRP STRENGTHENED STEEL MEMBERS SUBJECTED TO AXIAL COMPRESSION

S. Abeygunasekera<sup>1</sup>, J. C. P. H. Gamage<sup>2</sup>, S.Fawzia<sup>3</sup>

<sup>1</sup>Postgraduate, Department of Civil Engineering, University of Moratuwa, Sri Lanka  
Telephone: +94777175042  
E-mail: [Sampath@cinec.edu](mailto:Sampath@cinec.edu)

<sup>2</sup>Senior Lecturer, Department of Civil Engineering, University of Moratuwa, Sri Lanka  
Telephone: +94112650567-8 (Ext 2201); Fax: +94112651216  
E-mail: [kamage@Uom.lk](mailto:kamage@Uom.lk)

<sup>3</sup>Lecturer, School of Civil Engineering and Built Environment, Faculty of Science and Engineering,  
Queensland University of Technology, Australia  
Telephone: +61 7 3138 1012  
E-mail: [sabrina.fawzia@qut.edu.au](mailto:sabrina.fawzia@qut.edu.au)

## Abstract

This paper focuses on the use of externally bonded Carbon Fiber Reinforced Polymer (CFRP) materials to strengthen steel plates subjected to compression. A fully slender steel section was selected in this test programme. CFRP strengthened steel plates and non strengthened plates were tested to fail under compressive load. The middle part of the strut was strengthened using CFRP sheet. The length of the strengthened zone was varied. Eight specimens were tested in this test programme. The test results showed a significant strength gain of 47% and delaying of lateral torsional buckling failure mode of strengthened members. This study confirms that there is great potential to increase the short term performance of CFRP strengthened steel structure under axial compression.

**Keywords:** *CFRP/steel composites, Bond length, Bond performance, Axial Compression*

## 1.0 Introduction

Strength of steel structures may be deficient due to external factors such as corrosion, increased load and aging. Replacing of structures with new structures is relatively expensive and makes an inconvenience for users of such structures. CFRP is an attractive solution applying in Aerospace industry and Automobile industry for more than 50 years to retrofit metallic members. Since 1980s Civil Engineers have been successfully applied this technique for retrofitting civil engineering structures (Sveinsdottir, 2012). Mainly such structures are based on concrete or steel. In addition CFRP can use for strengthen timber and masonry structures. Considerable amount of researches were focused on strengthening of concrete structures. Nowadays there are many applications in retrofitting steel members in buildings, bridges and towers using Fibre Reinforced Polymer (FRP) materials. Steel bridge girders, pin jointed trusses and steel frames can be taken as examples. In this study, the short term performance of retrofitted members subjected to uni axial compressive load was investigated. Considerable amount of research has been conducted to investigate performance of Carbon Fiber Reinforced Polymer (CFRP) materials for strengthening steel structures in countries such as Australia and UK. However, the relative humidity

level of these countries is lower than in Sri Lanka. The humidity at the installation phase may affect on bond performance of polymeric adhesives. In this composite system, two part epoxy adhesive is used to create the bond between CFRP and steel and it is very sensitive to humidity in the installation phase (Gamage 2009). The high relative humidity level in Sri Lanka may affect on the composite performance. Therefore, it is important to investigate the short term performance of the system before exploring long term performance such as the composite performance when the system subjected to cyclic loading and environmental changes. There is a high potential to apply this technology in retrofitting deficient railway and road bridges in Sri Lanka because our road networks have more than 4000 steel bridges and most of them are constructed under British colonial periods. Some of these bridges have been constructed about 50 to 100 years ago (Munasighe 2011). No research studies have been conducted in Sri Lanka to evaluate the feasibility of CFRP applications in strengthening steel structures. Therefore, this research is focused on short term performance of CFRP strengthened steel plates subjected to axial compression.

## 2.0 Experimental programme

A total of eight specimens were tested in this preliminary test programme. The specimen details are listed in Table 1. Specimens were prepared using structural steel plate with dimensions 50 mm x 5 mm cross section and 450 mm length.

Table 1: The summary of test specimens

Specimen Series	Bond Length(mm)	No of Specimen
S1 and S2	No CFRP	2
S3 and S4	100	2
S5 and S6	150	2
S7 and S8	200	2

## 2.1 Materials

In this study CFRP sheets were used to strengthen steel plates. The main characteristics of Carbon fibres are their strength and Young's modulus. A commercially available epoxy adhesive type in Sri Lanka market was selected for this test series to examine the feasibility to make bond between CFRP and steel. The manufacturer provided material properties of CFRP sheet and two part epoxy adhesive are listed in Table 2.

Table 2: Material properties

Properties	CFRP(According to Manufacturer )	Epoxy(According to Manufacturer)
Material Type	MBrace CF130	J-BWeld
Cure time	N/A	15-24 Hours
Set time	N/A	20-25 Minutes
Tensile Strength	2600Mpa	27.3MPa
Thickness	0.146mm	NA

## 2.2. Specimen preparation

Surface preparation of the steel plate is very important to ensure effective load transfer between steel plate and CFRP sheet. The steel plates with dimensions 450 mm length 50 mm width and 5mm thickness were used for strengthening. The selected surface preparation technique should have facility for practical applications and also environmentally safe. Most effective way for the surface preparation is recommended as grit blasting (Schnerch 2006). However, the grit blasting method is not available in University of Moratuwa laboratories. Therefore an angle grinder was used for surface preparation of samples and resulted surface is shown in Fig.1 (a). Acetone used for the clean surface. A thin layer of primer coat was applied on the prepared and cleaned steel surface according to manufacturer's guidelines as shown in Fig. 1(b) and the samples were kept to cure about 1 hour before bonding applications. Then a thin layer of adhesive was uniformly applied on to the primed steel surfaces. Then a layer of CFRP is bonded on top of the adhesive layer. The excess epoxy and air bubbles were removed using a ribbed roller moving in the direction of fibres. Here used single layer of CFRP. The prepared samples are shown in Fig. 1(c). Finally samples were kept 24 hours to cure according to manufacturer provided guidelines. The schematic diagram of test specimens with 200 mm CFRP bond length is shown in Figure 2.

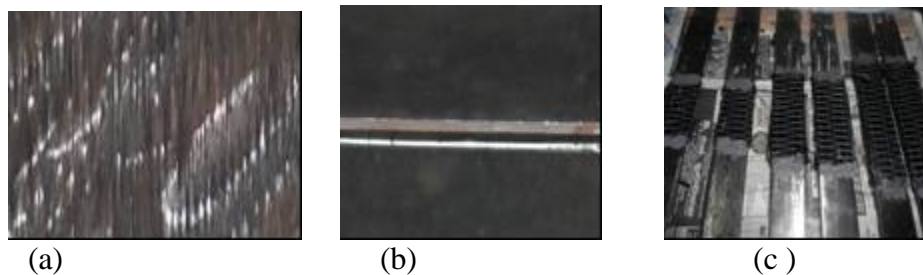


Figure 1: (a) Grinded surface, (b) After application of primer, (c) prepared specimens

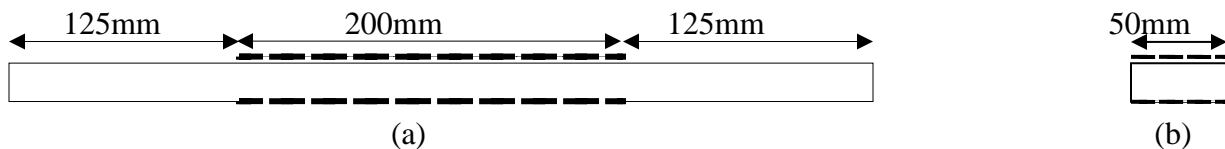


Figure 2: The schematic diagram of CFRP strengthened specimen, (a) Front elevation, (b) Cross section

The test was planned to determine the compressive load capacity of specimens. The specimens were fixed in the Amsler testing machine and uniaxial compressive load was applied gradually with idealised pinned support conditions at end as shown in Fig 3(b). Two dial gauges were fixed at the opposite sides of the

specimens at the middle to measure the midspan deflection. The schematic diagram of test setup is given in Figure 3(a)

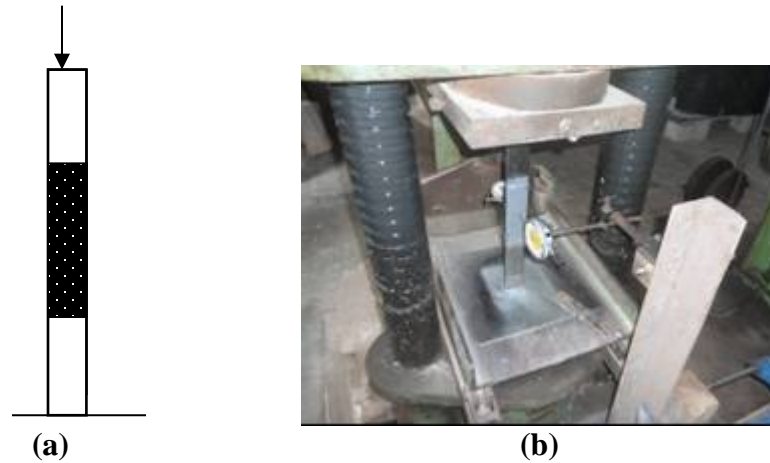


Fig 3:(a) Schematic diagram of test setup , (b)Test setup Apparatus

### 3. Experimental results and discussion

Each of test series, the mid point deflection of individual specimens was measured. The summary of test results is shown in Table 3. Test specimens S3-S8 were strengthened using CFRP and bond length was varied from 100mm to 200mm. When consider the overall length of specimens S3 and S4 was covered 22.2% of surface area with CFRP. The average strength gain of these specimens was 28%. Sample S5 and S6 were strengthened with 150 mm long CFRP sheet which is 33.3 % of gross surface area of the specimen. The average strength gain noted in those specimens was 47.1% with respect to control specimens. It was the maximum compressive load carrying capacity that observed in this test series. A lower strength gain was noted in the specimens with longest bond length than medium bond length. Reason for this behaviour may be an effect of effective bond length. On the other hand this may be happened due to experimental errors or imperfect bond between CFRP and steel in these specimens.

Table 3: The summary of test results

Specimen Series	Bond Length(mm)	Average Failure Load(kN)	Percentage strengthen gain (%)
S1, S2	NA	3.7	NA
S3, S4	100	4.7	28.0
S5, S6	150	5.3	47.1
S7, S8	200	4.9	33.7

Behaviour of load / mid span deflection of these specimens are shown in Figure 4. When the bond length increases magnitude of compressive load capacity also increases in specimens strengthened with 100 mm long CFRP sheet. It is shown at curves S3-S6.

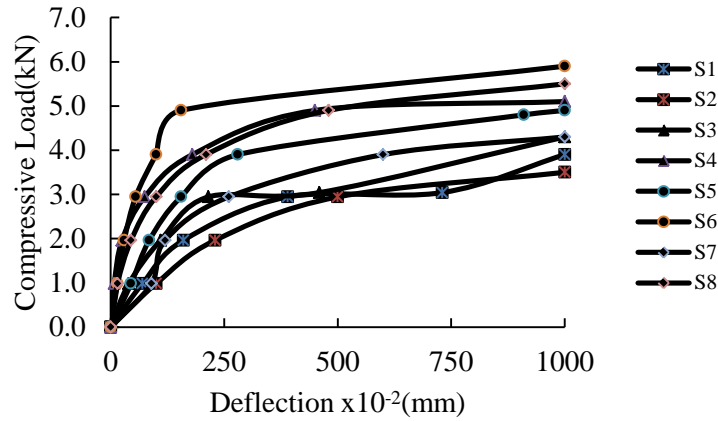
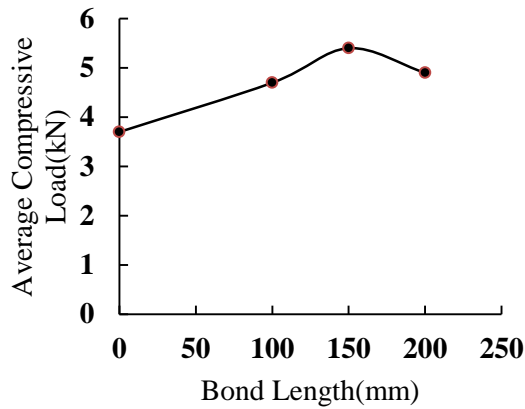
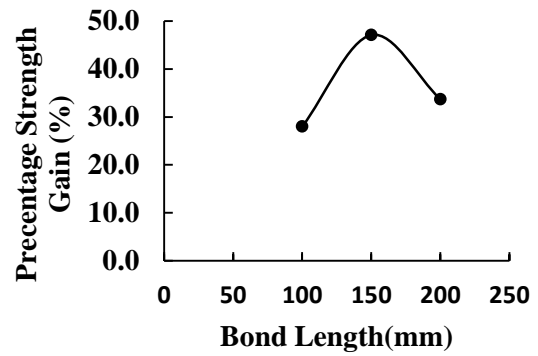


Figure 4

Specimens S1, S2 are from non strengthened series and average failure load was calculated as a 3.7 kN. This series is considered as a control specimens. The average strength gain and percentage strength gain were noted from these specimens and it is shown in Figures 5(a) and 5(b) respectively. Figure 5(a) indicates that the average compressive load capacity linearly increases with bond length.



(a)



(b)

Figure 5: (a)Average Load- deflection relationship (b)Percentage strength gain Bond lengthwith bond length

#### 4. Conclusions and recommendations

CFRP strengthened steel struts were tested under uni-axial compressive load to determine the performance of CFRP/steel composites. The following observations and conclusions are made.

- The compression load carrying capacity of steel was enhanced considerably with installation of CFRP sheet in steel struts
- On average 28% to 47% strength gain was noticed when the bond length varies from 100 mm to 200 mm and delaying of buckling failure mode was noticed.
- The selected two part adhesive showed good performance however the short pot life of 20 minutes is a critical issue for practical applications.

#### Acknowledgement

I would like to express my gratitude towards Finco Engineering (Pvt) Ltd, Sri Lanka for their kind co-operation on providing CFRP materials and the laboratory staff of University of Moratuwa for their support for this initial test programme.

#### References

Gamage, J.C.P.H., Al-Mahaidi, R. and Wong, M.B. (2009) "Durability of CFRP Strengthened Concrete Members under Extreme temperature and humidity", Australian Journal of Structural Engineering (AJSE), Vol.9, No2.

Munsinghe, M.G.J .2011 ,Study to Recommend a Steel Truss System With Minimum Steel Quantity Usage For Medium Span Bridges, MEng Thesis , University of Moratuwa,Sri Lanka.pp22-23.

Schnerch.D.Dawood.M, and Razkalla,S,2006, '*Proposed Design Guidelines For Strengthening of Steel Bridges With FRP Materials*', Journal of Construction and Building Material 21 (1001-1110), North Carolina state University,USA.

Sveinsdottir, S.L.2012. Experimental Research on Strengthening of Concrete Beams by The Use of Epoxy Adhesive And Cement Based Bonding Material, MSience Thesis ,Haskolinn, Reykjavik Univercity Iceland.